frontiers | Research Topics

Reassessing the immune system contribution in multiple sclerosis: Therapeutic target, biomarkers of disease and immune pathogenesis

Edited by
Maria Teresa Cencioni, Roberta Magliozzi and Luisa María Villar

Published in
Frontiers in Immunology
Frontiers in Neurology

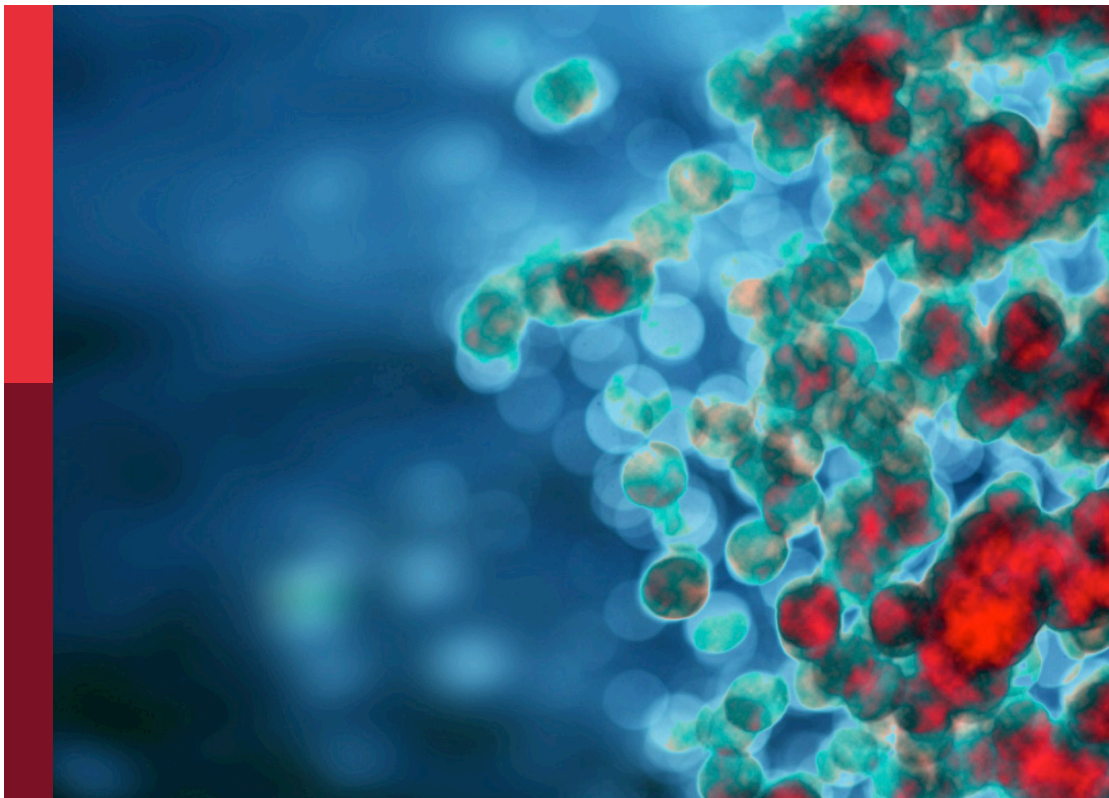

ISSN 1664-8714
ISBN 978-2-83252-014-7
DOI 10.3389/978-2-83252-014-7

About Frontiers

Frontiers is more than just an open access publisher of scholarly articles: it is a pioneering approach to the world of academia, radically improving the way scholarly research is managed. The grand vision of Frontiers is a world where all people have an equal opportunity to seek, share and generate knowledge. Frontiers provides immediate and permanent online open access to all its publications, but this alone is not enough to realize our grand goals.

Frontiers journal series

The Frontiers journal series is a multi-tier and interdisciplinary set of open-access, online journals, promising a paradigm shift from the current review, selection and dissemination processes in academic publishing. All Frontiers journals are driven by researchers for researchers; therefore, they constitute a service to the scholarly community. At the same time, the *Frontiers journal series* operates on a revolutionary invention, the tiered publishing system, initially addressing specific communities of scholars, and gradually climbing up to broader public understanding, thus serving the interests of the lay society, too.

Dedication to quality

Each Frontiers article is a landmark of the highest quality, thanks to genuinely collaborative interactions between authors and review editors, who include some of the world's best academicians. Research must be certified by peers before entering a stream of knowledge that may eventually reach the public - and shape society; therefore, Frontiers only applies the most rigorous and unbiased reviews. Frontiers revolutionizes research publishing by freely delivering the most outstanding research, evaluated with no bias from both the academic and social point of view. By applying the most advanced information technologies, Frontiers is catapulting scholarly publishing into a new generation.

What are Frontiers Research Topics?

Frontiers Research Topics are very popular trademarks of the *Frontiers journals series*: they are collections of at least ten articles, all centered on a particular subject. With their unique mix of varied contributions from Original Research to Review Articles, Frontiers Research Topics unify the most influential researchers, the latest key findings and historical advances in a hot research area.

Find out more on how to host your own Frontiers Research Topic or contribute to one as an author by contacting the Frontiers editorial office: frontiersin.org/about/contact

Reassessing the immune system contribution in multiple sclerosis: Therapeutic target, biomarkers of disease and immune pathogenesis

Topic editors

Maria Teresa Cencioni — Imperial College London, United Kingdom
Roberta Magliozzi — University of Verona, Italy
Luisa María Villar — Ramón y Cajal University Hospital, Spain

Citation

Cencioni, M. T., Magliozzi, R., Villar, L. M., eds. (2023). *Reassessing the immune system contribution in multiple sclerosis: Therapeutic target, biomarkers of disease and immune pathogenesis*. Lausanne: Frontiers Media SA.
doi: 10.3389/978-2-83252-014-7

Table of contents

frontiers in Neurology

ORIGINAL RESEARCH
published: 07 October 2021
doi: 10.3389/fneur.2021.716548

Evaluation of Natalizumab Pharmacokinetics and Pharmacodynamics: Toward Individualized Doses

*Jose M. Serra López-Matencio[1], Yaiza Pérez García[2], Virginia Meca-Lallana[3], Raquel Juárez-Sánchez[2], Angeles Ursa[2], Lorena Vega-Piris[4], Dora Pascual-Salcedo[2], Annick de Vries[5], Theo Rispens[5] and Cecilia Muñoz-Calleja[2,6]**

[1] Servicio de Farmacia, Hospital Universitario de La Princesa, Madrid, Spain, [2] Servicio de Inmunología, Hospital de La Princesa, Madrid, Spain, [3] Servicio de Neurologia, Hospital Universitario de La Princesa, Madrid, Spain, [4] Fundación Biomédica, Hospital de La Princesa, Madrid, Spain, [5] Department of Immunopathology, Sanquin Research and Landsteiner Laboratory, Amsterdam University Medical Centre, University of Amsterdam, Amsterdam, Netherlands, [6] School of Medicine, Universidad Autónoma de Madrid, Madrid, Spain

OPEN ACCESS

Edited by:
Luisa María Villar, Ramón y Cajal University Hospital, Spain

Reviewed by:
Allan G. Kermode, University of Western Australia, Australia
Roberto Alvarez-Lafuente, Instituto de Investigación Sanitaria del Hospital Clínico San Carlos, Spain

***Correspondence:**
Cecilia Muñoz-Calleja
munozcallejacecilia@gmail.com

Specialty section:
This article was submitted to Multiple Sclerosis and Neuroimmunology, a section of the journal Frontiers in Neurology

Received: 07 June 2021
Accepted: 07 September 2021
Published: 07 October 2021

Citation:
Serra López-Matencio JM, Pérez García Y, Meca-Lallana V, Juárez-Sánchez R, Ursa A, Vega-Piris L, Pascual-Salcedo D, de Vries A, Rispens T and Muñoz-Calleja C (2021) Evaluation of Natalizumab Pharmacokinetics and Pharmacodynamics: Toward Individualized Doses. Front. Neurol. 12:716548. doi: 10.3389/fneur.2021.716548

Background: Plasma concentration of natalizumab falls above the therapeutic threshold in many patients who, therefore, receive more natalizumab than necessary and have higher risk of progressive multifocal leukoencephalopathy.

Objective: To assess in a single study the individual and treatment characteristics that influence the pharmacokinetics and pharmacodynamics of natalizumab in multiple sclerosis (MS) patients in the real-world practice.

Methods: Prospective observational study to analyse the impact of body weight, height, body surface area, body mass index, gender, age, treatment duration, and dosage scheme on natalizumab concentrations and the occupancy of α4-integrin receptor (RO) by natalizumab.

Results: Natalizumab concentrations ranged from 0.72 to 67 μg/ml, and RO from 26 to 100%. Body mass index inversely associated with natalizumab concentration (beta = −1.78; $p \leq 0.001$), as it did body weight (beta = −0.34; $p = 0.001$), but not height, body surface area, age or gender Extended vs. standard dose scheme, but not treatment duration, was inversely associated with natalizumab concentration (beta = −7.92; $p = 0.016$). Similar to natalizumab concentration, body mass index (beta = −1.39; $p = 0.001$) and weight (beta = −0.31; $p = 0.001$) inversely impacted RO. Finally, there was a strong direct linear correlation between serum concentrations and RO until 9 μg/ml (rho = 0.71; $p = 0.003$). Nevertheless, most patients had higher concentrations of natalizumab resulting in the saturation of the integrin.

Conclusions: Body mass index and dosing interval are the main variables found to influence the pharmacology of natalizumab. Plasma concentration of natalizumab and/or RO are wide variable among patients and should be routinely measured to personalize treatment and, therefore, avoid either over and underdosing.

Keywords: natalizumab, pharmacokinetics, pharmacodynamics, multiple sclerosis, α4-integrin, dose scheme, efficacy, progressive multifocal leukoencephalopathy PML

INTRODUCTION

Natalizumab is a recombinant humanized anti-α4-integrin antibody against the α subunit (CD49d) of α4 integrins [α4β1 (VLA-4) and α4β7], that prevents the extravasation of inflammatory leukocytes across the blood-brain barrier into the central nervous system (1, 2). Natalizumab is currently indicated as a single disease modifying therapy in highly active relapsing remitting multiple sclerosis (RRMS) (3–5). The drug reduces multiple sclerosis relapses very effectively; nevertheless, it is associated with progressive multifocal leukoencephalopathy (PML), a potentially fatal complication caused by the reactivation of latent John Cunningham virus (JCV). Established risk factors for PML include: the level of anti JCV antibodies in serum as assessed by an anti-JCV antibody index; the use of immunosuppressant therapy before natalizumab initiation; and the duration of natalizumab treatment (6, 7).

The mechanisms underlying the development of PML associated with natalizumab are not completely understood but in all likelihood include, among others, the inhibition of the trafficking of immune cells like antigen presenting cells and anti-viral Th1 lymphocytes to the central nervous system (8, 9), therefore hampering the elimination of the JVC. The magnitude of this extravasation blockade is almost certainly related to the degree of saturation of the α4-integrin. Since demonstrating the presence of a concentration-dependent increase of α4-integrin saturation (10, 11), the PML risk seems to be linked to natalizumab serum concentrations (12–14).

Natalizumab is approved at a fixed dose of 300 mg IV every 4 weeks for the treatment of RRMS in adult patients, allowing natalizumab concentrations to be maintained at levels which ensure continuous maximal α4β1 integrin receptor saturation (15). However, many monoclonal antibodies are dosed on an individual basis (16, 17).

Whereas in the AFFIRM trial the average concentration on the steady state ranged between 23 and 29 μg/ml (11). It is known that plasma concentrations of natalizumab between 1 and 2 μg/ml are enough for most patients to reach saturation of α4-integrin [>80% of receptor occupancy (RO)]. Also that receptor desaturation (saturation <50%) only happens when natalizumab serum concentrations fall below 1 μg/mL (18). This suggests that most patients are overdosed by following the approved guidelines. In addition, considerable variation in natalizumab levels was found among patients in several studies (5, 10, 11, 19) despite administering the same dosage. As a consequence, many clinicians throughout the world now utilize alternative dosing schedules, mainly the extended interval dose (EID), to the standard interval dose (SID) (20–22).

We believe that optimizing natalizumab doses for individual patients is necessary to avoid either relapses or side-effects of the drug. To achieve this, it is necessary to know the impact of different parameters, including: body weight, height, body surface area, body mass index (BMI), age, gender, treatment duration and dosing intervals which influence the pharmacology of natalizumab. However, very few studies (19) have considered, in the real-world practice, both the personal and treatment characteristics altogether in the pharmacokinetics (PK) and pharmacodynamics (PD) of this therapeutic antibody.

MATERIALS AND METHODS

Patients and Study Design

This study is a prospective, observational, nonrandomized, open-label study performed at La Princesa Hospital (Madrid, Spain). For the study were enrolled 32 patients receiving natalizumab for relapsing into various forms of RRMS between 2014 and 2019. The eligibility criteria were: a diagnosis of RRMS according to the applicable panel criteria (23), age of 18 years or older and receiving natalizumab treatment with a minimum of six consecutive infusions. Exclusion criteria were: patients who did not give their informed consent in writing to take part in the study, patients who did not follow the treatment and patients who did not meet the above criteria.

Blood samples were collected immediately prior to the next natalizumab infusion. For some analyses, patients were divided into two groups based on the time interval since the previous natalizumab infusion: SID (26–33 days) or EID (34–41 days). These ranges were chosen after considering the bibliography, in which an interval of 3.5–4.5 weeks was considered standard, and an interval of more than 5 weeks was considered as extended (19–21). Body surface area was calculated with the Du Bois formula (24) and BMI was calculated as body-weight/height^2 (25). At least two serum samples and a maximum of four were drawn from each patient with a difference between samples of 1–5 months. Twenty three patients contributed with two samples, eight with three and one with four.

All samples were obtained at least 7 months after the first dose of natalizumab, therefore the drug had reached the steady state in all patients (10, 26). The longest time from the beginning of the treatment to the extraction of the peripheral blood samples was 54 months. In the case of SID and EID, the interval between sample collection and start of treatment is comparable (30.8 months for SID and 35.61 for EID) according to a two-sample t-test with equal variances, p-value = 0.1789. In total, 74 samples were collected: 30 corresponded to the SID group (40.54%), and 44 to the EID one (59.45%).

The study was classified as a "Postauthorization-Observational Study with drugs" by the Spanish Drug Agency and approved by the ethics committee of La Princesa Hospital (2634A; AMB-NAT-2015-01) and written, informed consent was provided by all research participants. Expanded disability scale score (EDSS), annualized relapse rate (ARRR), age, gender, body weight, treatment duration, and other clinical parameters were obtained from the Hospital medical records.

Natalizumab Serum Concentrations

Serum concentrations of natalizumab were measured at Sanquin Laboratories (Amsterdam) by an ELISA technique, previously described (27). Briefly, the technique requires specific polyclonal rabbit anti-natalizumab F (ab) 2 fragments as capture reagent and a mouse anti-human IgG4 (anti-hIgG4) monoclonal antibody for detection.

α4-Integrin Saturation (RO)

The RO was measured by flow cytometry with an anti-human IgG4-PE to reveal the binding of natalizumab to the surface of the lymphocytes. Three aliquots of whole peripheral blood were washed twice with phosphate-buffered saline to eliminate soluble IgG4 immunoglobulins present in the plasma of the patients to which anti-IgG4-PE could be bound. One of the aliquots was incubated with saturating natalizumab (10 μg/mL) for 1 h at 4°C temperature whereas the remaining two were kept in ice without natalizumab. After incubation, immunofluorescence was carried out against the following human molecules with the next panel of labeled antibodies: CD4-FITC, IgG4-PE, CD19-PerCP, CD3-V500, and CD8-APC-H7 (BD Biosciences, San José, CA). One of the tubes without natalizumab was used for fluorescence minus one (FMO)-PE control. The incubation was made in darkness for 30 min at 4°C. Then, red blood cells were lysed with FACS lysing solution (BD Biosciences, San José, CA) for 10 min and the remaining leukocytes were suspended with phosphate-buffered saline−1% fetal calf serum. The percentage of the different lymphoid subsets and the mean fluorescence intensity (MFI) of the PE signal were measured with a FACSCanto II flow cytometer (BD Biosciences, San José, CA) collecting 100,000 nucleated events. The percentage of natalizumab saturation was calculated from the MFI in each sample by the following formula: MFI – hIgG4-PE signal (without natalizumab)/MFI – hIgG4-PE signal (with natalizumab) × 100.

Statistics

Sample size predetermination was focused on the association between RO and plasma levels. Assuming a minimum correlation = 0.50, an alpha risk of 0.05 and a beta risk of 0.20, we obtained a sample of 30 patients.

Variables analyzed included serum concentration of natalizumab, α4-integrin saturation (RO), weight, height, body surface area, BMI, age, gender, time to treatment start, and dose scheme [either as continuous or categoric variable (SID vs. EID)].

Descriptive analysis of the sample: quantitative variables were described by their measures of central tendency (mean) and dispersion (standard deviation); qualitative variables were described by their proportion and number of patient. Differences of mean were analyzed by *t*-test. Homoscedasticity was tested with Levened and since the *t*-test is a robust test ($n \geq 30$), normality was not checked. Heteroscedasticity variables were analyzed with an unequal variance *t*-test. Spearman's correlation (rho) was used for association analysis of quantitative variables. A linear regression model was applied to control for possible confounding variables. A 95% CI was calculated for all estimates. A $p < 0.05$ was considered statistically significant. All analyses were performed using Stata version 13.

RESULTS

Patient Demographics

The 32 patients enrolled for the study experienced at least 1 relapse in the previous 12 months before being treated with natalizumab and their characteristics are summarized in **Table 1**.

TABLE 1 | Patient demographic and clinical characteristics.

Participants (*n*)	32
Male [*n* (%)]	15 (49%)
Female [*n* (%)]	17 (51%)
Age [Mean ± SD]	40.60 ± 8.61
Weight (kg) [Mean ± SD]	72.75 ± 14.71
Height [Mean ± SD]	170.80 ± 8.14
JC virus positive [*n* (%)]	11 (33.33%)
JC virus index [Mean ± SD]	0.47 ± 0.25
Treatment duration, years [Mean ± SD]	4.51 ± 2.68
Dose interval length, days [Mean ± SD]	33.2 ± 3.21
Days prior infusion by scheme [Mean ± SD]	*SID* 29.87 ± 1.96
	EID 35.47 ± 1.42
NTZ doses [Mean ± SD]	53.18 ± 31.04
Patients with prior treatment [n (%)]	
Interferon	27 (81.81%)
Glatiramer acetate	15 (45.45%)
Dimethyl fumarate	8 (24.24%)
Fampridine	3 (9.09%)
Reasons for abandonment of prior treatment	1 (3.03%)
Efficacy reasons	18 (66.6%)
Intolerability	7 (25.92%)
Lack of compliance	2 (6.06%)

SD, standard deviation; JCV, JC virus; SID, standard interval dose; EID, extended interval dose.

According to the Expanded Disability Status Scale (EDSS) (23), 26 patients (81.25%) presented mild to moderate impairment (EDSS ≤4), while 6 (18.75%) patients presented mild to moderate disability (EDSS between 4 and 7): no patient exceeded (EDSS > 7) thus unable to walk beyond ∼5 m. The mean (SD) EDSS score at the start of the study was 2.599 ± 1.520 while at the end it was 2.484 ± 1.486.

No participant missed a scheduled dose of natalizumab and all patients received the full 300 mg dose. There were no major adverse events that could have prevented the administration of a dose to a patient. All patients were radiologically stable and did not relapse during the study.

Natalizumab Serum Concentrations

The serum concentration of natalizumab was highly varied, ranging from 0.72 to 67 μg/ml: the concentration was constant over time for the same patient and most individuals. A variation in concentration of more than 15 ug/ml was observed in four patients. The rest of the patients had quite a good concordance in serum concentrations amongst samples from the same individual. However, variation among serum natalizumab concentrations between one individual and another were high, ranging from 1–2 to 50 or more μg/ml.

In view of these observations, we analyzed individual factors which could affect the PK and PD of natalizumab, including body weight, height, body surface area, BMI, age, gender, dose scheme, and duration of treatment.

Among individual characteristics, we found a negative linear relationship between serum concentrations of natalizumab and patient body weight (rho = −0.404; $p < 0.001$; **Figure 1A**), body surface area (−0.3624; $p = 0.0015$; **Figure 1B**), and BMI (−0.4933; $p = 0.0000$; **Figure 1C**), when considered as continuous variables. Similarly, when we analyzed the correlation between serum concentration and the interval between doses in each sample we saw a slight negative correlation between post-infusion days and plasma concentration of natalizumab (rho = −0.2389; $p = 0.0403$; **Figure 1D**). This correlation between body weight and natalizumab concentrations was seen with similar strength in both treatment schemes (SID rho = −0.41 $p < 0.04$ vs. EID rho = −0.42 $p < 0.002$; data not shown).

Multivariate analysis confirmed that body weight, BMI and dose interval influence the serum levels of natalizumab (**Tables 2**, **3**).

Finally, we found a weak association between natalizumab serum concentration and patient age ($p = 0.033$; data not shown) while the duration of the treatment did not influence the serum levels of the drug (data not shown).

α4-Integrin Receptor Occupancy

To evaluate the PD of natalizumab we measured the RO in the T-cells from the peripheral blood of patients by using flow cytometry. Just as with natalizumab concentrations we analyzed the impact of different individual characteristics as well as the scheme of treatment on the RO of natalizumab.

The evaluation of natalizumab occupancy of α4-integrin also revealed high variability among patients, ranging from 44 to 100% (data not shown). Natalizumab occupancy of α4-integrin was weakly inversely related to the body weight when the whole cohort was considered (rho = −0.28; $p = 0.02$; **Figure 2A**). Similar correlations were obtained with both body surface area and BMI (rho = −0.2885; $p = 0.0127$; rho = −0.2232; $p = 0.0559$; **Figures 2B,C**). When patients were divided on SID or EID scheme of treatment, natalizumab occupancy of α4-integrin was related to body weight only in those patients treated with the EID scheme (rho = −0.416, $p = 0.003$). Actually, most patients with values of RO below 70% were high weight individuals from the EID scheme. In addition, the treatment scheme did not influence the RO, either as a categorical (SID or EID: 88.41 vs. 85.67, $p = 0.367$) or continuous variable (rho = 0.02; $p = 0.853$; **Figure 2D**).

Similarly, the age, gender or treatment duration were not related to the RO neither considering patients as a whole cohort nor divided by the SID or EID scheme of treatment (data not shown). The multivariate analysis confirmed the inverse association between RO and body weight (beta = −0.31; $p = 0.001$) and BMI (beta = −1.39; $p = 0.001$; **Tables 4**, **5**).

The Receptor Occupancy Depended on the Serum Concentration of Natalizumab

Finally, we wanted to confirm the dependence of the RO on the plasma concentration of natalizumab in our cohort of patients. A weak association was found between both parameters in the cohort of patients (rho = 0.256, $p = 0.027$; **Figure 3**); in the case for male patients (rho = 0.477, $p = 0.019$); in the group of patients above 40 years old (rho = 0.453, $p = 0.04$); and in the EID scheme (rho = 0.416, $p = 0.003$). A multivariate analysis confirmed that the higher the natalizumab concentration the higher the RO adjusted of gender, age and scheme of treatment (**Table 6**).

The weak association between RO and plasma levels of natalizumab in the whole cohort was due to the fact that for over 10 μg/ml there was no correlation between RO and plasma concentration of natalizumab (**Figure 3**). In the light of this, correlations of up to 10 μg/ml and above 10 μg/ml were calculated separately: the values were for up to 10 μg/ml rho = 0.58 ($p = 0.006$) and above 10 μg/ml rho = 0.23 ($p = 0.091$). Moreover, the cut-off point with the highest statistic correlation between both parameters was 9 μg/ml (rho = 0.71; $p = 0.003$).

DISCUSSION

Our study adds insights on how the individual characteristics of the patients which mostly influence the PK (natalizumab serum concentration) and the PD (natalizumab RO) of natalizumab in 32 effectively treated RRMS patients for a long period of time with no major adverse reactions (data given in **Table 1**).

The long-standing experience reached with natalizumab in clinical trials and in observational studies offers strong evidence of its effectiveness in RRMS patients (3–5). However, there has been some concern for the patient safety since natalizumab was linked to some cases of PML (6, 7). Established risk factors for PML include the level of anti JCV antibodies in serum as assessed by anti-JCV antibody index, the use of immunosuppressant therapy before natalizumab initiation, and the duration of natalizumab treatment (6, 7). Moreover, it is more than likely that the EID scheme would develop this severe disease to a lesser extent and that this scheme could effectively control the RRMS in the same way. To confirm this possibility several studies were carried out by different authors (11, 18–22, 27–29). Currently, there are two clinical trials in this field, one assessing the effect of a planned 12-week dosing interruption on the drug PK (NCT04048577), and another to evaluate the impact of switching the patients from SID to EID on the effectiveness of natalizumab (NCT04580381).

The evaluation of natalizumab serum concentrations in our patients revealed a broad range (over 60-fold) of values, showing the pharmacological variability that exists among patients. The majority of patients had concentrations of 5 μg/ml or greater, including two patients with concentrations >50 μg/ml. This means that most patients were over-treated (19, 20), since concentrations higher than 5 μg/ml were related to complete saturation of the α4-integrin in most patients. This could increase the patient's risk of developing PML (29).

Our data demonstrate that serum concentration of natalizumab is inversely related with patient's weight, in agreement with previous studies (19, 30, 31), as well as with body surface area and BMI. Therefore, these parameters should be taken into consideration when deciding the scheme for natalizumab.

Similar to other studies the treatment scheme also impacted the plasma concentration of natalizumab, that was higher in the

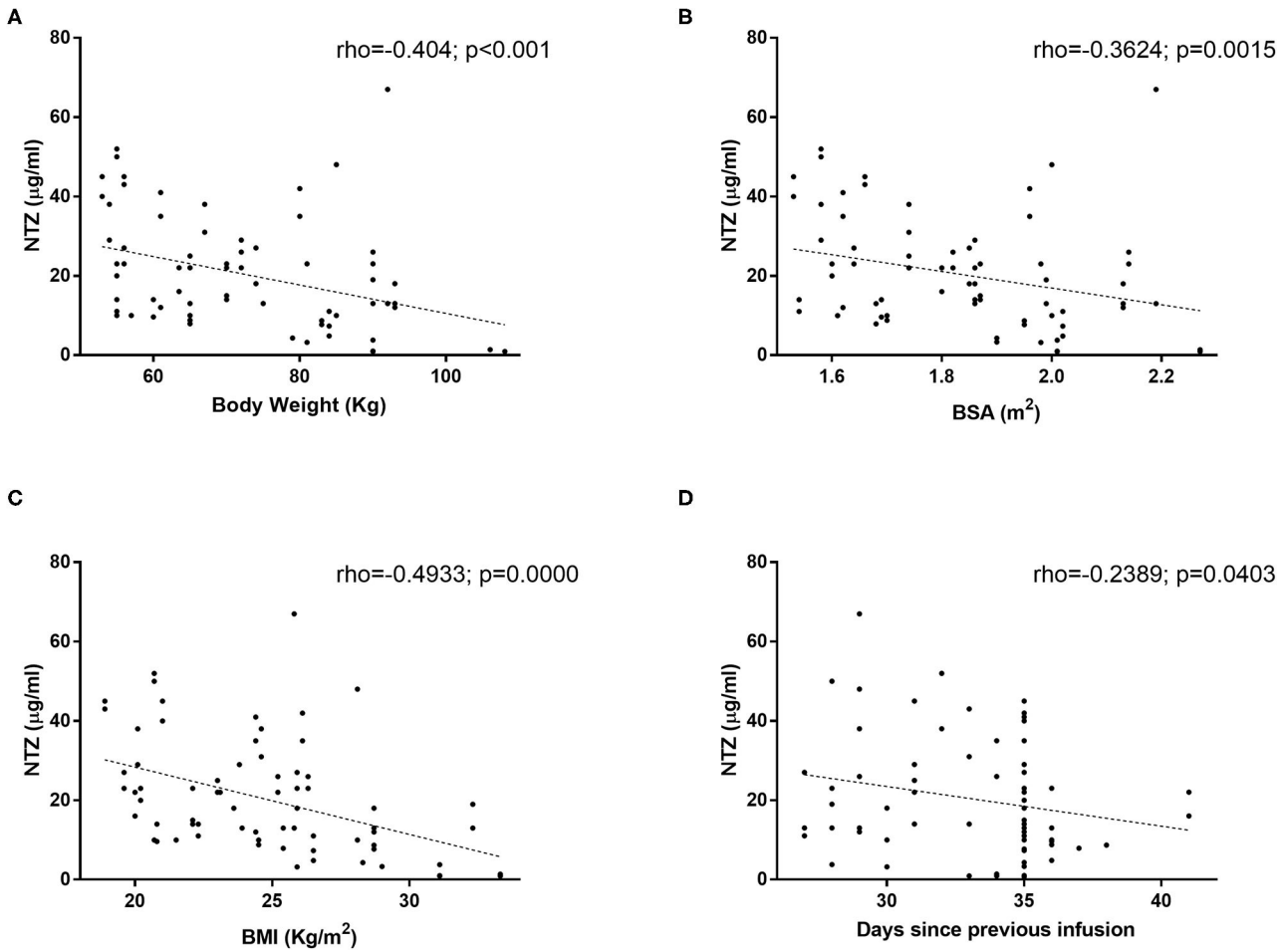

FIGURE 1 | Natalizumab serum concentration correlation to **(A)** body weight, **(B)** Body Surface Area (BSA), **(C)** Body Mass Index (BMI), and **(D)** scheme doses. Natalizumab concentration was measured with ELISA as described by Rispens et al. in 74 samples from 32 patients. Spearman's correlation (rho) was used for association analysis of quantitative variables.

TABLE 2 | Multivariate analysis for drug serum levels and body weight (variables are considered as continuous).

Natalizumab µg/ml	β	[95% Conf. Interval]	P-value
Weight (kg)	−0.3736135	−0.5905907 to 0.1566363	0.001
Age (years)	0.1156723	0.479519 to 0.2661744	0.548
Dose scheme (days)	−1.123487	−2.119463 to 0.1275116	0.028
Cons.	89.53663	52.32627 to 126.747	0.000

TABLE 3 | Multivariate analysis for drug serum levels and BMI (variables are considered as continuous).

Natalizumab µg/ml	β	[95% Conf. Interval]	P-value
BMI (Kg/m2)	−1.779968	−2.597465 to −0.9624717	0.000
Age (years)	−0.0439754	−0.4149139 to 0.3269631	0.814
Dose scheme (days)	−1.192826	−2.148883 to −0.2367683	0.015
Cons.	105.8316	67.78114 to 143.882	0.000

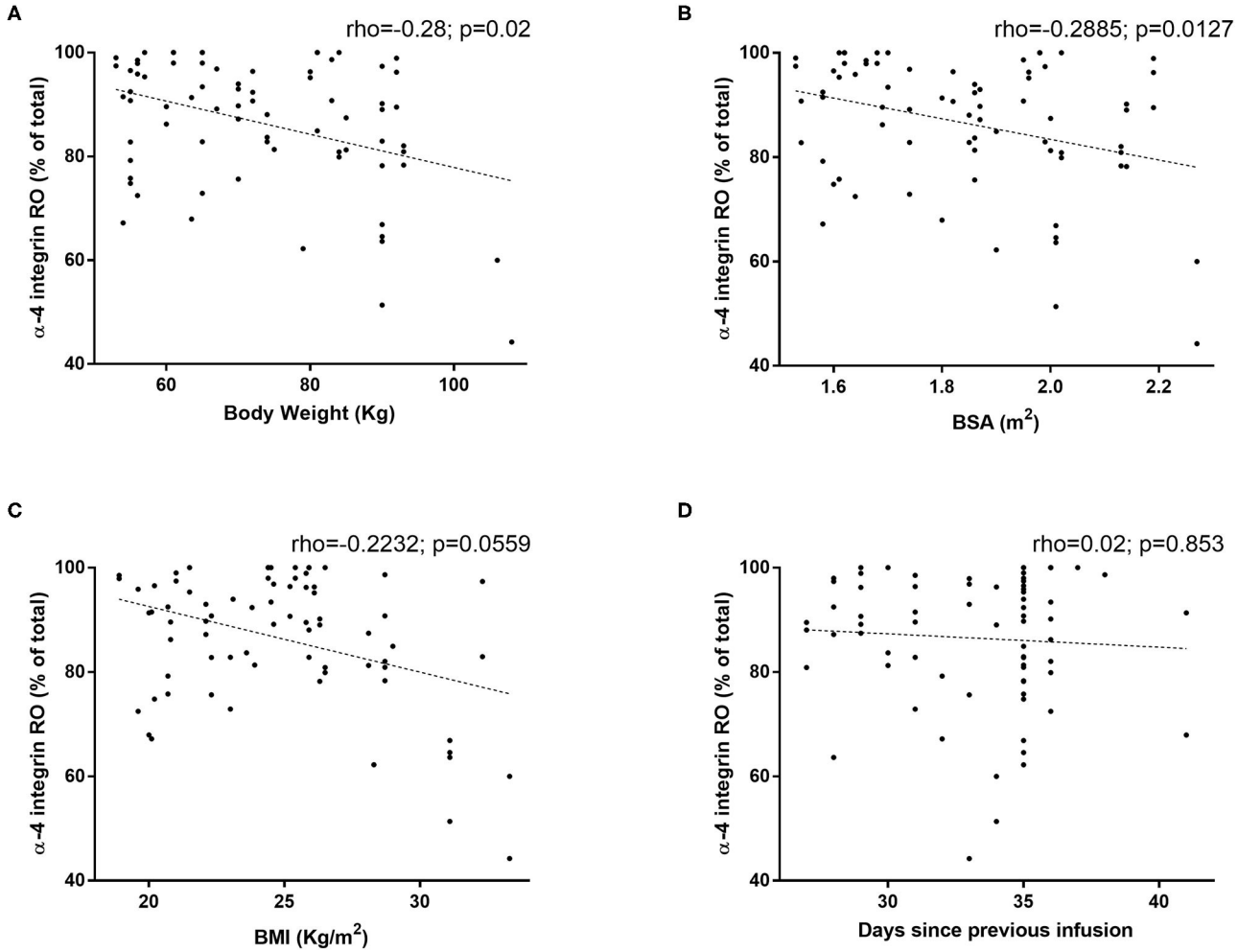

FIGURE 2 | Correlation of receptor occupancy of α4-integrin by natalizumab to **(A)** body weight, **(B)** Body Surface Area (BSA), **(C)** Body Mass Index (BMI), and **(D)** scheme doses. The receptor occupancy of natalizumab was measured by flow cytometry, with an anti-human IgG4-PE, by revealing the binding of natalizumab to the surface of the lymphocytes in 74 samples from 32 patients. Spearman's correlation (rho) was used for association analysis of quantitative variables.

TABLE 4 | Multivariate analysis for receptor occupancy of α4-integrin and body weight (variables are considered as continuous).

RO (% of total)	β	[95% Conf. Interval]	P-value
Weight (Kg)	−0.3124683	−0.4981626 to −0.126774	0.001
Treatment duration (years)	0.9801092	−0.0592339 to 2.019452	0.064
Cons.	104.8731	90.08744 to 119.6587	0.000

TABLE 5 | Multivariate analysis for receptor occupancy of α4-integrin and BMI (variables are considered as continuous).

RO (% of total)	β	[95% Conf. Interval]	P-value
Age (years)	0.1634503	0.2065952 to 0.5334958	0.381
Dose scheme (days)	−0.5334701	−1.43738 to 0.37044	0.243
Treatment duration (years)	0.0029582	−0.1976502 to 0.2035667	0.977
BMI (Kg/m2)	−1.398437	−2.172268 to −0.6246052	0.001
Cons.	132.2103	96.08135 168.3393	0.000

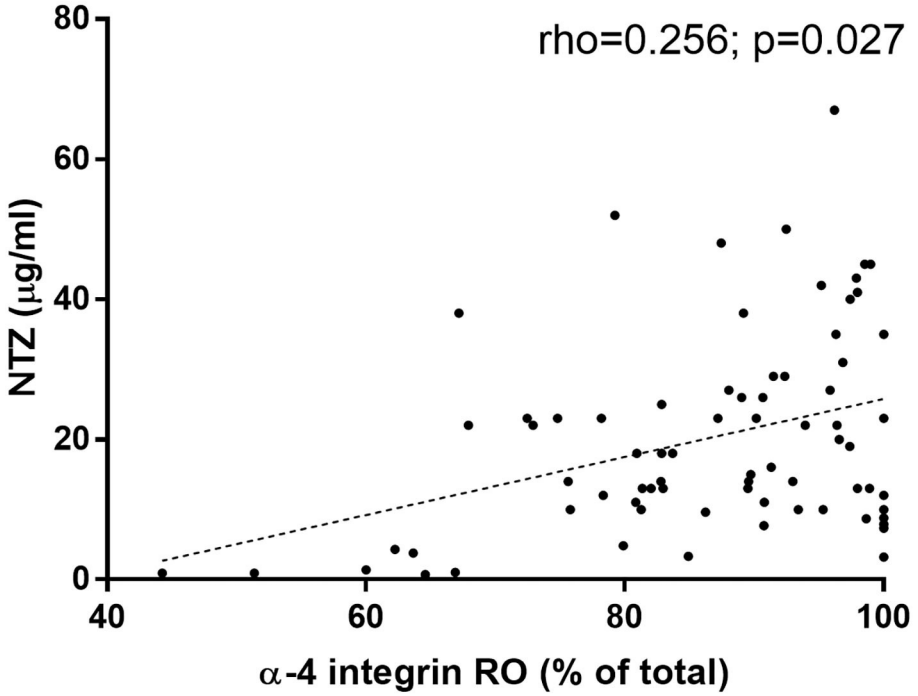

FIGURE 3 | Receptor occupancy of α4-integrin by natalizumab correlates to natalizumab serum concentration. Natalizumab concentration was measured with ELISA as described by Rispens et al. The receptor occupancy of natalizumab was measured by flow cytometry with an anti-human IgG4-PE, by revealing the binding of natalizumab to the surface of the lymphocytes in 74 samples from 32 patients.

TABLE 6 | Multivariate analysis confirming the relation between natalizumab concentration and receptor occupancy of α4-integrin.

RO (% of total)	β	[95% Conf. Interval]	P-value
Natalizumab (ug/ml)	0.2310722	0.0354729 to 0.4266714	0.021
Weight (Kg)	−0.229495	−0.4227673 to −0.0362227	0.021
Treatment duration (years)	0.9835752	−0.0242292 to 1.99138	0.056
Cons.	94.135	77.15946 to 111.1105	0.000

SID scheme (19, 21, 22). The selected patients from the SID group could, therefore, switch to the EID group since no patient relapsed during the study. Several studies after natalizumab discontinuation indicate that MS disease activity is suppressed for at least 6 weeks after the last administration of the drug (12, 14). Furthermore, 2 retrospective studies have suggested that natalizumab efficacy is not compromised by EID regimens (21, 22).

When stratified by gender, natalizumab serum concentrations were lower in men, both in the whole cohort and in the different dose schedules. However, no effect of gender was observed in the multivariate analysis, suggesting that those differences were actually related to weight differences between the sexes. Treatment duration did not influence the natalizumab serum concentrations, which is in line with other study (31). These findings reopen the discussion on whether a longer course of treatment could be supported without increasing the risk of PML (32, 33).

Regarding natalizumab RO, it has always been assumed that values between 70 and 80% were necessary for optimal drug efficacy. However, different studies show that much lower levels (around 20%) would be enough to keep the patient without significant disease activity (18, 34). This is supported by our study here where we found RO values under 70% and even some under 60% in stable patients.

In the individual characteristics that affect the RO, we found that occupancy of α4-integrin is weakly inversely related to the body weight and BMI when the whole cohort was considered. The fact that most patients were beyond saturation levels may explain the low significance, in accordance with a previous study (10). The relationship of RO and body weight found in the whole cohort was only maintained in the EID cohort, this may be due to the fact that many of our samples for EID were from heavier patients. There are no significant differences in RO values when dividing patients by the scheme of treatment,

in contrast with other studies whereby those were greater in SID (19, 21). This may be a reflection of our study design, in which the EID samples were collected at ∼5 weeks post infusion (**Table 1**), while in these other studies the time was longer, around 6 weeks. This would mean that the treatment could be extended at least 1 week without significant changes in RO.

Finally, in our cohort of patients we confirmed and characterized the correlation between the RO and the plasma concentration of natalizumab. In fact, we have described that a concentration of natalizumab of 9 μg/ ml is the cut-off point where the strongest correlation between these variables: when the natalizumab concentration increases, the α4ß1-integrin saturation increases rapidly from ∼40% to 80%, but the curve flattens beyond this value. In other studies this cut-off was established at 10 μg/ml (10). It appears that physicians should avoid concentrations higher than 9 μg/ml because there is no PD advantage or clinical benefits. Furthermore, we should seek lower concentrations to obtain even lower RO values since RO values below 50% have been sufficient to keep patients without radiological and clinical disease activity, either in our study or others (18, 34). Nevertheless, we are conscious that stability on MRI and lack of clinical relapses in the short term of observation are unequivocally not identical to lack of clinical progression, neurodegeneration, and axonal loss over the longer term.

In summary, with the current approved fixed dose, there is a wide pharmacological variability between patients that prescribing clinicians should be aware and take into account. Among the individual characteristics, body weight, BMI, and the treatment scheme, had a significant impact on the pharmacology of natalizumab. In addition, RO strongly depends on natalizumab serum concentrations up to ∼9 μg/ml while higher concentrations result in the saturation of the integrin in most patients. As a consequence, the majority of our patients were overtreated. Conversely, testing levels may be extremely useful to prevent inadvertent underdosing of patients, specifically those in whom extended dosing is exhibited. The possibility of underdosing should dominate clinical concerns in this group of patients. To pursue these possible outcomes larger studies will be necessary.

In summary, the authors strong argue that either the RO and/or the serum concentration of natalizumab should be routinely measured in every patient, with the aim of personalizing treatment without loss of efficacy.

DATA AVAILABILITY STATEMENT

The raw data supporting the conclusions of this article will be made available by the authors, without undue reservation.

ETHICS STATEMENT

The studies involving human participants were reviewed and approved by the Ethics Committee of La Princesa Hospital. The patients/participants provided their written informed consent to participate in this study.

AUTHOR CONTRIBUTIONS

JMSL-M and CM-C: conception, data collection, analysis, and writing. YP: data collection and sample analysis. VM-L: conception, data collection, and critical revision. RJ-S: sample analysis. LV-P: analysis and critical revision. DP-S: critical revision. AV: sample analysis and critical revision. TR: sample analysis and critical revision. All authors contributed to the article and approved the submitted version.

FUNDING

This work was supported by a grant PI018/01163 from the Fondo de Investigaciones Sanitarias, Instituto de Investigación Carlos III, Ministerio de Sanidad y Consumo, Spain, to CM-C who also was cofinanced by FEDER funds.

ACKNOWLEDGMENTS

We thank Lawrence Baron for linguistic and grammatical editing of the manuscript and Ana Marcos Jiménez for editing of the figures.

REFERENCES

1. Yednock TA, Cannon C, Fritz LC, Sanchez-Madrid F, Steinman L, Karin N. Prevention of experimental autoimmune encephalomyelitis by antibodies against alpha 4 beta 1 integrin. *Nature.* (1992) 356:63–6. doi: 10.1038/356063a0
2. Léger OJ, Yednock TA, Tanner L, Horner HC, Hines DK, Keen S, et al. Humanization of a mouse antibody against human alpha-4 integrin: a potential therapeutic for the treatment of multiple sclerosis. *Hum Antibodies.* (1997) 8:3–16. doi: 10.3233/HAB-1997-8102
3. European Commission (2006). *Renewing and Amending the Marketing Authorisation for the Medicinal Product for Human Use and Quot; Tysabri - Natalizumab and Quot; granted by Decision C.* Available online at: http://ec.europa.eu/health/documents/community-register/2016/20160418134501/dec_134501_en.pdf (accessed March 1, 2017).
4. Rudick R, Polman C, Clifford D, Miller D, Steinman L. Natalizumab: bench to bedside and beyond. *JAMA Neurol.* (2013) 70:172–82. doi: 10.1001/jamaneurol.2013.598
5. Polman CH, O'Connor PW, Havrdova E, Hutchinson M, Kappos L, Miller DH, et al. A randomized, placebo-controlled trial of natalizumab for relapsing multiple sclerosis. *N Engl J Med.* (2006) 354:899–910. doi: 10.1056/NEJMoa044397
6. Langer-Gould A, Atlas SW, Green AJ, Bollen AW, Pelletier D. Progressive multifocal leukoencephalopathy in a patient treated with natalizumab. *N Engl J Med.* (2005) 353:375–81. doi: 10.1056/NEJMoa051847
7. Kleinschmidt-DeMasters BK, Tyler KL. Progressive multifocal leukoencephalopathy complicating treatment with natalizumab and interferon beta-1a for multiple sclerosis. *N Engl J Med.* (2005) 353:369–74. doi: 10.1056/NEJMoa051782
8. Del Pilar Martin M, Cravens PD, Winger R, Frohman EM, Racke MK, Eagar TN. Decrease in the numbers of dendritic cells and CD4+ T cells

in cerebral perivascular spaces due to natalizumab. *Arch Neurol.* (2008) 65:1596–603. doi: 10.1001/archneur.65.12.noc80051
9. Paroni M, Maltese V, De Simone M, Ranzani V, Larghi P, Fenoglio C, et al. Recognition of viral and self-antigens by TH1 and TH1/TH17 central memory cells in patients with multiple sclerosis reveals distinct roles in immune surveillance and relapses. *J Allergy Clin Immunol.* (2017) 140:797–808. doi: 10.1016/j.jaci.2016.11.045
10. Muralidharan KK, Kuesters G, Plavina T, Subramanyam M, Mikol DD, Gopal S, et al. Population pharmacokinetics and target engagement of natalizumab in patients with multiple sclerosis. *J Clin Pharmacol.* (2017) 57:1017–30. doi: 10.1002/jcph.894
11. Fox RJ, Cree BA, De Seze J, Gold R, Hartung H-P, Jeffery D, et al. MS disease activity in RESTORE: a randomized 24-week natalizumab treatment interruption study. *Neurology.* (2014) 82:1491–8. doi: 10.1212/WNL.0000000000000355
12. Frohman EM, Monaco MC, Remington G, Ryschkewitsch C, Jensen PN, Johnson K, et al. JC virus in CD34+ and CD19+ cells in patients with multiple sclerosis treated with natalizumab. *JAMA Neurol.* (2014) 71:596–602. doi: 10.1001/jamaneurol.2014.63
13. Major EO, Frohman EM, Douek D. JC viremia in natalizumab treated patients with multiple sclerosis. *N Engl J Med.* (2013) 368:2240–1. doi: 10.1056/NEJMc1214233
14. Berkovich R, Togasaki DM, Cen SY, Steinman L. CD4 cell response to interval therapy with natalizumab. *Ann Clin Transl Neurol.* (2015) 2:570–4. doi: 10.1002/acn3.190
15. European Medicine Agency (EMA) (2020). Natalizumab: Summary of Product Characteristics. http://www.ema.europa.eu/docs/en_GB/document_library/EPAR_-_Product_Information/human/000603/WC500044686.pdf (accessed March 1, 2020).
16. European Medicine Agency (EMA). *Tocilizumab: Summary of Product Characteristics.* (2020). Available online at: https://www.ema.europa.eu/en/medicines/human/EPAR/roactemra (accessed March 1, 2020).
17. European Medicine Agency (EMA). *Rituximab: Summary of Product Characteristics.* (2020). Available online at: https://www.ema.europa.eu/en/documents/productinformation/mabthera-epar-product-information_en.pdf (accessed March 1, 2020).
18. Khatri BO, Man S, Giovannoni G, Koo AP, Lee JC, Tucky B, et al. Effect of plasma exchange in accelerating natalizumab clearance and restoring leukocyte function. *Neurology.* (2009) 72:402–9. doi: 10.1212/01.wnl.0000341766.59028.9d
19. Foley JF, Goelz S, Hoyt T, Christensen A, Metzger RR. Evaluation of natalizumab pharmacokinetics and pharmacodynamics with standard and extended interval dosing. *Mult Scler Relat Disord.* (2019) 31:65–71. doi: 10.1016/j.msard.2019.03.017
20. Yamout BI, Sahraian MA, Ayoubi NE, Tamim H, Nicolas J, Khoury SJ, et al. Efficacy and safety of natalizumab extended interval dosing. *Mult Scler Relat Disord.* (2018) 24:113–6. doi: 10.1016/j.msard.2018.06.015
21. Bomprezzi R, Pawate S. Extended interval dosing of natalizumab: a two-center, 7-year experience. *Ther Adv Neurol Disord.* (2014) 7:227–31. doi: 10.1177/1756285614540224
22. Zhovtis RL, Frohman TC, Foley J, Kister I, Weinstock-Guttman B, Tornatore C, et al. Extended interval dosing of natalizumab in multiple sclerosis. *J Neurol Neurosurg Psychiatry.* (2016) 87:885–9. doi: 10.1136/jnnp-2015-312940
23. Thompson A, Banwell B, Barkoff F, Carroll WM, Coetzee T, Comi G, et al. Diagnosis of multiple sclerosis: 2017 revisions of the McDonald Criteria. *Lancet Neurol.* (2018) 17:162–73. doi: 10.1016/S1474-4422(17)30470-2
24. Du Bois D, Du Bois EF. A formula to estimate the approximate surface area if height and weight be known. *Arch of Int Med.* (1916) 17:863–71. doi: 10.1001/archinte.1916.00080130010002
25. Deurenberg P, Weststrate JA, Seidell JC. Body mass index as a measure of body fatness: age- and sex-specific prediction formulas. *Br J Nutr.* (1991) 65:105. doi: 10.1079/BJN19910073
26. Calabresi PA, Giovannoni G, Confavreux C, Galetta SL, Havrdova E, Hutchinson M, et al. The incidence and significance of anti-natalizumab antibodies: results from AFFIRM and SENTINEL. *Neurology.* (2007) 69:1391–403. doi: 10.1212/01.wnl.0000277457.17420.b5
27. Rispens T, Leeuwen A, Vennegoor A, Killestein J, Aalberse RC, Wolbink GJ, et al. Measurement of serum levels of natalizumab, an immunoglobulin G4 therapeutic monoclonal antibody. *Anal Biochem.* (2011) 411:271–6. doi: 10.1016/j.ab.2011.01.001
28. Sehr T, Proschmann U, Thomas K, Marggraf M, Straube E, Reichmann H, et al. New insights into the pharmacokinetics and pharmacodynamics of natalizumab treatment for patients with multiple sclerosis, obtained from clinical and *in vitro* studies. *J Neuroinflammation.* (2016) 13:164. doi: 10.1186/s12974-016-0635-2
29. Van Kempen ZL, Leurs CE, Witte BI, de Vries A, Wattjes MP, Rispens T, et al. The majority of natalizumab-treated MS patients have high natalizumab concentrations at time of re-dosing. *Mult Scler.* (2017) 24:805–10. doi: 10.1177/1352458517708464
30. Zhovtis RL, Foley JF, Chang I, Kister I, Cutter G, Metzger RR, et al. Risk of natalizumab-associated PML in patients with MS is reduced with extended interval dosing. *Neurology.* (2019) 93:e1452–62.
31. van Kempen ZLE, Hoogervorst ELJ, Wattjes MP, Kalkers NF, Mostert JP, Lissenberg-Witte BI, et al. Personalized extended interval dosing of natalizumab in MS - a prospective multicenter trial. *Neurology.* (2020) 95:e745–54. doi: 10.1212/WNL.0000000000009995
32. Bloomgren G, Richman S, Hotermans C, Subramanyam M, Goelz S, Natarajan A, et al. Risk of natalizumab-associated progressive multifocal leukoencephalopathy. *N Engl J Med.* (2012) 366:1870–80. doi: 10.1056/NEJMoa1107829
33. Ho PR, Koendgen H, Campbell N, et al. Risk of natalizumab-associated progressive multifocal leukoencephalopathy in patients with multiple sclerosis: a retrospective analysis of data from four clinical studies. *Lancet Neurol.* (2017) 16:925–33. doi: 10.1016/S1474-4422(17)30282-X
34. Plavina T, Muralidharan KK, Kuesters G, Mikol D, Evans K, Subramanyam M, et al. Reversibility of the effects of natalizumab on peripheral immune cell dynamics in MS patients. *Neurology.* (2017) 89:1584–93. doi: 10.1212/WNL.0000000000004485

Conflict of Interest: The authors declare that the research was conducted in the absence of any commercial or financial relationships that could be construed as a potential conflict of interest.

Publisher's Note: All claims expressed in this article are solely those of the authors and do not necessarily represent those of their affiliated organizations, or those of the publisher, the editors and the reviewers. Any product that may be evaluated in this article, or claim that may be made by its manufacturer, is not guaranteed or endorsed by the publisher.

frontiers in Immunology

ORIGINAL RESEARCH
published: 08 October 2021
doi: 10.3389/fimmu.2021.760546

Role of B Cell Profile for Predicting Secondary Autoimmunity in Patients Treated With Alemtuzumab

*Paulette Esperanza Walo-Delgado[1], Enric Monreal[2], Silvia Medina[1], Ester Quintana[3], Susana Sainz de la Maza[2], José Ignacio Fernández-Velasco[1], Paloma Lapuente[1], Manuel Comabella[4], Lluis Ramió-Torrentà[3], Xavier Montalban[4], Luciana Midaglia[4], Noelia Villarrubia[1], Angela Carrasco-Sayalero[1], Eulalia Rodríguez-Martín[1], Ernesto Roldán[1], José Meca-Lallana[5], Roberto Alvarez-Lafuente[6], Jaime Masjuan[2], Lucienne Costa-Frossard[2] and Luisa Maria Villar[1]**

[1] Department of Immunology, Ramón y Cajal University Hospital, Instituto Ramón y Cajal de Investigación Sanitaria (IRYCIS), Red Española de Esclerosis Múltiple (REEM), Madrid, Spain, [2] Department of Neurology, Ramón y Cajal University Hospital, IRYCIS, Red Española de Esclerosis Múltiple (REEM), Madrid, Spain, [3] Neuroimmunology and Multiple Sclerosis Unit, Neurology Department, Neurodegeneration and Neuroinflammation Research Group, Biomedical Research Institute (IDIBGI), Red Española de Esclerosis Múltiple (REEM), Girona, Spain, [4] Servei de Neurologia-Neuroimmunologia, Centre d'Esclerosi Múltiple de Catalunya (Cemcat), Institut de Recerca Vall d'Hebron (VHIR), Hospital Universitari Vall d'Hebron, Universitat Autònoma de Barcelona, Red Española de Esclerosis Múltiple (REEM), Barcelona, Spain, [5] Department of Neurology, Virgen de la Arrixaca University Hospital, Murcia, Spain, [6] Grupo de Investigación de Factores Ambientales en Enfermedades Degenerativas, Instituto de Investigación Sanitaria del Hospital Clínico San Carlos, Hospital Clínico San Carlos, Red Española de Esclerosis Múltiple (REEM), Madrid, Spain

OPEN ACCESS

Edited by:
Jorge Correale,
Fundación Para la Lucha Contra las Enfermedades Neurológicas de la Infancia (FLENI), Argentina

Reviewed by:
Hans-Peter Hartung,
Heinrich Heine University of Düsseldorf, Germany
Wendy Gilmore,
University of Southern California, United States

***Correspondence:**
Luisa Maria Villar
luisamaria.villar@salud.madrid.org

Specialty section:
This article was submitted to Multiple Sclerosis and Neuroimmunology, a section of the journal Frontiers in Immunology

Received: 18 August 2021
Accepted: 21 September 2021
Published: 08 October 2021

Citation:
Walo-Delgado PE, Monreal E, Medina S, Qiuntana E, Sainz de la Maza S, Fernández-Velasco JI, Lapuente P, Comabella M, Ramió-Torrentà L, Montalban X, Midaglia L, Villarrubia N, Carrasco-Sayalero A, Rodríguez-Martín E, Roldán E, Meca-Lallana J, Alvarez-Lafuente R, Masjuan J, Costa-Frossard L and Villar LM (2021) Role of B Cell Profile for Predicting Secondary Autoimmunity in Patients Treated With Alemtuzumab. Front. Immunol. 12:760546. doi: 10.3389/fimmu.2021.760546

Objective: To explore if baseline blood lymphocyte profile could identify relapsing remitting multiple sclerosis (RRMS) patients at higher risk of developing secondary autoimmune adverse events (AIAEs) after alemtuzumab treatment.

Methods: Multicenter prospective study including 57 RRMS patients treated with alemtuzumab followed for 3.25 [3.5-4.21] years, (median [interquartile range]). Blood samples were collected at baseline, and leukocyte subsets determined by flow cytometry. We had additional samples one year after the first cycle of alemtuzumab treatment in 39 cases.

Results: Twenty-two patients (38.6%) developed AIAEs during follow-up. They had higher B-cell percentages at baseline (p=0.0014), being differences mainly due to plasmablasts/plasma cells (PB/PC, p=0.0011). Those with no AIAEs had higher percentages of CD4+ T cells (p=0.013), mainly due to terminally differentiated (TD) (p=0.034) and effector memory (EM) (p=0.031) phenotypes. AIAEs- patients also showed higher values of TNF-alpha-producing CD8+ T cells (p=0.029). The percentage of PB/PC was the best variable to differentiate both groups of patients. Baseline values >0.10% closely associated with higher AIAE risk (Odds ratio [OR]: 5.91, 95% CI: 1.83-19.10, p=0.004). When excluding the 12 patients with natalizumab, which decreases blood PB/PC percentages, being the last treatment before alemtuzumab, baseline PB/PC >0.1% even predicted more accurately the risk of AIAEs (OR: 11.67, 95% CI: 2.62-51.89, p=0.0007). The AIAEs+ group continued having high percentages of PB/PC after a year of alemtuzumab treatment (p=0.0058).

Conclusions: A PB/PC percentage <0.1% at baseline identifies MS patients at low risk of secondary autoimmunity during alemtuzumab treatment.

Keywords: multiple sclerosis, side effects, autoimmunity, disease modifying treatments, alemtuzumab, biomarkers, B cells

INTRODUCTION

Alemtuzumab (Lemtrada®; Sanofi, Paris, France) is a humanized monoclonal antibody approved for the treatment of relapsing-remitting multiple sclerosis (RRMS). It is administered as two annual courses and proved to be efficacious for patients with highly inflammatory disease, resulting in prolonged remission periods (1).

Alemtuzumab targets CD52, a molecule expressed at high levels by T and B lymphocytes (2). It causes a selective depletion of these cells *via* antibody and complement dependent cytotoxicity and apoptosis (3). T and B-cell repopulation begins within weeks, with a distinctive pattern; B cells undergo faster repopulation, while T cells remain depleted longer (4). Repopulation associates with increases of regulatory CD56bright natural killer (NK) cells (2), and regulatory T cells and with a reduction of the production of pro-inflammatory cytokines (5). This can explain the long duration of clinical effects in the absence of continuous treatment. As a counterpart, frequent adverse events associated with alemtuzumab include infusion-associated reactions, infections, and mainly autoimmune adverse events (AIAEs) (6, 7). The most frequent AIAEs are those involving the thyroid gland, observed in about 38% of patients treated with alemtuzumab (8). Other secondary AIAEs initially described in the clinical trials included immune thrombocytopenia and nephropathies. In the post-marketing setting, new ones have also been reported (9, 10). These side effects, although mild in most cases, limit the use of this drug. Therefore, reliable biomarkers predicting patient individual risk for developing autoimmunity, and hence, guide patient selection for this particular therapy, would be of great clinical importance.

We aimed to explore if the blood lymphocyte profile before alemtuzumab treatment initiation and after a year of treatment could identify MS patients at high risk of AIAEs.

MATERIALS AND METHODS

Study Design

This was a multicenter prospective longitudinal exploratory study including 59 patients diagnosed with RRMS according to 2010 McDonald criteria (11) who were initiating treatment with alemtuzumab. Patients were consecutively recruited in five Spanish hospitals.

Patients

Patients were followed for 3.55 [3.25-4.21] years (median [25%-75% interquartile range (IQR)]) after alemtuzumab treatment initiation. All patients received two courses of alemtuzumab (12 mg/d IV on five consecutive days at baseline and 12 mg/day IV on three consecutive days 12 month later). Five patients received an additional course for presenting new clinical relapses after the second course. Clinical and demographic data of patients at study inclusion are described in **Table 1**.

Patient Follow-Up

Patients were evaluated every three months to assess the appearance of new AIAEs, the occurrence of new relapses and the Expanded Disability Status Scale (EDSS) score. MRI scans were performed at baseline and yearly after treatment initiation. Analytical tests, including blood count, serum analyses of renal

TABLE 1 | Clinical and demographic features of patients.

Variable	Patients (n = 59)
Sex (F/M)	39/20
Age at disease onset [years] – median (IQR)	28 (23-33.6)
Age at treatment onset [years] – median (IQR)	37 (30-44)
Disease duration [years] – median (IQR)	7.0 (3.0-11.5)
EDSS score at treatment onset – median (IQR)	2.75 (1.5-3.63)
Annualized relapse rate in the two previous years – median (IQR)	0.83 (0.63-1.75)
Previous disease modifying treatments (Yes/No)	46/13
Number of previous treatments - median (range)	2 (0-6)
Last treatment (Number of patients)	
None	14
IFN-beta/GA/Teriflunomide/DMF	19
Fingolimod	13
Natalizumab	13
Time of follow-up since alemtuzumab treatment onset [years] – median (IQR)	3.55 (3.25-4.21)
Alemtuzumab curses (Number of patients)	
Two courses	54
Three courses	5

n, number of patients; F, Female; M, male; EDSS, Expanded Disability Status Scale; IQR, 25%-75% interquartile range; IFN, Interferon; GA, Glatiramer acetate; DMF, Dimethyl fumarate.

and thyroid function were performed monthly, while the presence of anti-glomerular basement membrane and anti-thyroid antibodies (including anti-thyroid peroxidase, anti-thyroglobulin and anti-thyroid-stimulating hormone receptor) was tested every three months.

Patients were trained to recognize symptoms suggestive of AIAEs early, and promptly inform the treating physician. AIAEs were defined as the appearance of any autoimmune events during follow-up, with special attention paid to thyroid-associated events, immune thrombocytopenia and autoimmune nephropathy.

Sample Collection

Blood samples were collected before initiating alemtuzumab and in 39 cases, one year after. Peripheral blood mononuclear cells (PBMCs) were obtained from heparinized whole blood (20 mL) by Ficoll density gradient centrifugation (Abbott) and cryopreserved in aliquots of 5x10 (6) cells until studied. Aditionally, fresh blood was collected in an EDTA tube to explore total cell counts in a Coulter counter.

Monoclonal Antibodies

Leukocyte subpopulations were assessed using the following monoclonal antibodies: CD3-PerCP, CD3-BV421, CD4-APC-H7, CD8-FITC, CD8-APC-H7, CD14-APC-H7, CD19-PE-Cy7, CD20-FITC, CD24-FITC, CD25-PE-Cy7, CD27-PE, CD38-APC-H7, CD45-V500, CD45RO-APC, CD56-APC, CD127-BV421 and CCR7-PE. Intracellular cytokines were stained using the next panel: Interleukin (IL)-10-PE, Interferon (IFN)-gamma-FITC, Granulocyte-Macrophage Colony Stimulating Factor (GM-CSF)-PE, Tumor necrosis factor (TNF)-alpha-PerCP-Cy5.5 and IL-17A -APC. All monoclonal antibodies were purchased from BD Biosciences, except IL-17A-APC, from R&D Systems.

Flow Cytometry Analyses

To study surface antigens, cells were stained with the respective monoclonal antibodies during 30 min at 4°C in the dark, washed with saline and analyzed in a FACSCanto II flow cytometer (BD Biosciences), as described before (12).

For intracytoplasmic cytokine detection, cells were stimulated with phorbol-12-myristate-13-acetate (PMA, Merck) and Ionomycin (Merck), in presence of Brefeldin A (GolgiPlug, BD Biosciences) and Monensin (GolgiStop, BD Biosciences), and then incubated 4 h at 37°C in 5% CO2 atmosphere. For the analysis of IL-10 producing B cells, PBMC were incubated prior to stimulation with CpG oligonucleotide (InvivoGen) for 20 h. After incubation, surface markers were stained, then the cellular membrane permeabilized with Cytofix/Cytoperm Kit (BD Biosciences), and incubated with intracellular antibodies, following the same protocol previously described (12).

Cells were analyzed using FACSDiva Software V.8.0 (BD Biosciences). A minimum amount of 5x10 (4) events were acquired. Gating strategy is defined in **Figure 1**.

Statistical Analysis

Data were analyzed using the Prism 8.0 (GraphPad Software) and Stata 14 (StataCorp) statistical packages. Mann–Whitney U tests were used to explore continuous variables. ROC curves were used to establish cut-off values and Fisher's exact tests to analyze categorical variables. p values below 0.05 were considered as significant.

The missing data were not imputed since the proportion was less than 10% in all variables and we can assume that they were missing completely at random.

Standard Protocol Approvals, Registrations, and Patient Consents

The study was approved by the ethics committee of the Ramón y Cajal University Hospital. All patients signed a written informed consent form before inclusion.

RESULTS

Fifty-nine RRMS patients initiating alemtuzumab were included. To avoid bias due to previous autoimmune diseases, one patient was excluded for presenting previous autoimmune pathology. One patient was lost during follow-up. Fifty-seven RRMS patients were finally studied. Twenty-two (38.6%) experienced AIAEs during follow-up. Twenty-one of them presented autoimmune thyroid alterations, and the remaining one developed autoimmune thrombocytopenia. No significant differences were found in clinical and demographic characteristics at baseline or during follow-up between patients showing AIAEs (AIAEs+) and patients who did not develop AIAEs (AIAEs-) (**Table 2**).

Flow Cytometry Analyses

We studied leukocyte profiles at baseline. Results are shown in **Tables 3** and **4**. When exploring innate immunity, represented by monocytes and NK cells, no significant differences in cellular percentages were observed between AIAEs+ and AIAEs- patients. We did not find differences either in regulatory T and NK as well as in IL-10 producing B and T cells. By contrast, there was an increase in the percentages of CD4+ T cells (p=0.012) in AIAEs- group, mainly due to effector memory (EM, p=0.031) and terminally differentiated (TD, p=0.034) subsets. In addition, AIAEs-patients showed an augment of CD8 T cells producing TNF-alpha (p=0.03). However, the highest differences between AIAEs+ and AIAEs- patients was found in B cells (**Figure 2**). Those acquiring AIAEs showed higher percentages of B cells (p=0.0014), being differences mainly due to plasmablasts/plasma cells (PB/PC, p=0.0011) and to a lesser extent to naïve cells (p=0.013). No significant differences were found in other B cell subsets or in cytokine producing B cells.

We measured absolute cell counts in all lymphocyte subsets associated with autoimmunity. The relative augment of PB/PC present in AIAEs+ patients was also found when exploring total cell numbers (p=0.024). No significant differences in absolute cell numbers were found in any other cell subset (**Supplementary Table 1**).

Finally, we explored if changes observed at baseline remained after a year of alemtuzumab treatment. We studied PBMCs obtained before administering the second cycle of the drug in

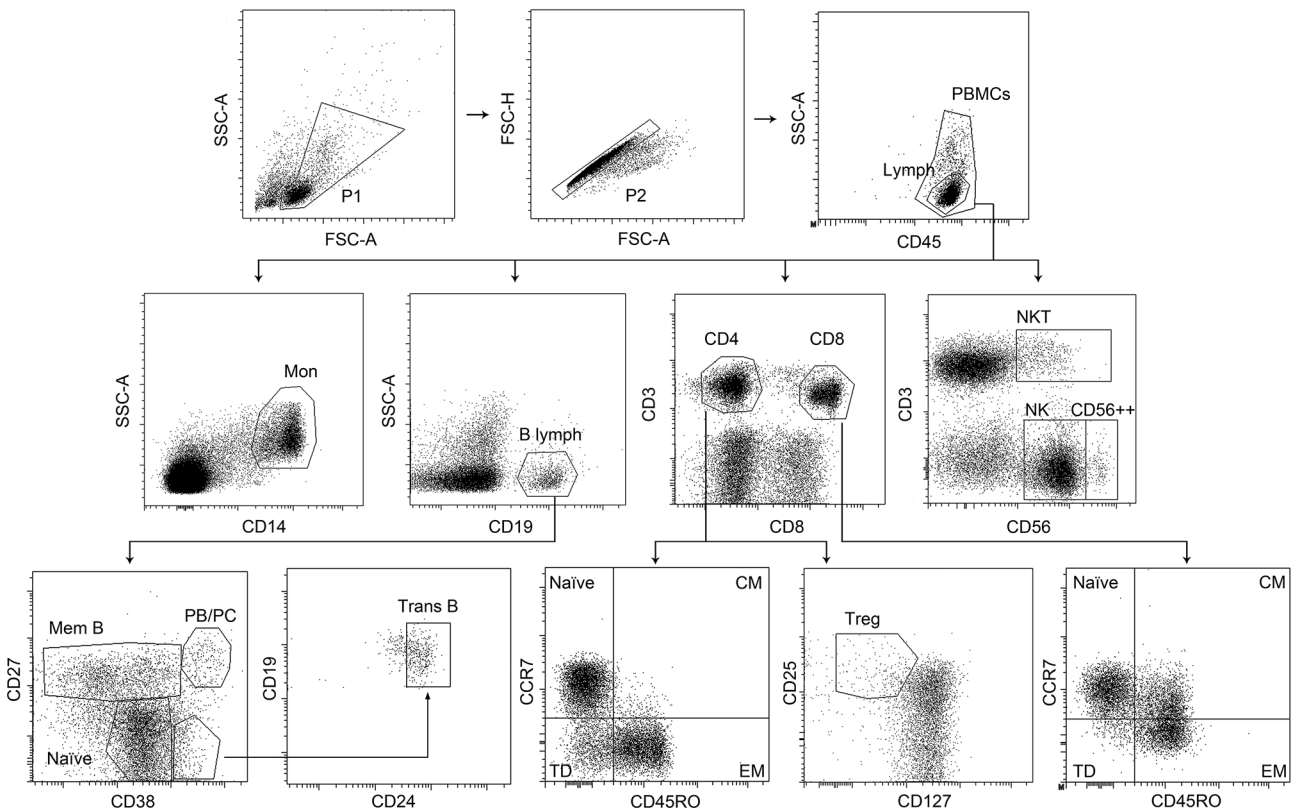

FIGURE 1 | Gating strategy showing representative images for flow cytometry analysis. Peripheral blood mononuclear cells (PBMC) were first gated for excluding debris and apoptotic cells (gate P1) and duplets (gate P2). Lymphocytes were recognized by CD45 staining and low SSC (gate Lymph). Monocytes were recognized as CD14++ cells with intermediate SSC (gate Mon). B cells were detected by the expression of CD19 (gate B lymph) and subdivided by CD27 staining into memory cells: CD27+ (gate Mem B), naïve: CD27- (gate Naïve), plasmablasts/plasma cells: CD27hi, CD38hi (gate PB/PC), and transitional B cells: CD27-, CD38hi, CD24hi, (gate Trans B). Total CD4+ T cells were identified as CD3+ CD8- T cells (gate CD4), and CD8+ T cells were gated as CD3+ CD8++ cells (gate CD8). CD4 and CD8 T cells were classified as naïve: CCR7+ CD45RO– (gate Naïve), central memory: CCR7+ CD45RO+ (gate CM), effector memory: CCR7– CD45RO+ (gate EM), and terminally differentiated: CCR7– CD45RO– (gate TD). CD4+ T regulator cells were identified as CD25hi and CD127-/low (gate Treg). NK cells were identified based on their CD56 expression intensity and CD3 co-expression into CD56+ CD3- (gate NK), CD56+ CD3+ (gate NKT), and CD56++ CD3- (gate CD56++). FSC-A= Forward Scatter-Area; FSC-H= Forward Scatter-Height; SSC-A= Side Scatter-Area.

39 of the patients studied at baseline (13 of AIAEs+ group and 26 of the AIAEs- one). Results are shown in **Table 5**. PB/PC remained high in AIAEs+ patients a year after administering the first alemtuzumab cycle (p= 0.0058). Representative examples are shown in **Figure 3**. No differences were observed in other cell subsets at this point.

Our data suggest that the percentages of PB/PC at baseline could be a good tool to identify patients with low risk of autoimmunity when treated with alemtuzumab. To address this issue we performed a ROC curve analysis [area under the curve (AUC)=0.75, p=0.001; sensitivity=77.1, specificity=63.6] and established a cut-off value of 0.10. Fourteen out of 22 patients presenting AIAEs but only eight of the 35 AIAEs- patients had a percentage of PB/PC higher than 0.10 [Odds ratio (OR) 5.91, 95% CI 1.83-19.10, p=0.004, **Figure 4A**]. To improve the sensitivity of the assay, we next explored if the heterogeneity found in AIAEs group could be related to previous treatment, since it has been described that natalizumab diminishes the concentration of blood plasmablasts (13, 14). We found that five of the eight AIAEs patients who presented a percentages of PB/PC at baseline <0,1%, received natalizumab as the last treatment prior to alemtuzumab. In fact, PB/PC percentages did not differ in patients previously treated with natalizumab who showed or not AIAEs [AIAEs+ median (IQR)=0.07 (0.06-0.09); AIAEs- median (IQR)=0.05 (0.05-0.07), p=ns]. We explored the effect of the previous treatment with natalizumab in other leukocyte subsets, and did not find any significant changes from our results with the whole cohort.

As a consequence, we performed a new ROC curve analysis on the PB/PC percentages excluding patients who received natalizumab as the last treatment before alemtuzumab. This improved the results (AUC 0.80, p=0.0007; sensitivity=75.0, specificity=82.4). The best cut-off value was again 0.1. Results of the new analysis clearly improved those obtained with the whole cohort (OR=11.67 95% CI 2.62-51.89, p=0.0007, **Figure 4B**).

TABLE 2 | Clinical and demographic characteristics of patients classified according to the appearance of autoimmune adverse events.

Variable	AIAEs+ (n = 22)	AIAEs- (n = 35)	p value
Sex (F/M).	16/6	21/14	ns
Age at disease onset [years] – median (IQR).	26.5 (23-33)	30 (25-36)	ns
Age at alemtuzumab treatment onset [years] – median (IQR)	36 (31-39)	37 (30-47)	ns
Disease duration [years] – median (IQR)	7.0 (1.0-12.0)	7 (3-11.2)	ns
EDSS score at treatment onset – median (IQR).	2.00 (1.5-4.0)	3.0 (2.0-3.5)	ns
Relapse rate in the two previous years – median (IQR)	0.86 (0.51-2.75)	0.78 (0.64-1.61)	ns
Time of follow-up since alemtuzumab treatment onset [years] – median (IQR)	3.78 (3.41-4.59)	3.47 (3.18-3.99)	ns
Number of previous treatments - median (range)	2.5 (0-5)	2.0 (0-6)	ns
Prior treatment (Number of patients)			ns
None (n=14)	7	7	
IFN-beta/GA/Teriflunomide/DMF (n=19)	3	16	
Fingolimod (n=12)	7	5	
Natalizumab (n=12)	5	7	

n, number of patients; AIAEs, Autoimmune adverse events (n=22, consisting of 21 patients with autoimmune thyroiditis, and one patient with autoimmune thrombocytopenia); F, Female; M, male; IQR=25%-75% interquartile range; ns, not significant; EDSS, Expanded Disability Status Scale; IFN, Interferon-beta; GA, Glatiramer acetate; DMF, Dimethyl fumarate. p-values were obtained using Mann–Whitney U tests for continuous variables and Fisher's exact tests for categorical variables.

DISCUSSION

The search for biomarkers predicting the appearance of new AIAEs after alemtuzumab treatment is of the utmost importance, since these side effects limit the use of this drug, which has proven to be very efficacious in patients with highly active MS (1).

The data obtained in the pivotal phase III trials suggested that the pattern of T- and B-cell depletion and repopulation following alemtuzumab could influence the appearance of secondary autoimmunity (15). However, repopulation kinetics of the peripheral lymphocyte subsets are comparable between patients with or without AIAEs (16).

On the other hand, high serum levels of IL-21, a cytokine promoting T and B-cell differentiation and antibody production, were proposed as predictors of secondary autoimmunity after alemtuzumab treatment (17–19). However ulterior analyses limited its use as a biomarker since there is some overlapping between patients who develop AAIEs and those who not, and detection tests currently available could not distinguish accurately between both groups of patients (20). Likewise, pre-treatment presence of serum anti-thyroid autoantibodies associated with increased risk for clinical onset of thyroid autoimmunity after alemtuzumab treatment (21), but this biomarker would only benefit a small group of patients.

TABLE 3 | Percentages of peripheral blood mononuclear cells at baseline.

		AIAEs+, n = 22 median (IQR)	AIAEs-, n = 35 median (IQR)	p value
Innate immune cells	NK CD56dim	15.0 (9.58-20.3)	12.2 (8.51-17.7)	ns
	NKT	2.67 (1.58-3.99)	3.30 (1.84-5.80)	ns
	Monocytes	11.3 (8.44-20.1)	13.2 (8.33-21.8)	ns
Regulatory cells	Regulatory T cells	2.08 (1.66–3.34)	2.33 (1.50-3.40)	ns
	NK CD56 bright	0.97 (0.76-1.35)	0.97 (0.55-1.13)	ns
	CD4 IL-10+	0.17 (0.10-0.31)	0.14 (0.10-0.20)	ns
	CD8 IL-10+	0.11 (0.04-0.20)	0.11 (0.06-0.26)	ns
	CD19 IL-10+	0.19 (0.09-0.30)	0.23 (0.10-0.35)	ns
T cells	Total T cells	47.4 (39.7-56.3)	53.3 (48.8-63.8)	0.020
	Total CD4+ T cells	32.4 (26.4-39.9)	41.8 (34.9-45.3)	0.013
	CD4+ Naïve	17.9 (12.7-25.6)	18.9 (10.3-28.5)	ns
	CD4+ CM	8.56 (7.0-10.2)	9.42 (7.76-12.5)	ns
	CD4+ EM	3.83 (3.01-6.64)	7.21 (3.40-11.2)	0.031
	CD4+ TD	1.05 (0.70-1.54)	1.60 (0.93-2.20)	0.034
	Total CD8+ T cells	10.4 (8.14-14.3)	9.19 (6.75-17.1)	ns
	CD8+ Naïve	5.10 (2.93-7.62)	3.27 (1.80-5.60)	ns
	CD8+ CM	0.44 (0.30-0.81)	0.31 (0.24-0.65)	ns
	CD8+ EM	2.22 (1.58-3.35)	1.93 (1.15-3.10)	ns
	CD8+ TD	2.59 (1.45-3.22)	2.40 (0.96-6.40)	ns
B cells	Total B cells	7.95 (5.10-13.1)	5.79 (3.90-6.66)	0.0014
	Transitional B cells	0.09 (0.03-0.20)	0.04 (0.03-0.10)	ns
	Naïve	4.10 (2.44-9.94)	2.46 (1.65-3.90)	0.013
	Memory	2.11 (1.30-3.21)	1.60 (1.25-2.97)	ns
	Plasmablasts/Plasma cells	0.13 (0.08-0.23)	0.07 (0.05-0.10)	0.0011

AIAEs, Autoimmune adverse events; IQR, 25%-75% interquartile range; ns, not significant; NK, Natural Killer cells; NKT, Natural Killer T cells; CM, central memory; EM, effector memory; TD, terminally differentiated. Percentages were calculated over total peripheral blood mononuclear cells. p-values were obtained using Mann–Whitney U test.

TABLE 4 | Percentages of T and B cells producing pro-inflammatory cytokines at baseline.

		AIAEs+, n = 22 median (IQR)	AIAEs-, n = 35 median (IQR)	p value
CD4+ T cells	CD4+ TNF-alpha+	13.2 (9.57-17.1)	16.9 (12.9-22.1)	ns
	CD4+ GM-CSF+	1.30 (0.79-1.66)	1.37 (0.97-2.47)	ns
	CD4+ IFN-gamma+	2.60 (2.08-4.50)	3.88 (2.27-5.50)	ns
	CD4+ IL-17+	0.17 (0.09-0.31)	0.12 (0.09-0.20)	ns
CD8+ T cells	CD8+ TNF-alpha+	3.39 (1.98-5.36)	5.42 (3.15-8.02)	0.029
	CD8+ GM-CSF+	0.59 (0.30-1.01)	0.74 (0.50-1.07)	ns
	CD8+ IFN-gamma+	2.48 (1.47-4.05)	3.11 (1.78-4.86)	ns
	CD8+ IL-17+	0.06 (0.03-0.10)	0.09 (0.04-0.10)	ns
B cells	TNF-alpha+	1.70 (1.10-2.99)	2.42 (1.33-5.54)	ns
	GM-CSF+	0.32 (0.18-0.58)	0.30 (0.20-0.40)	ns

AIAEs, Autoimmune adverse events; IQR, 25%-75% interquartile range; ns, not significant; IL, Interleukin; TNF, Tumor necrosis factor; GM-CSF, Granulocyte-Macrophage Colony Stimulating Factor; IFN, Interferon. Percentages were calculated over total peripheral blood mononuclear cells. p-values were obtained using Mann–Whitney U test.

MS is a heterogeneous disease with different immunological mechanisms playing a main role in the inflammatory response (22). Our group focused on studying the immune cell profile before alemtuzumab treatment, assessing both the absolute counts and percentages of the peripheral blood mononuclear cells.

Patients who later developed autoimmunity presented some subtle differences at baseline on T cells, including lower percentages of CD4+ T cells, particularly of terminally differentiated and effector memory cells, and also lower values of CD8+ T cells producing TNF-alpha.

The highest differences were found on B cells, particularly in plasmablasts/plasma cells (PB/PC), which were significantly higher at baseline on patients who later developed autoimmunity. These effector cells, which produce immunoglobulins at a high rate, were implicated in autoimmune responses in MS, where some blood plasmablasts are autoreactive and recognize brain gray matter

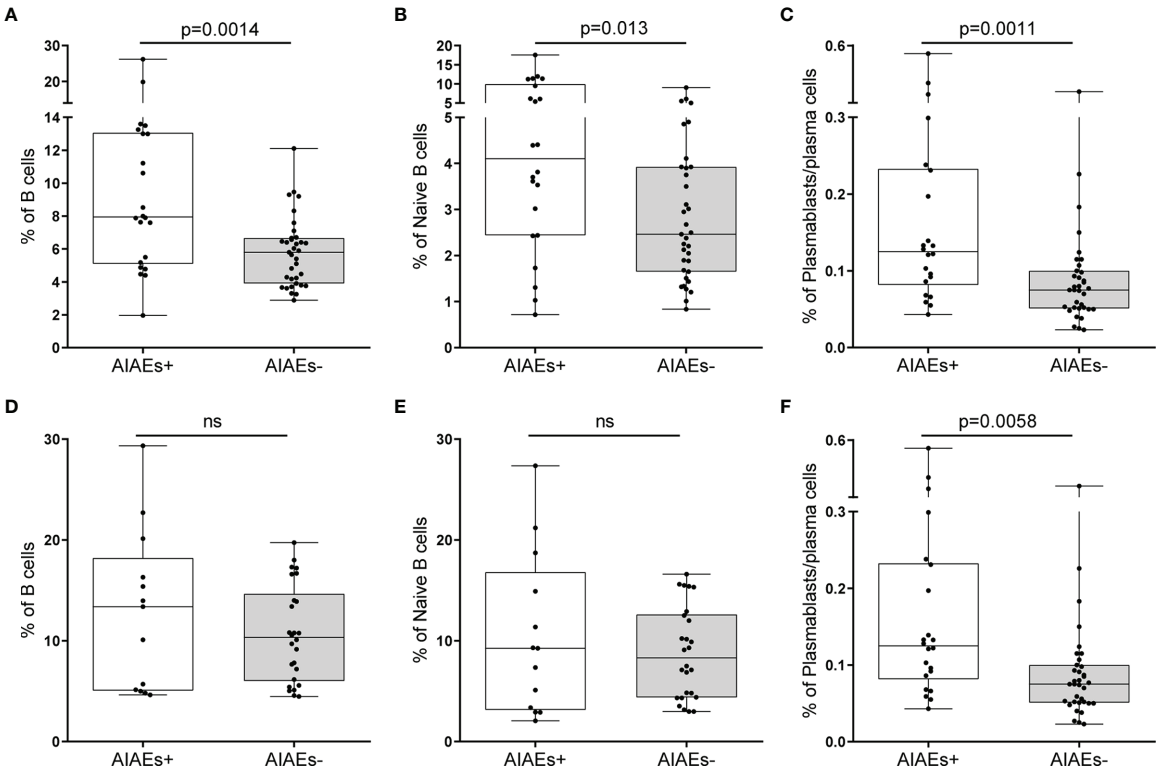

FIGURE 2 | Percentages of cell subsets classified according to the presence or absence of adverse autoimmune events (AIAEs). Percentages of total B cells **(A, D)**, naïve B cells **(B, E)** and plasmablasts **(C, F)** at baseline **(A–C)** and at 12 months of alemtuzumab treatment onset **(D–F)** in 22 patients who developed AIAEs (+) and 35 who did not (-). All percentages are relative to total peripheral blood mononuclear cells. Median values and 25%-75% interquartile range are shown in plots. p-value were obtained using Mann–Whitney U test. ns, not significant.

TABLE 5 | Percentages of cell subsets one year after first cycle of treatment in patients with secondary autoimmunity who had associations with baseline subsets.

		AIAEs+, n = 13 median (IQR)	AIAEs-, n = 26 median (IQR)	p value
T cells	CD4 T cells	22.0 (17.5-27.4)	18.9 (15.0-21.3)	ns
	CD4 EM	2.55 (2.00-3.67)	4.15 (2.08-6.08)	ns
	CD4 TD	0.70 (0.39-1.19)	0.90 (0.60-1.45)	ns
	CD8+ TNF-alpha	2.30 (1.92-7.64)	2.63 (1.15-3.17)	ns
B cells	Total B cells	13.4 (5.06-18.2)	10.3 (6.00-14.7)	ns
	Naïve	9.25 (3.14-16.8)	8.29 (4.37-12.6)	ns
	Plasmablasts/plasma cells	0.17 (0.09-0.28)	0.09 (0.05-0.10)	0.0058

AIAEs, Autoimmune adverse events; EM, effector memory; IQR, 25%-75% interquartile range; ns, not significant; TD, terminally differentiated. Percentages were calculated over total peripheral blood mononuclear cells. p-values were obtained using Mann–Whitney U test.

antigens, what produces and perpetuates an autoimmune response directed toward neurons (23).

When exploring the ability of these cells to predict secondary autoimmunity at baseline, we found that this was not the case in patients treated previously with natalizumab, who mostly presented a lower percentage of plasmablasts. This agrees with previous data showing that natalizumab and no other disease modifying drugs diminish the percentages of plasmablasts in blood (14, 15, 24).

We also observed that those patients who presented at baseline a lymphocyte profile associated with a high probability of developing AIAE, one year after the first cycle of treatment continued presenting high percentages of PB/PC. This may be due to the poor expression of CD52, the target molecule of alemtuzumab, in plasmablasts (25) and mostly in antibody secreting cells (26), which may minimize the effect of this drug in these B cell subsets.

Naïve B cell repopulation is completed about six months after administrating alemtuzumab, while that of CD8+ T cells lasts for a year and reconstitution of memory B cells and of CD4+ T cells and may last more than two years (6, 15). Additionally, the ratios between activated and regulatory cells seem to decrease in patients treated with alemtuzumab during reconstitution (27). This may contribute to the long quality responses reached after the administration of this drug and to the delay in the onset of secondary autoimmunity (6–8). However, when repopulation is

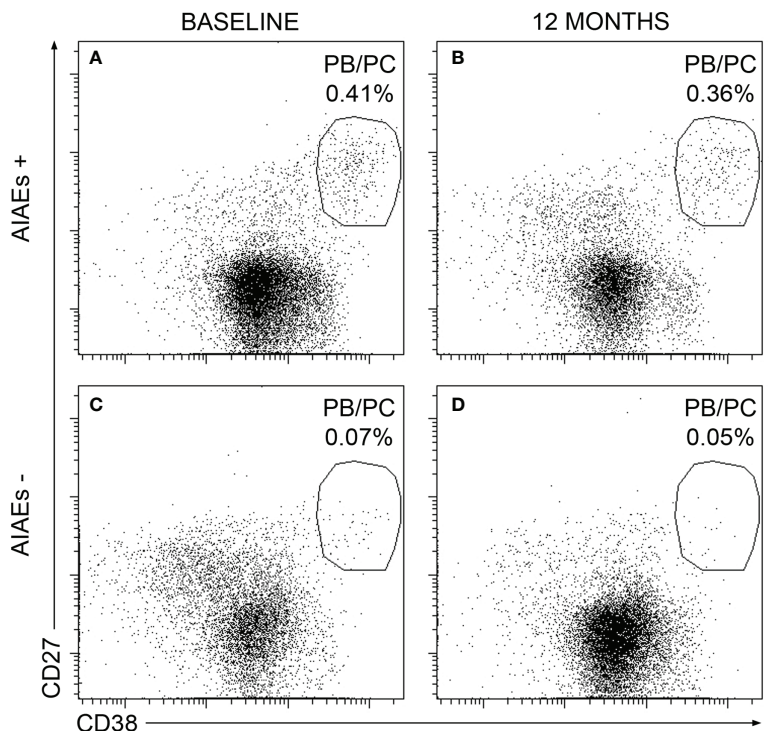

FIGURE 3 | Representative dot plots showing plasmablasts/plasma cells percentages from a AIAEs+ and AIAEs- patient at baseline and after one year of treatment. Percentages of plasmablasts/plasma cells from a AIAEs+ patient at baseline **(A)** and after a one year of treatment **(B)** and from a AIAEs- patient at baseline **(C)** and after one year of treatment **(D)**. Percentages are relative to total peripheral blood mononuclear cells.

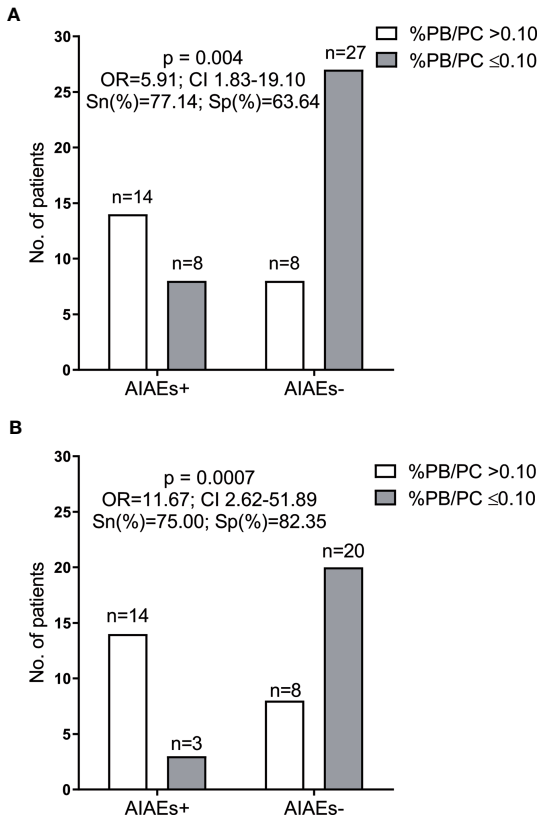

FIGURE 4 | Number of patients with (+) and without (-) autoimmune adverse events (AIAEs) classified according to plasmablasts/plasma cells percentages before alemtuzumab treatment initiation. **(A)** Analysis performed in all patients included in the study (n=57); **(B)** Analysis performed excluding patients who received natalizumab as the last treatment before alemtuzumab (n=45). AIAES, autoimmune adverse events; PB/PC, plasmablasts/plasma cells; N, number; OR, odds ratio; CI, confidence interval. ROC curves were used to establish cut-off values. p-value was obtained using Fisher's exact tests.

completed, the proportion of regulatory T, B and NK cells decreases in patients treated with alemtuzumab (27). The coincidence of lower values of regulatory cells with high numbers of plasmablasts may increase the risk of developing other antibody-mediated autoimmune diseases, as those mainly occurring after alemtuzumab treatment (8). This was observed in our series, where baseline percentages of plasmablasts > 0.10 clearly predicted a higher risk of secondary autoimmunity after alemtuzumab. These data suggest that the immunological mechanisms predominating in individual patients not only influence the response to treatment in MS (28) but can have a clear influence on the side effects.

Although these findings should be validated in larger cohorts with longer follow-up periods, our results suggest that to assess baseline percentages of plasmablasts could be a useful tool to identify MS patients at high risk of autoimmunity upon alemtuzumab treatment, with the limitation of previous treatment, since PB/PC percentages should not be assessed in patients receiving Natalizumab as the last drug before Alemtuzumab initiation.

DATA AVAILABILITY STATEMENT

The original contributions presented in the study are included in the article/**Supplementary Material**. Further inquiries can be directed to the corresponding author.

ETHICS STATEMENT

The studies involving human participants were reviewed and approved by Ethics committee of the Ramón y Cajal University Hospital. The patients/participants provided their written informed consent to participate in this study.

AUTHOR CONTRIBUTIONS

PEWD played a major role in performing experiments, acquisition and analysis of data and drafted the manuscript; EM contributed to statistical analyses and data adquisition. SM, JIFV, PL and NV collected samples and performed flow cytometry experiments; ER and ER-M supervised flow cytometry studies. ACS performed auto-antibody quantification; SSM, MC, EQ, LR-T, XM, LM, JM-L, RA-L, LCF, and JM visited MS patients, contributed to patient inclusion and collected clinical data; LMV designed and supervised the study and revised the draft. All authors revised the manuscript and approved the final version.

FUNDING

This work was supported by grants from Red Española de Esclerosis Múltiple (REEM) (RD16/0015/0001; RD16/0015/0004; RD16/0015/0006; RD16/0015/0013) and PI18/00572 integrated in the Plan Estatal I+D+I and co-funded by ISCIII-Subdirección General de Evaluación and Fondo Europeo de Desarrollo Regional (FEDER, "Una manera de hacer Europa").

ACKNOWLEDGMENTS

Authors acknowledge AI Pérez Macías and S Ortega for their excellent technical support.

SUPPLEMENTARY MATERIAL

The Supplementary Material for this article can be found online at: https://www.frontiersin.org/articles/10.3389/fimmu.2021.760546/full#supplementary-material

REFERENCES

1. Cohen JA, Coles AJ, Arnold DL, Confavreux C, Fox EJ, Hartung HP, et al. Alemtuzumab Versus Interferon Beta 1a as First-Line Treatment for Patients With Relapsing-Remitting Multiple Sclerosis: A Randomised Controlled Phase 3 Trial. *Lancet* (2012) 380(9856):1819–28. doi: 10.1016/S0140-6736(12)61769-3
2. Gross CC, Ahmetspahic D, Ruck T, Schulte-Mecklenbeck A, Schwarte K, Jörgens S, et al. Alemtuzumab Treatment Alters Circulating Innate Immune Cells in Multiple Sclerosis. *Neurol Neuroimmunol Neuroinflamm* (2016) 3(6):e289. doi: 10.1212/NXI.0000000000000289
3. Buonomo AR, Zappulo E, Viceconte G, Scotto R, Borgia G, Gentile I. Risk of Opportunistic Infections in Patients Treated With Alemtuzumab for Multiple Sclerosis. *Expert Opin Drug Saf* (2018) 17(7):709–17. doi: 10.1080/14740338.2018.1483330
4. Thompson SA, Jones JL, Cox AL, Compston DA, Coles AJ. B-Cell Reconstitution and BAFF After Alemtuzumab (Campath-1H) Treatment of Multiple Sclerosis. *J Clin Immunol* (2010) 30(1):99–105. doi: 10.1007/s10875-009-9327-3
5. Zhang X, Tao Y, Chopra M, Ahn M, Marcus KL, Choudhary N, et al. Differential Reconstitution of T Cell Subsets Following Immunodepleting Treatment With Alemtuzumab (Anti-CD52 Monoclonal Antibody) in Patients With Relapsing-Remitting Multiple Sclerosis. *J Immunol* (2013) 191(12):5867–74. doi: 10.4049/jimmunol.1301926
6. Ziemssen T, Thomas K. Alemtuzumab in the Long-Term Treatment of Relapsing-Remitting Multiple Sclerosis: An Update on the Clinical Trial Evidence and Data From the Real World. *Ther Adv Neurol Disord* (2017) 10(10):343–59. doi: 10.1177/1756285617722706
7. Tuohy O, Costelloe L, Hill-Cawthorne G, Bjornson I, Harding K, Robertson N, et al. Alemtuzumab Treatment of Multiple Sclerosis: Long-Term Safety and Efficacy. *J Neurol Neurosurg Psychiatry* (2015) 86(2):208–15. doi: 10.1136/jnnp-2014-307721
8. Coles AJ, Cohen JA, Fox EJ, Giovannoni G, Hartung HP, Havrdova E, et al. Alemtuzumab CARE-MS II 5-Year Follow-Up: Efficacy and Safety Findings. *Neurology* (2017) 89(11):1117–26. doi: 10.1212/WNL.0000000000004354
9. Ruck T, Pfeuffer S, Schulte-Mecklenbeck A, Gross CC, Lindner M, Metze D, et al. Vitiligo After Alemtuzumab Treatment: Secondary Autoimmunity Is Not All About B Cells. *Neurology* (2018) 91(24):e2233–7. doi: 10.1212/WNL.0000000000006648
10. Comini-Frota ER, Campos APF, Neto APG, Christo PP. Acquired Hemophilia A and Other Autoimmune Diseases After Alemtuzumab Therapy for Multiple Sclerosis: A Report of Two Cases. *Mult Scler Relat Disord* (2020) 44:102181. doi: 10.1016/j.msard.2020.102181
11. Polman CH, Reingold SC, Banwell B, Clanet M, Cohen JA, Filippi M, et al. Diagnostic Criteria for Multiple Sclerosis: 2010 Revisions to the McDonald Criteria. *Ann Neurol* (2011) 69(2):292–302. doi: 10.1002/ana.22366
12. Medina S, Villarrubia N, Sainz de la Maza S, Lifante J, Costa-Frossard L, Roldán E, et al. Optimal Response to Dimethyl Fumarate Associates in MS With a Shift From an Inflammatory to a Tolerogenic Blood Cell Profile. *Mult Scler* (2018) 24(10):1317–27. doi: 10.1177/1352458517717088
13. Cuculiza Henriksen A, Ammitzbøll C, Petersen ER, McWilliam O, Sellebjerg F, von Essen MR, et al. Natalizumab Differentially Affects Plasmablasts and B Cells in Multiple Sclerosis. *Mult Scler Relat Disord* (2021) 52:102987. doi: 10.1016/j.msard.2021.102987
14. Kemmerer CL, Pernpeintner V, Ruschil C, Abdelhak A, Scholl M, Ziemann U, et al. Differential Effects of Disease Modifying Drugs on Peripheral Blood B Cell Subsets: A Cross Sectional Study in Multiple Sclerosis Patients Treated With Interferon-β, Glatiramer Acetate, Dimethyl Fumarate, Fingolimod or Natalizumab. *PloS One* (2020) 15(7):e0235449. doi: 10.1371/journal.pone.0235449
15. Baker D, Herrod SS, Alvarez-Gonzalez C, Giovannoni G, Schmierer K. Interpreting Lymphocyte Reconstitution Data From the Pivotal Phase 3 Trials of Alemtuzumab. *JAMA Neurol* (2017) 74(8):961–9. doi: 10.1001/jamaneurol.2017.0676
16. Wiendl H, Carraro M, Comi G, Izquierdo G, Kim HJ, Sharrack B, et al. Lymphocyte Pharmacodynamics Are Not Associated With Autoimmunity or Efficacy After Alemtuzumab. *Neurol Neuroimmunol Neuroinflamm* (2019) 7(1):e635. doi: 10.1212/NXI.0000000000000635
17. Costelloe L, Jones J, Coles A. Secondary Autoimmune Diseases Following Alemtuzumab Therapy for Multiple Sclerosis. *Expert Rev Neurother* (2012) 12(3):335–41. doi: 10.1586/ern.12.5
18. Jones JL, Phuah CL, Cox AL, Thompson SA, Ban M, Shawcross J, et al. IL-21 Drives Secondary Autoimmunity in Patients With Multiple Sclerosis, Following Therapeutic Lymphocyte Depletion With Alemtuzumab (Campath-1h). *J Clin Invest* (2009) 119(7):2052–61. doi: 10.1172/JCI37878
19. Long D, Chen Y, Wu H, Zhao M, Lu Q. Clinical Significance and Immunobiology of IL-21 in Autoimmunity. *J Autoimmun* (2019) 99:1–14. doi: 10.1016/j.jaut.2019.01.013
20. Azzopardi L, Thompson SA, Harding KE, Cossburn M, Robertson N, Compston A, et al. Predicting Autoimmunity After Alemtuzumab Treatment of Multiple Sclerosis. *J Neurol Neurosurg Psychiatry* (2014) 85(7):795–8. doi: 10.1136/jnnp-2013-307042
21. Reindl M. Anti-Thyroid Autoantibodies as Biomarkers for Alemtuzumab Associated Thyroid Autoimmunity. *EBioMedicine* (2019) 47:22–23. doi: 10.1016/j.ebiom.2019.08.065
22. Kuhlmann T, Ludwin S, Prat A, Antel J, Brück W, Lassmann H. An Updated Histological Classification System for Multiple Sclerosis Lesions. *Acta Neuropathol* (2017) 133(1):13–24. doi: 10.1007/s00401-016-1653-y
23. Lisak RP, Benjamins JA, Nedelkoska L, Barger JL, Ragheb S, Fan B, et al. Secretory Products of Multiple Sclerosis B Cells Are Cytotoxic to Oligodendroglia In Vitro. *J Neuroimmunol* (2012) 246(1-2):85–95. doi: 10.1016/j.jneuroim.2012.02.015
24. Fernández-Velasco JI, Kuhle J, Monreal E, Meca-Lallana V, Meca-Lallana J, Izquierdo G, et al. Effect of Ocrelizumab in Blood Leukocytes of Patients With Primary Progressive Ms. *Neurol Neuroimmunol Neuroinflamm* (2021) 8(2):e940. doi: 10.1212/NXI.0000000000000940
25. Baker D, Ali L, Saxena G, Pryce G, Jones M, Schmierer K, et al. The Irony of Humanization: Alemtuzumab, the First, But One of the Most Immunogenic, Humanized Monoclonal Antibodies. *Front Immunol* (2020) 11:124. doi: 10.3389/fimmu.2020.00124
26. Ellebedy AH, Jackson KJL, Kissick HT, Nakaya HI, Davis CW, Roskin KM, et al. Defining Antigen-Specific Plasmablast and Memory B Cell Subsets in Human Blood After Viral Infection or Vaccination. *Nat Immunol* (2016) 17(10):1226–34. doi: 10.1038/ni.3533
27. Gilmore W, Lund BT, Li P, Levy AM, Kelland EE, Akbari O, et al. Repopulation of T, B, and NK Cells Following Alemtuzumab Treatment in Relapsing-Remitting Multiple Sclerosis. *J Neuroinflamm* (2020) 17(1):189. doi: 10.1186/s12974-020-01847-9
28. Alenda R, Costa-Frossard L, Alvarez-Lafuente R, Espejo C, Rodríguez-Martín E, de la Maza SS, et al. Blood Lymphocyte Subsets Identify Optimal Responders to IFN-Beta in MS. *J Neurol* (2018) 265(1):24–31. doi: 10.1007/s00415-017-8625-6

Conflict of Interest: EM received research grants, travel support or honoraria for speaking engagements from Biogen, Merck, Novartis, Roche, and Sanofi-Genzyme. SS received payment for lecturing or travel expenses from Almirall, Biogen, Merck-Serono, Novartis Roche, Sanofi-Genzyme, and Teva. MC has received compensation for consulting services and speaking honoraria from Bayer Schering Pharma, Merk Serono, Biogen-Idec, Teva Pharmaceuticals, Sanofi-Aventis, Genzyme, and Novartis. LR-T has received speaking honoraria and travel expenses for scientific meetings and has participated in advisory boards in the past years with Bayer Schering Pharma, Biogen, EMD Merck Serono, Sanofi Genzyme, Novartis, Sanofi-Aventis, Teva Phramaceuticals, Almirall and Roche. XM has received speaking honoraria and travel expenses for participation in scientific meetings, has been a steering committee member of clinical trials or participated in advisory boards of clinical trials in the past years with Actelion, Alexion, Bayer, Biogen, Celgene, EMD Serono, Genzyme, Immunic, Medday, Merck KGaA, Darmstadt Germany, Mylan, Nervgen, Novartis, Roche, Sanofi-Genzyme, Teva MSIF and NMSS. LM has received travel funding from Genzyme, Roche, Biogen Idec and Novartis, and personal fee for lectures from Roche. JM-L received grants and consulting or speaking fees from Almirall, Biogen, Celgene, Genzyme, Merck, Novartis, Roche and Teva. RA-L reports grants and personal fees from Merck Serono, personal fees and non-financial support from Biogen IDEC, grants, personal fees and non-financial support from Novartis Pharmaceuticals S.A., grants and personal fees from Genzyme, non-financial support from TEVA Pharma, S.L. LC-F received speaker fees, travel support, and/

or served on advisory boards by Biogen, Sanofi, Merck, Bayer, Novartis, Roche, Teva, Celgene, Ipsen, Biopas, Almirall. LV received research grants, travel support or honoraria for speaking engagements from Biogen, Merck, Novartis, Roche, Sanofi-Genzyme and Bristol-Myers.

The remaining authors declare that the research was conducted in the absence of any commercial or financial relationships that could be construed as a potential conflict of interest.

Publisher's Note: All claims expressed in this article are solely those of the authors and do not necessarily represent those of their affiliated organizations, or those of the publisher, the editors and the reviewers. Any product that may be evaluated in this article, or claim that may be made by its manufacturer, is not guaranteed or endorsed by the publisher.

frontiers in Immunology

BRIEF RESEARCH REPORT
published: 21 October 2021
doi: 10.3389/fimmu.2021.768682

Growth Factors and Their Roles in Multiple Sclerosis Risk

Hui Lu[1*†], *Peng-Fei Wu*[2,3†], *Deng-Lei Ma*[4], *Wan Zhang*[3,5] *and Meichen Sun*[1]

[1] Department of Neurology, Xuanwu Hospital, Capital Medical University, Beijing, China, [2] Center for Medical Genetics & Hunan Key Laboratory of Medical Genetics, School of Life Sciences, Central South University, Changsha, China, [3] Department of Neurology, Beth Israel Deaconess Medical Center, Harvard Medical School, Boston, MA, United States, [4] Department of Pharmacy, Xuanwu Hospital, Capital Medical University, Beijing, China, [5] Department of Biology, Boston University, Boston, MA, United States

OPEN ACCESS

Edited by:
Luisa María Villar, Ramón y Cajal University Hospital, Spain

Reviewed by:
Elena Urcelay, Health Research Institute of the Hospital Clínico San Carlos (IdISSC), Spain
Silvia Corrochano, Instituto de Investigación Sanitaria del Hospital Clínico San Carlos, Spain

***Correspondence:**
Hui Lu
erjihuixin@163.com

[†]These authors have contributed equally to this work

Specialty section:
This article was submitted to Multiple Sclerosis and Neuroimmunology, a section of the journal Frontiers in Immunology

Received: 01 September 2021
Accepted: 07 October 2021
Published: 21 October 2021

Citation:
Lu H, Wu P-F, Ma D-L, Zhang W and Sun M (2021) Growth Factors and Their Roles in Multiple Sclerosis Risk. Front. Immunol. 12:768682. doi: 10.3389/fimmu.2021.768682

Background: Previous studies have suggested essential roles of growth factors on the risk of Multiple Sclerosis (MS), but it remains undefined whether the effects are causal.

Objective: We applied Mendelian randomization (MR) approaches to disentangle the causal relationship between genetically predicted circulating levels of growth factors and the risk of MS.

Methods: Genetic instrumental variables for fibroblast growth factor (FGF) 23, growth differentiation factor 15 (GDF15), insulin growth factor 1 (IGF1), insulin-like growth factor binding proteins 3 (IGFBP3) and vascular endothelial growth factor (VEGF) were obtained from up-to-date genome-wide association studies (GWAS). Summary-level statistics of MS were obtained from the International Multiple Sclerosis Genetics Consortium, incorporating 14,802 subjects with MS and 26,703 healthy controls of European ancestry. Inverse-variance weighted (IVW) MR was used as the primary method and multiple sensitivity analyses were employed in this study.

Results: Genetically predicted circulating levels of FGF23 were associated with risk of MS. The odds ratio (OR) of IVW was 0.63 (95% confidence interval [CI], 0.49–0.82; $p < 0.001$) per one standard deviation increase in circulating FGF23 levels. Weighted median estimators also suggested FGF23 associated with lower MS risk (OR = 0.67; 95% CI, 0.51-0.87; $p = 0.003$). While MR-Egger approach provided no evidence of horizontal pleiotropy (intercept = -0.003, $p = 0.95$). Results of IVW methods provided no evidence for causal roles of GDF1, IGF1, IGFBP3 and VEGF on MS risks, and additional sensitivity analyses confirmed the robustness of these null findings.

Conclusion: Our results implied a causal relationship between FGF23 and the risk of MS. Further studies are warranted to confirm FGF23 as a genetically valid target for MS.

Keywords: multiple sclerosis, growth factors, fibroblast growth factor 23, Mendelian randomization, genetic epidemiology

INTRODUCTION

Multiple sclerosis (MS) is the most common chronic autoimmune disease affecting the central nervous system. The incidence of MS is 2.1 per 100,000 persons/year and approximately 2.8 million people live with MS worldwide (1). It is the leading non-traumatic neurological cause of disability in young individuals (2). The typical pathology of MS is focal areas of demyelination, inflammation and glial reaction in brain, spinal cord and optic nerve (3). The clinical characteristics of MS are intermittent and recurrent episodes of neurological dysfunction, eventually leading to disability and impaired cognition (3). The etiology and mechanisms of MS remain not fully understood. The need for continued studies is compelling to improve our understanding of its nosogenesis.

Growth factors are regulating cytokines in the pathways of cell proliferation, differentiation and activation. Previous studies have suggested growth factors as risk factors for MS and important players in the initiation and progression of MS.

Fibroblast growth factor (FGF) regulates various biological functions, including cellular proliferation, survival, migration and differentiation (4). FGF23 is a critical player in vitamin D metabolism. It is mainly released from osteoblasts. It inhibits 1α-hydroxylase and stimulates 24α-hydroxylase, resulting in the conversion of 25-hydroxyvitamin D into 24,25-dihydroxyvitamin D instead of into 1,25-dihydroxyvitamin D. Growth differentiation factor-15 (GDF15) belongs to the transforming growth factor beta superfamily. It regulates inflammation and apoptosis in various diseases (5–7). Levels of serum GDF15 were positively correlated with the Expanded Disability Status Scale of MS patients (8). Insulin-like growth factor-1 (IGF1) protects the survival of neurons and glia cells, stimulates the regeneration of myelin and promotes proliferation and differentiation of glia cells (9). It can also attenuate the damage of the blood-brain barrier (BBB) and alleviate immune-mediated inflammation (10, 11). Low levels of serum IGF1 in serum were demonstrated to be associated with susceptibility to MS (12), and were also associated with cognitive impairment and fatigue in MS (13). The bioavailability of IGF1 is regulated by insulin-like growth factor binding proteins (IGFBP). IGFBP3 is the most abundant IGFBP in human serum (14). Rather than controlling IGF activity, IGFBP3 can directly inhibit cell growth (15). In several studies, decreased levels of IGFBP3 and reduced bioavailability of IGF1 were reported in the serum of MS patients (16, 17). Vascular endothelial growth factor (VEGF), also called vascular permeability factor, mediates endothelial-specific mitogenesis, increases capillary permeability, and contributes to BBB breakdown (18). Additionally, VEGF induces major histocompatibility complex (MCH I & II) expression in the brain, and is a chemo attractant to monocytes (19). Upregulation of VEGF was detected in serum and central nervous tissue in MS patients (20).

We hypothesize that growth factors have essential function in the initiation of MS, thus establishing the causal relationship between circulating levels of growth factors and MS risk is important from clinical perspective. However, confined by methodological defects (such as residual confounding and reverse causality), traditional observational studies are unable to ascertain the causal relationships between exposures and corresponding diseases (21). Mendelian randomization (MR) is a method to exploit causality by using genetic variants as proxies (instrumental variables) to predict the effect of the exposure on disease risk (22). Since the assortment of alleles at meiosis is random and germline genetic variants are fixed at conception, MR studies are unaffected by the disease process and can avoid confounding and reverse causality.

Leveraging up-to-date genome-wide association studies (GWASs), we conducted a two-sample MR analysis to detangle the potential causal roles of growth factors on MS risk in this study.

MATERIALS AND METHODS

Based on public summary-level data derived from GWAS, we conducted a two-sample MR study to investigate the causal association of serum levels of FGF23, GDF1, IGF1, IGFBP3 and VEGF with MS (**Figure 1**). No additional consent from participants or ethical approval was required other than what had been completed in prior studies.

Genetic instruments for FGF23 were extracted from a meta-analysis of GWAS conducted by the ReproGen Alliance, consisting of 7 studies with 16,624 European participants (the mean age was ranged from 36.4 to 78.0 years old and 54.5% were women) (23). The GWAS data of FGF23 were adjusted for sex, age and top ten components of ancestry in linear regression (23). A meta-analysis of GWAS consisting 4 community-based cohorts with 5440 individuals of European ancestry (the mean age was 62 years and 53% were women) was utilized to obtain GDF15 genetic associations (24). Genetic instruments for serum IGF1 levels were selected from a GWAS of 451,993 European-descent individuals (the mean age was 56.5 years and 54% were women) in UK Biobank repository (25). Effect estimates for SNPs associated with IGFBP3 were obtained from a meta-analysis including 13 studies with up to 18, 995 individuals (8053 men and 10 942 women) (26). Genetic predictors of VEGF were obtained from a meta-analysis of GWAS including 16, 112 individuals (the mean age was 54.8 years and 54% were women) (27).

We obtained 7, 5, 318, 4 and 10 instrumental variables for FGF23 (23), GDF15 (24), IGF1 (25), IGFBP3 (26) and VEGF (27), respectively. All instrumental SNPs were strongly associated with the above circulating growth factors ($p < 5 \times 10^{-8}$). We checked linkage disequilibrium ($r^2 > 0.01$ within 1Mb window) between instrumental SNPs with 1000 Genomes EUR reference panel. Summary statistics of MS were retrieved from a recent GWAS (28) conducted by the International Multiple Sclerosis Genetics Consortium in 14,802 cases and 26,703 healthy controls of the European descent (**Supplementary Table 1**). For Instrumental variables which were not present in summary statistics of MS, proxied SNPs ($r^2 \geq 0.8$) were utilized if available. Effect estimates of palindromic variants were directly

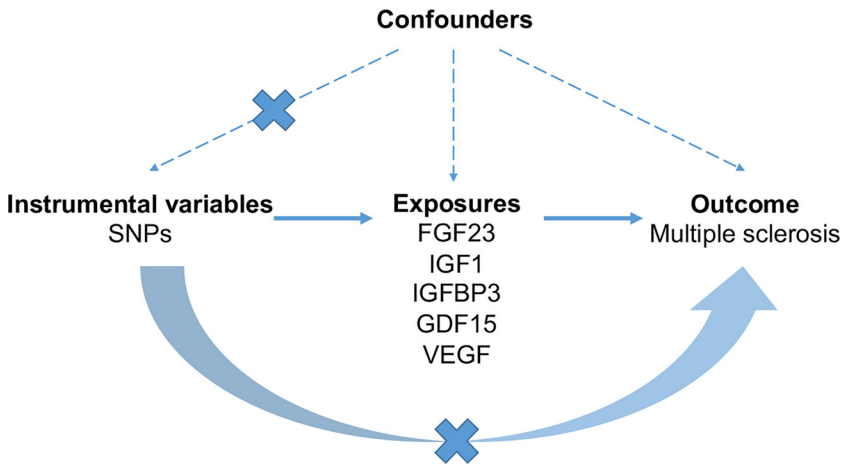

FIGURE 1 | The schematic diagram demonstrating concept of the MR design. Three key assumptions underlay standard selection procedure of instrumental SNPs. First, selected SNPs were robustly associated ($p < 5 \times 10^{-8}$) with exposures of interest. Second, later-life confounders of the exposure-outcome link scarcely existed, given that genetic variants were inherited at gamete formation when randomized allocation of instrumental variant alleles among the large population were determined. Thirdly, the exclusion-restriction assumption, that instrumental SNPs affected the outcome only though the exposure, were examined by sensitivity analyses. FGF23, fibroblast growth factor 23; GDF15, growth differentiation factor 15; IGF1, insulin-like growth factor 1; IGFBP3, insulin-like growth factor-binding protein 3; VEGF, vascular endothelial growth factor; MS, multiple sclerosis; SNP, Single-nucleotide polymorphism.

utilized since datasets downloaded from the GWAS Catalog were harmonized in terms of the forward strand. Since odds ratio (OR) was commonly reported for dichotomized traits, we made further harmonization, that is, OR in summary statistics of MS underwent log-transformation to get log-OR, which was equivalent to beta for continuous exposures. Demographic information of participants was provided in detail in original studies. The exposure and outcome datasets were merged with regard to each instrumental SNP and its effect allele, and the harmonized datasets (**Supplementary Tables 2–6**) were subject for ensuing analyses.

We conducted MR analyses using the TwoSampleMR package (29) in the R 3.6.1 software. Causal estimate by each instrumental variable SNP_k can be derived by dividing its effect on the outcome Y_k by its effect on the exposure X_k, that is, the Wald ratio Y_k/X_k and the associated standard error $\sigma Y_k/X_k$. To combine causal estimates from multiple SNPs, the inverse-variance-weighted (IVW) method was employed as the primary approach (30), with the causal estimate $\hat{\beta}_{IVW}$ and related standard error $\hat{\sigma}_{IVW}$ given by two formulae:

$$\hat{\beta}_{IVW} = \frac{\Sigma \quad X_k Y_k \sigma_{Y_k}^{-2}}{\Sigma \quad X_k^2 \sigma_{Y_k}^{-2}}$$

$$\hat{\sigma}_{IVW} = \sqrt{\frac{1}{\Sigma \quad X_k^2 \sigma_{Y_k}^{-2}}}$$

Two complementary approaches, weighted median and MR-Egger were also conducted (31, 32), since IVW estimates would be biased if not all instrumental variables were valid. Weighted median estimator was based on the relaxed assumption that more than 50% of variants were valid (32). MR-Egger regression was capable of identifying and adjusting for unbalanced horizontal pleiotropy by the regression intercept and slope, respectively (31). Forest plots were presented to visualize MR results, where causal estimates on the risk of MS were reported in OR and related confidence intervals (CI) in terms of one standard deviation increase in circulating levels of growth factors. Scatter plots and leave-one-out plots were depicted to examine the robustness of primary MR results. Bonferroni-corrected significance threshold at $p < 0.05/5$ was utilized.

RESULTS

MR Analysis of FGF23 on the Risk of MS

As shown in **Figure 2**, primary MR analysis by the IVW method showed that circulating levels of FGF23 affected the risk of MS (OR = 0.63; 95% CI, 0.49-0.82; $p = 4.7 \times 10^{-4}$). Weighted median estimators also suggested that FGF23 was associated with lower MS risk (OR = 0.67; 95% CI, 0.51-0.87; $p = 3.1 \times 10^{-3}$). Notably, by the MR-Egger approach assessing the causal effect of FGF23 on MS, there was no evidence of horizontal pleiotropy (intercept = -0.003, $p = 0.95$), but the causal estimate (OR = 0.66) was accompanied by a wide 95% CI (0.21-2.03), indicating a comprised power ($p = 0.49$). In the scenario, we considered primarily the causal estimate by the IVW approach, and the effect of FGF23 on MS was deemed significant. After examining the scatter plot and leave-one-out plot (**Figure 3**), there was no evidence supporting the existence of outlier SNPs, indicating negligible heterogeneity among all instrumental variants.

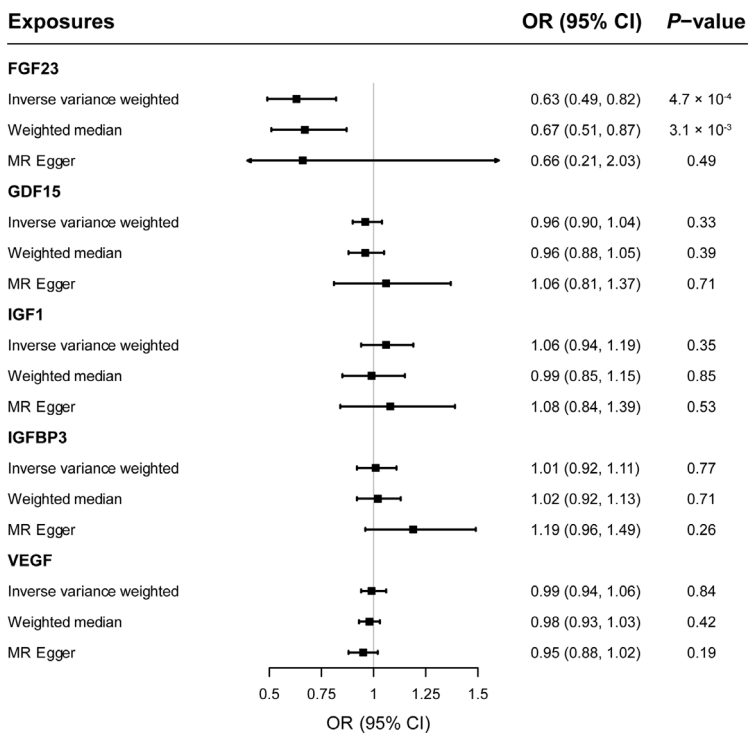

FIGURE 2 | The forest plot delineating causal estimates of growth factors on multiple sclerosis. CI, confidence interval; FGF23, fibroblast growth factor 23; GDF15, growth differentiation factor 15; IGF1, insulin-like growth factor 1; IGFBP3, insulin-like growth factor-binding protein 3; VEGF, vascular endothelial growth factor; MS, multiple sclerosis; SNP, Single-nucleotide polymorphism; OR, odds ratio.

Causal Estimates of GDF15, IGF1, IGFBP3, and VEGF on MS

Overall, genetically predicted concentrations of GDF15, IGF1, IGFBP3 and VEGF were not associated with the risk of MS. Primary MR results (**Figure 2**) demonstrated that there was no causal relationship between GDF15 and MS (OR = 0.96; 95% CI, 0.90-1.04; $p = 0.33$); neither did the causal effect of IGF1 (OR = 1.06; 95% CI, 0.94-1.19; $p = 0.35$), IGFBP3 (OR = 1.01; 95% CI, 0.92-1.11; $p = 0.77$), or VEGF (OR = 0.99; 95% CI, 0.94-1.06; $p = 0.84$) on MS reach nominal significance. Likewise, two additional MR methods, weighted median and MR-Egger gave similar causal estimates (all $p > 0.05$). Scatter plots (**Supplementary Figure 1**)

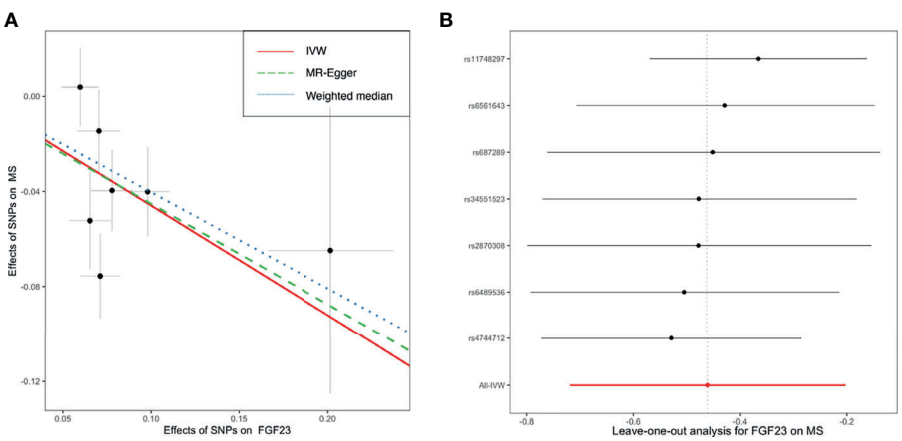

FIGURE 3 | The scatter plot **(A)** and leave-one-out plot **(B)** in the Mendelian randomization analysis of circulating FGF23 on the risk of MS. FGF23, fibroblast growth factor 23; IVW, inverse variance weighted; MS, multiple sclerosis; SNP, Single-nucleotide polymorphism.

and leave-one-out plots (**Supplementary Figure 2**) indicated no presence of outlying instrumental variables, which would exert unproportionate effects on the MR estimates otherwise.

DISCUSSION

In this MR study, we found that genetically predicted decreased circulating FGF23 levels may be associated with increased risk of MS. Meanwhile, we didn't find any causal relationship between circulating levels of GDF15, IGF1, IGFBP3 and VEGF and MS risk.

Primarily, FGF23 leads to decreased levels of phosphate, 1,25-dihydroxyvitamin D and parathyroid hormone in circulation (33, 34). Low vitamin D levels and low sun exposure have been generally recognized as risk factors for MS (35). The klotho–FGF23–vitamin D axis is fundamental in the regulation of calcium and phosphorus metabolisms. In addition, FGF23 is also secreted from neurons or the choroid plexus which can disrupt the integrity of BBB and alter the phosphate metabolism in cerebrospinal fluid (33). So it was postulated that the disequilibrium of FGF23 was associated with MS. But observational studies showed inconsistent results. A recent cohort study including 91 MS patients didn't find any difference ($p = 0.65$) between MS patient and healthy controls in plasma FGF23 concentrations (36). Another cohort study including 14 relapsing-remitting MS (RRMS) patients also found that FGF23 concentrations in MS patients were comparable to controls ($p = 0.59$) (37). While a previous observational study including 32 RRMS patients found overexpression of FGF23 in MS patients ($p < 0.01$) and an association of high FGF23 levels (approximately 2.5-fold higher) with comorbidities such as cardiovascular diseases in MS (33). Stein et al. revealed a disequilibrium of the PTH-FGF23-vitamin D axis in RRMS, with higher plasma FGF23 in winter ($p = 0.04$) and comparable FGF23 levels in summer ($p = 0.14$) (38). The discrepancies of these observational studies might be caused by confounding, reverse causation, and selection bias et al.

Interestingly, although FGF23 was regarded as a negative regulator of calcitriol biosynthesis, we found that genetically predicted FGF23 was inversely associated with risk of MS in this study. Similar to our result, Aleagha et al. also reported a significant negative correlation between FGF23 in cerebrospinal fluid and the Expanded Disability Status Scale of patients with RRMS (37). The result of a recent MR study suggested no strong evidence for the association between FGF23 and serum levels of 25-hydroxyvitamin D (p = 0.28) or calcium (p = 0.37) (39). So we hypothesize that the potential protective effect of FGF23 on MS is probably not *via* vitamin D pathways. The contradictory results by Ellidag et al. (33) and Stein et al. (38) might be caused by the effects of treatments in RRMS patients since previous studies have indicated that the expression of FGF23 might be influenced by medication (40).

Since only a few SNPs were available for FGF23, verification of our result with larger GWAS data with more genetic instruments (including rare variants) is needed. And more basic investigations are required to elucidate the underlying mechanisms related to the effect of FGF23 on MS. Our result also implied a potential therapeutic role of FGF23 for the treatment of MS. Since our study adopted serum FGF23, FGF23 might not need to cross BBB to exert a therapeutic effect and peripheral use of FGF23 might be helpful (41). Further clinical trials are warranted to explore the potential therapeutic effects of FGF23 in MS patients.

The main strength of our study is leveraging large-sample genetic data from several sources to clarify causal relationships between growth factors and MS. For these traits, we utilized up-to-date and largest GWASs as of December 31, 2020 in this study. Summary statistics of IGF1 were released recently, the GWAS incorporated ~467,000 participants from UK Biobank which has been the largest cohort worldwide. However, samples sizes of the other four exposures were relatively restricted, especially for GDF15; accordingly, number of instrumental variables at genome-wide significance and variance explained for concerned exposures by them were largely limited. In this scenario, we would have insufficient power to detect weak causal effects, and thus should be cautious with the strength of evidence provided by this study. It has been known that with the sample size increasing, more significant loci will be identified by GWASs. Last two decades have witnessed great advancement in sequencing technology and their availability and affordability. GWASs in larger populations can be expected in the future, and once summary statistics available, it is necessary to update these MR analyses to get new findings. Phenotypic observational studies cannot avoid the bias from confounding variables and reverse causation, thus spurious interplay between exposure and diseases may arise (42). Randomized controlled trials (RCTs) are less influenced by such defects of observational studies, but large-scale RCTs are very expensive. MR is a powerful method to infer the causality and could enable more robust understandings of causal molecular biology (41). Besides, MR imitates RCTs since genetic variants were randomly allocated at conception (43). And SNPs mimic lifelong exposure to medications which makes MR the nature's RCTs (43). Meanwhile, MR studies are effectively blind (41). It is proposed that drugs with genetic evidence might be twice likely to proceed from Phase I to approval (44). So MR is an economic and efficient way to screen possible drug targets. Leveraging population level data, we provide genetic support for prioritizing FGF23 as a potential treatment for MS.

Although MR provides reliable evidence of causation, it cannot replace RCTs as the best approach evaluating drug efficacy. Rather than disease progression, GWASs pertain to disease risk. The effects of MR instruments mimic low-dose exposure across the entire life-course and usually have smaller effects, whereas drugs are prescribed later in life and generally have larger effects (45). So MR is more suitable to study public health policies or preventative interventions, and less in predicting the outcome of RCTs which only last years and measure progression (41). Secondly, given largely unknown aspects of human genomes, MR studies are subject to the presence of linkage disequilibrium, cryptic relatedness, genetic heterogeneity, pleiotropy, canalization or co-variable

adjustment. Thirdly, MR is unable to assess potential non-linear relationships between risk factors and MS. Fourthly, our GWAS data were sampled from European ancestry populations. While MR minimizes the risk of population stratification and false-positive GWAS signals, heterogeneity across different populations limits generalization of the results to other populations with different genetic backgrounds. Lastly, the effect of FGF23 on MS might be sex specific, but sex-specific analysis cannot be implemented due to lack of relevant genetic summary statistical data.

In conclusion, our MR results supported a potential causality between decreased FGF23 levels and higher risk of MS.

DATA AVAILABILITY STATEMENT

The original contributions presented in the study are included in the article/**Supplementary Material**. Further inquiries can be directed to the corresponding author.

AUTHOR CONTRIBUTIONS

HL: study design, funding acquisition, literature research, data acquisition and manuscript preparation. P-FW: data analysis and statistical analysis. D-LM: manuscript editing and manuscript revision. WZ: manuscript editing and manuscript revision. MS: manuscript editing. All authors contributed to the article and approved the submitted version.

FUNDING

This work was supported by scientific research and cultivation plan of Beijing Municipal Hospital (grant PX2021036).

ACKNOWLEDGMENTS

The authors are grateful to the International Multiple Sclerosis Genetics Consortium for conducting GWAS and sharing summary-level data on multiple sclerosis. We extend our sincere thanks to Cassianne Robinson-Cohen, Jiyang Jiang, Daniela Zanetti, Alexander Teumer, and Seung Hoan Choi et al. for conducting GWAS and sharing summary-level data on growth factors.

SUPPLEMENTARY MATERIAL

The Supplementary Material for this article can be found online at: https://www.frontiersin.org/articles/10.3389/fimmu.2021.768682/full#supplementary-material

REFERENCES

1. Walton C, King R, Rechtman L, Kaye W, Leray E, Marrie RA, et al. Rising Prevalence of Multiple Sclerosis Worldwide: Insights From the Atlas of MS, Third Edition. *Mult Scler* (2020) 26(14):1816–21. doi: 10.1177/1352458520970841
2. Lo J, Chan L, Flynn S. A Systematic Review of the Incidence, Prevalence, Costs, and Activity and Work Limitations of Amputation, Osteoarthritis, Rheumatoid Arthritis, Back Pain, Multiple Sclerosis, Spinal Cord Injury, Stroke, and Traumatic Brain Injury in the United States: A 2019 Update. *Arch Phys Med Rehabil* (2021) 102(1):115–31. doi: 10.1016/j.apmr.2020.04.001
3. Reich DS, Lucchinetti CF, Calabresi PA. Multiple Sclerosis. *N Engl J Med* (2018) 378(2):169–80. doi: 10.1056/NEJMra1401483
4. Turner N, Grose R. Fibroblast Growth Factor Signalling: From Development to Cancer. *Nat Rev Cancer* (2010) 10(2):116–29. doi: 10.1038/nrc2780
5. Fujita Y, Ito M, Kojima T, Yatsuga S, Koga Y, Tanaka M. GDF15 is a Novel Biomarker to Evaluate Efficacy of Pyruvate Therapy for Mitochondrial Diseases. *Mitochondrion* (2015) 20:34–42. doi: 10.1016/j.mito.2014.10.006
6. Fujita Y, Taniguchi Y, Shinkai S, Tanaka M, Ito M. Secreted Growth Differentiation Factor 15 as a Potential Biomarker for Mitochondrial Dysfunctions in Aging and Age-Related Disorders. *Geriatr Gerontol Int* (2016) 16 Suppl 1:17–29. doi: 10.1111/ggi.12724
7. Lehtonen JM, Forsström S, Bottani E, Viscomi C, Baris OR, Isoniemi H, et al. FGF21 Is a Biomarker for Mitochondrial Translation and mtDNA Maintenance Disorders. *Neurology* (2016) 87(22):2290–9. doi: 10.1212/WNL.0000000000003374
8. Nohara S, Ishii A, Yamamoto F, Yanagiha K, Moriyama T, Tozaka N, et al. GDF-15, a Mitochondrial Disease Biomarker, Is Associated With the Severity of Multiple Sclerosis. *J Neurol Sci* (2019) 405:116429. doi: 10.1016/j.jns.2019.116429
9. Chesik D, Wilczak N, De Keyser J. The Insulin-Like Growth Factor System in Multiple Sclerosis. *Int Rev Neurobiol* (2007) . 79:203–26. doi: 10.1016/S0074-7742(07)79009-8
10. Liu X, Yao DL, Webster H. Insulin-Like Growth Factor I Treatment Reduces Clinical Deficits and Lesion Severity in Acute Demyelinating Experimental Autoimmune Encephalomyelitis. *Mult Scler* (1995) 1(1):2–9. doi: 10.1177/135245859500100102
11. Yao DL, Liu X, Hudson LD, Webster HD. Insulin-Like Growth Factor I Treatment Reduces Demyelination and Up-Regulates Gene Expression of Myelin-Related Proteins in Experimental Autoimmune Encephalomyelitis. *Proc Natl Acad Sci USA* (1995) 92(13):6190–4. doi: 10.1073/pnas.92.13.6190
12. Shahbazi M, Abdolmohammadi R, Ebadi H, Farazmandfar T. Novel Functional Polymorphism in IGF-1 Gene Associated With Multiple Sclerosis: A New Insight to MS. *Mult Scler Relat Disord* (2017) 13:33–7. doi: 10.1016/j.msard.2017.02.002
13. Nageeb RS, Hashim NA, Fawzy A. Serum Insulin-Like Growth Factor 1 (IGF-1) in Multiple Sclerosis: Relation to Cognitive Impairment and Fatigue. *Egypt J Neurol Psychiatr Neurosurg* (2018) 54(1):25. doi: 10.1186/s41983-018-0026-y
14. Stewart CE, Bates PC, Calder TA, Woodall SM, Pell JM. Potentiation of Insulin-Like Growth Factor-I (IGF-I) Activity by an Antibody: Supportive Evidence for Enhancement of IGF-I Bioavailability *In Vivo* by IGF Binding Proteins. *Endocrinology* (1993) 133(3):1462–5. doi: 10.1210/endo.133.3.7689959
15. Perks CM, Holly JM. IGF Binding Proteins (IGFBPs) and Regulation of Breast Cancer Biology. *J Mammary Gland Biol Neoplasia* (2008) 13(4):455–69. doi: 10.1007/s10911-008-9106-4
16. Lanzillo R, Di Somma C, Quarantelli M, Ventrella G, Gasperi M, Prinster A, et al. Insulin-Like Growth Factor (IGF)-I and IGF-Binding Protein-3 Serum Levels in Relapsing-Remitting and Secondary Progressive Multiple Sclerosis Patients. *Eur J Neurol* (2011) 18(12):1402–6. doi: 10.1111/j.1468-1331.2011.03433.x
17. Akcali A, Bal B, Erbagci B. Circulating IGF-1, IGFB-3, GH and TSH Levels in Multiple Sclerosis and Their Relationship With Treatment. *Neurol Res* (2017) 39(7):606–11. doi: 10.1080/01616412.2017.1321711
18. Proescholdt MA, Jacobson S, Tresser N, Oldfield EH, Merrill MJ. Vascular Endothelial Growth Factor is Expressed in Multiple Sclerosis Plaques and can Induce Inflammatory Lesions in Experimental Allergic Encephalomyelitis Rats. *J Neuropathol Exp Neurol* (2002) 61(10):914–25. doi: 10.1093/jnen/61.10.914

19. Proescholdt MA, Heiss JD, Walbridge S, Mühlhauser J, Capogrossi MC, Oldfield EH, et al. Vascular Endothelial Growth Factor (VEGF) Modulates Vascular Permeability and Inflammation in Rat Brain. *J Neuropathol Exp Neurol* (1999) 58(6):613–27. doi: 10.1097/00005072-199906000-00006
20. Su JJ, Osoegawa M, Matsuoka T, Minohara M, Tanaka M, Ishizu T, et al. Upregulation of Vascular Growth Factors in Multiple Sclerosis: Correlation With MRI Findings. *J Neurol Sci* (2006) 243(1-2):21–30. doi: 10.1016/j.jns.2005.11.006
21. Emdin CA, Khera AV, Kathiresan S. Mendelian Randomization. *JAMA* (2017) 318(19):1925–6. doi: 10.1001/jama.2017.17219
22. Davies NM, Holmes MV, Davey Smith G. Reading Mendelian Randomisation Studies: A Guide, Glossary, and Checklist for Clinicians. *BMJ* (2018) 362:k601. doi: 10.1136/bmj.k601
23. Robinson-Cohen C, Bartz TM, Lai D, Ikizler TA, Peacock M, Imel EA, et al. Genetic Variants Associated With Circulating Fibroblast Growth Factor 23. *J Am Soc Nephrol* (2018) 29(10):2583–92. doi: 10.1681/ASN.2018020192
24. Jiang J, Thalamuthu A, Ho JE, Mahajan A, Ek WE, Brown DA, et al. A Meta-Analysis of Genome-Wide Association Studies of Growth Differentiation Factor-15 Concentration in Blood. *Front Genet* (2018) 9:97. doi: 10.3389/fgene.2018.00097
25. Zanetti D, Gustafsson S, Assimes TL, Ingelsson E. Comprehensive Investigation of Circulating Biomarkers and Their Causal Role in Atherosclerosis-Related Risk Factors and Clinical Events. *Circ Genom Precis Med* (2020) 13(6):e002996. doi: 10.1161/CIRCGEN.120.002996
26. Teumer A, Qi Q, Nethander M, Aschard H, Bandinelli S, Beekman M, et al. Genomewide Meta-Analysis Identifies Loci Associated With IGF-I and IGFBP-3 Levels With Impact on Age-Related Traits. *Aging Cell* (2016) 15 (5):811–24. doi: 10.1111/acel.12490
27. Choi SH, Ruggiero D, Sorice R, Song C, Nutile T, Vernon Smith A, et al. Six Novel Loci Associated With Circulating VEGF Levels Identified by a Meta-Analysis of Genome-Wide Association Studies. *PloS Genet* (2016) 12(2): e1005874. doi: 10.1371/journal.pgen.1005874
28. International Multiple Sclerosis Genetics Consortium. Multiple Sclerosis Genomic Map Implicates Peripheral Immune Cells and Microglia in Susceptibility. *Science* (2019) 365(6460):eaav7188. doi: 10.1126/science.aav7188
29. Hemani G, Zheng J, Elsworth B, Wade KH, Haberland V, Baird D, et al. The MR-Base Platform Supports Systematic Causal Inference Across the Human Phenome. *Elife* (2018) 7:e34408. doi: 10.7554/eLife.34408
30. Burgess S, Butterworth A, Thompson SG. Mendelian Randomization Analysis With Multiple Genetic Variants Using Summarized Data. *Genet Epidemiol* (2013) 37(7):658–65. doi: 10.1002/gepi.21758
31. Bowden J, Davey Smith G, Burgess S. Mendelian Randomization With Invalid Instruments: Effect Estimation and Bias Detection Through Egger Regression. *Int J Epidemiol* (2015) 44(2):512–25. doi: 10.1093/ije/dyv080
32. Bowden J, Smith GD, Haycock PC, Burgess S. Consistent Estimation in Mendelian Randomization With Some Invalid Instruments Using a Weighted Median Estimator. *Genet Epidemiol* (2016) 40(4):304–14. doi: 10.1002/gepi.21965
33. Ellidag HY, Yilmaz N, Kurtulus F, Aydin O, Eren E, Inci A, et al. The Three Sisters of Fate in Multiple Sclerosis: Klotho (Clotho), Fibroblast Growth Factor-23 (Lachesis), and Vitamin D (Atropos). *Ann Neurosci* (2016) 23 (3):155–61. doi: 10.1159/000449181
34. Shimada T, Hasegawa H, Yamazaki Y, Muto T, Hino R, Takeuchi Y, et al. FGF-23 Is a Potent Regulator of Vitamin D Metabolism and Phosphate Homeostasis. *J Bone Miner Res* (2004) 19(3):429–35. doi: 10.1359/JBMR.0301264
35. Jakimovski D, Guan Y, Ramanathan M, Weinstock-Guttman B, Zivadinov R. Lifestyle-Based Modifiable Risk Factors in Multiple Sclerosis: Review of Experimental and Clinical Findings. *Neurodegener Dis Manag* (2019) 9 (3):149–72. doi: 10.2217/nmt-2018-0046
36. Vlot MC, Boekel L, Kragt J, Killestein J, van Amerongen BM, de Jonge R, et al. Multiple Sclerosis Patients Show Lower Bioavailable 25(Oh)D and 1,25(OH)(2)D, But No Difference in Ratio of 25(OH)D/24,25(Oh)(2)D and FGF23 Concentrations. *Nutrients* (2019) 11(11):2774. doi: 10.3390/nu11112774
37. Emami Aleagha MS, Siroos B, Allameh A, Shakiba S, Ranji-Burachaloo S, Harirchian MH. Calcitriol, But Not FGF23, Increases in CSF and Serum of MS Patients. *J Neuroimmunol* (2019) 328:89–93. doi: 10.1016/j.jneuroim.2018.12.011
38. Stein MS, Ward GJ, Butzkueven H, Kilpatrick TJ, Harrison LC. Dysequilibrium of the PTH-FGF23-Vitamin D Axis in Relapsing Remitting Multiple Sclerosis; a Longitudinal Study. *Mol Med* (2018) 24(1):27. doi: 10.1186/s10020-018-0028-3
39. Wang Y, Wang H, Chen P. Higher Fibroblast Growth Factor 23 Levels Are Causally Associated With Lower Bone Mineral Density of Heel and Femoral Neck: Evidence From Two-Sample Mendelian Randomization Analysis. *Front Public Health* (2020) 8:467. doi: 10.3389/fpubh.2020.00467
40. Moe SM, Chen NX, Newman CL, Organ JM, Kneissel M, Kramer I, et al. Anti-Sclerostin Antibody Treatment in a Rat Model of Progressive Renal Osteodystrophy. *J Bone Miner Res* (2015) 30(3):499–509. doi: 10.1002/jbmr.2372
41. Storm CS, Kia DA, Almramhi M, Wood NW. Using Mendelian Randomization to Understand and Develop Treatments for Neurodegenerative Disease. *Brain Commun* (2020) 2(1):fcaa031. doi: 10.1093/braincomms/fcaa031
42. Smith GD, Ebrahim S. 'Mendelian Randomization': Can Genetic Epidemiology Contribute to Understanding Environmental Determinants of Disease. *Int J Epidemiol* (2003) 32(1):1–22. doi: 10.1093/ije/dyg070
43. Evans DM, Davey Smith G. Mendelian Randomization: New Applications in the Coming Age of Hypothesis-Free Causality. *Annu Rev Genomics Hum Genet* (2015) 16:327–50. doi: 10.1146/annurev-genom-090314-050016
44. Nelson MR, Tipney H, Painter JL, Shen J, Nicoletti P, Shen Y, et al. The Support of Human Genetic Evidence for Approved Drug Indications. *Nat Genet* (2015) 47(8):856–60. doi: 10.1038/ng.3314
45. Gill D, Georgakis MK, Walker VM, Schmidt AF, Gkatzionis A, Freitag D, et al. Mendelian Randomization for Studying the Effects of Perturbing Drug Targets. *Wellcome Open Res* (2021) 6:16. doi: 10.12688/wellcomeopenres.16544.2

Conflict of Interest: The authors declare that the research was conducted in the absence of any commercial or financial relationships that could be construed as a potential conflict of interest.

frontiers in Neurology

ORIGINAL RESEARCH
published: 26 October 2021
doi: 10.3389/fneur.2021.719088

C-Reactive Protein Levels and Gadolinium-Enhancing Lesions Are Associated With the Degree of Depressive Symptoms in Newly Diagnosed Multiple Sclerosis

Yavor Yalachkov[1], Victoria Anschuetz[1], Jasmin Jakob[1,2], Martin A. Schaller-Paule[1], Jan Hendrik Schaefer[1], Annemarie Reilaender[1], Lucie Friedauer[1], Marion Behrens[1] and Christian Foerch[1]*

[1] Department of Neurology, University Hospital Frankfurt, Frankfurt, Germany, [2] Department of Neurology, Universitätsmedizin Mainz, Mainz, Germany

OPEN ACCESS

Edited by:
Maria Teresa Cencioni, Imperial College London, United Kingdom

Reviewed by:
Brigit De Jong, VU University Medical Center, Netherlands
Alice Mariottini, University of Florence, Italy

***Correspondence:**
Yavor Yalachkov
yavor.yalachkov@kgu.de

Specialty section:
This article was submitted to Multiple Sclerosis and Neuroimmunology, a section of the journal Frontiers in Neurology

Received: 01 June 2021
Accepted: 27 September 2021
Published: 26 October 2021

Citation:
Yalachkov Y, Anschuetz V, Jakob J, Schaller-Paule MA, Schaefer JH, Reilaender A, Friedauer L, Behrens M and Foerch C (2021) C-Reactive Protein Levels and Gadolinium-Enhancing Lesions Are Associated With the Degree of Depressive Symptoms in Newly Diagnosed Multiple Sclerosis. Front. Neurol. 12:719088. doi: 10.3389/fneur.2021.719088

Background: Inflammation is essential for the pathogenesis of multiple sclerosis (MS). While the immune system contribution to the development of neurological symptoms has been intensively studied, inflammatory biomarkers for mental symptoms such as depression are poorly understood in the context of MS. Here, we test if depression correlates with peripheral and central inflammation markers in MS patients as soon as the diagnosis is established.

Methods: Forty-four patients were newly diagnosed with relapsing-remitting MS, primary progressive MS or clinically isolated syndrome. Age, gender, EDSS, C-reactive protein (CRP), albumin, white blood cells count in cerebrospinal fluid (CSF WBC), presence of gadolinium enhanced lesions (GE) on T1-weighted images and total number of typical MS lesion locations were included in linear regression models to predict Beck Depression Inventory (BDI) score and the depression dimension of the Symptoms Checklist 90-Revised (SCL90RD).

Results: CRP elevation and GE predicted significantly BDI (CRP: $p = 0.007$; GE: $p = 0.019$) and SCL90RD (CRP: $p = 0.004$; GE: $p = 0.049$). The combination of both factors resulted in more pronounced depressive symptoms ($p = 0.04$). CSF WBC and EDSS as well as the other variables were not correlated with depressive symptoms.

Conclusions: CRP elevation and GE are associated with depressive symptoms in newly diagnosed MS patients. These markers can be used to identify MS patients exhibiting a high risk for the development of depressive symptoms in early phases of the disease.

Keywords: multiple sclerosis, depression, inflammation, C-reactive protein, gadolinium enhancing lesion

INTRODUCTION

Depression has a higher prevalence among multiple sclerosis (MS) patients as compared to non-MS-subjects (1) and is one of the most common comorbidities in MS (2, 3). It has a detrimental impact on patients' quality of life (4) as well as employment outcome (5) and is associated with an increased risk of disability worsening (6), resulting in adverse long term outcome (7).

Studies showing that physical disability predicts depression in MS (8) suggest that neurological deficits accumulate over time and lead to depressive symptoms. However, depression has been reported also for early MS and clinically isolated syndrome (CIS) patients (9–12), where physical disability is mostly mild or even non-existent. These observations indicate the existence of other mechanisms for the development of depression in MS.

One factor which has been shown to play a key role for the emergence of depressive symptoms in MS independent of disability is inflammation in the central nervous system (CNS). MS patients with an acute relapse have higher depression scores compared to patients in remission (13). Furthermore, tumor necrosis factor-α (TNF- α), interleukin-1β (IL-1β), and interleukin-6 (IL-6) measured in the cerebrospinal fluid of MS patients correlate with depression scores (13, 14).

On the other hand, major depression (MDD) studies stress the importance of peripheral inflammation markers. Thus, proinflammatory cytokines and molecules such as TNF-α, IL-6, interleukin 1 (IL-1), soluble interleukin 2-receptor (sIL-2R), and C-reactive protein (CRP) measured in serum are increased in patients with depression as compared to healthy subjects (15–18). Similar findings have been reported for MS: CRP levels are elevated in patients with as compared to those without a relapse and correlate with depression severity (19). Furthermore, increased IL-6 as well as decreased interleukin-4 (IL-4) and albumin in serum discriminate MS patients with from those without depression (20).

Treating depression in MS as early as possible and targeting its inflammatory mechanisms adequately require simultaneous investigations of peripheral and central markers of inflammation as early as the MS diagnosis is established. Such studies are largely lacking and it is not known whether both peripheral and central inflammatory processes are linked to depressive symptoms in newly diagnosed MS. We hypothesized that serological, CSF laboratory and CNS imaging markers of inflammation in patients with initial diagnosis of CIS, relapsing-remitting MS (RRMS) or primary progressive MS (PPMS) correlate with their depression scores.

MATERIALS AND METHODS

The study was approved by the ethics committee of University Hospital Frankfurt and carried out in accordance with The Code of Ethics of the World Medical Association (Declaration of Helsinki) for experiments involving humans. Written informed consent was obtained from all subjects. Patients were referred to the Department of Neurology at the University Hospital Frankfurt between 2017 and 2019 due to suspected demyelinating CNS disease either based on a clinical observation or on MRI imaging results. All patients underwent a neurological examination, laboratory tests, lumbar puncture, and MRI imaging as a part of a well-established diagnostic work-up based on the current guidelines of the German Neurological Society as well as the Competence Network Multiple Sclerosis. Patients were screened for eligibility and agreed to participate in the study and undergo additional measurements including Beck Depression Inventory (BDI) (21) and Symptom Checklist-90-R (22). BDI was used to assess depressive symptoms. As a validation of the results, additionally the Symptom Checklist-90-R (22) was applied and its depression dimension (SCL90RD) was entered into further analysis. Participants were included only if the diagnostic work-up resulted in the diagnosis of a relapsing-remitting multiple sclerosis (RRMS), primary progressive multiple sclerosis (PPMS) or clinically isolated syndrome (CIS) according to the 2010 revised McDonald criteria (23). The first participants were measured 2017 before the latest revisions of the McDonald criteria were officially published (24). At this time, we had already diagnosed and included several patients based on the McDonald 2010 criteria, therefore decided to keep these eligibility criteria unchanged. Exclusion criteria were diagnosis of secondary progressive multiple sclerosis or diagnosis of concurring neurological disease as a result of the diagnostic work-up ($n = 4$), determinable cause of an infection ($n = 2$), insufficient knowledge of German language to fill out the questionnaires or refusal to participate ($n < 10$).

Patients were interviewed and examined by a neurologist. Their degree of physical disability was estimated with the help of the Kurtzke Expanded Disability Status Scale (EDSS) (25). C-reactive protein (CRP, mg/dl) and albumin (g/l) were measured in serum as markers of peripheral inflammation. If multiple measurements were available, the ones with the greatest proximity in time to the questionnaires were used. CRP was considered elevated if it was ≥0.5 mg/dl. In this case, physical examination and laboratory testing were performed, including auscultation of the lungs and urinalysis. If a determinable cause of infection was found, the participant was excluded from further analysis. White blood cells count in CSF (CSF WBC/μl) was used as a marker of central inflammation. Gadolinium enhancement (GE) on T1-weighted imaging in at least one of the following: cerebral, spinal or orbit MRI imaging was another marker of CNS inflammation. We computed for each participant also the total number of typical MS lesion locations (juxtacortical, periventricular, infratentorial, and spinal) with T2- or FLAIR-hyperintense lesions ("MS lesions," number of typical locations with MS lesions varying between 1 and 4).

Some patients were treated with intravenous methylprednisolone (IVMP) for their neurological symptoms. CSF acquisition was done always prior to IVMP. To consider any possible influence of IVMP on depressive symptoms, patients were grouped according to the time between IVMP and BDI/SCL90RD: the first group did not receive any IVMP or the interval between IVMP and BDI/SCL90RD was >14 days (ΔIVMP-BDI/SCL90RD > 14 days), while the second group was treated with IVMP within 14 days before the BDI measurement (ΔIVMP-BDI/SCL90RD ≤ 14 d). To consider the influence of IVMP on GE, patients were grouped according

to the time between IVMP and MRI measurement: the first group did not receive any IVMP or the interval between IVMP and MRI was >14 days (ΔIVMP-MRI > 14 d), while the second group was treated with IVMP within 14 days before MRI (ΔIVMP-MRI ≤ 14 d).

First, a multiple linear regression was computed with BDI as dependent variable. Age, gender, EDSS, CRP elevation, albumin, CSF WBC, GE, and MS lesions were employed as independent variables. Next, a second multiple linear regression with the same independent variables but with SCL90RD as dependent variable was computed to validate our first results. Linear relationship was verified by inspecting the respective scatter plots of independent and dependent variables. Normal distribution of the residuals was verified by inspecting the respective P-P plots. There was no evidence of multicollinearity (highest correlation $r = -0.417$, lowest Tolerance statistics = 0.625, and highest VIF statistic = 1.6). Independence of residuals was tested by determining Durbin–Watson statistic (Durbin–Watson = 2.5 for BDI and 2.25 for SCL90RD). Homoscedasticity was tested by inspecting a graph plot of the standardized values predicted by the respective model against the standardized residuals. The lack of influential cases biasing the model was verified by determining Cook's Distance (all Cook's Distance values < 1).

To understand better the interaction between peripheral and central inflammation, we computed two further univariate general linear models with BDI and SCL90RD as dependent variables and the two markers which contributed significantly to the variance in the linear regression analyses (CRP elevation and GE, see section Results) as independent variables.

To assess the effects of steroid treatment on depressive symptoms, a multivariate general linear model was computed with BDI and SCL90RD as dependent variables and ΔIVMP-BDI/SCL90RD as an independent variable. To assess the effects of steroid treatment on acute inflammation seen in MRI, a Fisher's exact test was computed with GE and ΔIVMP-MRI.

Finally, we tested in an exploratory analysis whether disease type and fatigue measurements might affect our findings. Fatigue measurements were available from clinical routine diagnostics (The Fatigue Scale for Motor and Cognitive Functions, FMSC) (26) for some but not all subjects ($n = 40$). We computed an additional multiple linear regression like the ones mentioned above but with "disease type" (RRMS, CIS, or PPMS) and "FSMC total score" as additional independent variables. Since MS disease type can affect not only depression but also inflammation, we also computed a Fisher's exact test with disease type and CRP elevation.

RESULTS

One patient was excluded due to the combination of CRP elevation and an acute venous leg ulcer and another one due to a still active urinary tract infection in antibiotic treatment at the time of measurement. The data of the remaining 44 subjects were entered into the analysis. Their demographic data is shown in **Table 1**. The medical history of the patients is reported in **Table 2**.

TABLE 1 | Descriptive statistics of the studied sample.

		n	x	SD
Gender	Female	32		
	Male	12		
Diagnosis	RRMS	31		
	CIS	8		
	PPMS	5		
CRP	Elevated	6		
	Normal	38		
MS lesion locations	1	7		
	2	11		
	3	12		
	4	14		
GE + in at least one	Yes	30		
MRI imaging	No	14		
ΔIVMP-MRI	>14 days	32		
	≤14 days	12		
ΔIVMP-BDI	>14 days	18		
	≤14 days	26		
Age (years)			35.68	10.63
EDSS			2.02	1.28
CSF WBC (/μl)			11.09	11.78
Albumin (g/l)			44.95	4.60
BDI			6.77	6.25
SCL90RD			0.64	0.62

n, number of patients in the respective category; x, mean value; SD, standard deviation; RRMS, relapsing-remitting multiple sclerosis; CIS, clinically isolated syndrome; PPMS, primary progressive multiple sclerosis; CRP, C-reactive protein (elevated: ≥0.50 mg/dl; normal <0.50 mg/dl); MS lesion locations, total number of typical MS lesion locations (juxtacortical, periventricular, infratentorial, and spinal) per subject with T2- or FLAIR-hyperintense lesions; GE +, gadolinium enhancement in T1-weighted imaging; ΔIVMP-MRI > 14 days, no steroid treatment or the interval between IVMP and MRI was >14 days; ΔIVMP-MRI ≤ 14 days, interval between IVMP and MRI ≤ 14 days; ΔIVMP-BDI/SCL90RD > 14 days, no steroid treatment or the interval between IVMP and BDI/SCL90RD was > 14 days; ΔIVMP-BDI/SCL90RD ≤ 14 days, interval between IVMP and BDI/SCL90RD ≤ 14 days; EDSS, Expanded Disability Status Scale; CSF WBC, white blood cells count in the cerebrospinal fluid; BDI, Beck Depression Inventory; SCL90RD, depression dimension of the Symptoms Checklist-90-Revised.

The multiple linear regression model with BDI as dependent variable was significant ($R = 0.603$, $R^2 = 0.364$, adjusted $R^2 = 0.218$, $F = 2.502$, df1 = 8, df2 = 35, and $p = 0.029$). Two independent variables contributed significantly to the model: CRP elevation (ß = 0.431, $t = 2.87$, and $p = 0.007$) and GE (ß = 0.362, $t = 2.46$, and $p = 0.019$, see **Table 3**).

The multiple linear regression model with SCL90RD as a dependent variable was significant ($R = 0.609$, $R^2 = 0.371$, adjusted $R^2 = 0.227$, $F = 2.583$, df1 = 8, df2 = 35, and $p = 0.025$). Two independent variables contributed significantly to the model: CRP elevation (ß = 0.461, $t = 3.09$, and $p = 0.004$) and GE (ß = 0.298, $t = 2.04$, and $p = 0.049$, see **Table 3**). The other variables, CSF WBC, EDSS, age, gender, albumin, and total number of typical MS lesion locations, were not predictive for depressive symptoms.

Both CRP elevation and GE were entered as independent variables in two further general linear models in order to

TABLE 2 | Past medical history and medications reported in the sample.

Medical history	Medication
Arterial hypertension (x 1)	Estradiol (x 1)
Bronchial asthma (x 1)	Levothyroxine (x 9)
Carpal tunnel syndrome (x 1)	Oral contraceptives (x 2)
Chronic back pain (x 1)	Orthomol (x 1)
Coccygeal fistula (x 1)	Progesterone (x 1)
Depression (x 1)	Salbutamol (x 1)
Epilepsy (x 1)	Sumatriptan (x 2)
Factor V Leiden (x 1)	Vitamin D (x 1)
Hashimoto thyroiditis (x 3)	
Hypothyreosis (x 5)	
Lactose intolerance (x 1)	
Migraine (x 4)	
Obesity (x 1)	
Spondylarthritis (x 1)	
Status post autoimmune thyroiditis (x 1)	
Status post Bell's palsy (x 1)	
Status post benign tumor resection (x 1)	
Status post herpes zoster infection (x 2)	
Status post Lyme disease (x 1)	
Status post other fracture (x 1)	
Status post pelvic fracture (x 1)	
Status post sinusitis (x 1)	
Status post strabismus correction (x 1)	
Status post tonsillectomy (x 1)	
Status post type C gastritis type (x 1)	
Status post vestibular neuritis (x 1)	

TABLE 3 | Details from the two multiple linear regressions.

			95% CI for B				
	B	SE B	LB	UB	β	*t*	*p*
BDI							
Age	0.02	0.10	−0.19	0.22	0.03	0.16	n.s.
Gender	2.58	2.10	−1.68	6.85	0.19	1.23	n.s.
EDSS	0.46	0.71	−0.98	1.90	0.09	0.65	n.s.
CRP elevation	7.77	2.70	2.28	13.26	0.43	2.87	0.007
Albumin	0.26	0.22	−0.20	0.71	0.19	1.14	n.s.
CSF WBC	0.10	0.09	−0.08	0.27	0.18	1.14	n.s.
GE	4.81	1.95	0.84	8.78	0.36	2.46	0.019
MS lesion locations	−0.92	0.88	−2.70	0.86	−0.16	−1.05	n.s.
SCL90RD							
Age	0.00	0.01	−0.02	0.02	−0.02	0.02	n.s.
Gender	0.12	0.21	−0.30	0.54	−0.30	0.54	n.s.
EDSS	0.10	0.07	−0.04	0.25	−0.04	0.25	n.s.
CRP elevation	0.82	0.27	0.28	1.37	0.28	1.37	0.004
Albumin	0.01	0.02	−0.03	0.06	−0.03	0.06	n.s.
CSF WBC	0.00	0.01	−0.01	0.02	−0.01	0.02	n.s.
GE	0.39	0.19	0.00	0.78	0.00	0.78	0.049
MS lesion locations	−0.17	0.09	−0.35	0.00	−0.35	0.00	n.s.

BDI, Beck Depression Inventory (dependent variable); SCL90RD, depression dimension of the Symptoms Checklist-90-Revised (dependent variable); B, unstandardized B coefficient; SE B, standard error of the B coefficient; 95% CI, 95% confidence interval; LB, lower bound; UB, upper bound; β, standardized beta coefficient; t, t-value; p, p-value; n.s., not significant; EDSS, Expanded Disability Status Scale; CRP elevation, C-reactive protein elevation (elevated: ≥ 0.50 mg/dl; normal < 0.50 mg/dl); CSF WBC, white blood cells count in the cerebrospinal fluid; GE +, gadolinium enhancement in T1-weighted imaging.

exploratory illustrate the interaction between peripheral and central inflammation markers in the context of depression in newly diagnosed MS. With regard to BDI, CRP elevation and GE exhibited significant main effects (CRP elevation: $F = 7.113$, $p = 0.011$; GE: $F = 9.087$, $p = 0.004$) and the interaction between the two factors was significant, too (CRP elevation × GE: $F = 4.492$, $p = 0.04$). Elevated CRP values or presence of gadolinium enhancement on the T1-weighted MR imaging resulted into higher BDI scores (CPR normal: x = 5.7, SD = 4.4; CRP elevated: x = 13.8, SD = 11.2; GE –: x = 4.4, SD = 3.5; GE +: x = 7.9, SD = 6.9), while the combination of both elevated CRP and gadolinium enhancement had a particularly strong impact on the depression score (x = 18, SD = 11.5). Vice versa, the majority of patients with normal CRP levels and lack of GE in MRI exhibited normal BDI scores. However, either GE in MRI or CRP elevation were associated with BDI scores corresponding on average to a minimal or mild depression, while patients with both CRP elevation and GE in MRI had BDI scores which corresponded to at least a moderate depression (21). A similar pattern was revealed with regard to SCL90RD. Here, however, only CRP elevation reached significance ($F = 8.428$, $p = 0.006$), while GE ($F = 3.737$, $p > 0.05$) and the interaction between the both factors ($F = 1.202$, $p > 0.05$) failed to do so.

The multivariate general linear model did not reveal any significant effects of the time interval between IVMP treatment and the depression questionnaires on the BDI/SCL90RD scores ($F = 0.121$, $p > 0.05$). The Fisher's exact test revealed no significant effects of the time interval between IVMP treatment and MRI imaging on the presence of GE ($p > 0.05$).

The exploratory linear regression with BDI as dependent variable and with additional independent variables (disease type and FSMC total score additionally to age, gender, EDSS, CRP elevation, albumin, CSF WBC, GE, and MS lesions) was significant ($R = 0.696$, $R^2 = 0.485$, adjusted $R^2 = 0.307$, $F = 2.726$, df1 = 10, df2 = 29, and $p = 0.017$). Like in the initial analysis, two independent variables contributed significantly to the model: CRP elevation (ß = 0.373, $t = 2.312$, and $p = 0.028$) and GE (ß = 0.381, $t = 2.522$, and $p = 0.017$). Disease type and fatigue measurements did not reach significance ($p > 0.05$). The Fisher's exact test revealed no significant effects of the disease type on CRP elevation ($p > 0.05$).

DISCUSSION

In the current study, depressive symptoms of patients with newly diagnosed RRMS, CIS, or PPMS were linked to peripheral and central markers of inflammation. More precisely,

patients with elevated CRP or presence of GE on T1-weighted MRI-imaging were more likely to score higher on depression scales BDI and SCL90RD. Further analysis showed that the link between CRP/GE and depression is even more pronounced if both inflammation markers are simultaneously present.

The role of CRP elevation has been highlighted so far mainly by studies with MDD patients (15–17, 27). Recent findings suggest that inflammation contributes to the emergence of depression, since elevated CRP predicts the subsequent development of depressive symptoms (28). The pathophysiological mechanisms are complex and involve different pathways: peripherally released signals including CRP and cytokines cause an inflammatory response in the CNS, altering production, metabolism and transport of mood-related neurotransmitters and affecting neuronal growth and survival (27). Further mechanisms, including oxidative stress, cytokine-induced glutamate dysregulating and excitotoxicity as well as maladaptive hypothalamic-pituitary-adrenal (HPA) axis functioning have been suggested (19, 20, 27). CRP elevation might be distinctly relevant for therapeutic decisions, too. Thus, a treatment with the monoclonal antibody infliximab, an TNF-α antagonist, resulted in a greater reduction of depressive symptoms in a subset of medication resistant MDD patients with high baseline CRP levels (29). Furthermore CRP is among the inflammatory signal molecules with the strongest relationships with depression (15, 16) and is easily obtained and analyzed in hospital laboratories, rendering it readily utilizable in a clinical context (27).

The source of CRP elevation in MS patients seems even more complex than in MDD. CRP is higher during MS relapses and associated with EDSS, predictive for later progression and decreasing during interferon beta 1a therapy (30–32). Therefore, peripheral inflammation is probably linked to general disease activity in MS, too. However, interactions with environmental factors might lead to an increased risk for the emergence of depression as has been shown for MDD: adults diagnosed with MDD who have a history of early maltreatment exhibit higher CRP levels than those without such a history (33). Thus, MS-related inflammation coupled with external events which also boost inflammatory responses might be crucial for the development of depressive symptoms in early MS.

CNS inflammation markers might contribute further to understanding the role of the immune system in the context of depression. Generally, GE on T1-weighted MRI imaging indicates a disrupted blood-brain barrier and characterizes active MS lesions (34). In our sample, the presence of active lesions was significantly associated with the degree of depressive symptoms. This extends earlier findings (13, 35), confirming the link between CNS inflammatory lesions and mood disorders in MS and validating it with regard to newly diagnosed patients. While it can be argued that active lesions induce neurological impairment and that depressive symptoms arise only as a result from the newly emerging physical disability, our findings do not support this notion. Indeed, the degree of depressive symptoms did not correlate with EDSS. Furthermore, GE was present in a multitude of CNS regions (e.g., spinal, infratentorial, or optic nerve lesions), which implies that mood alterations in the context of newly diagnosed MS occur also without direct lesions to the limbic system. Rather, depressive symptoms may be triggered by more general inflammatory mechanisms. Moreover, the total number of typical MS lesion locations with T2- or FLAIR-hyperintense lesions was not correlated to the mood symptoms, suggesting that the degree of disease activity in MS is not determining for the emergence of depression in newly diagnosed patients. However, since all our patients were newly diagnosed and were thus exposed to a novel, stressful situation (new symptoms, initial uncertainty, major diagnosis, etc.), a more complex interplay between CNS inflammation and external factors seems possible here, too. Interestingly, major negative stressful events predict increased risk for GE in MRI imaging in MS patients (36). Thus, an interaction between inflammatory MS-related processes and confrontation with a spectrum of novel, potentially stressful events such as physical disability and major diagnosis may have contributed to the development of depressive symptoms in our sample.

CRP elevation and GE did not explain the whole variance of depression in our sample. Similarly, it has been estimated that only 47% of depression patients whose scores are above the clinical threshold had a CRP level $\geq$ 0.3 mg/dl and only 29% had a CRP level $\geq$ 0.5 g/dl (27, 37), suggesting an essential but perhaps not sufficient role of peripheral inflammation for the emergence of depression and a more pronounced relevance for a subset of depressed individuals. Interestingly, we demonstrated an interaction between peripheral and central inflammation leading to more pronounced depression scores, which points at a possible mutually augmenting effect of peripheral and central inflammatory agents. The correlational nature of our results does not allow us to imply causation but one possible, hypothetical mechanism would be a common pathway of inflammation starting in the periphery and resulting in blood-brain barrier breakdown, unfolding inflammation in CNS and triggering depressive symptoms in early MS. Similar interactions between peripheral and central processes have been shown for MDD, where high CRP levels are associated with gray matter volume reductions (38) as well as with reduced functional connectivity in a widely-distributed brain network (39, 40). It would be highly relevant to follow-up whether the depressive symptoms persist in the further course of MS and if the initial peripheral and central inflammation parameters are predictive for their future development.

MS disease type has previously been shown to be relevant for depression and inflammation (4, 41, 42). Similarly, fatigue might affect or co-occur with depression (42, 43). However, in our exploratory linear regression analysis, disease type and fatigue were not associated with BDI, while CRP and GE presence were again significant predictors for depressive symptoms. Furthermore, CRP elevation did not differ between the three investigated disease types. The small sample size as well as the fact that we did not include SPMS patients could have

contributed to these findings. An interesting yet purely tentative notion refers to the fact that we studied newly diagnosed patients only. Thus, the pathophysiological underpinnings of inflammation and depression might be very similar across different MS disease forms during early disease stages and the effect of fatigue on depression might grow in later stages of the disease (41).

There are several limitations to our study. First, we employed a cross-sectional design, which does not allow us to determine a causal relationship between the measured inflammation and degree of depressive symptoms. For this purpose, a prospective design would be necessary. Second, the sample size was moderate. We included only patients with newly established diagnosis, thus leaving out effects of immunomodulatory therapy, accumulated physical disability or other disease-related confounding variables. However, this reduced the power of the study and may have contributed to the lack of significant effects regarding inflammation markers such as albumin and CSF WBC. Especially with regard to CSF WBC the results are surprising since CSF inflammatory markers such as TNF-α and IL-1β measured in the cerebrospinal fluid of treatment-naive MS patients correlate with depression scores (13, 14). The insufficient power of the study due to our conservative inclusion criteria would explain the lack of positive findings regarding CSF. Another possible explanation is that in this study we focused on the CSF WBC, while leaving out other, possibly more specific inflammatory markers such as TNF-α and IL-1β. Second, measurements were done as a part of a diagnostic work-up tailored for the clinical routine, which did not allow us to standardize all the parameters (e.g., MRI scanner, time of lumbar puncture and blood sample collection, IVMP treatment, etc.). While we did not observe any effects of IVMP treatment on the primary outcome parameters, a prospective, standardized approach with predetermined parameters would have increased the methodological quality and validity of our results. This is, however, a common challenge of studies in the clinical setting, when patients without an established diagnosis are referred to the emergency department at night and cannot wait with the IVMP treatment because of pronounced neurological disability. Similarly, it is difficult to determine the time interval between communicating the diagnosis to the patients and the measurements of depression and inflammation markers, since many patients are referred for a diagnostic work-up with a suspected diagnosis which they already know of. However, standardizing the measurements of this time interval as far as possible would limit the influence of external factors such as diagnosis communication on subjects' mood. Finally, we employed only self-assessment instruments such as BDI and SCL90R. Using clinical interviews which are available for depressive symptoms would increase the validity of the results.

Despite the above-mentioned limitations, our study contributes several important findings to the scientific debate. First, we demonstrate that the relationship between inflammation and depression is seen not only in patients with a prolonged disease history but also in newly diagnosed MS when the disease is presumably in its initial stages. Furthermore, the reported findings are not affected by immunomodulatory and symptomatic therapy. Moreover, contrary to the common expectation that depressive symptoms are seen in MS only when neurological impairment is strongly pronounced, we demonstrate that even in a sample of newly diagnosed MS patients with little to none accumulated physical disability (average EDSS = 2.02, SD = 1.28) there is a link between inflammation and depression. Studies focusing on adults with a major depressive disorder seldomly employ MRI with contrast-agent or perform a cerebrospinal fluid analysis. As illustrated in this study, investigating interactions between inflammation and depression in newly diagnosed MS patients, in whom those examinations are part of the diagnostic work-up, seems particularly promising. Of course, the chronic inflammation typical for MS remains an important issue to tackle when interpreting the data. Prospective studies investigating the link between inflammation and depression simultaneously in both newly diagnosed MS and MDD patients in early stages of the disease might be essential in addressing this issue.

In our study we demonstrated that peripheral (CRP) and central (GE on T1-weighted MRI imaging) inflammation markers are associated with the degree of depressive symptoms in newly diagnosed patients with RRMS, PPMS, and CIS. Understanding which MS patients exhibit higher risk for depressive symptoms would facilitate the development of eligible therapeutic options, targeting depression-relevant inflammatory pathways.

DATA AVAILABILITY STATEMENT

The raw data supporting the conclusions of this article will be made available by the authors, without undue reservation.

ETHICS STATEMENT

The study was reviewed and approved by Ethics Committee of University Hospital Frankfurt. The patients/participants provided their written informed consent to participate in this study.

AUTHOR CONTRIBUTIONS

YY: drafting/revision of the manuscript for content, including medical writing for content, major role in the acquisition of data, study concept or design, and analysis or interpretation of data. VA and MB: major role in the acquisition of data and analysis or interpretation of data. JJ, JS, AR, and LF: major role in the acquisition of data. MS-P: drafting/revision of the manuscript for content, including medical writing for content, and major role in the acquisition of data. CF: drafting/revision of the manuscript for content, including medical writing for content, and study concept or design. All authors contributed to the article and approved the submitted version.

REFERENCES

1. Persson R, Lee S, Yood MU, Wagner MR, Minton N, Niemcryk S, et al. Incident depression in patients diagnosed with multiple sclerosis: a multi-database study. *Eur J Neurol.* (2020) 27:1556–60. doi: 10.1111/ene.14314
2. Marrie RA, Cohen J, Stuve O, Trojano M, Sørensen PS, Reingold S, et al. A systematic review of the incidence and prevalence of comorbidity in multiple sclerosis: overview. *Mult Scler.* (2015) 21:263–81. doi: 10.1177/1352458514564491
3. Magyari M, Sorensen PS. Comorbidity in multiple sclerosis. *Front Neurol.* (2020) 11:851. doi: 10.3389/fneur.2020.00851
4. Yalachkov Y, Soydaş D, Bergmann J, Frisch S, Behrens M, Foerch C, et al. Determinants of quality of life in relapsing-remitting and progressive multiple sclerosis. *Mult Scler Relat Disord.* (2019) 30:33–7. doi: 10.1016/j.msard.2019.01.049
5. Chen J, Taylor B, Winzenberg T, Palmer AJ, Kirk-Brown A, van Dijk P, et al. Comorbidities are prevalent and detrimental for employment outcomes in people of working age with multiple sclerosis. *Mult Scler.* (2020) 26:1550–9. doi: 10.1177/1352458519872644
6. Binzer S, McKay KA, Brenner P, Hillert J, Manouchehrinia A. Disability worsening among persons with multiple sclerosis and depression: a Swedish cohort study. *Neurology.* (2019) 93:e2216–e23. doi: 10.1212/WNL.0000000000008617
7. McKay KA, Tremlett H, Fisk JD, Zhang T, Patten SB, Kastrukoff L, et al. Psychiatric comorbidity is associated with disability progression in multiple sclerosis. *Neurology.* (2018) 90:e1316–e23. doi: 10.1212/WNL.0000000000005302
8. Jones KH, Jones PA, Middleton RM, Ford DV, Tuite-Dalton K, Lockhart-Jones H, et al. Physical disability, anxiety and depression in people with MS: an internet-based survey *via* the UK MS Register. *PLoS One.* (2014) 9:e104604. doi: 10.1371/journal.pone.0104604
9. Di Legge S, Piattella MC, Pozzilli C, Pantano P, Caramia F, Pestalozza IF, et al. Longitudinal evaluation of depression and anxiety in patients with clinically isolated syndrome at high risk of developing early multiple sclerosis. *Mult Scler.* (2003) 9:302–6. doi: 10.1191/1352458503ms921oa
10. Lode K, Bru E, Klevan G, Myhr KM, Nyland H, Larsen JP. Depressive symptoms and coping in newly diagnosed patients with multiple sclerosis. *Mult Scler.* (2009) 15:638–43. doi: 10.1177/1352458509102313
11. Nourbakhsh B, Julian L, Waubant E. Fatigue and depression predict quality of life in patients with early multiple sclerosis: a longitudinal study. *Eur J Neurol.* (2016) 23:1482–6. doi: 10.1111/ene.13102
12. Glukhovsky L, Kurz D, Brandstadter R, Leavitt VM, Krieger S, Fabian M, et al. Depression and cognitive function in early multiple sclerosis: multitasking is more sensitive than traditional assessments. *Mult Scler.* (2020) 27:1276–1283. doi: 10.1177/1352458520958359
13. Rossi S, Studer V, Motta C, Polidoro S, Perugini J, Macchiarulo G, et al. Neuroinflammation drives anxiety and depression in relapsing-remitting multiple sclerosis. *Neurology.* (2017) 89:1338–47. doi: 10.1212/WNL.0000000000004411
14. Brenner P, Granqvist M, Königsson J, Al Nimer F, Piehl F, Jokinen J. Depression and fatigue in multiple sclerosis: relation to exposure to violence and cerebrospinal fluid immunomarkers. *Psychoneuroendocrinology.* (2018) 89:53–8. doi: 10.1016/j.psyneuen.2018.01.002
15. Howren MB, Lamkin DM, Suls J. Associations of depression with C-reactive protein, IL-1, and IL-6: a meta-analysis. *Psychosom Med.* (2009) 71:171–86. doi: 10.1097/PSY.0b013e3181907c1b
16. Dowlati Y, Herrmann N, Swardfager W, Liu H, Sham L, Reim EK, et al. A meta-analysis of cytokines in major depression. *Biol Psychiatry.* (2010) 67:446–57. doi: 10.1016/j.biopsych.2009.09.033
17. Liu Y, Ho RC-M, Mak A. Interleukin (IL)-6, tumour necrosis factor alpha (TNF-α) and soluble interleukin-2 receptors (sIL-2R) are elevated in patients with major depressive disorder: a meta-analysis and meta-regression. *J Affect Disord.* (2012) 139:230–9. doi: 10.1016/j.jad.2011.08.003
18. Pedraz-Petrozzi B, Neumann E, Sammer G. Pro-inflammatory markers and fatigue in patients with depression: a case-control study. *Sci Rep.* (2020) 10:9494. doi: 10.1038/s41598-020-66532-6
19. Katarina V, Gordana T, Svetlana MD, Milica B. Oxidative stress and neuroinflammation should be both considered in the occurrence of fatigue and depression in multiple sclerosis. *Acta Neurol Belg.* (2020) 120:853–61. doi: 10.1007/s13760-018-1015-8
20. Kallaur AP, Lopes J, Oliveira SR, Simão ANC, Reiche EMV, Almeida ERD, et al. Immune-inflammatory and oxidative and nitrosative stress biomarkers of depression symptoms in subjects with multiple sclerosis: increased peripheral inflammation but less acute neuroinflammation. *Mol Neurobiol.* (2016) 53:5191–202. doi: 10.1007/s12035-015-9443-4
21. Beck AT, Steer RA, Brown G. *PsycTESTS Dataset* (1996).
22. Derogatis LR, Savitz KL. The SCL-90-R, brief symptom inventory, and matching clinical rating scales. In: *The Use of Psychological Testing for Treatment Planning and Outcomes Assessment, 2nd Edn.* Mahwah, NJ: Lawrence Erlbaum Associates Publishers (1999). p. 679–724.
23. Polman CH, Reingold SC, Banwell B, Clanet M, Cohen JA, Filippi M, et al. Diagnostic criteria for multiple sclerosis: 2010 revisions to the McDonald criteria. *Ann Neurol.* (2011) 69:292–302. doi: 10.1002/ana.22366
24. Thompson AJ, Banwell BL, Barkhof F, Carroll WM, Coetzee T, Comi G, et al. Diagnosis of multiple sclerosis: 2017 revisions of the McDonald criteria. *Lancet Neurol.* (2018) 17:162–73. doi: 10.1016/S1474-4422(17)30470-2
25. Kurtzke JF. Rating neurologic impairment in multiple sclerosis: an expanded disability status scale (EDSS). *Neurology.* (1983) 33:1444–52. doi: 10.1212/WNL.33.11.1444
26. Penner IK, Raselli C, Stöcklin M, Opwis K, Kappos L, Calabrese P. The Fatigue Scale for Motor and Cognitive Functions (FSMC): validation of a new instrument to assess multiple sclerosis-related fatigue. *Mult Scler.* (2009) 15:1509–17. doi: 10.1177/1352458509348519
27. Kiecolt-Glaser JK, Derry HM, Fagundes CP. Inflammation: depression fans the flames and feasts on the heat. *Am J Psychiatry.* (2015) 172:1075–91. doi: 10.1176/appi.ajp.2015.15020152
28. Valkanova V, Ebmeier KP, Allan CL. CRP, IL-6 and depression: a systematic review and meta-analysis of longitudinal studies. *J Affect Disord.* (2013) 150:736–44. doi: 10.1016/j.jad.2013.06.004
29. Raison CL, Rutherford RE, Woolwine BJ, Shuo C, Schettler P, Drake DF, et al. A randomized controlled trial of the tumor necrosis factor antagonist infliximab for treatment-resistant depression: the role of baseline inflammatory biomarkers. *JAMA Psychiatry.* (2013) 70:31–41. doi: 10.1001/2013.jamapsychiatry.4
30. Soilu-Hänninen M, Koskinen JO, Laaksonen M, Hänninen A, Lilius E-M, Waris M. High sensitivity measurement of CRP and disease progression in multiple sclerosis. *Neurology.* (2005) 65:153–5. doi: 10.1212/01.WNL.0000167129.90918.f5
31. Guzel I, Mungan S, Oztekin ZN, Ak F. Is there an association between the Expanded Disability Status Scale and inflammatory markers in multiple sclerosis? *J Chin Med Assoc.* (2016) 79:54–7. doi: 10.1016/j.jcma.2015.08.010
32. Shu Y, Li R, Qiu W, Chang Y, Sun X, Fang L, et al. Association of serum gamma-glutamyltransferase and C-reactive proteins with neuromyelitis optica and multiple sclerosis. *Mult Scler Relat Disord.* (2017) 18:65–70. doi: 10.1016/j.msard.2017.09.021
33. Danese A, Moffitt TE, Pariante CM, Ambler A, Poulton R, Caspi A. Elevated inflammation levels in depressed adults with a history of childhood maltreatment. *Arch Gen Psychiatry.* (2008) 65:409–15. doi: 10.1001/archpsyc.65.4.409
34. Gonzalez-Scarano F, Grossman RI, Galetta S, Atlas SW, Silberberg DH. Multiple sclerosis disease activity correlates with gadolinium-enhanced magnetic resonance imaging. *Ann Neurol.* (1987) 21:300–6. doi: 10.1002/ana.410210312
35. Fassbender K, Schmidt R, Mössner R, Kischka U, Kühnen J, Schwartz A, et al. Mood disorders and dysfunction of the hypothalamic-pituitary-adrenal axis in multiple sclerosis: association with cerebral inflammation. *Arch Neurol.* (1998) 55:66–72. doi: 10.1001/archneur.55.1.66
36. Burns MN, Nawacki E, Kwasny MJ, Pelletier D, Mohr DC. Do positive or negative stressful events predict the development of new brain lesions in people with multiple sclerosis? *Psychol Med.* (2014) 44:349–59. doi: 10.1017/S0033291713000755
37. Rethorst CD, Bernstein I, Trivedi MH. Inflammation, obesity, and metabolic syndrome in depression: analysis of the 2009-2010 National Health and Nutrition Examination Survey (NHANES). *J Clin Psychiatry.* (2014) 75:e1428–32. doi: 10.4088/JCP.14m09009

38. Opel N, Cearns M, Clark S, Toben C, Grotegerd D, Heindel W, et al. Large-scale evidence for an association between low-grade peripheral inflammation and brain structural alterations in major depression in the BiDirect study. *J Psychiatry Neurosci.* (2019) 44:423–31. doi: 10.1503/jpn.180208
39. Kraynak TE, Marsland AL, Wager TD, Gianaros PJ. Functional neuroanatomy of peripheral inflammatory physiology: a meta-analysis of human neuroimaging studies. *Neurosci Biobehav Rev.* (2018) 94:76–92. doi: 10.1016/j.neubiorev.2018.07.013
40. Yin L, Xu X, Chen G, Mehta ND, Haroon E, Miller AH, et al. Inflammation and decreased functional connectivity in a widely-distributed network in depression: centralized effects in the ventral medial prefrontal cortex. *Brain Behav Immun.* (2019) 80:657–66. doi: 10.1016/j.bbi.2019.05.011
41. Giovannoni G, Miller DH, Losseff NA, Sailer M, Lewellyn-Smith N, Thompson AJ, et al. Serum inflammatory markers and clinical/MRI markers of disease progression in multiple sclerosis. *J Neurol.* (2001) 248:487–95. doi: 10.1007/s004150170158
42. Mills RJ, Young CA. The relationship between fatigue and other clinical features of multiple sclerosis. *Mult Scler.* (2011) 17:604–12. doi: 10.1177/1352458510392262
43. Valentine TR, Alschuler KN, Ehde DM, Kratz AL. Prevalence, co-occurrence, and trajectories of pain, fatigue, depression, and anxiety in the year following multiple sclerosis diagnosis. *Mult Scler.* (2021). doi: 10.1177/13524585211023352 Availabe online at: https://journals.sagepub.com/doi/10.1177/13524585211023352

Conflict of Interest: YY has been supported by travel grants from Novartis and Sanofi Genzyme, has received an honorarium for active participation in an advisory board by Sanofi Genzyme as well as speaking honoraria by Roche and Sanofi Genzyme. CF reports speaker honoraria and honoraria for participating in advisory boards from Alexion, Novartis, Teva, Merck, Sanofi-Genzyme, and Roche and he received research support from Novartis and Sanofi-Genzyme.

The remaining authors declare that the research was conducted in the absence of any commercial or financial relationships that could be construed as a potential conflict of interest.

frontiers in Immunology

HYPOTHESIS AND THEORY
published: 01 November 2021
doi: 10.3389/fimmu.2021.757302

Cumulative Roles for Epstein-Barr Virus, Human Endogenous Retroviruses, and Human Herpes Virus-6 in Driving an Inflammatory Cascade Underlying MS Pathogenesis

*Ute-Christiane Meier[1,2], Richard Christopher Cipian[3], Abbas Karimi[4], Ranjan Ramasamy[5] and Jaap Michiel Middeldorp[6]**

[1] Institut für Laboratoriumsmedizin, Klinikum der Universität München, München, Germany, [2] Department of Psychological Medicine, Institute of Psychiatry, Psychology and Neuroscience, King's College London, London, United Kingdom, [3] Department of Biology, Crafton Hills College, Yucaipa, CA, United States, [4] Department of Molecular Medicine, Faculty of Advanced Medical Sciences, Tabriz University of Medical Sciences, Tabriz, Iran, [5] ID-FISH Technology Inc., Miltipas, CA, United States, [6] Department of Pathology, Amsterdam University Medical Center, VUMC, Amsterdam, Netherlands

OPEN ACCESS

Edited by:
Maria Teresa Cencioni, Imperial College London, United Kingdom

Reviewed by:
Andre Ortlieb Guerreiro Cacais, Karolinska Institutet (KI), Sweden
Shinji Oki, National Center of Neurology and Psychiatry, Japan

***Correspondence:**
Jaap Michiel Middeldorp
j.middeldorp@amsterdamumc.nl

Specialty section:
This article was submitted to Multiple Sclerosis and Neuroimmunology, a section of the journal Frontiers in Immunology

Received: *11 August 2021*
Accepted: *11 October 2021*
Published: *01 November 2021*

Citation:
Meier U-C, Cipian RC, Karimi A, Ramasamy R and Middeldorp JM (2021) Cumulative Roles for Epstein-Barr Virus, Human Endogenous Retroviruses, and Human Herpes Virus-6 in Driving an Inflammatory Cascade Underlying MS Pathogenesis. Front. Immunol. 12:757302. doi: 10.3389/fimmu.2021.757302

Roles for viral infections and aberrant immune responses in driving localized neuroinflammation and neurodegeneration in multiple sclerosis (MS) are the focus of intense research. Epstein-Barr virus (EBV), as a persistent and frequently reactivating virus with major immunogenic influences and a near 100% epidemiological association with MS, is considered to play a leading role in MS pathogenesis, triggering localized inflammation near or within the central nervous system (CNS). This triggering may occur directly *via* viral products (RNA and protein) and/or indirectly *via* antigenic mimicry involving B-cells, T-cells and cytokine-activated astrocytes and microglia cells damaging the myelin sheath of neurons. The genetic MS-risk factor HLA-DR2b (DRB1*1501β, DRA1*0101α) may contribute to aberrant EBV antigen-presentation and anti-EBV reactivity but also to mimicry-induced autoimmune responses characteristic of MS. A central role is proposed for inflammatory EBER1, EBV-miRNA and LMP1 containing exosomes secreted by viable reactivating EBV+ B-cells and repetitive release of EBNA1-DNA complexes from apoptotic EBV+ B-cells, forming reactive immune complexes with EBNA1-IgG and complement. This may be accompanied by cytokine- or EBV-induced expression of human endogenous retrovirus-W/-K (HERV-W/-K) elements and possibly by activation of human herpesvirus-6A (HHV-6A) in early-stage CNS lesions, each contributing to an inflammatory cascade causing the relapsing-remitting neuro-inflammatory and/or progressive features characteristic of MS. Elimination of EBV-carrying B-cells by antibody- and EBV-specific T-cell therapy may hold the promise of reducing EBV activity in the CNS, thereby limiting CNS inflammation, MS symptoms and possibly reversing disease. Other approaches targeting HHV-6 and HERV-W and limiting

inflammatory kinase-signaling to treat MS are also being tested with promising results. This article presents an overview of the evidence that EBV, HHV-6, and HERV-W may have a pathogenic role in initiating and promoting MS and possible approaches to mitigate development of the disease.

Keywords: Epstein-Barr virus, human endogenous retrovirus-W, inflammatory cascade, molecular mimicry, multiple sclerosis, human herpesvirus-6

INTRODUCTION

Multiple sclerosis (MS) is a debilitating neurological condition with a strong autoimmune component and a significant cause of neurological impairment in young adults. MS is characterized by episodic, localized and progressive demyelination as the final result of focal inflammatory lesions, causing progressive or reiterating neuroinflammatory and neurodegenerative changes of the white and gray matter (1). The disease is characterized by immune cell infiltration from the periphery into the central nervous system (CNS), causing localized inflammation and demyelination with axonal damage, leading to autonomic, sensorimotor, and cognitive impairments. The severity and clinical phenotype is dependent on the frequency and distribution of CNS inflammatory lesions as well as the cellular composition and activation status of such lesions (1, 2). Intensive research has focused on autoreactive T- and B-cells as causal mediators, although the trigger for inflammation and autoreactivity remains obscure (1).

The diagnosis of MS is based on neurological examination, magnetic resonance imaging (MRI) and the presence of oligoclonal bands in the cerebrospinal fluid (3, 4). Immunomodulatory therapies are used for the treatment of MS. These disease-modifying treatments (DMTs) reduce the incidence of relapses and impact on progression by dampening the inflammatory signaling and reducing the entry of lymphocytes into the brain (5). The etiology of MS is unknown, but the immune system is thought to be pivotal in the development of MS in genetically predisposed individuals, in addition to environmental risk factors such as smoking, deficiency in sun exposure/vitamin D, and infection (6, 7). There is growing evidence indicating a causal role for viral pathogens in MS, serving as inflammatory agents activating astrocytes and microglia directly or indirectly (8, 9). Several viruses, including Epstein-Barr virus (EBV), Human Herpesvirus-6 (HHV-6), Varicella-zoster virus, John Cunningham virus, and human endogenous retroviruses (HERVs), have been studied in the context of MS. Except for HERVs, these viruses are persistent and cause life-long infections with "cellular stress-triggered" reactivation cycles that may be associated with the relapsing nature of MS (10, 11).

Here we present a hypothesis and testable model (**Figure 1**) suggesting a leading role of EBV infected B-cells in triggering the clinical MS phenotypes in genetically susceptible individuals (i.c. HLA-DR2b) by causing direct focal inflammation near and subsequently within the CNS, inducing reactivation of endogenous viruses (HERVs and HHV6A) and mimicry-driven autoimmunity within the CNS. This inflammatory cascade, overall and in time, leads to deranged (self- and virus-reactive) immune responses with reiterating and/or progressive inflammatory signaling in CNS-resident lymphocytes, glia-cells and astrocytes, associating with destruction of myelin producing oligodendrocytes (ODCs), together causing damage to the protective myelin sheath of neurons leading to axonal damage and progressive neurological disability (2, 9).

EPSTEIN-BARR VIRUS AND MULTIPLE SCLEROSIS

A Brief Description of EBV Biology and Life Cycle

EBV is a γ1 human herpesvirus (HHV4, lymphocryptovirus) that persistently infects up to 95 percent of humans worldwide mainly during childhood. Primary infection in young adults is often symptomatic and referred to as glandular fever or infectious mononucleosis (IM). EBV transforms and immortalizes B-lymphocytes during initial infection as an essential part of its life cycle, but persists as a quiescent (latent) virus in a small number of circulating resting memory B-cells and is thought to infect epithelial cells for virus replication and spread (12–14). Importantly, the bulk of EBV-carrying B-cells appear to home to lymphoid tissues in the head and neck region, proximal to the CNS (15). Dysregulated EBV-infection is associated with several pathologies, including neurological, hematological and autoimmune diseases, e.g. chronic-active EBV infection, MS, Rheumatoid Arthritis (RA) and Systemic Lupus Erythematosus (SLE), as well as multiple cancers, including distinct types of lymphoma and carcinoma (16–20).

EBV is a double-stranded DNA virus encoding approximately 100 open reading frames, which are expressed in tightly

Abbreviations: ANO, Anoctamin; BBB, blood-brain-barrier; BCR, B-cell receptor; BTK, Bruton tyrosine kinase; CMV, human cytomegalovirus; CNS, central nervous system; CRYAb, α-B crystallin; CSF, cerebrospinal fluid; CTL, cytotoxic T-lymphocytes; EAE, experimental autoimmune encephalitis EBV, Epstein-Barr Virus; EBER, EBV encoded small RNA; EBNA, Epstein-Barr nuclear antigen; HIV, human immunodeficiency virus; HERV, human endogenous retrovirus; HHV-6, human Herpesvirus-6; HLA, human leukocyte antigen; HSV, Herpes Simplex Virus; IM, infectious mononucleosis; IFN, Interferon; LMP, Latent membrane protein; MAPK, mitogen-activated protein kinase; MBP, myelin basic protein; MOG, myelin oligodendrocyte glycoprotein; MS, Multiple sclerosis; NFL, neurofilament light chain; PLP, Proteolipid protein; PPMS, primary progressive MS; RRMS, relapsing-remitting MS; SPMS, secondary progressive MS; RASGRP, RAS guanyl nucleotide-releasing protein; TCR, T-cell receptor.

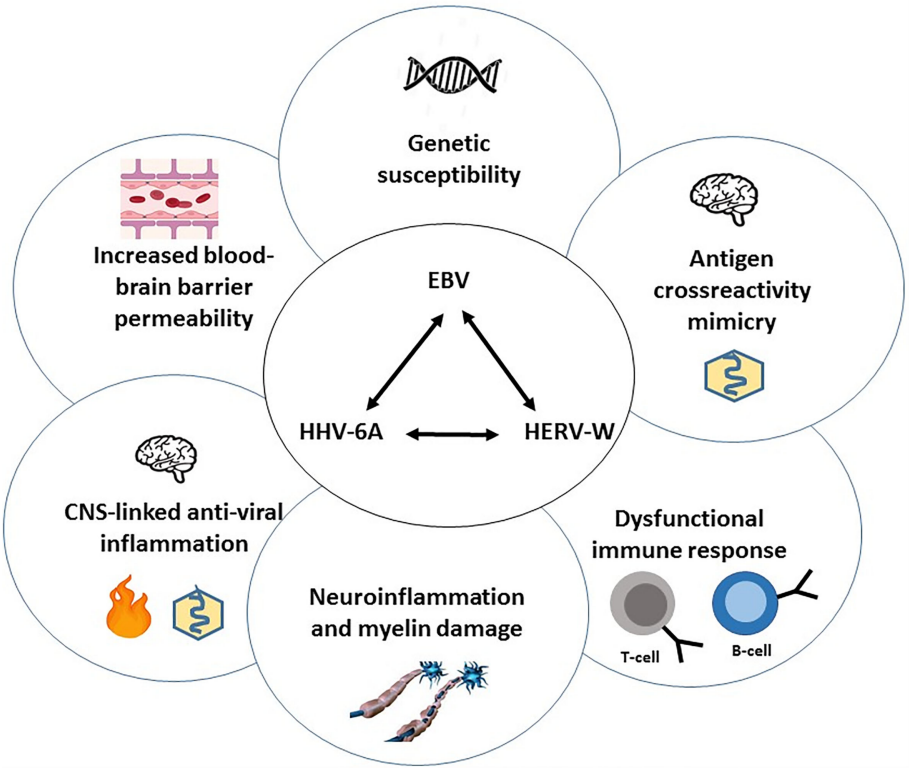

FIGURE 1 | Overview of the central viral cascade causing dysregulation of immune responses, localized CNS-inflammation and neuronal damage underlying MS-pathogenesis. A central role is proposed for Epstein-Barr virus (EBV), a persistent and frequently reactivating virus, that is associated with Multiple Sclerosis (MS) in genetically susceptible individuals (HLA-DRB*1501). Following ("stress"-induced) EBV reactivation in quiescent latency-I EBV-carrying B-cells in lymphoid tissues near the CNS, EBV-encoded gene products, - such as EBER1, miRNA and LMP1 in exosomes secreted by viable reactivating B-cells (latency-II/-III) and EBNA1-DNA complexes released from apoptotic EBV+ B-cells and possibly forming reactive immune complexes with locally produced anti-EBNA1-IgG -, together trigger anti-viral T-/B-/NK-cell-, antibody- and cytokine responses (Type-I IFN, TNF-α, IL-6, -10, -17A) causing localized inflammation. This is associated with spread of viral products, immune complexes, cytokines and the infiltration of (cross-)? reactive lymphocytes *via* a compromised blood-brain barrier causing aberrant activation of CNS-resident microglia and astrocytes and damage to oligodendrocytes (ODCs), leading to CNS inflammatory lesions as characteristic feature of MS. EBV itself and inflammatory cytokines may trigger the expression of endogenous germline-encoded viral sequences (MSRV or HERV-K/-W and HHV6A) in reactive lymphocytes and in inflammatory glia/astrocytes/ODC, which further enhance the localized CNS inflammation. In this inflammatory milieu, shared epitopes between (endogenous) viral and neuronal self-antigens may trigger autoimmune responses in susceptible individuals (HLA-DRB*1501), thus perpetuating CNS inflammation and causing pathogenic microglia activation and neuronal damage in an episodic (CIS), recurrent (RRMS) or progressive (SPMS, PPMS) virus-driven and auto-reactive pathogenic process. Interference with virus-driven inflammatory signaling, reconstitution of a quiescent immunological balance, remyelination and repair of damaged neurons are therefore key to future treatment and curative approaches in MS.

regulated latent (transforming and persistent) and replicative (reproductive) gene clusters (21–23). Genes expressed during latency encode proteins like EBV-nuclear-antigen-1 (EBNA-1), essential for viral genome maintenance in dividing cells, linking the viral genome to host cell chromosomes and affecting host gene-expression and the latent membrane proteins-1 and -2 (LMP-1, -2), crucial for inducing and maintaining an immortalized transformed state (default program of latent gene expression, *Latency-II*). During initial B-cell transformation and immortalization, additional EBV nuclear proteins (EBNA-2 to EBNA-6) are expressed (transformation program, *Latency-III*), but their activity is quickly limited by gene silencing *via* CpG-promotor methylation within- and strong T-cell control against Latency-II/-III activated EBV^+ B-cells (14, 24). The Latency-II and -III stages are only sporadically detectable in lymphoid follicles, where EBV-infected B-cells can proliferate and mimic a germinal center activation program (25). In healthy EBV carriers EBV persists for life in a small number of quiescent circulating memory B-lymphocytes, expressing only EBNA-1 protein when these cells divide (True Latency program, *Latency-I*) (26). Upon cognate antigen encounter within lymphoid tissues, these memory B-cells can switch to IgG-producing plasma cells (13). The molecular switch of memory B-cell to Ig-producing plasma cell activates a three stage EBV lytic-cycle with ultimate virion release and apoptotic cell death. Induction of the lytic phase requires initial triggering of immediate-early viral gene expression encoding highly immunogenic transcription factors Zta and Rta (step-1), followed by early genes encoding enzymes for nucleotide metabolism and viral DNA replication (step-2) and late genes encoding proteins involved in virion assembly (step-3) (27). Virus-encoded small nuclear and nucleolar RNAs and over 40

microRNAs encoded in two gene clusters are abundantly expressed during latent and lytic stages and modulate host gene expression and inflammatory responses, associating with distinct EBV-driven diseases (28–31). Host immune surveillance against EBV is constantly active at a high level (~1% of all T-cells are EBV-antigen responsive) and predominantly directed at latency-II/-III and immediate early gene products, preventing latent B-cell proliferation and lytic activation of EBV (24).

Humoral Immune Responses Against EBV in MS

The serological evidence for EBV being a risk factor for MS is strong and growing, although the high levels of EBV seropositivity in adults make it hard to establish such association unequivocally. However, recent large-scale studies have revealed a near 100 percent EBV seropositive rate in MS patients, which is significantly higher compared to age-, gender- and population-matched controls (32, 33). The increased IgG seropositivity in MS patients particularly involves responses to proteins coded for by EBV latent genes (esp. EBNA-1) rather than lytic genes (EA, VCA), and is virus-specific because no elevated antibody levels to human cytomegalovirus (CMV) or Herpes simplex virus (HSV) are significantly linked to MS (32, 34). The risk of MS increased more than two-fold after a history of IM, as opposed to subclinical primary EBV infection (35, 36). The risk was further substantially elevated in individuals with an IM history and HLA Class II DR2b (DRB1*1501 β, DRA1*0101 α), which is the strongest genetic risk factor for MS (37). Furthermore, specific increases in serum anti-EBNA-1 antibody levels preceded the onset of clinically apparent MS by several years, showed increases during conversion from a clinically isolated syndrome (CIS) to definite MS and associated with active MRI lesions in established MS (38–41). Overall, anti-EBNA-1 antibodies are specifically elevated in MS and thought to originate from the periphery as the levels of anti-EBNA-1 antibodies relative to total IgG were higher in the serum compared to CSF in the majority of relapsing-remitting MS patients (34, 42). Importantly, EBNA-1 forms dimers and multimeric complexes tightly bound to viral and host DNA, which are released upon apoptotic death of EBV-infected host cells as induced by the lytic switch and/or anti-EBV cytotoxic T-cell (CTL) responses (see **Figure 2**). Such EBNA-1-DNA complexes are stable and highly immunogenic and human anti-EBNA-1 antibodies specifically recognize surface epitopes of such complexes (**Figure 2**, epitopes depicted in top section), but not the intramolecular dimer and DNA-interacting regions of EBNA-1 (43, 44). This suggests that anti-EBNA-1 antibody responses are driven by apoptotic EBNA-1-DNA complexes directly (via BCR on B-cells) or indirectly (via phagocytosis and/or Fc-/Complement receptor-mediated uptake and presentation in specialized antigen-presenting cells, APC) thus triggering anti-EBNA-1 T- and B-cell responses. Oligoclonal bands, which are found in the CSF of most MS patients, contain immunoglobulins that recognize EBNA-1 and intrathecal IgG from MS patients recognized defined EBNA-1 epitopes thus implying local anti-EBNA-1 antibody production that can lead to immune (complex)-mediated pathology (45). Interestingly, more recent detailed epitope mapping studies have confirmed the prevalence of anti-EBNA-1 IgG and IgM in CSF and sera from MS-patients, and revealed possible cross-reactive peptide mimicry epitopes, as will be detailed later (46, 47). The presence of high levels of anti-EBNA-1 antibodies and oligoclonal bands in CSF may reflect increased activation and locoregional multiplication with subsequent T-cell mediated apoptotic elimination of B-cells that are latently infected with EBV (26).

Cellular Immune Responses Against EBV

EBV-reactive T lymphocytes are abundant in the circulation of EBV carriers and pivotal in controlling EBV homeostasis by eliminating undesired and potentially dangerous (re)activated EBV-infected B-cells (24). It is estimated that in healthy EBV carriers about 1% of all circulating T-cells are responsive to EBV-derived antigenic peptides, with latency-associated and immediate early lytic proteins being prime targets (23). CD4+ T cell responses are dominantly directed against EBNA-1, recognizing 12-15 mer peptide epitopes located within the stable EBNA-1/DNA dimer structure, suggesting complete complex degradation "*in trans*" in APCs (myeloid dendritic or B cells) before presentation on MHC-II to CD4+ T cells (48) (see **Figure 2**, epitopes in top section). On the other hand, CD8+ cytotoxic T cells (CTLs), which recognize MHC-I associated 8-mer peptides processed "*in cis*" by the host cell proteasome and presented on the surface of EBV infected cells, are much less abundant and very restricted in epitope recognition (24, 44, 49). Importantly, elevated EBNA-1 specific T-cell responses are detectable during initial stages (CIS) of MS and are predictive for symptomatic MS progression in parallel with anti-EBNA1 serology (40). Aberrant EBV-specific T-cell control has been found in MS patients, as will be detailed here below.

EBV Persistence and Dysregulation of EBV Homeostasis in MS

Throughout life, EBV remains immunologically silent (*Latency-I*) in small numbers of B- cells (1 in 10^5) in the blood, which home to the head and neck lymphoid tissues (15). EBV-infected B-cells periodically reactivate during lymph node passage to form new EBV+ B-cells (Latency-II/-III) or become plasma cells that may reproduce virus (lytic stage), leading to virus shedding in saliva and blood, but both types of reactivation are tightly controlled by CTLs to EBV latency-II/-III and immediate early lytic antigens to prevent B-cell lymphoproliferation (24). Importantly, physiological and immunological stressors can trigger inflammatory events that reactivate EBV from latency and drive multiplication of EBV-carrying B-cells (50, 51). Such aberrant state of EBV latency and/or reactivation proximal to the CNS may deregulate and enhance local (anti-EBV) inflammatory responses by release of exosomes (see **Figure 2**, lower section) containing EBV-encoded immunomodulatory RNAs (EBER1, miRNA) and proteins (LMP1). These exosomes may influence locoregional cellular functions and cytokine milieu (30, 31). CTL-mediated elimination of EBV+ B-cells may create apoptotic bodies

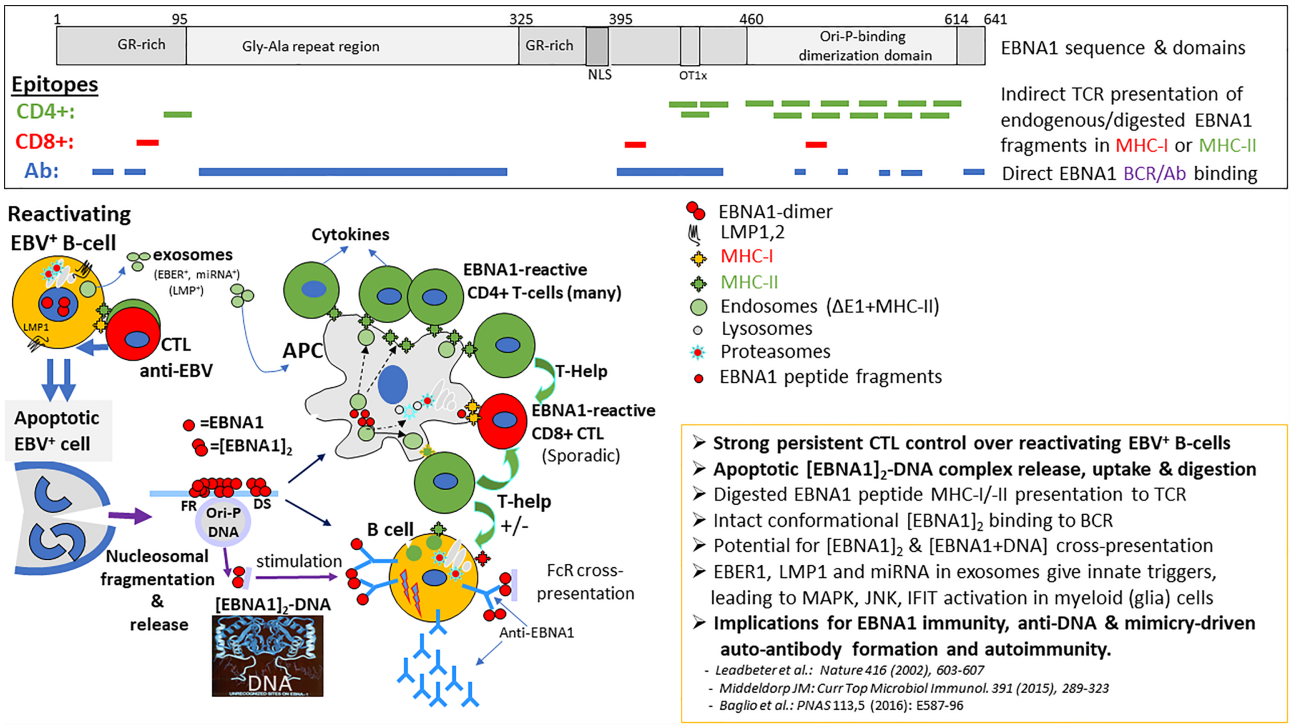

FIGURE 2 | Processing, presentation and position of EBNA-1 epitopes for CD4+, CD8+ T-cells and antibodies (B-cells). Viable persistent and "reactivating" EBV infected B-cells secrete EBER1 and LMP1 containing exosomes in the head & neck lymphoid microenvironment, continuously activating resident myeloid cells (possibly including microglia and astrocytes) for innate inflammatory signaling and increased antigen-uptake, digestion and presentation. Such innate signals may attract and pre-activate T- and B-cells to the inflammatory site. In EBV carriers, lifelong strong adaptive CD4+ and CD8+ cytotoxic T-cell immunosurveillance exists against replicating latent (Latency-I,-II,-III) and reactivating (Latency-III, Lytic) EBV-infected B-cells recognizing viral peptides bound to surface MHC-I or MHC-II molecules, resulting in release of pro-inflammatory cytokines. This T-cell surveillance is causing repetitive apoptotic cell death of EBV-infected cells and release of nuclear content as apoptotic bodies, enhancing the local inflammatory milieu. Such apoptotic bodies contain EBNA1-DNA (and host protein) complexes which are taken-up by antigen-presenting cells (APC), digested and presented in MHC-II for further CD4+ T-help and cytokine activation. EBNA1-dimers and multimeric EBNA1-DNA complexes also bind to the B-cell receptor (BCR) on B-cells, directly triggering anti-EBNA1 antibody responses, supported by local CD40 T-cell interactions and cytokines (IL4, IL10, IL17A). Prevalent anti-EBNA1 antibodies may form (complement-containing) immune complexes with released EBNA1-dimer/-DNA resulting in Fc-receptor (FcR) uptake into APC's and processing for MHC-II cross-presentation. Binding to B-cell receptor (IgM-IgD) directly triggers anti-EBNA1 antibody responses and possible anti-self autoimmune responses mediated by EBNA1-bound DNA and host nuclear proteins (i.c. ORC-complex) or *via* the mimicry domains within the EBNA1 sequence (see **Table 1**).

containing EBNA1 that will be taken-up by local APC and induce further anti-EBV T-cell activation and associated (IL-17A) cytokine release. These locally produced cytokines are further affecting normal immune balances, triggering blood-brain-barrier (BBB) permeation and possible local oligodendrocyte (ODC) disfunction (52–54). Episodes of (natural or therapy-induced) immune suppression and T-cell dysfunction are clearly related to and provide evidence for the importance of a well-balanced immune control over EBV-reactivation and B-cell proliferation (17, 55). Several studies have addressed in detail the T-cell operators and viral targets involved in maintaining a life-long balanced immune control over EBV and their potential exhaustion and dysregulation in MS (24, 56, 57).

Aberrant T-cell responses in CSF and CNS have been widely associated with MS, and a dysregulated T-/B-cell interaction may be fundamental to MS pathogenesis (58–60). The trigger(s) for initiating and maintaining this dysregulated immune balance in the CNS remains elusive. Intrathecal EBV-specific T-cell responses against EBV and/or auto-antigens have been identified and may be involved in MS pathogenesis (61–65). These can reflect autoreactive EBV-infected B-cells entering the CSF from the blood (Pender's hypothesis (66); and becoming activated locally, thus triggering inflammatory signaling and initiating EBV-specific or auto- (cross-) reactive CTL responses in the CNS. Alternatively, inflammation or stress-induced activation of (EBV-carrying) B-cells in meninges or locoregional lymphoid tissues may trigger cytokine responses and/or EBV encoded small-RNA (EBER)-induced inflammation *via* exosome secretion (**Figure 2**, lower section) that affect BBB integrity and allows anti-EBV immune cell passage and activation of microglia and astrocytes and dysfunctional of ODCs that together cause neuronal damage (2, 31, 51, 67–72).

Support for the hypothesis that anti-EBV inflammatory responses may be associated with the onset of MS came from reports of high levels of CTL activation against EBV but not CMV in the course of early MS (73). Studies on the

characterization of CTLs to latent and lytic EBV antigens in relapsing-remitting MS (RRMS) found an expansion of CTLs specific for lytic EBV antigens (Zta/BZLF1 and BMLF1) during active disease in untreated MS patients but not in patients treated with natalizumab (74). Furthermore, the frequency of CTLs specific for EBV lytic and latent antigens was higher in active and inactive MS patients than in controls (74). More recently, activated EBV-specific CD8+ T-cells were found to predominate in CSF of MS patients compared to non-MS controls (63). Characterization of CD4+ T-cell responses in MS patients also showed dysregulation with strikingly elevated frequencies of EBNA-1-specific CD4+ memory T cells, with increased proliferative capacity and enhanced IFN-γ production (40, 75). T-helper (Th) cell responses to three other latent and three other lytic immunodominant EBV antigens and CMV epitopes did not differ between patients and controls suggesting that EBNA-1 specific Th1 cells in MS are capable of sustaining autoimmunity (75). Multiple auto-antigen targets have been defined for CNS-derived T-cells, some of which are specifically expressed on activated EBV-carrying B-cells and share MHC-II restricted antigenic epitopes with EBV proteins, in particular EBNA-1, as will be detailed later (63–65, 76).

EBV Status and the MS Brain

Disruption of the BBB facilitates translocation of EBV-infected B-cells, inflammatory cytokines (i.c. IFN-1, TNF-α, IL17A), exosomes as well as anti-EBV antibodies and EBV-specific immune cells. One important question, which warrants further study, is how EBV and/or its products enter the MS brain during inflammatory events that (temporarily or chronically) permeate the BBB and whether such entrance is an early (triggering) or late (bystander) event in MS pathogenesis. As EBV resides in B-cells, which are able to traverse the "inflammation-damaged" BBB and traffic into CNS, its presence could be a mere bystander phenomenon. Recent studies indicate that epigenetic manipulation, for instance by inflammatory cytokines, can drive activation and CNS infiltration of EBV-infected B-cells (77). On the other hand, during periods of (EBV-related)? inflammation in locoregional lymphoid patches in the parenchyma, EBV+ B-cells and EBV-products in exosomes produced by such B-cells may cross the BBB and be taken-up by microglia cells to cause localized CNS inflammation (31, 78, 79). This would fit well with the characteristic $MAPK^{ERK}$ activation status of microglia and astrocytes in MS lesions, which are not directly infected with EBV (2, 9).

The detection of EBV in the MS brain is not without controversy (80). Although initial PCR studies failed to find traces of EBV genome in MS-related CNS tissue biopsies (81), a 2007 report of abundant EBV infection and widespread EBV reactivation in acute MS but not in other inflammatory central nervous diseases triggered much attention (82). However, despite rigorous efforts, these findings could not be confirmed in subsequent studies by others (83–85). Additional studies demonstrated localized EBV-infection in both MS and control brains (86, 87). Early studies reported meningeal B-cells within specific structures, referred to as tertiary lymphoid follicles with a germinal center-like architecture and denoted as major sites of EBV persistence in the MS brain (82), which however were found mostly negative for EBV in other studies (83, 84). The reasons for these opposite findings may be due to technical issues, such as degradation of RNA, the use of different MS tissues, differences in reagents, and non-specific staining of EBER+ cells by *in-situ* hybridization leading to cytoplasmic instead of nuclear staining (80). More recent studies, using similar techniques have detected EBV in sporadic cells in 90% of MS cases compared to only 24% of non-MS cases with other neuropathologies with EBV-infection being present in microglia and astrocytes, besides B-cells (88). The presence of EBV-infected B cells in or near the CNS and the anti-EBV immune responses in CSF of MS patient implicates that EBV-related products released from "activated" infected cells (i.e. EBNA-1-DNA complexes and/or EBER-containing exosomes) may provide persistent triggers for local (neuro-)inflammation. Further detailed analysis of laser-cut CNS and meningeal tissue lesions suggested low-level EBV presence and prevalent activated EBV latency or restricted (abortive) viral reactivation capable of triggering localized anti-EBV T-cell responses in CNS of patients with active progressive MS (61, 87, 89).

If EBV is finally incriminated, how could latent infection play a role? Latent EBV-infection may activate innate immune responses and thereby drive neuroinflammation in the MS brain (86). The detection of EBER+ cells in active white matter MS lesions was linked to the overexpression of the innate cytokine interferon-α (IFN-α) by cells with the morphology of microglia and macrophages (86). IFN-α is part of the type-I interferon family and an important player in anti-viral immunity. Its biological effect is distinct from IFN-β, which is also used to treat MS as discussed below. Latent EBV infection may contribute to neuroinflammation by triggering IFN-α production, as supported by the findings that EBERs can bind to Toll-like receptor 3 and potentially other intracellular receptors such as retinoic acid-inducible gene 1 (RIG-I) and elicit IFN-α production (31). However, these findings were not exclusive to the MS brain, as EBER+ cells were also found in cases of stroke and CNS lymphoma (86). This is also supported by more recent studies (87). Interestingly, recent studies have revealed a link between innate iNKT cells and B-cell responses, which would substantiate the potential role of EBV-derived inflammatory products (EBER-1 in exosomes, EBNA-1-DNA complexes) as triggers for dysregulated (autoimmune) B-cell responses (90). Whether MS-triggering EBV activity is located within the CNS or its boundaries remains to be determined, as well as whether such EBV activity is an MS initiating event or a consequence of (autoimmune)? inflammation.

EBV Status and Lymph Nodes in MS

Despite the dogma that the CNS has "immune privilege" to mitigate immunological damage to neurons, neuroimmune interactions may play an important role in the MS brain. There is increasing evidence for an intimate interaction between the brain and the immune system in the dural sinuses (91). Lymphatic vessels in the meninges provide an important link between the CNS and peripheral immune system and can play a role in autoimmunity in MS (91). Vessels in the dura

mater that drain CSF from the brain to the cervical lymph nodes and pathogens in lymph nodes can lead to the initiation of immune responses. B-cells seem to traffic freely across the tissue barrier, with the majority of B-cell maturation occurring outside of the CNS in the secondary lymphoid tissue (92). Furthermore, CNS B-cells have access to lymphoid tissue where they may encounter antigen and experience activation and affinity maturation.

There is evidence to suggest that cervical lymph nodes may serve as a latent viral reservoir due to dysregulated EBV activation (61, 87, 89). Histopathological findings of MS tissue from cerebral hemisphere, brain stem, and cervical lymph node of a patient with primary progressive MS (PPMS), who died of an ischemic stroke, showed EBER+ cells within B-cell follicles in the paracortex of the cervical lymph node (93).

EBV and Molecular Mimicry in MS

Autoimmunity can be caused by TCR-independent bystander mechanism or by cross-recognition of autoantigens when antigenic epitopes shared between a pathogen and host generate a cross-reactive B- or T-cell response that breaks self-tolerance and causes antibodies or T-cells respectively to damage host tissues. The concept of molecular mimicry at the level of T-cells causing the autoimmune disease was first elaborated by Ebringer in 1979 (94). A molecular mimicry hypothesis for MS has been proposed, whereby epitopes in viral pathogens, such as EBV, endogenous retroviruses, HHV-6 cross-react with epitopes in brain proteins and elicit cross-reactive B- or T-cell responses, which create inflammatory triggers and immunopathology (95–97).

EBV is thought to lead to marked immune activation and stimulate autoreactive T-cells *via* molecular mimicry between foreign agents and myelin peptides (98). These findings are supported by mechanistic studies into the structure of the T cell receptor (TCR) from an MS patient, which recognized both a DRB1*1501-restricted myelin basic protein (MBP) peptide and a DRB5*0101-restricted EBV peptide. Both HLA-peptide complexes revealed a marked degree of structural similarity at the surface presented for TCR recognition, which provided structural evidence for molecular mimicry involving Class-II HLA molecules (99). Recent studies in a humanized mouse model confirm a central role for HLA-DR15 restriction elements in causing aberrant anti-EBV immune responses with risk of autoimmunity (100).

Prior studies addressing the possibility of molecular mimicry in MS found clonally expanded EBNA-1-specific CD4+ T-cells that potentially contributed to the development of MS by cross-recognition with myelin antigens (75, 101). MS patients showed increased T-cell responses to EBNA-1 but not to other EBV-encoded proteins nor to other viruses such as influenza, HSV-1 and CMV. An expanded reservoir of EBNA-1-specific central memory CD4+Th1 precursors and Th1 (but not Th17) polarized effector cells recognized myelin antigens more frequently than other autoantigens that are not associated with MS (101). More recent findings shed light on how EBV may trigger mimicry-based autoimmunity, suggesting a crucial role for EBNA-1 in inducing mimicry-based self-reactivity as summarized in **Table 1** and visualized in **Figure 2**. Antigenic products induced by EBV within (e.g. alpha B-crystallin (CRYab) (105, 106, 114), or released from EBV infected B-cells (i.c. EBNA-1-DNA, LMP1,2 in exosomes, Lytic phase components) are thought to activate HLA-DR/peptide reactive CD4+ T-cells, which then respond to potentially "pathogenic" self-peptides or autoantigens with EBV-related amino acid sequence homology (= mimicry) such as myelin basic protein (MBP), myelin oligodendrocyte glycoprotein (MOG), neurofilament light chain (NFL). Multiple putative cross-reactive epitopes in human and EBV proteins interacting with IgG from CSF or serum from MS patients have been identified (**Table 1**). A recently identified pathogenic self-peptide is derived from the RAS Guanyl Releasing Protein 2 (RASGRP2), which is expressed by B-cells but also in neurons and other brain cells. B-cells presenting RASGRP2-derived peptides are thought to trigger autoreactive T-cells, similar to CRYab (65, 76, 102, 104, 114). These HLA-DR-self peptide-reactive CD4+ T-cells can cross the BBB and enter the brain where they orchestrate an autoimmune attack by producing inflammatory mediators leading to demyelination and axonal injury.

A structural approach to investigate molecular mimicry identified a structurally related pair of peptides from EBNA-1 and β-synuclein, a brain protein implicated in MS (102). Binding experiments showed the binding of the predicted peptides to HLA DR2b with characteristics comparable a with the well-known Th-epitope in myelin basic protein (MBP). Structural modeling of the peptides with HLA DR2b revealed binding to the peptide-binding cleft similar to MBP and relative conservation of the surface exposed, potential TCR contact residues in the two peptides. This suggests that molecular mimicry is possible between the EBNA-1 and β-synuclein peptides.

A recent study presented a case for molecular mimicry between Anoctamin 2 (ANO2) and EBNA- 1 associates with MS risk (104). ANO2 is a chloride channel protein expressed in the CNS. MS patients showed increased autoantibody reactivity to ANO2 with high sequence similarity between epitopes in ANO2 and EBNA-1 (**Table 1**).

Whether antigenic mimicry is a cause or consequence of MS-related inflammation and is driven by the mimicry-domains in EBNA-1 remains to be established.

EBV and Reactivation of Human Endogenous Viruses

The regular (stress-triggered) reactivation of EBV in or near the CNS with associated activation of host genes and release of EBV-encoded components, together with the loco-regional (anti-virus/-self) inflammatory cytokine responses triggered by and against EBV, may set-of a number of cellular signaling events in actively responsive as well as bystander cells (B-/T-cells, glia-astrocytes, ODCs). These EBV-induced molecular events may lead to changes in transcriptional control/activation of viral sequences encoded within the germline genome, in particular endogenous retroviruses (HERV) and integrated HHV6A (each individually detailed further below). Well known examples are the induction of HERV-K18 (115, 116) and HERV-W (117)

TABLE 1 | Overview of viral proteins involved in antigen mimicry in MS.

Virus	Viral protein	Self-protein	Nature of cross-reaction	Study	Reference
EBV	EBNA-1	β-Synuclein	HLA DR2b binding (potentially CD4+ T-cells)	Ramasamy et al. (2020),	(102)
	EBNA-1	α-Synuclein, CRYAb, MBP, MOG & neurofilament light chain	Cross-reactivity of anti-EBNA1 peptide-specific antibodies with human brain protein extracts and purified brain proteins and identification of sequence homologies	Vertelman & Middeldorp (unpublished), Middeldorp (2015)	(44)
	EBNA-1	MBP	Serum antibodies in MS patients	Jog et al. (2020)	(103)
	EBNA-1	Mix of myelin proteins	CD4+ T cells	Lünemann et al. (2008)	(101)
	EBNA-1	Anoctamin 2	Antibodies in MS patients	Tengvall et al. (2019)	(104)
	EBNA-1	Alpha-B Crystallin (CRYAb)	Serum and CSF antibodies in MS cases	Hecker et al. (2016)	(46)
			EBV+ LCL and MS-CNS lesions	Van Sechel et al. (1999)	(105)
				Van Noort et al. (2010)	(106)
	EBNA-1	hnRNP-L	Serum antibodies in MS	Lindsay et al. (2016)	(107)
	DNA-polymerase	MBP	CD4+ T-cells	Wucherpfennig & Strominger (1995)	(98)
	BFRF3 (VCA-p18)	Septin-9	Antibodies in MS patients	Lindsey (2017)	(108)
	BRRF2	Mitochondrial antigens	Serum antibodies in MS	Dooley et al. (2016)	(109)
	LMP-1	MBP	CSF antibodies in MS and Mouse immunizations	Lomakin et al. (2017)	(110)
	LMP-1	a-Synuclein	Monoclonal antibody on human brain tissue	Woulfe et al. (2016) Middeldorp, unpublished	(111)
	Multiple	Multiple	Pentapeptide epitope homology	Kanduc and Shoenfeld, (2020)	(112)
	BZLF1	Unknown	CD8+ T-cells in MS brain	Serafini et al. (2019)	(61)
HHV-6	U24	MBP	CD4+ T-cells and antibodies in patients	Tejada-Simon et al. (2003)	(113)
pHERV-W	env	MOG	HLA DR2b binding (potentially CD4+ T-cells)	Ramasamy et al. (2020)	(102)

gene-products by EBV infection in B-cells and/or cytokine-driven reactivation (118) of these endogenous viruses. The induced HERV-K18/-W proteins may serve as "superantigens" further inducing polyclonal Vβ TCR-driven activation and associated cytokine releases (119). On the other hand, it has been described that endogenous retroviral elements (i.c. HERV-W-env (Syncytin-1) may enhance lytic viral gene expression of gamma-herpesviruses in latently infected B-cells, making the interaction two-sided (120). Dysregulated (virus- or cytokine-induced) expression of HERV-K/-W elements have clear implications for the pathogenesis of multiple neurological disease, including MS (121), secondary to the initial triggering by EBV-driven mechanisms. Of relevance is the possible induction of mitogen-activated protein kinase extracellular signal-regulated protein kinase (MAPK-ERK) (122) pathway in HERV-W-ENV expressing cells, which is characteristic of MS glia-cell activation (9). Together, these observations strengthen the 3-viral cascade hypothesis (123), with EBV as leading pathogen (**Figure 1**) and comprising a multi-factorial interaction of virus-, altered self or mimicry- and cytokine-driven inflammatory pathogenic events underlying the different manifestation of MS disease, being non-progressive (CIS), reiterating (RRMS) and progressive (SPMS, PPMS) with increasing neurological damage.

Future Studies on the Relationship Between EBV and MS

Defining the roles of autoimmune responses as cause or consequence in the pathogenesis of MS and their potential link to viral antigen mimicry and auto-reactive EBV-infected B-cells merits further analysis. This also holds for the putative inflammatory role(s) of EBV-derived components (EBERs in exosomes and/or EBNA1-DNA complexes) in triggering loco-regional activation of the MS-characteristic inflammatory MAPK pathway in microglia (2, 9). The role and mechanism of EBV and cytokines on activating other endogenous viruses, such as HERVs and HHV-6 also deserves attention (9). Since all MS patients are EBNA-1-IgG positive, the involvement of EBNA-1-IgG immune complex formation and inflammation near CNS should be further analysed. Single cell sorting could be utilized to provide more definitive proof on the presence and status of EBV (analysis of viral DNA and RNAs) in the MS brain and nearby regional lymphoid tissues (61, 89). Frozen tissue containing (pre-)active HLA-DR+ lesions with reactive glia-cell and ODC-clusters from MS cases will be needed to perform single-cell B cell receptor (BCR) and TCR sequencing as was recently done on Alzheimer's patient biopsy material (124). Cell types can be selected based on cell-specific protein markers and many features may be used simultaneously to classify cells by molecular analysis (125). EBV-specific TCRs have been detected in the CSF from patients with Alzheimer's disease. However, these data are not direct evidence of a causal link between EBV and Alzheimer's disease (124). A search for EBV-DNA, EBER1-RNA, EBV encoded miRNA or EBNA-1/LMP-1 in combination with single cell analysis of CNS cell type-specific RNA, T-cell lineage and TCR sequence has not yet been conducted in in MS patients to our knowledge, but methods to do so are being developed (126, 127). Similarly, the presence, frequency and level of HERV-K/-W RNA as well as HHV6A gene-expression in defined cell types in MS-related (early) CNS lesions requires further analysis. Other interesting topics include the link between bacterial infection (periodontitis, inflammatory bowel disease, etc.), short-chain fatty acids, and vitamin D status or

"stress" factors and their influence on (chronic or repeated) EBV reactivation in causing neuroinflammation, exemplified by the well-defined effects of butyric acid, butyrate derivatives and glucocorticoids on ODC activation, triggering B-cell proliferation and switching EBV from tight latency into reactivation and lytic replication (128–131).

Therapeutic Approaches Targeting EBV-Infection in MS

Efforts to develop antiviral strategies for treating MS are underway. Interferon-β (IFN-β) is one of the first-line treatments of MS and an important player in antiviral immunity. However the mechanism by which the therapeutic effect takes place remains somewhat elusive to date. It is thought that IFN-β has antiproliferative effects and down-regulates T-cell activation by altering the expression of proteins involved in antigen presentation, and promotes the differentiation of activated T cells away from a Th1 response (pro-inflammatory) and towards a Th2 response (anti-inflammatory). Clinically effective IFN-β therapy was associated with a downregulation of proliferative T-cell responses to EBNA-1 and showed efficacy in reducing pHERV-W and HHV6-A plasma viral loads, two additional viral risk factors in the context of MS, as will be described further below (132, 133).

New monoclonal antibody-based treatments targeting B-cells have recently been introduced and proven highly successful in reducing MS clinical symptoms. The idea that these treatments impact on the B-cell-tropic EBV warrants further study (8, 134). The B-cell depleting antibody ocrelizumab significantly reduced annual relapse rate and dramatically limited the appearance of new Gadolinium-enhanced T2 lesions, as well as disability progression (135). However, this treatment proved less effective in more advanced progressive stages of MS and is not considered curative. The use of haemopoietic stem cell transplantation (HSCT) has been suggested as curative MS-treatment aiming at the elimination of pathogenic reactive lymphoid cells and to re-boost the immune system. Interestingly, autologous HSCT may deplete EBV from the pathogenic equation, as early studies indicated complete elimination of endogenous EBV by HSCT (136). However, EBV-elimination is not guaranteed after HSCT and the HLA-DR based genetic susceptibility for MS remains, whereas the health risks associated with HSCT are considerable and HSCT may not be suitable for all categories of MS (137).

Studies examining the effect of antiviral and antiretroviral drugs on MS disease activity are currently planned. In past antiviral trials targeting herpes virus, treatment only reduced lytic viral replication without affecting latent virus. Several nucleoside analogs have been shown *in-vitro* to impact EBV lytic replication including acyclovir and penciclovir, ganciclovir and tenofovir (138). A case report described the resolution of MS symptoms, which remained subsided for more than 12 years (139), in a MS patient diagnosed with HIV after starting HIV antiretroviral therapy. It is interesting to speculate to what extent the observed benefits reflect an impact of anti-retroviral therapy on neuroinflammation and on EBV-mediated disease mechanism.

A novel strategy is currently tested to eliminate EBV-infected B-cells using an EBV-specific CD8+ T-cell therapy. Autologous or allogeneic infusion-cell therapy studies by Pender and colleagues have focused on inducing CTL activity against latent EBV proteins (140). A phase-1 trial of autologous EBV-specific T-cell therapy in progressive MS showed short-term clinical improvement in 7 out of 10 patients and noted no serious adverse effects. The patients were treated with four escalating doses of *in vitro*-expanded autologous EBV-specific T-cells targeting EBNA-1, LMP1 and LMP2A. Clinical improvement following treatment was associated with the potency of EBV-specific reactivity of the administered T-cells. However, the beneficial effect was sustained in a limited number of cases in this trial (141).

Targeting neuroinflammation *via* Fc- (FcR), B-cell (BCR) and Toll-like receptor signaling may also be achieved with Bruton's tyrosine kinase (BTK) inhibitors. BTK is a signaling molecule involved in maturation and activation of B-cells through BCR and FcR. BTK has been demonstrated to also play an important role in signaling pathways of multiple Toll-like receptors (142, 143). The BTK inhibitor AG126 has recently been tested in experimental autoimmune encephalomyelitis (EAE), the animal model of MS, and reduced clinical symptoms, immune cell infiltration in the CNS, microglia activation and myelin damage, and decreased Th17 differentiation. BTK inhibitors also impacted LMP2A mediated IL-10 production crucial for EBV survival by increasing STAT3 phosphorylation *via* a PI3K/BTK-dependent pathway (144). A recent clinical trial examined the BTK inhibitor evobrutinib in a phase 2 clinical trial in MS. Patients with RRMS who received 75 mg of evobrutinib once daily had significantly fewer enhancing lesions during weeks 12 through 24 than those who received placebo (145). However, there was no significant difference with placebo for the other dosing regimes, nor in the annualized relapse rate or disability progression at any dose. A second oral BTK-inhibitor tolebrutinib, capable of passing the BBB, was also evaluated in a phase-2b trial with similar beneficial effects for the highest 60 mg dose with minimal side-effects (146). Newer BTK inhibitors are being developed, which more specifically inhibit BCR and FcR mediated signaling in B-cells and myeloid cells, which may have impact on the proposed reactive T-/B-cell and EBV-EBNA1 antigen-driven inflammation in MS lesions (147). Alternative options to reduce neuroinflammation in MS include inhibition of fibroblast growth factor receptor and MAPK-signaling (9, 148, 149) or use of ursolic acid, a well-tolerated oral drug that reduced neuroinflammation and stimulates remyelinisation (150).

Suppressing the function of EBNA-1, as crucial viral gene for EBV DNA maintenance in B-cells, is being tested for treatment of EBV-driven cancers, including lymphomas and carcinomas. Such an approach may also prove relevant for MS treatment, provided that EBV within B-cells indeed is a master player in MS pathogenesis (151, 152).

HUMAN HERPESVIRUS 6 AND MS

A Brief Description of HHV-6

Human herpesvirus 6 (HHV-6) is a ubiquitous β-herpesvirus associated with a number of clinical disorders including MS. Two

closely but biologically distinct variants (HHV-6A and HHV-6B) have been described with different tropisms. Although some authors have described a possible relation between HHV-6B and MS (153), HHV-6A is more strongly associated with MS (154, 155). HHV-6 has a seroprevalence rate of 70 to 90 percent in the human population (156). Most adults become infected as infants and have seroconverted by the age of two. There have been reports of neuroinvasion and persistence of HHV-6 in children with neurological complications, e.g. febrile seizures and encephalitis (156, 157). The virus can reactivate, especially in cases of immune deficiency, such as in acquired immune deficiency syndrome (158). HHV-6 also has the capacity to be inherited in a Mendelian fashion in up to one percent of the population as chromosomally integrated HHV-6 in which the complete HHV-6 genome is integrated into the telomere of every chromosome (159).

HHV-6 Infection and MS

A question of interest is how HHV-6 can cause or contribute to neuroinflammation in MS as it is considered a risk factor for MS (160). New animal models have recently been established, mainly for HHV-6A and reproduced some pathological features seen in humans. Animal models have been slow to develop because rodents lack CD46, the receptor for cellular entry of the virus. It is hypothesized that HHV-6 can modulate the functions of the CD46 receptor by binding to it and levels of soluble CD46 are increased in the serum of patients with MS (161). Studies in a CD46 transgenic murine model of HHV-6A infection described persistent infection of the brain (162) with infiltrating lymphocytes in periventricular areas of the brain indicative of neuroinflammation. HHV-6A triggered chemokine and cytokine production *via* stimulation of Toll-like receptor 9. The marmoset model showed that animals inoculated intravenously with HHV-6A exhibited neurologic symptoms, while marmosets inoculated with HHV-6A intranasally stayed asymptomatic (163). Other studies showed that HHV-6A can enter the CNS *via* the olfactory pathway (164).

Several groups have reported the presence of HHV-6A in MS plaques and normal-appearing white matter within the MS brain as well as in normal controls (155, 165). A groundbreaking report in 1995 obtained evidence that HHV-6 was a common commensal virus of the brain expressed in neurons and glial cells (165). Expression of HHV-6 antigens was observed in oligodendrocytes in MS cases, but not in various controls. Moreover, in MS patients, nuclear HHV-6 staining in oligodendrocytes was most commonly associated with MS plaques. These findings were later confirmed and HHV-6A genome-containing cells, including ODCs, were detected in biopsy specimens of acute MS lesions (166). In addition, an association was found between HHV-6A reactivation and disease activity in RRMS and secondary progressive MS (SPMS) (167). The increase of the anti-HHV-6A/B IgG and IgM titers predicted clinical relapses and highlighted their usefulness as disease biomarker of clinical response to the different disease-modifying treatments (DMTs) (155). In addition, increased IgM serum antibody responses to HHV-6 early antigen (p41/38) were detected in patients with RRMS when compared to patients with primary progressive MS (PPMS), SPMS, patients with other neurologic disease, patients with other autoimmune diseases, and normal controls (168).

HHV-6 and Molecular Mimicry in MS

Molecular mimicry between HHV-6 and brain proteins has been suggested and may help understand the potential role of HHV-6 infection in the activation of autoimmunity and its implication in the pathogenesis of MS (**Table 1**). Sequence similarity between MBP residues 93-105 and the U24 protein of HHV-6 has been identified (113). The precursor frequency of cross-reactive CD4+ T-cells recognizing peptides from MBP and U24 were significantly elevated in MS patients compared to healthy controls.

HHV6A has also been found to activate a HERV-K18-encoded superantigen, which in turn activated T-cells carrying receptors of the Vβ13 family (169). T-cell clones, activated in this way, had TCRs that recognized the immunodominant encephalitogenic MBP peptide (residues 83-99) presented by HLA DR2b, thereby demonstrating the potential for causing immunopathology in HLA DR2b-positive MS patients (113).

Transactivation of EBV and HERV by HHV-6

Transactivation can be triggered by viral proteins, also called transactivators, which act in trans (i.e. intermolecularly) in the same co-infected host cell. The transactivation of EBV by HHV-6 was described whereby HHV-6 upregulated the immediate-early EBV Zebra gene transcription through a cyclic AMP-responsive element associated with the Zebra gene (170, 171). Additional studies showed that HHV-6 variant A, but not variant B, infected EBV+ve B-cells activated the endogenous latent EBV genome through a BZLF-1-dependent mechanism (172).

HHV-6A also transactivated other viruses. HHV-6A and HHV-6B induced transcriptional activation of the endogenous retroviral superantigen HERV-K18 (169, 173). An interesting recent study reported that HHV-6A increased the expression the envelope protein of a pathogenic version of HERV-W in human glial cell lines, supporting the hypothesis that HHV-6 infection may promote neuroinflammation (174).

HUMAN ENDOGENOUS RETROVIRUS W

A Brief Description on HERVs

Human endogenous retroviruses (HERVs) are remnants of ancient RNA viruses that have DNA copies of their genome incorporated into the human genome (175). HERVs compose approximately 8% of human DNA, although many HERVs have undergone loss of function mutations in critical genes or become highly truncated (176, 177). The possible roles of different HERV family members in MS have been comprehensively reviewed recently, including how immune activation, inflammation, and oxidative stress can influence the transcription of HERV genes (178). HERV-W family members have particularly attracted attention. Among the 13 HERV-W loci with full-length *env* genes coding for viral envelope proteins in the human genome

(179), only a single gene located in chromosome 7q21.2 and coding for Syncytin-1 has an uninterrupted open reading frame. Syncytin-1 has evolved or undergone exaptation to perform an important fusogenic function in human placentation in the fusion of cytotrophoblasts to form the placental syncytiotrophoblast (180). Another HERV env protein termed Syncytin-2 from a different HERV family, HERV- FRD, has also been similarly exapted to play an essential fusogenic role in forming the placental syncytiotrophoblast (181).

HERV-W Envelope Proteins and MS

An MS-associated retrovirus termed MSRV, also a member of the HERV-W family, has been particularly implicated in MS because virus particles and reverse transcriptase activity were detected in MS patients (182). MSRV env protein has been found to be present in microglia associated with myelinated axons in MS lesions, and implicated in inflammatory myelin and neuron damaging activity by microglia *in vitro* (183). A humanized IgG4 monoclonal antibody to MSRV env has been reported in a clinical trial to show a neuroprotective effect in RRMS (184). MSRV env has also been detected in macrophages, astrocytes and infiltrating lymphocytes within lesions (185). The MSRV env is 87% identical to Syncytin-1 in amino acid sequence by BLAST analysis (95), and to clearly differentiate the two proteins and their origins, which has in the past caused confusion in the literature, MSRV is now referred to as pathogenic HERV-W or pHERV-W (183). The genomic origin of the pHERV-W env protein remains a puzzle in view of the absence of a full-length gene for a HERV-W env protein other than Syncytin-1. However, it has been proposed that pHERV-W env may be derived from a HERV-W gene on the X chromosome at Xq22.3, which has a premature stop codon at position 39, through a process of somatic mutation or trans-splicing (186).

HLA Class II DR2b (composed of the DRB1*1501 β chain that pairs with a relatively invariant DRA1*0101 α chain) is the strongest genetic risk factor for multiple sclerosis (187). pHERV-W env, Syncytin-1 and Syncytin-2 on one hand and the three myelin proteins that are principal targets of an autoimmune response in multiple sclerosis (MBP, PLP and MOG) showed sequence similarities between potential Th cell epitopes within pairs of viral and myelin peptides predicted to bind HLA DR2b (95). A set of the sequence homologous peptides from pHERV-W env, Syncytin-1, Syncytin-2, and MOG were shown to bind to HLA DR2b molecules in an *in-vitro* assay (102). These results were consistent with a molecular mimicry hypothesis (95, 102) that brings together the genetic (i.e. HLA) and viral (i.e. HERV-W) factors that influence susceptibility to MS (**Table 1**). Furthermore, it is speculated that EBV may provide the necessary immune activation and inflammatory stimuli that permits transcription of the pHERV-W env gene (95, 102), and also that the EBV protein EBNA-1 may provide the trans-splicing activity needed to synthesize the full-length pHERV-W env protein (102). It has also been postulated that HHV-6 may synergize with pHERV-W to initiate MS (174).

Syncytin-1, Syncytin-2, and MS

Syncytin-1 binds to the Na-dependent amino acid transporter-1 and -2 (ASCT1 and ASCT2) (188), which are also expressed in neurons and glia (189). It has been suggested that Syncytin-1 expression increases in monocytes during infections and MS relapses, two conditions reflecting inflammation (119). Syncytin-1 has been reported to be up-regulated in activated lymphocytes, monocytes, and effector NK cells, suggesting a role in the first steps of immune cell activation (119). However, these studies used a commercial antibody against an unknown peptide of unspecified length from the N-terminus of the Syncytin-1 protein, and it is possible that this antibody recognizes pHERV-W env instead of Syncytin-1 in the targeted tissues because of the 87% amino acid sequence identity between the two proteins. Therefore, further clarification is needed on whether these studies (119) detect and differentiate pHERV-W env and Syncytin-1.

However, the immunological role of potential MOG-cross-reactive Th cell epitopes potentially present in Syncytins-1 and -2 are an enigma that needs resolution. It is possible that these epitopes in these two 'natural', and therefore potentially tolerogenic, human proteins may have an immune regulatory role in preventing molecular mimicry-led immune damage. The 87% amino acid sequence identity between Syncytin-1 to pHERV-W env and the 38% amino acid sequence identity between Syncytin-2 and pHERV-W env by BLAST analysis make further study of Syncytin-1 and -2 important. Both Syncytins-1 and -2 functions have immunosuppressive functions (190). Syncytin 2 decreased Th1 cytokine production (191), and Syncytin-1 inhibited production of TNF-α, IFN-γ, and CXCL10 (192). However, such immunosuppressive functions have not been demonstrated for pHERV-W env, which instead shows inflammatory properties (183, 185, 192). The basis for the differences in immunological properties of three homologous proteins pHERV-W env, Syncytin-1 and Syncytin-2, however, remain to be fully elucidated. Differences in fusogenic functions are related to differences in amino acid sequences because only Syncytin-1 and Syncytin-2, and not pHERV-W env, have sites for cleavage by the protease furin that is necessary for initiating membrane fusion of cytotrophoblasts to form syncytiotrophoblasts in the placenta (190). The putative 16-amino acid immunosuppressive domain of Syncytin-1 differs from the corresponding sequence in pHERV-W env by a charge-altering glutamic acid to lysine change (102) that may eliminate immunosuppression. Differential binding of monoclonal antibodies to Syncytin-1 and pHERV-W env demonstrate antigenic differences and there also differences in membrane localization and oligomerization properties of the two proteins (193). Furthermore, Syncytins 1&2 are mainly expressed in the developing placenta and are also present as components of placental exosomes formed in a tolerogenic environment, while pHERV-W env is known to be produced in an inflammatory environment in the CNS (183, 185). These differences between the two Syncytins and pHERV-W env may be pertinent to their varying roles in the etiology of MS, and require further investigation.

pHERV-W and MS

As virus particles displaying reverse transcriptase activity, pHERV-W has been particularly implicated in MS (194–196).

It has been shown that the expression of the pHERV-W env gene product is significantly elevated in brain lesions in MS plaques and associated with the extent of active demyelination and inflammation (171, 172, 174, 175). pHERV-W can induce T-cell responses and pro-inflammatory cytokines release (197, 198). Sequencing pHERV-W in MS prompted the initial link between the HERV-W family and MS (199). pHERV-W mediates T-cells to cause neuropathology *in-vivo* (200). The HERV-W gene at Xq22.3 has been suggested as the potential cause for the higher prevalence of MS in women. However, the reported role of pHERV-W load in peripheral blood mononuclear cells (PBMCs) as a biomarker for MS needs more investigation (201).

During efficacious therapy with IFN-β, a longitudinal evaluation of patients revealed that viremia fell rapidly below detection limits; notably however, one patient, after initial clinical and virological benefit, had pHERV-W rescue, preceding strong disease progression and therapy failure (202). It was suggested that the evaluation of plasma pHERV-W could be considered the first prognostic marker for the individual patient to monitor disease progression and therapy outcome (203). A study of patients with optic neuritis, a disease frequently prodromic to MS, makes this possibility stronger as patients had significantly higher pHERV-W positivity than control groups (203).

Approaches Targeting pHERVs MS

One approach focusing on the postulated role of pHERV-W in the etiology of MS has been to initiate clinical trials with temelimab, an IgG4 humanized monoclonal antibody against the proinflammatory pHERV-W env (184, 204). Additional first attempts have been made in a clinical study with the HIV integrase strand inhibitor, raltegravir, which did not impact on disease activity but found interesting correlations between HERV-W markers, EBV shedding and new MRI lesions, independent from treatment effects (205). Other attempts are being made to induce tolerance and/or induce regulatory T-cells in MS, against specific encephalogenic peptide epitopes. Tolerogenic dendritic cells pulsed with peptides shown promise in preliminary clinical trials (206). Novel approaches have shown promise in mouse models of EAE for inducing regulatory CD8+ T cells (207) and regulatory CD4+T cells (208).

THE INFLAMMATORY CASCADE IN MS PATHOGENESIS

Our understanding of the underlying immunopathology of MS is still incomplete. We propose that EBV, pHERVs and HHV-6A are part of an inflammatory cascade with mimicry-driven autoimmunity contributing to the pathogenesis of MS in genetically susceptible individuals (**Figure 1**). Based on the strong epidemiological link between EBV and MS our hypothesis predicts a leading pathogenic role for EBV and its products (**Figure 2**) in triggering CNS-localized inflammatory lesions characteristic of MS. This is paralleled by endogenous virus reactivation and interaction between the 3 viruses within and beyond the CNS-proximal immune system and points to testable pathogenic parameters and targeted treatment options.

In summary: EBV-infected B-cells in Latency-I programme circulate in blood and home to head and neck lymphoid tissues near the CNS, especially to meninges or brain lymphatics linked to Ring of Waldeyer lymphoid system, including tonsils (209–211). The EBV genome gets activated during passage through these lymphoid structures to replicate and produce new Lat-II/III B-cells (proliferative blast stage) that switch to the resting stage again (Lat-I/-0) when leaving lymphoid structures and re-entering the circulation (25). However, defined epigenetic triggers including hormonal stress factors, other infections (bacterial or viral) and related products or induced inflammatory cytokines may lead to EBV lytic reactivation and/or uncontrolled proliferation of EBV-infected B-cells and release of EBV products like EBNA-1-DNA complexes and EBER-exosomes, thus inducing or enhancing local inflammation and antigenic cross-presentation (**Figure 2**). EBV-infected B-cells are normally successfully eliminated by EBV-specific T-cells, however, overstimulation and uncontrolled proliferation may induce a state of T-cell exhaustion as seen in infectious mononucleosis, X-linked lymphoproliferative syndrome and HIV infection, allowing EBV-positive B-cells to escape T-cell surveillance (8, 56, 57, 62). Overactive EBV-Lat-III B-cells may then trigger further local inflammation and activation of endogenous pHERV-W/-K and HHV-6A in regional virus- or cytokine-activated cell types (lymphocytes, microglia, astrocytes and oligodendrocytes (**Figure 1**). This localized inflammation impacts on the integrity of the blood-brain barrier and facilitates translocation of (EBV-infected) B-cells, inflammatory cytokines, exosomes as well as anti-EBV antibodies (esp. anti-EBNA1), immune complexes and EBV-specific immune cells.

This basically EBV-driven process may lead to the activation of CNS-resident myeloid cells (microglia, astrocytes) into an M1-state (2, 9) and triggering pHERVs and HHV-6 together driving auto-reactive immune responses and damage to CNS-resident microglia and ODCs leading to neuronal damage by targeting and other neural self-antigens *via* molecular mimicry (**Table 1**). By eliminating EBV from the equation (i.e. by HSCT, anti-B-cell or anti-EBV T-cell therapy), and by inhibiting specific receptor-driven signaling (BTK, MAPK-ERK, JAK/STAT) or inducing the natural silencers of these signaling pathways (DUSP6), the multi-component inflammatory cascade underlying MS may be halted (2, 9, 210), overall reducing glia cells and astrocyte activation and inducing myelin damage repair to ultimately restore neural functions.

CONCLUDING REMARKS

Although gaps remain in our detailed understanding of the etiology of MS, the role of physiological, hormonal or

cytokine-induced stress conditions triggering reactivation of persistent viral infections and driving aberrant innate and adaptive antiviral immune responses in MS deserves further attention. There is increasing evidence that an inability to adequately control reactivating infection with EBV, pHERV-W and HHV-6 in or near the CNS contributes to the immunopathology in MS, with MHC-II and antigenic mimicry enhancing the autoimmune component of MS pathogenesis. Additional investigations will help understand the conundrum of environmental triggers, reactivating viruses and genetic susceptibility factors in MS.

AUTHOR CONTRIBUTIONS

Draft and revision of the manuscript for content: RC, U-CM, JM, RR, and AK. Figure: JM; Table: RR, U-CM, and JM. All authors contributed to the article and approved the submitted version.

ACKNOWLEDGMENTS

The authors wish to thank dr. George ten Bosch for helpful discussions and Nuria Vakil for drafting **Figure 1**.

REFERENCES

1. Reich DS, Lucchinetti CF, Calabresi PA. Multiple Sclerosis. *N Engl J Med* (2018) 378(2):169–80. doi: 10.1056/NEJMra1401483
2. Absinta M, Maric D, Gharagozloo M, Garton T, Smith MD, Jin J, et al. A Lymphocyte–Microglia–Astrocyte Axis in Chronic Active Multiple Sclerosis. *Nature* (2021) 597(7878):709–14. doi: 10.1038/s41586-021-03892-7
3. Thompson AJ, Banwell BL, Barkhof F, Carroll WM, Coetzee T, Comi G, et al. Diagnosis of Multiple Sclerosis: 2017 Revisions of the McDonald Criteria. *Lancet Neurol* (2018) 17(2):162–73. doi: 10.1016/s1474-4422(17)30470-2
4. Filippi M, Preziosa P, Banwell BL, Barkhof F, Ciccarelli O, De Stefano N, et al. Assessment of Lesions on Magnetic Resonance Imaging in Multiple Sclerosis: Practical Guidelines. *Brain* (2019) 142(7):1858–75. doi: 10.1093/brain/awz144
5. Chen BY, Ghezzi C, Villegas B, Quon A, Radu CG, Witte ON, et al. (18)F-FAC PET Visualizes Brain-Infiltrating Leukocytes in a Mouse Model of Multiple Sclerosis. *J Nucl Med* (2020) 61(5):757–63. doi: 10.2967/jnumed.119.229351
6. Belbasis L, Bellou V, Evangelou E, Ioannidis JP, Tzoulaki I. Environmental Risk Factors and Multiple Sclerosis: An Umbrella Review of Systematic Reviews and Meta-Analyses. *Lancet Neurol* (2015) 14(3):263–73. doi: 10.1016/s1474-4422(14)70267-4
7. Ramagopalan SV, Dobson R, Meier UC, Giovannoni G. Multiple Sclerosis: Risk Factors, Prodromes, and Potential Causal Pathways. *Lancet Neurol* (2010) 9(7):727–39. doi: 10.1016/S1474-4422(10)70094-6
8. Bar-Or A, Pender MP, Khanna R, Steinman L, Hartung HP, Maniar T, et al. Epstein-Barr Virus in Multiple Sclerosis: Theory and Emerging Immunotherapies. *Trends Mol Med* (2020) 26(3):296–310. doi: 10.1016/j.molmed.2019.11.003
9. Ten Bosch GJ, Bolk J, Hart B, Laman JD. Multiple Sclerosis Is Linked to MAPK ERK Overactivity in Microglia. *J Mol Med (Berlin)* (2021) 99(8):1033–42. doi: 10.1007/s00109-021-02080-4
10. Tarlinton RE, Martynova E, Rizvanov AA. Role of Viruses in the Pathogenesis of Multiple Sclerosis. *Viruses* (2020) 12(6):643. doi: 10.3390/v12060643
11. Guan Y, Jakimovski D, Ramanathan M, Weinstock-Guttman B, Zivadinov R. The Role of Epstein-Barr Virus in Multiple Sclerosis: From Molecular Pathophysiology to *In Vivo* Imaging. *Neural Regener Res* (2019) 14(3):373–86. doi: 10.4103/1673-5374.245462
12. Balfour HHJr., Odumade OA, Schmeling DO, Mullan BD, Ed JA, Knight JA, et al. Behavioral, Virologic, and Immunologic Factors Associated With Acquisition and Severity of Primary Epstein-Barr Virus Infection in University Students. *J Infect Dis* (2013) 207(1):80–8. doi: 10.1093/infdis/jis646
13. Hadinoto V, Shapiro M, Sun CC, Thorley-Lawson DA. The Dynamics of EBV Shedding Implicate a Central Role for Epithelial Cells in Amplifying Viral Output. *PLoS Pathog* (2009) 5(7):e1000496. doi: 10.1371/journal.ppat.1000496
14. Price AM, Luftig MA. Dynamic Epstein-Barr Virus Gene Expression on the Path to B-Cell Transformation. *Adv Virus Res* (2014) 88:279–313. doi: 10.1016/b978-0-12-800098-4.00006-4
15. Laichalk LL, Hochberg D, Babcock GJ, Freeman RB, Thorley-Lawson DA. The Dispersal of Mucosal Memory B Cells: Evidence From Persistent EBV Infection. *Immunity* (2002) 16(5):745–54. doi: 10.1016/s1074-7613(02)00318-7
16. Maghzi A-H, Marta M, Bosca I, Savoj M-R, Etemadifar M, Giovannoni G, et al. Epstein–Barr Virus and Multiple Sclerosis. *Neuroinflamm: Elsevier* (2011) 25–37. doi: 10.1016/b978-0-12-384913-7.00002-2
17. Thorley-Lawson DA. Epstein-Barr Virus: Exploiting the Immune System. *Nat Rev Immunol* (2001) 1(1):75–82. doi: 10.1038/35095584
18. Shannon-Lowe C, Rickinson A. The Global Landscape of EBV-Associated Tumors. *Front Oncol* (2019) 9:713. doi: 10.3389/fonc.2019.00713
19. Häusler M, Ramaekers VT, Doenges M, Schweizer K, Ritter K, Schaade L. Neurological Complications of Acute and Persistent Epstein-Barr Virus Infection in Paediatric Patients. *J Med Virol* (2002) 68(2):253–63. doi: 10.1002/jmv.10201
20. Okuno Y, Murata T, Sato Y. Defective Epstein-Barr Virus in Chronic Active Infection and Haematological Malignancy. *Nat Microbiol* (2019) 4(3):404–13. doi: 10.1038/s41564-018-0334-0
21. Tempera I, Lieberman PM. Epigenetic Regulation of EBV Persistence and Oncogenesis. *Semin Cancer Biol* (2014) 26:22–9. doi: 10.1016/j.semcancer.2014.01.003
22. Middeldorp JM, Brink AA, van den Brule AJ, Meijer CJ. Pathogenic Roles for Epstein-Barr Virus (EBV) Gene Products in EBV-Associated Proliferative Disorders. *Crit Rev Oncol Hematol* (2003) 45(1):1–36. doi: 10.1016/s1040-8428(02)00078-1
23. Skalsky RL, Cullen BR. EBV Noncoding RNAs. *Curr Top Microbiol Immunol* (2015) 391:181–217. doi: 10.1007/978-3-319-22834-1_6
24. Hislop AD, Taylor GS, Sauce D, Rickinson AB. Cellular Responses to Viral Infection in Humans: Lessons From Epstein-Barr Virus. *Annu Rev Immunol* (2007) 25:587–617. doi: 10.1146/annurev.immunol.25.022106.141553
25. Thorley-Lawson DA. EBV Persistence–Introducing the Virus. *Curr Top Microbiol Immunol* (2015) 390(Pt 1):151–209. doi: 10.1007/978-3-319-22822-8_8
26. Hochberg D, Middeldorp JM, Catalina M, Sullivan JL, Luzuriaga K, Thorley-Lawson DA. Demonstration of the Burkitt's Lymphoma Epstein-Barr Virus Phenotype in Dividing Latently Infected Memory Cells *In Vivo*. *Proc Natl Acad Sci U S A* (2004) 101(1):239–44. doi: 10.1073/pnas.2237267100
27. Murata T. Encyclopedia of EBV-Encoded Lytic Genes: An Update. *Adv Exp Med Biol* (2018) 1045:395–412. doi: 10.1007/978-981-10-7230-7_18
28. Iwakiri D. Epstein-Barr Virus-Encoded RNAs: Key Molecules in Viral Pathogenesis. *Cancers (Basel)* (2014) 6(3):1615–30. doi: 10.3390/cancers6031615
29. Qiu J, Cosmopoulos K, Pegtel M, Hopmans E, Murray P, Middeldorp J, et al. A Novel Persistence Associated EBV miRNA Expression Profile is Disrupted in Neoplasia. *PLoS Pathog* (2011) 7(8):e1002193. doi: 10.1371/journal.ppat.1002193
30. Iizasa H, Kim H, Kartika AV, Kanehiro Y, Yoshiyama H. Role of Viral and Host microRNAs in Immune Regulation of Epstein-Barr Virus-Associated Diseases. *Front Immunol* (2020) 11:367. doi: 10.3389/fimmu.2020.00367
31. Baglio SR, van Eijndhoven MA, Koppers-Lalic D, Berenguer J, Lougheed SM, Gibbs S, et al. Sensing of Latent EBV Infection Through Exosomal Transfer of 5'pppRNA. *Proc Natl Acad Sci U S A* (2016) 113(5):E587–96. doi: 10.1073/pnas.1518130113

32. Dobson R, Kuhle J, Middeldorp J, Giovannoni G. Epstein-Barr-Negative MS: A True Phenomenon? *Neurol Neuroimmunol Neuroinflamm* (2017) 4(2): e318. doi: 10.1212/nxi.0000000000000318
33. Abrahamyan S, Eberspächer B, Hoshi MM, Aly L, Luessi F, Groppa S, et al. Complete Epstein-Barr Virus Seropositivity in a Large Cohort of Patients With Early Multiple Sclerosis. *J Neurol Neurosurg Psychiatry* (2020) 91 (7):681–6. doi: 10.1136/jnnp-2020-322941
34. Jafari N, van Nierop GP, Verjans GM, Osterhaus AD, Middeldorp JM, Hintzen RQ. No Evidence for Intrathecal IgG Synthesis to Epstein Barr Virus Nuclear Antigen-1 in Multiple Sclerosis. *J Clin Virol* (2010) 49(1):26–31. doi: 10.1016/j.jcv.2010.06.007
35. Handel AE, Williamson AJ, Disanto G, Handunnetthi L, Giovannoni G, Ramagopalan SV. An Updated Meta-Analysis of Risk of Multiple Sclerosis Following Infectious Mononucleosis. *PLoS One* (2010) 5(9):e12496. doi: 10.1371/journal.pone.0012496
36. Thacker EL, Mirzaei F, Ascherio A. Infectious Mononucleosis and Risk for Multiple Sclerosis: A Meta-Analysis. *Ann Neurol* (2006) 59(3):499–503. doi: 10.1002/ana.20820
37. Disanto G, Hall C, Lucas R, Ponsonby AL, Berlanga-Taylor AJ, Giovannoni G, et al. Assessing Interactions Between HLA-DRB1*15 and Infectious Mononucleosis on the Risk of Multiple Sclerosis. *Mult Scler* (2013) 19 (10):1355–8. doi: 10.1177/1352458513477231
38. Munger KL, Levin LI, O'Reilly EJ, Falk KI, Ascherio A. Anti-Epstein-Barr Virus Antibodies as Serological Markers of Multiple Sclerosis: A Prospective Study Among United States Military Personnel. *Mult Scler* (2011) 17 (10):1185–93. doi: 10.1177/1352458511408991
39. Farrell RA, Antony D, Wall GR, Clark DA, Fisniku L, Swanton J, et al. Humoral Immune Response to EBV in Multiple Sclerosis Is Associated With Disease Activity on MRI. *Neurology* (2009) 73(1):32–8. doi: 10.1212/WNL.0b013e3181aa29fe
40. Lunemann JD, Tintore M, Messmer B, Strowig T, Rovira A, Perkal H, et al. Elevated Epstein-Barr Virus-Encoded Nuclear Antigen-1 Immune Responses Predict Conversion to Multiple Sclerosis. *Ann Neurol* (2010) 67 (2):159–69. doi: 10.1002/ana.21886
41. Ascherio A, Munger KL. Environmental Risk Factors for Multiple Sclerosis. Part I: The Role of Infection. *Ann Neurol* (2007) 61(4):288–99. doi: 10.1002/ana.21117
42. Sisay S, Lopez-Lozano L, Mickunas M, Quiroga-Fernandez A, Palace J, Warnes G, et al. Untreated Relapsing Remitting Multiple Sclerosis Patients Show Antibody Production Against Latent Epstein Barr Virus (EBV) Antigens Mainly in the Periphery and Innate Immune IL-8 Responses Preferentially in the CNS. *J Neuroimmunol* (2017) 306:40–5. doi: 10.1016/j.jneuroim.2017.02.017
43. Chen MR, Middeldorp JM, Hayward SD. Separation of the Complex DNA Binding Domain of EBNA-1 Into DNA Recognition and Dimerization Subdomains of Novel Structure. *J Virol* (1993) 67(8):4875–85. doi: 10.1128/jvi.67.8.4875-4885.1993
44. Middeldorp JM. Epstein-Barr Virus-Specific Humoral Immune Responses in Health and Disease. *Curr Top Microbiol Immunol* (2015) 391:289–323. doi: 10.1007/978-3-319-22834-1_10
45. Wang Z, Kennedy PG, Dupree C, Wang M, Lee C, Pointon T, et al. Antibodies From Multiple Sclerosis Brain Identified Epstein-Barr Virus Nuclear Antigen 1 & 2 Epitopes Which Are Recognized by Oligoclonal Bands. *J Neuroimmune Pharmacol* (2021) 16(3):567–80. doi: 10.1007/s11481-020-09948-1
46. Hecker M, Fitzner B, Wendt M, Lorenz P, Flechtner K, Steinbeck F, et al. High-Density Peptide Microarray Analysis of IgG Autoantibody Reactivities in Serum and Cerebrospinal Fluid of Multiple Sclerosis Patients. *Mol Cell Proteomics* (2016) 15(4):1360–80. doi: 10.1074/mcp.M115.051664
47. Capone G, Calabrò M, Lucchese G, Fasano C, Girardi B, Polimeno L, et al. Peptide Matching Between Epstein-Barr Virus and Human Proteins. *Pathog Dis* (2013) 69(3):205–12. doi: 10.1111/2049-632x.12066
48. Leen A, Meij P, Redchenko I, Middeldorp J, Bloemena E, Rickinson A, et al. Differential Immunogenicity of Epstein-Barr Virus Latent-Cycle Proteins for Human CD4(+) T-Helper 1 Responses. *J Virol* (2001) 75(18):8649–59. doi: 10.1128/jvi.75.18.8649-8659.2001
49. Meij P, Leen A, Rickinson AB, Verkoeijen S, Vervoort MB, Bloemena E, et al. Identification and Prevalence of CD8(+) T-Cell Responses Directed Against Epstein-Barr Virus-Encoded Latent Membrane Protein 1 and Latent Membrane Protein 2. *Int J Cancer* (2002) 99(1):93–9. doi: 10.1002/ijc.10309
50. Godbout JP, Glaser R. Stress-Induced Immune Dysregulation: Implications for Wound Healing, Infectious Disease and Cancer. *J Neuroimmune Pharmacol* (2006) 1(4):421–7. doi: 10.1007/s11481-006-9036-0
51. Miller AH, Raison CL. The Role of Inflammation in Depression: From Evolutionary Imperative to Modern Treatment Target. *Nat Rev Immunol* (2016) 16(1):22–34. doi: 10.1038/nri.2015.5
52. Casiraghi C, Dorovini-Zis K, Horwitz MS. Epstein-Barr Virus Infection of Human Brain Microvessel Endothelial Cells: A Novel Role in Multiple Sclerosis. *J Neuroimmunol* (2011) 230(1-2):173–7. doi: 10.1016/j.jneuroim.2010.08.003
53. Larochelle C, Wasser B, Jamann H, Löffel JT, Cui Q-L, Tastet O, et al. Pro-Inflammatory T Helper 17 Directly Harms Oligodendrocytes in Neuroinflammation. *Proc Natl Acad Sci* (2021) 118(34):e2025813118. doi: 10.1073/pnas.2025813118
54. Salloum N, Hussein HM, Jammaz R, Jiche S, Uthman IW, Abdelnoor AM, et al. Epstein-Barr Virus DNA Modulates Regulatory T-Cell Programming in Addition to Enhancing Interleukin-17A Production *via* Toll-Like Receptor 9. *PLoS One* (2018) 13(7):e0200546. doi: 10.1371/journal.pone.0200546
55. Damania B, Münz C. Immunodeficiencies That Predispose to Pathologies by Human Oncogenic γ-Herpesviruses. *FEMS Microbiol Rev* (2019) 43(2):181–92. doi: 10.1093/femsre/fuy044
56. Pender MP, Burrows SR. Epstein-Barr Virus and Multiple Sclerosis: Potential Opportunities for Immunotherapy. *Clin Transl Immunol* (2014) 3(10):e27. doi: 10.1038/cti.2014.25
57. Pender MP, Csurhes PA, Burrows JM, Burrows SR. Defective T-Cell Control of Epstein-Barr Virus Infection in Multiple Sclerosis. *Clin Transl Immunol* (2017) 6(1):e126. doi: 10.1038/cti.2016.87
58. Venken K, Hellings N, Liblau R, Stinissen P. Disturbed Regulatory T Cell Homeostasis in Multiple Sclerosis. *Trends Mol Med* (2010) 16(2):58–68. doi: 10.1016/j.molmed.2009.12.003
59. van Langelaar J, Rijvers L, Smolders J, van Luijn MM. B and T Cells Driving Multiple Sclerosis: Identity, Mechanisms and Potential Triggers. *Front Immunol* (2020) 11:760. doi: 10.3389/fimmu.2020.00760
60. Schafflick D, Xu CA. Integrated Single Cell Analysis of Blood and Cerebrospinal Fluid Leukocytes in Multiple Sclerosis. *Nat Commun* (2020) 11(1):247. doi: 10.1038/s41467-019-14118-w
61. Serafini B, Rosicarelli B, Veroni C, Mazzola GA, Aloisi F. Epstein-Barr Virus-Specific CD8 T Cells Selectively Infiltrate the Brain in Multiple Sclerosis and Interact Locally With Virus-Infected Cells: Clue for a Virus-Driven Immunopathological Mechanism. *J Virol* (2019) 93(24):e00980–19. doi: 10.1128/jvi.00980-19
62. Lossius A, Johansen JN, Vartdal F, Robins H, Jūratė Šaltytė B, Holmøy T, et al. High-Throughput Sequencing of TCR Repertoires in Multiple Sclerosis Reveals Intrathecal Enrichment of EBV-Reactive CD8+ T Cells. *Eur J Immunol* (2014) 44(11):3439–52. doi: 10.1002/eji.201444662
63. van Nierop GP, Mautner J, Mitterreiter JG, Hintzen RQ, Verjans GM. Intrathecal CD8 T-Cells of Multiple Sclerosis Patients Recognize Lytic Epstein-Barr Virus Proteins. *Mult Scler* (2016) 22(3):279–91. doi: 10.1177/1352458515588581
64. Fransen NL, Hsiao CC, van der Poel M, Engelenburg HJ, Verdaasdonk K, Vincenten MCJ, et al. Tissue-Resident Memory T Cells Invade the Brain Parenchyma in Multiple Sclerosis White Matter Lesions. *Brain* (2020) 143 (6):1714–30. doi: 10.1093/brain/awaa117
65. Jelcic I, Al Nimer F, Wang J, Lentsch V, Planas R, Jelcic I, et al. Memory B Cells Activate Brain-Homing, Autoreactive CD4(+) T Cells in Multiple Sclerosis. *Cell* (2018) 175(1):85–100.e23. doi: 10.1016/j.cell.2018.08.011
66. Pender MP. The Essential Role of Epstein-Barr Virus in the Pathogenesis of Multiple Sclerosis. *Neuroscientist* (2011) 17(4):351–67. doi: 10.1177/1073858410381531
67. Minagar A, Alexander JS. Blood-Brain Barrier Disruption in Multiple Sclerosis. *Mult Scler* (2003) 9(6):540–9. doi: 10.1191/1352458503ms965oa
68. Ortiz GG, Pacheco-Moisés FP, Macías-Islas M, Flores-Alvarado LJ, Mireles-Ramírez MA, González-Renovato ED, et al. Role of the Blood-Brain Barrier in Multiple Sclerosis. *Arch Med Res* (2014) 45(8):687–97. doi: 10.1016/j.arcmed.2014.11.013
69. Horng S, Therattil A, Moyon S, Gordon A, Kim K, Argaw AT, et al. Astrocytic Tight Junctions Control Inflammatory CNS Lesion Pathogenesis. *J Clin Invest* (2017) 127(8):3136–51. doi: 10.1172/jci91301
70. Ponath G, Park C, Pitt D. The Role of Astrocytes in Multiple Sclerosis. *Front Immunol* (2018) 9:217. doi: 10.3389/fimmu.2018.00217

71. Dong Y, Yong VW. When Encephalitogenic T Cells Collaborate With Microglia in Multiple Sclerosis. *Nat Rev Neurol* (2019) 15(12):704–17. doi: 10.1038/s41582-019-0253-6
72. Kunkl M, Frascolla S, Amormino C, Volpe E. Tuosto L. T Helper Cells: The Modulators of Inflammation in Multiple Sclerosis. *Cells* (2020) 9(2):482. doi: 10.3390/cells9020482
73. Jilek S, Schluep M, Meylan P, Vingerhoets F, Guignard L, Monney A, et al. Strong EBV-Specific CD8+ T-Cell Response in Patients With Early Multiple Sclerosis. *Brain* (2008) 131(Pt 7):1712–21. doi: 10.1093/brain/awn108
74. Angelini DF, Serafini B, Piras E, Severa M, Coccia EM, Rosicarelli B, et al. Increased CD8+ T Cell Response to Epstein-Barr Virus Lytic Antigens in the Active Phase of Multiple Sclerosis. *PLoS Pathog* (2013) 9(4):e1003220. doi: 10.1371/journal.ppat.1003220
75. Lünemann JD, Edwards N, Muraro PA, Hayashi S, Cohen JI, Münz C, et al. Increased Frequency and Broadened Specificity of Latent EBV Nuclear Antigen-1-Specific T Cells in Multiple Sclerosis. *Brain* (2006) 129(Pt 6):1493–506. doi: 10.1093/brain/awl067
76. Geginat J, Paroni M, Pagani M, Galimberti D, De Francesco R, Scarpini E, et al. The Enigmatic Role of Viruses in Multiple Sclerosis: Molecular Mimicry or Disturbed Immune Surveillance? *Trends Immunol* (2017) 38 (7):498–512. doi: 10.1016/j.it.2017.04.006
77. Soldan SS, Su C, Lamontagne RJ, Grams N, Lu F, Zhang Y, et al. Epigenetic Plasticity Enables CNS-Trafficking of EBV-Infected B Lymphocytes. *PLoS Pathog* (2021) 17(6):e1009618. doi: 10.1371/journal.ppat.1009618
78. Zomer A, Vendrig T, Hopmans ES, van Eijndhoven M, Middeldorp JM, Pegtel DM. Exosomes: Fit to Deliver Small RNA. *Commun Integr Biol* (2010) 3(5):447–50. doi: 10.4161/cib.3.5.12339
79. Pegtel DM, Peferoen L, Amor S. Extracellular Vesicles as Modulators of Cell-to-Cell Communication in the Healthy and Diseased Brain. *Philos Trans R Soc Lond B Biol Sci* (2014) 369(1652):20130516. doi: 10.1098/rstb.2013.0516
80. Lassmann H, Niedobitek G, Aloisi F, Middeldorp JM. Epstein-Barr Virus in the Multiple Sclerosis Brain: A Controversial Issue–Report on a Focused Workshop Held in the Centre for Brain Research of the Medical University of Vienna, Austria. *Brain* (2011) 134(Pt 9):2772–86. doi: 10.1093/brain/awr197
81. Morré SA, van Beek J, De Groot CJ, Killestein J, Meijer CJ, Polman CH, et al. Is Epstein-Barr Virus Present in the CNS of Patients With MS? *Neurology* (2001) 56(5):692. doi: 10.1212/wnl.56.5.692
82. Serafini B, Rosicarelli B, Franciotta D, Magliozzi R, Reynolds R, Cinque P, et al. Dysregulated Epstein-Barr Virus Infection in the Multiple Sclerosis Brain. *J Exp Med* (2007) 204(12):2899–912. doi: 10.1084/jem.20071030
83. Peferoen LA, Lamers F, Lodder LN, Gerritsen WH, Huitinga I, Melief J, et al. Epstein Barr Virus is Not a Characteristic Feature in the Central Nervous System in Established Multiple Sclerosis. *Brain* (2010) 133(Pt 5):e137. doi: 10.1093/brain/awp296
84. Willis SN, Stadelmann C, Rodig SJ, Caron T, Gattenloehner S, Mallozzi SS, et al. Epstein-Barr Virus Infection Is Not a Characteristic Feature of Multiple Sclerosis Brain. *Brain* (2009) 132(Pt 12):3318–28. doi: 10.1093/brain/awp200
85. Sargsyan SA, Shearer AJ, Ritchie AM, Burgoon MP, Anderson S, Hemmer B, et al. Absence of Epstein-Barr Virus in the Brain and CSF of Patients With Multiple Sclerosis. *Neurology* (2010) 74(14):1127–35. doi: 10.1212/WNL.0b013e3181d865a1
86. Tzartos JS, Khan G, Vossenkamper A, Cruz-Sadaba M, Lonardi S, Sefia E, et al. Association of Innate Immune Activation With Latent Epstein-Barr Virus in Active MS Lesions. *Neurology* (2012) 78(1):15–23. doi: 10.1212/WNL.0b013e31823ed057
87. Moreno MA, Or-Geva N, Aftab BT, Khanna R, Croze E, Steinman L, et al. Molecular Signature of Epstein-Barr Virus Infection in MS Brain Lesions. *Neurol Neuroimmunol Neuroinflamm* (2018) 5(4):e466. doi: 10.1212/nxi.0000000000000466
88. Hassani A, Corboy JR, Al-Salam S, Khan G. Epstein-Barr Virus is Present in the Brain of Most Cases of Multiple Sclerosis and may Engage More Than Just B Cells. *PLoS One* (2018) 13(2):e0192109. doi: 10.1371/journal.pone.0192109
89. Veroni C, Serafini B, Rosicarelli B, Fagnani C, Aloisi F. Transcriptional Profile and Epstein-Barr Virus Infection Status of Laser-Cut Immune Infiltrates From the Brain of Patients With Progressive Multiple Sclerosis. *J Neuroinflammation* (2018) 15(1):18. doi: 10.1186/s12974-017-1049-5
90. Vomhof-DeKrey EE, Yates J, Hägglöf T, Lanthier P, Amiel E, Veerapen N, et al. Cognate Interaction With iNKT Cells Expands IL-10-Producing B Regulatory Cells. *Proc Natl Acad Sci U S A* (2015) 112(40):12474–9. doi: 10.1073/pnas.1504790112
91. Rustenhoven J, Drieu A, Mamuladze T, de Lima KA, Dykstra T, Wall M, et al. Functional Characterization of the Dural Sinuses as a Neuroimmune Interface. *Cell* (2021) 184(4):1000–16.e27. doi: 10.1016/j.cell.2020.12.040
92. Stern JN, Yaari G, Vander Heiden JA, Church G, Donahue WF, Hintzen RQ, et al. B Cells Populating the Multiple Sclerosis Brain Mature in the Draining Cervical Lymph Nodes. *Sci Transl Med* (2014) 6(248):248ra107. doi: 10.1126/scitranslmed.3008879
93. Serafini B, Rosicarelli B, Aloisi F, Stigliano E. Epstein-Barr Virus in the Central Nervous System and Cervical Lymph Node of a Patient With Primary Progressive Multiple Sclerosis. *J Neuropathol Exp Neurol* (2014) 73(7):729–31. doi: 10.1097/nen.0000000000000082
94. Ebringer A. Ankylosing Spondylitis, Immune-Response-Genes and Molecular Mimicry. *Lancet* (1979) 1(8127):1186. doi: 10.1016/s0140-6736(79)91861-0
95. Ramasamy R, Joseph B, Whittall T. Potential Molecular Mimicry Between the Human Endogenous Retrovirus W Family Envelope Proteins and Myelin Proteins in Multiple Sclerosis. *Immunol Lett* (2017) 183:79–85. doi: 10.1016/j.imlet.2017.02.003
96. Kakalacheva K, Munz C, Lunemann JD. Viral Triggers of Multiple Sclerosis. *Biochim Biophys Acta* (2011) 1812(2):132–40. doi: 10.1016/j.bbadis.2010.06.012
97. Chastain EM, Miller SD. Molecular Mimicry as an Inducing Trigger for CNS Autoimmune Demyelinating Disease. *Immunol Rev* (2012) 245(1):227–38. doi: 10.1111/j.1600-065X.2011.01076.x
98. Wucherpfennig KW, Strominger JL. Molecular Mimicry in T Cell-Mediated Autoimmunity: Viral Peptides Activate Human T Cell Clones Specific for Myelin Basic Protein. *Cell* (1995) 80(5):695–705. doi: 10.1016/0092-8674(95)90348-8
99. Lang HL, Jacobsen H, Ikemizu S, Andersson C, Harlos K, Madsen L, et al. A Functional and Structural Basis for TCR Cross-Reactivity in Multiple Sclerosis. *Nat Immunol* (2002) 3(10):940–3. doi: 10.1038/ni835
100. Zdimerova H, Murer A, Engelmann C, Raykova A, Deng Y, Gujer C, et al. Attenuated Immune Control of Epstein–Barr Virus in Humanized Mice Is Associated With the Multiple Sclerosis Risk Factor HLA-Dr15. *Eur J Immunol* (2021) 51(1):64–75. doi: 10.1002/eji.202048655
101. Lünemann JD, Jelcić I, Roberts S, Lutterotti A, Tackenberg B, Martin R, et al. EBNA1-Specific T Cells From Patients With Multiple Sclerosis Cross React With Myelin Antigens and Co-Produce IFN-Gamma and IL-2. *J Exp Med* (2008) 205(8):1763–73. doi: 10.1084/jem.20072397
102. Ramasamy R, Mohammed F, Meier UC. HLA DR2b-Binding Peptides From Human Endogenous Retrovirus Envelope, Epstein-Barr Virus and Brain Proteins in the Context of Molecular Mimicry in Multiple Sclerosis. *Immunol Lett* (2020) 217:15–24. doi: 10.1016/j.imlet.2019.10.017
103. Jog NR, McClain MT, Heinlen LD, Gross T, Towner R, Guthridge JM, et al. Epstein Barr Virus Nuclear Antigen 1 (EBNA-1) Peptides Recognized by Adult Multiple Sclerosis Patient Sera Induce Neurologic Symptoms in a Murine Model. *J Autoimmun* (2020) 106:102332. doi: 10.1016/j.jaut.2019.102332
104. Tengvall K, Huang J, Hellstrom C, Kammer P, Bistrom M, Ayoglu B, et al. Molecular Mimicry Between Anoctamin 2 and Epstein-Barr Virus Nuclear Antigen 1 Associates With Multiple Sclerosis Risk. *Proc Natl Acad Sci U S A* (2019) 116(34):16955–60. doi: 10.1073/pnas.1902623116
105. van Sechel AC, Bajramovic JJ, van Stipdonk MJ, Persoon-Deen C, Geutskens SB, van Noort JM. EBV-Induced Expression and HLA-DR-Restricted Presentation by Human B Cells of Alpha B-Crystallin, a Candidate Autoantigen in Multiple Sclerosis. *J Immunol* (1999) 162(1):129–35.
106. van Noort JM, Bsibsi M, Gerritsen WH, van der Valk P, Bajramovic JJ, Steinman L, et al. Alphab-Crystallin Is a Target for Adaptive Immune Responses and a Trigger of Innate Responses in Preactive Multiple Sclerosis Lesions. *J Neuropathol Exp Neurol* (2010) 69(7):694–703. doi: 10.1097/NEN.0b013e3181e4939c
107. Lindsey JW, deGannes SL, Pate KA, Zhao X. Antibodies Specific for Epstein-Barr Virus Nuclear Antigen-1 Cross-React With Human Heterogeneous Nuclear Ribonucleoprotein L. *Mol Immunol* (2016) 69:7–12. doi: 10.1016/j.molimm.2015.11.007
108. Lindsey JW. Antibodies to the Epstein-Barr Virus Proteins BFRF3 and BRRF2 Cross-React With Human Proteins. *J Neuroimmunol* (2017) 310:131–4. doi: 10.1016/j.jneuroim.2017.07.013

109. Dooley MM, de Gannes SL, Fu KA, Lindsey JW. The Increased Antibody Response to Epstein-Barr Virus in Multiple Sclerosis Is Restricted to Selected Virus Proteins. *J Neuroimmunol* (2016) 299:147–51. doi: 10.1016/j.jneuroim.2016.08.016
110. Lomakin Y, Arapidi GP, Chernov A, Ziganshin R, Tcyganov E, Lyadova I, et al. Exposure to the Epstein-Barr Viral Antigen Latent Membrane Protein 1 Induces Myelin-Reactive Antibodies *In Vivo*. *Front Immunol* (2017) 8:777. doi: 10.3389/fimmu.2017.00777
111. Woulfe J, Gray MT, Ganesh MS, Middeldorp JM. Human Serum Antibodies Against EBV Latent Membrane Protein 1 Cross-React With α-Synuclein. *Neurol Neuroimmunol Neuroinflamm* (2016) 3(4):e239. doi: 10.1212/nxi.0000000000000239
112. Kanduc D, Shoenfeld Y. From Anti-EBV Immune Responses to the EBV Diseasome *via* Cross-Reactivity. *Glob Med Genet* (2020) 7(2):51–63. doi: 10.1055/s-0040-1715641
113. Tejada-Simon MV, Zang YC, Hong J, Rivera VM, Zhang JZ. Cross-Reactivity With Myelin Basic Protein and Human Herpesvirus-6 in Multiple Sclerosis. *Ann Neurol* (2003) 53(2):189–97. doi: 10.1002/ana.10425
114. Bajramović JJ, Plomp AC, Goes A, Koevoets C, Newcombe J, Cuzner ML, et al. Presentation of Alpha B-Crystallin to T Cells in Active Multiple Sclerosis Lesions: An Early Event Following Inflammatory Demyelination. *J Immunol* (2000) 164(8):4359–66. doi: 10.4049/jimmunol.164.8.4359
115. Sutkowski N, Conrad B, Thorley-Lawson DA, Huber BT. Epstein-Barr Virus Transactivates the Human Endogenous Retrovirus HERV-K18 That Encodes a Superantigen. *Immunity* (2001) 15(4):579–89. doi: 10.1016/s1074-7613(01)00210-2
116. Hsiao FC, Tai AK, Deglon A, Sutkowski N, Longnecker R, Huber BT. EBV LMP-2A Employs a Novel Mechanism to Transactivate the HERV-K18 Superantigen Through its ITAM. *Virology* (2009) 385(1):261–6. doi: 10.1016/j.virol.2008.11.025
117. Mameli G, Madeddu G, Mei A, Uleri E, Poddighe L, Delogu LG, et al. Activation of MSRV-Type Endogenous Retroviruses During Infectious Mononucleosis and Epstein-Barr Virus Latency: The Missing Link With Multiple Sclerosis? *PLoS One* (2013) 8(11):e78474. doi: 10.1371/journal.pone.0078474
118. Morandi E, Tarlinton RE, Gran B. Multiple Sclerosis Between Genetics and Infections: Human Endogenous Retroviruses in Monocytes and Macrophages. *Front Immunol* (2015) 6:647. doi: 10.3389/fimmu.2015.00647
119. Garcia-Montojo M, Rodriguez-Martin E, Ramos-Mozo P, Ortega-Madueño I, Dominguez-Mozo MI, Arias-Leal A, et al. Syncytin-1/HERV-W Envelope is an Early Activation Marker of Leukocytes and Is Upregulated in Multiple Sclerosis Patients. *Eur J Immunol* (2020) 50(5):685–94. doi: 10.1002/eji.201948423
120. Frey TR, Akinyemi IA, Burton EM, Bhaduri-McIntosh S, McIntosh MT. An Ancestral Retrovirus Envelope Protein Regulates Persistent Gammaherpesvirus Lifecycles. *Front Microbiol* (2021) 12:708404. doi: 10.3389/fmicb.2021.708404
121. Gruchot J, Kremer D, Küry P. Neural Cell Responses Upon Exposure to Human Endogenous Retroviruses. *Front Genet* (2019) 10:655. doi: 10.3389/fgene.2019.00655
122. Zhou Y, Liu L, Liu Y, Zhou P, Yan Q, Yu H, et al. Implication of Human Endogenous Retrovirus W Family Envelope in Hepatocellular Carcinoma Promotes MEK/ERK-Mediated Metastatic Invasiveness and Doxorubicin Resistance. *Cell Death Discov* (2021) 7(1):177. doi: 10.1038/s41420-021-00562-5
123. Tao C, Simpson S Jr, Taylor BV, van der Mei I. Association Between Human Herpesvirus & Human Endogenous Retrovirus and MS Onset & Progression. *J Neurol Sci* (2017) 372:239–49. doi: 10.1016/j.jns.2016.11.060
124. Gate D, Saligrama N, Leventhal O, Yang AC, Unger MS, Middeldorp J, et al. Clonally Expanded CD8 T Cells Patrol the Cerebrospinal Fluid in Alzheimer's Disease. *Nature* (2020) 577(7790):399–404. doi: 10.1038/s41586-019-1895-7
125. Alsema AM, Jiang Q, Kracht L, Gerrits E, Dubbelaar ML, Miedema A, et al. Profiling Microglia From Alzheimer's Disease Donors and Non-Demented Elderly in Acute Human Postmortem Cortical Tissue. *Front Mol Neurosci* (2020) 13:134. doi: 10.3389/fnmol.2020.00134
126. Bar-Or A, Li R. Cellular Immunology of Relapsing Multiple Sclerosis: Interactions, Checks, and Balances. *Lancet Neurol* (2021) 20(6):470–83. doi: 10.1016/s1474-4422(21)00063-6
127. Clark IC, Gutiérrez-Vázquez C, Wheeler MA, Li Z, Rothhammer V, Linnerbauer M, et al. Barcoded Viral Tracing of Single-Cell Interactions in Central Nervous System Inflammation. *Science* (2021) 372(6540):eabf1230. doi: 10.1126/science.abf1230
128. Alvarenga MOP, Frazão DR, de Matos IG, Bittencourt LO, Fagundes NCF, Rösing CK, et al. Is There Any Association Between Neurodegenerative Diseases and Periodontitis? A Systematic Review. *Front Aging Neurosci* (2021) 13:651437. doi: 10.3389/fnagi.2021.651437
129. Haase S, Wilck N, Haghikia A, Gold R, Mueller DN, Linker RA. The Role of the Gut Microbiota and Microbial Metabolites in Neuroinflammation. *Eur J Immunol* (2020) 50(12):1863–70. doi: 10.1002/eji.201847807
130. Koike R, Nodomi K, Watanabe N, Ogata Y, Takeichi O, Takei M, et al. Butyric Acid in Saliva of Chronic Periodontitis Patients Induces Transcription of the EBV Lytic Switch Activator BZLF1: A Pilot Study. *In Vivo* (2020) 34(2):587–94. doi: 10.21873/invivo.11811
131. Novalic Z, van Rossen T, Greijer A, Middeldorp J. Agents and Approaches for Lytic Induction Therapy of Epstein-Barr Virus Associated Malignancies. *Med Chem* (2016) 6:449–66. doi: 10.4172/2161-0444.1000384
132. Alvarez-Lafuente R, De Las Heras V, Bartolomé M, Picazo JJ, Arroyo R. Beta-Interferon Treatment Reduces Human Herpesvirus-6 Viral Load in Multiple Sclerosis Relapses But Not in Remission. *Eur Neurol* (2004) 52(2):87–91. doi: 10.1159/000079936
133. Petersen T, Møller-Larsen A, Ellermann-Eriksen S, Thiel S, Christensen T. Effects of Interferon-Beta Therapy on Elements in the Antiviral Immune Response Towards the Human Herpesviruses EBV, HSV, and VZV, and to the Human Endogenous Retroviruses HERV-H and HERV-W in Multiple Sclerosis. *J Neuroimmunol* (2012) 249(1-2):105–8. doi: 10.1016/j.jneuroim.2012.04.013
134. Meier UC, Giovannoni G, Tzartos JS, Khan G. Translational Mini-Review Series on B Cell Subsets in Disease. B Cells in Multiple Sclerosis: Drivers of Disease Pathogenesis and Trojan Horse for Epstein-Barr Virus Entry to the Central Nervous System? *Clin Exp Immunol* (2012) 167(1):1–6. doi: 10.1111/j.1365-2249.2011.04446.x
135. Mulero P, Midaglia L, Montalban X. Ocrelizumab: A New Milestone in Multiple Sclerosis Therapy. *Ther Adv Neurol Disord* (2018) 11:1756286418773025. doi: 10.1177/1756286418773025
136. Gratama JW, Oosterveer MA, Zwaan FE, Lepoutre J, Klein G, Ernberg I. Eradication of Epstein-Barr Virus by Allogeneic Bone Marrow Transplantation: Implications for Sites of Viral Latency. *Proc Natl Acad Sci U S A* (1988) 85(22):8693–6. doi: 10.1073/pnas.85.22.8693
137. Miller AE, Chitnis T, Cohen BA, Costello K, Sicotte NL, Stacom R. Autologous Hematopoietic Stem Cell Transplant in Multiple Sclerosis: Recommendations of the National Multiple Sclerosis Society. *JAMA Neurol* (2021) 78(2):241–6. doi: 10.1001/jamaneurol.2020.4025
138. Drosu NC, Edelman ER. Tenofovir Prodrugs Potently Inhibit Epstein-Barr Virus Lytic DNA Replication by Targeting the Viral DNA Polymerase. *Proc Natl Acad Sci U S A* (2020) 117(22):12368–74. doi: 10.1073/pnas.2002392117
139. Maruszak H, Brew BJ, Giovannoni G, Gold J. Could Antiretroviral Drugs be Effective in Multiple Sclerosis? A Case Report. *Eur J Neurol* (2011) 18(9):e110–1. doi: 10.1111/j.1468-1331.2011.03430.x
140. Pender MP, Csurhes PA, Smith C, Douglas NL, Neller MA, Matthews KK, et al. Epstein-Barr Virus-Specific T Cell Therapy for Progressive Multiple Sclerosis. *JCI Insight* (2018) 3(22):e124714. doi: 10.1172/jci.insight.124714
141. Ioannides ZA, Csurhes PA, Douglas NL, Mackenroth G, Swayne A, Thompson KM, et al. Sustained Clinical Improvement in a Subset of Patients With Progressive Multiple Sclerosis Treated With Epstein-Barr Virus-Specific T Cell Therapy. *Front Neurol* (2021) 12:652811. doi: 10.3389/fneur.2021.652811
142. Marron TU, Martinez-Gallo M, Yu JE, Cunningham-Rundles C. Toll-Like Receptor 4-, 7-, and 8-Activated Myeloid Cells From Patients With X-Linked Agammaglobulinemia Produce Enhanced Inflammatory Cytokines. *J Allergy Clin Immunol* (2012) 129(1):184–90.e1-4. doi: 10.1016/j.jaci.2011.10.009
143. Menzfeld C, John M, van Rossum D, Regen T, Scheffel J, Janova H, et al. Tyrphostin AG126 Exerts Neuroprotection in CNS Inflammation by a Dual Mechanism. *Glia* (2015) 63(6):1083–99. doi: 10.1002/glia.22803
144. Incrocci R, Barse L, Stone A, Vagvala S, Montesano M, Subramaniam V, et al. Epstein-Barr Virus Latent Membrane Protein 2a (LMP2A) Enhances IL-10 Production Through the Activation of Bruton's Tyrosine Kinase and STAT3. *Virology* (2017) 500:96–102. doi: 10.1016/j.virol.2016.10.015
145. Montalban X, Arnold DL, Weber MS, Staikov I, Piasecka-Stryczynska K, Willmer J, et al. Placebo-Controlled Trial of an Oral BTK Inhibitor in Multiple Sclerosis. *N Engl J Med* (2019) 380(25):2406–17. doi: 10.1056/NEJMoa1901981

146. Reich DS, Arnold DL, Vermersch P, Bar-Or A, Fox RJ, Matta A, et al. Safety and Efficacy of Tolebrutinib, an Oral Brain-Penetrant BTK Inhibitor, in Relapsing Multiple Sclerosis: A Phase 2b, Randomised, Double-Blind, Placebo-Controlled Trial. *Lancet Neurol* (2021) 20(9):729–38. doi: 10.1016/s1474-4422(21)00237-4
147. Bame E, Tang H, Burns JC, Arefayene M, Michelsen K, Ma B, et al. Next-Generation Bruton's Tyrosine Kinase Inhibitor BIIB091 Selectively and Potently Inhibits B Cell and Fc Receptor Signaling and Downstream Functions in B Cells and Myeloid Cells. *Clin Trans Immunol* (2021) 10(6): e1295. doi: 10.1002/cti2.1295
148. Rajendran R, Böttiger G, Dentzien N, Rajendran V, Sharifi B, Ergün S, et al. Effects of FGFR Tyrosine Kinase Inhibition in OLN-93 Oligodendrocytes. *Cells* (2021) 10(6):1318. doi: 10.3390/cells10061318
149. Suo N, Guo YE, He B, Gu H, Xie X. Inhibition of MAPK/ERK Pathway Promotes Oligodendrocytes Generation and Recovery of Demyelinating Diseases. *Glia* (2019) 67(7):1320–32. doi: 10.1002/glia.23606
150. Zhang Y, Li X, Ciric B, Curtis MT, Chen WJ, Rostami A, et al. A Dual Effect of Ursolic Acid to the Treatment of Multiple Sclerosis Through Both Immunomodulation and Direct Remyelination. *Proc Natl Acad Sci U S A* (2020) 117(16):9082–93. doi: 10.1073/pnas.2000208117
151. Soldan SS, Anderson EM, Frase DM, Zhang Y, Caruso LB, Wang Y, et al. EBNA1 Inhibitors Have Potent and Selective Antitumor Activity in Xenograft Models of Epstein-Barr Virus-Associated. *Gastric Cancer* (2021) 24(5):1076–88. doi: 10.1007/s10120-021-01193-6
152. Jiang L, Lung HL, Huang T, Lan R, Zha S, Chan LS, et al. Reactivation of Epstein–Barr Virus by a Dual-Responsive Fluorescent EBNA1-Targeting Agent With Zn2+-Chelating Function. *Proc Natl Acad Sci* (2019) 116 (52):26614–24. doi: 10.1073/pnas.1915372116
153. Höllsberg P, Kusk M, Bech E, Hansen HJ, Jakobsen J, Haahr S. Presence of Epstein-Barr Virus and Human Herpesvirus 6B DNA in Multiple Sclerosis Patients: Associations With Disease Activity. *Acta Neurol Scand* (2005) 112 (6):395–402. doi: 10.1111/j.1600-0404.2005.00516.x
154. Soldan SS, Leist TP, Juhng KN, McFarland HF, Jacobson S. Increased Lymphoproliferative Response to Human Herpesvirus Type 6A Variant in Multiple Sclerosis Patients. *Ann Neurol* (2000) 47(3):306–13. doi: 10.1002/1531-8249(200003)47:3<306::aid-ana5>3.0.co;2-a
155. Ortega-Madueño I, Garcia-Montojo M, Dominguez-Mozo MI, Garcia-Martinez A, Arias-Leal AM, Casanova I, et al. Anti-Human Herpesvirus 6A/B IgG Correlates With Relapses and Progression in Multiple Sclerosis. *PLoS One* (2014) 9(8):e104836. doi: 10.1371/journal.pone.0104836
156. Hall CB, Long CE, Schnabel KC, Caserta MT, McIntyre KM, Costanzo MA, et al. Human Herpesvirus-6 Infection in Children. A Prospective Study of Complications and Reactivation. *N Engl J Med* (1994) 331(7):432–8. doi: 10.1056/nejm199408183310703
157. Caserta MT, Hall CB, Schnabel K, McIntyre K, Long C, Costanzo M, et al. Neuroinvasion and Persistence of Human Herpesvirus 6 in Children. *J Infect Dis* (1994) 170(6):1586–9. doi: 10.1093/infdis/170.6.1586
158. Knox KK, Carrigan DR. Active Human Herpesvirus (HHV-6) Infection of the Central Nervous System in Patients With AIDS. *J Acquir Immune Defic Syndr Hum Retrovirol* (1995) 9(1):69–73.
159. Zhang E, Bell AJ, Wilkie GS, Suárez NM, Batini C, Veal CD, et al. Inherited Chromosomally Integrated Human Herpesvirus 6 Genomes Are Ancient, Intact, and Potentially Able To Reactivate From Telomeres. *J Virol* (2017) 91 (22):e01137-17. doi: 10.1128/jvi.01137-17
160. Leibovitch EC, Jacobson S. Evidence Linking HHV-6 With Multiple Sclerosis: An Update. *Curr Opin Virol* (2014) 9:127–33. doi: 10.1016/j.coviro.2014.09.016
161. Kawano M, Seya T, Koni I, Mabuchi H. Elevated Serum Levels of Soluble Membrane Cofactor Protein (CD46, MCP) in Patients With Systemic Lupus Erythematosus (SLE). *Clin Exp Immunol* (1999) 116(3):542–6. doi: 10.1046/j.1365-2249.1999.00917.x
162. Reynaud JM, Jégou JF, Welsch JC, Horvat B. Human Herpesvirus 6A Infection in CD46 Transgenic Mice: Viral Persistence in the Brain and Increased Production of Proinflammatory Chemokines *via* Toll-Like Receptor 9. *J Virol* (2014) 88(10):5421–36. doi: 10.1128/jvi.03763-13
163. Leibovitch E, Wohler JE, Cummings Macri SM, Motanic K, Harberts E, Gaitán MI, et al. Novel Marmoset (Callithrix Jacchus) Model of Human Herpesvirus 6A and 6B Infections: Immunologic, Virologic and Radiologic Characterization. *PLoS Pathog* (2013) 9(1):e1003138. doi: 10.1371/journal.ppat.1003138
164. Harberts E, Yao K, Wohler JE, Maric D, Ohayon J, Henkin R, et al. Human Herpesvirus-6 Entry Into the Central Nervous System Through the Olfactory Pathway. *Proc Natl Acad Sci U S A* (2011) 108(33):13734–9. doi: 10.1073/pnas.1105143108
165. Challoner PB, Smith KT, Parker JD, MacLeod DL, Coulter SN, Rose TM, et al. Plaque-Associated Expression of Human Herpesvirus 6 in Multiple Sclerosis. *Proc Natl Acad Sci U S A* (1995) 92(16):7440–4. doi: 10.1073/pnas.92.16.7440
166. Goodman AD, Mock DJ, Powers JM, Baker JV, Blumberg BM. Human Herpesvirus 6 Genome and Antigen in Acute Multiple Sclerosis Lesions. *J Infect Dis* (2003) 187(9):1365–76. doi: 10.1086/368172
167. Chapenko S, Millers A, Nora Z, Logina I, Kukaine R, Murovska M. Correlation Between HHV-6 Reactivation and Multiple Sclerosis Disease Activity. *J Med Virol* (2003) 69(1):111–7. doi: 10.1002/jmv.10258
168. Soldan SS, Berti R, Salem N, Secchiero P, Flamand L, Calabresi PA, et al. Association of Human Herpes Virus 6 (HHV-6) With Multiple Sclerosis: Increased IgM Response to HHV-6 Early Antigen and Detection of Serum HHV-6 DNA. *Nat Med* (1997) 3(12):1394–7. doi: 10.1038/nm1297-1394
169. Tai AK, Luka J, Ablashi D, Huber BT. HHV-6A Infection Induces Expression of HERV-K18-Encoded Superantigen. *J Clin Virol* (2009) 46 (1):47–8. doi: 10.1016/j.jcv.2009.05.019
170. Flamand L, Stefanescu I, Ablashi DV, Menezes J. Activation of the Epstein-Barr Virus Replicative Cycle by Human Herpesvirus 6. *J Virol* (1993) 67 (11):6768–77. doi: 10.1128/jvi.67.11.6768-6777.1993
171. Flamand L, Menezes J. Cyclic AMP-Responsive Element-Dependent Activation of Epstein-Barr Virus Zebra Promoter by Human Herpesvirus 6. *J Virol* (1996) 70(3):1784–91. doi: 10.1128/JVI.70.3.1784-1791.1996
172. Cuomo L, Angeloni A, Zompetta C, Cirone M, Calogero A, Frati L, et al. Human Herpesvirus 6 Variant A, But Not Variant B, Infects EBV-Positive B Lymphoid Cells, Activating the Latent EBV Genome Through a BZLF-1-Dependent Mechanism. *AIDS Res Hum Retroviruses* (1995) 11(10):1241–5. doi: 10.1089/aid.1995.11.1241
173. Turcanova VL, Bundgaard B, Hollsberg P. Human Herpesvirus-6B Induces Expression of the Human Endogenous Retrovirus K18-Encoded Superantigen. *J Clin Virol* (2009) 46(1):15–9. doi: 10.1016/j.jcv.2009.05.015
174. Charvet B, Reynaud JM, Gourru-Lesimple G, Perron H, Marche PN, Horvat B. Induction of Proinflammatory Multiple Sclerosis-Associated Retrovirus Envelope Protein by Human Herpesvirus-6A and CD46 Receptor Engagement. *Front Immunol* (2018) 9:2803. doi: 10.3389/fimmu.2018.02803
175. Johnson WE. Origins and Evolutionary Consequences of Ancient Endogenous Retroviruses. *Nat Rev Microbiol* (2019) 17(6):355–70. doi: 10.1038/s41579-019-0189-2
176. Lander ES, Linton LM, Birren B, Nusbaum C, Zody MC, Baldwin J, et al. Initial Sequencing and Analysis of the Human Genome. *Nature* (2001) 409 (6822):860–921. doi: 10.1038/35057062
177. Karimi A, Esmaili N, Ranjkesh M, Zolfaghari MA. Expression of Human Endogenous Retroviruses in Pemphigus Vulgaris Patients. *Mol Biol Rep* (2019) 46(6):6181–6. doi: 10.1007/s11033-019-05053-6
178. Morris G, Maes M, Murdjeva M, Puri BK. Do Human Endogenous Retroviruses Contribute to Multiple Sclerosis, and if So How? *Mol Neurobiol* (2019) 56(4):2590–605. doi: 10.1007/s12035-018-1255-x
179. de Parseval N, Lazar V, Casella JF, Benit L, Heidmann T. Survey of Human Genes of Retroviral Origin: Identification and Transcriptome of the Genes With Coding Capacity for Complete Envelope Proteins. *J Virol* (2003) 77 (19):10414–22. doi: 10.1128/jvi.77.19.10414-10422.2003
180. Mi S, Lee X, Li X, Veldman GM, Finnerty H, Racie L, et al. Syncytin is a Captive Retroviral Envelope Protein Involved in Human Placental Morphogenesis. *Nature* (2000) 403(6771):785–9. doi: 10.1038/35001608
181. Lokossou AG, Toudic C, Barbeau B. Implication of Human Endogenous Retrovirus Envelope Proteins in Placental Functions. *Viruses* (2014) 6 (11):4609–27. doi: 10.3390/v6114609
182. Perron H, Lalande B, Gratacap B, Laurent A, Genoulaz O, Geny C, et al. Isolation of Retrovirus From Patients With Multiple Sclerosis. *Lancet* (1991) 337(8745):862–3. doi: 10.1016/0140-6736(91)92579-q
183. Kremer D, Gruchot J, Weyers V, Oldemeier L, Göttle P. pHERV-W Envelope Protein Fuels Microglial Cell-Dependent Damage of Myelinated Axons in

Multiple Sclerosis. *Proc Natl Acad Sci U S A* (2019) 116(30):15216–25. doi: 10.1073/pnas.1901283116
184. Hartung H-P, Derfuss T, Cree BA, Sormani MP, Selmaj K, Stutters J, et al. Efficacy and Safety of Temelimab in Multiple Sclerosis: Results of a Randomized Phase 2b and Extension Study. *Multiple Sclerosis J* (2021), 13524585211024997. doi: 10.1177/13524585211024997
185. van Horssen J, van der Pol S, Nijland P, Amor S, Perron H. Human Endogenous Retrovirus W in Brain Lesions: Rationale for Targeted Therapy in Multiple Sclerosis. *Mult Scler Relat Disord* (2016) 8:11–8. doi: 10.1016/j.msard.2016.04.006
186. Ruprecht K, Mayer J. On the Origin of a Pathogenic HERV-W Envelope Protein Present in Multiple Sclerosis Lesions. *Proc Natl Acad Sci U S A* (2019) 116(40):19791–2. doi: 10.1073/pnas.1911703116
187. International Multiple Sclerosis Genetics C and Wellcome Trust Case Control C, Sawcer S, Hellenthal G, Pirinen M, Spencer CC, et al. Genetic Risk and a Primary Role for Cell-Mediated Immune Mechanisms in Multiple Sclerosis. *Nature* (2011) 476(7359):214–9. doi: 10.1038/nature10251
188. Antony JM, Deslauriers AM, Bhat RK, Ellestad KK, Power C. Human Endogenous Retroviruses and Multiple Sclerosis: Innocent Bystanders or Disease Determinants? *Biochim Biophys Acta* (2011) 1812(2):162–76. doi: 10.1016/j.bbadis.2010.07.016
189. Antony JM, Ellestad KK, Hammond R, Imaizumi K, Mallet F, Warren KG, et al. The Human Endogenous Retrovirus Envelope Glycoprotein, Syncytin-1, Regulates Neuroinflammation and its Receptor Expression in Multiple Sclerosis: A Role for Endoplasmic Reticulum Chaperones in Astrocytes. *J Immunol* (2007) 179(2):1210–24. doi: 10.4049/jimmunol.179.2.1210
190. Chen CP, Chen LF, Yang SR, Chen CY, Ko CC, Chang GD, et al. Functional Characterization of the Human Placental Fusogenic Membrane Protein Syncytin 2. *Biol Reprod* (2008) 79(5):815–23. doi: 10.1095/biolreprod.108.069765
191. Lokossou AG, Toudic C, Nguyen PT, Elisseeff X, Vargas A, Rassart É, et al. Endogenous Retrovirus-Encoded Syncytin-2 Contributes to Exosome-Mediated Immunosuppression of T Cells†. *Biol Reprod* (2020) 102(1):185–98. doi: 10.1093/biolre/ioz124
192. Tolosa JM, Schjenken JE, Clifton VL, Vargas A, Barbeau B, Lowry P, et al. The Endogenous Retroviral Envelope Protein Syncytin-1 Inhibits LPS/PHA-Stimulated Cytokine Responses in Human Blood and Is Sorted Into Placental Exosomes. *Placenta* (2012) 33(11):933–41. doi: 10.1016/j.placenta.2012.08.004
193. Charvet B, Pierquin J, Brunel J, Gorter R, Quétard C, Horvat B, et al. Human Endogenous Retrovirus Type W Envelope From Multiple Sclerosis Demyelinating Lesions Shows Unique Solubility and Antigenic Characteristics. *Virol Sin* (2021). doi: 10.1007/s12250-021-00372-0
194. Mameli G, Astone V, Arru G, Marconi S, Lovato L, Serra C, et al. Brains and Peripheral Blood Mononuclear Cells of Multiple Sclerosis (MS) Patients Hyperexpress MS-Associated Retrovirus/HERV-W Endogenous Retrovirus, But Not Human Herpesvirus 6. *J Gen Virol* (2007) 88(Pt 1):264–74. doi: 10.1099/vir.0.81890-0
195. Dolei A. Endogenous Retroviruses and Human Disease. *Expert Rev Clin Immunol* (2006) 2(1):149–67. doi: 10.1586/1744666x.2.1.149
196. Nissen KK, Laska MJ, Hansen B, Terkelsen T, Villesen P, Bahrami S, et al. Endogenous Retroviruses and Multiple Sclerosis-New Pieces to the Puzzle. *BMC Neurol* (2013) 13:111. doi: 10.1186/1471-2377-13-111
197. Arneth B. Up-To-Date Knowledge About the Association Between Multiple Sclerosis and the Reactivation of Human Endogenous Retrovirus Infections. *J Neurol* (2018) 265(8):1733–9. doi: 10.1007/s00415-018-8783-1
198. Arru G, Mameli G, Astone V, Serra C, Huang YM, Link H, et al. Multiple Sclerosis and HERV-W/MSRV: A Multicentric Study. *Int J BioMed Sci* (2007) 3(4):292–7.
199. Grandi N, Tramontano E. HERV Envelope Proteins: Physiological Role and Pathogenic Potential in Cancer and Autoimmunity. *Front Microbiol* (2018) 9:462. doi: 10.3389/fmicb.2018.00462
200. Firouzi R, Rolland A, Michel M, Jouvin-Marche E, Hauw JJ, Malcus-Vocanson C, et al. Multiple Sclerosis-Associated Retrovirus Particles Cause T Lymphocyte-Dependent Death With Brain Hemorrhage in Humanized SCID Mice Model. *J Neurovirol* (2003) 9(1):79–93. doi: 10.1080/13550280390173328
201. Perron H, Bernard C, Bertrand JB, Lang AB, Popa I, Sanhadji K, et al. Endogenous Retroviral Genes, Herpesviruses and Gender in Multiple Sclerosis. *J Neurol Sci* (2009) 286(1-2):65–72. doi: 10.1016/j.jns.2009.04.034
202. Garcia-Montojo M, Dominguez-Mozo M, Arias-Leal A, Garcia-Martinez Á, De las Heras V, Casanova I, et al. The DNA Copy Number of Human Endogenous Retrovirus-W (MSRV-Type) Is Increased in Multiple Sclerosis Patients and is Influenced by Gender and Disease Severity. *PLoS One* (2013) 8(1):e53623. doi: 10.1371/journal.pone.0053623
203. Mameli G, Serra C, Astone V, Castellazzi M, Poddighe L, Fainardi E, et al. Inhibition of Multiple-Sclerosis-Associated Retrovirus as Biomarker of Interferon Therapy. *J Neurovirol* (2008) 14(1):73–7. doi: 10.1080/13550280701801107
204. Porchet H, Vidal V, Kornmann G, Malpass S. Curtin F. A High-Dose Pharmacokinetic Study of a New IgG4 Monoclonal Antibody Temelimab/GNbAC1 Antagonist of an Endogenous Retroviral Protein pHERV-W Env. *Clin Ther* (2019) 41(9):1737–46. doi: 10.1016/j.clinthera.2019.05.020
205. Gold J, Marta M, Meier UC, Christensen T, Miller D, Altmann D, et al. A Phase II Baseline *Versus* Treatment Study to Determine the Efficacy of Raltegravir (Isentress) in Preventing Progression of Relapsing Remitting Multiple Sclerosis as Determined by Gadolinium-Enhanced MRI: The INSPIRE Study. *Mult Scler Relat Disord* (2018) 24:123–8. doi: 10.1016/j.msard.2018.06.002
206. Zubizarreta I, Florez-Grau G, Vila G, Cabezon R, Espana C, Andorra M, et al. Immune Tolerance in Multiple Sclerosis and Neuromyelitis Optica With Peptide-Loaded Tolerogenic Dendritic Cells in a Phase 1b Trial. *Proc Natl Acad Sci U S A* (2019) 116(17):8463–70. doi: 10.1073/pnas.1820039116
207. Saligrama N, Zhao F, Sikora MJ, Serratelli WS, Fernandes RA, Louis DM, et al. Opposing T Cell Responses in Experimental Autoimmune Encephalomyelitis. *Nature* (2019) 572(7770):481–7. doi: 10.1038/s41586-019-1467-x
208. Krienke C, Kolb L, Diken E, Streuber M, Kirchhoff S, Bukur T, et al. A Noninflammatory mRNA Vaccine for Treatment of Experimental Autoimmune Encephalomyelitis. *Science* (2021) 371(6525):145–53. doi: 10.1126/science.aay3638
209. Croese T, Castellani G, Schwartz M. Immune Cell Compartmentalization for Brain Surveillance and Protection. *Nat Immunol* (2021) 22(9):1083–92. doi: 10.1038/s41590-021-00994-2
210. Kumar N, Sharma N, Mehan S. Connection Between JAK/STAT and Pparγ Signaling During the Progression of Multiple Sclerosis: Insights Into the Modulation of T-Cells and Immune Responses in the Brain. *Curr Mol Pharmacol* (2021). doi: 10.2174/1874467214666210301121432
211. Louveau A, Herz J, Alme MN, Salvador AF, Dong MQ, Viar KE, et al. CNS Lymphatic Drainage and Neuroinflammation Are Regulated by Meningeal Lymphatic Vasculature. *Nat Neurosci* (2018) 21(10):1380–91. doi: 10.1038/s41593-018-0227-9

Conflict of Interest: RR is a scientific advisor to IDFISH Technology Inc.

The remaining authors declare that the research was conducted in the absence of any commercial or financial relationships that could be construed as a potential conflict of interest.

Publisher's Note: All claims expressed in this article are solely those of the authors and do not necessarily represent those of their affiliated organizations, or those of the publisher, the editors and the reviewers. Any product that may be evaluated in this article, or claim that may be made by its manufacturer, is not guaranteed or endorsed by the publisher.

frontiers in Immunology

ORIGINAL RESEARCH
published: 11 November 2021
doi: 10.3389/fimmu.2021.763323

Parkinson's Disease Is Associated With Dysregulation of Circulatory Levels of lncRNAs

Kasra Honarmand Tamizkar[1], Pooneh Gorji[2], Mahdi Gholipour[1], Bashdar Mahmud Hussen[3], Mehrdokht Mazdeh[4], Solat Eslami[5,6], Mohammad Taheri[7,8] and Soudeh Ghafouri-Fard[9]**

[1] Phytochemistry Research Center, Shahid Beheshti University of Medical Sciences, Tehran, Iran, [2] Men's Health and Reproductive Health Research Center, Shahid Beheshti University of Medical Sciences, Tehran, Iran, [3] Department of Pharmacognosy, College of Pharmacy, Hawler Medical University, Erbil, Iraq, [4] Neurophysiology Research Center, Hamadan University of Medical Sciences, Hamadan, Iran, [5] Dietary Supplements and Probiotic Research Center, Alborz University of Medical Sciences, Karaj, Iran, [6] Department of Medical Biotechnology, School of Medicine, Alborz University of Medical Sciences, Karaj, Iran, [7] Skull Base Research Center, Loghman Hakim Hospital, Shahid Behehsti University of Medical Sciences, Tehran, Iran, [8] Institute of Human Genetics, Jena University Hospital, Jena, Germany, [9] Department of Medical Genetics, School of Medicine, Shahid Behehsti University of Medical Sciences, Tehran, Iran

Long non-coding RNAs (lncRNAs) have been recently reported to be involved in the pathoetiology of Parkinson's disease (PD). Circulatory levels of lncRNAs might be used as markers for PD. In the present work, we measured expression levels of *HULC*, *PVT1*, *MEG3*, *SPRY4-IT1*, *LINC-ROR* and *DSCAM-AS1* lncRNAs in the circulation of patients with PD *versus* healthy controls. Expression of *HULC* was lower in total patients compared with total controls (Expression ratio (ER)=0.19, adjusted P value<0.0001) as well as in female patients compared with female controls (ER=0.071, adjusted P value=0.0004). Expression of *PVT1* was lower in total patients compared with total controls (ER=0.55, adjusted P value=0.0124). Expression of *DSCAM-AS1* was higher in total patients compared with total controls (ER=5.67, P value=0.0029) and in male patients compared with male controls (ER=9.526, adjusted P value=0.0024). Expression of *SPRY4-IT* was higher in total patients compared with total controls (ER=2.64, adjusted P value<0.02) and in male patients compared with male controls (ER=3.43, P value<0.03). Expression of *LINC-ROR* was higher in total patients compared with total controls (ER=10.36, adjusted P value<0.0001) and in both male and female patients compared with sex-matched controls (ER=4.57, adjusted P value=0.03 and ER=23.47, adjusted P value=0.0019, respectively). Finally, expression of *MEG3* was higher in total patients compared with total controls (ER=13.94, adjusted P value<0.0001) and in both male and female patients compared with sex-matched controls (ER=8.60, adjusted P value<0.004 and ER=22.58, adjusted P value<0.0085, respectively). ROC

OPEN ACCESS

Edited by:
Roberta Magliozzi, University of Verona, Italy

Reviewed by:
Hikoaki Fukaura, Saitama Medical University, Japan
Rezvan Noroozi, Jagiellonian University, Poland
Amin Safa, Complutense University of Madrid, Spain

***Correspondence:**
Mohammad Taheri
Mohammad_823@yahoo.com
Soudeh Ghafouri-Fard
s.ghafourifard@sbmu.ac.ir

Specialty section:
This article was submitted to Multiple Sclerosis and Neuroimmunology, a section of the journal Frontiers in Immunology

Received: *23 August 2021*
Accepted: *22 October 2021*
Published: *11 November 2021*

Citation:
Honarmand Tamizkar K, Gorji P, Gholipour M, Hussen BM, Mazdeh M, Eslami S, Taheri M and Ghafouri-Fard S (2021) Parkinson's Disease Is Associated With Dysregulation of Circulatory Levels of lncRNAs. Front. Immunol. 12:763323. doi: 10.3389/fimmu.2021.763323

curve analysis revealed that MEG3 and LINC-ROR have diagnostic power of 0.77 and 0.73, respectively. Other lncRNAs had AUC values less than 0.7. Expression of none of lncRNAs was correlated with age of patients, disease duration, disease stage, MMSE or UPDRS. The current study provides further evidence for dysregulation of lncRNAs in the circulation of PD patients.

Keywords: Parkinson's disease, lncRNA, HULC, PVT1, MEG3, SPRY4-IT1, LINC-ROR, DSCAM-AS1

INTRODUCTION

As a progressive neurodegenerative condition, Parkinson's disease (PD) affects 2-3% of the whole population age more than 65 years with a gradually increasing incidence (1). This disorder is characterized by resting tremor, bradykinesia, rigidity of muscles, balance disturbances, postural instability and a number of non-motor manifestations, particularly cognitive dysfunction which affects the vast majority of PD patients (2). PD is associated with alteration of expression and activity of several genes, particularly those related with dopamine-dependent oxidative stress (3). Many genetic and environmental risk factors of PD converge in pathways inducing cell death in dopaminergic neurons. In fact, high level of dopamine in cytoplasm of nigral neurons has been associated with dopamine oxidation and production of reactive oxygen species which have detrimental effects on these neurons (3). Cumulatively, dopamine-associated oxidative stress, dysfunction of synaptic vesicles and misfolding of α-synuclein produce an extending vicious cycle which perpetually results in death of dopaminergic neurons (3). PD has been associated with dysregulation of several transcripts among them are long non-coding RNAs (lncRNAs) (4). LncRNAs have possible role in brain development. A multi-disciplinary study of four highly conserved and brain-expressed lncRNA has shown that lncRNAs are functional transcripts with important roles in the development of vertebrate brain. This speculation is based on the observed preservation of lncRNAs across various amniotes, obvious conservation of their exons structures, and resemblances in lncRNA signature throughout the embryonic and early postnatal phases (5).

A number of lncRNAs affect pathoetiology of PD. For instance, *NEAT1* has been shown to promote the MPTP-associated autophagy in PD *via* increasing the stability of PINK1 protein (6). Moreover, *HOTAIR* has been found to target miR-126-5p to facilitate progression of PD *via* RAB3IP (7). A recent study has reported lower plasma levels of *MEG3* in PD patients compared with control group. Notably, authors have reported negative correlations between *MEG3* levels and Hoehn & Yahr (H&Y) stage and Non-Motor Symptoms Scale (NMSS) score in PD group. However, expression of this lncRNA has been positively correlated with Mini-Mental State Examination (MMSE) and Montreal Cognitive Assessment (MoCA) scores. Thus, authors have suggested close relation between *MEG3* expression and worsening of non-motor symptoms, cognitive impairments, and PD stage (8).

In the present work, we measured expression levels of *HULC*, *PVT1*, *MEG3*, *SPRY4-IT1*, *LINC-ROR* and *DSCAM-AS1* lncRNAs in the circulation of patients with PD *versus* healthy controls. These lncRNAs have been suggested to affect immune responses and participate in the pathoetiology of immune-related disorders of nervous system (9). Moreover, expressions of *LINC-ROR*, *MEG3* and *SPRY4-IT1* have been shown to be higher in patients with schizophrenia compared with healthy subjects (10). These lncRNAs might also affect pathoetiology of PD, since they can influence fundamental processes in this disorder such as autophagy. For instance, *HULC* has been found to target ATG7 (11), an autophagy related gene with crucial functions in the development of PD (12). Moreover, *PVT1* can induce cytoprotective autophagy (13). *MEG3* triggers autophagy through modulation of activity of ATG3 (14). The role of *LINC-ROR* in regulation of autophagy has been investigated in the context of cancer (15). These lncRNAs might also affect neurotoxic events. For instance, *SPRY4-IT1* has been shown to modulate ketamine-associated neurotoxicity in human embryonic stem cell-originated neurons (16). Besides, *DSCAM-AS1* has interaction with hnRNPL (17), an RNA-binding protein with possible role in the etiology of PD (18). However, their role of the development of PD has been less studied.

MATERIALS AND METHODS

Patient and Controls

The present project was performed using the blood specimens collected from 50 cases of PD (Female/male ratio: 13/37) and 58 healthy individuals (Female/male ratio: 20/38). Patients were enlisted during January 2020-April 2021 from Farshchian, Hamadan, Iran. PD cases were diagnosed based on criteria proposed by the International Parkinson and Movement Disorder Society (19). Exclusion criteria were current or chronic infections, neoplastic conditions or any systemic disorder. H&Y staging system was used for evaluation of the functional disability associated with PD (20). Moreover, the MMSE was used as a screening tool for PD dementia, with values below 26 showing possible dementia (21). Moreover, Unified Parkinson's Disease Rating Scale (UPDRS) was used as a rating tool to estimate the severity and progression of PD (22). Persons enlisted in the control group had no personal or family history of any neuropsychiatric disorder. The study protocol was confirmed by ethical committee of Shahid Beheshti University of

Medical Sciences. All PD patients and controls signed the informed consent forms.

Expression Assays

A total of 5 mL of peripheral blood was collected from PD patients and healthy persons in EDTA-blood collection tubes. Total RNA was extracted from these specimens using GeneAll extraction kit (Seoul, South Korea). The quality and quantity of RNA were assessed using gel electrophoresis and Nanodrop equipment. Afterwards, cDNA was made from roughly 75 ng of RNA using BioFact™ kit (Seoul, South Korea). The Ampliqon real time PCR master mix (Denmark) was used for making PCR reactions. Primers were designed so that the amplicon contains exon-intron boundary. Tests were accomplished in StepOnePlus™ RealTime PCR System (Applied Biosystems, Foster city, CA, USA). **Table 1** shows primers sequences. PCR program comprised a preliminary activation stage for 5 minutes at 94°C, and 40 cycles at 94°C for 15 seconds and 60°C for 45 seconds.

Statistical Methods

The Statistical Package for the Social Sciences (SPSS) v.18.0 (SPSS Inc., Chicago, IL) was used for statistical assessments. Graphics were created using GraphPad Prism version 9.0 for Windows, GraphPad Software, La Jolla California USA. Expressions of lncRNAs in each sample were calculated using the Efficiency adjusted Ct of normalizer gene (B2M) - Efficiency adjusted Ct of target gene (comparative –delta Ct method). A two-way ANOVA was used to analyze effects of disease and gender on expression level of lncRNA in peripheral blood of patients and controls. Tukey *post hoc* test was used for multiple comparisons between subgroups. The "– delta Ct" Data in the figures were plotted as box and whisker plots (including the median [line], mean [cross], interquartile range [box], and minimum and maximum values. The delta delta Ct value was determined by subtracting the delta Ct of the control sample from the individual delta Ct of the test sample. The fold change of the test sample relative to the control sample was determined by $2^{-\text{delta delta Ct}}$ and was shown as lower limit-mean and upper limit in the figures and table. The correlations between transcript levels of lncRNAs were evaluated using regression model and Bonferroni correction for multiple comparisons. The partial correlation between expression levels and age of study participants, disease stage (Hoehn & Yahr stage), disease duration, MMSS and UPDRES was described by R and P values. The receiver operating characteristic (ROC) curves were depicted to appraise the diagnostic power of expression levels of lncRNAs. Youden's J parameter was measured to find the optimum threshold. P value < 0.05 was considered as significant. The significance of difference in mean values of lncRNAs expression (mean of –delta Ct method) between two subgroups of patients using L-DOPA and other drugs was computed using the t-test. Dynamic principal component analysis of lncRNA expression profile was used to cluster samples *via* Gene Expression software (GenEx SW, Multid Analysis AB, Göteborg, Sweden). Normalized values were used for principal component analysis. Heatmaps were generated by using GenEx software.

RESULTS

General Data of Cases

Table 2 shows the clinical data and demographic information of PD cases.

Expression Assays

Expression of *HULC* was lower in total patients compared with total controls (Expression ratio (ER)=0.19, adjusted P value<0.0001) as well as in female patients compared with female controls (ER=0.071, adjusted P value=0.0004). Expression of *PVT1* was lower in total patients compared with total controls (ER=0.55, adjusted P value=0.0124). Expression of *DSCAM-AS1* was higher in total patients compared with total controls (ER=5.67, P value=0.0029) and in male patients compared with male controls (ER=9.526, adjusted P value=0.0024). Expression of *SPRY4-IT* was higher in total patients compared with total controls (ER=2.64, adjusted P value<0.02) and in male patients compared with male controls (ER=3.43, P value<0.03). Expression of *LINC-ROR* was higher in

TABLE 1 | Primer sequences.

Gene	Primer sequence		Primer length	Product size
HULC	Forward primer	ACGTGAGGATACAGCAAGGC	20	75
	Reverse primer	AGAGTTCCTGCATGGTCTGG	20	
PVT1	Forward primer	CCCATTACGATTTCATCTC	19	131
	Reverse primer	GTTCGTACTCATCTTATTCAA	21	
MEG3	Forward primer	TGGCATAGAGGAGGTGAT	18	111
	Reverse primer	GGAGTGCTGTTGGAGAATA	19	
SPRY4-IT1	Forward primer	AGCCACATAAATTCAGCAGA	20	115
	Reverse primer	GATGTAGGATTCCTTTCA	18	
LINC-ROR	Forward primer	TATAATGAGATACCACCTTA	20	170
	Reverse primer	AGGAACTGTCATACCGTTTC	20	
DSCAM-AS1	Forward primer	TCAGTGTCGCTACAGGGGAT	20	118
	Reverse primer	GGAGGAGGGACAGAGAAGGA	20	
B2M	Forward primer	AGATGAGTATGCCTGCCGTG	20	105
	Reverse primer	GCGGCATCTTCAAACCTCCA	20	

TABLE 2 | General data of cases.

Parameters	Groups		Values
Sex (number)	Male		37
	Female		13
Age [Years, mean ± SD (range)]	Male		69.64 ± 10.59 (47-89)
	Female		66.46 ± 12.6 (38-85)
Duration [Years, mean ± SD (range)]	Male		3.18 ± 3.65 (1-12)
	Female		5.38 ± 9.76 (1-36)
MMSE [mean ± SD (range)]	Male		22.84 ± 3.032 (17-29)
	Female		23.08 ± 2.499 (19-26)
UPDRS [mean ± SD (range)]	Male		23.92 ± 7.418 (13-41)
	Female		26.31 ± 9.437 (16-42)
Hoehn & Yahr stage (number)	I	Male	8
		Female	3
	II	Male	18
		Female	5
	III	Male	11
		Female	5
Drug administration (number)	L-DOPA		46
	Bromocriptine, Amantadine, Quetiapine		4

total patients compared with total controls (ER=10.36, adjusted P value<0.0001) and in both male and female patients compared with sex-matched controls (ER=4.57, adjusted P value=0.03 and ER=23.47, adjusted P value=0.0019, respectively). Finally, expression of *MEG3* was higher in total patients compared with total controls (ER=13.94, adjusted P value<0.0001) and in both male and female patients compared with sex-matched controls (ER=8.60, adjusted P value<0.004 and ER=22.58, adjusted P value<0.0085, respectively) (**Table 3**).

Figures 1 and **2** show relative expression of expression levels of lncRNAs and their fold changes in PD patients *versus* controls.

ROC curve analysis revealed that MEG3 and LINC-ROR have diagnostic power of 0.77 and 0.73, respectively (**Figure 3**). Other lncRNAs had AUC values less than 0.7.

Table 4 shows sensitivity, specificity and AUC values of each lncRNA in separation of PD cases from controls. This type of analysis was repeated for distinct sex-based groups. *HULC* and *PVT1* could differentiate only between female subgroups. On the other hand, *DSCAM-AS1* and *SPRY4-IT* could differentiate only between male subgroups.

Expression of none of lncRNAs was correlated with age of patients, disease duration, disease stage, MMSE or UPDRS (**Table 5**).

Expressions of lncRNAs were significantly correlated with each other in both PD patients and controls (**Table 6**).

Finally, we compared expression levels of lncRNAs in patients receiving L-DOPA *versus* those being under treatment with other drugs (**Figure 4**). This analysis revealed no significant difference in expression of lncRNAs between these two groups.

TABLE 3 | The results of expression study of lncRNAs in peripheral blood of patients with PD compared with healthy controls.

lncRNAs		Total patients *vs.* Controls (50 *vs.* 58)	Male patients *vs.* Male Controls (37 *vs.* 38)	Female patients *vs.* Female Controls (13 *vs.* 20)	Female patients *vs.* Male patients 13 *vs.* 37)
HULC	Expression ratio (Lower Limit-Upper Limit)	0.19 (0.130-0.279)	0.513 (0.339-0.775)	0.071 (0.037-0.134)	0.962 (0.318-1)
	Adjusted P Value	<0.0001*	0.3746	0.0004	0.757
PVT1	Expression ratio (Lower Limit-Upper Limit)	0.55 (0.435-0.696)	0.619 (0.479-0.799)	0.49 (0.33-0.727)	0.962 (0.673-1.375)
	Adjusted P Value	0.0124*	0.2430	0.2770	0.999
DSCAM-AS1	Expression ratio (Lower Limit-Upper Limit)	5.672 (3.208-10.029)	9.526 (5.124-17.71)	3.375 (1.296-8.784)	0.116 (0.048-0.276)
	Adjusted P Value	0.0029*	0.0024*	0.5826	0.0683
SPRY4-IT	Expression ratio (Lower Limit-Upper Limit)	2.64 (1.735-4.019)	3.434 (2.174-5.432)	2.03 (1-4.106)	0.913 (0.482-1.728)
	Adjusted P Value	<0.0227	<0.0397*	<0.7471	0.9999
LINC-ROR	Expression ratio (Lower Limit-Upper Limit)	10.36 (6.236-17.21)	4.575 (2.634-7.948)	23.47 (10.014-55.024)	0.854 (0.395-1.848)
	Adjusted P Value	<0.0001*	0.0345*	0.0019*	0.9970
MEG3	Expression ratio (Lower Limit-Upper Limit)	13.94 (7.86-24.706)	8.603 (4.615-16.037)	22.58 (8.639-59.014)	1.392 (0.583-3.321)
	P-value	<0.0001	<0.0044*	<0.0085*	0.9811

The expression ratio of each gene (mean, lower limit and upper limit) is shown as the ratio of expression of the first group compared to the second group in each column.
** shows significance.*

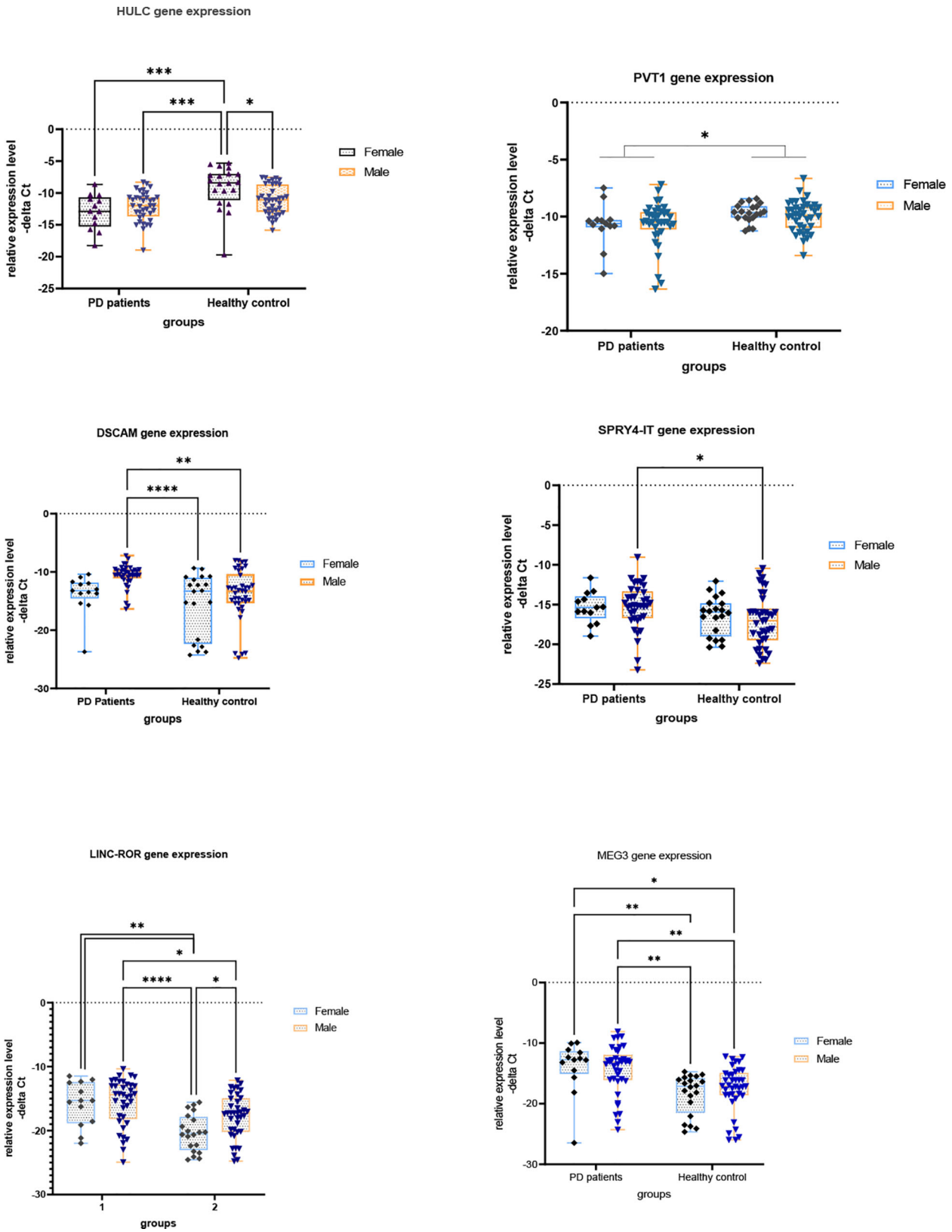

FIGURE 1 | Relative expression levels of lncRNAs in PD patients *versus* controls (*P value < 0.05, **P value < 0.001, ***P < 0.001 and ****P value < 0.0001).

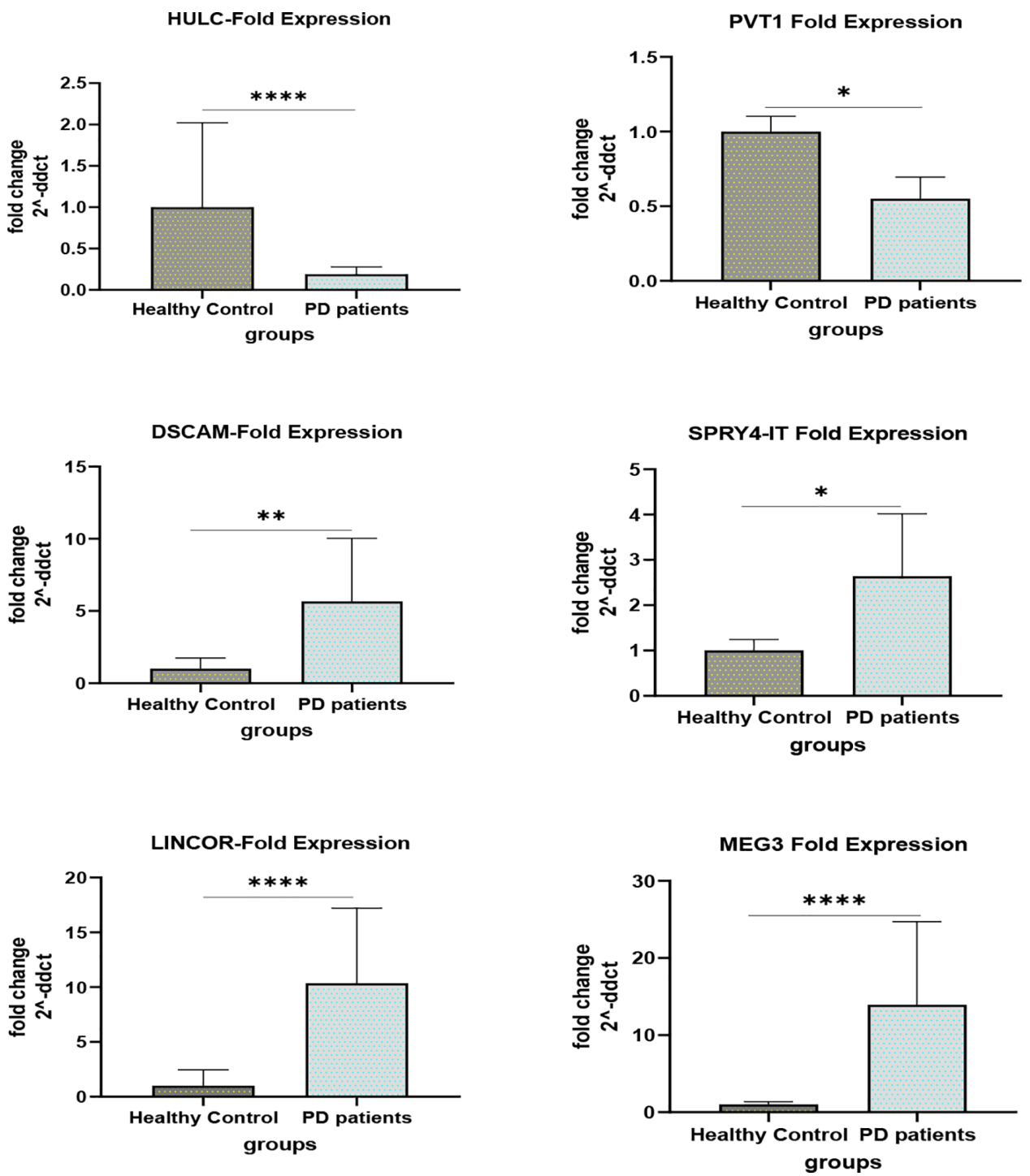

FIGURE 2 | Fold changes of lncRNAs in PD patients *versus* controls (*P value < 0.05, **P value < 0.001 and ****P value < 0.0001).

Principal component analysis (PCA) was performed on 6 lncRNA expression profiles in patients with PD compared with healthy control. PCA of the 6 lncRNAs expression data could not clearly clusters samples collected from healthy controls (blue squares) and patients with Parkinson (green squares) into their respective groups (**Figure 5**).

Then, dynamic principal component analysis (DPCA) was performed on the lncRNA results from the analyzed samples to

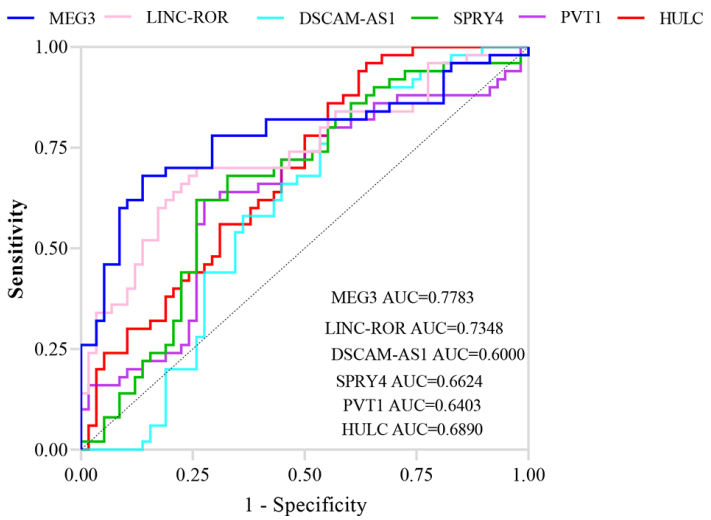

FIGURE 3 | ROC curves showing the power of lncRNAs in separation of PD patients from controls.

determine how the 6 differentially expressed lncRNAs were distributed among the samples from PD patients and healthy controls. DPCA excluded lncRNA PVT1 with low standard deviation. Thus, 5 lncRNAs expression data were used to clusters samples collected from healthy controls (blue squares) and patients with PD (green squares) into their respective groups. As shown in **Figure 6**, the DPCA almost clearly separated the samples collected from healthy controls (blue squares) and patients with PD (green squares) into their respective groups.

Finally, we depicted Log2 Fold Change Heat Map for lncRNA levels (**Figure 7**). Most of patient samples (A1-A50) were located on the left side with increased expression of lncRNAs studied in this work.

DISCUSSION

In the present work, we measured expression levels of 6 lncRNAs in the circulation of patients with PD *versus* healthy controls. Expression of *HULC* was lower in total patients compared with total controls as well as in female patients compared with female controls. This lncRNA has a role in regulation of immune response, since up-regulation of *HULC* has been shown to has a necessary role in pro-inflammatory responses in the course of LPS-associated sepsis (23). In addition, *HULC* has a role in regulation of apoptosis. Experiments in the contexts of various neoplasms have indicated an anti-apoptotic role for *HULC* (24, 25). This function of *HULC* has not been assessed in neurons. If this lncRNA exerts similar role in neurons, down-regulation of *HULC* in the circulation of patients with PD might be associated with higher apoptosis of neurons. It has been widely accepted that apoptosis of nigral dopaminergic neurons has essential roles in the development of PD (26). Various mechanisms including both intrinsic and extrinsic routes participate in the degeneration of dopaminergic neurons in this disorder (26). However, the exact position of *HULC* within this complicated network of apoptosis-related mechanisms needs to be clarified.

Expression of *PVT1* was lower in total patients compared with total controls. *PVT1* silencing has been shown to induce apoptosis and inhibit cell cycle transition *via* modulating EFGR pathway (27). Experiment in animal model of PD has shown the impact of EGFR signaling in cell death of dopaminergic neurons in the course of neuro-apoptosis (28).

Expressions of *DSCAM-AS1* and *SPRY4-IT* were higher in total patients compared with total controls and in male patients compared with male controls. *DSCAM-AS1* has been previously reported as an Estrogen receptor α-dependent lncRNA with critical roles in the regulation of cell growth and migration (29). Since estrogen and some selective estrogen receptor modulators have been suggested as possible therapeutic options for PD (30), identification of the molecular mechanism of participation of *DSCAM-AS1* in the pathetiology of PD has clinical significance. The observed sex-biased dysregulation of this lncRNA among PD patients further support the interaction between estrogen receptor and this lncRNA. *SPRY4-IT1* has been shown to modulate ketamine-associated neurotoxicity in human embryonic stem cell-originated neurons *via* EZH2 (16). Up-regulation of this lncRNA in the circulatory blood of PD patients might be a compensatory mechanism to decrease PD-associated neuron loss.

Expressions of *LINC-ROR* and *MEG3* were higher in total patients compared with total controls and in both male and female patients compared with sex-matched controls. *LINC-ROR* has been shown to regulate apoptosis through influencing p53 ubiquitination *via* regulation of miR-204-5p/MDM2 axis (31). *MEG3* has been shown to affect neuron apoptosis through miR-181b-12/15-LOX signaling (32). Thus, modulation of apoptotic pathways is possible mechanism of participation of these lncRNAs in PD.

TABLE 4 | Sensitivity, specificity and AUC values of each lncRNA in separation of PD cases from controls.

	HULC				PVT1				DSCAM-AS1				SPRY4-IT				LINC-ROR				MEG3			
	AUC ± SD	Sensitivity	Specificity	P Value	AUC ± SD	Sensitivity	Specificity	P Value	AUC ± SD	Sensitivity	Specificity	P Value	AUC ± SD	Sensitivity	Specificity	P Value	AUC ± SD	Sensitivity	Specificity	P Value	AUC ± SD	Sensitivity	Specificity	P Value
Total patients *vs.* total normal controls (50 *vs.* 58)	0.68 ± 0.050	0.96	0.36	0.0007	0.64 ± 0.054	0.62	0.72	0.0122	0.6 ± 0.055	0.84	0.43	0.074	0.66 ± 0.052	0.62	0.74	0.0037	0.73 ± 0.049	0.7	0.74	<0.0001	0.77 ± 0.047	0.68	0.86	<0.0001
Female patients *vs.* Female normal controls (13 *vs.* 20)	0.84 ± 0.068	0.92	0.75	0.0009	0.74 ± 0.10	0.84	0.85	0.018	0.53 ± 0.10	0.92	0.3	0.76	0.62 ± 0.09	0.76	0.5	0.23	0.68 ± 0.06	0.70	0.63	0.005	0.85 ± 0.08	0.77	0.83	0.0006
Male patients *vs.* Male normal controls (37 *vs.* 38)	0.6 ± 0.006	0.22	0.94	0.13	0.59 ± 0.06	0.54	0.68	0.14	0.73 ± 0.06	0.86	0.73	0.0005	0.67 ± 0.06	0.83	0.5	0.0089	0.68 ± 0.062	0.70	0.63	0.0057	0.73 ± 0.059	0.75	0.68	0.0004

TABLE 5 | The results of partial correlation between expression of lncRNAs and age, Disease duration, Disease stage, MMSE and UPDRS [Controlled for sex, Diseases duration was classified into 3 ranges (1-5, 6-10 and more than 10 years)].

Parameters	Age		HULC		PVT1		DSCAM-AS1		SPRY4-IT		LINC-ROR		MEG3		Disease stage (Hoehn & Yahr stage)		Disease duration		MMSE		UPDRS	
	R	P value	R	P value	R	P value	R	P value	R	P value	R	P value	R	P value	R	P value	R	P value	R	P value	R	P value
Age	1	0	0.06	0.64	0.051	0.72	-0.079	0.58	-0.05	0.71	0.23	0.1	0.15	0.30	0.14	0.31	-0.09	0.49	-0.61*	0.000002	0.11	0.43
Disease duration	-0.09	0.49	-0.13	0.354	-0.07	0.63	-0.046	0.75	0.048	0.7385	-0.04	0.768	-0.01	0.91	0.6*	0.000004	1	0	-0.39*	0.005577	0.52*	0.0001
Disease stage (Hoehn & Yahr stage)	0.14	0.31	-0.05	0.7	0.007	0.96	-0.05	0.7	0.02	0.87	0.04	0.73	0.07	0.60	1	0	0.6*	0.000004	-0.54*	0.000048	0.70*	1.4167E-8
MMSE	-0.61	0.000002	-0.09	0.53	0.033	0.81	0.044	0.76	0.014	0.92	-0.13	0.37	-0.06	0.64	-0.5	0.000048	-0.39*	0.005577	1	0	-0.33*	0.02
UPDRS	0.11	0.43	-0.11	0.41	0.052	0.72	-0.005	0.970	-0.039	0.78	0.078	0.59	0.15	0.27	0.70*	1.4167E-8	0.52*	0.000103	-0.33*	0.02035	1	0

** shows significance.*

TABLE 6 | Correlations between expressions of lncRNAs in study groups.

DSCAM-AS1	Controls	0.48*	0.0001								
	Patients	0.66*	<0.0001								
SPRY4-IT	Controls	0.45*	0.0004	0.63*	<0.0001						
	Patients	0.51*	0.0001	0.49*	0.0003						
LINC-ROR	Controls	0.31	0.0167	0.63*	<0.0001	0.57*	<0.0001				
	Patients	0.53*	<0.0001	0.45	0.001	0.55*	<0.0001				
MEG3	Controls	0.33*	0.0096	0.60*	<0.0001	0.42*	0.0008	0.61*	<0.0001		
	Patients	0.46*	0.0006	0.35	0.0123	0.25	0.0738	0.49*	0.0003		
PVT1	Controls	0.46*	0.0003	0.43*	0.0006	0.36	0.0051	0.47*	0.0002	0.44*	0.0006
	Patients	0.34	0.0138	0.40	0.0035	0.32	0.0207	0.58*	<0.0001	0.55*	<0.0001
		R	P Value	R	P Value	R	P Value	R	P Value	R	P Value
		HULC		DSCAM-AS1		SPRY4-IT		LINC-ROR		MEG3	

Correlations between expressions of lncRNAs in study groups (R values are presented; after correction for multiple comparisons (Bonferroni correction), P value less than 0.0016 was accepted as significant.

** shows significance.*

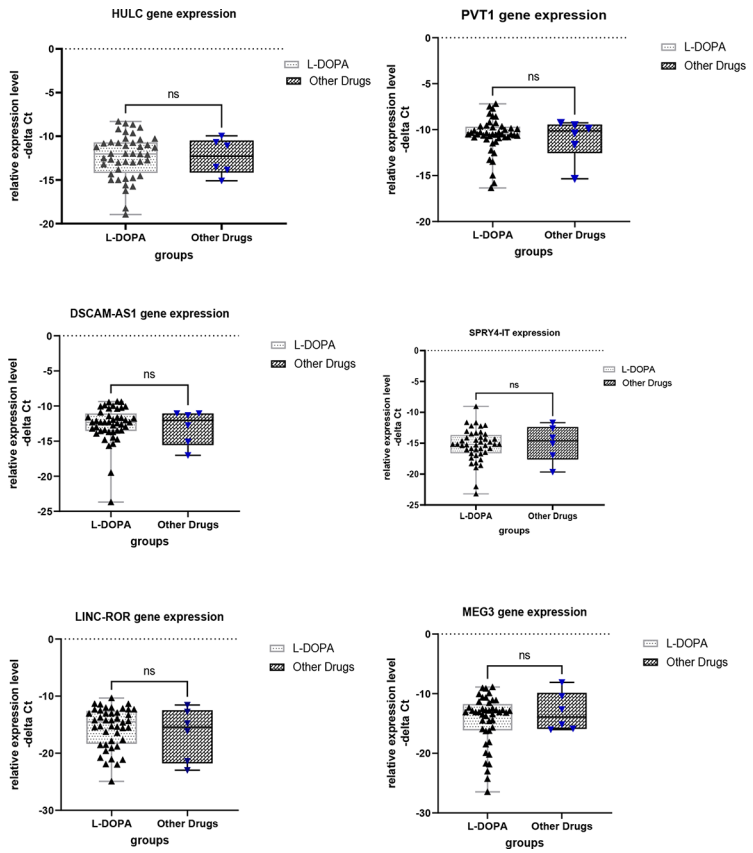

FIGURE 4 | Comparison of expression levels of lncRNAs between patients receiving L-DOPA and those under treatment with other drugs. ns, not significant.

ROC curve analysis revealed that *MEG3* and *LINC-ROR* have diagnostic power of 0.77 and 0.73, respectively. Other lncRNAs had AUC values less than 0.7. Thus, *MEG3* and *LINC-ROR* are possible markers for PD.

Expression of none of lncRNAs was correlated with age of patients, disease duration, disease stage, MMSE or UPDRS. The current study provides further evidence for dysregulation of lncRNAs in the circulation of PD patients. Therefore,

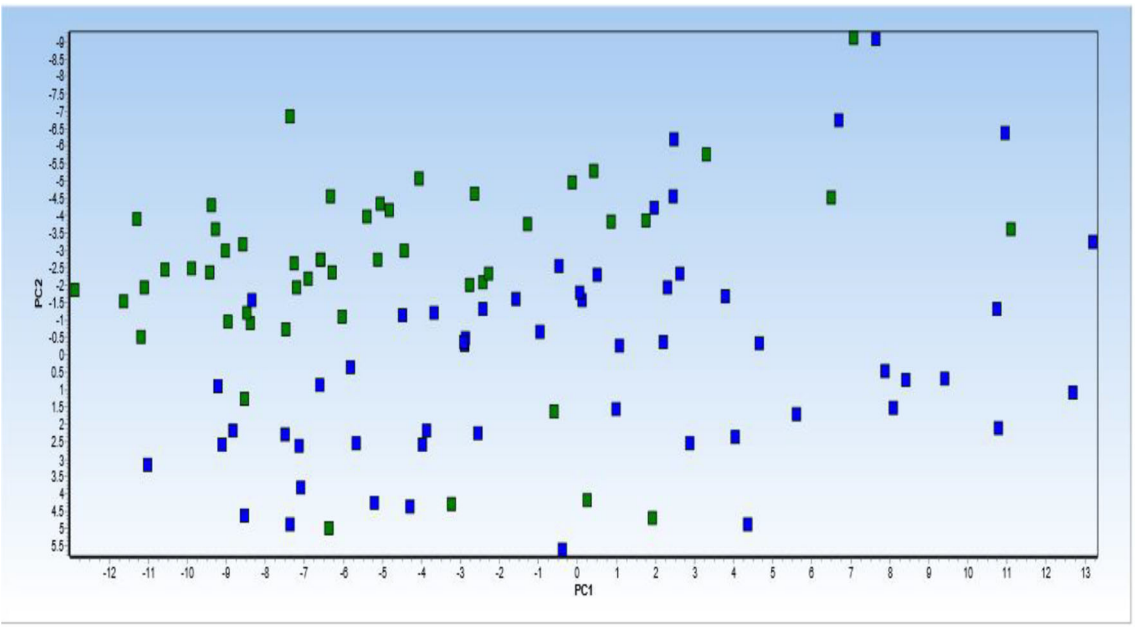

FIGURE 5 | Principal component analysis (PCA) of 6 lncRNA expression profiles in patients with Parkinson diseases compared with healthy control. PCA of the 6 lncRNAs expression data could not clearly clusters samples collected from healthy controls (blue squares) and patients with Parkinson (green squares) into their respective groups. Normalized values were used for principal component analysis.

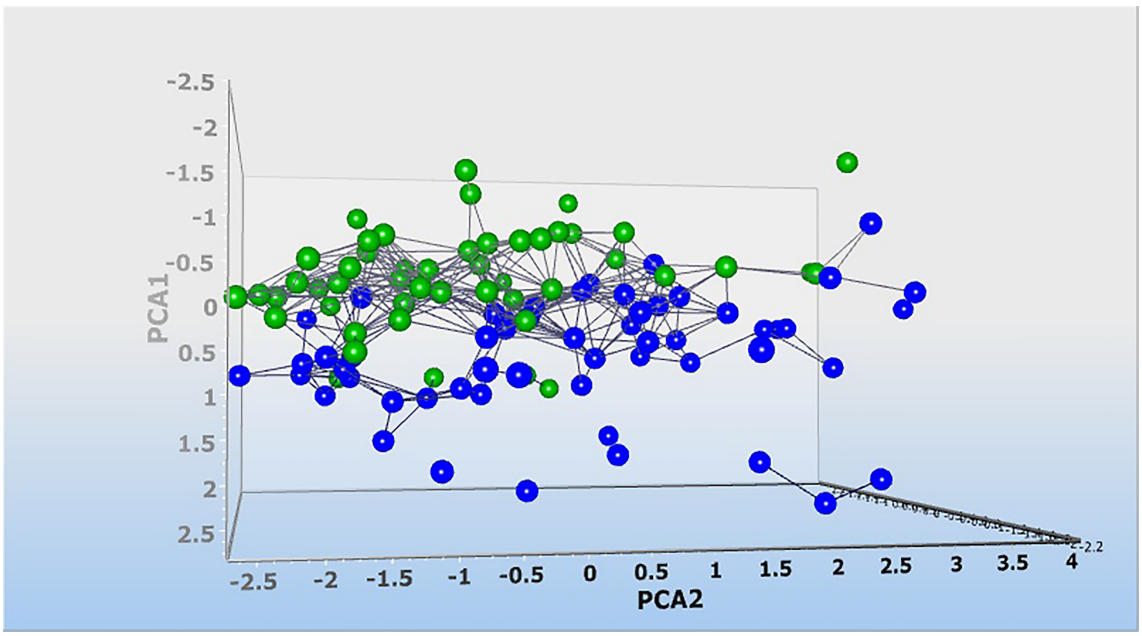

FIGURE 6 | Dynamic principal component analysis (DPCA) of 6 lncRNA expression profiles. DPCA was used to filter out and exclude lncRNA with low standard deviation. LncRNA PVT1 was excluded and 5 lncRNA expression data were used to clusters samples collected from healthy controls (blue squares) and patients with Parkinson (green squares) into their respective groups. Normalized values were used for principal component analysis.

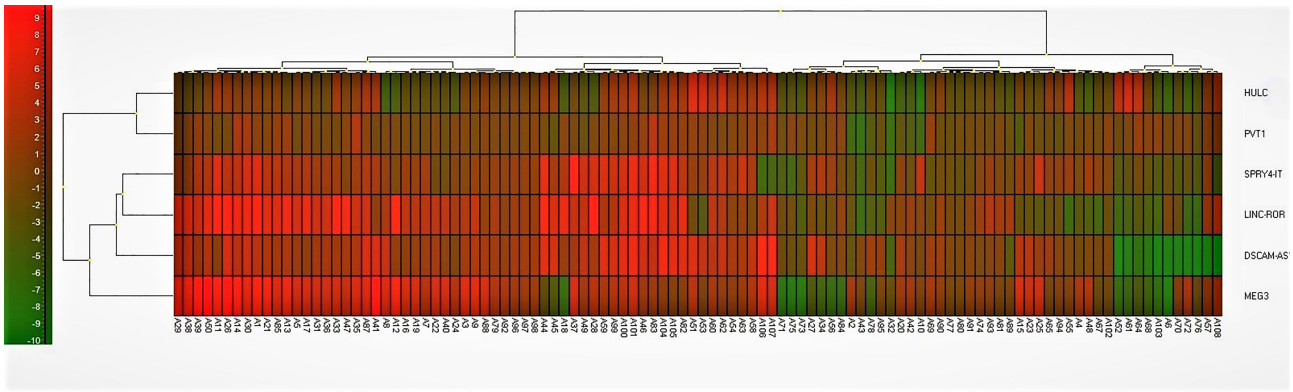

FIGURE 7 | Log2 Fold Change Heat Map. A heat map for the subjects with Parkinson diseases and healthy control. Log2 fold change was calculated based on delta Ct value compared to the control samples. Red color implies increased expression while green implies decreased expression. LncRNAs on the right are clustered using a hierarchical clustering method (Ward's method, Euclidean distances) and 5 clusters were found. Cluster 1 = HULC and PVT1; Cluster 2 = SPRY4-IT; Cluster 3 = LINC-ROR; Cluster 4 = DSCAM-AS1; Cluster 5 = MEG3. Most of patient samples (A1-A50) were located on the left side with increased expression of lncRNAs studied in this work.

expression level of these lncRNAs is independent from PD course.

Moreover, the DPCA almost clearly separated the samples collected from healthy controls and patients with PD into their respective groups. This suggests that the observed lncRNA differences are associated with the pathophysiology of PD, and these lncRNA might constitute an important biomarker signature for PD.

In conclusion, the current study shows dysregulation of lncRNAs in the circulation of PD patients. The study has limitations regarding small sample size and lack of inclusion of drug-naïve patients. Moreover, it is important to characterize each lncRNA in detail, such as the structure and function of each lncRNA, and to quantify the role of lncRNA in PD in multinational multicenter studies.

DATA AVAILABILITY STATEMENT

The raw data supporting the conclusions of this article will be made available by the authors, without undue reservation.

ETHICS STATEMENT

The study protocol was confirmed by ethical committee of Shahid Beheshti University of Medical Sciences. The patients/participants provided their written informed consent to participate in this study. Written informed consent was obtained from the individual(s) for the publication of any potentially identifiable images or data included in this article.

AUTHOR CONTRIBUTIONS

SG-F wrote the draft and revised it. MT and BH designed and supervised the study. SE analyzed the data. KH, MG, and PG performed the experiment. All authors contributed to the article and approved the submitted version.

FUNDING

The current study was supported by a grant from Shahid Beheshti University of Medical Sciences.

REFERENCES

1. Poewe W, Seppi K, Tanner CM, Halliday GM, Brundin P, Volkmann J, et al. Parkinson Disease. *Nat Rev Dis Primers* (2017) 3(1):1–21. doi: 10.1038/nrdp.2017.13
2. Marsili L, Rizzo G, Colosimo C. Diagnostic Criteria for Parkinson's Disease: From James Parkinson to the Concept of Prodromal Disease. *Front Neurol* (2018) 9:156. doi: 10.3389/fneur.2018.00156
3. Lotharius J, Brundin P. Pathogenesis of Parkinson's Disease: Dopamine, Vesicles and α-Synuclein. *Nat Rev Neurosci* (2002) 3(12):932–42. doi: 10.1038/nrn983
4. Rezaei O, Nateghinia S, Estiar MA, Taheri M, Ghafouri-Fard S. Assessment of the Role of non-Coding Rnas in the Pathophysiology of Parkinson's Disease. *Eur J Pharmacol* (2021) 896:173914. doi: 10.1016/j.ejphar.2021.173914
5. Chodroff RA, Goodstadt L, Sirey TM, Oliver PL, Davies KE, Green ED, et al. Long Noncoding RNA Genes: Conservation of Sequence and Brain Expression Among Diverse Amniotes. *Genome Biol* (2010) 11(7):1–16. doi: 10.1186/gb-2010-11-7-r72
6. Yan W, Chen ZY, Chen JQ, Chen HM. Lncrna NEAT1 Promotes Autophagy in MPTP-Induced Parkinson's Disease Through Stabilizing PINK1 Protein. *Biochem Biophys Res Commun* (2018) 496(4):1019–24. doi: 10.1016/j.bbrc.2017.12.149
7. Lin Q, Hou S, Dai Y, Jiang N, Lin Y. Lncrna HOTAIR Targets Mir-126-5p to Promote the Progression of Parkinson's Disease Through RAB3IP. *Biol Chem* (2019) 400(9):1217–28. doi: 10.1515/hsz-2018-0431
8. Quan Y, Wang J, Wang S, Zhao J. Association of the Plasma Long non-Coding RNA MEG3 With Parkinson's Disease. *Front Neurol* (2020) 11. doi: 10.3389/fneur.2020.532891

9. Gholipour M, Taheri M, Mehvari Habibabadi J, Nazer N, Sayad A, Ghafouri-Fard S. Dysregulation of Lncrnas in Autoimmune Neuropathies. *Sci Rep* (2021) 11(1):1–9. doi: 10.1038/s41598-021-95466-w
10. Fallah H, Azari I, Neishabouri SM, Oskooei VK, Taheri M, Ghafouri-Fard S. Sex-Specific Up-Regulation of Lncrnas in Peripheral Blood of Patients With Schizophrenia. *Sci Rep* (2019) 9(1):1–8. doi: 10.1038/s41598-019-49265-z
11. Chen S, Wu D-D, Sang X-B, Wang L-L, Zong Z-H, Sun K-X, et al. The Lncrna HULC Functions as an Oncogene by Targeting ATG7 and ITGB1 in Epithelial Ovarian Carcinoma. *Cell Death Dis* (2017) 8(10):e3118–e. doi: 10.1038/cddis.2017.486
12. Niu XY, Huang HJ, Zhang JB, Zhang C, Chen WG, Sun CY, et al. Deletion of Autophagy-Related Gene 7 in Dopaminergic Neurons Prevents Their Loss Induced by MPTP. *Neuroscience* (2016) 339:22–31. doi: 10.1016/j.neuroscience.2016.09.037
13. Huang F, Chen W, Peng J, Li Y, Zhuang Y, Zhu Z, et al. Lncrna PVT1 Triggers Cyto-Protective Autophagy and Promotes Pancreatic Ductal Adenocarcinoma Development *via* the Mir-20a-5p/ULK1 Axis. *Mol Cancer* (2018) 17(1):98–. doi: 10.1186/s12943-018-0845-6
14. Xiu Y-L, Sun K-X, Chen X, Chen S, Zhao Y, Guo Q-G, et al. Upregulation of the Lncrna Meg3 Induces Autophagy to Inhibit Tumorigenesis and Progression of Epithelial Ovarian Carcinoma by Regulating Activity of ATG3. *Oncotarget* (2017) 8(19):31714–25. doi: 10.18632/oncotarget.15955
15. Chen W, Yang J, Fang H, Li L, Sun J. Relevance Function of Linc-ROR in the Pathogenesis of Cancer. *Front Cell Dev Biol* (2020) 8:696. doi: 10.3389/fcell.2020.00696
16. Huang J, Xu Y, Wang F, Wang H, Li L, Deng Y, et al. Long Noncoding RNA SPRY4-IT1 Modulates Ketamine-Induced Neurotoxicity in Human Embryonic Stem Cell-Derived Neurons Through EZH2. *Dev Neurosci* (2021) 43(1):9–17. doi: 10.1159/000513535
17. Niknafs YS, Han S, Ma T, Speers C, Zhang C, Wilder-Romans K, et al. The Lncrna Landscape of Breast Cancer Reveals a Role for DSCAM-AS1 in Breast Cancer Progression. *Nat Commun* (2016) 7(1):1–13. doi: 10.1038/ncomms12791
18. Costain WJ, Mishra RK. PLG Regulates Hnrnp-L Expression in the Rat Striatum and Pre-Frontal Cortex: Identification by Ddpcr. *Peptides* (2003) 24 (1):137–46. doi: 10.1016/S0196-9781(02)00286-3
19. Postuma RB, Berg D, Stern M, Poewe W, Olanow CW, Oertel W, et al. MDS Clinical Diagnostic Criteria for Parkinson's Disease. *Movement Disord Off J Movement Disord Soc* (2015) 30(12):1591–601. doi: 10.1002/mds.26424
20. Poewe W. Global Scales to Stage Disability in PD: The Hoehn and Yahr Scale. *Rating Scales Parkinsons Dis* (2012) 115–22. doi: 10.1093/med/9780199783106.003.0258
21. Arevalo-Rodriguez I, Smailagic N, Roqué I Figuls M, Ciapponi A, Sanchez-Perez E, Giannakou A, et al. Mini-Mental State Examination (MMSE) for the Detection of Alzheimer's Disease and Other Dementias in People With Mild Cognitive Impairment (MCI). *Cochrane Database Syst Rev* (2015) 2015(3): CD010783–CD. doi: 10.1002/14651858.CD010783.pub2
22. Ebersbach G, Baas H, Csoti I, Müngersdorf M, Deuschl G. Scales in Parkinson's Disease. *J Neurol* (2006) 253(4):iv32–5. doi: 10.1007/s00415-006-4008-0
23. Chen Y, Fu Y, Song Y-F, Li N. Increased Expression of Lncrna UCA1 and HULC is Required for Pro-Inflammatory Response During LPS Induced Sepsis in Endothelial Cells. *Front Physiol* (2019) 10:608. doi: 10.3389/fphys.2019.00608
24. Zhao Y, Guo Q, Chen J, Hu J, Wang S, Sun Y. Role of Long non-Coding RNA HULC in Cell Proliferation, Apoptosis and Tumor Metastasis of Gastric Cancer: A Clinical and *In Vitro* Investigation. *Oncol Rep* (2014) 31(1):358–64. doi: 10.3892/or.2013.2850
25. Li Y, Liu JJ, Zhou JH, Chen R, Cen CQ. Lncrna HULC Induces the Progression of Osteosarcoma by Regulating the Mir-372-3p/HMGB1 Signalling Axis. *Mol Med (Cambridge Mass)* (2020) 26(1):26. doi: 10.1186/s10020-020-00155-5
26. Singh S, Dikshit M. Apoptotic Neuronal Death in Parkinson's Disease: Involvement of Nitric Oxide. *Brain Res Rev* (2007) 54(2):233–50. doi: 10.1016/j.brainresrev.2007.02.001
27. Li W, Zheng Z, Chen H, Cai Y, Xie W. Knockdown of Long non-Coding RNA PVT1 Induces Apoptosis and Cell Cycle Arrest in Clear Cell Renal Cell Carcinoma Through the Epidermal Growth Factor Receptor Pathway. *Oncol Lett* (2018) 15(5):7855–63. doi: 10.3892/ol.2018.8315
28. Kim IS, Koppula S, Park SY, Choi DK. Analysis of Epidermal Growth Factor Receptor Related Gene Expression Changes in a Cellular and Animal Model of Parkinson's Disease. *Int J Mol Sci* (2017) 18(2):430. doi: 10.3390/ijms18020430
29. De Bortoli M, Miano V, Ferrero G, Annaratone L, Coscujuela L, Castellano I, et al. DSCAM-AS1, a Breast Cancer Specific and Estrogen Receptor Alpha-Dependent Long Noncoding RNA, is a Key Component of the Pathway Controlling Cell Growth and Migration. In: *Cancer Research*. PHILADELPHIA, PA: AMER ASSOC CANCER RESEARCH 615 CHESTNUT ST, 17TH FLOOR (2017).
30. Baraka AM, Korish AA, Soliman GA, Kamal H. The Possible Role of Estrogen and Selective Estrogen Receptor Modulators in a Rat Model of Parkinson's Disease. *Life Sci* (2011) 88(19-20):879–85. doi: 10.1016/j.lfs.2011.03.010
31. Gao H, Wang T, Zhang P, Shang M, Gao Z, Yang F, et al. Linc-ROR Regulates Apoptosis in Esophageal Squamous Cell Carcinoma *via* Modulation of P53 Ubiquitination by Targeting Mir-204-5p/MDM2. *J Cell Physiol* (2020) 235 (3):2325–35. doi: 10.1002/jcp.29139
32. Liu X, Hou L, Huang W, Gao Y, Lv X, Tang J. The Mechanism of Long non-Coding RNA MEG3 for Neurons Apoptosis Caused by Hypoxia: Mediated by Mir-181b-12/15-LOX Signaling Pathway. *Front Cell Neurosci* (2016) 10:201–. doi: 10.3389/fncel.2016.00201

Conflict of Interest: The authors declare that the research was conducted in the absence of any commercial or financial relationships that could be construed as a potential conflict of interest.

Publisher's Note: All claims expressed in this article are solely those of the authors and do not necessarily represent those of their affiliated organizations, or those of the publisher, the editors and the reviewers. Any product that may be evaluated in this article, or claim that may be made by its manufacturer, is not guaranteed or endorsed by the publisher.

frontiers in Immunology

ORIGINAL RESEARCH
published: 07 December 2021
doi: 10.3389/fimmu.2021.753929

Identification and Clinical Validation of Key Extracellular Proteins as the Potential Biomarkers in Relapsing-Remitting Multiple Sclerosis

*Meng Li, Hongping Chen, Pengqi Yin, Jihe Song, Fangchao Jiang, Zhanbin Tang, Xuehui Fan, Chen Xu, Yingju Wang, Yang Xue, Baichao Han, Haining Wang, Guozhong Li and Di Zhong**

Department of Neurology, First Affiliated Hospital, Harbin Medical University, Harbin, China

OPEN ACCESS

Edited by:
Maria Teresa Cencioni, Imperial College London, United Kingdom

Reviewed by:
Alice Mariottini, University of Florence, Italy
Yoshiki Takai, Tohoku University Hospital, Japan

***Correspondence:**
Di Zhong
sjnkzhongdi@163.com

Specialty section:
This article was submitted to Multiple Sclerosis and Neuroimmunology, a section of the journal Frontiers in Immunology

Received: *05 August 2021*
Accepted: *12 November 2021*
Published: *07 December 2021*

Citation:
Li M, Chen H, Yin P, Song J, Jiang F, Tang Z, Fan X, Xu C, Wang Y, Xue Y, Han B, Wang H, Li G and Zhong D (2021) Identification and Clinical Validation of Key Extracellular Proteins as the Potential Biomarkers in Relapsing-Remitting Multiple Sclerosis. Front. Immunol. 12:753929. doi: 10.3389/fimmu.2021.753929

Background: Multiple sclerosis (MS) is a demyelinating disease of the central nervous system (CNS) mediated by autoimmunity. No objective clinical indicators are available for the diagnosis and prognosis of MS. Extracellular proteins are most glycosylated and likely to enter into the body fluid to serve as potential biomarkers. Our work will contribute to the in-depth study of the functions of extracellular proteins and the discovery of disease biomarkers.

Methods: MS expression profiling data of the human brain was downloaded from the Gene Expression Omnibus (GEO). Extracellular protein-differentially expressed genes (EP-DEGs) were screened by protein annotation databases. GO and KEGG were used to analyze the function and pathway of EP-DEGs. STRING, Cytoscape, MCODE and Cytohubba were used to construct a protein-protein interaction (PPI) network and screen key EP-DEGs. Key EP-DEGs levels were detected in the CSF of MS patients. ROC curve and survival analysis were used to evaluate the diagnostic and prognostic ability of key EP-DEGs.

Results: We screened 133 EP-DEGs from DEGs. EP-DEGs were enriched in the collagen-containing extracellular matrix, signaling receptor activator activity, immune-related pathways, and PI3K-Akt signaling pathway. The PPI network of EP-DEGs had 85 nodes and 185 edges. We identified 4 key extracellular proteins IL17A, IL2, CD44, IGF1, and 16 extracellular proteins that interacted with IL17A. We clinically verified that IL17A levels decreased, but Del-1 and resolvinD1 levels increased. The diagnostic accuracy of Del-1 (AUC: 0.947) was superior to that of IgG (AUC: 0.740) with a sensitivity of 82.4% and a specificity of 100%. High Del-1 levels were significantly associated with better relapse-free and progression-free survival.

Conclusion: IL17A, IL2, CD44, and IGF1 may be key extracellular proteins in the pathogenesis of MS. IL17A, Del-1, and resolvinD1 may co-regulate the development of MS and Del-1 is a potential biomarker of MS. We used bioinformatics methods to explore the biomarkers of MS and validated the results in clinical samples. The study provides a theoretical and experimental basis for revealing the pathogenesis of MS and improving the diagnosis and prognosis of MS.

Keywords: relapsing-remitting multiple sclerosis, bioinformatics analysis, extracellular protein, protein-protein interactions, biomarkers

INTRODUCTION

Multiple sclerosis (MS), an autoimmune, chronic inflammatory demyelinating disease of the central nervous system, is the number one cause of neurological disability among adults, affecting women twice to three times as often as men (1–3). It is one of the main disability diseases in the global population (4). The clinical features of MS are dissemination in space and time (5). Relapsing-remitting multiple sclerosis (RRMS) mostly occurs in the early onset of MS patients, accounting for about 85% of all MS types. It is the initial phase of MS, which is characterized by reversible episodes of neurological deficits (known as relapsing) that often last for days or weeks, and can be completely relieved after the acute phase (known as remitting) (6). The pathogenesis of RRMS remains incompletely understood, but both genes and environment are believed to contribute (7). At present, it has been found that RRMS in mainly caused by cellular immunity, humoral immunity, and cellular crosstalk in which a variety of extracellular signaling molecules play an important role. They trigger central nervous system inflammation, making immune cell (mainly T cells, B cells, and macrophages) derived from peripheral blood move to the central nervous system and destruct the oligodendrocytes or neurons, resulting in demyelination and axonal damage eventually At present, it has been found that RRMS is mainly caused by cellular immunity, humoral immunity, and a variety of extracellular signaling molecules (8). They can trigger central nervous system inflammation, make immune cells (mainly T cells, B cells, and macrophages) move to the central nervous system, destruct oligodendrocytes or neurons with microglia, and cause demyelination and axonal damage eventually (3). Disease-modifying therapies have gradually been confirmed clinically to be effective in reducing the relapse of RRMS patients, implying that immune regulation plays an important role in RRMS (9). Up to now, subjected to the atypical clinical presentations, RRMS is still difficult to diagnose and lacks effective therapeutic targets. Therefore, the search for biological markers with high sensitivity and specificity is particularly important for studying disease pathogenesis, improving diagnosis, improving prognosis, and providing patients with more personalized treatment strategies.

In recent years, many studies have found that some molecules in the extracellular environment of CNS, mainly secreted proteins, have immunomodulatory effects (10). They are an essential component of the crosstalk between RRMS immune cells (11). Extracellular proteins can be detected in clinical tissues and some body fluids, they may be potential biomarkers or therapeutic targets of RRMS (12–15).

Bioinformatics analysis of transcriptional profiling from microarray is a new method to explore the pathogenesis of autoimmune disorders, identify disease biomarkers and discover therapeutic targets (16). Several MS transcriptomic profiling studies found that the gene expression profiles in peripheral blood of MS patients changed significantly, suggesting that differentially expressed mRNAs and proteins they encoded may be involved in the pathogenesis of MS (17, 18). Due to the scarcity of brain tissue samples from MS patients, there is not much analysis of brain tissue expression profiles in MS. However, the environment in which the lesions are located can most directly reflect the pathological process of the disease. Therefore, analyzing the brain tissue expression profile of MS patients is particularly important for studying the mechanism and biomarkers of MS.

The Gene Expression Omnibus (GEO) database contains the most disease microarray expression profile data so far (19). In this study, we downloaded the MS human brain tissue microarray gene expression profile (GSE5839) from the GEO database, and used R software to screen out the differentially expressed genes (DEGs) between MS human brain tissue and normal human brain tissue samples. Then we selected the extracellular protein-differentially expressed genes (EP-DEGs) from DEGs. Subsequently,we used Gene Ontology (GO) and Kyoto Encyclopedia of Genes and Genomes (KEGG) databases to perform biological function enrichment and pathway enrichment analysis of EP-DEGs. A protein-protein interaction (PPI) network of EP-DEGs had also been established to screen out functional modules and hub genes and extracellular molecules that interacted with hub genes. Finally, cerebrospinal fluid (CSF) samples of RRMS patients and control were collected to validate the expression of key EP-DEGs and their correlation with clinical data at the protein level. This study aims to identify key extracellular proteins that may be involved in the pathogenesis of RRMS, find biomarkers that can improve the diagnosis and prognosis of RRMS clinically, and explore new therapeutic targets.

MATERIALS AND METHODS

Data Acquisition and Processing

The NCBI GEO database (http://www.ncbi.nlm.nih.gov/geo) is an open-access platform for data. It contains the most microarray

chip and high-throughput sequencing gene expression profile data to date (20). We download the pre-processed MS human brain tissue microarray dataset (GSE5839) from GEO, which is established on Affymetrix Human Genome U133A Array (HG-U133A). The dataset contains 3 MS patients and 1 non-neurological control brain tissue sample (21). Patients are included according to 2017 McDonald diagnostic criteria, and the patients have not received immunomodulatory treatment. Exclusion criteria includes other inflammatory diseases or autoimmune disorders. We use the Biobase package to normalize the data. According to the annotation information on the platform, the probes are labeled with gene symbols, and multiple probes corresponding to the same gene are randomly selected to remove duplicates, and then the gene expression matrix is obtained.

Screening of DEGs and EP-DEGs

The limma package in R is currently a powerful method for analyzing DEGs (22). We used it to screen DEGs between patients and control in the GSE5839 dataset. $p<0.05$ and $|\log2$ fold change (FC)$| \geq 1$ were set as the threshold values of DEG identification. After that, we used the Uniprot database to download the extracellular protein gene list GO:0005576 and the Human Protein Atlas (HPA) protein annotation database to download the extracellular protein gene list (23, 24). The two lists were intersected with DEGs. We take the union of the results obtained by the two methods to screen out EP-DEGs, and then analyzed the differential expression of EP-DEGs between the MS group and the control group.

Functional Enrichment and Pathway Analysis of EP-DEGs

We used the enrichGO and enrichKEGG functions of the ClusterProfiler package in Bioconductor (http://bioconductor.org/packages/release/bioc/html/clusterProfer.html) to perform GO and KEGG enrichment analysis on EP-DEGs. Using the human genome as a background reference, choosing $P<0.05$ and count ≥ 2 as cut-off values, we identified the biological processes (BPs), cellular components (CCs), and molecular functions (MFs) of EP-DEGs. We divided EP-DEGs into up-regulated and down-regulated groups, then performed KEGG pathway enrichment analysis on them respectively. Using $P<0.05$ and count ≥ 2 as cut-off values, we identified the EP-DEGs enriched pathways. Finally, we used the dotplot and barplot in ClusterProfiler package to show the results of enrichment analysis.

Construction of the PPI Network of the EP-DEGs and Gene Expression Analysis

The STRING database (http://string-db.org) was used to assess protein-protein interactions (PPIs) in functional protein association network using core factors as query proteins. A PPI network of EP-DEGs was constructed on STRING11.0 (25). Cytoscape visualization was used, with a confidence score>0.4 and a hiding of the unconnected genes. To screen for interactions supported by published literature, we chose text mining evidence. Molecular Complex Detection (MCODE) was applied on Cytoscape to find functional clusters of genes in the PPI network with a degree cutoff=2, node score cutoff=0.2, k-core=2, and max depth=100 (26). The modules with established scores>5 were screened out. We used the CytoHubba plug-in in Cytoscape to find the Top10 node genes in 10 ways, and took the intersection to screen the hub genes. The MCC method is the most accurate in CytoHubba (27). From the selected hub genes, we selected the highest MCC score down-regulated hub gene IL17A as the key gene, and used CytoHubba to predict the first station gene that interacted with it.

Study Population and Clinical Data Collection

We collected 51 patients with RRMS in the First Affiliated Hospital of Harbin Medical University (Harbin, China) from January 2018 to December 2019, and 20 patients with primary headache as the controls. The entry criteria of the experimental group were strictly in accordance with the McDonald 2017 diagnostic criteria. The entry criteria of the control group were diagnosed according to the International Classification of Headache Disorders (ICHD3) criteria for primary headache (28). Both groups were excluded from patients with other demyelinating diseases, autoimmune diseases, CNS infectious diseases, infections in the past 30 days, or secondary headache. Patients who received immunomodulatory therapies before baseline sampling were excluded. Clinical data of patients were recorded, including name, gender, age, first symptoms, disease course, attack frequency, CSF oligoclonal bands, CSF IgG content, CSF white blood cell count (WBC) and CSF total protein content, to name but a few. Patients were followed up at admission, discharge, 1, 3, 6 months after discharge, and every 6 months for the next years. Study design and the purpose were explained for the participants and informed consent were obtained. The study was approved by the Ethics Committee of First Affiliated Hospital of Harbin Medical University.

Clinical Outcomes

Two clinical outcomes were used in this study. 1) Clinical relapse. 2) Disability progression. After 6 months from baseline, an EDSS score increase of ≥1 (if baseline EDSS>0) or 1.5 points (if baseline EDSS=0) was defined as disability progress. A new clinical relapse was defined as patient-reported symptoms or objectively observed signs typical for an acute inflammatory demyelinating event in the central nervous system with a duration of at least 24 h, and within one month, in the absence of fever or infection.

CSF Collection Analysis

Cerebrospinal fluid samples obtained by lumbar puncture were collected and stored at -80°C. Samples were immediately transferred into the tubes for ELISA detection. Del-1 (Wuhan Boster), IL17A (Shanghai Enzyme Immunoassay), and resolvinD1 (Shanghai Enzyme Immunoassay) ELISA kits were used to detect the content of Del-1, IL17A, and resolvinD1 in CSF respectively, two technical replicates (wells) for each sample. The protocols of ELISA were performed according to the kit's

instructions: dilute the standard, add 100μl of the sample to the wells of the ELISA kit, incubate the kit at 37°C for 90 minutes. add 100μl of biotin-labeled antibody to the working solution, incubate at 37°C for 60 minutes. Wash the plate, add 100μl of enzyme-labeled reagent, incubate at 37°C for 30 minutes. Wash the plate, add 90mul of color reagent to each well, incubate for 20 minutes at 37°C in the dark. Add 100μl of stop solution to each well to stop the reaction. Measure the OD values at 450 nm by a microplate reader. Calculate the actual content of CSF Del-1, IL17A, and resolvinD1 according to the equation. The flow chart for this study is shown in **Figure 1**.

Statistical Methods

Biobase package, limma package, ClusterProfiler package, pROC package of R and Cytoscape V3.8.2 software were used to analyze public gene expression data. SPSS V25.0 and GraphPad V8.0.2 software were used for statistical analysis of clinical data. The measurement data are described as mean±SD (normal distribution) or median (P25, P75). Two-tailed independent sample t-test or wilcoxon rank sum test were used to compare the mean difference between the two groups. Correlations were determined by Pearson or Spearman's analysis. TheAUC was used to evaluate the diagnostic performance of all models, and the differences were compared by the DeLong test. Relapse-free and progression-free survival curves were built using the Log-rank (Mantel-Cox) method. Difference were considered statistically significant at *p<0.05, **p<0.01, ***p<0.001.

RESULTS

Identification of DEGs

To compare the difference in gene expression between the MS group and the control group, differential gene expression analysis

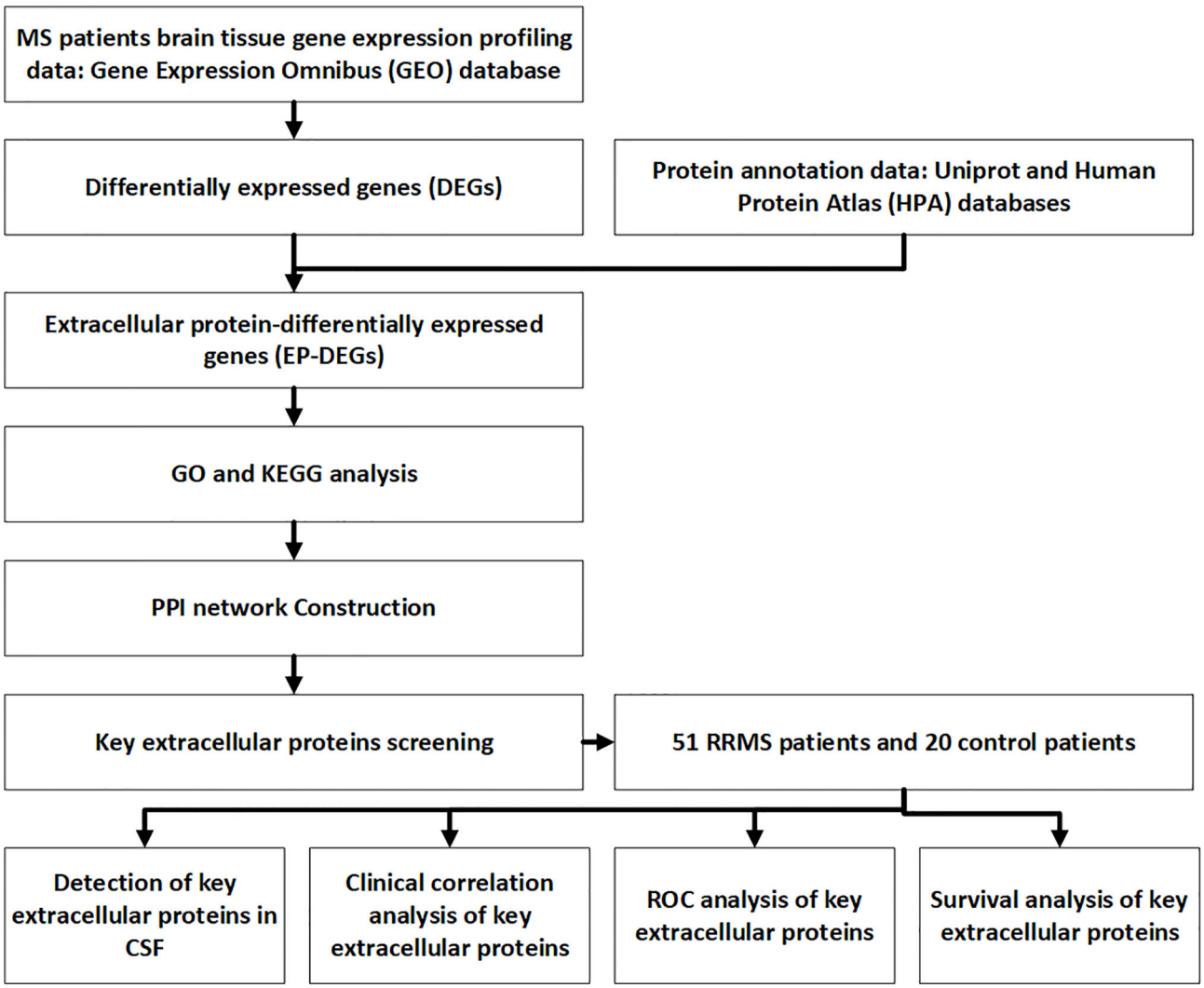

FIGURE 1 | Flow chart of the study.

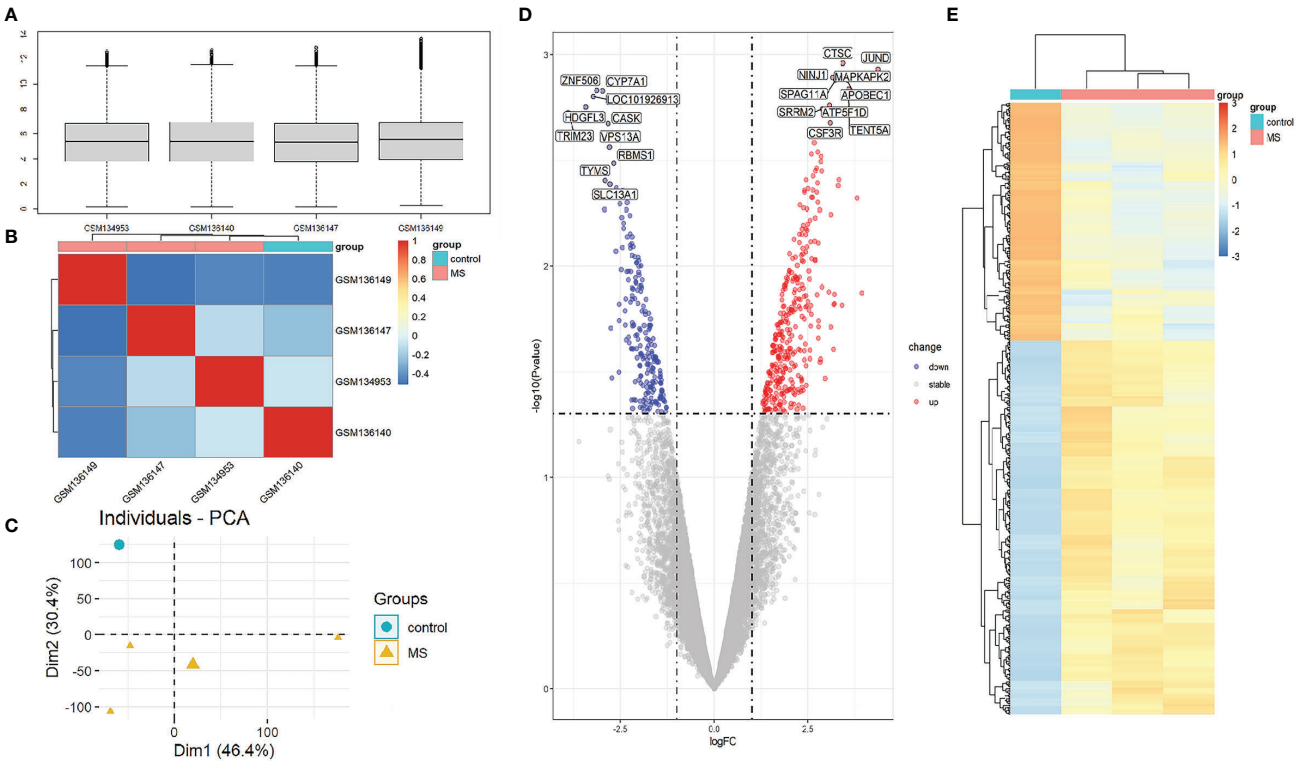

FIGURE 2 | Analysis of gene expression correlation and differential gene expression between MS group and control group in the dataset. **(A)** Boxplot of gene probe expression levels among samples. There was no significant difference in the median and the upper and lower quartile. **(B)** Correlation heatmap between samples. Compared with the control group, the intra-group correlation in the MS group was stronger. **(C)** PCA principal-component analysis. The center points of the MS group and the control group are far apart in space, indicating that the principal components are different. **(D)** Volcano map of all DEGs in the MS group and the control group analyzed by the limma R package. The top 10 up-regulated and down-regulated genes with the smallest P-value are marked on the map. **(E)** Heatmap of all DEGs in MS group and control group.

between samples was performed. The median, upper and lower quartiles, maximum and minimum values of the four sample genes in the GSE5839 data set are basically the same (**Figure 2A**). Correlation analysis showed that the intra-group correlation in the MS group was stronger (**Figure 2B**). Principal-component analysis showed that the center of the MS group and the control group were far apart,indicating that there were differences in gene expression between the MS group and the control group (**Figure 2C**). Differential gene expression analysis set |logFC|≥1 and P<0.05 as DEGs, and a total of 540 DEGs were screened (**Sup 1**). The top three up-regulated genes with the smallest P-value are CTSC, JUND, and NINJ1, and down-regulated genes are ZNF506, CYP7A1, and LOC101926913 (**Figure 2D**). The DEGs heat map showed that DEGs were consistently up-regulated or down-regulated in the MS group, which was significantly different from the control group (**Figure 2E**).

Screening of EP-DEGs

To find out the genes encoding extracellular proteins that are differentially expressed in the MS group and the control group, we refer to the annotated extracellular protein genes in existing public libraries, screen out EP-DEGs from DEGs and analyze them. The genes encoding extracellular proteins annotated in the HPA database were intersected with DEGs, and 69 EP-DEGs were screened out. The genes encoding extracellular proteins annotated in the Uniprot database were intersected with DEGs, and 132 EP-DEGs were screened out. The EP-DEGs obtained by these two methods were unionized, and only one gene was not overlapped. A total of 133 EP-DEGs were screened, 87 up-regulated and 46 down-regulated (**Figure 3A** and **Sup 2**). The top 10 up-regulated genes with the smallest P-value in the MS group and control group were CTSC, NINJ1, MAPKAPK2, SPAG11A, CSF3R, CTRB2, MERTK, PLEKHO2, NAGA and KRT13. The top 10 down-regulated genes were HDGFL3, KITLG, ANGPT4, ADCY1, OSM, SLC4A4, PSG5, ENPEP, MMP1 and FGF20 (**Figure 3B**, **Table 1** and **Sup 3**). The heatmap of EP-DEGs up-regulated and down-regulated in the first 30 with the smallest P-value shows that SLC4A4, IL17A, ADH6, OSM, and ADCY1 are significantly down-regulated in MS and the clustering distance is close (**Figure 3C**).

GO and KEGG Pathway Enrichment Analysis of EP-DEGs

To study the function of EP-DEGs, we performed GO and KEGG enrichment analysis on EP-DEGs. The enrichGO function in the ClusterProfiler package is used to enrich EP-DEGs from BP, CC

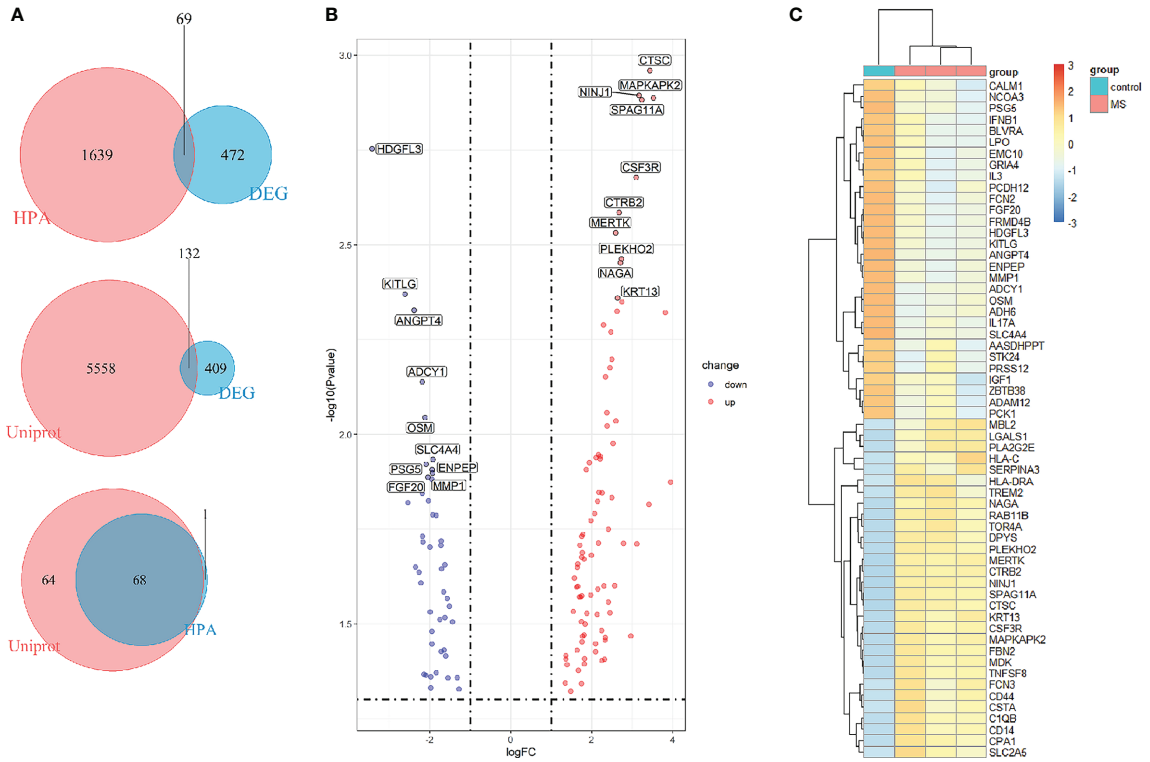

FIGURE 3 | Screening of differentially expressed genes encoding extracellular proteins. **(A)** The genes encoding extracellular proteins annotated in the HPA database were intersected with DEGs, 69 EP-DEGs were screened out. The genes encoding extracellular proteins annotated in the Uniprot database were intersected with DEGs, 132 EP-DEGs were screened out. The genes screened by the two methods were combined to obtain a total of 133 EP-DEGs. **(B)** Volcano map of EP-DEGs in MS group and control group. Mark the top 10 up-regulated and down-regulated genes with the smallest P-value. **(C)** Heatmap of the top 30 up-regulated and down-regulated EP-DEGs.

TABLE 1 | Top twenty EP-DEGs in RRMS human brain tissues (GSE5839).

symbol	logFC	AveExpr	P.Value
CTSC	3.433656544	4.538716532	0.001096231
NINJ1	3.164096409	5.651057054	0.001274412
MAPKAPK2	3.51814957	3.486609084	0.001296023
SPAG11A	3.231901028	3.959978671	0.001309249
CSF3R	3.092993263	4.424081607	0.002097986
CTRB2	2.672838909	4.437588589	0.002595307
MERTK	2.591990121	3.791989497	0.002937676
PLEKHO2	2.731264198	6.234314693	0.003439064
NAGA	2.70318136	4.290420426	0.003526288
KRT13	2.633039893	3.353291543	0.004368255
HDGFL3	-3.428978333	2.240764475	0.001763368
KITLG	-2.609629361	1.62774048	0.004262401
ANGPT4	-2.39160971	3.151151163	0.004698345
ADCY1	-2.187618912	3.19217583	0.007254208
OSM	-2.118575941	2.490019385	0.00901236
SLC4A4	-1.920336454	1.924320091	0.011628523
PSG5	-2.090113143	3.110487048	0.011968366
ENPEP	-1.945700755	1.611113762	0.012368029
MMP1	-1.931833585	1.672140212	0.012628526
FGF20	-2.048333614	2.481671697	0.012946904

and MF respectively. EP-DEGs were mainly enriched in positive regulation of cell adhesion, regulation of cell-cell adhesion of BPs, collagen-containing extracellular matrix of CCs, and signaling receptor activator activity and receptor-ligand activity of MFs (**Figure 4**). The cnetplot function in the ClusterProfiler package is used to display the genes enriched in the top 5 processes with the smallest P-value of BPs, CCs, and MFs. Among them, MDK, LGALS1, CD74, PYCARD, BMP7, IL2, IGF1, IL13, KITLG, ANGPT4, OSM, IL3, EDIL3, TNFSF8 are enriched in at least two aspects of BPs, CCs and MFs (**Figure 5**). With reference to the human genome, the enrichKEGG function in the ClusterProfiler package is used to enrich the up-regulated and down-regulated genes in the KEGG pathway respectively, and the up-regulated genes are enriched in Staphylococcus aureus infection, complement and coagulation cascades, cytokine-cytokine receptor interaction, and autoimmune thyroid disease. Down-regulated genes are enriched in the PI3K-Akt signaling pathway, pathways in cancer, rap1 signaling pathway, and ras signaling pathway (**Figures 6A, B**).

Establishment of PPI Network and Identification of Hub Genes

In order to study the interaction between the proteins corresponding to EP-DEGs, the STRING database was used to construct a PPI network of 133 EP-DEGs. Cytoscape software was used to visualize the total PPI network (**Figure 7A**). The PPI network consists of 85 nodes and 185 edges. The darker the color and the wider the edge, the stronger the evidence for the interaction between proteins (see **Supplementary Figure 2** for the legend). The MCODE plug-in in Cytoscape is used to construct functional modules. The results show that there is only one module with an established score>5, consisting of 9 genes and 34 edges (**Figure 7B**). The 10 topological methods of the CytoHubba plug-in in Cytoscape were used to screen top10 hub genes. There are 4 genes in all 10 methods, namely IL17A, IL2, CD44, IGF1 (**Table 2** and **Figure 7C**). IL17A is the gene that exists in the functional module, and the down-regulated gene with the highest score in the MCC method (the most accurate method) (27). CytoHubba was used to construct the first node gene to interact with IL17A. A total of 16 genes were screened out (**Figure 7D**), 10 were up-regulated and 6 were down-regulated.

Levels of IL17A, Del-1 and ResolvinD1 and Their Correlation With Clinical Data

In order to verify the key extracellular proteins identified, 51 RRMS patients and 20 patients with primary headache who excluded CNS infectious diseases and recent infections were included (see **Tables 3**, **4** and **Supplementary Material 10** for patient baseline data), and the patients' CSF was collected to detect IL17A, Del-1 (encoded by the EDIL3 gene) levels. It has been reported in the literature that there is a regulatory relationship between IL17A, Del-1 and resolvinD1, so the level of resolvinD1 in the CSF of RRMS patients was also detected (29). Del-1 and resolvinD1 levels were elevated in RRMS patients, and IL17A levels were reduced in RRMS patients (**Figures 8A–C**). Correlation analysis of the three extracellular molecules and clinical indicators revealed that the level of resolvinD1 was positively correlated with Del-1 in the CSF of RRMS patients, and the level of resolvinD1 was negatively correlated with protein and IgA (**Figures 8D–F**).

Del-1 Diagnostic Efficacy and Survival Analysis

In order to study the predictive effect of Del-1 on the diagnosis and prognosis of RRMS, ROC curve and survival analysis were

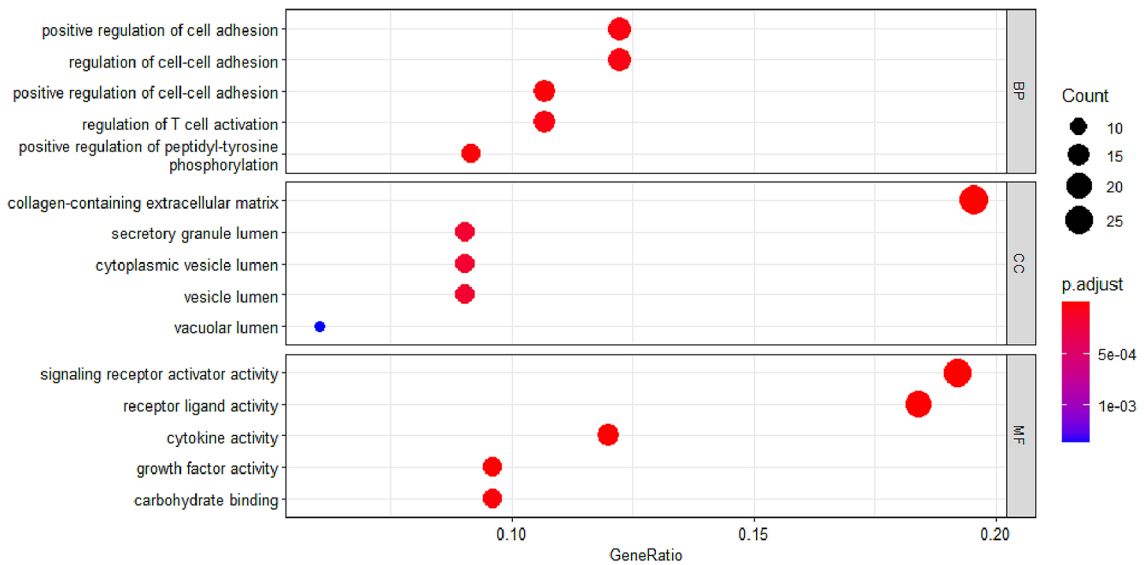

FIGURE 4 | GO enrichment of EP-DEGs. The dotplots show the Top5 processes enriched by EP-DEGs in BPs, CCs and MFs.

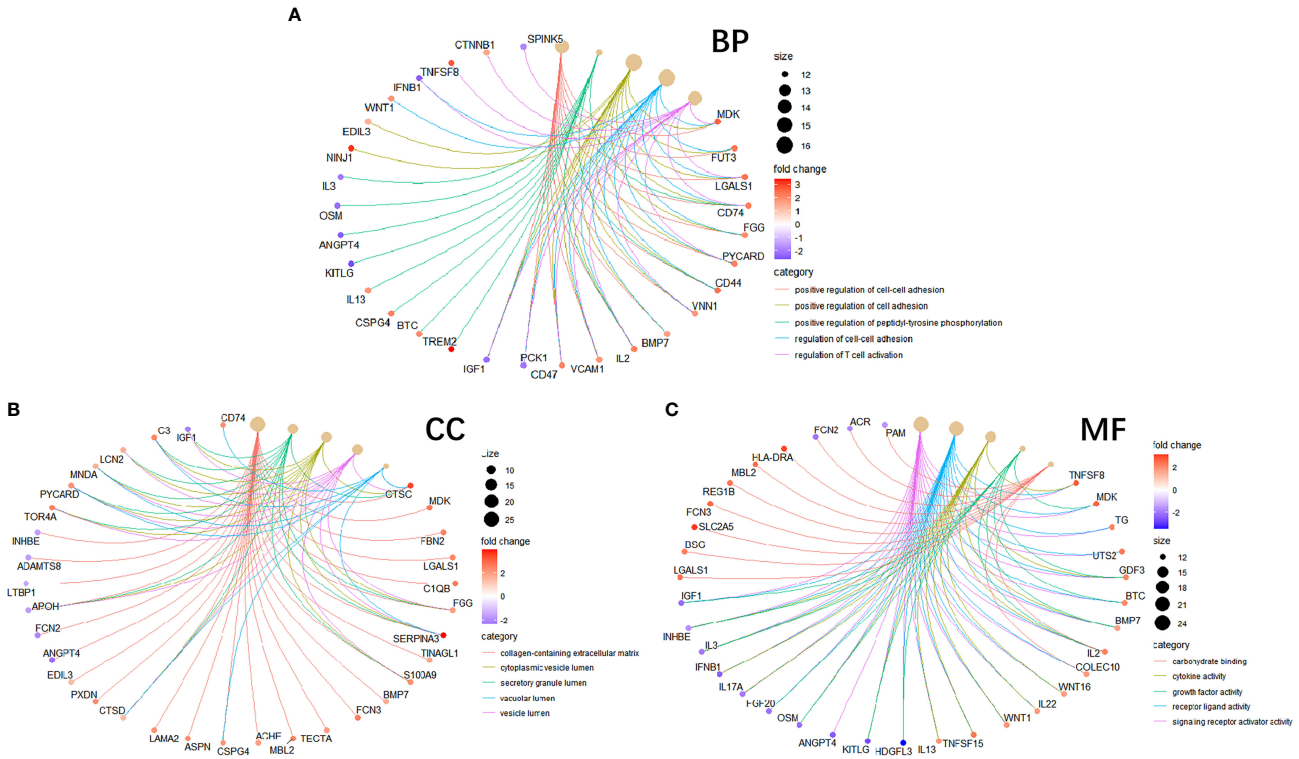

FIGURE 5 | Circle graph in GO enrichment of EP-DEGs. **(A–C)** The circle graph shows the EP-DEGs enriched in the Top5 GO categories of BPs, CCs, and MFs, respectively. The yellow points represent the GO categories, the color of the line delivered by a point indicates the category of the point in the legend, the size of a point indicates the number of the genes it includes.

performed. Del-1 had high accuracy in the diagnosis of RRMS (AUC = 0.947, 95%CI = 0.898-0.996), and IgG had certain accuracy in the diagnosis of RRMS (AUC = 0.740, 95%CI = 0.623-0.857) (**Figure 9A**), In the diagnostic model of RRMS, the diagnostic efficacy of Del-1 was better than that of IgG, and the result was statistically significant (DeLong's test, P = 0.002). The cut-off value of Del-1 was 1623.882pg/ml, the Sensitivity% corresponding to this cut-off value was 82.4%, and the Specificity% was 100%. Del-1 was divided into high and low groups according to the median, and survival analysis was performed in RRMS patients (**Figures 9B, C**). The results showed that the median relapse-free survival time in the high Del-1 group was 30 months, and the median relapse-free survival time in the low Del-1 group was 13.5 months, the difference was statistically significant [HR=1.89(0.89-3.59)], P=0.044). The probability of progression-free survival in the high Del-1 group

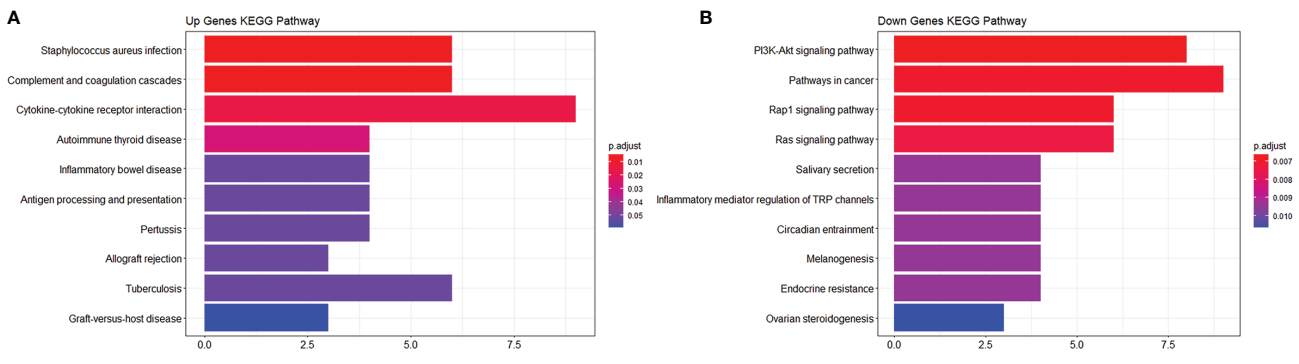

FIGURE 6 | KEGG enrichment analysis of EP-DEGs. **(A, B)** respectively show the pathways to which up-regulated genes and down-regulated genes are enriched.

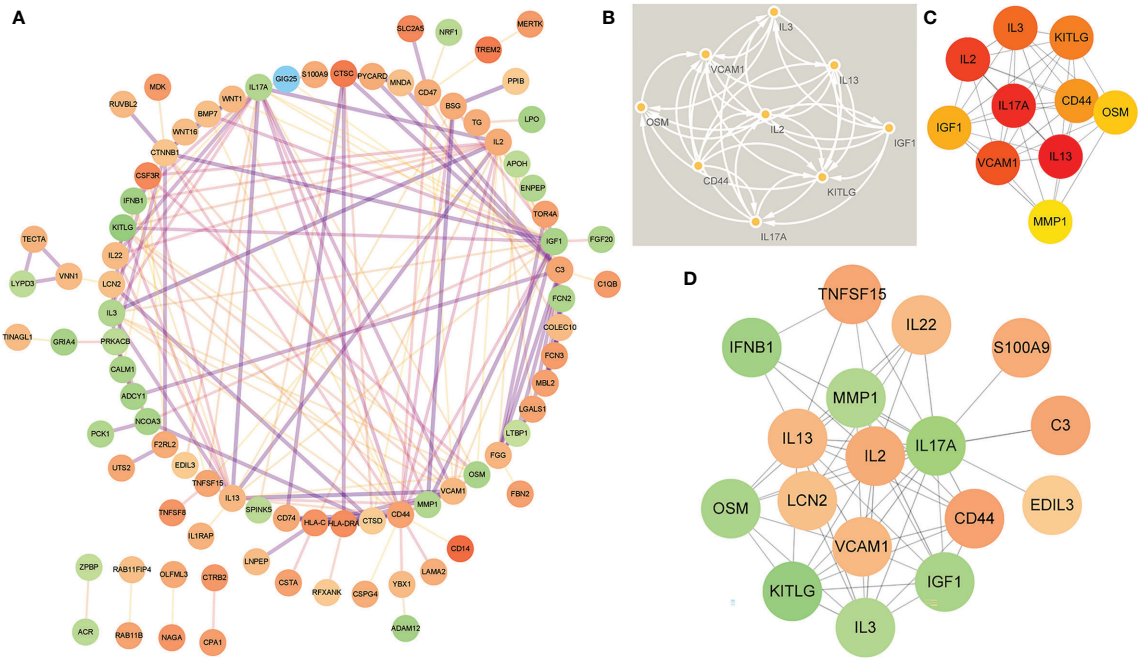

FIGURE 7 | Construction of PPI network of EP-DEGs and screening of hub genes. **(A)** The STRING database is used to construct the PPI network of EP-DEGs, with 85 nodes and 185 edges (the legend is in the **Supplementary Material**). **(B)** The node gene cluster with the highest score constructed by the MCODE plug-in in Cytoscape consists of 9 genes. **(C)** The Cytohubba is used to construct the Top10 hub genes. The figure shows the Top10 hub genes constructed by the MCC method. **(D)** The Cytohubba was used to predict the first stop node genes that interact with IL17A. A total of 16 genes were predicted, 10 up-regulated and 6 down-regulated.

was always higher than 50% during the follow-up period, and the median progression-free survival time in the high Del-1 group was 46 months, the difference was statistically significant [HR=3.46(1.21-9.86)], P=0.034).

DISCUSSION

Biological Processes in Which EP-DEGs May Participate in MS

We analyzed the GSE5839 dataset and obtained a total of 541 DEGs. Among the top 3 up-regulated and top 3 down-regulated genes, only 2 genes were marked as extracellular proteins in the Genecards database. Because some nuclear proteins and cytoplasmic proteins cannot be detected in the body fluids of clinical patients, this analysis method did not focus on finding intracellular biomarkers of the disease. We compared DEGs with extracellular protein gene lists in the protein annotation database Uniprot and HPA, and a total of 133 EP-DEGs were screened. We compared the EP-DEGs obtained from the two databases. It was interesting that 68 of the 69 EP-DEGs selected from the HPA database overlapped with Uniprot, and only 1 gene did not overlap, which reflected these two database had good consistency in the annotation of extracellular proteins. GO enrichment showed that EP-DEGs were enriched in collagen-containing extracellular matrix, signaling receptor activator activity,

TABLE 2 | Top10 EP-DEGs by 10 topological analysis methods of CytoHubba.

MCC	MNC	Degree	EPC	BottleNeck	EcCentricity	Closeness	Radiality	Betweeness	Stress
IL13	IL2	CD44	IL2	IL2	IL2	CD44	IL2	CD44	CD44
IL17A	CD44	IL2	IL17A	CD44	CD44	IL2	CD44	C3	IL2
IL2	IL13	IGF1	CD44	IGF1	IGF1	IL17A	IL17A	IL2	C3
VCAM1	IL17A	IL13	IL13	C3	C3	IGF1	IGF1	IGF1	IGF1
IL3	VCAM1	IL17A	IGF1	CTNNB1	IL17A	VCAM1	VCAM1	IL17A	IL17A
KITLG	IGF1	C3	VCAM1	IL17A	IL13	IL13	IL13	CTNNB1	CTNNB1
CD44	IL3	VCAM1	IL3	IL13	VCAM1	C3	IL3	CD47	CD47
IGF1	KITLG	CTNNB1	KITLG	CTSD	CSF3R	IL3	C3	LCN2	VCAM1
OSM	OSM	IL3	OSM	CD47	IL3	CTNNB1	KITLG	IL13	LCN2
MMP1	MMP1	KITLG	MMP1	VCAM1	KITLG	KITLG	MMP1	PRKACB	IL3

TABLE 3 | Clinicopathological characteristics of RRMS patients and control samples (N = 71).

Patient demographics and laboratory information	RRMS (N = 51)	Control (N = 20)	P value
Average age	36.12±10.28	37.90±13.19	0.547
Sex (female)	39 (76.47%)	15 (75.00%)	0.238
Oligoclonal band positive	20 (39.2%)	0	0.001**
CSF IgG (mg/L)	32.7 (21.9-54.5)	20.2 (14.85-28.3)	0.002**
CSF IgA (mg/L)	2.85 (1.76-4.14)	2.23 (1.4-2.67)	0.056
CSF IgM (mg/L)	0.45 (0.29-0.89)	0.32 (0.23-0.41)	0.049*
CSF Alb (mg/L)	172 (138-204)	162.5 (124.5-199)	0.494
CSF total cell count (10^6/L)	5 (0-10)	1 (0-6.5)	0.122
CSF WBC count (10^6/L)	1 (0-4)	0 (0-1.5)	0.26
CSF protein (mg/L)	328.53 (282.84-403.98)	287.52 (238.04-351.98)	0.089

*$p < 0.05$, **$p < 0.01$.

receptor-ligand activity and positive regulation of cell adhension processes. This indicated that extracellular proteins might be mainly secreted into the extracellular matrix by specific cells in the pathological process of MS. They bound to receptors on specific cells as ligands, transmitted signals for cell-to-cell communication, and mediate processes such as cell migration and adhesion. The GO enrichment circle map shows that MDK, LGALS1, CD74, PYCARD, BMP7, IL2, IGF1, IL13, KITLG, ANGPT4, OSM, IL3, EDIL3, and TNFSF8 were enriched in multiple biological processes. These genes might play a more important role in MS. KEGG enrichment analysis showed that up-regulated EP-DEGs were mainly enriched in certain inflammatory pathways, complement pathways and cytokine-cytokine receptor pathways. The result indicated that extracellular proteins in MS might be mainly some cytokines, which mainly activated immunity-related pathways. Down-regulation of EP-DEGs mainly enriched in PI3K-Akt signaling pathway. Studies had found that the PI3K-Akt signaling pathway played an immune-regulatory role in the development of regulatory T cells (30) and the inflammation process of periodontitis (29). An FTY720 analog in the EAE model could inhibit the progression of inflammation by inhibiting the PI3K-Akt signaling pathway (31). These results collectively suggested that the PI3K-Akt signaling pathway might play a regulatory role in the progression of MS inflammation.

IL17A and EDIL3 May Be the Key Extracellular Proteins in the Pathogenesis of MS

After analyzing the PPI network of EP-DEGs, we found that IL17A, IL2, CD44, and IGF1 were simultaneously present in the Top10 hub genes screened by 10 CytoHubba topology methods and the functional gene modules constructed by MCODE. The involvement of IL17A in the pathological process of MS has been confirmed (32), but the changes of IL17A content in the serum and CSF of MS patients are controversial. Increases in IL17A in the acute phase of MS have commonly been reported (33), but other studies have found no changes or even reductions (13). The results of this study showed that the expression of IL17A was down-regulated, and the verification at the protein level also showed that IL17A was down-regulated. The patients included in this study were not in the active acute phase, so we speculate that IL17A levels may increase in the early stage of MS inflammation, and IL17A levels gradually decrease as the inflammation subsides, but this speculation needs to be further verified.

Del-1 Could Be Related to the Relapse and Progression of RRMS

The extracellular environment of the brain and spinal cord is CSF. There are a large number of extracellular proteins in CSF that act as messengers to transmit signals (34). Therefore, we detected the levels of IL17A, Del-1 and resolvinD1 in the CSF of MS patients to verify the key extracellular proteins predicted by bioinformatics analysis. The levels of IL17A decreased, the levels of Del-1 and resolvinD1 increased, the trend was consistent with the prediction. Del-1 and resolvinD1 levels were positively correlated, Del-1 and IL17A levels exhibited the opposite trends. The results were consistent with previous literature reports, suggesting that Del-1, IL17A and resolvinD1 might interact with each other to regulate the occurrence and

TABLE 4 | Baseline characteristics of RRMS patients (N = 51).

Patient baseline characteristics	Enrolled RRMS patients (N = 51)
Frequency of relapses/year	0.91±0.76
Disease duration at admission	2.93±3.52
EDSS score at admission	1.17±0.51
Disease Course/day (from this relapse date to lumber puncture date)	18.49±18.37
Comorbidities	
History of hypertension,n (%)	6 (11.76)
History of diabetes,n (%)	0

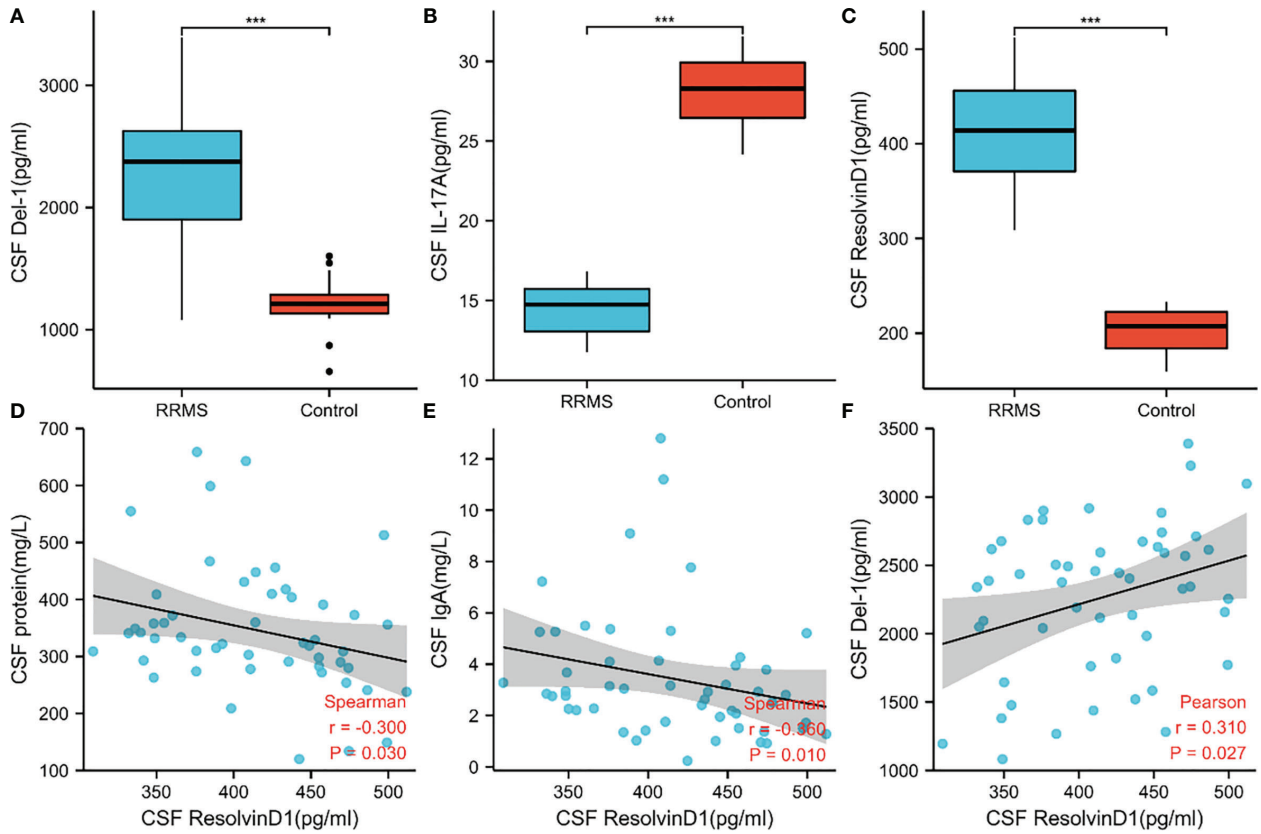

FIGURE 8 | Levels of IL17A, Del-1, and resolvinD1 in CSF of RRMS patients and their correlation with clinical data. **(A–C)** Del-1 and resolvinD1 levels were elevated in RRMS patients, and IL17A level were reduced in RRMS patients. **(D–F)** ResolvinD1 was positively correlated with Del-1, resolvinD1 was negatively correlated with protein and IgA. ***p < 0.001.

development of MS. Moreover, Del-1 had high accuracy in the diagnosis and prognostic stratification of MS, suggesting that Del-1 might be helpful to the diagnosis of MS. Compared to the high Del-1 group, the median relapse-free survival time and median progression-free survival time in the low Del-1 group was lower, indicating that the baseline Del-1 levels may be related to the relapse and progression of the disease. Whether the patients received immunomodulatory therapies, age, sex, sleep and stress might be the potential confounders in survival analysis. Additionally, no differences in age or sex existed between the groups, moreover, we excluded the patients who had ever received immunomodulatory therapies, which might be the potential confounders in survival analysis, therefore, these aspects may not affect the results. Other aspects are needed to be investigated in detail in the following studies.

Limitations

This study has some limitations. At present, most of the MS gene expression data in the publically available datasets comes from human peripheral blood, and the human brain tissue gene expression data is relatively few, so the small sample sizes may cause bias in the results. In the future, more MS human brain tissue expression profiles will be needed for further analysis. In the process of screening extracellular proteins, two protein annotation databases were used, but the evidence for protein localization of these annotation databases is mainly derived from published literature. The evidence is not complete, and some extracellular proteins may be missed. We validated the key EP-DEGs at the protein level, not at the transcription level. Because the trends of gene changes at the transcription level may not be fully consistent with the trends at the protein level, the potential mechanism needs to be further explored.

CONCLUSION

In this study, 1) we analyzed the gene expression profiles of MS human brain tissue and screened out 133 EP-DEGs. 2) We predicted the biological processes and pathways they participate in. 3) We also predicted 4 key extracellular proteins and 16 extracellular proteins that may interact with IL17A. 4) We validated the levels of IL17A, Del-1, and resolvinD1 in clinical

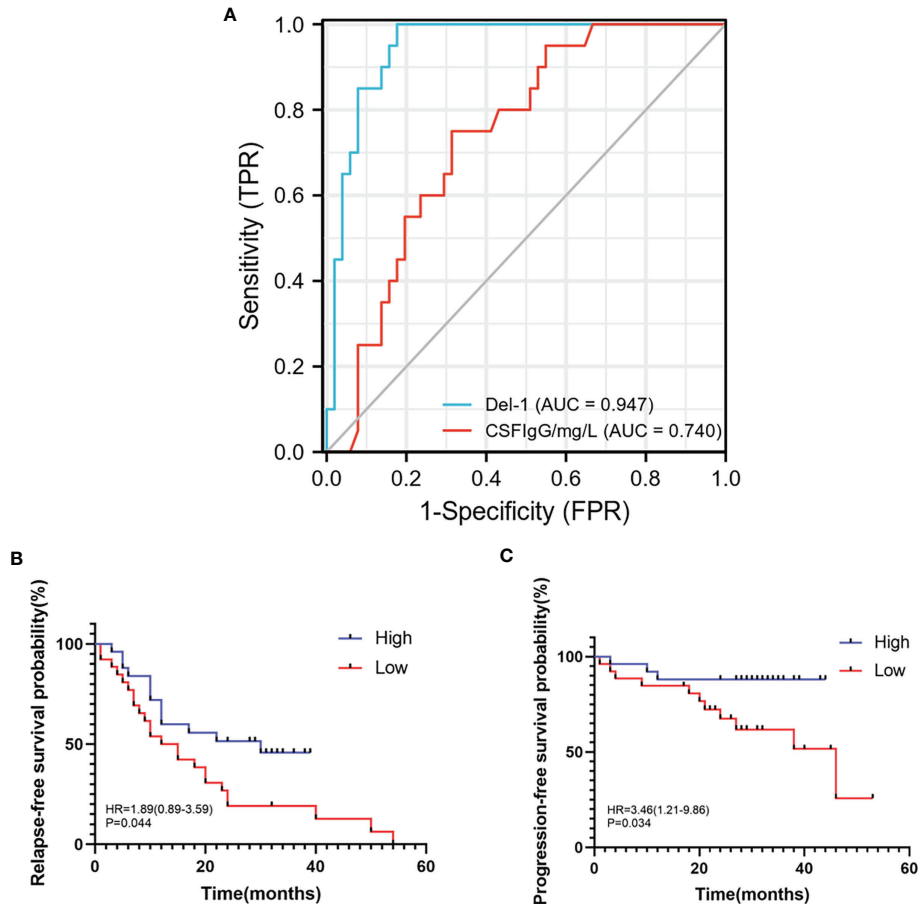

FIGURE 9 | ROC, relapse-free survival, progression-free survival curves of Del-1 in RRMS. **(A)** The area under the ROC curve of Del-1 (AUC=0.947), which is higher than that of IgG (AUC=0.740). **(B)** The median relapse-free survival time was 30 months in the high Del-1 group, the median relapse-free survival time was 13.5 months in the low Del-1 group, the difference was statistically significant (P=0.044). **(C)** The probability of progression-free survival in the high Del-1 group was always higher than 50% during the follow-up period, and the median progression-free survival time in the low Del-1 group was 46 months, the difference was statistically significant (P=0.034).

samples, performed survival analysis on Del-1, and found that Del-1 may be related to the relapse and progression of RRMS. The purpose of this study is to provide bioinformatics and clinical evidence for the discovery of potential biomarkers of MS.

DATA AVAILABILITY STATEMENT

Publicly available datasets were analyzed in this study. This data can be found here: https://www.ncbi.nlm.nih.gov/geo/query/acc.cgi?acc=GSE5839, NCBI GEO GSE5839.

ETHICS STATEMENT

The studies involving human participants were reviewed and approved by The Ethics Committee of First Affiliated Hospital of Harbin Medical University (No. 2019118). The patients/participants provided their written informed consent to participate in this study. Written informed consent was obtained from the individual(s) for the publication of any potentially identifiable images or data included in this article.

AUTHOR CONTRIBUTIONS

ML conceived the idea, searched relevant information, and performed all bioinformatics analysis. Then ML collected the CSF of RRMS patients and control group patients, detected the levels of extracellular proteins by ELISA and followed up the patients. JS, FJ, and ZT helped ML to collect the CSF, and XF, CX, YW, BH, and HW helped ML to record and arrange the clinical data. Finally, ML drafted and finalized the article. DZ has been committed to studying the molecular immunomodulation effects in neuro-autoimmune diseases. She proposed the point that we should search for more

detected biomarkers in body fluids of MS patients to improve the diagnosis and prognosis of MS. DZ reviewed and revised the manuscript many times. GL contributed to this manuscript by setting follow-up schedules, providing suggestions to reviewers' comments, and modifying the manuscript. HC, PY, and YX reviewed the manuscript and provided many comments. All authors agree to be accountable for the content of the work. All authors contributed to the article and approved the submitted version.

FUNDING

This work was supported by the National Natural Science Foundation of China (No. 81873773) and the Foundation of the First Affiliated Hospital of Harbin Medical University, China (Grant No. 2019M18).

ACKNOWLEDGMENTS

The authors gratefully acknowledge the data provided by patients and researchers participating in GEO.

SUPPLEMENTARY MATERIAL

The Supplementary Material for this article can be found online at: https://www.frontiersin.org/articles/10.3389/fimmu.2021.753929/full#supplementary-material

REFERENCES

1. Teunissen CE, Dijkstra C, Polman C. Biological Markers in CSF and Blood for Axonal Degeneration in Multiple Sclerosis. *Lancet Neurol* (2005) 4(1):32–41. doi: 10.1016/s1474-4422(04)00964-0
2. Disorders GNGroup., C. Global, Regional, and National Burden of Neurological Disorders During 1990-2015: A Systematic Analysis for the Global Burden of Disease Study 2015. *Lancet Neurol* (2017) 16(11):877–97. doi: 10.1016/s1474-4422(17)30299-5
3. Reich DS, Lucchinetti CF, Calabresi PA. Multiple Sclerosis. *N Engl J Med* (2018) 378(2):169–80. doi: 10.1056/NEJMra1401483
4. Mansilla MJ, Presas-Rodríguez S, Teniente-Serra A, González-Larreategui I, Quirant-Sánchez B, Fondelli F, et al. Paving the Way Towards an Effective Treatment for Multiple Sclerosis: Advances in Cell Therapy. *Cell Mol Immunol* (2021) 18(6):1353–74. doi: 10.1038/s41423-020-00618-z
5. Thompson AJ, Banwell BL, Barkhof F, Carroll WM, Coetzee T, Comi G, et al. Diagnosis of Multiple Sclerosis: 2017 Revisions of the McDonald Criteria. *Lancet Neurol* (2018) 17(2):162–73. doi: 10.1016/s1474-4422(17)30470-2
6. Filippi M, Bar-Or A, Piehl F, Preziosa P, Solari A, Vukusic S, et al. Multiple Sclerosis. *Nat Rev Dis Primers* (2018) 4(1):43. doi: 10.1038/s41572-018-0041-4
7. Consortium., I.M.S.G. Low-Frequency and Rare-Coding Variation Contributes to Multiple Sclerosis Risk. *Cell* (2018) 175(6):1679–87.e1677. doi: 10.1016/j.cell.2018.09.049
8. Akbarian F, Tabatabaiefar MA, Shaygannejad V, Shahpouri MM, Badihian N, Sajjadi R, et al. Upregulation of MTOR, RPS6KB1, and EIF4EBP1 in the Whole Blood Samples of Iranian Patients With Multiple Sclerosis Compared to Healthy Controls. *Metab Brain Dis* (2020) 35(8):1309–16. doi: 10.1007/s11011-020-00590-7
9. Biolato M, Bianco A, Lucchini M, Gasbarrini A, Mirabella M, Grieco A. The Disease-Modifying Therapies of Relapsing-Remitting Multiple Sclerosis and Liver Injury: A Narrative Review. *CNS Drugs* (2021) 35(8):861–80. doi: 10.1007/s40263-021-00842-9
10. Hu WT, Howell JC, Ozturk T, Gangishetti U, Kollhoff AL, Hatcher-Martin JM, et al. CSF Cytokines in Aging, Multiple Sclerosis, and Dementia. *Front Immunol* (2019) 10:480. doi: 10.3389/fimmu.2019.00480
11. Ransohoff RM. Immune-Cell Crosstalk in Multiple Sclerosis. *Nature* (2018) 563(7730):194–5. doi: 10.1038/d41586-018-07063-z
12. Raphael I, Webb J, Stuve O, Haskins W, Forsthuber T. Body Fluid Biomarkers in Multiple Sclerosis: How Far We Have Come and How They Could Affect the Clinic Now and in the Future. *Expert Rev Clin Immunol* (2015) 11(1):69–91. doi: 10.1586/1744666x.2015.991315
13. Bai Z, Chen D, Wang L, Zhao Y, Liu T, Yu Y, et al. Cerebrospinal Fluid and Blood Cytokines as Biomarkers for Multiple Sclerosis: A Systematic Review and Meta-Analysis of 226 Studies With 13,526 Multiple Sclerosis Patients. *Front Neurosci* (2019) 13:1026. doi: 10.3389/fnins.2019.01026
14. Deisenhammer F, Zetterberg H, Fitzner B, Zettl UK. The Cerebrospinal Fluid in Multiple Sclerosis. *Front Immunol* (2019) 10:726. doi: 10.3389/fimmu.2019.00726
15. Paul A, Comabella M, Gandhi R. Biomarkers in Multiple Sclerosis. *Cold Spring Harb Perspect Med* (2019) 9(3):a029058. doi: 10.1101/cshperspect.a029058
16. Mendiola AS, Ryu JK, Bardehle S, Meyer-Franke A, Ang KK, Wilson C, et al. Transcriptional Profiling and Therapeutic Targeting of Oxidative Stress in Neuroinflammation. *Nat Immunol* (2020) 21(5):513–24. doi: 10.1038/s41590-020-0654-0
17. Hundeshagen A, Hecker M, Paap BK, Angerstein C, Kandulski O, Fatum C, et al. Elevated Type I Interferon-Like Activity in a Subset of Multiple Sclerosis Patients: Molecular Basis and Clinical Relevance. *J Neuroinflamm* (2012) 9:140. doi: 10.1186/1742-2094-9-140
18. Nickles D, Chen HP, Li MM, Khankhanian P, Madireddy L, Caillier SJ, et al. Blood RNA Profiling in a Large Cohort of Multiple Sclerosis Patients and Healthy Controls. *Hum Mol Genet* (2013) 22(20):4194–205. doi: 10.1093/hmg/ddt267
19. Barrett T, Troup DB, Wilhite SE, Ledoux P, Evangelista C, Kim IF, et al. NCBI GEO: Archive for Functional Genomics Data Sets–10 Years on. *Nucleic Acids Res* (2011) 39(Database issue):D1005–10. doi: 10.1093/nar/gkq1184
20. Barrett T, Wilhite SE, Ledoux P, Evangelista C, Kim IF, Tomashevsky M, et al. NCBI GEO: Archive for Functional Genomics Data Sets–Update. *Nucleic Acids Res* (2013) 41(Database issue):D991–5. doi: 10.1093/nar/gks1193
21. Padden M, McQuaid S, Brankin B. P9: Microarray Analysis of Brain Tissue From Multiple Sclerosis and Non-Neurological Control Samples. *J Anat* (2004) 205(6):530. doi: 10.1016/j.jneuroim.2004.03.011
22. Ritchie ME, Phipson B, Wu D, Hu Y, Law CW, Shi W, et al. Limma Powers Differential Expression Analyses for RNA-Sequencing and Microarray Studies. *Nucleic Acids Res* (2015) 43(7):e47. doi: 10.1093/nar/gkv007
23. Uhlén M, Fagerberg L, Hallström BM, Lindskog C, Oksvold P, Mardinoglu A, et al. Proteomics. Tissue-Based Map of the Human Proteome. *Science* (2015) 347(6220):1260419. doi: 10.1126/science.1260419
24. Consortium., T.U. UniProt: The Universal Protein Knowledgebase in 2021. *Nucleic Acids Res* (2021) 49(D1):D480–9. doi: 10.1093/nar/gkaa1100
25. Szklarczyk D, Gable AL, Lyon D, Junge A, Wyder S, Huerta-Cepas J, et al. STRING V11: Protein-Protein Association Networks With Increased Coverage, Supporting Functional Discovery in Genome-Wide Experimental Datasets. *Nucleic Acids Res* (2019) 47(D1):D607–13. doi: 10.1093/nar/gky1131
26. Bader GD, Hogue CW. An Automated Method for Finding Molecular Complexes in Large Protein Interaction Networks. *BMC Bioinf* (2003) 4:2. doi: 10.1186/1471-2105-4-2
27. Chin CH, Chen SH, Wu HH, Ho CW, Ko MT, Lin CY. Cytohubba: Identifying Hub Objects and Sub-Networks From Complex Interactome. *BMC Syst Biol* (2014) 8(Suppl 4):S11. doi: 10.1186/1752-0509-8-s4-s11
28. (IHS)., H.C.C.o.t.I.H.S. Headache Classification Committee of the International Headache Society (IHS) The International Classification of Headache Disorders, 3rd Edition. *Cephalalgia* (2018) 38(1):1–211. doi: 10.1177/0333102417738202
29. Maekawa T, Hosur K, Abe T, Kantarci A, Ziogas A, Wang B, et al. Antagonistic Effects of IL-17 and D-Resolvins on Endothelial Del-1

Expression Through a GSK-3beta-C/EBPbeta Pathway. *Nat Commun* (2015) 6:8272. doi: 10.1038/ncomms9272
30. Pompura SL, Dominguez-Villar M. The PI3K/AKT Signaling Pathway in Regulatory T-Cell Development, Stability, and Function. *J Leukoc Biol* (2018) 103:1065–76. doi: 10.1002/jlb.2mir0817-349r
31. da Silva LC, Lima IVA, da Silva MCM, Corrêa TA, de Souza VP, de Almeida MV, et al. A New Lipophilic Amino Alcohol, Chemically Similar to Compound FTY720, Attenuates the Pathogenesis of Experimental Autoimmune Encephalomyelitisby PI3K/Akt Pathway Inhibition. *Int Immunopharmacol* (2020) 88:106919. doi: 10.1016/j.intimp.2020.106919
32. McGinley AM, Sutton CE, Edwards SC, Leane CM, DeCourcey J, Teijeiro A, et al. Interleukin-17a Serves a Priming Role in Autoimmunity by Recruiting IL-1-Producing Myeloid Cells That Promote Pathogenic T Cells. *Immunity* (2020) 52(2):342–56.e346. doi: 10.1016/j.immuni.2020.01.002
33. Luchtman DW, Ellwardt E, Larochelle C, Zipp F. IL-17 and Related Cytokines Involved in the Pathology and Immunotherapy of Multiple Sclerosis: Current and Future Developments. *Cytokine Growth Factor Rev* (2014) 25(4):403–13. doi: 10.1016/j.cytogfr.2014.07.013
34. Bastos P, Ferreira R, Manadas B, Moreira PI, Vitorino R. Insights Into the Human Brain Proteome: Disclosing the Biological Meaning of Protein Networks in Cerebrospinal Fluid. *Crit Rev Clin Lab Sci* (2017) 54(3):185–204. doi: 10.1080/10408363.2017.1299682

Conflict of Interest: The authors declare that the research was conducted in the absence of any commercial or financial relationships that could be construed as a potential conflict of interest.

Publisher's Note: All claims expressed in this article are solely those of the authors and do not necessarily represent those of their affiliated organizations, or those of the publisher, the editors and the reviewers. Any product that may be evaluated in this article, or claim that may be made by its manufacturer, is not guaranteed or endorsed by the publisher.

frontiers in Immunology

REVIEW
published: 07 December 2021
doi: 10.3389/fimmu.2021.774002

Long Non-Coding RNAs, Novel Offenders or Guardians in Multiple Sclerosis: A Scoping Review

Abbas Jalaiei[1,2], Mohammad Reza Asadi[1], Hani Sabaie[1,2], Hossein Dehghani[3], Jalal Gharesouran[2], Bashdar Mahmud Hussen[4], Mohammad Taheri[5,6], Soudeh Ghafouri-Fard[7] and Maryam Rezazadeh[1,2]**

[1] Molecular Medicine Research Center, Tabriz University of Medical Sciences, Tabriz, Iran, [2] Department of Medical Genetics, Faculty of Medicine, Tabriz University of Medical Sciences, Tabriz, Iran, [3] Department of Molecular Medicine, School of Medicine, Birjand University of Medical Sciences, Birjand, Iran, [4] Department Pharmacognosy, College of Pharmacy, Hawler Medical University, Erbil, Iraq, [5] Skull Base Research Center, Loghman Hakim Hospital, Shahid Beheshti University of Medical Sciences, Tehran, Iran, [6] Institute of Human Genetics, Jena University Hospital, Jena, Germany, [7] Department of Medical Genetics, School of Medicine, Shahid Beheshti University of Medical Sciences, Tehran, Iran

OPEN ACCESS

Edited by:
Luisa María Villar,
Ramón y Cajal University Hospital, Spain

Reviewed by:
Francesca Gilli,
Dartmouth College, United States
Paul Roy Heath,
The University of Sheffield, United Kingdom

***Correspondence:**
Soudeh Ghafouri-Fard
s.ghafourifard@sbmu.ac.ir
Maryam Rezazadeh
Rezazadehm@tbzmed.ac.ir

Specialty section:
This article was submitted to Multiple Sclerosis and Neuroimmunology, a section of the journal Frontiers in Immunology

Received: 10 September 2021
Accepted: 08 November 2021
Published: 07 December 2021

Citation:
Jalaiei A, Asadi MR, Sabaie H, Dehghani H, Gharesouran J, Hussen BM, Taheri M, Ghafouri-Fard S and Rezazadeh M (2021) Long Non-Coding RNAs, Novel Offenders or Guardians in Multiple Sclerosis: A Scoping Review. Front. Immunol. 12:774002. doi: 10.3389/fimmu.2021.774002

Multiple sclerosis (MS), a chronic inflammatory demyelinating disease of the central nervous system, is one of the most common neurodegenerative diseases worldwide. MS results in serious neurological dysfunctions and disability. Disturbances in coding and non-coding genes are key components leading to neurodegeneration along with environmental factors. Long non-coding RNAs (lncRNAs) are long molecules in cells that take part in the regulation of gene expression. Several studies have confirmed the role of lncRNAs in neurodegenerative diseases such as MS. In the current study, we performed a systematic analysis of the role of lncRNAs in this disorder. In total, 53 studies were recognized as eligible for this systematic review. Of the listed lncRNAs, 52 lncRNAs were upregulated, 37 lncRNAs were downregulated, and 11 lncRNAs had no significant expression difference in MS patients compared with controls. We also summarized some of the mechanisms of lncRNA functions in MS. The emerging role of lncRNAs in neurodegenerative diseases suggests that their dysregulation could trigger neuronal death *via* still unexplored RNA-based regulatory mechanisms. Evaluation of their diagnostic significance and therapeutic potential could help in the design of novel treatments for MS.

Keywords: lncRNAs, multiple sclerosis, neurodegenerative disease, polymorphism, expression

INTRODUCTION

Multiple sclerosis (MS) is a chronic inflammatory demyelinating disease of the central nervous system (CNS) and one of the most common neurodegenerative diseases worldwide (1). Pathogenic mechanisms underlying MS development have not been determined up to now. Clinically, different MS subtypes have been identified, including relapsing–remitting (RR), secondary progressive (SP), and primary progressive (PP) subtypes. These subtypes are heterogeneous among

affected individuals in terms of clinical course as well as genetic background (2). Complex interactions between genetic susceptibility and environmental factors lead to this neurodegenerative disease. Both innate and adaptive immune-mediated inflammatory mechanisms contribute to the demyelination and neurodegeneration in the context of MS. Previous studies have demonstrated that the inflammatory immune cells such as CD4 T-helper cells (Th1 and Th17) are the main contributors in disease pathogenesis (3, 4). The presence of these cells in the CNS is associated with neuronal demyelination, which can subsequently result in neuroinflammation and neurodegeneration (5, 6). Th17 cells that produce IL-17 are regarded as important inflammatory effectors in this disorder (7). However, the impact of Th17 cells in the pathogenesis of MS is not entirely dependent on the production of this cytokine, and it is supposed that an array of inflammatory factors is responsible in this regard (8). For example, expression of high amounts of the C-C chemokine receptor 6 (CCR6) on the cell surface of Th17 cells (9) facilitates the entry of these cells into the CNS *via* the choroid plexus (10). Th17 cells also participate in the pathoetiology of MS through production of other proinflammatory cytokines including TNF-α (11).

In recent years, genome-wide association studies (GWAS) and genetic mapping have nominated several candidate loci and variants in autoimmune conditions. However, MS pathogenesis cannot be explained by the genetic susceptibility factors alone. A large amount of evidence has revealed that long non-coding RNAs (lncRNAs) have critical roles in the regulation of cellular immunological pathways and autoimmunity. This new class of non-coding RNA (ncRNAs) contains a large part of the transcriptional output in the human genome but low protein-coding potential (12).

In the current review, we focus on recent reports performed on the roles of lncRNAs in MS pathogenesis. Then, we illustrate the role of some specific lncRNAs and their target genes. Therefore, our manuscript provides new insights into understanding the molecular etiology, diagnosis, and management of MS.

Long Non-Coding RNA Classification and Function

LncRNAs are a class of ncRNAs with sizes more than 200 nt and no protein-coding potential. They are commonly transcribed by RNA Pol II (13). LncRNAs have been detected in a variety of species such as animals, plants, and prokaryotes. The majority of them have a 5′ cap structure, multiple exons, and 3′ polyadenylated tails and are spliced in a way similar to mRNAs (14). Since lncRNAs do not encode proteins, they used to be called as "dark matter." However, recent studies have demonstrated that they are regulatory molecules and play important roles in several biological processes (14, 15), including gene expression at the epigenetic, transcriptional, and posttranscriptional levels. The vital mechanisms of epigenetic regulation consist of DNA methylation, histone modification, and ncRNA-mediated regulation. Emerging evidence revealed that the normal execution of biological events is controlled by a combination of ncRNAs and transcription factor (TF)-mediated epigenetic modifications (16). Studies on the role of lncRNAs suggest that their dysregulation could trigger neuronal death *via* still unexplored RNA-based regulatory mechanisms (17). Gene signature in human CNS is precisely regulated by several mechanisms. LncRNAs have a substantial impact on normal neural development, so their abnormal expression affects development and progression of neurodegenerative diseases (18).

According to databases such as the NONCODE (version v5.0) (19), the number of lncRNAs in human has been estimated to be higher than the number of protein-coding genes. The classification of lncRNAs is based on subcellular localization, function, interaction with the protein-coding gene, their size, and their association with protein-encoding genes. Based on their association with protein-encoding genes, they can be categorized to different classes such as sense, intergenic, bidirectional, intronic, antisense, and divergent lncRNAs (20, 21). Long intergenic non-coding RNA (lincRNA) genes are an important group of ncRNAs that participate in many biological processes, such as regulation of gene expression. They also play an essential role in many autoimmune and inflammatory diseases (22). In the current study, we performed a systematic analysis of the role of lncRNAs in MS.

METHODS

Review question: Which lncRNAs have been dysregulated in multiple sclerosis?

Inclusion/Exclusion Criteria

The inclusion criteria were as follows: 1) original studies, 2) studies focusing on the expression of lncRNAs in MS patients, 3) studies that confirmed results by RT-PCR, 4) studies with a sample of blood or tissue of human or animal model, and 5) studies that evaluated polymorphisms on lncRNAs. The following documents were excluded from this study: letters, reviews, *in vitro* studies, or papers with insufficient data.

Search Strategy

The current scoping review was performed according to the PRISMA statement (23). PubMed, Web of Science, ProQuest, and Scopus databases were searched to identify all published studies up to August 10, 2021.

Study Selection

Following the abovementioned search method, all obtained papers were loaded into EndNote version 20. Then, duplicate studies were removed. The title and abstracts of the remaining studies were evaluated, and their full texts were screened using the inclusion criteria. Then, lncRNAs with a role in the pathogenesis of MS were included.

Data Extraction

The required data were extracted using a self-constructed data extraction table. Author and year of publication, origin, sample

type, studied patients, method for lncRNA analysis, identified lncRNAs and expression pattern, and polymorphisms were extracted from the studies.

Figure 1 shows the flowchart of the study.

RESULTS

As shown in **Figure 1**, a total of 931 studies were identified through searching PubMed, Web of Science, ProQuest, and Scopus databases, and 26 studies were identified from other databases. After removing duplicated articles, 716 studies remained. In the next step, based on the evaluation of titles and abstracts, 656 studies were excluded and 60 studies remained. The full text of the articles was evaluated based on our inclusion criteria. After evaluation of the full text, seven studies were removed due to lack of inclusion criteria. At last, 53 studies remained for our systematic review. Among the included studies, 47 studies were conducted on human samples (24–70), 7 studies used animal models (45, 71–76), and only 1 research was conducted on both human samples and animal model (45). Also, 33 studies were conducted in the Iranian population (24–26, 28–34, 36, 38–43, 45–55, 57, 58, 61, 66, 67), 9 studies were in China (68–76), 5 studies were in Egypt (37, 62–65), 4 studies were in Italy (27, 35, 59, 60), 1 study was in Russia (44), and 1 study was in the Netherlands (56). A total of 44 studies evaluated the expression of lncRNAs in MS patients (24, 26–31, 34–43, 45, 46, 48, 50–54, 56–61, 63–65, 67–76), while 9 other studies analyzed polymorphisms of lncRNAs (25, 32, 33, 44, 47, 49, 55, 62, 66). The details of the included studies are summarized in **Tables 1**, **2**.

Recently, several studies revealed the involvement of lncRNAs in the pathogenesis of MS. **Figure 2** demonstrates the function of several lncRNAs that are involved in the pathogenesis of MS.

The Role of LncRNAs in the Pathophysiology of MS

LncRNAs Participating in Adaptive Immune Response or Inflammation

Linc-MAF-4 and lnc-DDIT4 are two upregulated lncRNAs in MS patients which are involved in the regulation of immune responses and inflammation (69, 70). DDIT4 is a cytoplasmic protein that is upregulated during DNA damage. Also, it inhibits the mTORC1 pathway which is a crucial regulator of the immune response (77). Since the mTOR pathway causes differentiation of Th17 and subsequent production of IL-17, it can be a key pathogenic player in MS (78, 79). Lnc-DDIT4 directly binds to and increases DDIT4 expression; thus, it suppresses the differentiation of Th17 (69). Therefore, lnc-DDIT4 might directly regulate Th17 cell differentiation and contribute to the pathogenesis of MS. Linc-MAF-4 is a lincRNA located in the minus strand of 16q23.2, almost 150 kb apart from the gene encoding MAF (19). This lincRNA has an important role in regulating differentiation of Th1/2 cells. MAF is the Th2 lineage-specific TF facilitating Th2 differentiation (70). Linc-MAF-4 is a Th1 lineage-specific factor that recruits chromatin remodeling factors LSD1 and EZH2 to inhibit MAF transcription and elevate Th1 differentiation and IFN-γ production (15). So, linc-MAF-4 can contribute in the pathogenesis of MS. Another study has identified six lncRNAs with abnormal expression in MS. ENSG00000231898.3 (MYO3B-AS1), XLOC_009626, and XLOC_010881 were upregulated, while ENSG00000233392.1 (AC104809.2), ENSG00000259906.1 (AC120045.1), and XLOC_010931 showed downregulation (68).

LincR-Gng2-5′, LincR-Epas1-3′as, and LincR-Ccr2-5′AS

LincR-Gng2-5′ and lincR-Epas1-3 loci were firstly identified by Hu et al. in Th1 and Th2 cells regulated by signal transducer and activator of transcription 4 (STAT4) and (STAT6), respectively (22). According to the data from lncRNAdb (80), LNCipedia (version 5.2), and Ensemble genome browser 99, LincR-Gng2-5′ is located on chromosome 14q22.1 on the plus strand and has a transcript size of 1,233 bp. LincR-Epas1-3′as is located on chromosome 2p.21 on the positive strand and has 758 bp length. They are located in an important place rich in genes with immune regulatory functions. Since they act as enhancers, they might participate in the regulation of neighboring genes, thus modulating immune responses (63). LincR-Gng2-5′ is upregulated in MS patients, while LincR-Epas1-3′as is downregulated in these patients. Dysregulation of these lncRNAs has a role in the pathoetiology of MS through affecting the balance between Th1 and Th2 cells (22, 81). LincR-Ccr2-5′AS is another lncRNA that is expressed in Th2 and has association with GATA-binding protein 3 (GATA3), the "master regulator" of Th2. Shaker et al. have reported the downregulation of lincR-Ccr2-5′AS in MS patients and the subsequent decrease in the production of Th2 cytokines (64).

GSTT1-AS1 and IFNG-AS1

Glutathione S-transferase, Theta1-Anti Sense1 (GSTT1-AS1), also known as lncRNA-CD244, is a novel 284-bp lncRNA, located on the minus strand 22q11.23 with partial overlap with 5′ UTR of the *GSTT1* gene (19, 82). This lncRNA was originally discovered as an lncRNA with a crucial role in the pathogenesis of tuberculosis (83). Ganji et al. show downregulation of GSTT1-AS1 in MS patients. Since this lncRNA suppresses the expression of TNF and INFG through recruitment of the epigenetic complex PRC2 and *via* the EZH2 enzyme complex, it might be involved in the pathogenesis of MS (36).

IFNG-AS1 has been firstly identified as a transcript with a possible role in the regulation of immune system function (84). Also known as Tmevpg1, it is a 1,791-bp intergenic lncRNA located on the plus strand on 12q15 (19), adjacent to the *INFG* gene (85). It has been shown to be dysregulated in several immune-related disorders (83, 86). This lincRNA acts as an important checkpoint for the expression of IFNG in Th1 cells (87).

AC007278.2 (Expression in T Cells)

Another lncRNA is a 1,200-bp intronic lncRNA, AC007278.2, also known as Lnc-IL18R1-1. This lncRNA is located on the plus strand of the 2q12.1 chromosome and has two exons (19). AC007278.2 has a specific expression in Th1 cells. It is located within the introns of the protein-coding genes *IL18RAP* and *IL18R1*, with important roles in Th1 cell differentiation (43).

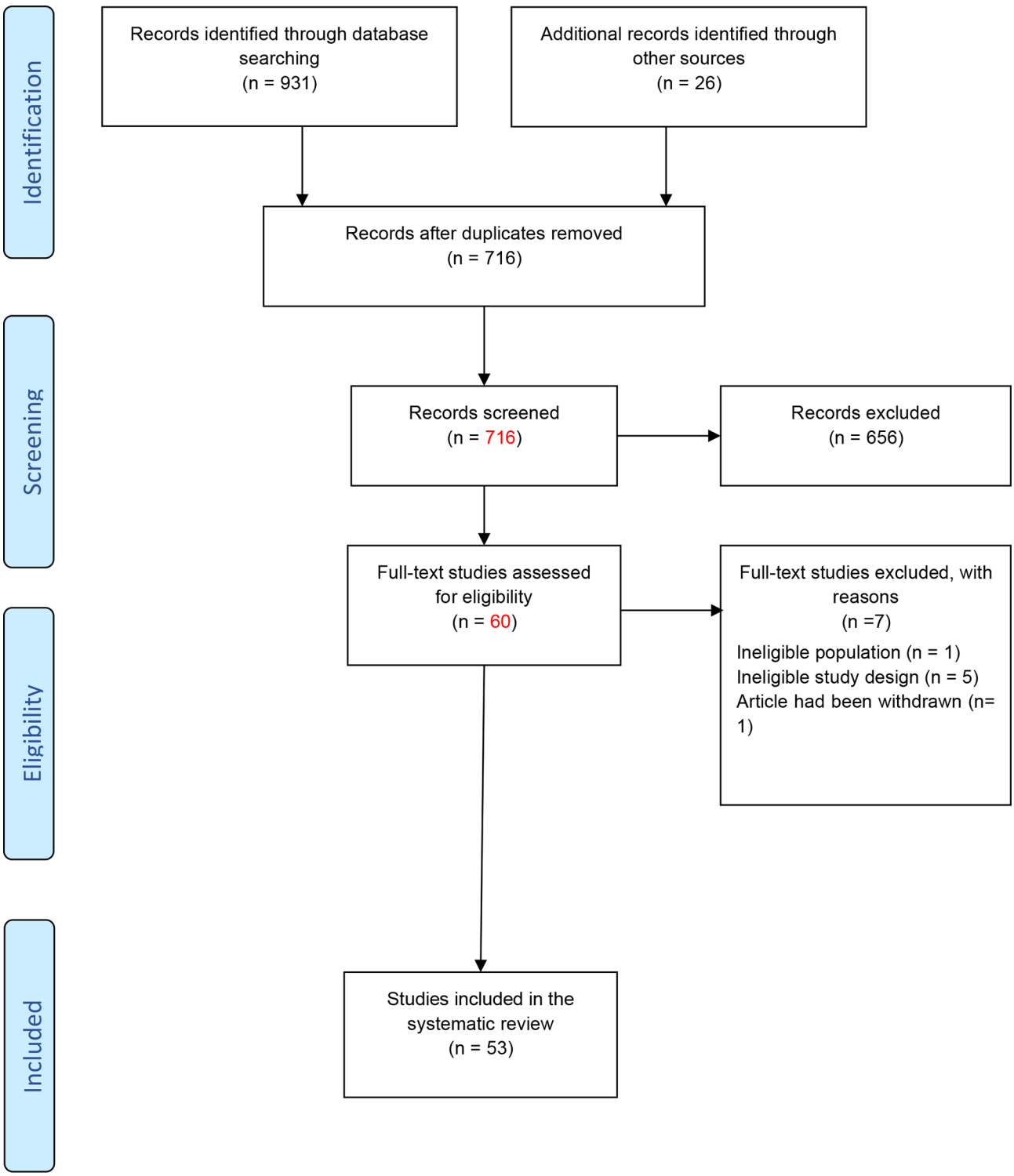

FIGURE 1 | Flowchart of the study (23).

TABLE 1 | Details of the included human studies.

Author	Year	Origin	LncRNA measurement technique	Sample type	Number of studied patients	Identified lncRNA/expression pattern	Polymorphism	Ref
Bahrami et al.	2021	Iran	RT-PCR	PBMCs	50 RRMS 50 controls	Lnc-DC ↑		(24)
Bahrami et al.	2020	Iran	T-ARMS PCR	PBMCs	300 patients 300 controls		TRPM2-AS1, rs933151 HNF1A-AS1, rs7953249	(25)
Bina et al.	2017	Iran	RT- PCR	PBMCs	36 RRMS 30 Controls	lnc-IL-7R [NS]		(26)
Cardamone et al.	2019	Italy	Microarray assay validation by RT-PCR	PBMCs	190 cases 182 controls	MALAT1 ↑		(27)
Dastmalchi et al.	2018	Iran	RT-PCR	PBMCs	50 RRMS 50 controls	NEAT1 ↑ TUG1 ↑ PANDA ↑		(28)
Dastmalchi et al.	2018	Iran	TaqMan RT-PCR	PBMCs	50 RRMS 50 controls	UCA1 ↑ CCAT2 ↑		(29)
Dehghanzad et al.	2020	Iran	RT-PCR	PBMCs	39 MS 32 controls	TOB1-AS1 ↑		(30)
Eftekharian et al.	2019	Iran	T-ARMS-PCR Confirmed by the Sanger method	PBMCs	428 MS 505 controls		MALAT1 rs619586, rs3200401	(32)
Eftekharian et al.	2019	Iran	T-ARMS PCR	PBMCs	400 MS 410 controls	GAS5 ↑	rs2067079 rs6790	(33)
Eftekharian et al.	2019	Iran	TaqMan RT-PCR	PBMCs	50 RRMS 50 controls	NNT-AS1 ↑		(34)
Eftekharian et al.	2017	Iran	TaqMan RT-PCR	PBMCs	50 RRMS 50 controls	THRIL ↑ FAS-AS1 ↓ PVT1 ↓		(31)
Fenoglio et al.	2018	Italy–Belgium	Real-time PCR validated with TaqMan and lastly confirmed by droplet digital PCR	PBMCs	27 RRMS 13 PPMS 31 controls	MALAT1 ↓, MEG9 ↓, NRON ↓, ANRIL ↓, TUG1 ↓, XIST ↓, SOX2OT ↓, GOMAFU ↓, HULC ↓, BACE-1AS ↓		(35)
Ganji et al.	2019	Iran	RT-PCR	PBMCs	50 RRMS 50 controls	GSTT1-AS1 ↓ IFNG-AS1 ↓		(36)
Ghaiad et al.	2020	Egypt	RT-PCR	PBMCs	72 MS 28 controls	APOA1-AS1 ↑ IFNG-AS1 ↑ RMRP ↑		(37)
Gharesouran et al.	2019	Iran	TaqMan RT-PCR	PBMCs	50 RRMS 50 controls	MALAT1 ↑ HOTAIRM1 ↑		(39)
Gharesouran et al.	2019	Iran	TaqMan RT-PCR	PBMCs	50 RRMS 50 controls	OIP5-AS1 ↓		(40)
Gharesouran et al.	2018	Iran	TaqMan RT-PCR	PBMCs	50 RRMS 50 controls	GAS5 ↑		(38)
Gharzi et al.	2018	Iran	RT-PCR	PBMCs	50 RRMS 50 controls	BDNF-AS1 [NS]		(41)
Ghoveud et al.	2020	Iran	RT-PCR	PBMCs	50 RRMS 25 controls	RP11-530C5.1 ↑ AL928742.12 ↓		(42)
Hosseini et al.	2019	Iran	RT-PCR	PBMCs	50 RRMS 25 controls	AC007278.2 ↑ IFNG-AS1-001 ↑ IFNG-AS1-003 ↑		(43)
Kozin et al.	2020	Russia	PCR-RFLP performed by TaqMan RT-PCR	PBMCs	444 RRMS 96 SPMS 406 controls		PVT1 rs2114358 rs4410871	(44)
Masoumi et al.	2019	Iran	RT-PCR	Human brain tissue	5 RRMS 5 controls	MALAT1 ↓		(45)
Mazdeh et al.	2019	Iran	RT-PCR	PBMCs	50 RRMS 50 controls	AFAP1-AS1 ↑		(46)
Mazdeh et al.	2019	Iran	T-ARMS PCR	PBMCs	402 RRMS 392 controls		LncRNA H19 rs2839698 rs217727	(47)
Moradi et al.	2020	Iran	RT-PCR confirmed by RFLP	PBMCs	300 RRMS 300 controls		GAS5, rs55829688 and NR3C1, rs6189/6190, rs56149945, rs41423247	(49)

(Continued)

TABLE 1 | Continued

Author	Year	Origin	LncRNA measurement technique	Sample type	Number of studied patients	Identified lncRNA/expression pattern	Polymorphism	Ref
Moradi et al.	2019	Iran	RT-PCR	PBMCs	20 RRMS 10 controls	NR003531.3(MEG3a) ↓ AC00061.2_201 [NS] AC007182-6 [NS]		(48)
Pahlevan Kakhki et al.	2019	Iran, North Khorasan, Sistani	RT-PCR	PBMCs	North Khorasan 30 MS, 30 controls	THRIL, North Khorasan ↑		(51)
					Sistani 21 MS, 21 controls	Sistani ↓ lnc-DC [NS] both groups		
Pahlevan Kakhki et al.	2018	Iran	RT-PCR	PBMCs	42 RRMS 32 controls	HOTAIR ↑ ANRIL [NS]		(50)
Patoughi et al.	2020	Iran	RT-PCR	PBMCs	50 RRMS 50 controls	PINK1-AS ↑		(53)
Patoughi et al.	2019	Iran	TaqMan RT-PCR	PBMCs	50 RRMS 50 controls	GAS8-AS1 ↑		(52)
Rahmani et al.	2020	Iran	RT-PCR	PBMCs	83 RRMS 44 controls	RORC ↑ DDX5 ↑ RMRP ↑		(54)
Rezazadeh et al.	2018	Iran	T-ARMS-PCR	PBMCs	410 RRMS 419 controls		ANRIL, rs1333045, rs4977574, rs1333048, rs10757278	(55)
Rodríguez-Lorenzo	2020	Netherlands	Ref-seq validated by RT-PCR	Brain tissue	6 MS patients 6 controls	HIF1A-AS3 ↑		(56)
Safa et al.	2020	Iran	RT-PCR	PBMCs	50 RRMS 50 controls	LINC00305 ↓ lnc-MKI67IP-3 ↓ HNF1A-AS1↓ MIR31HG [NS] NKILA [NS] ADINR [NS] CHAST [NS] DICER1-AS1 [NS]		(57)
Safa et al.	2020	Iran	RT-PCR	Venous blood	40 RRMS 40 controls	SPRY4-IT1 ↓ HOXA-AS2 ↓ LINC-ROR ↓ MEG3 ↓		(58)
Santoro et al.	2020	Italy	RT-PCR	Serum	16 SPMS, 12 PPMS 8 controls	TUG1 ↑ LINC00293 ↑ RP11-29G8.3 ↑		(59)
Santoro et al.	2016	Italy	RT-PCR	Serum	12 RRMS 12 controls	NEAT1 ↑ TUG1 ↑ RN7SKRNA ↑		(60)
Sayad et al.	2019	Iran	TaqMan RT-PCR	PBMCs	50 RRMS 50 controls	HULC ↑		(61)
Senousy et al.	2020	Egypt	TaqMan RT-PCR	Serum	108 RRMS 104 controls	GAS5 ↑	rs2067079 rs1625579	(62)
Shaker et al.	2021	Egypt	RT-PCR	PBMCs	74 RRMS, SPMS 60 controls	LincR-Ccr2-5′AS ↓ THRIL ↑		(64)
Shaker et al.	2019	Egypt	RT-PCR	PBMCs	42 RRMS 18 SPMS 60 controls	LincR-Gng2-5′ ↑ LincREpas1-3′as ↓		(63)
Shaker et al.	2019	Egypt	RT-PCR	Serum	45 RRMS 45 controls	MALAT1 T ↑ lnc-DC ↑		(65)
Taheri et al.	2020	Iran	T-ARMS-PCR	PBMCs	403 MS patients 420 controls		HOTAIR, rs12826786, rs1899663, rs4759314	(66)
Teimuri et al.	2019	Iran	RT-PCR	PBMCs	25 RRMS 25 SPMS	AL450992.2 ↓ AC009948.5 ↓		(67)

(Continued)

TABLE 1 | Continued

Author	Year	Origin	LncRNA measurement technique	Sample type	Number of studied patients	Identified lncRNA/expression pattern	Polymorphism	Ref
					25 controls	RP11-98D18.3 ↓ AC007182.6 ↓		
Zhang et al.	2018	China	Microarray assay validation by RT-PCR	PBMCs	36 RRMS 26 controls	lncDDIT4 ↑		(69)
Zhang et al.	2017	China	RT-PCR	PBMCs	34 RRMS 26 controls	Linc-MAF4 ↑		(70)
Zhang et al.	2016	China	RT-PCR	PBMCs	26 RRMS	MYO3B-AS1 (ENSG00000231898.3) ↑		(68)
					26 controls	AC104809.2 (ENSG00000233392.1) ↓ AC120045.1 (ENSG00000259906.1) ↓ LncRNA XLOC_010931 ↓ LncRNA XLOC_009626 ↑ LncRNA XLOC_010881 ↑		

RT-PCR, real-time PCR; T-ARMS-PCR, tetra-primer amplification refractory mutation system-PCR; PBMCs, peripheral blood mononuclear cells; RRMS, relapsing–remitting multiple sclerosis; SPMS, secondary progressive multiple sclerosis; upregulation, ↑; downregulation, ↓; NS, not significant; rs, reference SNP.

Several studies revealed significant correlations between IL18RAP and IL18R1 and their association with the lncRNA AC007278.2. On the other hand, elevated expression of IL18RAP and IL18R1 is involved in the differentiation of Th1 cells and the pathogenesis MS. During Th1 differentiation, STAT4 and IL-12 recruit chromatin remodeling complexes. Induction of histone acetylases and DNA methylases promotes the expression of IL18RAP and IL18R1 and the release of IL-18 and IL-12 which trigger the differentiation of Th1 and the release of pro-inflammatory cytokines and eventually the progression of MS (43, 88, 89).

TOB1-AS1

TOB1 antisense RNA 1 (TOB1-AS1) is transcribed from the opposite orientation of the *TOB1* gene on chromosome 17q21.33, a region with an important role in maintaining immune tolerance (19). Dehghanzad et al. demonstrated the abnormal expression levels of TOB1-AS1 and its targets genes *TOB1*, *TSG*, and *SKP2* in the blood of MS. Downregulation of TOB1-AS1 might cause dysregulation of the target genes and participate in the progression of MS (30). TOB1-AS1 enhances the expression of the *TOB1* gene *via* suppressing the production of IL-2 (90). An *in vitro* study revealed the positive feedback between TOB1 and S-phase kinase-associated protein 2 (SKP2). Elevation of TOB1-AS1 levels causes increased TOB1 and thus increased the TSG levels (30).

RMRP

Rahmani et al. demonstrated that RORC, DDX5, and RMRP have been significantly upregulated in patients with MS (54). RORC and DDX5 can affect MS pathogenesis through regulation of Th17 differentiation and the production of inflammatory cytokines such as IL-17A, IL-17F, and IL-22.

LncRNAs With Roles in Innate Immune Response

Lnc-DC and THRIL

TNF and HNRNPL-related immunoregulatory long non-coding RNA (THRIL) is a lincRNA located on the minus strand of the 12q24.31 chromosome. This lncRNA plays an important role in the regulation of the innate immune system (19). This lncRNA has been among the dysregulated lncRNAs in MS (31). THRIL

TABLE 2 | Details of the included animal studies.

Author	Year	Origin	LncRNA measurement technique	Sample type	Type of EAE model	Identified lncRNA/expression pattern	Ref
Bian et al.	2020	China	Microarray assay validation by q-PCR	Spleen tissue	Not mentioned	GM15575 ↑	(71)
Duan et al.	2018	China	RT-PCR	Microglia	Cuprizone-induced demyelination	HOTAIR ↑	(72)
Guo et al.	2017	China	Microarray confirmed by RT-PCR	Spleen tissue	Myelin oligodendrocyte glycoprotein (MOG) peptide-induced EAE	1700040D17Rik ↓	(73)
Liu et al.	2021	China	RT-PCR	Spinal cords or astrocyte	MOG peptide-induced EAE	GM13568 ↑	(74)
Masoumi et al.	2019	Iran	RT-PCR	Lumbar spinal cord tissue	MOG peptide-induced EAE	MALAT1 ↓	(45)
Sun et al.	2017	China	Microarray assay validation by RT-PCR	Microglia	MOG peptide-induced EAE	GAS5 ↑	(75)
Yue et al.	2019	China	RT-PCR Western blot	Microglia BV2 cells	MOG peptide-induced EAE	TUG1 ↑	(76)

RT-PCR, real-time PCR; EAE, autoimmune encephalomyelitis; upregulation, ↑; downregulation, ↓.

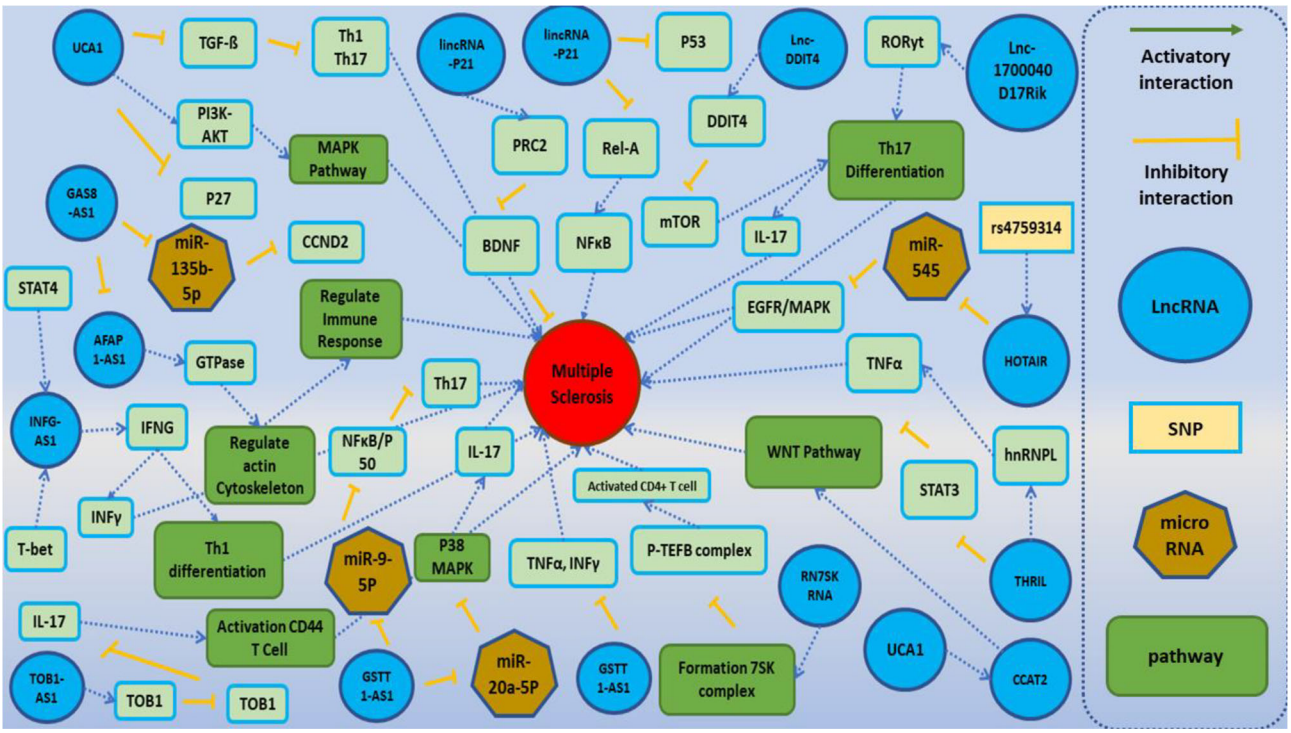

FIGURE 2 | A schematic diagram of the role of several lncRNAs involved in the modulation of the main molecular cascades in multiple sclerosis (MS). One of the main pathophysiological mechanisms associated with the MS involves T cells subsets [regulatory T cells (Treg), Th1, Th2, and Th17 cells]. Dysregulation of these subsets activates inflammatory cascades and cytokine secretion and ultimately leads to demyelination within the brain and spinal cord and neuronal damage. Lnc-DC has been shown to be upregulated in PBMCs of MS patients. Upregulation of this lncRNA activates Toll-like receptor 4 (TLR4) and TLR9. TLR4 has a central role in the secretion of inflammatory cytokines such as IL-1, IL-6, and IL-17 and suppresses Treg cells. Also, TLR4 increases the differentiation of Th17 through inhibition of miR-30a (24, 65). Moreover, lnc-DDIT4 is upregulated in the PBMCs of MS patients. This lncRNA binds to DDIT4 and regulates immune response and differentiation of Th17 (69). BDNF-AS has a role in the recruitment of PRC2 and inhibition of the neuroprotective factor BDNF (41). GSTT1-AS1 inhibits the progression of MS through inhibition of secretion of IFN-γ and TNF-α (36). TUG1 activates p38 MAPK signaling pathway through suppression of miR-20a-5p, so downregulation of TUG1 decreases Th17 differentiation. UCA1 has a role in the regulation of activity of PI3K–AKT, ERK1/2, and MAPK cascades and Th17 differentiation. Also, this lncRNA has interaction with another lncRNA, namely, CCAT2. CCAT2 induces WNT cascade signaling and enhances the production of inflammatory cytokines (28, 59).

regulates TNF-α expression *via* its interaction with heterogeneous nuclear ribonucleoprotein L (hnRNPL) and persuades a transcriptional-activating complex, finally connecting to the TNF-α promoter (91). THRIL can suppress STAT3 (51).

Lnc-DC (also known as Wfdc21) is a non-coding RNA gene on the minus strand of chromosome 17q23.1, which was firstly identified by Wang et al. to have an important role in the differentiation of dendritic cells and the regulation of the immune response (92, 93). Lnc-DC positively regulates STAT3 resulting in the differentiation of monocyte cell to dendritic cells (92). This lncRNA is involved in the pathogenesis of sepsis (93), coronary artery disease (94), pre-eclampsia (95), MS (51), and systemic lupus erythematosus (SLE) (96). Xie et al. showed the role of lnc-Dc on the regulation of TLR4 (93). Lnc-DC through the TLR9/STAT3 axis can regulate apoptosis and immune responses, thus can participate in the pathogenesis of MS (97, 98). Bahrami et al. demonstrated the upregulation of lnc-DC level in HLADRB1*15:01-negative MS patients compared with healthy controls (24).

LncRNAs Having a Role in Response to DNA Damage

LincRNA-p21 (Expression in T Cell)

P21-associated ncRNA DNA damage-activated (PANDA) is a lincRNA located on the minus strand 6p21.2. It has a role in response to DNA damage in a p53-dependent pathway (15). Dastmalchi et al. revealed the upregulation of this lncRNA in the peripheral blood of MS patients (28). PANDA controls the cell cycle through suppression of proapoptotic-related genes (15, 99). Dysregulation of the expression of this lncRNA in oligodendrocytes and neurons is associated with the release of free radicals and activation of the apoptosis process (100).

LncRNAs Involved in the Regulation of the Cell Cycle

TUG1, UCA1, and CCAT2

UCA1, CCAT2, and TUG1 are a subgroup of lncRNAs that have a role in the regulation of the cell cycle. UCA1 is located in the plus strand of chromosome 19p13.12 (19). It participates in the

pathogenesis of several cancers such as colorectal, breast, and bladder cancer through increasing cell proliferation, apoptosis-resistant cells, invasion, and drug resistance induction (101). UCA1 *via* modulation of the PI3K–AKT, ERK1/2, and MAPK pathways can regulate the proliferation of cells in various cancers (102). Dastmalchi et al. revealed the upregulation of UCA1 in the blood of MS patients. This lncRNA *via* inhibiting cell cycle inhibitors such as p27 may cause increased proliferation of T cells (29).

CCAT2 is an intergenic lncRNA on the plus strand of the 8q24.21 chromosome (19). This lncRNA acts as an oncogene and participates in the metastasis, chromosomal instability, and tumor growth in colon cancer (103). Both UCA1 and CCAT2 can regulate the expression of genes participating in WNT pathway (104).

Fenoglio et al. showed the downregulation of TUG1 in MS patients compared with controls (35). TUG1 exerts a repressor function *via* recruitment of the PRC2 complex. Its promoter has many conserved binding sites for p53, thus after DNA damage, p53 regulates cell cycle and apoptosis *via* upregulation of TUG1 (35, 105, 106). TUG1 has been found to be upregulated in the serum and PBMCs of RRMS patients (28, 59, 60). TUG1 targets and suppresses different miRNAs such as miR-20a-5p, which has a role in the regulation of p38 MAPK signaling pathway. p38 MAPK promotes the production of proinflammatory cytokines. Downregulation of miR-20a-5p by TUG1 activates p38 MAPK signaling and MS progression (60).

The growth arrest-specific 5 (GAS5) has been recognized as a lncRNA with a possible role in normal growth arrest in T cells. This lncRNA plays a central role in the suppression of glucocorticoid receptor (GR). Gharesouran et al. revealed the correlation between GAS5 and nuclear receptor subfamily 3 group C member 1 (NR3C1) (38). Sun et al. demonstrated that GAS5 can inhibit the transcription factor IRF4, thus suppressing the generation of T cells (75).

LncRNAs With a Role in the CNS

GOMAFU

MIAT or GOMAFU is a lincRNA on the plus strand of 22q12.2 (19), which is highly expressed in the CNS and is suggested to have an important role in regulating the neural stem cell differentiation into oligodendrocytes (107). Fenoglio et al. showed the downregulation of this lncRNA in the blood of MS patients (35). GOMAFU using its repetitive sequence binds to the splicing factor 1 (SF1) protein and prevents the function of the spliceosome complex. Thus, deregulation of GOMAFU causes advent of alternative splicing patterns (108). GOMAFU has a possible role in inflammatory and neurodegenerative processes (35).

OIP5-AS1

OIP5-AS1 (Cyrano) was firstly detected in zebrafish models and it was suggested that it has a role in the development of the CNS (109). Kim et al. revealed that OIP5-AS1 causes a reduction in the stability a cyclin G-associated kinase (GAK) mRNA with important roles for mitotic progression (110). It seems that this lncRNA exerts its role in the suppression of cell proliferation through reducing GAK levels by associating with the RNA-binding proteins (RBPs) like HUR1 (ELAV-like protein 1). HuR1 is a protein that in humans is encoded by the ELAVL1 and is regarded as a member of the ELAVL proteins. HUR1 contains three RNA-binding domains and binds to cis-acting AU-rich elements. Since the *HuR1* gene is expressed in astrocytes, it might have a role in autoimmune diseases such as encephalomyelitis and MS (111).

BDNF-AS

Brain-derived neurotrophic factor-antisense RNA (BDNF-AS) is a 191-kb-long conserved lncRNA (112), located in the opposite orientation of BDNF on the 11p14.1. It negatively regulates the expression of BDNF at the mRNA and protein levels (113). BDNF is a neuroprotective factor that is synthesized in the brain and is expressed at a high level in the CNS. It has diverse functions such as the promotion of neuronal survival and elevation of growth, maturation, and synaptic plasticity. BDNF is produced and released by neurons and immune cells such as T and B cells under the circumstance of inflammation of the CNS in MS patients (114). BDNF-AS recruits PRC2 and inhibits BDNF expression (113).

Other LncRNAs

NEAT1

This lncRNA has been shown to be upregulated in MS patients compared with healthy individuals (59). NEAT1 plays an important role in the formation of paraspeckle, a nuclear body that comprises numerous protein factors. NEAT1 has been shown to be co-localized with splicing factor proline/glutamine-rich (SFPQ) and NonPOU domain containing, octamer-binding (NONO) (115). Also, NEAT1 is activated by the Toll-like receptor 3 (TLR3)–p38 pathway in antiviral response or endogenous agonists that bind to TLR3 (116, 117). Imamura et al. revealed that upregulation of NEAT1 causes activation and excess IL-8 production *via* enhancing the relocation of SFPQ proteins from the IL-8 promoter (118).

RN7SK RNA

The lincRNA 7SK small nuclear (RN7SK RNA) is transcribed from the plus strand of the 6p12.2 chromosome. It is involved in the formation of the 7SK snRNP complex with other specific proteins (HEXIM1/2, LARP7, and PIP7S) that can inhibit approximately half of the activity of the cellular kinase P-TEFb complex (119, 120). The P-TEFb complex and its protein component Cdk9/cyclin T1 heterodimer have a role in the activation of CD4+ T cells. So, upregulated RN7SK RNA may cause disturbance in the P-TEFb complex with resulting regulation effects on CD4+ T cells, thus participating in autoimmune diseases such as idiopathic inflammatory myopathy (IIM) and MS (59).

AFAP1-AS1

Actin Filament-Associated Protein 1 Antisense RNA 1 (AFAP1-AS1) is a conserved non-coding RNA transcribed from the plus strand of chromosome 4p16.1 on the opposite strand of the AFAP1 locus. This lncRNA regulates the expression of AFAP1 at the translation level (121). AFAP1-AS1 was found to modulate

AFAP1 and act as an adapter molecule that links other proteins such as SRC and PKC with a hypothetical function in blood–brain barrier (BBB) integrity. BBB dysfunction in MS patients allows the enormous influx of immune cells into the brain and, after a series of interactions, leads to demyelination (122). Based on the bioinformatics analyses, AFAP1-AS1 affected the expression of molecules with a vital role in the actin cytoskeleton signaling pathway such as multiple small GTPase family members. As small GTPases are involved in the regulation of immunity and inflammation response, its dysregulation leads to disease progression in many diseases such as autoimmune diseases (123). Upregulation of AFAP1-AS1 promotes metastasis *via* modulation actin filament integrity (124). Due to its antiapoptotic properties in peripheral immune cells, it might be involved in the pathogenesis of MS (40).

GAS8-AS1

A previous study showed that GAS8-AS1 is a tumor suppressor and regulates the expression of another lncRNA, namely, AFAP1-AS1 (125). GAS8-AS1 has been downregulated, while AFAP-AS1 has been upregulated in MS patients. Regarding the role of AFAP1-AS1 in the pathogenesis and progression of MS, it can be hypothesized that dysregulation of GAS8-AS1 might be involved in the pathogenesis of MS (40, 125). Zha et al. revealed that GAS8-AS1 negatively regulated the expression of UCA1. UCA1 has been shown to regulate various signaling pathways such as FGFR1/ERK and TGF-β (126). TGF-β has a role in the inflammatory condition and acts as an anti-inflammatory factor to inhibit Th1 and Th17 cells (127), so upregulation of GAS8-AS1 resulting in the downregulation of UCA1 and reduced TGF-β might cause progression and aggregate MS.

PINK1-AS

PTEN-induced kinase 1-AS (PINK1-AS) is an intronic non-coding RNA transcribed from the minus strand of chromosome 1p36.12 on the opposite strand of the PINK1 locus. This lncRNA regulates the expression of PINK1. Patoughi et al. (53) revealed the upregulation of the expression level of the PINK1-AS in male MS patients compared with male healthy controls. This might be due to the existence of a gender-based regulatory direction for PINK1-AS expression or variance in the pathogenic process of disease in female and male MS patients. PINK1 is a serine/threonine kinase that preserves the mitochondria and supports its normal function (128). Further studies by Fenoglio et al. have identified 10 lncRNAs with abnormal expression. These lncRNAs consist of MALAT1, MEG9, NRON, ANRIL, TUG1, XIST, SOX2OT, GOMAFU, HULC, and BACE-1AS (35).

The highly upregulated liver cancer (HULC) is another lncRNA found to be upregulated in MS patients in one study (61), whereas Fenoglio et al. have reported an opposite result (35). This lncRNA attaches to miR-200a-3p and also acts as an endogenous sponge for miR-122. Since miR-122 has an anti-inflammatory effect and is significantly downregulated in the blood of MS patients, HULC may be involved in the progression of MS. On the other hand, HULC activates miR-200a-3p/ZEB1 signaling. miR-200a plays an important role in the regulation of the TLR4 pathway and ZEB1 has a neuroprotective protein (129).

Dysregulated LncRNAs in the Animal Model of MS

One of the useful animal models of MS is EAE mice that share several characteristics with MS. However, there are few studies in this area. Yue et al. (76) demonstrated the abnormal activity of the TUG1/miR-9-5p/NF-κB1/p50 axis in the mouse model of MS. In fact, upregulation of TUG1 causes suppression of miR-9-5p and an increase in the expression of NF-κB1/p50. This transcription factor causes activation of Th17 cell and the production of IL-17 and IL-6. NF-κB also regulates matrix metalloproteinases (MMPs). Downregulation of TUG1 leads to increased levels of miR-9-5p and a decrease in NF-κB1/p50.

Another study by Guo and colleagues showed that lncRNA-1700040D17Rik is a specific mouse lincRNA that is located adjacent to the *RORγt* gene on chromosome 3 and is downregulated in EAE (73). Then, an *in vitro* approach revealed that IL23R-CHR is a soluble IL23R that counteracts IL-23 and blocks its signaling pathway, thus inhibiting differentiation of Th17 cell (130). These findings demonstrated that 1700040D17Rik regulates the expression of RORγt, which is an essential transcription factor for Th17 (73).

Liu et al. revealed that IL-9 inducing lncRNA Gm13568 in astrocytes has interaction with CBP/P300. It promotes Notch1 pathway activation and is involved in the construction of inflammatory cytokines in astrocytes in the progression of EAE development (74).

Variants Within LncRNAs and Association With MS

According to the important roles of lncRNAs in the regulation of immune responses, it is expected that functional variants within their coding region or adjacent to them can affect the risk of MS. However, there are few studies on this issue. Bahrami et al. have evaluated the association between rs933151 and rs7953249 polymorphisms in TRPM2-AS and HNF1-AS1, respectively, and MS risk in the Iranian population. They revealed that rs7953249 within HNF1-AS1 has an association with C-reactive protein (CRP) (25).

Taheri et al. assessed the association between three SNPs (rs12826786, rs1899663, and rs4759314) within HOTAIR and MS in 403 Iranian MS patients and 420 controls. Their results showed that the G allele of rs4759314 might be involved in the risk of MS (66).

CONCLUSION

In conclusion, the pathogenesis of MS is highly complex including several molecular signaling pathways. Most of the abovementioned studies have assessed the expression of lncRNAs in serum or PBMCs. Although several of these lncRNAs have essential roles in the CNS processes, modulation of peripheral immune responses is the most appreciated route of participation of lncRNAs in the pathogenesis of MS. Few studies have assessed the expressions of lncRNAs in the brain tissues of EAE models. An important study in this field has identified dysregulation of Gm14005, Gm12478, mouselincRNA1117,

AK080435, and mouselincRNA0681 in brain tissues of affected animals. Notably, inflammation has been among the mostly enriched pathways among dysregulated genes (131). This observation further emphasized the importance of inflammation-related lncRNAs in the pathoetiology of MS.

In the current review, we highlighted the function of various lncRNAs in the MS pathway. Although few studies have addressed this issue, it is predicted that genomic variation within lncRNAs affecting their function or expression may contribute to the risk of MS or response of subjects to treatments. It has been determined that lncRNAs have roles in the development of the immune system and nerve cells. Further studies are required for understanding the mechanism of lncRNA involvement in the pathogenesis of MS.

AUTHOR CONTRIBUTIONS

AJ, MT, BH, and SG-F wrote the draft and revised it. MR, HS, JG, and MA collected the data and designed the figures. HD performed the bioinformatics analysis. All authors contributed to the article and approved the submitted version.

ACKNOWLEDGMENTS

This article is the result of a student dissertation approved by Tabriz University of Medical Sciences code 66211. We also want to thank the Molecular Medicine Research Center of Tabriz University of Medical Sciences for their collaboration.

REFERENCES

1. Yamout BI, Alroughani R. Multiple Sclerosis. *Semin Neurol* (2018) 38 (2):212–25. doi: 10.1055/s-0038-1649502
2. Multiple Sclerosis. *Nat Rev Dis Primers* (2018) 4(1):44. doi: 10.1038/s41572-018-0046-z
3. Yadav SK, Mindur JE, Ito K, Dhib-Jalbut S. Advances in the Immunopathogenesis of Multiple Sclerosis. *Curr Opin Neurol* (2015) 28 (3):206–19. doi: 10.1097/WCO.0000000000000205
4. Broux B, Stinissen P, Hellings N. Which Immune Cells Matter? The Immunopathogenesis of Multiple Sclerosis. *Crit Rev™ Immunol* (2013) 33 (4):283–306. doi: 10.1615/CritRevImmunol.2013007453
5. Galli E, Hartmann FJ, Schreiner B, Ingelfinger F, Arvaniti E, Diebold M, et al. GM-CSF and CXCR4 Define a T Helper Cell Signature in Multiple Sclerosis. *Nat Med* (2019) 25(8):1290–300. doi: 10.1038/s41591-019-0521-4
6. Capone A, Bianco M, Ruocco G, De Bardi M, Battistini L, Ruggieri S, et al. Distinct Expression of Inflammatory Features in T Helper 17 Cells From Multiple Sclerosis Patients. *Cells* (2019) 8(6):533. doi: 10.3390/cells8060533
7. Brucklacher-Waldert V, Stuerner K, Kolster M, Wolthausen J, Tolosa E. Phenotypical and Functional Characterization of T Helper 17 Cells in Multiple Sclerosis. *Brain* (2009) 132(12):3329–41. doi: 10.1093/brain/awp289
8. Volpe E, Battistini L, Borsellino G. Advances in T Helper 17 Cell Biology: Pathogenic Role and Potential Therapy in Multiple Sclerosis. *Mediators Inflammation* (2015) 2015. doi: 10.1155/2015/475158
9. Acosta-Rodriguez EV, Napolitani G, Lanzavecchia A, Sallusto F. Interleukins 1β and 6 But Not Transforming Growth Factor-β Are Essential for the Differentiation of Interleukin 17–Producing Human T Helper Cells. *Nat Immunol* (2007) 8(9):942–9. doi: 10.1038/ni1496
10. Reboldi A, Coisne C, Baumjohann D, Benvenuto F, Bottinelli D, Lira S, et al. CC Chemokine Receptor 6–Regulated Entry of T H-17 Cells Into the CNS Through the Choroid Plexus Is Required for the Initiation of EAE. *Nat Immunol* (2009) 10(5):514. doi: 10.1038/ni.1716
11. McGeachy MJ, Bak-Jensen KS, Chen YI, Tato CM, Blumenschein W, McClanahan T, et al. TGF-β and IL-6 Drive the Production of IL-17 and IL-10 by T Cells and Restrain TH-17 Cell–Mediated Pathology. *Nat Immunol* (2007) 8(12):1390–7. doi: 10.1038/ni1539
12. Wan P, Su W, Zhuo Y. The Role of Long Noncoding RNAs in Neurodegenerative Diseases. *Mol Neurobiol* (2017) 54(3):2012–21. doi: 10.1007/s12035-016-9793-6
13. Sun M, Kraus WL. From Discovery to Function: The Expanding Roles of Long Noncoding RNAs in Physiology and Disease. *Endocrine Rev* (2015) 36 (1):25–64. doi: 10.1210/er.2014-1034
14. Ma L, Bajic VB, Zhang Z. On the Classification of Long Non-Coding RNAs. *RNA Biol* (2013) 10(6):924–33. doi: 10.4161/rna.24604
15. Aune TM, Spurlock CFIII. Long Non-Coding RNAs in Innate and Adaptive Immunity. *Virus Res* (2016) 212:146–60. doi: 10.1016/j.virusres.2015.07.003
16. Wu H, Zhao M, Yoshimura A, Chang C, Lu Q. Critical Link Between Epigenetics and Transcription Factors in the Induction of Autoimmunity: A Comprehensive Review. *Clin Rev Allergy Immunol* (2016) 50(3):333–44. doi: 10.1007/s12016-016-8534-y
17. Riva P, Ratti A, Venturin M. The Long Non-Coding RNAs in Neurodegenerative Diseases: Novel Mechanisms of Pathogenesis. *Curr Alzheimer Res* (2016) 13 (11):1219–31. doi: 10.2174/1567205013666160622112234
18. Quan Z, Zheng D, Qing H. Regulatory Roles of Long Non-Coding RNAs in the Central Nervous System and Associated Neurodegenerative Diseases. *Front Cell Neurosci* (2017) 11:175. doi: 10.3389/fncel.2017.00175
19. Fang S, Zhang L, Guo J, Niu Y, Wu H, Li H, et al. NONCODEV5: A Comprehensive Annotation Database for Long Non-Coding RNAs. *Nucleic Acids Res* (2018) 46(D1):D308–14. doi: 10.1093/nar/gkx1107
20. Laurent GS, Wahlestedt C, Kapranov P. The Landscape of Long Noncoding RNA Classification. *Trends Genet* (2015) 31(5):239–51. doi: 10.1016/j.tig.2015.03.007
21. Quinn JJ, Chang HY. Unique Features of Long Non-Coding RNA Biogenesis and Function. *Nat Rev Genet* (2016) 17(1):47. doi: 10.1038/nrg.2015.10
22. Hu G, Tang Q, Sharma S, Yu F, Escobar TM, Muljo SA, et al. Expression and Regulation of Intergenic Long Noncoding RNAs During T Cell Development and Differentiation. *Nat Immunol* (2013) 14(11):1190–8. doi: 10.1038/ni.2712
23. Moher D, Liberati A, Tetzlaff J, Altman DGThe PRISMA Group. Preferred Reporting Items for Systematic Reviews and Meta-Analyses: The PRISMA Statement. *Int J Surg* (2010) 8(5):336–41. doi: 10.1016/j.ijsu.2010.02.007
24. Bahrami T, Taheri M, Javadi S, Omrani MD, Karimipour M. Expression Analysis of Long Non-Coding RNA Lnc-DC in HLA-DRB1*15:01-Negative Patients With Multiple Sclerosis: A Probable Cause for Gender Differences in Multiple Sclerosis Susceptibility? *J Mol Neurosci* (2021) 71(4):821–5. doi: 10.1007/s12031-020-01704-7
25. Bahrami T, Taheri M, Javadi S, Omrani MD, Karimipour M. Associations Between Genomic Variants in lncRNA-TRPM2-AS and lncRNA-HNF1A-AS1 Genes and Risk of Multiple Sclerosis. *J Mol Neurosci* (2020) 70(7):1050–5. doi: 10.1007/s12031-020-01504-z
26. Bina P, Kakhki MD, Sahraian MA, Behmanesh M. The Expression of lnc-IL-7R Long Non-Coding RNA Dramatically Correlated With Soluble and Membrane-Bound Isoforms of IL-7Ra Gene in Multiple Sclerosis Patients. *Neurosci Lett* (2017) 642:174–8. doi: 10.1016/j.neulet.2017.01.068
27. Cardamone G, Paraboschi EM, Solda G, Cantoni C, Supino D, Piccio L, et al. Not Only Cancer: The Long Non-Coding RNA MALAT1 Affects the Repertoire of Alternatively Spliced Transcripts and Circular RNAs in Multiple Sclerosis. *Hum Mol Genet* (2019) 28(9):1414–28. doi: 10.1093/hmg/ddy438
28. Dastmalchi R, Ghafouri-Fard S, Omrani MD, Mazdeh M, Sayad A, Taheri M. Dysregulation of Long Non-Coding RNA Profile in Peripheral Blood of Multiple Sclerosis Patients. *Mult Scler Relat Disord* (2018) 25:219–26. doi: 10.1016/j.msard.2018.07.044
29. Dastmalchi R, Omrani MD, Mazdeh M, Arsang-Jang S, Movafagh A, Sayad A, et al. Expression of Long Non-Coding RNAs (UCA1 and CCAT2) in the Blood of Multiple Sclerosis Patients: A Case-Control Study. *Iranian Red Crescent Med J* (2018) 20(8). doi: 10.5812/ircmj.66334

30. Dehghanzad R, Kakhki MP, Alikhah A, Sahraian MA, Behmanesh M. The Putative Association of TOB1-AS1 Long Non-Coding RNA With Immune Tolerance: A Study on Multiple Sclerosis Patients. *Neuromol Med* (2020) 22 (1):100–10. doi: 10.1007/s12017-019-08567-1
31. Eftekharian MM, Ghafouri-Fard S, Soudyab M, Omrani MD, Rahimi M, Sayad A, et al. Expression Analysis of Long Non-Coding RNAs in the Blood of Multiple Sclerosis Patients. *J Mol Neurosci* (2017) 63(3-4):333–41. doi: 10.1007/s12031-017-0982-1
32. Eftekharian MM, Noroozi R, Komaki A, Mazdeh M, Ghafouri-Fard S, Taheri M. MALAT1 Genomic Variants and Risk of Multiple Sclerosis. *Immunol Investig* (2019) 48(5):549–54. doi: 10.1080/08820139.2019.1576728
33. Eftekharian MM, et al. GAS5 Genomic Variants and Risk of Multiple Sclerosis. *Neurosci Lett* (2019) 701:54–7. doi: 10.1016/j.neulet.2019.02.028
34. Eftekharian MM, et al. Nicotinamide Nucleotide Transhydrogenase Expression Analysis in Multiple Sclerosis Patients. *Int J Neurosci* (2019) 129(12):1256–60. doi: 10.1080/00207454.2019.1660655
35. Fenoglio C, et al. LncRNAs Expression Profile in Peripheral Blood Mononuclear Cells From Multiple Sclerosis Patients. *J Neuroimmunol* (2018) 324:129–35. doi: 10.1016/j.jneuroim.2018.08.008
36. Ganji M, et al. Expression Analysis of Long Non-Coding RNAs and Their Target Genes in Multiple Sclerosis Patients. *Neurol Sci* (2019) 40(4):801–11. doi: 10.1007/s10072-019-3720-3
37. Ghaiad HR, et al. Long Noncoding RNAs APOA1-AS, IFNG-AS1, RMRP and Their Related Biomolecules in Egyptian Patients With Relapsing-Remitting Multiple Sclerosis: Relation to Disease Activity and Patient Disability. *J Adv Res* (2020) 21:141–50. doi: 10.1016/j.jare.2019.10.012
38. Gharesouran J, et al. The Growth Arrest-Specific Transcript 5 (GAS5) and Nuclear Receptor Subfamily 3 Group C Member 1 (NR3C1): Novel Markers Involved in Multiple Sclerosis. *Int J Mol Cell Med* (2018) 7(2):102–10. doi: 10.22088/IJMCM.BUMS.7.2.102
39. Gharesouran J, et al. A Novel Regulatory Function of Long Non-Coding RNAs at Different Levels of Gene Expression in Multiple Sclerosis. *J Mol Neurosci* (2019) 67(3):434–40. doi: 10.1007/s12031-018-1248-2
40. Gharesouran J, et al. Integrative Analysis of OIP5-AS1/HUR1 to Discover New Potential Biomarkers and Therapeutic Targets in Multiple Sclerosis. *J Cell Physiol* (2019) 234(10):17351–60. doi: 10.1002/jcp.28355
41. Gharzi V, et al. Expression Analysis of BDNF Gene and BDNF-AS Long Noncoding RNA in Whole Blood Samples of Multiple Sclerosis Patients: Not Always a Negative Correlation Between Them. *Iran J Allergy Asthma Immunol* (2018) 17(6):548–56. doi: 10.18502/ijaai.v17i6.619
42. Ghoveud E, et al. Potential Biomarker and Therapeutic LncRNAs in Multiple Sclerosis Through Targeting Memory B Cells. *NeuroMol Med* (2020) 22(1):111–20. doi: 10.1007/s12017-019-08570-6
43. Hosseini A, et al. LncRNAs Associated With Multiple Sclerosis Expressed in the Th1 Cell Lineage. *J Cell Physiol* (2019) 234(12):22153–62. doi: 10.1002/jcp.28779
44. Kozin M, et al. Mitonuclear Interactions Influence Multiple Sclerosis Risk. *Gene* (2020) 758:144962. doi: 10.1016/j.gene.2020.144962
45. Masoumi F, et al. Malat1 Long Noncoding RNA Regulates Inflammation and Leukocyte Differentiation in Experimental Autoimmune Encephalomyelitis. *J Neuroimmunol* (2019) 328:50–9. doi: 10.1016/j.jneuroim.2018.11.013
46. Mazdeh M, et al. Long Non-Coding RNA AFAP1-AS1 Is Upregulated in a Subset of Multiple Sclerosis Patients. *Clin Exp Neuroimmunol* (2019) 10 (2):105–9. doi: 10.1111/cen3.12513
47. Mazdeh M, et al. Single Nucleotide Polymorphisms of lncRNA H19 Are Not Associated With Risk of Multiple Sclerosis in Iranian Population. *Meta Gene* (2019) 21. doi: 10.1016/j.mgene.2019.100592
48. Moradi A, et al. Evaluation of the Expression Levels of Three Long Non-Coding RNAs in Multiple Sclerosis. *Cell J* (2019) 22(2):165–70.
49. Moradi M, et al. Role of NR3C1 and GAS5 Genes Polymorphisms in Multiple Sclerosis. *Int J Neurosci* (2020) 130(4):407–12. doi: 10.1080/00207454.2019.1694019
50. Pahlevan Kakhki M, et al. HOTAIR But Not ANRIL Long Non-Coding RNA Contributes to the Pathogenesis of Multiple Sclerosis. *Immunology* (2018) 153(4):479–87. doi: 10.1111/imm.12850
51. Pahlevan Kakhki M, et al. Differential Expression of STAT3 Gene and its Regulatory Long Non-Coding RNAs, Namely lnc-DC and THRIL, in Two Eastern Iranian Ethnicities With Multiple Sclerosis. *Neurol Sci* (2020) 41 (3):561–8. doi: 10.1007/s10072-019-04092-y
52. Patoughi M, et al. GAS8 and its Naturally Occurring Antisense RNA as Biomarkers in Multiple Sclerosis. *Immunobiology* (2019) 224(4):560–4. doi: 10.1016/j.imbio.2019.04.005
53. Patoughi M, et al. Expression Analysis of PINK1 and PINK1-AS in Multiple Sclerosis Patients Versus Healthy Subjects. *Nucleosides Nucleotides Nucleic Acids* (2020) 40(2):157–65. doi: 10.1080/15257770.2020.1844229
54. Rahmani S, Noorolyai S, Ayromlou H, Shahgoli VK, Shanehbandi D, Baghbani E, et al. The Expression Analyses of RMRP, DDX5, and RORC in RRMS Patients Treated With Different Drugs Versus Naive Patients and Healthy Controls. *Gene* (2021) 769:145236. doi: 10.1016/j.gene.2020.145236
55. Rezazadeh M, et al. Association Study of ANRIL Genetic Variants and Multiple Sclerosis. *J Mol Neurosci* (2018) 65(1):54–9. doi: 10.1007/s12031-018-1069-3
56. Rodríguez-Lorenzo S, Francisco DM, Vos R, van Het Hof B, Rijnsburger M, Schroten H, et al. Altered Secretory and Neuroprotective Function of the Choroid Plexus in Progressive Multiple Sclerosis. *Acta Neuropathol Commun* (2020) 8(1):1–3. doi: 10.1186/s40478-020-00903-y
57. Safa A, et al. Dysregulation of NF-κb-Associated lncRNAs in Multiple Sclerosis Patients. *J Mol Neurosci* (2021) 71(1):80–8. doi: 10.1007/s12031-020-01628-2
58. Safa A, et al. Downregulation of Cancer-Associated lncRNAs in Peripheral Blood of Multiple Sclerosis Patients. *J Mol Neurosci* (2020) 70(10):1533–40. doi: 10.1007/s12031-020-01646-0
59. Santoro M, et al. Expression Profile of Long Non-Coding RNAs in Serum of Patients With Multiple Sclerosis. *J Mol Neurosci* (2016) 59(1):18–23. doi: 10.1007/s12031-016-0741-8
60. Santoro M, et al. A Pilot Study of lncRNAs Expression Profile in Serum of Progressive Multiple Sclerosis Patients. *Eur Rev Med Pharmacol Sci* (2020) 24(6):3267–73.
61. Sayad A, et al. Hepatocellular Carcinoma Up-Regulated Long Non-Coding RNA: A Putative Marker in Multiple Sclerosis. *Metab Brain Dis* (2019) 34 (4):1201–5. doi: 10.1007/s11011-019-00418-z
62. Senousy MA, et al. LncRNA GAS5 and miR-137 Polymorphisms and Expression Are Associated With Multiple Sclerosis Risk: Mechanistic Insights and Potential Clinical Impact. *ACS Chem Neurosci* (2020) 11 (11):1651–60. doi: 10.1021/acschemneuro.0c00150
63. Shaker OG, et al. Correlation Between LincR-Gng2-5'and LincR-Epas1-3'as With the Severity of Multiple Sclerosis in Egyptian Patients. *Int J Neurosci* (2020) 130(5):515–21. doi: 10.1080/00207454.2019.1695610
64. Shaker OG, et al. lincR-Ccr2-5 ' AS and THRIL as Potential Biomarkers of Multiple Sclerosis. *Egyptian J Med Hum Genet* (2021) 22(1). doi: 10.1186/s43042-021-00151-2
65. Shaker OG, et al. LncRNAs, MALAT1 and lnc-DC as Potential Biomarkers for Multiple Sclerosis Diagnosis. *Biosci Rep* (2019) 39(1). doi: 10.1042/BSR20181335
66. Taheri M, Noroozi R, Sadeghpour S, Omrani MD, Ghafouri-Fard S. The Rs4759314 SNP Within Hotair lncRNA Is Associated With Risk of Multiple Sclerosis. *Multiple Sclerosis Relat Disord* (2020) 40:101986. doi: 10.1016/j.msard.2020.101986
67. Teimuri S, et al. Integrative Analysis of lncRNAs in Th17 Cell Lineage to Discover New Potential Biomarkers and Therapeutic Targets in Autoimmune Diseases. *Mol Ther Nucleic Acids* (2018) 12:393–404. doi: 10.1016/j.omtn.2018.05.022
68. Zhang F, et al. Expression Profile of Long Noncoding RNAs in Peripheral Blood Mononuclear Cells From Multiple Sclerosis Patients. *CNS Neurosci Ther* (2016) 22(4):298–305. doi: 10.1111/cns.12498
69. Zhang F, et al. DDIT4 and Associated Lncddit4 Modulate Th17 Differentiation Through the DDIT4/TSC/mTOR Pathway. *J Immunol* (2018) 200(5):1618–26. doi: 10.4049/jimmunol.1601689
70. Zhang F, et al. Linc-MAF-4 Regulates Th1/Th2 Differentiation and Is Associated With the Pathogenesis of Multiple Sclerosis by Targeting MAF. *FASEB J* (2017) 31(2):519–25. doi: 10.1096/fj.201600838R
71. Bian Z, et al. Gm15575 Functions as a ceRNA to Up-Regulate CCL7 Expression Through Sponging miR-686 in Th17 Cells. *Mol Immunol* (2020) 125:32–42. doi: 10.1016/j.molimm.2020.06.027
72. Duan C, Liu Y, Li Y, Chen H, Liu X, Chen X, et al. Sulfasalazine Alters Microglia Phenotype by Competing Endogenous RNA Effect of miR-136-5p

and Long Non-Coding RNA HOTAIR in Cuprizone-Induced Demyelination. *Biochem Pharmacol* (2018) 155:110–23. doi: 10.1016/j.bcp.2018.06.028
73. Guo W, Lei W, Yu D, Ge Y, Chen Y, Xue W, et al. Involvement of lncRNA-1700040D17Rik in Th17 Cell Differentiation and the Pathogenesis of EAE. *Int Immunopharmacol* (2017) 47:141–9. doi: 10.1016/j.intimp.2017.03.014
74. Liu X, Zhou F, Wang W, Chen G, Zhang Q, Lv R, et al. IL-9-Triggered lncRNA Gm13568 Regulates Notch1 in Astrocytes Through Interaction With CBP/P300: Contribute to the Pathogenesis of Experimental Autoimmune Encephalomyelitis. *J Neuroinflamm* (2021) 18(1):1–5. doi: 10.1186/s12974-021-02156-5
75. Sun DY, Yu Z, Fang X, Liu M, Pu Y, Shao Q, et al. LncRNA GAS5 Inhibits Microglial M2 Polarization and Exacerbates Demyelination. *EMBO Rep* (2017) 18(10):1801–16. doi: 10.15252/embr.201643668
76. Yue P, Jing L, Zhao X, Zhu H, Teng J. Down-Regulation of Taurine-Up-Regulated Gene 1 Attenuates Inflammation by Sponging miR-9-5p *via* Targeting NF-κb1/P50 in Multiple Sclerosis. *Life Sci* (2019) 233:116731. doi: 10.1016/j.lfs.2019.116731
77. Powell JD, et al. Regulation of Immune Responses by mTOR. *Annu Rev Immunol* (2012) 30:39–68. doi: 10.1146/annurev-immunol-020711-075024
78. Lock C, Hermans G, Pedotti R, Brendolan A, Schadt E, Garren H, et al. Gene-Microarray Analysis of Multiple Sclerosis Lesions Yields New Targets Validated in Autoimmune Encephalomyelitis. *Nat Med* (2002) 8(5):500–8. doi: 10.1038/nm0502-500
79. Matusevicius D, Kivisäkk P, He B, Kostulas N, Özenci V, Fredrikson S, et al. Interleukin-17 mRNA Expression in Blood and CSF Mononuclear Cells Is Augmented in Multiple Sclerosis. *Multiple Sclerosis J* (1999) 5(2):101–4. doi: 10.1191/135245899678847275
80. Amaral PP, Clark MB, Gascoigne DK, Dinger ME, Mattick JS. LncRNAdb: A Reference Database for Long Noncoding RNAs. *Nucleic Acids Res* (2011) 39 (suppl_1):D146–51. doi: 10.1093/nar/gkq1138
81. Ransohoff JD, Wei Y, Khavari PA. The Functions and Unique Features of Long Intergenic Non-Coding RNA. *Nat Rev Mol Cell Biol* (2018) 19(3):143. doi: 10.1038/nrm.2017.104
82. Stelzer G, Rosen N, Plaschkes I, Zimmerman S, Twik M, Fishilevich S, et al. The GeneCards Suite: From Gene Data Mining to Disease Genome Sequence Analyses. *Curr Protoc Bioinf* (2016) 54(1):1.30. 1–1.30. 33.
83. Wang Y, Zhong H, Xie X, Chen CY, Huang D, Shen L, et al. Long Noncoding RNA Derived From CD244 Signaling Epigenetically Controls CD8+ T-Cell Immune Responses in Tuberculosis Infection. *Proc Natl Acad Sci* (2015) 112 (29):E3883–92. doi: 10.1073/pnas.1501662112
84. Luo M, Liu X, Meng H, Xu L, Li Y, Li Z, et al. IFNA-AS1 Regulates CD4+ T Cell Activation in Myasthenia Gravis Though HLA-Drb1. *Clin Immunol* (2017) 183:121–31. doi: 10.1016/j.clim.2017.08.008
85. Aune TM, Crooke PS, Spurlock CF. Long Noncoding RNAs in T Lymphocytes. *J Leukocyte Biol* (2016) 99(1):31–44. doi: 10.1189/jlb.1RI0815-389R
86. Stein N, Berhani O, Schmiedel D, Duev-Cohen A, Seidel E, Kol I, et al. IFNG-AS1 Enhances Interferon Gamma Production in Human Natural Killer Cells. *Iscience* (2019) 11:466–73. doi: 10.1016/j.isci.2018.12.034
87. Collier SP, Collins PL, Williams CL, Boothby MR, Aune TM. Cutting Edge: Influence of Tmevpg1, a Long Intergenic Noncoding RNA, on the Expression of Ifng by Th1 Cells. *J Immunol* (2014) 192(1):533–3. doi: 10.4049/jimmunol.1390068
88. Yu Q, Chang HC, Ahyi AN, Kaplan MH. Transcription Factor-Dependent Chromatin Remodeling of Il18r1 During Th1 and Th2 Differentiation. *J Immunol* (2008) 181(5):3346–52. doi: 10.4049/jimmunol.181.5.3346
89. Gutcher I, et al. Interleukin 18–Independent Engagement of Interleukin 18 Receptor-α Is Required for Autoimmune Inflammation. *Nat Immunol* (2006) 7(9):946–53. doi: 10.1038/ni1377
90. Tzachanis D, Freeman GJ, Hirano N, van Puijenbroek AA, Delfs MW, Berezovskaya A, et al. Tob Is a Negative Regulator of Activation That Is Expressed in Anergic and Quiescent T Cells. *Nat Immunol* (2001) 2 (12):1174–82. doi: 10.1038/ni730
91. Li Z, Chao TC, Chang KY, Lin N, Patil VS, Shimizu C, Head SR, et al. The Long Noncoding RNA THRIL Regulates Tnfα Expression Through its Interaction With hnRNPL. *Proc Natl Acad Sci* (2014) 111(3):1002–7. doi: 10.1073/pnas.1313768111
92. Wang P, Xue Y, Han Y, Lin L, Wu C, Xu S, et al. The STAT3-Binding Long Noncoding RNA lnc-DC Controls Human Dendritic Cell Differentiation. *Science* (2014) 344(6181):310–3. doi: 10.1126/science.1251456
93. Xie Z, Guo Z, Liu J. Whey Acidic Protein/Four-Disulfide Core Domain 21 Regulate Sepsis Pathogenesis in a Mouse Model and a Macrophage Cell Line *via* the Stat3/toll-Like Receptor 4 (TLR4) Signaling Pathway. *Med Sci Moni: Int Med J Exp Clin Res* (2018) 24:4054. doi: 10.12659/MSM.907176
94. Alikhah A, Kakhkia MP, Ahmadi A, Dehghanzad R, Boroumand MA, Behmanesh M. The Role of lnc-DC Long Non-Coding RNA and SOCS1 in the Regulation of STAT3 in Coronary Artery Disease and Type 2 Diabetes Mellitus. *J Diabetes Its Complic* (2018) 32(3):258–65. doi: 10.1016/j.jdiacomp.2017.12.001
95. Zhang W, Zhou Y, Ding Y. Lnc-DC Mediates the Over-Maturation of Decidual Dendritic Cells and Induces the Increase in Th1 Cells in Preeclampsia. *Am J Reprod Immunol* (2017) 77(6):e12647. doi: 10.1111/aji.12647
96. Wu G-C, Li J, Leng RX, Li XP, Li XM, Wang DG, et al. Identification of Long Non-Coding RNAs GAS5, Linc0597 and lnc-DC in Plasma as Novel Biomarkers for Systemic Lupus Erythematosus. *Oncotarget* (2017) 8 (14):23650. doi: 10.18632/oncotarget.15569
97. Zhuang L, Tian J, Zhang X, Wang H, Huang C. Lnc-DC Regulates Cellular Turnover and the HBV-Induced Immune Response by TLR9/STAT3 Signaling in Dendritic Cells. *Cell Mol Biol Lett* (2018) 23(1):1–9. doi: 10.1186/s11658-018-0108-y
98. Zhou Y, Fang L, Peng L, Qiu W. TLR9 and its Signaling Pathway in Multiple Sclerosis. *J Neurol Sci* (2017) 373:95–9. doi: 10.1016/j.jns.2016.12.027
99. Kim C, Kang D, Lee EK, Lee JS. Long Noncoding RNAs and RNA-Binding Proteins in Oxidative Stress, Cellular Senescence, and Age-Related Diseases. *Oxid Med Cell Longevity* (2017) 2017. doi: 10.1155/2017/2062384
100. Abedin K, et al. Oxidative DNA Damage in the Spinal Cord in Multiple Sclerosis. *Neuropathol Appl Neurobiol* (2002) 28(2):168–8. doi: 10.1046/j.1365-2990.2002.39286_53.x
101. Tehrani SS, et al. Multiple Functions of Long Non-Coding RNAs in Oxidative Stress, DNA Damage Response and Cancer Progression. *J Cell Biochem* (2018) 119(1):223–36. doi: 10.1002/jcb.26217
102. Yang C, et al. Long Non-Coding RNA UCA1 Regulated Cell Cycle Distribution *via* CREB Through PI3-K Dependent Pathway in Bladder Carcinoma Cells. *Gene* (2012) 496(1):8–16. doi: 10.1016/j.gene.2012.01.012
103. Xue Y, et al. Long Noncoding RNA CCAT2 as an Independent Prognostic Marker in Various Carcinomas: Evidence Based on Four Studies. *Int J Clin Exp Med* (2016) 9(2):2567–72.
104. Ong MS, et al. 'Lnc'-Ing Wnt in Female Reproductive Cancers: Therapeutic Potential of Long Non-Coding RNAs in Wnt Signalling. *Br J Pharmacol* (2017) 174(24):4684–700. doi: 10.1111/bph.13958
105. Khalil AM, et al. Many Human Large Intergenic Noncoding RNAs Associate With Chromatin-Modifying Complexes and Affect Gene Expression. *Proc Natl Acad Sci* (2009) 106(28):11667–72. doi: 10.1073/pnas.0904715106
106. Li J, et al. LncRNA TUG1 Acts as a Tumor Suppressor in Human Glioma by Promoting Cell Apoptosis. *Exp Biol Med* (2016) 241(6):644–9. doi: 10.1177/1535370215622708
107. Mercer TR, et al. Long Noncoding RNAs in Neuronal-Glial Fate Specification and Oligodendrocyte Lineage Maturation. *BMC Neurosci* (2010) 11(1):14. doi: 10.1186/1471-2202-11-14
108. Barry G, et al. The Long Non-Coding RNA Gomafu Is Acutely Regulated in Response to Neuronal Activation and Involved in Schizophrenia-Associated Alternative Splicing. *Mol Psychiatry* (2014) 19(4):486–94. doi: 10.1038/mp.2013.45
109. Arunkumar G, et al. LncRNA OIP5-AS1 Is Overexpressed in Undifferentiated Oral Tumors and Integrated Analysis Identifies as a Downstream Effector of Stemness-Associated Transcription Factors. *Sci Rep* (2018) 8(1):1–13. doi: 10.1038/s41598-018-25451-3
110. Kim J, et al. LncRNA OIP5-AS1/cyrano Suppresses GAK Expression to Control Mitosis. *Oncotarget* (2017) 8(30):49409. doi: 10.18632/oncotarget.17219
111. Chen J, et al. Posttranscriptional Gene Regulation of IL-17 by the RNA-Binding Protein HuR Is Required for Initiation of Experimental Autoimmune Encephalomyelitis. *J Immunol* (2013) 191(11):5441–50. doi: 10.4049/jimmunol.1301188

112. Pruunsild P, et al. Dissecting the Human BDNF Locus: Bidirectional Transcription, Complex Splicing, and Multiple Promoters. *Genomics* (2007) 90(3):397–406. doi: 10.1016/j.ygeno.2007.05.004
113. Modarresi F, et al. Inhibition of Natural Antisense Transcripts *In Vivo* Results in Gene-Specific Transcriptional Upregulation. *Nat Biotechnol* (2012) 30(5):453–9. doi: 10.1038/nbt.2158
114. Yoshimura S, Ochi H, Isobe N, Matsushita T, Motomura K, Matsuoka T, et al. Altered Production of Brain-Derived Neurotrophic Factor by Peripheral Blood Immune Cells in Multiple Sclerosis. *Multiple Sclerosis J* (2010) 16(10):1178–88. doi: 10.1177/1352458510375706
115. Sasaki YT, Ideue T, Sano M, Mituyama T, Hirose T. Menε/β Noncoding RNAs Are Essential for Structural Integrity of Nuclear Paraspeckles. *Proc Natl Acad Sci* (2009) 106(8):2525–30. doi: 10.1073/pnas.0807899106
116. Bsibsi M, Bajramovic JJ, Vogt MH, van Duijvenvoorden E, Baghat A, Persoon-Deen C, et al. The Microtubule Regulator Stathmin Is an Endogenous Protein Agonist for TLR3. *J Immunol* (2010) 184(12):6929–37. doi: 10.4049/jimmunol.0902419
117. Wu G-C, Pan HF, Leng RX, Wang DG, Li XP, Li XM, et al. Emerging Role of Long Noncoding RNAs in Autoimmune Diseases. *Autoimmun Rev* (2015) 14(9):798–805. doi: 10.1016/j.autrev.2015.05.004
118. Imamura K, Imamachi N, Akizuki G, Kumakura M, Kawaguchi A, Nagata K, et al. Long Noncoding RNA NEAT1-Dependent SFPQ Relocation From Promoter Region to Paraspeckle Mediates IL8 Expression Upon Immune Stimuli. *Mol Cell* (2014) 53(3):393–406. doi: 10.1016/j.molcel.2014.01.009
119. Markert A, Grimm M, Martinez J, Wiesner J, Meyerhans A, Meyuhas O, et al. The La-Related Protein LARP7 Is a Component of the 7SK Ribonucleoprotein and Affects Transcription of Cellular and Viral Polymerase II Genes. *EMBO Rep* (2008) 9(6):569–75. doi: 10.1038/embor.2008.72
120. He N, Jahchan NS, Hong E, Li Q, Bayfield MA, Maraia RJ, et al. A La-Related Protein Modulates 7SK snRNP Integrity to Suppress P-TEFb-Dependent Transcriptional Elongation and Tumorigenesis. *Mol Cell* (2008) 29(5):588–99. doi: 10.1016/j.molcel.2008.01.003
121. Bo H, Gong Z, Zhang W, Li X, Zeng Y, Liao Q, et al. Upregulated Long Non-Coding RNA AFAP1-AS1 Expression Is Associated With Progression and Poor Prognosis of Nasopharyngeal Carcinoma. *Oncotarget* (2015) 6 (24):20404. doi: 10.18632/oncotarget.4057
122. Kamphuis W, Derada Troletti C, Reijerkerk A, Romero I, de Vries EH. The Blood-Brain Barrier in Multiple Sclerosis: microRNAs as Key Regulators. *CNS Neurol Disorders-Drug Targets (Formerly Curr Drug Targets-CNS Neurol Disorders)* (2015) 14(2):157–67. doi: 10.2174/1871527314666150116125246
123. Reedquist KA, Tak PP. Suppl 2: Signal Transduction Pathways in Chronic Inflammatory Autoimmune Disease: Small GTPases. *Open Rheumatol J* (2012) 6:259. doi: 10.2174/1874312901206010259
124. Zhang J-Y, Weng M-Z, Song F-B, Xu Y-G, Liu Q, Wu J-Y, et al. Long Noncoding RNA AFAP1-AS1 Indicates a Poor Prognosis of Hepatocellular Carcinoma and Promotes Cell Proliferation and Invasion *via* Upregulation of the RhoA/Rac2 Signaling. *Int J Oncol* (2016) 48(4):1590–8. doi: 10.3892/ijo.2016.3385
125. Zhao Y, Chu Y, Sun J, Song R, Li Y, Xu F. LncRNA Gas8-AS Inhibits Colorectal Cancer (CRC) Cell Proliferation by Downregulating lncRNA AFAP1-As1. *Gene* (2019) 710:140–4. doi: 10.1016/j.gene.2019.05.040
126. Zha Z, Han Q, Liu W, Huo S. lncRNA GAS8-AS1 Downregulates lncRNA UCA1 to Inhibit Osteosarcoma Cell Migration and Invasion. *J Orthopaedic Surg Res* (2020) 15(1):1–6. doi: 10.1186/s13018-020-1550-x
127. Tuosto L. Targeting Inflammatory T Cells in Multiple Sclerosis: Current Therapies and Future Challenges. *Austin J Mult Scler Neuroimmunol* (2015) 2(1):1009. doi: 10.26420/austinjmultsclerneuroimmunol.2015.1009
128. Scheele C, Petrovic N, Faghihi MA, Lassmann T, Fredriksson K, Rooyackers O, et al. The Human PINK1 Locus Is Regulated *In Vivo* by a Non-Coding Natural Antisense RNA During Modulation of Mitochondrial Function. *BMC Genomics* (2007) 8(1):1–13. doi: 10.1186/1471-2164-8-74
129. Wendlandt EB, Graff JW, Gioannini TL, McCaffrey AP, Wilson ME. The Role of microRNAs miR-200b and miR-200c in TLR4 Signaling and NF-κb Activation. *Innate Immun* (2012) 18(6):846–55. doi: 10.1177/1753425912443903
130. Guo W, Luo C, Wang C, Wang Yh, Wang X, Gao Xd, et al. Suppression of Human and Mouse Th17 Differentiation and Autoimmunity by an Endogenous Interleukin 23 Receptor Cytokine-Binding Homology Region. *Int J Biochem Cell Biol* (2014) 55:304–10. doi: 10.1016/j.biocel.2014.09.019
131. Liu X, Zhang Q, Wang W, Zuo D, Wang J, Zhou F, et al. Analysis of Long Noncoding RNA and mRNA Expression Profiles in IL-9-Activated Astrocytes and EAE Mice. *Cell Physiol Biochem* (2018) 45(5):1986–98. doi: 10.1159/000487975

Conflict of Interest: The authors declare that the research was conducted in the absence of any commercial or financial relationships that could be construed as a potential conflict of interest.

Publisher's Note: All claims expressed in this article are solely those of the authors and do not necessarily represent those of their affiliated organizations, or those of the publisher, the editors and the reviewers. Any product that may be evaluated in this article, or claim that may be made by its manufacturer, is not guaranteed or endorsed by the publisher.

GLOSSARY

lncRNA	long non-coding RNA
MS	multiple sclerosis
RT-PCR	real-time polymerase chain reaction
AFAP1-AS1	actin filament-associated protein 1 antisense RNA 1
RRMS	relapsing–remitting multiple sclerosis
SPMS	secondary progressive multiple sclerosis
CNS	central nervous system
HOTAIR	Hox transcript antisense intergenic RNA
miRNAs	microRNAs
CD4+ T cells	T helper cells
CD8+ T cells	cytotoxic T cells
GWAS	genome-wide association studies
BDNF	brain-derived neurotrophic factor
BDNF-AS	BDNF antisense RNA
NR3C1	nuclear receptor subfamily 3 group C member 1
PRC2	polycarbonate 2 suppressor complex
DDIT4	DNA-damage-inducible transcript 4
mTORC1	mammalian target of rapamycin complex 1
lncDDIT4	lncRNA DDIT4
Th17	T helper 17 cell
Tregs	regulatory T cells
IFN-γ	interferon gamma
hnRNPs	heterogeneous nuclear ribonucleoproteins
DC	dendritic cells
lnc-DC	lncRNA expressed in DC
PANDA	P21-associated ncRNA DNA damage-activated
FAS-AS1	FAS antisense transcript 1
linc-MAF-4	A lncRNA
THRIL	TNF-α and heterogeneous nuclear ribonucleoprotein L
PVT1	plasmacytoma variant translocation 1
GAK	cyclin G-associated kinase
HuR1	Huantigen R
SIRT1	silent information regulator 1
OIP5-AS1	OIP5 antisense RNA 1
TUG1	taurine-upregulated gene
IL-8	interleukin 8
SFPQ	splicing factor proline- and glutamine-rich
IL-17	interleukin 17
STAT4	*signal transducer and activator of transcription 4*
EZH2	enhancer of zeste homolog 2
TNF-α	tumor necrosis factor alpha
TLR4	Toll-like receptor 4
NF-κB	nuclear factor kappa-light-chain-enhancer of activated B cells
MAPK	mitogen-activated protein kinase
PI3K	phosphoinositide 3-kinases
ERK1/2	extracellular signal-regulated kinases 1/2
AKT	protein kinase B
WNT	Wnt signaling pathway
SF1	splicing factor 1
GAK	G-associated kinase
NonPOU	non-POU domain-containing octamer-binding protein
P-TEFb	positive transcription elongation factor
BBB	blood–brain barrier
FGFR1	fibroblast growth factor receptor 1
ERK	extracellular signal-regulated kinase
TGF-β	transforming growth factor beta
CRP	C-reactive protein
PINK1-AS	PTEN-induced kinase 1-AS
HIF1-AS3	hypoxia-inducible factor 1-AS3
RMRP	RNA component of the mitochondrial RNA-processing endoribonuclease (RNase MRP)
GATA3	GATA-binding protein 3
GR	glucocorticoid receptor
HULC	highly upregulated liver cancer
ZEB1	zinc finger and homeodomain transcription factor 1

frontiers in Immunology

ORIGINAL RESEARCH
published: 08 December 2021
doi: 10.3389/fimmu.2021.770679

Long Non-Coding RNA- Associated Competing Endogenous RNA Axes in T-Cells in Multiple Sclerosis

Hani Sabaie[1,2], Zoha Salkhordeh[3], Mohammad Reza Asadi[4], Soudeh Ghafouri-Fard[5], Nazanin Amirinejad[6], Mahla Askarinejad Behzadi[6], Bashdar Mahmud Hussen[7], Mohammad Taheri[8,9] and Maryam Rezazadeh[1,2]**

[1] Molecular Medicine Research Center, Tabriz University of Medical Sciences, Tabriz, Iran, [2] Department of Medical Genetics, Faculty of Medicine, Tabriz University of Medical Sciences, Tabriz, Iran, [3] Department of Medical Genetics, Faculty of Medicine, Kerman University of Medical Sciences, Kerman, Iran, [4] Student Research Committee, Tabriz University of Medical Sciences, Tabriz, Iran, [5] Department of Medical Genetics, School of Medicine, Shahid Beheshti University of Medical Sciences, Tehran, Iran, [6] Department of Biology, Faculty of Sciences, Shahid Bahonar University of Kerman, Kerman, Iran, [7] Department of Pharmacognosy, College of Pharmacy, Hawler Medical University, Erbil, Iraq, [8] Men's Health and Reproductive Health Research Center, Shahid Beheshti University of Medical Sciences, Tehran, Iran, [9] Institute of Human Genetics, Jena University Hospital, Jena, Germany

OPEN ACCESS

Edited by:
Roberta Magliozzi,
University of Verona, Italy

Reviewed by:
Hikoaki Fukaura,
Saitama Medical University, Japan
Amin Safa,
Complutense University of Madrid, Spain
Rezvan Noroozi,
Jagiellonian University, Poland

***Correspondence:**
Mohammad Taheri
Mohammad_823@yahoo.com
Maryam Rezazadeh
Rezazadehm@tbzmed.ac.ir

Specialty section:
This article was submitted to Multiple Sclerosis and Neuroimmunology, a section of the journal Frontiers in Immunology

Received: 04 September 2021
Accepted: 22 November 2021
Published: 08 December 2021

Citation:
Sabaie H, Salkhordeh Z, Asadi MR, Ghafouri-Fard S, Amirinejad N, Askarinejad Behzadi M, Hussen BM, Taheri M and Rezazadeh M (2021) Long Non-Coding RNA- Associated Competing Endogenous RNA Axes in T-Cells in Multiple Sclerosis. Front. Immunol. 12:770679. doi: 10.3389/fimmu.2021.770679

Multiple sclerosis (MS) is an immune-mediated demyelinating and degenerative disease with unknown etiology. Inappropriate response of T-cells to myelin antigens has an essential role in the pathophysiology of MS. The clinical and pathophysiological complications of MS necessitate identification of potential molecular targets to understand the pathogenic events of MS. Since the functions and regulatory mechanisms of long non-coding RNAs (lncRNAs) acting as competing endogenous RNAs (ceRNAs) in MS are yet uncertain, we conducted a bioinformatics analysis to explain the lncRNA-associated ceRNA axes to clarify molecular regulatory mechanisms involved in T-cells responses in MS. Two microarray datasets of peripheral blood T-cell from subjects with relapsing-remitting MS and matched controls containing data about miRNAs (GSE43590), mRNAs and lncRNAs (GSE43591) were downloaded from the Gene Expression Omnibus database. Differentially expressed miRNAs (DEmiRNAs), mRNAs (DEmRNAs), and lncRNAs (DElncRNAs) were identified by the limma package of the R software. Protein-protein interaction (PPI) network and module were developed using the Search Tool for the Retrieval of Interacting Genes/Proteins (STRING) and the Molecular Complex Detection (MCODE) Cytoscape plugin, respectively. Using DIANA-LncBase and miRTarBase, the lncRNA-associated ceRNA axes was constructed. We conducted a Pearson correlation analysis and selected the positive correlations among the lncRNAs and mRNAs in the ceRNA axes. Lastly, DEmRNAs pathway enrichment was conducted by the Enrichr tool. A ceRNA regulatory relationship among Small nucleolar RNA host gene 1 (*SNHG1*), *hsa-miR-197-3p*, YOD1 deubiquitinase (*YOD1*) and zinc finger protein 101 (*ZNF101*) and downstream connected genes was identified. Pathway enrichment analysis showed that DEmRNAs were enriched in "Protein processing in endoplasmic reticulum" and "Herpes simplex virus 1 infection" pathways. To our

knowledge, this would be the first report of a possible role of *SNHG1/hsa-miR-197-3p/YOD1/ZNF101* axes in the pathogenesis of MS. This research remarks on the significance of ceRNAs and prepares new perceptions for discovering the molecular mechanism of MS.

Keywords: bioinformatics analysis, competing endogenous RNA, long non-coding RNA, microarray, multiple sclerosis

INTRODUCTION

Multiple sclerosis (MS) is the most frequent cause of non-traumatic neurological disability in young adult people (1). Estimates indicate that a total of 2.8 million individuals with MS live around the world (35.9 per 100,000 population) (2). In this degenerative disorder, the central nervous system is demyelinated through the mediation of the immune system. Yet, the main cause of MS is not known. MS presents in four clinical types: relapsing-remitting MS (RRMS), secondary progressive MS (SPMS), primary progressive MS (PPMS), and progressive relapsing MS (PRMS). RRMS is the most common subtype, which is represented by acute attacks (relapses) and then partially or fully recovered phases (remission) (3). Although the causes and etiologies underlie MS are not completely apprehended, there are proofs that it originates from multiple factors involving central and peripheral immunological tolerance mechanisms. An inappropriate T-cell response to myelin antigens is probably an important mechanism in MS pathogenesis (4). Emerging evidence indicates the potential of non-coding RNAs, especially long non-coding RNAs (lncRNAs) and the microRNAs (miRNAs), in the regulation of gene expression, providing novel prospects to understand the progression of MS (5–7). LncRNAs have major contributions to complex disorders (e.g., MS) through functioning as competing endogenous RNAs (ceRNAs) (8).

The ceRNA hypothesis suggests a cross-talk between both coding and non-coding RNAs through miRNA response elements (MREs), as miRNA complementary sequences, thereby forming a large-scale regulatory network in various parts of the transcriptome. Based on this supposition, through ceRNA regulatory mechanism, these two RNA transcripts will be indirectly correlated with miRNAs levels. Additionally, expression levels of these two RNA transcripts are positively correlated with each other (9). The consequence of disrupted balance of ceRNA cross-talk is well documented in a variety of disorders (10). Nevertheless, the roles and regulatory mechanisms of lncRNAs acting as ceRNAs in MS are still unclear.

As MS is complex in terms of both pathophysiological and clinical aspects, it is necessary to identify wide-ranging potential molecular targets to understand the pathogenic processes involved in MS. As the functions and regulatory mechanisms of lncRNAs role as ceRNAs in MS is not clear, bioinformatics analysis was done to clarify the lncRNA-associated ceRNA axes to explain molecular regulatory mechanisms involved in T-cells in MS.

METHODS

In the present study, we utilized a system biology methodology for mining data of the two microarray datasets of peripheral blood T-cell (GSE43590 and GSE43591) from patients with RRMS and matched controls, which are SubSeries of the SuperSeries GSE43592 (11). We intended to identify differentially expressed miRNAs (DEmiRNAs), mRNAs (DEmRNAs), and lncRNAs (DElncRNAs) and construct lncRNA-associated ceRNA axes. **Figure 1** summarizes the stages performed in the bioinformatics strategy. The study protocol was approved by Ethical Committee of Shahid Beheshti University of Medical Sciences and all methods were performed in accordance with the relevant guidelines and regulations.

Gene Expression Profile Data Collection

The miRNA profile data GSE43590 and lncRNA/mRNA profile data GSE43591 were obtained from the NCBI Gene Expression Omnibus database (GEO, https://www.ncbi.nlm.nih.gov/geo/). The platforms GPL14613 (miRNA-2) Affymetrix Multispecies miRNA-2 Array and GPL570 (HG-U133_Plus_2) Affymetrix Human Genome U133 Plus 2.0 Array were applied for GSE43590 and GSE43591 datasets, respectively. The GSE43590 included 11 peripheral blood samples from RRMS patients and nine from control subjects. The GSE43591 contained 20 peripheral blood samples, of which ten were from RRMS patients, and ten were served as controls.

Data Preprocessing and DEmRNAs, DElncRNAs, and DEmiRNAs Identification

Two datasets were analyzed separately. The Robust Multichip Average (RMA) was employed for background correction and quantile normalization of the entire raw data files (12). The quality was assessed by the AgiMicroRna Bioconductor package (version 2.40.0). The principal component analysis (PCA) was applied for a dimensional reduction analysis (13) to find similarities between each sample group by the ggplot2 package in R software version 4.0.3. Differential gene expression analysis (DGEA) was performed between RRMS and normal samples by the linear models for microarray data (limma) R package (14) in Bioconductor (https://www.bioconductor.org/) (15). The miRNAmeConverter Bioconductor package (16) was used to convert all miRNA names to miRBase v22. The previously applied methodology wasfor QA employed to detect lncRNA probes (17). We downloaded the full list of lncRNA genes with the approved HUGO Gene Nomenclature Committee (HGNC) symbols from

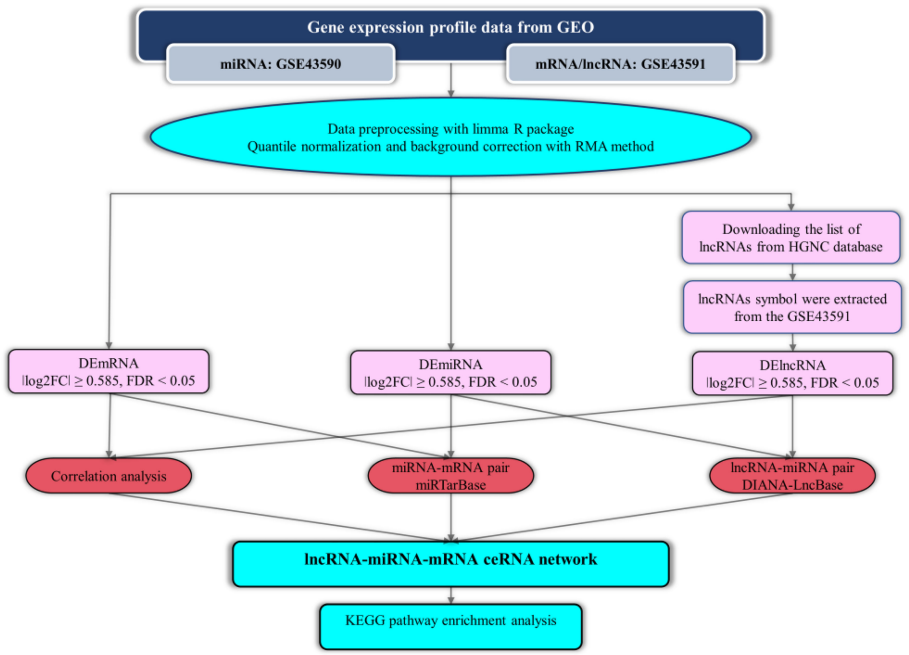

FIGURE 1 | Flow chart of bioinformatics analysis.

(https://www.genenames.org/) (18). Then, we compared the lncRNA gene list with our dataset gene symbols and chose the overlapped genes. Student t-test was utilized to detect statistically significant genes and the aberrantly expressed RNAs cut-off was set as: (1) a false discovery rate (adjusted *P*-value) < 0.05, and (2) | log2 fold change (log2FC)| ≥ 0.585. The heat map of DEmiRNAs and volcano plot of DEmRNAs/DElncRNAs were drawn using the Pheatmap (version 1.0.12) and ggplot2 packages of R.

Protein-Protein Interaction (PPI) Network Analysis and lncRNA-Associated ceRNA Axes Construction

PPIs were identified amongst the DEmRNAs using the Search Tool for the Retrieval of Interacting Genes/Proteins (STRING, https://string-db.org/) (19). For PPI network construction, a combined score of 0.4 (medium confidence) was selected. The PPI network was depicted using Cytoscape software (version 3.8.0) (20). In addition, the Molecular Complex Detection (MCODE) cytoscape plugin (version 2.0.0) was used to select most significant module in the PPI network (21). The experimentally validated interactions between miRNAs and lncRNAs were identified using DIANA-LncBase v3 (22). *Homo Sapiens* "Species" and high "miRNA Confidence Levels" were selected as criteria for the DIANA-LncBase query. Furthermore, we acquired the interactions between miRNAs and target mRNAs from miRTarBase (23), which were supported by experimental evidence. Next, a comparison was made between the obtained mRNAs and the previously attained mRNAs. Duplicated mRNAs were then utilized for constructing the lncRNA-miRNA-mRNA axes. LncRNAs, targeted mRNAs, and the interacted miRNAs were retrieved from the ceRNA axes based on the observed opposite expression pattern between the target mRNAs and lncRNAs. The ceRNA regulatory axes were generated by the Cytoscape software.

Correlation Analysis

We performed Pearson correlation analysis to find positive correlations between lncRNAs and mRNAs that were in the ceRNA axes. We used Hmisc (version 4.5.0) and psych (version 2.1.3) packages for the calculation of the correlations and visualization.

Kyoto Encyclopedia of Genes and Genomes (KEGG) Pathway Enrichment Analysis

The KEGG pathway enrichment analysis was done by the Enrichr tool (24, 25) for pathway enrichment for analyzing the DEmRNAs existing in the ceRNA axes.

RESULTS

DEmRNAs and DElncRNAs Identification

Background correction and normalization were performed prior to DGEA. The AgiMicroRna Bioconductor package was employed for controlling the quality of data. The spatial distribution of samples was demonstrated by a PCA plot (**Supplementary File S1**), which represents information concerning the structure of the examined data, and is helpful in finding similarities between samples. PCA showed that the

samples were heterogeneous. For noise reduction, few samples [GSM1065996, GSM1065997 (two control samples), and GSM1066022 (a patient sample)] were excluded from the analysis. As it is necessary to balance between noise reduction and sample size drop, only the most obvious outliers were removed. Three samples were excluded from further analysis: two control samples from GSE43590 and a RRMS sample from GSE43591.

Based on the criteria of adjusted *P*-value < 0.05, and (2) |log2 fold change (log2FC)| ≥ 0.585, a total of three human DEmiRNAs were identified from GSE43590, all of them being were downregulated. In the GSE43591 dataset, 19 DElncRNA (12 downregulated and seven upregulated), and 467 DEmRNA (307 downregulated and 160 upregulated) were screened. A heatmap for GSE43590 and a volcano plot for GSE43591 are shown in **Figure 2**. The details of DEGs are summarized in **Supplementary File S1**.

PPI Network Analysis and lncRNA-Associated ceRNA Axes Construction

Protein interactions amongst DEmRNAs were identified (cutoff score ≥ 0.4) using the online STRING tool. We eliminated non-interacting genes from the PPI network to simplify it. Furthermore, the highly connected module was detected by plugin MCODE. To elucidate the regulatory mechanism in T-cells in RRMS, we made regulatory ceRNA axes based on DElncRNA-DEmiRNA and DEmiRNA-DEmRNA interactions which were obtained from DIANA-LncBase and mirTarBase, respectively. DELncRNAs, targeted DEmRNAs, and also the interacted DEmiRNAs were deleted from the ceRNA axes in the opposite expression pattern present between DElncRNAs and the targeted DEmRNAs. In total, one key lncRNA (*SNHG1*: small nucleolar RNA host gene 1), one key miRNA (*hsa-miR-197-3p*), and two key mRNAs (*YOD1*: YOD1 deubiquitinase and *ZNF101*: zinc finger protein 101) were identified. The ceRNA axes in T-cell in MS and the downstream connected genes are depicted in **Figure 3**.

Correlation Analysis

The Pearson correlation analysis between lncRNA *SNHG1* and target mRNAs (*YOD1* and *ZNF101*) was conducted for the verification of the hypothesis that in the ceRNA axes, mRNA expression is positively regulated by lncRNA through interaction with miRNA (**Figure 4**). The results showed that expression of *SNHG1* is positively correlated with *YOD1* (r = 0.87, $P < 0.001$) and *ZNF101* (r = 0.86, $P < 0.001$).

KEGG Pathway Enrichment Analyses

The results of KEGG pathway enrichment analyses for DEmRNAs that were in the ceRNA axes are presented in **Figure 5**. The related pathways were "Protein processing in endoplasmic reticulum" and "Herpes simplex virus 1 infection".

DISCUSSION

Multiple reports have shown that ceRNA regulatory axes and connected networks act actively in various developmental procedures and pathological conditions, such as tumor formation and wide-ranging brain-related disorders (26, 27). The ceRNA is expressed differently according to tissue-related, cellular, and subcellular situations. There may be a variety of ceRNAs, including lncRNAs, circRNAs, pseudogenes, as well as mRNAs, in a network. LncRNAs, one of the main types of RNAs,

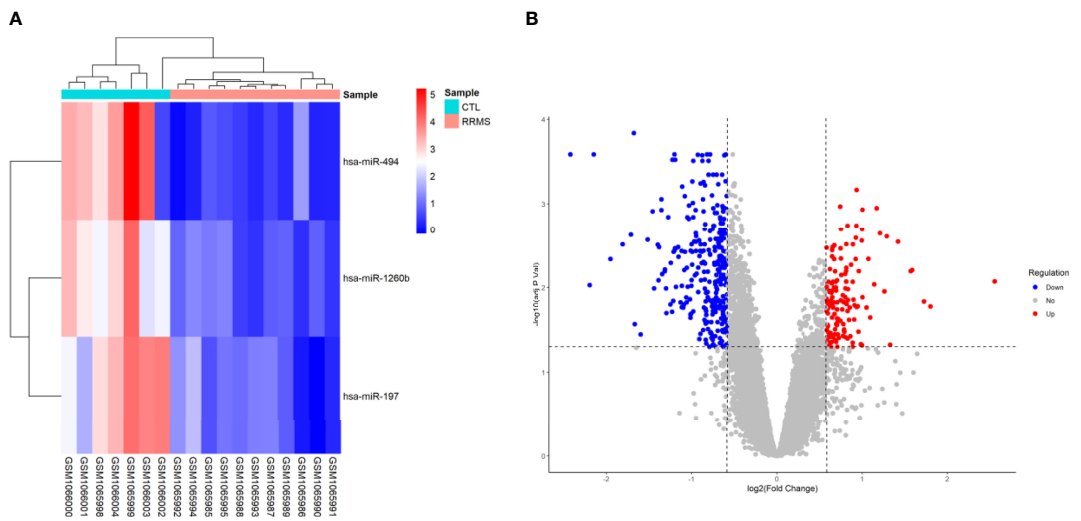

FIGURE 2 | Differentially expressed genes between relapsing-remitting multiple sclerosis (RRMS) samples and control (CTL) samples. **(A)** Heatmap of the DEmiRNAs in dataset GSE43590. The normalized relative expression values are in a range between zero and five. High expressed genes are shown in red, while those expressed at low levels are blue. **(B)** Volcano plot for the DEmRNAs and DElncRNAs in dataset GSE43591. The x-axis shows the log Fold Change, and the y-axis shows the -log10 (adjusted *P*-value). Upregulated and downregulated genes are represented by red and blue dots, respectively. The gray dots represent genes with no significant difference. The DEGs were screened according to a |(log2FC)≥ 0.585 and an adjusted *P*-value < 0.05.

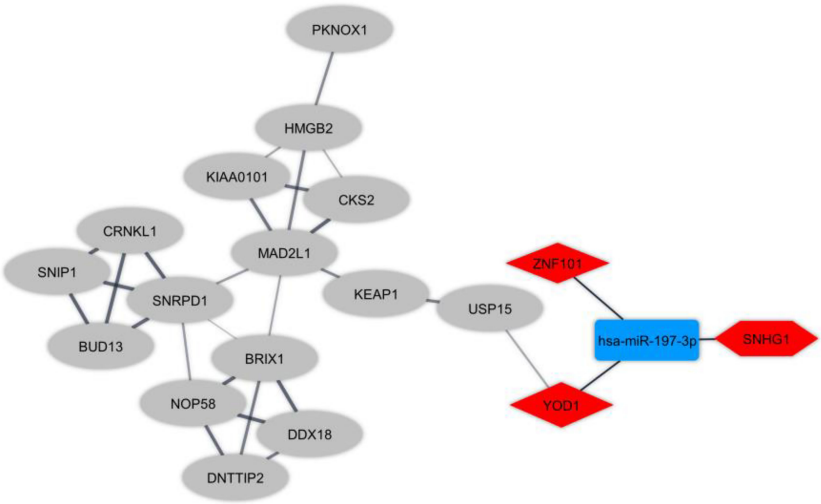

FIGURE 3 | The long non-coding RNA-associated competing endogenous RNA (ceRNA) axes in T-cell in Multiple sclerosis. The red and blue nodes represent the upregulation and downregulation, respectively. The hexagon nodes and the round rectangle nodes represent the lncRNA and miRNA, respectively. The diamond nodes represent miRNAs targeted mRNAs. The ellipse nodes represent downstream connected mRNAs.

are detected in the ceRNA machinery and significantly contribute to cellular mechanisms in both physiological and pathological situations (28). There is currently full agreement that lncRNAs are expressed variously according to tissue, cellular types, and developmental levels. Such a specific tissue dependence, in addition to subcellular dispersions, is a clear indication of the tight regulation of lncRNAs expression (29). As denoted in the theoretic notions, the ceRNA regulatory axes connected to lncRNAs can have a critical contribution to MS pathogenicity. Up to now, research on the ceRNA axes involved in MS has been insufficient, and it is necessary to further examine the corresponding expression patterns and mechanisms in MS.

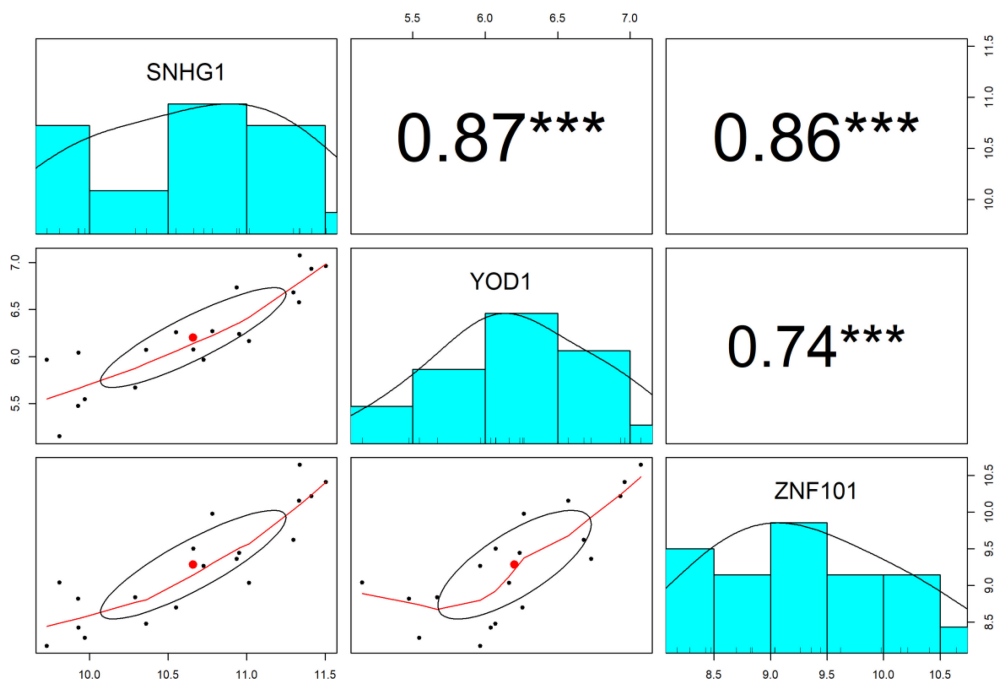

FIGURE 4 | The distribution of each variable is shown on the diagonal. The lower portion of the diagonal shows bivariate scatter plots with a fitted line. On the upper part of the diagonal, the correlation coefficients plus the significance level as stars are displayed. *** is significant correlation at *P*-value < 0.001.

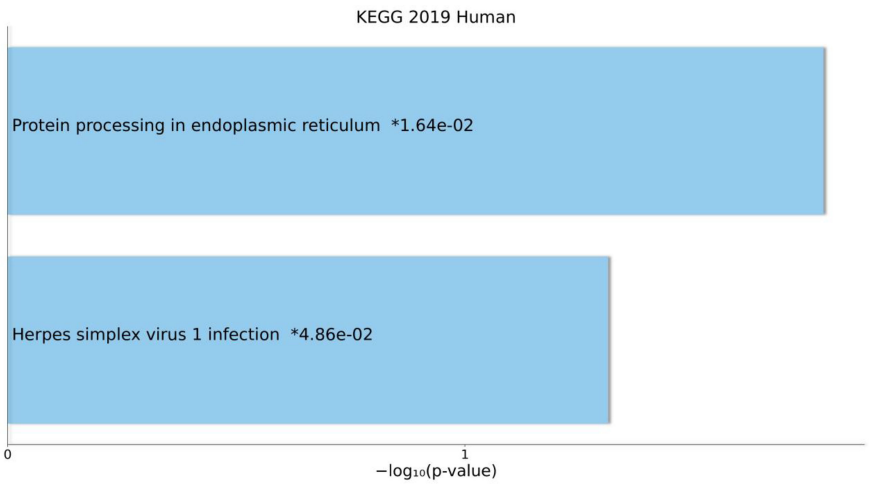

FIGURE 5 | Overall results of pathway enrichment analysis using Enrichr tool. The bar chart shows the enriched pathways, along with their corresponding *P*-values. Colored bars correspond to terms with significant *P*-values (<0.05). An asterisk (*) next to a *P*-value indicates the term also has a significant adjusted *P*-value (<0.05).

In the current study, we utilized a public database to download the expression profiles of peripheral blood T-cells from RRMS patients to assess the DEmiRNAs, DElncRNAs, and DEmRNAs in RRMS and normal samples and then construct lncRNA-miRNA-mRNA regulatory axes. According to these ceRNA axes and lncRNA-mRNA co-expression relationships, we found the lncRNA-miRNA-mRNA axes consisting of one lncRNA (*SNHG1*), one miRNA (*hsa-miR-197-3p*), and two mRNAs (*YOD1* and *ZNF101*).

A higher level of lncRNA *SNHG1* was detected in patients with RRMS in comparison with the controls. *SNHG1* is a recently described lncRNA involved in the development of several tumors and other types of disorders, including Alzheimer's disease (AD) and Parkinson's disease (PD). In line with our result, its upregulation has been seen in *in vitro* models of PD from neurons and microglia, mouse models, and AD *in vitro* models. It is involved in the pathogenesis of AD and PD through several complementary ceRNA mechanisms (27). To our knowledge, our research is the first to report the association between *SNHG1* and MS; thus, the reported result should be validated by extra investigations.

Conversely, the level of *hsa-miR-197-3p* was lower in RRMS patients in comparison with controls. In a profiling study using microarray analysis and validation by real-time polymerase chain reaction, *hsa-miR-197-3p* was identified as a downregulated significant regulatory miRNA in T-cells in RRMS (11), consistent with our result.

The expression of *YOD1* and *ZNF101* genes was increased in RRMS cases compared with controls. *YOD1* is a highly conserved deubiquitinase-like yeast ovarian tumor domain-containing protein 1 (OTU1) related to regulating the endoplasmic reticulum (ER)-associated degradation pathway. Indeed, *YOD1* is reported to be involved in the ER stress response induced by the mislocalization of unfolded proteins in mammalian cells. *YOD1* was shown to have elevated expression levels due to different stress conditions. Moreover, *YOD1* level upregulation was reported to be induced by neurogenic proteins, causing Huntington's disease and PD. The deubiquitinase YOD1 was proposed to contribute in the pathogenicity of neurodegenerative diseases by reducing ubiquitination of abnormal proteins and their degradation (30). Our result is in line with these findings. *ZNF101* was another gene in the ceRNA axes. Zinc finger proteins, including ZNF101 interact with nucleic acids and have lots of crucial activities, particularly regulation of transcription (31). In line with our result, a previous study reported that single nucleotide polymorphism rs1064395 in neurocan (*NCAN*) gene is associated with the upregulated expression level of *ZNF101* (32).

In the current study, KEGG pathway enrichment analysis also was conducted. The results showed that DEmRNAs that were in the ceRNA axes were enriched in "Protein processing in endoplasmic reticulum" and "Herpes simplex virus 1 infection" pathways, respectively. The unfolded protein response (UPR) happens to respond to ER stress resulting from the accretion of unfolded or misfolded proteins in the ER. The cytoprotective activities are promoted by the UPR to amend ER stress, but the influenced cells become apoptotic due to the UPR as a result of unresolved ER stress. The UPR is a central attribute of various disorders in humans, e.g., MS (33). Furthermore, an association between herpes simplex virus 1 (HSV-1) infection and demyelination has been reported in previous studies. Nonetheless, it is not certain whether HSV-1 is involved in MS etiology. Viruses, specifically HSV-1, may act as a risk factor for MS progression rather than a causative agent. This neurotropic pathogenic agent may mediate several molecular procedures (34).

There are some limitations in our study. Firstly, multiple parameters, including different methodologies, sample preparation, patient characteristics, platforms, and analyzing data, might influence the gene expression patterns. Secondly, a

small sample size can cause low statistical power. Lastly, the present findings need to be validated by confirmative experimental approaches as well as re-analysis of microarray gene expression profiles.

CONCLUSION

In conclusion, lncRNA *SNHG1* can serve as a ceRNA to regulate the expression of *YOD1* and *ZNF101* and downstream connected genes in T-cells in RRMS patients *via* sponging *hsa-miR-197-3p*. In our investigation, potential research targets are provided to examine molecular mechanisms that underpin the pathogenicity of MS.

DATA AVAILABILITY STATEMENT

The raw data supporting the conclusions of this article will be made available by the authors, without undue reservation.

AUTHOR CONTRIBUTIONS

MT, HS, BH, and MR wrote the manuscript and revised it. SG-F, NA, ZS, MAB, and MRA performed the bioinformatic analysis and collected the information. All authors contributed to the article and approved the submitted version.

FUNDING

The research protocol was approved & supported by Molecular Medicine Research Center, Tabriz University of Medical Sciences (grant number: 67290).

SUPPLEMENTARY MATERIAL

The Supplementary Material for this article can be found online at: https://www.frontiersin.org/articles/10.3389/fimmu.2021.770679/full#supplementary-material

REFERENCES

1. Koch-Henriksen N, Sørensen PS. The Changing Demographic Pattern of Multiple Sclerosis Epidemiology. *Lancet Neurol* (2010) 9(5):520–32. doi: 10.1016/S1474-4422(10)70064-8
2. Walton C, King R, Rechtman L, Kaye W, Leray E, Marrie RA, et al. Rising Prevalence of Multiple Sclerosis Worldwide: Insights From the Atlas of MS, Third Edition. *Mult Scler* (2020) 26(14):1816–21. doi: 10.1177/1352458520970841
3. Ghasemi N, Razavi S, Nikzad E. Multiple Sclerosis: Pathogenesis, Symptoms, Diagnoses and Cell-Based Therapy. *Cell J* (2017) 19(1):1–10. doi: 10.22074/cellj.2016.4867
4. Kasper LH, Shoemaker J. Multiple Sclerosis Immunology: The Healthy Immune System vs the MS Immune System. *Neurology* (2010) 74(Suppl 1): S2–8. doi: 10.1212/WNL.0b013e3181c97c8f
5. Yang X, Wu Y, Zhang B, Ni B. Noncoding RNAs in Multiple Sclerosis. *Clin Epigenet* (2018) 10(1):149. doi: 10.1186/s13148-018-0586-9
6. Sheng WH, Sheng KT, Zhao YX, Li H, Zhou JL, Yao HY, et al. Identifying the Biomarkers of Multiple Sclerosis Based on Non-Coding RNA Signature. *Eur Rev Med Pharmacol Sci* (2015) 19(19):3635–42.
7. Ghafouri-Fard S, Taheri M. A Comprehensive Review of Non-Coding RNAs Functions in Multiple Sclerosis. *Eur J Pharmacol* (2020) 879:173127. doi: 10.1016/j.ejphar.2020.173127
8. Ding Y, Li T, Yan X, Cui M, Wang C, Wang S, et al. Identification of Hub lncRNA ceRNAs in Multiple Sclerosis Based on ceRNA Mechanisms. *Mol Genet Genomics* (2021) 296(2):423–35. doi: 10.1007/s00438-020-01750-1
9. Salmena L, Poliseno L, Tay Y, Kats L, Pandolfi PP. A ceRNA Hypothesis: The Rosetta Stone of a Hidden RNA Language? *Cell* (2011) 146(3):353–8. doi: 10.1016/j.cell.2011.07.014
10. Sen R, Ghosal S, Das S, Balti S, Chakrabarti J. Competing Endogenous RNA: The Key to Posttranscriptional Regulation. *ScientificWorldJournal* (2014) 2014:896206. doi: 10.1155/2014/896206
11. Jernås M, Malmeström C, Axelsson M, Nookaew I, Wadenvik H, Lycke J, et al. MicroRNA Regulate Immune Pathways in T-Cells in Multiple Sclerosis (MS). *BMC Immunol* (2013) 14:32. doi: 10.1186/1471-2172-14-32
12. Irizarry RA, Hobbs B, Collin F, Beazer-Barclay YD, Antonellis KJ, Scherf U, et al. Exploration, Normalization, and Summaries of High Density Oligonucleotide Array Probe Level Data. *Biostatistics* (2003) 4(2):249–64. doi: 10.1093/biostatistics/4.2.249
13. Yeung KY, Ruzzo WL. Principal Component Analysis for Clustering Gene Expression Data. *Bioinf (Oxford England)* (2001) 17(9):763–74. doi: 10.1093/bioinformatics/17.9.763
14. Ritchie ME, Phipson B, Wu D, Hu Y, Law CW, Shi W, et al. Limma Powers Differential Expression Analyses for RNA-Sequencing and Microarray Studies. *Nucleic Acids Res* (2015) 43(7):e47. doi: 10.1093/nar/gkv007
15. Huber W, Carey VJ, Gentleman R, Anders S, Carlson M, Carvalho BS, et al. Orchestrating High-Throughput Genomic Analysis With Bioconductor. *Nat Methods* (2015) 12(2):115–21. doi: 10.1038/nmeth.3252
16. Haunsberger SJ, Connolly NM, Prehn JH. Mirnameconverter: An R/bioconductor Package for Translating Mature miRNA Names to Different Mirbase Versions. *Bioinf (Oxford England)* (2017) 33(4):592–3. doi: 10.1093/bioinformatics/btw660
17. Dashti S, Taheri M, Ghafouri-Fard S. An in-Silico Method Leads to Recognition of Hub Genes and Crucial Pathways in Survival of Patients With Breast Cancer. *Sci Rep* (2020) 10(1):18770. doi: 10.1038/s41598-020-76024-2
18. Braschi B, Denny P, Gray K, Jones T, Seal R, Tweedie S, et al. Genenames.org: The HGNC and VGNC Resources in 2019. *Nucleic Acids Res* (2019) 47(D1): D786–D92. doi: 10.1093/nar/gky930
19. Szklarczyk D, Gable AL, Lyon D, Junge A, Wyder S, Huerta-Cepas J, et al. STRING V11: Protein–Protein Association Networks With Increased Coverage, Supporting Functional Discovery in Genome-Wide Experimental Datasets. *Nucleic Acids Res* (2018) 47(D1):D607–13. doi: 10.1093/nar/gky1131
20. Shannon P, Markiel A, Ozier O, Baliga NS, Wang JT, Ramage D, et al. Cytoscape: A Software Environment for Integrated Models of Biomolecular Interaction Networks. *Genome Res* (2003) 13(11):2498–504. doi: 10.1101/gr.1239303
21. Bader GD, Hogue CWV. An Automated Method for Finding Molecular Complexes in Large Protein Interaction Networks. *BMC Bioinf* (2003) 4:2. doi: 10.1186/1471-2105-4-2
22. Karagkouni D, Paraskevopoulou MD, Tastsoglou S, Skoufos G, Karavangeli A, Pierros V, et al. DIANA-LncBase V3: Indexing Experimentally Supported miRNA Targets on Non-Coding Transcripts. *Nucleic Acids Res* (2020) 48(D1): D101–D10. doi: 10.1093/nar/gkz1036
23. Huang HY, Lin YC, Li J, Huang KY, Shrestha S, Hong HC, et al. Mirtarbase 2020: Updates to the Experimentally Validated microRNA-Target Interaction Database. *Nucleic Acids Res* (2020) 48(D1):D148–D54. doi: 10.1093/nar/gkz896
24. Chen EY, Tan CM, Kou Y, Duan Q, Wang Z, Meirelles GV, et al. Enrichr: Interactive and Collaborative HTML5 Gene List Enrichment Analysis Tool. *BMC Bioinf* (2013) 14:128. doi: 10.1186/1471-2105-14-128
25. Kuleshov MV, Jones MR, Rouillard AD, Fernandez NF, Duan Q, Wang Z, et al. Enrichr: A Comprehensive Gene Set Enrichment Analysis Web Server

2016 Update. *Nucleic Acids Res* (2016) 44(W1):W90–7. doi: 10.1093/nar/gkw377
26. Ala U. Competing Endogenous RNAs, Non-Coding RNAs and Diseases: An Intertwined Story. *Cells* (2020) 9(7):1574. doi: 10.3390/cells9071574
27. Moreno-García L, López-Royo T, Calvo AC, Toivonen JM, de la Torre M, Moreno-Martínez L, et al. Competing Endogenous RNA Networks as Biomarkers in Neurodegenerative Diseases. *Int J Mol Sci* (2020) 21 (24):9582. doi: 10.3390/ijms21249582
28. Cai Y, Wan J. Competing Endogenous RNA Regulations in Neurodegenerative Disorders: Current Challenges and Emerging Insights. *Front Mol Neurosci* (2018) 11:370–. doi: 10.3389/fnmol.2018.00370
29. Gloss BS, Dinger ME. The Specificity of Long Noncoding RNA Expression. *Biochim Biophys Acta* (2016) 1859(1):16–22. doi: 10.1016/j.bbagrm.2015.08.005
30. Tanji K, Mori F, Miki Y, Utsumi J, Sasaki H, Kakita A, et al. YOD1 Attenuates Neurogenic Proteotoxicity Through Its Deubiquitinating Activity. *Neurobiol Dis* (2018) 112:14–23. doi: 10.1016/j.nbd.2018.01.006
31. Bellefroid EJ, Marine JC, Ried T, Lecocq PJ, Rivière M, Amemiya C, et al. Clustered Organization of Homologous KRAB Zinc-Finger Genes With Enhanced Expression in Human T Lymphoid Cells. *EMBO J* (1993) 12 (4):1363–74. doi: 10.1002/j.1460-2075.1993.tb05781.x
32. Fransen NL, Crusius JBA, Smolders J, Mizee MR, van Eden CG, Luchetti S, et al. Post-Mortem Multiple Sclerosis Lesion Pathology is Influenced by Single Nucleotide Polymorphisms. *Brain Pathol* (2020) 30(1):106–19. doi: 10.1111/bpa.12760
33. Stone S, Lin W. The Unfolded Protein Response in Multiple Sclerosis. *Front Neurosci* (2015) 9:264–. doi: 10.3389/fnins.2015.00264
34. Bello-Morales R, Andreu S, López-Guerrero JA. The Role of Herpes Simplex Virus Type 1 Infection in Demyelination of the Central Nervous System. *Int J Mol Sci* (2020) 21(14):5026. doi: 10.3390/ijms21145026

Conflict of Interest: The authors declare that the research was conducted in the absence of any commercial or financial relationships that could be construed as a potential conflict of interest.

Publisher's Note: All claims expressed in this article are solely those of the authors and do not necessarily represent those of their affiliated organizations, or those of the publisher, the editors and the reviewers. Any product that may be evaluated in this article, or claim that may be made by its manufacturer, is not guaranteed or endorsed by the publisher.

frontiers in Immunology

ORIGINAL RESEARCH
published: 14 December 2021
doi: 10.3389/fimmu.2021.743010

Treatment With Cladribine Selects IFNγ+IL17+ T Cells in RRMS Patients – An *In Vitro* Study

Minodora Dobreanu[1,2,3†], *Doina Ramona Manu*[1†], *Ion Bogdan Mănescu*[2,3*], *Manuela Rozalia Gabor*[4], *Adina Huţanu*[2,3], *Laura Bărcuţean*[5,6] *and Rodica Bălaşa*[5,6]

[1] Department of Immunology, Centre for Advanced Medical and Pharmaceutical Research, "George Emil Palade" University of Medicine, Pharmacy, Science and Technology, Târgu Mureș, Romania, [2] Clinical Laboratory, County Emergency Clinical Hospital, Târgu Mureș, Romania, [3] Department of Laboratory Medicine, "George Emil Palade" University of Medicine, Pharmacy, Science and Technology, Târgu Mureș, Romania, [4] Department of Management and Economy, "George Emil Palade" University of Medicine, Pharmacy, Science and Technology, Târgu Mureș, Romania, [5] Neurology 1 Clinic, County Emergency Clinical Hospital, Târgu Mureș, Romania, [6] Department of Neurology, "George Emil Palade" University of Medicine, Pharmacy, Science and Technology, Târgu Mureș, Romania

OPEN ACCESS

Edited by:
Luisa María Villar, Ramón y Cajal University Hospital, Spain

Reviewed by:
Bonaventura Casanova, La Fe Hospital, Spain
Aurora Zanghì, University of Catania, Italy

***Correspondence:**
Ion Bogdan Mănescu
bogdan.manescu@umfst.ro

[†]These authors have contributed equally to this work and share first authorship

Specialty section:
This article was submitted to Multiple Sclerosis and Neuroimmunology, a section of the journal Frontiers in Immunology

Received: 17 July 2021
Accepted: 15 November 2021
Published: 14 December 2021

Citation:
Dobreanu M, Manu DR, Mănescu IB, Gabor MR, Huțanu A, Bărcuțean L and Bălașa R (2021) Treatment With Cladribine Selects IFNγ+IL17+ T Cells in RRMS Patients – An In Vitro Study. Front. Immunol. 12:743010. doi: 10.3389/fimmu.2021.743010

Background: Multiple sclerosis (MS) is an incurable autoimmune disease mediated by a heterogeneous T cell population (CD3+CD161+CXCR3–CCR6+IFNγ–IL17+, CD3+CXCR3+CCR6+IFNγ+IL17+, and CD3+CXCR3+IFNγ+IL17– phenotypes) that infiltrates the central nervous system, eliciting local inflammation, demyelination and neurodegeneration. Cladribine is a lymphocyte-depleting deoxyadenosine analogue recently introduced for MS therapy as a Disease Modifying Drug (DMD). Our aim was to establish a method for the early identification and prediction of cladribine responsiveness among MS patients.

Methods: An experimental model was designed to study the cytotoxic and immunomodulatory effect of cladribine. T cell subsets of naïve relapsing-remitting MS (RRMS) patients were analyzed *ex vivo* and *in vitro* comparatively to healthy controls (HC). Surviving cells were stimulated with rh-interleukin-2 for up to 14days. Cell proliferation and immunophenotype changes were analyzed after maximal (phorbol myristate acetate/ionomycin/monensin) and physiological T-cell receptor (CD3/CD28) activation, using multiparametric flow cytometry and xMAP technology.

Results: *Ex vivo* CD161+Th17 cells were increased in RRMS patients. *Ex vivo* to *in vitro* phenotype shifts included: decreased CD3+CCR6+ and CD3+CD161+ in all subjects and increased CD3+CXCR3+ in RRMS patients only; Th17.1 showed increased proliferation vs Th17 in all subjects; CD3+IL17+ and CD3+IFNγ+IL17+ continued to proliferate till day 14, CD3+IFNγ+ only till day 7. Regarding cladribine exposure: RRMS CD3+ cells were more resistant compared to HC; treated CD3+ cells proliferated continuously for up to 14 days, while untreated cells only up to 7 days; both HC/RRMS CD3+CXCR3+ populations increased from baseline till day 14; in RRMS patients vs HC, IL17 secretion from cladribine-treated cells increased significantly, in line with the observed proliferation of CD3+IL17+ and CD3+IFNγ+IL17+ cells; in both HC/RRMS, cladribine led to a significant

increase in CD3+IFNγ+ cells at day 7 only, having no further effect at day14. IFNγ and IL17 secreted in culture media decreased significantly from *ex vivo* to *in vitro*.

Conclusions: CD3+ subtypes showed different responsiveness due to selectivity of cladribine action, in most patients leading to *in vitro* survival/proliferation of lymphocyte subsets known as pathogenic in MS. This *in vitro* experimental model is a promising tool for the prediction of individual responsiveness of MS patients to cladribine and other DMDs.

Keywords: relapsing-remitting multiple sclerosis (RRMS), cladribine, T cells, IFNγ+IL17+ cells, Th17.1 cells, *in vitro*, disease modifying drug (DMD)

1 INTRODUCTION

Multiple Sclerosis (MS) is an incurable autoimmune disease affecting the central nervous system (CNS) and is associated with T cell-mediated immunopathology during all phases of the disease. Numerous genetic and pathological studies performed in the last decade point towards T and B cells, as essential players in MS pathogenesis. MS affects only the CNS, as an argument that T and B cells are recruited by CNS specific antigens (1). Activated T cells (CD3+) are capable of mounting an autoimmune response against myelin components, penetrating the blood-brain barrier, proliferating and subsequently secreting pro-inflammatory cytokines. These cytokines stimulate microglia, macrophages, astrocytes and B cells, resulting in demyelination and neurodegeneration (2, 3).

In the peripheral blood of MS patients, a large number of heterogeneous, IL17-producing CD3+ cells have been identified, especially during disease exacerbation (4, 5). In addition to a Th17 phenotype (CD3+CD4+CD161+CCR6+) characterized by IL17 production, and a classical Th1 phenotype (CD3+CD4+ CXCR3+) which is associated with production of IFNγ (6, 7), a heterogeneous CD3+ cell population has been shown to be implicated in MS pathogenesis: these cells express phenotypic markers of both Th1 and Th17 cells, but in varying levels and combinations, and also exhibit a mixed profile, characterized by a CCR6+CXCR3+ immunophenotype and concomitant secretion of IL17A and IFNγ (8–11). Furthermore, both IL17-producing CD3+CD4+ and CD3+CD8+ cells were highlighted in the peripheral blood and cerebrospinal fluid of MS patients in early stages of the disease (12–14). A clonal expansion of CD3+CD8+ cells takes place within the brain inflammatory microenvironment at the onset of disease, beginning with IL17 production (15–18). The number of CD3+CD8+ cells surpasses the number of CD3+CD4+ cells in the inflammatory infiltrate of active demyelinating plaques regardless of disease stage, duration or progression (19, 20).

Relapsing-remitting MS (RRMS) is the most common clinical form of MS, accounting for about 85% of all MS cases (21). RRMS patients may benefit from treatment, but individual response to a given therapy and the occurrence of adverse events are largely unpredictable. Thus, many patients need to change several drugs in order to stabilize their disease. Current therapy consists mainly of disease-modifying drugs (DMDs) with immunomodulatory or immunosuppressive action, targeting inflammation in patients in order to reduce the relapse rate and to delay progression (22, 23).

Cladribine was first synthesized in 1972, but only approved by the FDA in the early '90s for the treatment of certain leukaemias (24). In 2010, cladribine was approved for RRMS in Russia and Australia, but was later removed (24). Based on clinical data from the CLARITY, CLARITY-EXT, ORACLE-MS, and PREMIERE studies, in 2017 cladribine was approved in the EU for the treatment of active RRMS (24). In 2019, cladribine was also approved by the FDA for active RRMS and, as of July 2020, it is approved in more than 75 countries (24). This synthetic deoxyadenosine analog is a prodrug, which is incorporated into the DNA of proliferating cells (like activated lymphocytes), causing strand breakage, followed by p53 activation and programmed cell death (apoptosis) through the caspase system (25, 26).

Cladribine acts as a lymphocyte-depleting drug, but preferentially depletes memory B cells: in MS patients, Cladribine can deplete 40-50% of total T cells, and approximately 80% of total B cells (27, 28), but informations on the efficacy of this drug in RRMS are scarce (29). Moreover, in some patients cladribine is not able to stop the progression of disease and induce a long-lasting remission. Hence, methods able to predict responsiveness to cladribine would be very useful in the clinical setting, allowing for the early identification of cladribine (non-)responders and assisting clinicians in proper treatment selection. however, to date, little progress has been made in personalized therapy and response prediction in MS. It is essential to identify non-responders to a therapeutic molecule before the appearance of advanced neurological lesions. Additionally, side effects of immunosuppressants or monoclonal antibodies in MS patients, as well as specific risk-benefit ratios, should be established from the earliest stages of patient management. The aim of our study was to assess an experimental model that can characterize the changes in surviving T-cell subpopulations following cladribine exposure in order to create an algorithm of responsiveness to DMDs that could assist clinicians in choosing the best therapy for each patient, avoiding additional CNS lesions, disability progression, and unnecessary costs. Cytotoxic and immunomodulatory effects of cladribine on T cells from naïve RRMS patients were studied by tracking changes in phenotypic markers of aggressivity, such

as the T cell surface markers CXCR3, CCR6 and CD161, as well as the secretion of IFNγ and IL17. Such experimental models may prove useful for establishing a personalized approach to therapy in MS patients.

2 MATERIALS AND METHODS

2.1 T Cell Isolation and Activation

Our study was approved by the Committee for Ethical Research of the Emergency Clinical County Hospital of Târgu Mureş (decision no. 7,100/2018) and the experiments were performed according to the Declaration of Helsinki principles for experiments involving humans. For T cell isolation, peripheral blood from RRMS naïve patients and healthy donors (healthy controls, HC) was collected in heparinized tubes (Greiner Bio-One, cat. no. 455051). Automated complete blood counts (CBC) were performed using a Sysmex XS-800i hematology analyzer and hsCRP plasma levels were analyzed with a BN ProSpec System using N Latex CardioPhase hsCRP Reagent (Siemens, cat. no. OQIY 21). Samples with more than 10×10^9 white blood cells/L and/or hsCRP above 3 mg/L were excluded. Peripheral blood mononuclear cells (PBMCs) were isolated by Ficoll-Paque (Sigma, cat. no. H8889) density gradient centrifugation, using a standard operating procedure previously implemented in our laboratory (30), and cryopreserved with 10% DMSO at -140°C, until analysis. PBMCs were then cultured in RPMI-1640 medium containing L-glutamine (Sigma, cat. no. R8758) supplemented with 1% penicillin/1% streptomycin (Sigma A, cat. no. P4333) and 10% fetal bovine serum (FBS; Sigma, cat. no. F7524) at a density of $1\text{-}2\times10^6$ cells/mL.

Ex vivo analysis was performed after short-term maximal stimulation for 4-5 hours with 50 ng/mL phorbol 12-myristate 13-acetate (PMA; Sigma, cat. no. P-8139) and 1 µg/mL ionomycin (Sigma, cat. no. I-0634), in the presence of 0.1 µg/mL monensin (GolgiStop, BD Pharmingen, cat. no. 554724). Surface phenotype and intracellular cytokines were evaluated by multi-parametric flow cytometry analysis. An additional fraction of cells was subjected to physiological TCR activation with soluble NA/LE™ CD3 monoclonal (mAb) antibody (BD, clone HIT3a, cat. no. 555336) at a final concentration of 1 µg/mL, and CD28 mAb (BD, clone 28.2, cat. no. 555725) at a final concentration of 5 µg/mL, for 72 hours. Culture media were harvested for cytokine secretion analysis.

For *in vitro* medium-term analysis, thawed PBMCs were treated with CD3/CD28 mAbs for 72 hours, then transferred into media supplemented with 10 ng/mL recombinant human IL2 (rh-IL2; BD Pharmingen, cat. no. 554603) for a period of either 5 or 10 days. rh-IL2 was removed 20 hours prior to cell re-stimulation on day 7 and 14. The re-stimulations were performed with PMA/ionomycin/monensin for multi-parametric flow cytometric assessment of the phenotypic profile, and with CD3/CD28 mAbs for analysis of cytokine secretion in culture media. Cell culture and activation protocols were previously described by Korsen et al. (31).

Details of protocols are described in **Figure 1**.

2.2 *Ex Vivo* Versus *In Vitro* Maximally Activated T Cell Phenotypic Profile

Phenotypic profile analysis of T cell subsets in *ex vivo* (immediately after thawing cryopreserved cells) and *in vitro* (after maintaining thawed cells in culture for 7 and 14 days) samples consisted of immunostaining for cell surface markers, lineage-specific transcription factors, and intracellular cytokines. The first panel included specific fluorochrome-conjugated antibodies against cell surface biomarkers CD3, CD4, CD161, CXCR3, CCR6 and intracellular cytokines IFNγ and IL17. The expressions of lineage-specific transcription factors TBet and RORγt were measured with a secondary panel of fluorochrome-conjugated antibodies that tagged the same surface markers. The BD FACSAria III cytometer configuration as well as the antibodies used in the protocol are presented in **Table 1**. Data acquisition and analysis were performed using BD FACSDiva™ digital software. A minimum of 30,000 CD3+ events was acquired per sample. Details of cell gating strategy to identify the CD3+CD4+ cell population of interest by flow cytometry are shown in **Figure 2**.

2.3 The Cytotoxic Effect of Cladribine

TCR-activated cells were incubated for 48 hours with 10^{-7} M cladribine (Sigma Aldrich, cat. no. C4438) or in the absence of cladribine, as control samples. After the incubation period, the cytotoxic effect of cladribine was immediately assessed by absolute CBC using Sysmex XS 800i Hematology Analyzer, followed by a viability assay using the FACSAria III flow cytometer and Becton Dickinson Horizon™ Fixable Viability Stain 780 (FVS 780, BD cat. no. 565388). Necrotic cells were determined by higher levels of FVS 780, with a 10-20-fold increase in intensity over viable cells.

TCR-activated lymphocytes cultured for 48h with or without cladribine were transferred to a cladribine-free medium with rh-IL2 for up to 7 and 14 days. Lymphocytes were analyzed for viability at day 0 (before culture initiation) and at day 7 or 14, as described above.

The changes in absolute lymphocyte number reflected cell proliferation or depletion in response to the cytotoxic action of cladribine. Survival indexes were established as a ratio between absolute viable cell number without or after cladribine exposure, and initial absolute viable cell number. Proliferation indexes were calculated as a ratio of absolute viable cell number before and after 7 days and 14 days of culture with rh-IL2.

2.4 Evaluation of the Immunomodulatory Effect of Cladribine on the Cytokine Secretory Profile of TCR-Activated Cells

After 7-14 days of culturing cells exposed/unexposed to cladribine, lymphocytes were stimulated with PMA/ionomycin/monensin, and analyzed by flow cytometry for immunophenotypic changes. Immunophenotypic shifts were defined as changes in cell surface receptors (CD161, CXCR3, CCR6) and intracellular cytokines (IFNγ and IL17) expression in T cell subpopulations. The immunomodulatory effect of cladribine was quantified by flow cytometry as changes in the percentages of positive cell subpopulations, labeled with the

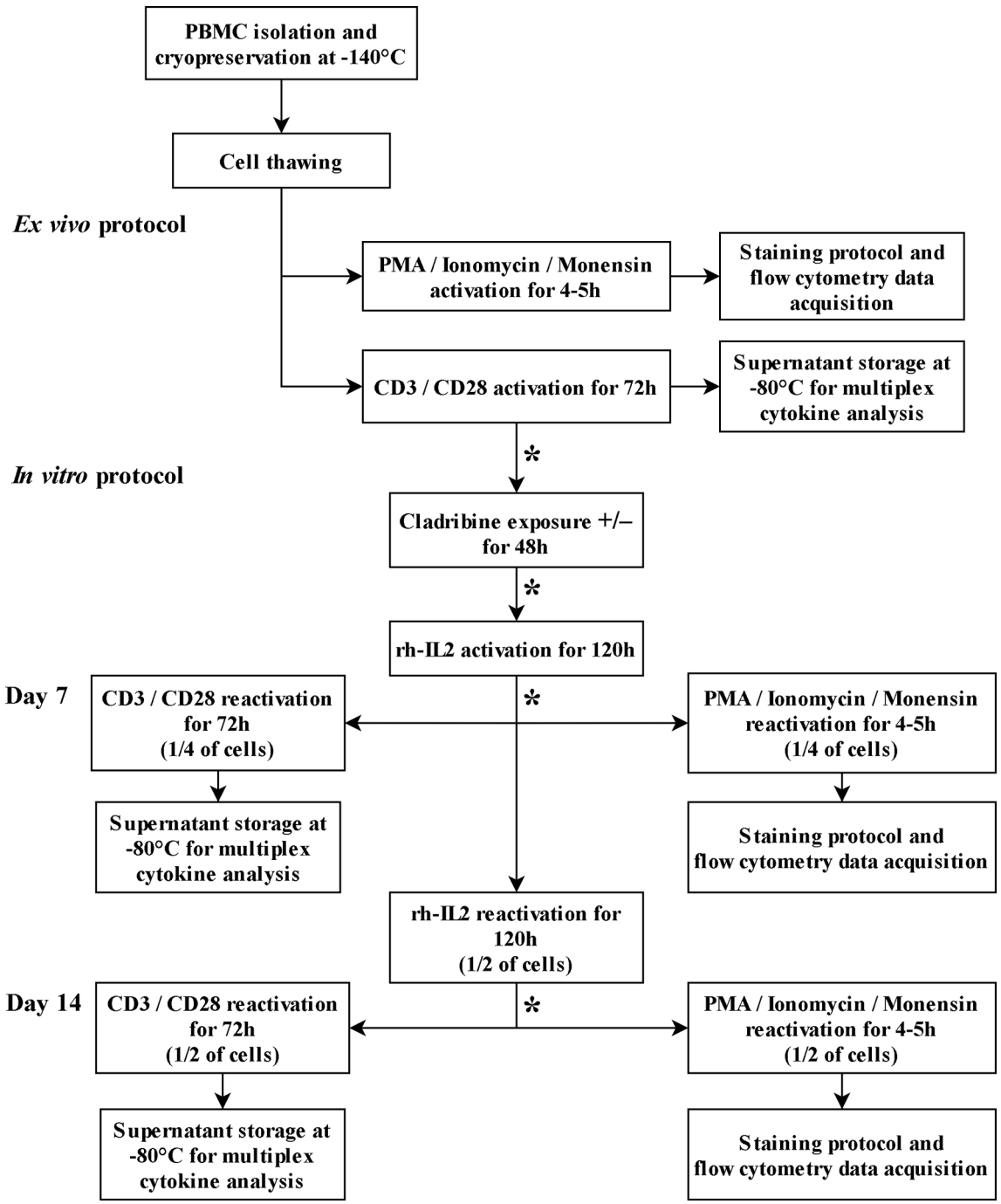

FIGURE 1 | T cell culture and activation protocols. The asterisk (*) between steps indicates cell wash, cell count, and viability assessments.

specific antibodies for antigens of interest, as listed in **Table 1**. The same antibody panels and cytometer configurations were used for the assessment of cladribine effect on *ex vivo* versus *in vitro* T cell phenotype.

The ideal method for *in vitro* activation of T cells should mimic the signaling events that occur during physiological activation, and agonistic antibodies against the TCR/CD3 complex with the co-stimulatory molecule CD28 are largely used for this purpose. In our study, the T cell signature of secreted cytokines was analyzed in *ex vivo* and *in vitro* lymphocytes at day 7 and day 14, after re-stimulation with CD3/CD28 mAbs for 72 hours. The supernatant was collected and stored at -80°C until analysis. The secreted cytokine profile associated with TCR-activated cells was measured using xMAP

TABLE 1 | Parameter specifications and BD FACSAria III cytometer configuration used for data acquisition.

Excitation LASER lines	Fluorochrome	Maximum emission (nm)	Band-Pass filters (nm)	Relative Brightness	Mouse antibody clone	Specificity
Violet (405 nm)	BD Horizon™ BV421	421	450/40	Brightest	B27	Human IFNγ/TBet
	BD Horizon™ BV510	510	530/30	Moderate	UCHT1	Human CD3
Blue (488 nm)	BD Pharmingen™ Alexa Fluor® 488	519	530/30	Moderate	1C6/CXCR3	Human CD183 (CXCR3)
	BD Pharmingen™ PE	578	575/26	Bright	DX12	Human CD161
	BD Pharmingen™ PE-Cy7™	785	780/60	Brightest	11A9	Human CD196 (CCR6)
Red (633 nm)	BD Pharmingen™ Alexa Fluor® 647	668	660/20	Bright	N49-653	Human IL17/RORγt
	BD Pharmingen™ Alexa Fluor® 700	719	730/45	Dim	SK3	Human CD4
	Fixable Viability Stain 780	780	780/60	–	–	Cell-surface and intracellular amines

Technology on FlexMap 3D Luminex analyzer and a cytokine panel, including IFNγ and IL17A built with ProcartaPlex™ Multiplex Kits from Invitrogen [Human High-Sensitivity Panel 9-plex, cat. no. EPXS090-12199-901]. Data were acquired and analyzed with xPONENT software for Luminex instruments.

2.5 Statistical Analysis

Statistical analysis of data was performed with GraphPad Prism 5.0 (GraphPad Software, San Diego, CA, USA) and SPSS 23.0. Graphs were generated with the same softwares.

In order to evaluate data distribution, Shapiro-Wilk and one-sample Kolmogorov-Smirnov with Lilliefors correction tests were used. If data exhibited normal distribution for continuous variables, the values were expressed as means with standard deviation (SD). For non-gaussian data, the median with interquartile 25%/75% range [IQR] was used, and for categorical variables as numbers (percentage), absolute and relative frequencies were used. *T*-test, median, two-sample Kolmogorov-Smirnov, and Mann-Whitney U tests were used to compare the variance/mean/median differences between groups. Wilcoxon signed-ranks test (two-related samples) was used for differences between time points (*ex vivo*/day 7/day 14). The percentage changes of immune cell subsets were calculated from absolute numbers in comparison to baseline. *P*-values were

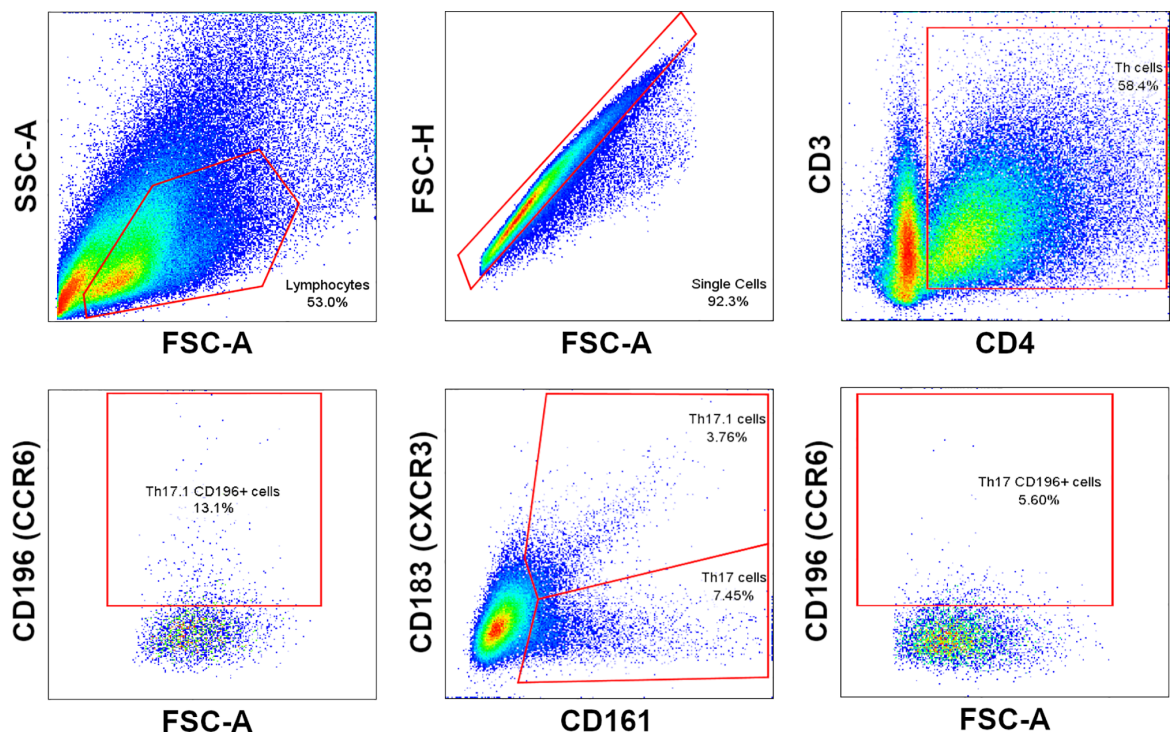

FIGURE 2 | Cell gating strategy to identify Th17 and Th17.1 cell subpopulations.

considered significant when equal to or lower than 0.05: $^{*}P \leq 0.05$, $^{**}P \leq 0.01$, $^{***}P \leq 0.005$, $^{****}P \leq 0.0001$.

The correlation between two sets of data was assessed by Spearman's or Pearson's test, depending on data distribution and type. Strength of correlation was classified as null/very weak ($|r| < 0.25$), acceptable ($0.25 \leq |r| < 0.5$), moderate ($0.5 \leq |r| < 0.75$), or very good ($|r| \geq 0.75$). Statistical testing was performed at the two-tailed α-level of 0.05.

3 RESULTS

Cellular analysis was performed for 34 RRMS patients and 17 HC. The RRMS group consisted of 32.35% males, while the control group was made up of 35.29% males ($p>0.05$). Mean ages were 35.9 years for the RRMS group and 33.2 years for the HC group ($p>0.05$).

3.1 T Cell Immunophenotype Shift From *Ex Vivo* to *In Vitro*

In *ex vivo* samples, the proportion of CD3+CD161+ cells was significantly increased in RRMS patients compared to HC ($p<0.05$) (**Figure 3A**).

The percentage of *ex vivo* CD3+CXCR3+ (**Figure 3B**) and CD3+CCR6+ cells (**Figure 3C**) was not significantly different in RRMS patients compared to HC. Compared to *ex vivo*, the CD3+CD161+ cell subpopulation at day 7 *in vitro* was significantly decreased in both RRMS patients (p=0.0002) and HC subjects (p=0.013). Compared to day 7, the percentage of CD3+CD161+ cells at day 14 decreased slightly in cultures from HC subjects and increased in RRMS patients ($p<0.05$) (**Figure 4A**). A significant increase in the CD3+CXCR3+ cell subpopulation was found in RRMS patients after 7 and 14 days in culture, relative to *ex vivo* cells ($p=0.018$ and $p=0.014$, respectively). For HC, non-significant variations of CD3+CXCR3+ cell subpopulations were found after 7 and 14 days in culture (**Figure 4B**). A significant decrease in the CD3+CCR6+ population was observed in RRMS patients ($p<0.0001$) and HC ($p=0.0075$) after 7 days in culture, with no further significant changes noted at day 14 (**Figure 4C**).

CD3+CD4+CD161+CXCR3+ cells (Th 17.1) from HC showed a significant *in vitro* proliferation under rh-IL2 at day 7 relative to *ex vivo* samples ($p<0.0001$), associated with a sustained increase at day 14 ($p=0.02$). For RRMS subjects, Th17.1 proliferation was significant in the first 7 days ($p<0.0001$) and also between days 7 and 14 ($p=0.0007$) (**Figure 5A**). *In vitro* cultivation led to loss of CCR6 expression. In both Th17 and Th17.1 cell populations (CD3+CD4+CD161+CXCR3− and CD3+CD4+CD161+CXCR3+, respectively), the percentage of CCR6+ cells decreased over time. The Th17 population in both HC and RRMS subjects rapidly lost CCR6 expression from the *ex vivo* stage to day 7 ($p<0.0001$). Subsequently, from day 7 to day 14, the loss was non-significant. CCR6 cell surface expression decreased non-significantly on Th17.1 cells in HC from *ex vivo* to day 7, and significantly until day 14 ($p=0.0013$). In RRMS subjects, CCR6 was lost rapidly on Th17.1 and Th17 cells from *ex vivo* to day 7 ($p<0.0001$), but afterward was non-significant – results that were consistent with the evolution of CCR6+ expression on CD3+ cells (**Figures 5B**, **4C**).

In *ex vivo* samples, the percentage of Th17.1 cells was significantly lower than that of Th17 (for HC, $p=0.0094$ and for RRMS, $p<0.0001$). However, in rh-IL2 culture conditions, the Th17.1 subpopulation became predominant at day 7 ($p=0.05$ for HC and $p=0.028$ for RRMS) and day 14 ($p=0.037$ for HC and $p=0.0009$ for RRMS patients) (**Figure 5A**).

3.2 *Ex Vivo* Versus *In Vitro* Cytokine Production Capacity of Activated T Cells

Flow cytometric analysis of the intracellular cytokine profile of CD3+ cells after short-term maximal activation revealed a significant increase in the percentage of CD3+IFNγ+ cells for HC and RRMS patients after 7 days in culture ($p=0.0024$ and $p=0.0005$, respectively), followed by a significant decrease at day

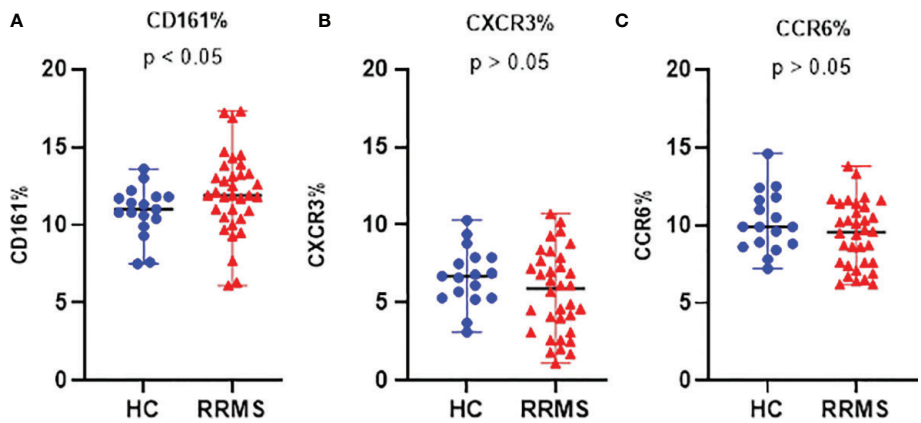

FIGURE 3 | The proportion of *ex vivo* CD161 **(A)**, CXCR3 **(B)**, and CCR6 **(C)** positive cells in HC and RRMS groups. Each dot represents one individual subject and horizontal bars indicate median values. Shown *p*-values were calculated using the median test.

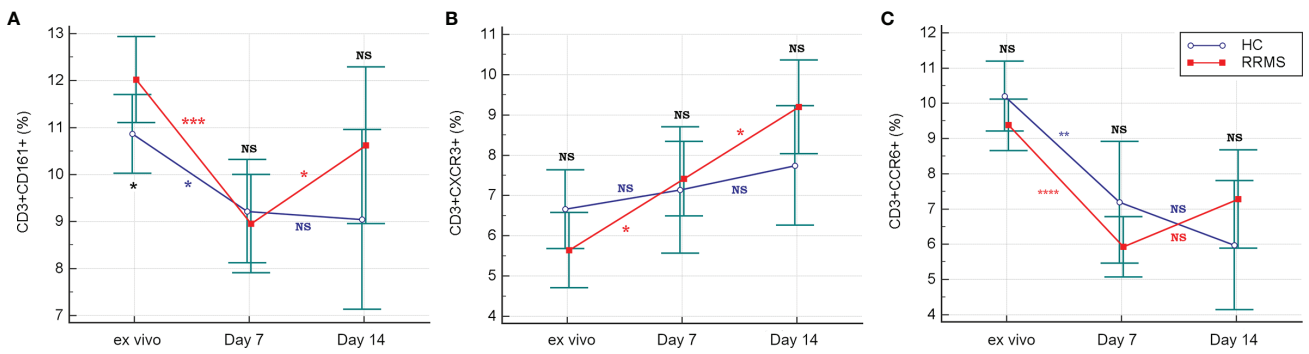

FIGURE 4 | The evolution of CD3+ cells expressing CD161 **(A)**, CXCR3 **(B)** and CCR6 **(C)** receptors in *ex vivo* samples to 7 and 14 days in culture with rh-IL2. Significance levels are graphically represented as follows: NS, non significant, $p>0.05$, *$p<0.05$, **$p<0.01$, ***$p<0.001$, ****$p<0.0001$.

14 ($p=0.013$ for HC and $p=0.015$ for RRMS subjects) (**Figure 6A**). The proportion of IL17-producing cells also increased in HC and RRMS patients from *ex vivo* up to day 7 (both $p<0.0001$), and additionally until day 14 ($p=0.0004$ for HC and $p=0.0006$ for RRMS subjects) (**Figure 6B**). Double-positive CD3+IFNγ+IL17+ cells increased in HC and RRMS patients after 7 days in culture, relative to cells analyzed *ex vivo* ($p<0.0001$ for RRMS subjects and $p=0.0001$ for HC) and continued to increase until day 14 ($p=0.0007$ for HC and $p=0.022$ for RRMS subjects) (**Figure 6C**). There was a significant increase in the CD3+IFNγ+IL17+ and CD3+IL17+ cell subpopulations, which proliferated well after rh-IL2 activation *in vitro*, in both HC and RRMS subjects.

Ex vivo TBet-positive cells, which correspond to Th1 and Th17.1 phenotypes, were significantly increased in RRMS compared to HC ($p<0.0001$). On the contrary, in *ex vivo*, CD3+RORγt+ cells, which correspond to Th17 and Th17.1 phenotypes, were significantly decreased in RRMS patients ($p<0.0001$).

The proportion of CD3+ cells positive for TBet (which is a transcriptional regulator of IFNγ), had non-significant variations in the HC group and a weakly significant increase ($p=0.036$) in RRMS patients between *ex vivo* status and day 14 of culture. Considering the evolution of CD3+IFNγ+ and CD3+TBet+ cells, shown in **Figures 6A, D**, the significant increase in the CD3+CXCR3+ cell population (**Figure 4B**) was probably due to a Th17.1 subpopulation, which was more resistant and proliferative in response to *in vitro* activation with rh-IL2.

In addition to the increased proportions of CD3+ IFNγ+IL17+ and CD3+IL17+ cell subpopulations, we observed an increase in the CD3+RORγt+ cell population from *ex vivo* to *in vitro* status at day 14, but only for RRMS patients. ($p<0.0001$ at day 7 and $p=0.035$ at day 14) (**Figure 6E**). The analysis also revealed an increase in both transcription factors (double-positive CD3+TBet+RORγt+ cells) at day 14 for HC ($p=0.0015$) as well as for RRMS patients ($p= 0.0004$) (**Figure 6F**).

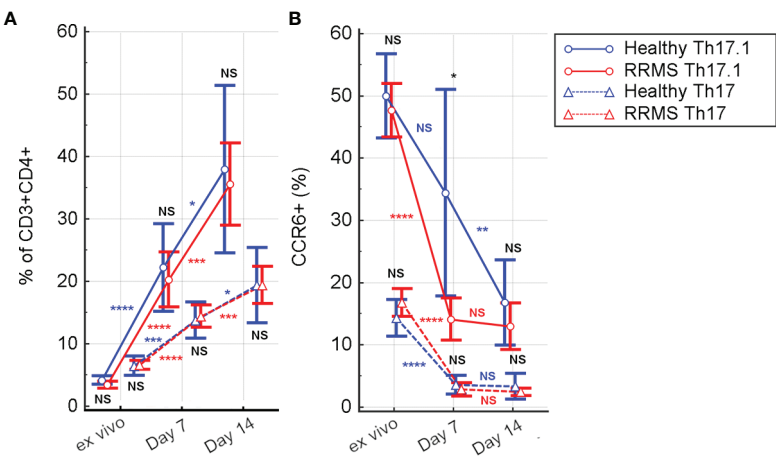

FIGURE 5 | The evolution of Th17 (CD3+CD4+CD161+CXCR3–) and Th17.1 (CD3+CD4+CD161+CXCR3+) cell subpopulations **(A)** and of CCR6 positive Th17 and Th17.1 cells **(B)** from *ex vivo* to 7 and 14 days in culture with rh-IL2. Significance levels are graphically represented as follows: NS, non significant, $p>0.05$, *$p<0.05$, **$p<0.01$, ***$p<0.001$, ****$p<0.0001$.

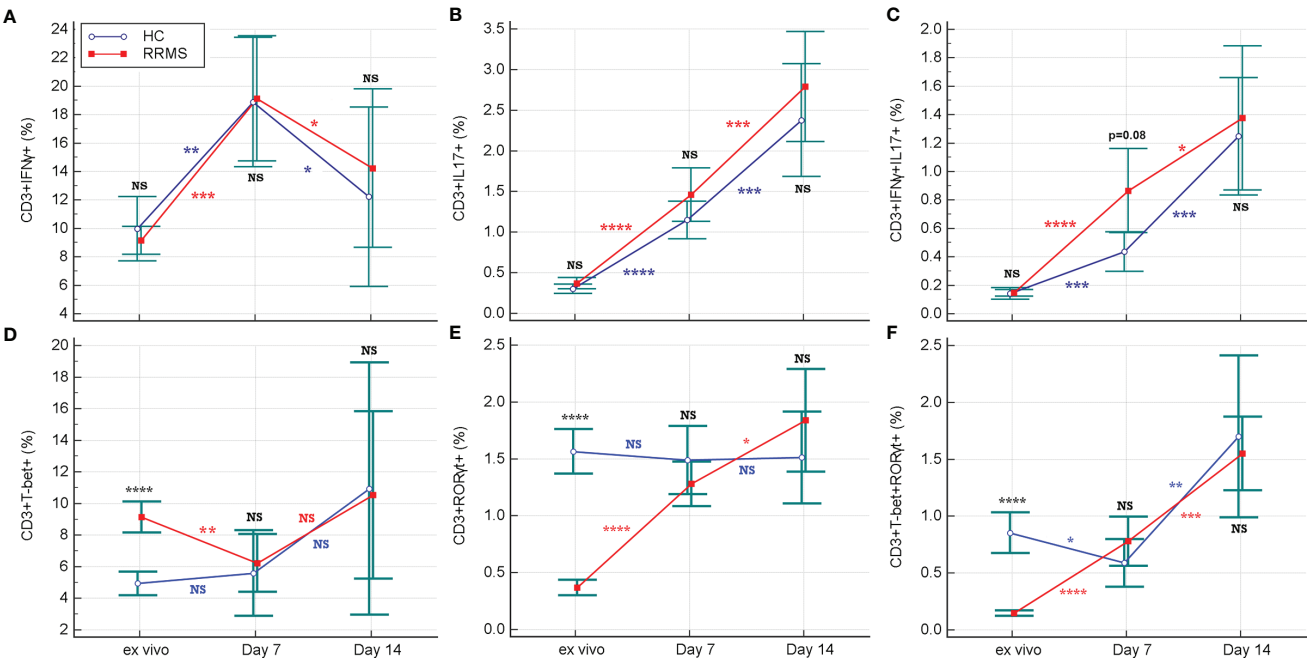

FIGURE 6 | Changes in the proportion of CD3+IFNγ+ and CD3+TBet+ **(A, D)**, CD3+IFNγ+IL17+ and CD3+TBet+RORγt+ **(B, E)**, CD3+IL17+ and CD3+RORγt+ **(C, F)** cell subpopulations from *ex vivo* stage to days 7 and 14 of culture with rh-IL2. Significance levels are graphically presented as follows: NS, non significant, $p>0.05$,*$p<0.05$, **$p<0.01$, ***$p<0.001$, ****$p<0.0001$.

3.3 The Effect of *In Vitro* Cladribine Exposure on T Cells

3.3.1 Proliferation of Surviving T Cells After Cladribine Cytotoxic Action

For HC, after 48hrs of cladribine exposure, a survival index of 0.42 was calculated, while the survival index of unexposed cells was 0.89 (p=0.0001). After rh-IL2 activation, the proliferation index of HC cells significantly increased by day 7 (p<0.0001 for untreated cells and p<0.001 for cladribine-treated cells). From day 7 to 14, the proliferation of untreated cells decreased significantly (p=0.031), while cladribine-treated cells continued to proliferate.

For RRMS subjects, the survival index calculated after 48hrs of cladribine exposure was 0.72 for treated cells and 1.28 for untreated cells. In cultures including rh-IL2, the proliferation indices of RRMS significantly increased by day 7, similarly in both cladribine-treated and untreated cells (p<0.0001). From day 7 to 14, the proliferation of cladribine-treated cells increased non-significantly, while decreasing non-significantly for untreated cells. Under rh-IL2, the proliferation index of cladribine-treated cells increased at day 7 and again at day 14 while for untreated cells, the proliferation index increased only at day 7 (**Figure 7**).

3.3.2 Immunomodulatory Effects of Cladribine

The difference between unexposed and cladribine-exposed CD3+CD161+ cells in HC subjects was non-significant at day 7 (p=0.072). However, the difference was significant at day 14 (p=0.005) due to the increased proliferation of CD3+CD161+ cells in cladribine-exposed versus unexposed samples. Conversely, in RRMS subjects, the difference between the percentage of CD3+CD161+ cells in cladribine-exposed versus unexposed cells was higher at day 7 (p=0.005) but was lost until day 14 (p=0.015) (**Figure 8A**).

A sustained increase in CD3+CXCR3+ cell subpopulations from HC exposed to cladribine, compared to unexposed, was noted at day 7 (p=0.003) and 14 (p<0.0001). CD3+CXCR3+ cells exposed to cladribine had better survival and proliferation profiles only in HC. CD3+CXCR3+ cells from RRMS subjects had similar survival and proliferation profiles at day 7 and day 14, regardless of exposure to cladribine (**Figure 8B**).

For CD3+CCR6+ cells from HC at day 7, a non-significant difference was found between unexposed and cladribine-exposed cells. However, due to the increased proliferation of exposed CD3+CCR6+ cells between day 7 and 14, this difference became significant at day 14 (p=0.002). In RRMS subjects, the percentages of CD3+CCR6+ cells were not significantly different between exposed and unexposed cells at 7 and 14 days. The loss of CCR6 expression was lower in HC than in RRMS patients treated with cladribine in the first week of culture (p=0.006) (**Figure 8C**).

On day 7, unexposed and cladribine-exposed CD3+IFNγ+ cell subpopulations from the HC group proliferated similarly (p=0.098). On day 14, a lower percentage of CD3+IFNγ+ cells

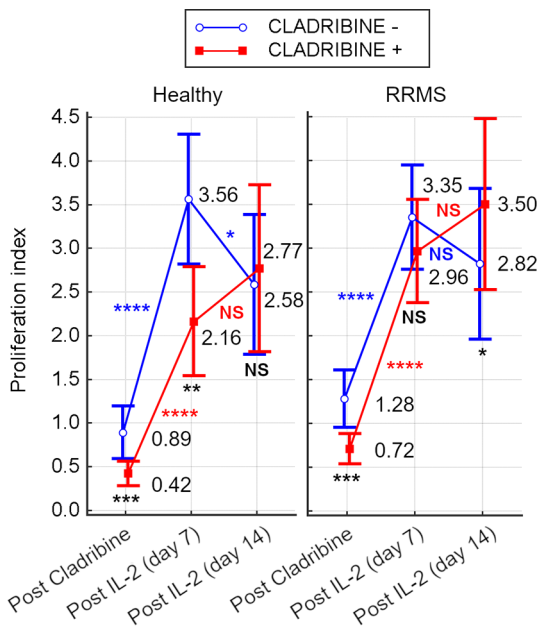

FIGURE 7 | Survival index of cells from HC and RRMS subjects after cladribine exposure and proliferation index after 7 days or 14 days of rh-IL2 activation in cultures. Significance levels are graphically presented as follows: NS, non significant (p>0.05), *p<0.05, **p<0.01, ***p<0.001, ****p<0.0001.

survived in culture. Unexposed cells exhibited especially poor survival. However, the difference between unexposed and cladribine-exposed CD3+IFNγ+ cell subpopulations remained non-significant. CD3+IFNγ+ cells from RRMS patients proliferated until day 7, with a weakly significant difference observed between exposed and unexposed cells (p=0.043). In the second week, the percentage of CD3+IFNγ+ cells decreased below *ex vivo* levels in both exposed and unexposed cells and the difference between them at day 14 was non-significant (**Figure 9A**). Cladribine exposure did not seem to significantly alter CD3+IFNγ+ cells proliferation in neither RRMS nor HC subjects.

HC CD3+IFNγ+IL17+ cells exposed to cladribine survived and proliferated better than unexposed cells until day 7 (p=0.036) and continued to fare significantly better (p=0.002) until day 14. For RRMS patients, the percentages of CD3+ IFNγ+IL17+ cells also increased up to day 14 compared to *ex vivo* but were significantly different only at day 14 (p=0.006) (**Figure 9B**).

Cladribine-exposed CD3+IL17+ cell subpopulations exhibited greater survivability and proliferation than unexposed cells at day 7, for both HC (p=0.002) and RRMS subjects (p=0.0001). However, on day 14, a significant increase of exposed versus unexposed CD3+IL17+ cells was observed only in RRMS subjects (p=0.004) (**Figure 9C**).

3.3.3 Secreted Cytokine Profile Changes in Response to Cladribine Treatment

The cytokine profile measured from culture media of TCR-stimulated cells revealed a significant decrease in IFNγ secreted by HC cells from the *ex vivo* stage to day 7 (p=0.001) and day 14 (p=0.002) of culture. For RRMS patients, a significant decrease in IFNγ secretion was also observed from the *ex vivo* stage to day 7 and day 14 (both p<0.0001). A similar decrease in IL17 secretion was measured from the *ex vivo* stage until day 7 (p=0.005 for HC and p<0.0001 for RRMS) and day 14 (p=0.001 for HC and p<0.0001 for RRMS). A general trend of IFNγ and IL17 secretion recovery is observed up to day 14 in both RRMS and HC subjects, regardless of cladribine exposure.

IFNγ secretion from cladribine-treated cells significantly increased at day 7 relative to untreated cells (p=0.049 for HC and p=0.013 for RRMS), but at day 14 the differences were no longer significant (p >0.05) (**Figure 10A**). IL17 secretion from cladribine-treated vs untreated cells increased non-significantly

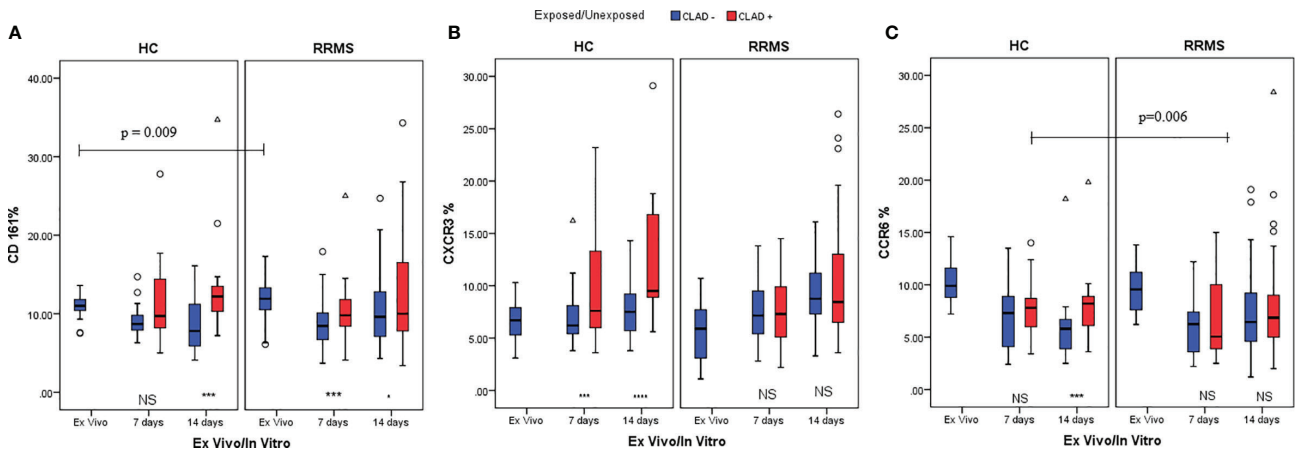

FIGURE 8 | HC and RRMS CD3+CD161+ **(A)**, CD3+CXCR3+ **(B)** and CD3+CCR6+ **(C)** cell population changes at day 7 and day 14, after cladribine treatment, represented as boxplot (median with error bars). NS, non significant (p > 0.05) *P*-values were considered significant when lower than 0.05 (*p ≤ 0.05, ***p ≤ 0.005, ****p ≤ 0.0001).

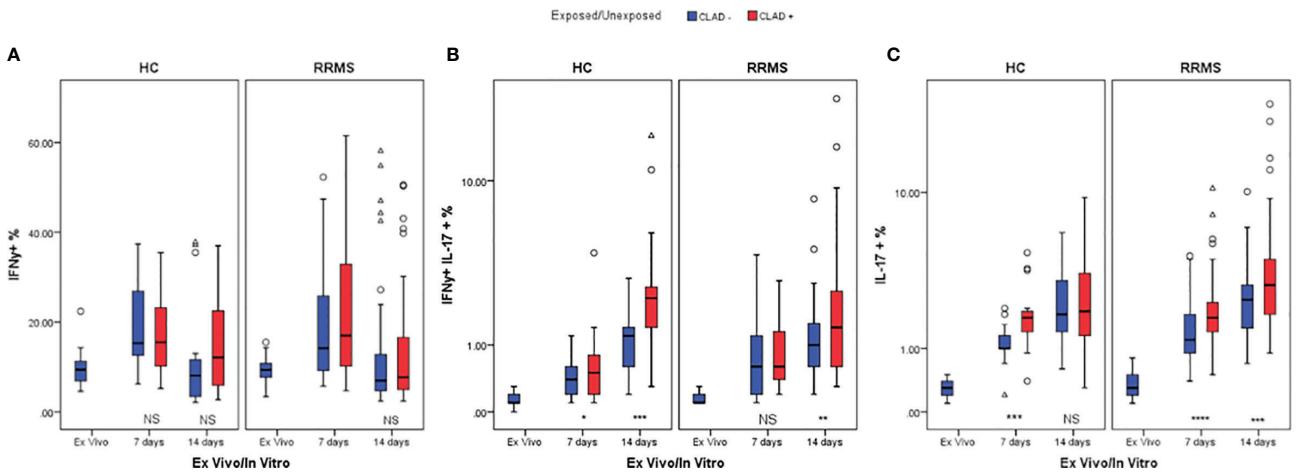

FIGURE 9 | HC and RRMS CD3+IFNγ+ **(A)**, CD3+IFNγ+IL17+ **(B)**, and CD3+IL17+ **(C)** cell percentages changes with cladribine treatment at day 7 and 14 represented as boxplot (median with error bars). NS, non significant (p > 0.05) *P*-values were considered significant when lower than 0.05 (*$p \leq 0.05$, **$p \leq 0.01$, ***$p \leq 0.005$, ****$p \leq 0.0001$).

for HC at day 7 and 14, but increased significantly for RRMS at both time points (p=0.027 at day 7 and p=0.007 at day 14) (**Figure 10B**).

4 DISCUSSION

4.1 The Surface T Cell Phenotype Shifts From *Ex Vivo* to *In Vitro* Status

T cells involved in MS pathogenesis express a combination of encephalitogenic molecules from cells with Th1 and Th17 phenotypes, eliciting CNS inflammation (32). Our study first highlighted the presence of CD161, CXCR3, and CCR6 on the surface of T cells in *ex vivo* samples, which is expected to mirror the *in vivo* status of the cells quite accurately. The *ex vivo* T cell phenotype was compared with the phenotypic profile of *in vitro* rh-IL2-activated cells in medium-term cultures that are often used to study the effect of therapeutic molecules in the pre-clinical phases of trials.

As described by Fergusson et al. (33), the C-type lectin CD161 binds lectin-like transcript 1 (LLT1) expressed by both activated antigen presenting cells and lymphocytes, leading to increased IFNγ production in T lymphocytes. CD161 is considered a

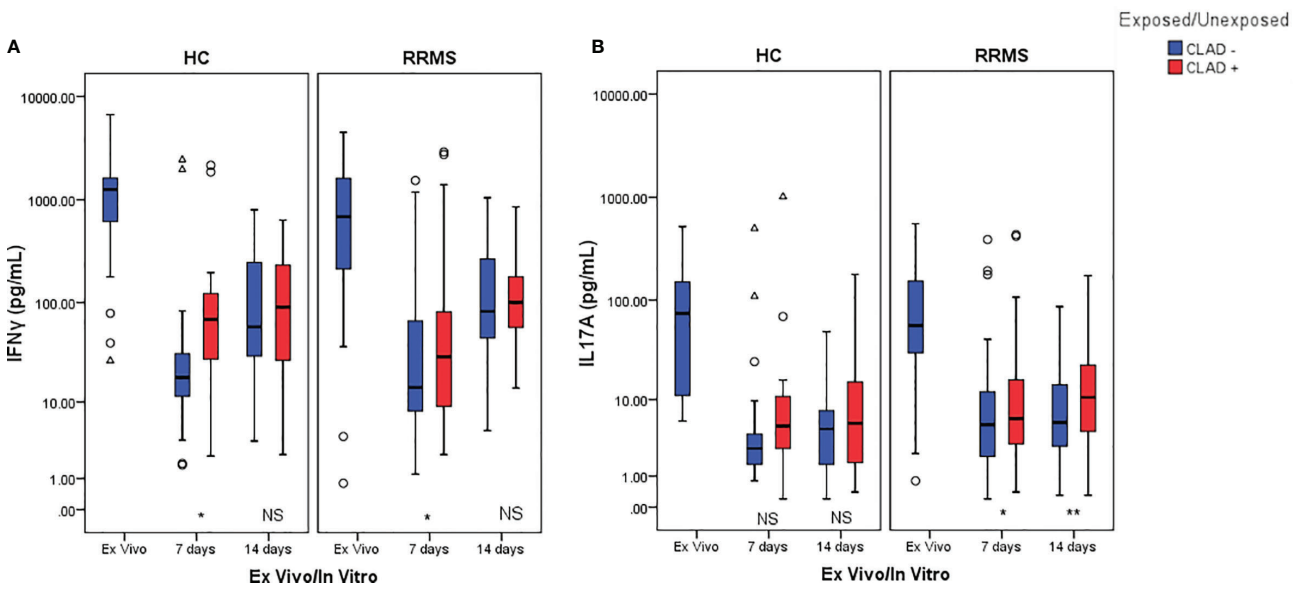

FIGURE 10 | Changes in IFNγ **(A)** and IL17 **(B)** secretion profiles after cladribine exposure represented as boxplot (median with error bars). NS, non significant (p > 0.05) *P*-values were considered significant when lower than 0.05 (*$p \leq 0.05$, **$p \leq 0.01$).

hallmark of Th17 cells and has been consistently associated with a memory phenotype in the adult circulation. Also, CD161 is involved in transendothelial migration in the absence of chemotactic stimuli by binding to acidic oligosaccharides on the endothelial cell surface (33). IL17 knockout mice exhibit delayed onset, reduced severity, and early recovery of experimental autoimmune encephalomyelitis (EAE), the murine model of MS. In humans, MS patients show increased IL17 levels (34), infiltration of CD3+IL17+ cells within MS brain lesions (35), and a significantly higher percentage of peripheral blood CD3+CD8+CD161^{high} cells compared to healthy subjects (15). Taken together, data from the literature provides sufficient evidence that CD161 is involved in MS pathogenesis in ways that are yet to be fully elucidated. As expected, in our study, a significantly higher percentage of CD3+CD161+ cells was observed in the *ex vivo* samples from RRMS patients compared to HC (**Figures 3A**, **4A**). Given that RRMS patients included in this study had no evidence of disease activity at the time of blood sampling, this finding suggests that increased CD3+CD161+ cell levels may serve as a potential biomarker for differentiating healthy individuals not only from relapsing MS patients but also from RRMS patients with no current evidence of disease activity. By the same logic, it could be speculated that an increased level of CD3+CD161+ cells (or an unexplained increase from the baseline) in yet undiagnosed future MS patients, may predict an upcoming clinically isolated syndrome as a first episode of MS. However, this is a speculation that remains to be addressed in future research. Regarding the *in vitro* evolution of CD3+CD161+ cells, the significant difference seen *ex vivo* between RRMS patients and HC is lost *in vitro*, with only an apparent recovery of RRMS CD3+CD161+ cells at day 14. Therefore, we consider that CD161 is not a suitable T cell marker for monitoring medium-term cultures using the activation protocol described in this paper.

As shown by Groom et al. (36), after initial T cell entry into the CNS, a subsequent inflow of T cells is mediated by CXCR3 (an interferon-inducible chemokine receptor). CXCR3 is associated with Th1 and CCR6+ Th1 cell phenotypes. CXCR3 binds three chemokines: CXCL9 (also known as MIG, monokine induced by gamma-interferon), CXCL10 (IP-10, interferon-induced protein of 10kDa), and CXCL11 (I-TAC, interferon-inducible T cell alpha chemoattractant), triggering the entry of CXCR3+ cells into the brain. Our analysis showed that the proportion of CD3+CXCR3+ cells from RRMS patients continued to significantly increase from *ex vivo* to 7 and then to 14 days in culture, while HC CD3+ CXCR3+ cells increased non-significantly between these three time points (**Figures 3B**, **4B**). Despite that, there was no significant difference between HC and RRMS CD3+CXCR3+ cells at neither time point. Since CXCR3 is an inflammation-driven, interferon-inducible molecule, this lack of significant difference *ex vivo* may too be related to the lack of evident disease activity in our RRMS patients at the time of blood sampling. Also, the continuous increase of this cell population *in vitro* is probably caused by increased levels of CD3+IL17+ and CD3+IFNγ+IL17+ cells, the two pathogenic populations that are the focus of this study (see similar patterns for **Figures 4B**, **5A**, **6B, C**).

According to Restorick et al. (37) and Lee et al. (38), CCR6 (chemokine receptor 6) binds CCL20 (chemokine ligand 20), and this CCR6-CCL20 axis is required for the initial wave of T cells entering the CNS. CCR6+ cells are the first cells recruited across the choroid plexus into the CNS, driving the activation of the endothelial barrier and reducing barrier integrity in the first phase of MS disease. It can be presumed that the gradual *in vitro* loss of CD3+CCR6+ (**Figure 4C**), CCR6+ Th17 and Th17.1 cells (**Figure 5B**) seen in this study was caused by the absence of CCL20 stimulation.

In summary, *ex vivo* levels of CD3+CD161+ cells are significantly higher in RRMS patients without evidence of disease activity, and may therefore have practical applications. In turn, *ex vivo* levels of CD3+CXCR3+ and CD3+CCR6+ cells are not significantly different between HC and patients. However, the situation is likely to change in relapsing patients with ongoing disease activity. As elicited by our *in vitro* experimental model, CD161 and especially CCR6 do not seem to be suitable T cell markers for monitoring cell cultures. CD3+ CXCR3+ cell percentages however seem to increase significantly in relation to pathogenic CD3+IL17+ and CD3+IFNγ+IL17+ cell populations.

4.2 *Ex Vivo* Versus *In Vitro* Cytokine Production Capacity of Maximally Activated T Cells

A peak of CD3+ cells with maximal IFNγ-producing capacity was identified at day 7 in culture for both HC and RRMS after rh-IL2 induction. Therefore, during the second week in culture, a resumption of TBet synthesis likely occurred and the percentage of CD3+TBet+ cells stabilized. As Ross et al. (39) described, in CD3+ cells activated with rh-IL2, TBX21 gene expression is triggered, followed by TBet transcription factor and IFNγ synthesis *via* a STAT5-dependent mechanism. CXCR3 synthesis is also driven by TBet (36), and IL2 promotes the proliferation of cells with Th1 phenotype (39).

Cell culture conditions determined a similar evolution pattern of CD3+IFNγ+ cells in both RRMS and HC subjects. Also, cladribine exposure does not seem to alter the proliferation of CD3+IFNγ+ cells.

In vitro rh-IL2 activation generated a significant increase in the CD3+IFNγ+IL17+ cell subpopulation for HC and RRMS subjects which, simultaneous with the evolution of CD3+CD161+ and CD3+CXCR3+ cells, was related to CD3+TBet+RORγt+ signaling at day 7 and day 14 of culture.

A significant increase in CD3+IL17+ cells was observed in HC and RRMS subjects. The number of CD3+RORγt+ cells remained constant for HC but increased in RRMS patients, which could also explain the evolution of CD3+CD161+ cells during the 14 days in culture. This evolution could have been a consequence of the proliferation of cells with a Th17 phenotype that also share differing degrees of Th1 features. The heterogeneous group of Th17 cells *in vitro* activated with rh-IL2 were found to exhibit good survivability and proliferation.

According to van Langelaar et al. (10), the heterogeneous cellular Th17 phenotype can be comprised of high

(CCR6+CXCR3−) and low (CCR6+CXCR3+) IL17A-producers, that is CCR6+CXCR3−CCR4+IFNγ+IL17^{high} Th17 cells, CCR6+CXCR3+CCR4−IFNγ+IL17^{low} Th17.1 cells, and CCR6+CXCR3+CCR4+IFNγ+IL17^{dim} Th17 double-positives cells. Th17.1 (Th1-like Th17) cells have a Th17 origin and are characterized by IL17 and IFNγ co-expression (due to co-expression of transcription factors TBet and RORγt) and the presence of CCR6 and CXCR3, with or without CCR4 expression on the cell surface. Th17.1 cells also showed CD161 expression, as an ex-Th17 phenotype, but with distinct pro-inflammatory Th1 features due to the co-expression of VLA-4, CD161, TBet, RORγt, IFNγ, IL17 and GM-CSF (10). Th17.1 cells are recruited to the CNS to mediate early MS disease activity and are predominantly accumulated in the blood of relapse-free patients (10). As Kalra et al. (5) demonstrated, this group shares features of Th17 and Th1 cells, but also contains non-classical Th1 cells (known as ex-Th17 or non-conventional Th1 cells), which are significantly more numerous in the CSF as compared to the peripheral blood. These IFNγ-secreting Th17 cells express TBX21, CCR6 and CXCR3 surface markers and RORγt, but are characterized by the absence of Th17-associated cytokines.

Acquaviva et al. (40) showed that the gene expression of both IL17 and C-type lectin CD161, controlled by the transcription factor RORγt, is not only a feature of Th17 cells but also of a particular CD3+CD8+ cell type. Hinks and Zhang (41) described CD8+CD161^{high} cells, known as mucosal-associated invariant T (MAIT) cells. Fergusson et al. (33) showed that 10% of MAIT cells display an upregulated expression of RORγt and CCR6, representing a Tc17 cell type with diminished cytotoxic potential due to a reduced amount of the Tbox transcription factor, Eomesodermin, IFNγ, and granzyme B in comparison with CD3+CD8+ effector cells. The frequency of CD3+CD8+CD161+ lymphocytes decreased in blood but increased in the inflamed site by infiltrating MS lesions. Seventy to eighty percent of CD3+CD8+ cells from active MS lesions are known to produce IL17 (40). Patients with MS have a significantly higher percentage of peripheral blood CD3+CD8+CD161^{high} cells, which secrete more IL17 than in healthy individuals. Furthermore, IFNγ and IFNγ/IL17 co-secreting CD3+CD8+ cells were identified, expressing intermediate or high CD161 levels, while CD3+CD4+ cells express intermediate levels of CD161 (40).

In summary, this study enabled the emphasis to be placed on CD3+ cell subpopulations involved in MS pathology. More specific, the proposed *in vitro* experimental protocol has proven very efficient at selecting pathogenic Th17 and especially Th17.1 populations (**Figure 5A**), and also pathogenic secretory CD3+ cell populations such as CD3+IL17+ and CD3+IFNγ+IL17+ (**Figures 6B, C**). We conclude that the protocol is appropriate for personalized *in vitro* T cell profile assessment by short- and medium-term activation and for the *in vitro* investigation of the effect of therapeutic drugs on such selected populations. One limitation of the present study was the lack of characterization of CD3+CD8+ cells and their specific contribution to the evolution of CD3+ cell subpopulations in culture with rh-IL2.

4.3 The Effect of *In Vitro* Cladribine Exposure on T Cells

Heterogeneous brain-infiltrating lymphocyte subsets are known to contribute to MS pathogenesis (32). A better knowledge of the particular phenotype shift and proliferation capacity of lymphocyte subsets in response to DMDs can help in developing a predictive algorithm of responsiveness in order to tailor the best therapy for each MS patient. Characterization of immune cell alterations occurring during the disease course and in response to treatment may support a better understanding of MS pathogenesis and the mechanism of action of DMDs (42).

4.3.1 Real-World Data on Cladribine Treatment for MS

Published in 2010, CLARITY was the first clinical trial on cladribine treatment for RRMS patients (43). This Phase III randomised controlled clinical trial demonstrated that treatment with oral cladribine significantly reduces the relapse rate, the risk of disability progression, and MRI measures of disease activity in RRMS patients (43). Subsequent clinical trials, clinical trials extensions, trial cohort follow-ups, and other studies have confirmed cladribine as a potent DMD for MS patients, with therapeutic efficiency lasting between 2-5 years or even up to 8 years in some individuals (29, 42, 44–49). Other ongoing clinical trials are aiming to further establish clear therapeutic indications for MS patients in various stages of the disease and clinical contexts (50).

Cladribine has been approved in the EU in 2017 and is currently indicated mostly for the treatment of patients with highly active RRMS. Regarding cladribine's efficacy and real-world applications compared to other drugs, a Class III evidence, CLARITY/i-MuST propensity score matched study on RRMS patients showed that cladribine-treated patients had: lower annualized relapse rates compared with interferon, glatiramer acetate, or dimethyl fumarate; similar annualized relapse rates compared to fingolimod; and higher annualized relapse rates compared to natalizumab (51). Moreover, the beneficial effect of oral cladribine was generally higher in patients with high disease activity (51). Similar results were observed in a cohort of RRMS patients where cladribine was proven superior to interferon, similar to fingolimod, and inferior to natalizumab (52). Similarly, a recent publication suggests that oral cladribine is significantly more effective in achieving NEDA-3 (no evidence of disease activity-3, a composite endpoint comprising 3 measurements of disease activity: lack of clinical relapse, lack of confirmed disability progression, and no disease activity on MRI) than dimethyl fumarate and teriflunomide, but has similar efficacy compared with fingolimod (53). According to a network meta-analysis regarding the effects of RRMS drugs on annualized relapse rates and confirmed disability progression in patients with active and highly active RRMS, cladribine was superior to glatiramer acetate and interferon, but similar to dimethyl fumarate and fingolimod (54). In the same network meta-analysis, when compared with other DMDs, cladribine was ranked 4th on a scale of efficacy for reduction of annualized relapse rate, after alemtuzumab, natalizumab, and ocrelizumab (54). However, regarding confirmed disease progression for 6 months, NEDA, and overall adverse event risk, oral cladribine did not differ significantly from most alternative DMDs (54). A recent study on 270 MS patients from Germany, reported that patients switching from natalizumab to cladribine tablets were prone to re-emerging disease activity (55). Similarly, recent

evidence from patients switching from natalizumab to other DMDs shows that cladribine has a higher risk for relapses and MRI activity than ocrelizumab, but similar to rituximab (56). Regarding confirmed disability progression, there was no difference between patients switching from natalizumab to either cladribine, ocrelizumab, or rituximab (56). Overall, cladribine seems to be a safe exit strategy in natalizumab-treated RRMS patients at high risk of progressive multifocal leukoencephalopathy (56).

All things considered, there's an increasing body of evidence from clinical trials and large studies in support of cladribine as a safe and efficient DMD in RRMS. However, despite these evidences and its superiority over other DMDs, the short- and long-term effects of cladribine on cells of the specific immune system are yet to be fully elucidated. Risk assessment is required before initiating cladribine therapy in MS patients, especially due to its lymphocyte-depleting effect which can cause severe lymphopenia. Moreover, cladribine treatment should ideally be initiated only for individuals responsive to this DMD. Hence, we aimed to assess the effect of cladribine on T cells phenotype as a means towards achieving the goal of precision medicine in RRMS patients.

4.3.2 The Cytotoxic Effect of Cladribine

As a result of the cytotoxic effect of cladribine, the initial T cell proliferation index after 48h of cladribine exposure was lower for treated cells from both HC and RRMS patients, compared to untreated cells. However, the median proliferation index was higher in RRMS patients compared to HC (untreated: 1.28 vs 0.89; treated: 0.72 vs 0.42; see **Figure 7**). These differences suggest that T cells of RRMS patients tend to proliferate (as opposed to T cells of HC) and are also more resistant to cladribine compared to T cells of HC. In both HC and RRMS, only treated T cells proliferated continuously until day 14, suggesting that T cells resistant to cladribine also display a consistent proliferative behavior. Given the meteoric rise of Th17 and especially Th17.1 *in vitro* (**Figure 5A**), it is safe to assume that these two pathogenic populations share a certain degree of cladribine resistance and proliferative behavior.

4.3.3 The Immunomodulatory Effect of Cladribine

Cellular subpopulations like Th17 and Th17.1 are very rare in the peripheral blood. Secretory profile assessment of T cells lineage using intracellular cytokines *in vitro* experimental protocol has been proven to be very efficient in the analysis of these T subpopulations. In cultures exposed to cladribine, CD3+CD161+ cells from HC were depleted until day 7, as in untreated cells; however, the exposed HC CD3+CD161+ cells proliferated up to day 14, which led to a significant difference between treated and untreated cells (**Figure 8A**). On day 7, there was a significantly higher percentage of treated CD3+CD161+ RRMS cells compared to untreated cells. The phenomenon of survival and proliferation after cladribine exposure continued for up to 14 days, further generating significantly higher percentages of CD161+ cells in cladribine treated cultures. CD3+CXCR3+ cells from HC were selected, surviving and proliferating well up to day 7 and day 14, with a significant difference observed between cladribine-treated and untreated cells. CD3+CXCR3+ cells from RRMS patients also proliferated well up to day 7 and day 14, with non-significant differences between cladribine-exposed and unexposed cell cultures (**Figure 8B**). The number of CD3+CCR6+ cells decreased only in the first week after cladribine exposure. In the second week, treated cells proliferated, highlighting a significant difference between untreated and cladribine-treated CD3+CCR6+ cells. The RRMS CD3+CCR6+ cell subpopulation was non-significantly modified in treated and untreated cell cultures on day 7 and day 14 (**Figure 8C**).

CD3+IFNγ+ cells from HC showed significant proliferation until day 7, followed by significant depletion at day 14, regardless of cladribine exposure. Cladribine-treated CD3+IFNγ+ cells from RRMS subjects also proliferated well during the first week, particularly compared to untreated cells. In the second week of culture, a similar depletion of untreated and treated cells was observed. The proliferation of the surviving CD3+ IFNγ+IL17+cells from HC and RRMS subjects was more intense during the second week after cladribine exposure (**Figure 9B**). Cladribine-treated CD3+IL17+ cells from both HC and RRMS proliferated more than untreated cells at day 7, and only cladribine-treated RRMS CD3+IL17+ cells proliferated significantly more compared to untreated cells at day 14. Overall, CD3+CXCR3+, CD3+IL17+, and CD3+IFNγ+IL17+ are the populations with the highest proliferation after cladribine exposure. It appears that cladribine selects these T cell subpopulations, which survive and proliferate well. The recovery of CD161+ and CCR6+ cells at day 14 after cladribine exposure was also observed.

On day 7, IFNγ secretion in culture media from cladribine-treated cells was significantly higher than in untreated cells in both HC and RRMS subjects. On day 14, there is a non-significant difference between untreated and cladribine-treated cells. Given the much higher proportion of IFNγ single-positive cells (corresponding to Th1) relative to the T cell subpopulation double-positive for IFNγ and IL17, it can be presumed that Th1 cells make the largest contribution to IFNγ secretion. Indeed, similarly, the appearance of IFNγ single-positive cells has also been linked to IFNγ secretion in culture media. Exposure to cladribine led to a significant increase in CD3+IFNγ+ cells at day 7 only in RRMS patients and then had no effect at day 14. The levels of IFNγ secretion were different only at day 7, after which point there was no significant difference, regardless of cladribine exposure, in both HC and RRMS patients. These results, together with the evolution of the T cell phenotype *in vitro* at 7 and 14 days, indicate that a 14-day, double-stimulation *in vitro* experimental protocol is not necessarily needed, as data collected at day 14 is mainly redundant compared to data collected at day 7. Hence, we propose that, in view of precision medicine approaches to MS treatment, a 7-day, one-stimulation, standard experimental protocol be used for the induction of significant and measurable individual and disease-specific changes *in vitro*. Here, we tried to establish a relation between intracellular cytokine production and culture media

cytokine levels. We emphasize that such efforts should be made in order to identify corresponding techniques that could replace costly and elaborate investigations like intracellular cytokine staining and multiparameter flow cytometry.

Despite the significant proliferation of cladribine-treated CD3+IL17+ cells at day 7, and of CD3+IFNγ+IL17+ cells at day 7 and day 14 of culture, IL17 secretion from HC cells was not different between untreated and treated cells at these time points. In RRMS patients, IL17 secretion from cladribine-treated cells was significantly higher at day 7 and day 14, in line with the proliferation of CD3+IL17+ and CD3+IFNγ+IL17+ cells exposed to cladribine.

As Korsen et al. (31) demonstrated, *in vitro* treatment with cladribine for 72 h, followed by PBMC culture for up to 58 days with IL2 and re-stimulation of surviving cells with anti-CD3/anti-CD28 antibodies or phytohemagglutinin, did not impair cell proliferation. Initial exposure of PBMCs from healthy subjects to cladribine only affected anti-inflammatory cytokine release. No significant changes were observed regarding IFNγ and IL17A secretion in culture media

An important issue is the influence of the different methods used for T cell activation. According to the cytokine profile determined by Olsen et al. (57), IFNγ and IL17 production were higher after T cell stimulation with PMA/ionomycin compared to anti-CD3/anti-CD28 mAbs. While T cell activation by anti-CD3/anti-CD28 mAbs is regarded as a physiological activation through the T-cell receptor complex (TCR), PMA/ionomycin activation triggers maximal cytokine production With appropriate concentration and stimulation time, PMA/ionomycin stimulation is useful to characterize cytokine production in poorly represented T cell subpopulations. While physiological activation may be the preferred option to assess the immune profile of T cells involved in MS, PMA/ionomycin activation provides more information on the immunomodulatory effect of DMDs such as cladribine. In this regard, the analysis of RRMS subjects, including those with outlier values, revealed an agreement between the results obtained by short maximal activation with PMA/ionomycin and by physiological activation with anti-CD3/anti-CD28 mAbs, only at day 7 in culture. On day 14, only the maximal activation provided significant results on the effect of cladribine (**Figures 9B, C**).

In a study recently published by Moser et al. (58), the immunological consequences of two cycles of therapy with oral cladribine for two years on 18 MS patients were investigated. The authors observed that CD3+CD4+ and CD3+CD8+ cells reached the lowest levels at month 15, followed by recovery at month 24. Memory and naïve T cytotoxic and helper cells were not altered by cladribine. Central memory and effector memory CD8+ cells, together with central memory Th17.1 (CD4+CD45RO+CCR7+ CXCR3+CCR6^{high}) cells, were depleted during the two-year period. Cladribine led to a depletion of Th1 and Th17.1 cells only at the end of year two, but no significant changes were noted in the cytokine expression profiles of Th1 and different Th17 subsets. In another study, Stuve et al. (59) analyzed the effects of 3.5 mg/kg cladribine administration after the first year of treatment. Cladribine intake led to a large reduction in B cells (approximately 80% at nadir), a moderate reduction in T cells (approximately 50% CD4+ and 40% CD8+ at nadir), and smaller reductions in NK cells (between 30% and 44% at nadir). The reductions were followed by a quick recovery towards baseline levels for CD16+/CD56+ and for CD19+ cells. The CD4+ and CD8+ T cells had a minimal and gradual recovery. Both memory and effector CD4+ T lymphocytes proportions decreased after treatment (63% and 54%, respectively, at nadir). CD4+ central memory remained lower at 48 weeks than at baseline, and CD4+ effector memory T cells were 16% higher at week 48 than at baseline.

All of the discussed findings raise the issue of cladribine action selectivity on different T cell subsets. Cladribine undergoes intracellular phosphorylation catalyzed by deoxycytidine kinase (DCK), generating active mononucleotide 2-chlorodeoxyadenosine 5'-triphosphate (2CdATP), which incorporates into DNA, blocking its synthesis and leading to cell death. DCK expression is variable in different types of lymphocytes, dependent on their degree of activation. Cells of the immune system present different sensitivities to cladribine, depending on the expression levels of DCK and two cytosolic 5-nucleotidases (5-NT) isoforms most involved in adenosine metabolism: higher DCK to 5-NT ratio means higher cladribine sensitivity (60). Among lymphocytes, DCK:5-NT is very high for B cells, intermediate for CD4+ T cells, and low for CD8+ T cells (60). The CLARITY clinical trial revealed that oral cladribine treatment was associated with a profound decline in lymphocyte counts from baseline (43). Although B cells are the most affected by cladribine, a gradual repopulation is seen toward the ends of both courses of treatment (27). On the other hand, T cell depletion was modest and dose-dependent, but sustained. Thus, Baker et al. hypothesized that the marked and long-lasting depletion of B cells is the key mechanism of action of cladribine in MS (27). However, given that major peripheral blood immune subsets such as CD4+/CD8+/CD19+ can not be used as biomarkers to predict disease activation following cladribine treatment, the authors also recognize that the mechanism of action of cladribine in MS is up to debate (27). It is likely that the pathogenic cells in MS are represented only by a minor population within any major cell subset. Therefore, cladribine's beneficial effect in MS may be explained by either one or both qualitative and quantitative changes in one or multiple lymphocyte subsets. An in depth analysis of the many immune subsets may be the key to uncovering the mechanism of action of cladribine in MS.

All things considered, B cells have been so far the lymphocyte population most studied in MS. However, given the important role of T cells in the pathogenesis and progression of MS, we consider that a more in depth investigation of this lymphocyte population is needed in order to further clarify its role in MS. Therefore, we aimed to analyze both the quantitative (survival/proliferation index) and qualitative (immunophenotype) effects of *in vitro* cladribine exposure on T cells from RRMS patients in order to identify an algorithm able to differentiate between cladribine responders and non-responders. This endeavor represents a step towards precision medicine in MS.

The different responsiveness of particular lymphocyte subtypes to cladribine action, such as the sustained proliferation of cladribine-treated cells during two weeks in culture, was highlighted in our study. At the individual level, we assessed the net effect of cladribine on the evolution of cytokine-producing CD3+ cell populations after 7 days in culture (see **Figure 11**). Net variation is expressed as absolute percentage of cell population from the parent CD3+ cell population and is calculated as follows: (% value in treated samples) – (% value in untreated samples). Due to their role in the pathology of MS, CD3+IFNγ+IL17+ followed by CD3+IL17+ cell populations were the main focus of this assessment. Despite the apparent heterogeneity, **Figure 11A** shows a continuous and mainly unidirectional variation of cladribine effect on cytokine-producing CD3+ populations at day 7, defined by significant positive correlations between the (primary aggressive) CD3+ IFNγ+IL17+ cell population and the CD3+IFNγ+ (Spearman's r=0.662, p<0.0001) and CD3+IL17+ (Spearman's r=0.356, p=0.038) cell populations. Interestingly, it should be noted that the top 10% of RRMS subjects on the list (**Figure 11A**; 4 RRMS patients: 06, 24, 15, and 27) presented systematically high values and were therefore classified as atypical for multiple parameters, including their response to short-term maximal activation with PMA/ionomycin/monensin, and to physiological stimulation. Given that, after cladribine exposure, all four subjects showed a significant net increase in all three cytokine-producing CD3+ cell populations (IFNγ+IL17+, IL17+, and IFNγ+), we consider these patients as possible drug-resistant or non-responders to cladribine. Inversely, most RRMS patients from the bottom 40% of the list (10 out of 14) show post-cladribine net variations of ≤ 0% for the CD3+IFNγ+IL17+ population and ≤ +0.5% for the CD3+IL17+ population. These negative net variations are caused by a lower prevalence of the pathogenic CD3+ cell populations in cladribine-treated samples compared to untreated samples, hinting at the suppressive role of cladribine on these pathogenic subsets. Hence, we consider these patients as possible responders to cladribine treatment. Moreover, based on the evolution of the CD3+IFNγ+ cell population, these responders can be further divided into two distinct types: type 1 (complete) responder (relative depletion of all 3 cell populations: CD3+IFNγ+IL17+, CD3+IL17+, and CD3+ IFNγ+) and type 2 (incomplete) responder (relative depletion of CD3+IFNγ+IL17+ and CD3+IL17+ cells and relative selection of CD3+IFNγ+ cells). In summary, data analysis at the individual level with emphasis on the highs and lows of the same group, revealed that in some patients cladribine could be very effective in depleting IL17 and IFNγ secretory CD3+ cells, while in others, it may select highly reactive lymphocyte species, such as CD3+ IFNγ+IL17+ and CD3+IL17+.

In HC, no similar pattern of responsiveness can be established. The bottom 50% of the list meets the main criterion of responsiveness used above for RRMS patients, that is a post-cladribine net variation of ≤ 0% for the CD3+ IFNγ+IL17+ cells. Another similarity between HC and RRMS responders is that, except for one, all HC responders show negative net variation for CD3+IFNγ+ cells. However, in contrast to the established RRMS pattern, all of these HC responders show a positive net variation of CD3+IL17+ cells, ranging from 0.1% to 1.3%. This notable difference between HC responders, where net variations of CD3+IL17+ cells are all > 0%, and RRMS responders, where net variations of CD3+IL17+ cells are mainly ≤ 0%, is also supported by a negative correlation between the two cell populations in HC (Spearman's r = -0.498, p=0.042). The HC subjects showing a non-responder behavior populate the upper 35% of the HC lot. However, once again in contrast to RRMS subjects, HC non-responders show mainly negative net variations for CD3+IFNγ+ cells whereas RRMS non-responders show highly positive net variations for CD3+ IFNγ+ cells. A noteworthy case is the top HC non-responder which was an apparently healthy 35-year-old male who passed the exclusion criteria with a hsCRP level of 2.27 mg/L and a WBC count of 7.18×10^9/L. The *ex vivo* levels of IFNγ and IL17A secreted in culture were as follows: IL17A 139.1 ng/mL (group range 5.8–519.8 ng/mL, median value 68.7 ng/mL, 4th largest value) and IFNγ 3671.3 ng/mL (group range 26.6–6666.9 ng/mL, median value 1167.5 ng/mL, 2nd largest value). Given the exaggerated response in *ex vivo* and *in vitro* experiments, we further investigated the levels of three inflammatory cytokines secreted in culture media: IL1β (3485 ng/mL), IL6 (17350 ng/mL), and TNFα (756 ng/mL). Given the described experimental behavior and cytokine levels together with the normal levels of hsCRP and WBC, we can only assume that this particular HC subject was going through the very early phase of an acute inflammation at the time of blood sampling.

A better knowledge of the particular phenotype shift and proliferation capacity of lymphocyte subsets in response to cladribine may help in developing a predictive algorithm of responsiveness in order to tailor the best therapy for each MS patient. This experimental model could be useful for precision therapy and to identify cladribine non-responders, to evaluate the behavior of Th1, Th17, Th17.1 cells from naïve MS patients in the presence of cladribine. As cladribine is an important member of immune reconstruction therapies, it is mandatory to determine what type of lymphocytes undergo this reconstruction process and what types are spared. In clinical practice there is no rebound of MS clinical or MRI activity even after recovery of T cell count, suggesting a degree of qualitative change after treatment with cladribine in the adaptive immune response (3, 61, 62).

A limitation of our study is patient-related since no relevant clinical data on the evolution of the investigated RRMS patients is available at the moment of writing. Therefore, only hypothetical, but no clear relations between the *ex vivo/in vitro* behavior of T cells and the clinical evolution of RRMS patients could be established. However, this is merely a temporal limitation as all RRMS patients included in this study are monitored periodically and, given the natural evolution of MS, more relevant clinical data will likely come to light over the following years.

The lately therapeutic developments seen in MS are unmatched in any field of neurology. Actually, modern treatment guidelines place the MS patient in the center of the

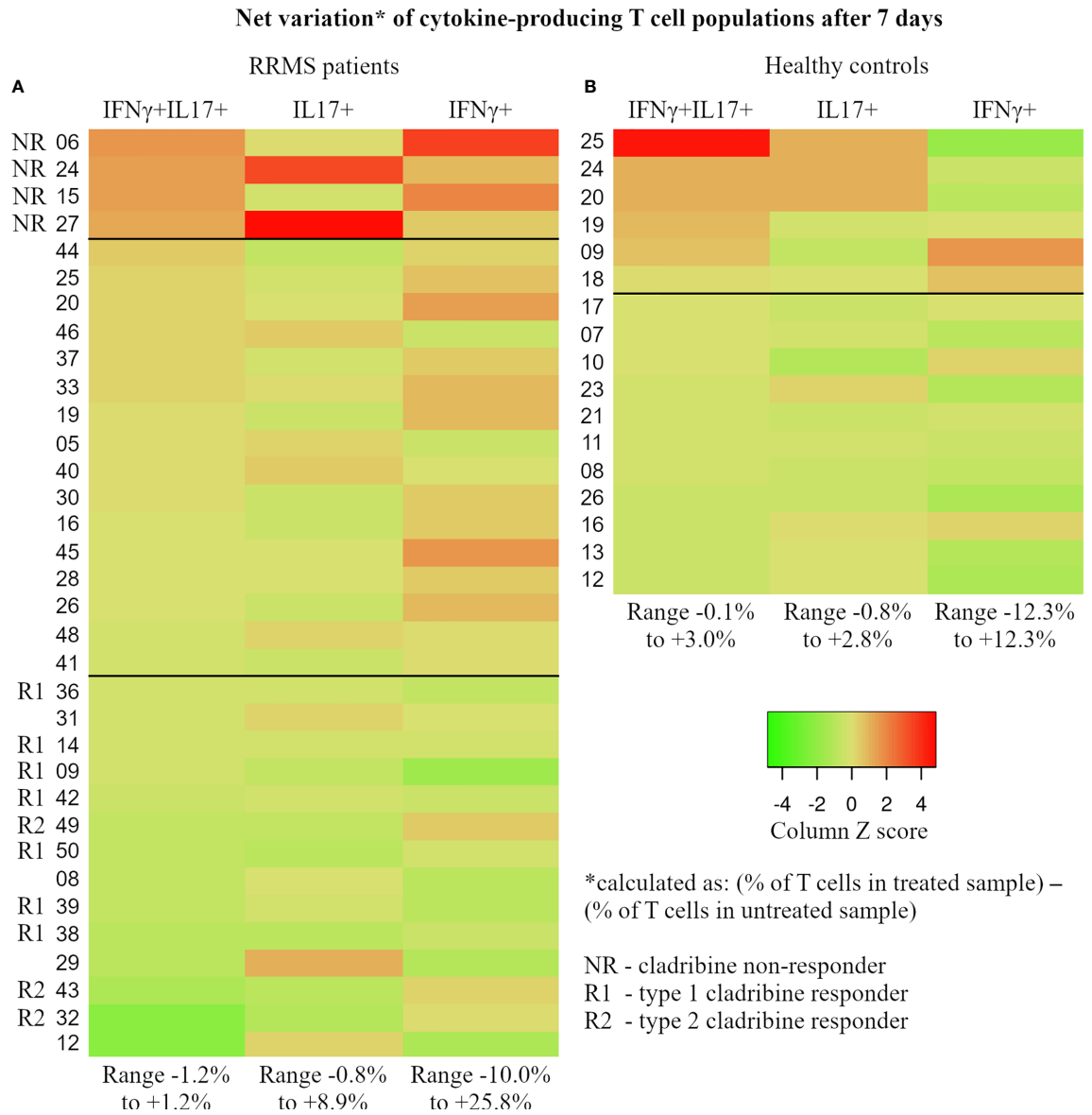

FIGURE 11 | For each subject, the percentage of IFNγ+IL17+, IL17+, and IFNγ+ T cells was determined at day 7 through flow cytometry from paired cladribine-exposed and unexposed samples. The net effect of cladribine on the cytokine-producing populations was calculated for each subject as follows: (cytokine-producing population as % of T cells in the cladribine-exposed sample) – (the same cytokine-producing population as % of T cells in the unexposed sample). Calculated values reflect the true effect of cladribine and were used to generate the 2 heatmaps in this figure (**A** – RRMS patients, **B** – healthy donors). Based on the observed trends and patterns, RRMS patients were divided into 3 groups that may reflect each subject's individual reaction to cladribine exposure: NR, non-responders (defined as net increase in all 3 cytokine-producing T cell populations after cladribine exposure), R1 – type 1 responders (defined as net decrease of all three cytokine-producing T cell populations), and R2 – type 2 responder (defined as net decrease of IFNγ+IL17+ and IL17+ T cells combined with net increase in IFNγ+ T cells). Note that HC and RRMS share the same color gradient. Also, the values are color coded based on Z score, while the range of absolute net % values for cell populations is presented at the bottom of each column.

treatment decision-making process for the improvement of MS management. There are nonresponders to DMDs among MS patients, but the amount of newly available DMDs on the market poses great challenges in selecting the right DMD for the right MS patients at the right moment. Hence, current interest and research targets to provide the tools and evidence for personalized medicine in MS. In the era of precision medicine, the decision to recommend treatment with cladribine to MS patients requires an understanding of cell responsiveness, which can be very different from patient to patient.

The experimental method we propose here could be the answer for the early prediction of the responsiveness of MS patient to cladribine. Additionally, this model may be extended to other DMDs.

DATA AVAILABILITY STATEMENT

The raw data supporting the conclusions of this article will be made available by the authors, without undue reservation.

ETHICS STATEMENT

The studies involving human participants were reviewed and approved by the Committee for Ethical Research of the County Emergency Clinical Hospital of Târgu Mureș (decision no. 7,100/2018). The patients/participants provided their written informed consent to participate in this study.

AUTHORS CONTRIBUTION

MD and RB conceived and designed the study. MD and DRM developed the methodologies. RB and LB provided patient samples and data. DM, DRM, AH and IBM analyzed data and performed experiments. MRG, LB and IBM performed statistical analysis of experimental data. MD and DRM analyzed data in the literature and drafted the manuscript. MD, AH and IBM technically revised the manuscript. MD and RB critically revised the manuscript for important intellectual content and approved the final version of the manuscript. All authors contributed to the article and approved the submitted version.

FUNDING

This work was supported by Merck Regional Grant for Central and Eastern Europe Countries 2017 Research Project (No. 548/2018). The funder was not involved in the study design, collection, analysis, interpretation of data, the writing of this article or the decision to submit it for publication. Fees for open access publication are supported by "George Emil Palade" University of Medicine, Pharmacy, Science and Technology, Târgu Mureș, Romania.

ACKNOWLEDGMENTS

The authors are grateful to the physicians and nurses from the Neurology 1 Clinic of the Emergency Clinical County Hospital of Târgu Mureș, who participated in our study.

REFERENCES

1. van Langelaar J, Rijvers L, Smolders J, Van Luijn MM. B and T Cells Driving Multiple Sclerosis: Identity, Mechanisms and Potential Triggers. *Front Immunol* (2020) 11:760. doi: 10.3389/fimmu.2020.00760
2. Peterson LK, Fujinami RS. Inflammation, Demyelination, Neurodegeneration and Neuroprotection in the Pathogenesis of Multiple Sclerosis. *J Neuroimmunol* (2007) 184(1-2):37–44. doi: 10.1016/j.jneuroim.2006.11.015
3. Balasa R, Maier S, Barcutean L, Stoian A, Motataianu A. The Direct Deleterious Effect of Th17 Cells in the Nervous System Compartment in Multiple Sclerosis and Experimental Autoimmune Encephalomyelitis: One Possible Link Between Neuroinflammation and Neurodegeneration. *Rev Romana Med Laborator* (2020) 28(1):9–17. doi: 10.2478/rrlm-2020-0005
4. Durelli L, Conti L, Clerico M, Boselli D, Contessa G, Ripellino P, et al. T-Helper 17 Cells Expand in Multiple Sclerosis and Are Inhibited by Interferon-Beta. *Ann Neurol* (2009) 65:499–509. doi: 10.1002/ana.21652
5. Kalra S, Lowndes C, Durant L, Strange RC, Al-Araji A, Hawkins CP, et al. Th17 Cells Increase in RRMS as Well as in SPMS, Whereas Various Other Phenotypes of Th17 Increase in RRMS Only. *Mult Scler J Exp Transl Clin* (2020) 6(1):2055217319899695. doi: 10.1177/2055217319899695
6. Annunziato F, Cosmi L, Santarlasci V, Maggi L, Liotta F, Mazzinghi B, et al. Phenotypic and Functional Features of Human Th17 Cells. *J Exp Med* (2007) 204(8):1849–61. doi: 10.1084/jem.20070663
7. Basdeo SA, Cluxton D, Sulaimani J, Moran B, Canavan M, Orr C, et al. Ex-Th17 (Nonclassical Th1) Cells Are Functionally Distinct From Classical Th1 and Th17 Cells and Are Not Constrained by Regulatory T Cells. *J Immunol* (2017) 198(6):2249–59. doi: 10.4049/jimmunol.1600737
8. Boniface K, Blumenschein WM, Brovont-Porth K, McGeachy MJ, Basham B, Desai B, et al. Human Th17 Cells Comprise Heterogeneous Subsets Including IFN-γ–Producing Cells With Distinct Properties From the Th1 Lineage. *J Immunol* (2010) 185(1):679–87. doi: 10.4049/jimmunol.1000366
9. Jones AP, Kermode AG, Lucas RM, Carroll WM, Nolan D, Hart PH. Circulating Immune Cells in Multiple Sclerosis. *Clin Exp Immunol* (2017) 187:193–203. doi: 10.1111/cei.12878
10. van Langelaar J, van der Vuurst de Vries RM, Janssen M, Wierenga-Wolf AF, Spilt IM, Siepman TA, et al. T Helper 17.1 Cells Associate With Multiple Sclerosis Disease Activity: Perspectives for Early Intervention. *Brain J Neurol* (2018) 141(5):1334–49. doi: 10.1093/brain/awy069
11. Kunkl M, Frascolla S, Amormino C, Volpe E, Tuosto L. T Helper Cells: The Modulators of Inflammation in Multiple Sclerosis. *Cells* (2020) 9(2):482. doi: 10.3390/cells9020482
12. Skulina C, Schmidt S, Dornmair K, Babbe H, Roers A, Rajewsky K, et al. Multiple Sclerosis: Brain-Infiltrating CD8+ T Cells Persist as Clonal Expansions in the Cerebrospinal Fluid and Blood. *Proc Natl Acad Sci USA* (2004) 101(8):2428–33. doi: 10.1073/pnas.0308689100
13. Huber M, Heink S, Grothe H, Guralnik A, Reinhard K, Elflein K, et al. A Th17-Like Developmental Process Leads to CD8(+) Tc17 Cells With Reduced Cytotoxic Activity. *Eur J Immunol* (2009) 39(7):1716–25. doi: 10.1002/eji.200939412
14. Salou M, Garcia A, Michel L, Gainche-Salmon A, Loussouarn D, Nicol B, et al. Expanded CD8 T-Cell Sharing Between Periphery and CNS in Multiple Sclerosis. *Ann Clin Transl Neurol* (2015) 2(6):609–22. doi: 10.1002/acn3.199
15. Annibali V, Ristori G, Angelini DF, Serafini B, Mechelli R, Cannoni S, et al. CD161(high)Cd8+T Cells Bear Pathogenetic Potential in Multiple Sclerosis. *Brain* (2011) 134(Pt 2):542–54. doi: 10.1093/brain/awq354
16. Salou M, Nicol B, Garcia A, Laplaud DA. Involvement of CD8(+) T Cells in Multiple Sclerosis. *Front Immunol* (2015) 6:604. doi: 10.3389/fimmu.2015.00604
17. Willing A, Jäger J, Reinhardt S, Kursawe N, Friese MA. Production of IL-17 by MAIT Cells Is Increased in Multiple Sclerosis and Is Associated With IL-7 Receptor Expression. *J Immunol* (2018) 200(3):974–82. doi: 10.4049/jimmunol.1701213
18. Beltrán E, Gerdes LA, Hansen J, Flierl-Hecht A, Krebs S, Blum H, et al. Early Adaptive Immune Activation Detected in Monozygotic Twins With Prodromal Multiple Sclerosis. *J Clin Invest* (2019) 129(11):4758–68. doi: 10.1172/JCI128475
19. Denic A, Wootla B, Rodriguez M. CD8(+) T Cells in Multiple Sclerosis. *Expert Opin Ther Targets* (2013) 17(9):1053–66. doi: 10.1517/14728222.2013.815726
20. Wagner CA, Roqué PJ, Goverman JM. Pathogenic T Cell Cytokines in Multiple Sclerosis. *J Exp Med* (2020) 217(1):e20190460. doi: 10.1084/jem.20190460
21. Tillery EE, Clements JN, Howard Z. What's New in Multiple Sclerosis? *Ment Health Clin* (2018) 7(5):213–20. doi: 10.9740/mhc.2017.09.213
22. Gajofatto A, Benedetti MD. Treatment Strategies for Multiple Sclerosis: When to Start, When to Change, When to Stop? *World J Clin Cases* (2015) 3(7):545–55. doi: 10.12998/wjcc.v3.i7.545
23. Wingerchuk DM, Weinshenker BG. Disease Modifying Therapies for Relapsing Multiple Sclerosis. *BMJ* (2016) 354:i3518. doi: 10.1136/bmj.i3518

24. Rammohan K, Coyle PK, Sylvester E, Galazka A, Dangond F, Grosso M, et al. The Development of Cladribine Tablets for the Treatment of Multiple Sclerosis: A Comprehensive Review. *Drugs* (2020) 80(18):1901–28. doi: 10.1007/s40265-020-01422-9
25. Schreiber K, Soelberg Sorensen P. Cladribine in the Treatment of Multiple Sclerosis. *Clin Invest* (2011) 1(2):317–26. doi: 10.4155/CLI.10.32
26. Baker D, Pryce G, Herrod SS, Schmierer K. Potential Mechanisms of Action Related to the Efficacy and Safety of Cladribine. *Mult Scler Relat Disord* (2019) 30:176–86. doi: 10.1016/j.msard.2019.02.018
27. Baker D, Herrod SS, Alvarez-Gonzalez C, Zalewski L, Albor C, Schmierer K. Both Cladribine and Alemtuzumab may Effect MS *via* B-Cell Depletion. *Neurol Neuroimmunol Neuroinflamm* (2017) 4(4):e360. doi: 10.1212/NXI.0000000000000360
28. Moser T, Akgün K, Proschmann U, Sellner J, Ziemssen T. The Role of TH17 Cells in Multiple Sclerosis: Therapeutic Implications. *Autoimmun Rev* (2020) 19(10):102647. doi: 10.1016/j.autrev.2020.102647
29. Leist TP, Comi G, Cree BA, Coyle PK, Freedman MS, Hartung HP, et al. Effect of Oral Cladribine on Time to Conversion to Clinically Definite Multiple Sclerosis in Patients With a First Demyelinating Event (ORACLE MS): A Phase 3 Randomised Trial. *Lancet Neurol* (2014) 13(3):257–67. doi: 10.1016/S1474-4422(14)70005-5
30. Şerban GM, Mănescu IB, Manu DR, Dobreanu M. Optimization of a Density Gradient Centrifugation Protocol for Isolation of Peripheral Blood Mononuclear Cells. *Acta Med Marisiensis* (2018) 64(2):83–90. doi: 10.2478/amma-2018-0011
31. Korsen M, Bragado Alonso S, Peix L, Bröker BM, Dressel A. Cladribine Exposure Results in a Sustained Modulation of the Cytokine Response in Human Peripheral Blood Mononuclear Cells. *PloS One* (2015) 10(6):e0129182. doi: 10.1371/journal.pone.0129182
32. Segal BM. The Diversity of Encephalitogenic CD4+ T Cells in Multiple Sclerosis and Its Animal Models. *J Clin Med* (2019) 8(1):120. doi: 10.3390/jcm8010120
33. Fergusson JR, Fleming VM, Klenerman P. CD161-Expressing Human T Cells. *Front Immunol* (2011) 2:36. doi: 10.3389/fimmu.2011.00036
34. Lock C, Hermans G, Pedotti R, Brendolan A, Schadt E, Garren H, et al. Gene-Microarray Analysis of Multiple Sclerosis Lesions Yields New Targets Validated in Autoimmune Encephalomyelitis. *Nat Med* (2002) 8(5):500–8. doi: 10.1038/nm0502-500
35. Tzartos JS, Friese MA, Craner MJ, Palace J, Newcombe J, Esiri MM, et al. Interleukin-17 Production in Central Nervous System-Infiltrating T Cells and Glial Cells Is Associated With Active Disease in Multiple Sclerosis. *Am J Pathol* (2008) 172(1):146–55. doi: 10.2353/ajpath.2008.070690
36. Groom JR, Luster AD. CXCR3 in T Cell Function. *Exp Cell Res* (2011) 317(5):620–31. doi: 10.1016/j.yexcr.2010.12.017
37. Restorick SM, Durant L, Kalra S, Hassan-Smith G, Rathbone E, Douglas MR, et al. CCR6+ Th Cells in the Cerebrospinal Fluid of Persons With Multiple Sclerosis are Dominated by Pathogenic Non-Classic Th1 Cells and GM-CSF-Only-Secreting Th Cells. *Brain Behav Immun* (2017) 64:71–9. doi: 10.1016/j.bbi.2017.03.008
38. Lee AYS, Körner H. The CCR6-CCL20 Axis in Humoral Immunity and T-B Cell Immunobiology. *Immunobiology* (2019) 224(3):449–54. doi: 10.1016/j.imbio.2019.01.005
39. Ross SH, Cantrell DA. Signaling and Function of Interleukin-2 in T Lymphocytes. *Annu Rev Immunol* (2018) 36:411–33. doi: 10.1146/annurev-immunol-042617-053352
40. Acquaviva M, Bassani C, Sarno N, Dalla Costa G, Romeo M, Sangalli F, et al. Loss of Circulating CD8+ CD161high T Cells in Primary Progressive Multiple Sclerosis. *Front Immunol* (2019) 10:1922. doi: 10.3389/fimmu.2019.01922
41. Hinks TSC, Zhang XW. MAIT Cell Activation and Functions. *Front Immunol* (2020) 11:1014. doi: 10.3389/fimmu.2020.01014
42. Giovannoni G, Soelberg Sorensen P, Cook S, Rammohan K, Rieckmann P, Comi G, et al. Safety and Efficacy of Cladribine Tablets in Patients With Relapsing Remitting Multiple Sclerosis: Results From the Randomized Extension Trial of the CLARITY Study. *Mult Scler* (2018) 24:1594–604. doi: 10.1177/1352458517727603
43. Giovannoni G, Comi G, Cook S, Rammohan K, Rieckmann P, Soelberg Sørensen P, et al. CLARITY Study Group. A Placebo-Controlled Trial of Oral Cladribine for Relapsing Multiple Sclerosis. *N Engl J Med* (2010) 362(5):416–26. doi: 10.1056/NEJMoa0902533
44. Thompson AJ, Baranzini SE, Geurts J, Hemmer B, Ciccarelli O. Multiple Sclerosis. *Lancet* (2018) 391(10130):1622–36. doi: 10.1016/S0140-6736(18)30481-1
45. Montalban X, Leist TP, Cohen BA, Moses H, Campbell J, Hicking C, et al. Cladribine Tablets Added to IFN-β in Active Relapsing MS: The ONWARD Study. *Neurol Neuroimmunol Neuroinflamm* (2018) 5(5):e477. doi: 10.1212/NXI.0000000000000477
46. Cook S, Leist T, Comi G, Montalban X, Giovannoni G, Nolting A, et al. Safety of Cladribine Tablets in the Treatment of Patients With Multiple Sclerosis: An Integrated Analysis. *Mult Scler Relat Disord* (2019) 29:157–67. doi: 10.1016/j.msard.2018.11.021
47. Patti F, Visconti A, Capacchione A, Roy S, Trojano MCLARINET-MS Study Group. Long-Term Effectiveness in Patients Previously Treated With Cladribine Tablets: A Real-World Analysis of the Italian Multiple Sclerosis Registry (CLARINET-Ms). *Ther Adv Neurol Disord* (2020) 13:1756286420922685. doi: 10.1177/1756286420922685
48. Lizak N, Hodgkinson S, Butler E, Lechner-Scott J, Slee M, McCombe PA, et al. Real-World Effectiveness of Cladribine for Australian Patients With Multiple Sclerosis: An MSBase Registry Substudy. *Mult Scler* (2021) 27(3):465–74. doi: 10.1177/1352458520921087
49. Moccia M, Lanzillo R, Petruzzo M, Nozzolillo A, De Angelis M, Carotenuto A, et al. Single-Center 8-Years Clinical Follow-Up of Cladribine-Treated Patients From Phase 2 and 3 Trials. *Front Neurol* (2020) 11:489. doi: 10.3389/fneur.2020.00489
50. Miravalle AA, Katz J, Robertson D, Hayward B, Harlow DE, Lebson LA, et al. CLICK-MS and MASTER-2 Phase IV Trial Design: Cladribine Tablets in Suboptimally Controlled Relapsing Multiple Sclerosis. *Neurodegener Dis Manage* (2021) 11(2):99–111. doi: 10.2217/nmt-2020-0059
51. Signori A, Saccà F, Lanzillo R, Maniscalco GT, Signoriello E, Repice AM, et al. Cladribine vs Other Drugs in MS: Merging Randomized Trial With Real-Life Data. *Neurol Neuroimmunol Neuroinflamm* (2020) 7(6):e878. doi: 10.1212/NXI.0000000000000878
52. Kalincik T, Jokubaitis V, Spelman T, Horakova D, Havrdova E, Trojano M, et al. MSBase Study Group. Cladribine Versus Fingolimod, Natalizumab and Interferon β for Multiple Sclerosis. *Mult Scler* (2018) 24(12):1617–26. doi: 10.1177/1352458517728812
53. Bartosik-Psujek H, Kaczyński Ł, Górecka M, Rolka M, Wójcik R, Zięba P, et al. Cladribine Tablets Versus Other Disease-Modifying Oral Drugs in Achieving No Evidence of Disease Activity (NEDA) in Multiple Sclerosis-A Systematic Review and Network Meta-Analysis. *Mult Scler Relat Disord* (2021) 49:102769. doi: 10.1016/j.msard.2021.102769
54. Siddiqui MK, Khurana IS, Budhia S, Hettle R, Harty G, Wong SL. Systematic Literature Review and Network Meta-Analysis of Cladribine Tablets Versus Alternative Disease-Modifying Treatments for Relapsing-Remitting Multiple Sclerosis. *Curr Med Res Opin* (2018) 34(8):1361–71. doi: 10.1080/03007995.2017.1407303
55. Pfeuffer S, Rolfes L, Hackert J, Kleinschnitz K, Ruck T, Wiendl H, et al. Effectiveness and Safety of Cladribine in MS: Real-World Experience From Two Tertiary Centres. *Mult Scler* (2021) 12:13524585211012227. doi: 10.1177/13524585211012227
56. Zanghì A, Gallo A, Avolio C, Capuano R, Lucchini M, Petracca M, et al. Exit Strategies in Natalizumab-Treated RRMS at High Risk of Progressive Multifocal Leukoencephalopathy: A Multicentre Comparison Study. *Neurotherapeutics* (2021) 18(2):1166–74. doi: 10.1007/s13311-021-01037-2
57. Olsen I, Sollid LM. Pitfalls in Determining the Cytokine Profile of Human T Cells. *J Immunol Methods* (2013) 390(1-2):106–12. doi: 10.1016/j.jim.2013.01.015
58. Moser T, Schwenker K, Seiberl M, Feige J, Akgun K, Haschke-Becher E, et al. Long-Term Peripheral Immune Cell Profiling Reveals Further Targets of Oral Cladribine in MS. *Ann Clin Transl Neurol* (2020) 7(11):2199–212. doi: 10.1002/acn3.51206
59. Stuve O, Soelberg Soerensen P, Leist T, Giovannoni G, Hyvert Y, Damian D, et al. Effects of Cladribine Tablets on Lymphocyte Subsets in Patients With Multiple Sclerosis: An Extended Analysis of Surface Markers. *Ther Adv Neurol Disord* (2019) 12:1756286419854986. doi: 10.1177/1756286419854986
60. Voo VTF, Butzkueven H, Stankovich J, O'Brien T, Monif M. The Development and Impact of Cladribine on Lymphoid and Myeloid Cells in Multiple Sclerosis. *Mult Scler Relat Disord* (2021) 52:102962. doi: 10.1016/j.msard.2021.102962

61. Comi G, Cook S, Giovannoni G, Rieckmann P, Sørensen PS, Vermersch P, et al. Effect of Cladribine Tablets on Lymphocyte Reduction and Repopulation Dynamics in Patients With Relapsing Multiple Sclerosis. *Mult Scler Relat Disord* (2019) 29:168–74. doi: 10.1016/j.msard.2019.01.038
62. Balasa R, Barcutean L, Balasa A, Motataianu A, Roman-Filip C, Manu D. The Action of TH17 Cells on Blood Brain Barrier in Multiple Sclerosis and Experimental Autoimmune Encephalomyelitis. *Hum Immunol* (2020) 81 (5):237–43. doi: 10.1016/j.humimm.2020.02.009

Conflict of Interest: The authors declare that the research was conducted in the absence of any commercial or financial relationships that could be construed as a potential conflict of interest.

frontiers in Immunology

ORIGINAL RESEARCH
published: 16 December 2021
doi: 10.3389/fimmu.2021.778204

Soluble Receptor Isoform of IFN-Beta (sIFNAR2) in Multiple Sclerosis Patients and Their Association With the Clinical Response to IFN-Beta Treatment

Pablo Aliaga-Gaspar[1,2†], Isaac Hurtado-Guerrero[1,3†], Nicolas Lundahl Ciano-Petersen[1,4], Patricia Urbaneja[1,4], Isabel Brichette-Mieg[1], Virginia Reyes[1,4], Jose Luis Rodriguez-Bada[1], Roberto Alvarez-Lafuente[5,6], Rafael Arroyo[7], Ester Quintana[6,8], Lluis Ramió-Torrentà[6,8,9,10], Ana Alonso[1,4], Laura Leyva[1,6], Oscar Fernández[11‡] and Begoña Oliver-Martos[1,4,6,12*‡]*

[1] Neuroimmunology and Neuroinflammation Group, Instituto de Investigación Biomédica de Málaga (IBIMA), Unidad de Gestión Clínica (UGC) Neurociencias, Hospital Regional Universitario de Málaga, Málaga, Spain, [2] Facultad de Medicina, Universidad de Málaga, Málaga, Spain, [3] Neuroinflammation Unit, Biotech Research and Innovation Centre (BRIC), Faculty of Health and Medical Sciences, Copenhagen Biocentre, University of Copenhagen, Copenhagen, Denmark, [4] Red Andaluza de Investigación Clínica y Traslacional en Neurología (Neuro-Reca), Málaga, Spain, [5] Grupo de Investigación de Factores Ambientales en Enfermedades Degenerativas, Instituto de Investigación Sanitaria del Hospital Clínico San Carlos (IdISSC), Madrid, Spain, [6] Red Española de Esclerosis Múltiple (REEM), Madrid, Spain, [7] Servicio de Neurología, Hospital Universitario Quirónsalud, Madrid, Spain, [8] Servicio de Neurología, Hospital Universitari de Girona Doctor Josep Trueta, Girona, Spain, [9] Girona Biomedical Research Institute (IDIBGI), Girona, Spain, [10] Medical Sciences Department, University of Girona, Girona, Spain, [11] Departmento de Farmacología, Facultad de Medicina, Universidad de Málaga, Málaga, Spain, [12] Departamento de Biología Celular, Genética y Fisiología, Área de Fisiología, Facultad de Ciencias, Universidad de Málaga, Málaga, Spain

Purpose: Interferon beta receptor 2 subunit (IFNAR2) can be produced as a transmembrane protein, but also as a soluble form (sIFNAR2) generated by alternative splicing or proteolytic cleavage, which has both agonist and antagonist activities for IFN-β. However, its role regarding the clinical response to IFN-β for relapsing-remitting multiple sclerosis (RRMS) is unknown. We aim to evaluate the *in vitro* short-term effects and after 6 and 12 months of IFN-β therapy on sIFNAR2 production and their association with the clinical response in MS patients.

Methods: Ninety-four RRMS patients were included and evaluated at baseline, 6 and 12 months from treatment onset. A subset of 41 patients were classified as responders and non-responders to IFN-β therapy. sIFNAR2 serum levels were measured by ELISA. mRNA expression for IFNAR1, IFNAR2 splice variants, MxA and proteases were assessed by RT-PCR. The short-term effect was evaluated in PBMC from RRMS patients after IFN-β stimulation *in vitro*.

Results: Protein and mRNA levels of sIFNAR2 increased after IFN-β treatment. According to the clinical response, only non-responders increased sIFNAR2 significantly at both protein and mRNA levels. sIFNAR2 gene expression correlated with the transmembrane isoform expression and was 2.3-fold higher. While MxA gene expression increased

OPEN ACCESS

Edited by:
Roberta Magliozzi,
University of Verona, Italy

Reviewed by:
Wakiro Sato,
National Center of Neurology and Psychiatry (Japan), Japan
Andreia Barroso,
IQVIA (Brazil), Brazil
Martina Severa,
National Institute of Health (ISS), Italy

***Correspondence:**
Begoña Oliver-Martos
begoliver@gmail.com
Oscar Fernández
oscar.fernandez.sspa@gmail.com

†These authors share first authorship

‡These authors share last authorship

Specialty section:
This article was submitted to Multiple Sclerosis and Neuroimmunology, a section of the journal Frontiers in Immunology

Received: *16 September 2021*
Accepted: *29 November 2021*
Published: *16 December 2021*

Citation:
Aliaga-Gaspar P, Hurtado-Guerrero I, Ciano-Petersen NL, Urbaneja P, Brichette-Mieg I, Reyes V, Rodriguez-Bada JL, Alvarez-Lafuente R, Arroyo R, Quintana E, Ramió-Torrentà L, Alonso A, Leyva L, Fernández O and Oliver-Martos B (2021) Soluble Receptor Isoform of IFN-Beta (sIFNAR2) in Multiple Sclerosis Patients and Their Association With the Clinical Response to IFN-Beta Treatment. Front. Immunol. 12:778204. doi: 10.3389/fimmu.2021.778204

significantly after treatment, IFNAR1 and IFNAR2 only slightly increased. After short-term IFN-β *in vitro* induction of PBMC, 6/7 patients increased the sIFNAR2 expression.

Conclusions: IFN-β administration induces the production of sIFNAR2 in RRMS and higher levels might be associated to the reduction of therapeutic response. Thus, levels of sIFNAR2 could be monitored to optimize an effective response to IFN-β therapy.

Keywords: alternative splicing, soluble receptors, IFNAR, interferon beta, multiple sclerosis

INTRODUCTION

Multiple sclerosis (MS) is the most prevalent chronic inflammatory autoimmune disease of the central nervous system, with a complex pathophysiology characterized by inflammation, demyelination, and axonal degeneration. Although in the last two decades the approval of several disease-modifying therapies have revolutionized the management of MS (1), IFN-β is still used as a first line therapeutic option because of benefit/risk profile and cost. A wide range of immunomodulatory effects have been associated to IFN-β, being able to reduce the antigen presentation, inhibit the proliferation of T cells, and shift cytokine production (2). However, despite the fact that this drug has been used for more than 25 years, its mechanism of action is not completely understood. It has been estimated that 20 to 50% of patients are non-responsive to the treatment (3), highlighting the need for biomarkers to predict treatment response.

Cytokine receptors are usually expressed by cells as transmembrane proteins, however, most of them are also secreted in soluble forms and can be detected in different human body fluids including the blood, the tears, the cerebrospinal fluid or the urine (4, 5). The generation of soluble receptors is an important mechanism by which the biological activity of cytokines is modulated due to their ability to bind them, acting as antagonists or agonists (6, 7), so that they can be used for therapeutic purposes (4).

There are two main mechanisms to generate soluble receptors: alternative splicing at the gene level and proteolytic cleavage at the protein level (8). On the one hand, alternative splicing is a mechanism to regulate gene expression that allows a single gene to code for multiple proteins isoforms and occurs in up to 94% of human genes (9). For instance, some isoforms of cytokine receptors generated by alternative splicing may lose the extracellular domain, which is subsequently secreted to the bloodstream (10). On the other hand, proteolytic cleavage of receptors on the cell surface is accomplished by a family of specialized enzymes called proteases, which result in the excision of the extracellular domain and its release into the bloodstream (11). Probably, the most important proteases in immunity and inflammation are metalloproteases of the ADAM family, notably ADAM17 (12, 13).

IFN-β is a cytokine that exerts its biological activity thought interaction with its cell surface receptor (IFNAR), which is composed of two functional subunits: IFNAR1 and IFNAR2, and the subsequent activation of the JAK-STAT signaling pathway (14). The IFNAR2 subunit has a soluble isoform (sIFNAR2) that can be generated by alternative splicing of the human IFNAR2 gene giving a transcript that lacks the transmembrane and cytoplasmic domain that was cloned in human and mouse (15, 16). Besides, the IFNAR2 subunit can be cleaved by specific proteases such as TNF-alpha converting enzyme (known as TACE or ADAMS) that releases the extracellular domain (17), as well as by presenilins (PSEN) that release the intracellular domain (18). As a result of both mechanisms, sIFNAR2 can be detected in body fluids (19) and has been found to be expressed at levels 10-fold higher than the transmembrane IFNAR2 transcripts in most mouse tissues (20).

Although type I interferon responses and their regulation are widely described in autoimmune diseases, including MS, the presence and action of the sIFNAR2 has not been explored, despite its ability of binding endogenous and exogenous IFN-β and modulating their activity (20–22). This capacity of modulate the IFN-β activity and its accessibility in serum makes sIFNAR2 an attractive target molecule to be considered in MS, due to the key role of endogenous IFN-β in the pathophysiology of MS and even more if we consider the use of exogenous IFN-β as a treatment. Accordingly, we previously demonstrated that untreated-MS patients had lower sIFNAR2 levels than healthy controls, patients with other inflammatory neurological diseases and MS patients treated with IFN-β, highlighting its value as a diagnostic biomarker for MS. Moreover, we proved that patients treated with IFN-β have higher circulating levels of sIFNAR2, in contrast to those treated with Glatiramer Acetate (GA) or Natalizumab (23).

Our aim was to assess the *in vitro* short-term effects and after 6 and 12 months of IFN-β treatment on the circulating sIFNAR2 levels and on the gene expression of the different IFNAR2 splice variants in MS patients, as well as their relation with the therapeutic response to IFN-β.

MATERIAL AND METHODS

Participant Centers and Subjects

Fifty-nine RRMS patients, defined according to the revised McDonald criteria (24) were recruited from the MS Unit at Malaga Regional Hospital (Malaga, Spain), before to start IFN-β treatment, and were followed at 6 and 12 months after IFN-β treatment onset (Cohort 1). Forty-one of them whose data of relapses, EDSS progression and MRI activity were available, were classified after one year of treatment as responders (R) or non-responders (NR) according to the Rio Score (25). Nineteen patients (46.35%) were considered non-responders according

to the occurrence of two or three positive variables during the first year of therapy (at least one relapse during the first year of therapy; an increase of at least one point in the EDSS score during the first year of therapy (confirmed at 6 months); three or more active lesions (either new or enlarging T2 lesions compared to baseline MRI scan or gadolinium-enhancing lesions) on the MRI performed after 1 year of therapy); the remaining twenty-two (53.65%) were considered responders.

An independent cohort including 25 MS patients from Dr. Josep Trueta University Hospital, Girona (Spain) and 10 MS patients from Hospital San Carlos, Madrid (Spain) was also analyzed at baseline and at 6 and 12 months after treatment onset for validation of the results (Cohort 2).

All participants in the study gave informed consent and the protocols were approved by the institutional ethical committee (Comité de Ética de la Investigación Málaga Nordeste. Project identification: DTS1800045).

Table 1

Sample Collection

For serum determinations, 3 ml of peripheral blood were collected in serum-separating tubes basally and after 6 and 12 months of treatment onset. For gene expression studies, peripheral blood samples were collected in EDTA tubes, only in patients from cohort 1. In all cases, the time elapsed between the administration of IFN-β and sampling was of at least 24 hours.

Samples were processed following standard procedures and frozen immediately after reception by the Malaga Hospital-IBIMA Biobank, as part of Andalusian Public Health System Biobank. PBMC were isolated using a ficoll-hypaque gradient, as described in the supplier's protocol (ICN Biomedicals Inc.). After that, cells were cryopreserved in RPMI-1640- 10% DMSO until use for RNA extraction.

Quantification of Soluble IFNAR2 by ELISA

sIFNAR2 levels were quantified with an ELISA previously developed and validated in our laboratory (26). First, a recombinant sIFNAR2 protein was cloned, expressed and purified and then used as standard curve in the ELISA (23, 26). Briefly, the plates were coated with 0.2-μg rabbit polyclonal anti-human IFNAR2 antibody (Abnova) overnight. After washing, the wells were blocked with a casein blocking buffer [2 hours, room temperature (RT)]. Then, 50 μL of each point of the standard curve or serum samples (diluted in half) were added to the wells in duplicate, and incubated for 1 hour. Mouse polyclonal anti-human IFNAR2 antibody (1 μg/mL in assay buffer; Abnova) was added and incubated (1 hour, RT). After washing again, 50-μL horseradish peroxidase (HRP)-conjugated goat anti-mouse IgG (H+L) adsorbed against human immunoglobulins was added and incubated (1 hour, RT). After three additional washes, 100 μL/well 3,3′,5,5′-tetramethylbenzidine (TMB) One Component HRP Microwell Substrate was added and incubated (10–15 minutes in the dark). Color development was done by adding 50 μL/well 1 N H2SO4. Optical density (OD) was measured at 450 nm in a VersaMax™ ELISA Microplate Reader (Molecular Devices)

Sample analysis. Each assay included a standard curve, two quality controls, and a negative control. sIFNAR2 concentration was calculated by OD interpolation from the samples and controls in the standard curve, that was established using a four-parameter curve fitting model by the SoftMax® Pro Software (Molecular Devices). Sample measurement was considered acceptable if the intra and inter assay coefficients of variation (CV) were <10% and <20% respectively (27). Here, the average of the intra and inter-assay CV was 3.6% and 13%, respectively.

Isolation of RNA and Quantitative Reverse Transcriptase-PCR

Total RNA was isolated from PBMC fromMS patients following the instructions of Aurum Total RNA Mini KIT (BioRad). RNA concentration and purity were analyzed in a NanoDrop 2000 Spectrophotometer. Total RNA (500 ng) was reverse-transcribed using the M-MLV retrotranscriptase (Sigma). Samples were run in the same reaction, and the resulting cDNA was controlled for purity and transcription efficiency on the NanoDrop.

RT² qPCR Primer Assay for Human IFNAR1, IFNAR2, MxA and PSEN 1 and 2 from Qiagen were used. Primers for ADAM17 and sIFNAR2 were designed with Primer3 (http://frodo.wi.mit.edu/primer3) and ordered to Isogen Life Science (**Supplementary Table 1**). For sIFNAR2 the design was carried out by taking into account that this isoform is the product of an alternative splicing, therefore, the primers must hybridize in a specific region, so that the

TABLE 1 | Clinical and demographic data.

	Cohort 1	Cohort 2	Responders†	Non responders†	P-value*
N	59	35	22	19	–
Female/Male	38/21	25/10	11/11	12/7	n.s.
EDSS score at baseline	1,08 ± 1,33	1,70 ± 0,87	0,97 ± 1,46	1,13 ± 1,21	0,039
IFN-β type (a)	12/7/32/2/0	4/22/8/0/3	4/0/18/0/0	4/4/10/1/0	–
EDSS score after one year of therapy	–	–	0,93 ± 1,48	1,71 ± 1,21	0,008
MRI activity (b)	–	–	13/1	8/3	<0,001
Number of relapses after one year of therapy	–	–	0 ± 0	1,26 ± 1,09	<0,001

(a) Treatment type: Avonex/Betaferon/Rebif/Extavia/Plegridy.

(b) MRI activity: Negative/Positive.

**P-values obtained by chi-square test (gender, MRI activity) or Mann-Whitney test.*

†From cohort 1.

n.s. (Non significant).

resulting amplified product is exclusive to this isoform (**Supplementary Figure 1**). RT-qPCR was performed in duplicate using iTaq Universal SYBR Green SMX (BioRad), and was run on a 7500 Fast Real-Time PCR System (Applied Biosystems). Relative expressions of genes were analysed by comparison of ΔΔCt values using GAPDH as raeference gene. MIQE Guidelines were considered for real time experiments (28).

Quantification of IFN-β in Serum by Luminex

IFN-β serum levels were assessed basally and after treatment using a customized Procartaplex Immunoassay (Thermo Fisher). 25 µL per well of antibody coupled beads and 50 µL per well of diluted patient serum were added into a 96 well plate and incubated overnight at 4°C. Each assay included a standard curve and all samples were performed in duplicate. Plates were processed following manufacturers' instructions and then read with a Bio-Plex® 200 system (Bio-Rad). The data obtained were processed with the Bioplex Manager 6.0 software (Bio-Rad) using a five-parameter curve fitting algorithm to analyse them.

Neutralizing Antibodies (NABs) Against IFN Beta by Cytopathic Effect Test (CPE Test)

Sera of IFNβ-treated patients were tested for the presence of NAbs against the three commercial forms of IFN-β (IFN-β 1a (Avonex, Biogen, Inc.), IFN-β 1b (Betaferon, Bayer Pharma AG) or IFN-β 1a (Rebif, Merck Serono Ltd) by a calibrated antiviral CPE test, as previously described by 29. Briefly, A549 cells were seeded in 96 well plates in 100 µl of DMEM medium supplemented with 2% FCS. After 24 h, serial dilutions of the patient sera were incubated for 1 h with IFN-β, and without IFN-β to control the presence of endogenous IFN-β in the patient serum. These dilutions were added to the A549 cell culture, seeded the day before. Each plate included a viral control which did not contain IFN-β, a cell control which did not contain virus, and a standard of IFN-β. After 24 h incubation, cells were infected with Encephalomyocarditis virus (EMCV) (except for the cell control). Twenty-four hours later, the cells were stained with crystal violet and the absorbance was read at 630 lambdas in a spectrophotometer. The neutralization titre was calculated according to 30 and expressed in 10-fold reduction units per millilitre (TRU/mL). Titres ≥20 TRU/mL were considered as positive.

Cell Cultures in the Presence of Recombinant IFN-β

PBMC isolated from 7 randomly untreated MS patients were thawed and suspended ($1x10^6$ cells mL-1) in pre-warmed RPMI-1640 medium, supplemented with 2 mM l-glutamine (MP Biomedicals, Irvine, CA, USA), 10% Fetal Bovine Serum (FBS) and 0.032 mg mL-1 gentamicin (Normon). Cells were washed by centrifugation and resuspended in RPMI-1640 complete medium with 2% FBS.

To evaluate the ability of recombinant IFN-β to induce the production of sIFNAR2, the cells were stimulated with 20 units/mL of IFN-β (Avonex) during 8 and 24 hours. A non-stimulated control was included each time. After that, the cells were collected for RNA extraction and cDNA conversion, as explained above. sIFNAR2, IFNAR2 and MxA were measured by real time PCR. MxA was considered as positive control since it is well known that its expression is clearly induced after IFN-β stimulation (31).

Statistical Analysis

As a non-normal distribution was established in the Kolmogorov–Smirnov test, non-parametric tests were used for comparison between groups. The results are expressed as median and interquartile ranges.

For each comparison, all groups were assigned equal sample sizes. The samples were not randomized, and untreated and treated samples were run in parallel in order to minimize the inter-assay variation. Wilcoxon Rank test (related samples analysis) was used to compare the variables (sIFNAR2, IFN-β and the gene expression of IFNAR1, IFNAR2 sIFNAR2, MxA and PSEN 1 and 2) before and after treatment.

To analyze the association or interdependence between the gene expression of IFN-β subunits and MxA, and between gene expression and protein levels, Spearman's Rho correlation analysis was used. Statistical significance was set at $p < 0.05$. Figures have been created with GraphPad Prism5 Software. *In vitro* results were represented using log10 for normalizing the data.

RESULTS

Serum Levels of Soluble IFNAR2 Increase With Long IFN-β Treatment

In the cohort 1, the first step was the confirmation that IFN-β treated patients increased circulating levels of IFN-β compared to the levels before the treatment onset (p=0.001) (**Figure 1**). Also, it was demonstrated that all the patients included were negative for NABs against the molecule of the IFN-β that were receiving.

Regarding sIFNAR2, we found increased levels at 6- and 12-months follow-up after IFN-β exposure compared to baseline levels, with significant differences at 6 months (p=0.008). This increase of sIFNAR2 levels was replicated in the cohort 2, being statistically significant at 6 months (p=0.0001) and at 12 months (p=0.0001).

Considering all the patients, serum sIFNAR2 levels were increased in 70.4% of the patients at 6 months of treatment and remained increased at 12 months in 60.3% of them. In **Supplementary Figure 2** the ΔsIFNAR2 has been represented for each patient.

Figure 1, **Table 2**

Serum Levels of Soluble IFNAR2 According to the IFN-β Response

Patients from cohort 1 whose data was available, were classified as responders (N=22) and non-responders (N=19) according to the Rio Score (25). In the follow-up study, responders maintained stable serum sIFNAR2 levels, however, non-responder patients showed a significant increase after 6 months of treatment (p=0.018), returning to baseline levels at 12 months.

Figure 2, **Table 3**

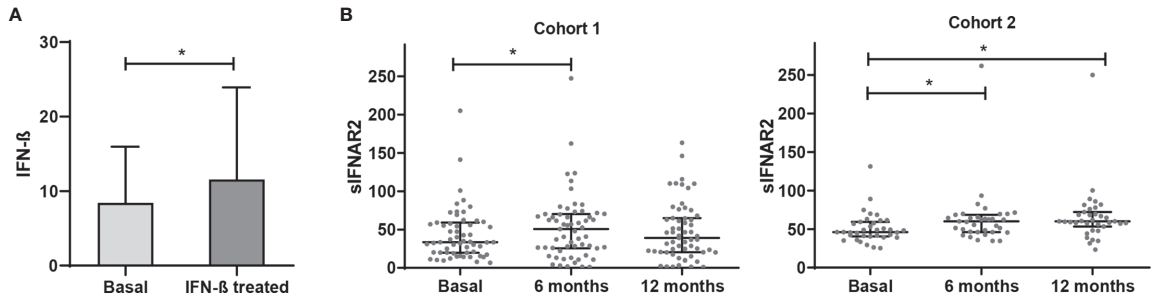

FIGURE 1 | IFN-β levels and longitudinal assessment of serum sIFNAR2 levels in MS patients. **(A)** Serum IFN-β levels measured in MS patients basally and after IFN-β therapy onset (N=59). Significant p-value is shown with asterisk. **(B)** Graphs comparing serum sIFNAR2 levels at baseline and after 6 and 12 months of IFN-β therapy onset in two independent cohorts (Cohort 1 N=59, Cohort 2 N=35). Each point represents an individual, and horizontal bars indicate the median values and interquartile ranges. Significant p-values are shown with asterisk.

sIFNAR2 Gene Expression Increases With IFN- β Treatment

Forty-one MS patients from cohort 1, who had available PBMC samples at baseline and after 6 of months of treatment onset, were included for the gene expression study of IFNAR1, the transmembrane and soluble transcripts of IFNAR2, and MxA gene. Although there was an increase in IFNAR1 and IFNAR2 gene expression after IFN-β treatment, those changes did not reach statistical significance. However, the expression of sIFNAR2 transcript and MxA gene were significantly increased after IFN-β treatment (p=0.017 and p<0.001 respectively).

Figure 3

IFNAR2 Splice Variants Under IFN-β Treatment

Transmembrane IFNAR2 and sIFNAR2 are products of an alternative splicing of IFNAR2 gene. The primer design carried out allowed the quantification of both splice variants independently. A strong positive correlation between the gene expression levels of IFNAR2 and sIFNAR2 before (r=0.636 p< 0.001) and after the IFN-β treatment (r=0.749 p<0.001) was observed.

Interestingly, the expression of sIFNAR2 was significantly greater compared to the transmembrane isoform before (1.35 vs 3.17; p<0.001) and after IFN-β treatment (1.65 vs 4.98 p<0.001).

Figure 4

IFNAR2 Splice Variants According to the IFN-β Response

The gene expression data of IFNAR1, IFNAR2, sIFNAR2 and MxA have been represented using a heat map (**Figure 5**). Comparison between responders and non-responders, showed no differences in the expression of any of the genes at baseline and after 6 months of therapy (A). The comparison between baseline and that after 6-month of therapy in both groups of patients (B) showed an increase more accentuated in responders after treatment, but there were not statistical differences in IFNAR1 and IFNAR2 gene expression. However, MxA expression increased significantly after treatment independently of the therapeutic response (p<0.001 and p=0.006, in responders and non-responders, respectively) and sIFNAR2 also increased in both groups of patients although significance was reached only in non-responders (p=0.020).

Figure 5

TABLE 2 | Serum sIFNAR2 levels in MS patients.

Cohort 1/Cohort 2	Basal	6 Months	12 Months
N	59/35	59/35	59/35
25% Percentile	19,59/40,44	25,61/45,94	20,41/53,3
Median	33,43/46,01	50,6/60,04	38,97/59,97
75% Percentile	59,16/59,44	70,16/68,44	65/72,15

Induction of Proteases by IFN-β

In order to evaluate the ability of IFN-β to induce the expression of proteases that have been described to cleave the transmembrane IFNAR2 subunit, the expression of ADAM17 and PSEN 1 and 2 have been measured at baseline and after 6 months of IFN-β therapy in patients of cohort 1. There was no increase in the expression of ADAM17 and PSEN 2 after treatment, however there was a significant increase in the expression of PSEN 1 (p=0.041).

Figure 6

sIFNAR2 Gene Expression Increases After Short-Term IFN-β Induction *In Vitro*

PBMC isolated from seven untreated MS patients were cultured to demonstrate the short-term induction of sIFNAR2 by IFN-β. MxA was also measured as positive control since it is well known to be induced by IFN-β (31). As expected, its expression was significantly increased after 8 hours of IFN-β induction (p=0.043). There was no change in the expression of sIFNAR2 after 8 hours of IFN-β induction, however all patients increased their sIFNAR2 expression after 24 h of induction (p=0.043), with the exception of one of them.

Figure 7

DISCUSSION

The treatment landscape has changed in MS over the past two decades and, currently, many drugs are approved for RRMS (32). Most of the recent drugs target specific molecules as a result of a

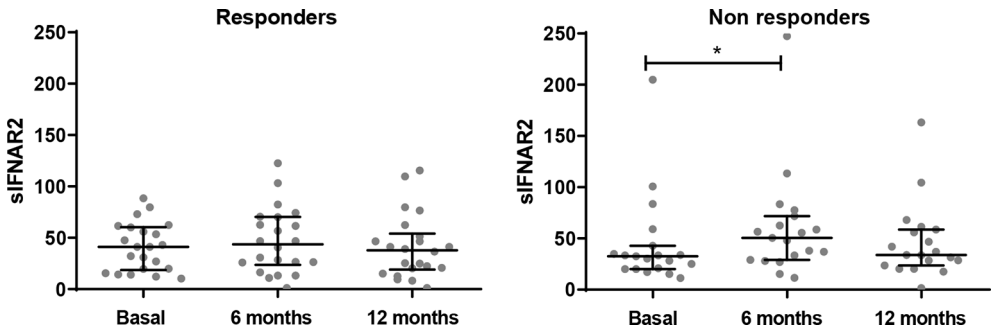

FIGURE 2 | Longitudinal assessment of serum sIFNAR2 levels in responder and non-responder patients. Graphs comparing serum sIFNAR2 levels at baseline and after 6 and 12 months of IFN-β therapy onset in responder (N=22) and non-responder patients (N=19). Each point represents an individual, and horizontal bars indicate the median values and interquartile ranges. Significant p-values are shown with asterisk.

better knowledge of the pathophysiology of the disease and have a rational drug design. However, IFN-β preparations have no clearly defined mechanisms of action despite being the first approved drug by the US Food and Drug Administration (FDA) for the treatment of MS in 1993, and continue being a first line treatment for MS. IFN-β plays an important role in the regulation of the immune system and has a wide range of immunomodulatory effects, but how these effects translate into the beneficial therapeutic effect in MS is still not understood. However, IFN-β can also have adverse effects (injection site reactions, nausea, headaches, fever, leukopenia, and other more serious although rare) (33); therefore, biomarkers to predict treatment response could avoid these undesirable side effects in patients that may not benefit of the treatment. Alternative splicing is a mechanism for regulating gene expression that allows a single gene to code for multiple protein isoforms. It occurs in up to 94% of human genes and the isoforms generated may have related, distinct or even opposing functions (9). Many relevant genes of the immune system have been shown to undergo alternative splicing, although the knowledge of how this mechanism may regulate the immune system are still limited (7). Nevertheless, an altered RNA of genes mediating immune signaling pathways has been repeatedly implicated in MS pathogenesis (34).

sIFNAR2 is able to bind circulating IFN-β and modulate its activity, as it may have agonist or antagonist properties (20). However, its role in the immune system is mostly unknown, despite that the human form was first cloned in 1995 (15). Therefore, we cloned a recombinant form analogous to human soluble IFNAR2 and recently demonstrated that it exerts antiviral, immunomodulatory and antiproliferative activities without IFN-β mediation (35). Regarding the native form, we developed an ELISA to detect sIFNAR2 in serum that was analytically validated (26). This ELISA uses a double antigen recognition and detects sIFNAR2 generated by both mechanisms, alternative splicing and proteolysis (26). Moreover, we observed that sIFNAR2 increased significantly in IFN-β-treated patients during the first year of therapy, in contrast to GA and natalizumab-treated patients (23). Herein, we assessed in depth the ability of IFN-β treatment to induce the production of sIFNAR2 and its potential relationship with the heterogeneity of the clinical response in MS patients treated with IFN-β.

TABLE 3 | Serum sIFNAR2 levels in MS patients according to IFN beta response.

Responders/Non-responders	Basal	6 Months	12 Months
N	22/19	22/19	22/19
25% Percentile	16,52/20,19	18,8/28,99	16,5/23,64
Median	37,61/32,58	35,58/50,6	30,91/33,83
75% Percentile	61,2/42,71	70,38/71,7	59,62/58,72

First, we analyzed the sIFNAR2 serum levels in a follow up study of two independent cohorts of MS patients and observed an increase of sIFNAR2 levels after 6 months of IFN-β administration in both cohorts. As aforementioned, IFN-β is able to bind either their membrane-bound receptors or their soluble counterparts (20), consequently, the action of the IFN-β could ultimately depend on the relative abundance of each isoform. Although there are soluble receptors that enhance the effect of their ligand, the majority of the known soluble cytokine receptors has antagonistic functions (4), which could explain that non-responder patients increased significantly sIFNAR2 levels at 6 months, in contrast to responder patients, who showed a non-significant increase. Interestingly, a study published in 1999 suggested that high serum levels of soluble sIFNAR2 suppressed the effectiveness of IFN therapy in patients with chronic hepatitis C (36). Both studies suggest an antagonist effect of sIFNAR2 at high levels that could have important implications if the IFN-β activities are neutralized, as previously described *in vitro* by *Mckenna et al.* (21). However, it should be considered that an opposite effect could be reached at low concentrations (21), being proposed as an important agonist of endogenous IFN actions in pathophysiological processes like septic shock (22). Beyond these studies, there are no recent research focused on the sIFNAR2/IFN-β relationship, which would be necessary for the optimization of the IFN-β treatment given the agonist and antagonist properties of sIFNAR2.

Regarding the gene expression follow-up study, the functional subunits of the receptor, IFNAR1 and IFNAR2, showed a slight increase after IFN-β therapy, while MxA increased significantly its expression, as expected. sIFNAR2 gene expression behaved similar to MxA, being significantly induced after treatment with

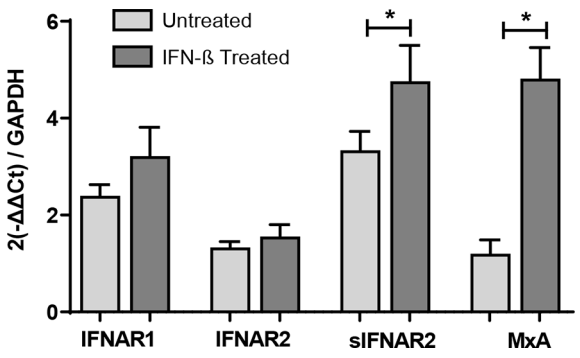

FIGURE 3 | Longitudinal assessment of IFNAR1, IFNAR2, sIFNAR2 and MxA gene expression. RNA relative expression of IFNAR1, IFNAR2, sIFNAR2 and MxA in PBMC from MS patients before and after 6 months of IFN-β therapy onset (N=41), assessed by real time-PCR using GAPDH as raeference gene. Significant p-values are shown with asterisk.

IFN-β. This up-regulation in the levels of sIFNAR2 over the first year of therapy was previously described by Gilli et al. in MS patients that were negative for neutralizing antibodies. According to the IFN-β clinical response, responder and non-responder patients increased sIFNAR2 after treatment but only non-responders reached statistical significance, in line to which was observed at protein levels. It has been described that non-responders had an activated type I IFN system in peripheral blood cells that was refractory to exogenous IFN-β (37). The elevated levels of circulating sIFNAR2 found in our study, acting as an antagonist to IFN-β, could be a plausible explanation of that absence of response observed in non-responders, but this has to be further studied.

As the transmembrane IFNAR2 and sIFNAR2 are products of an alternative splicing, we further analyzed the relationship between both spliced variants with the treatment. The relative expression of the transmembrane protein and its soluble counterpart showed a strong positive correlation, which was not modified by the IFN-β treatment. It should be highlighted that the expression of the sIFNAR2 was 2.3-fold higher compared to the transmembrane isoform before and after IFN-β therapy. The greater abundance of the mRNA transcript for the soluble isoform than for the transmembrane one was previously described in mouse tissues, where both transcripts were expressed ubiquitously and the ratio soluble:transmembrane IFNAR varied from 10:1 in the liver and other organs, to 1:1 in tissues involved in hematopoiesis, suggesting that both receptor isoforms should be regulated independently (20). However, a comprehensive study of human sIFNAR2 mRNA expression in normal tissue is still lacking, and hence there is limited information on normal relative expression levels.

As aforementioned, in addition to the alternative splicing, the soluble receptors of cytokines can also be generated by proteolytic cleavage. Cell membrane proteins undergo this cleavage at the cell surface, resulting in the release of a significant portion of their extracellular domain (11). ADAM17, proteolytically cleaves many substrates including the IFNAR2 receptor (17, 18). This led us to think that the serum levels of sIFNAR2 detected in MS patients after one year of IFN-β exposure could be the result of both alternative splicing but also importantly of proteolytic cleavage (or shedding). However, we did not find any induction of ADAM17 after IFN-β administration which suggests that serum sIFNAR2 was most probably the product of alternative splicing of the IFNAR2 gene rather than a proteolytically cleaved product of IFNAR2, in concordance with data observed in mouse (38). Regarding the presenilins, it has been described that they release the intracellular domain of IFNAR2 (18), although it is not clear whether this cleavage leads also to the release of the extracellular domain. We have found a significant increase in the expression of PSEN 1 in MS patients after IFN-β treatment, but its implication on the release of the intracellular domain of IFNAR2 is unknown and should be further studied.

We finally determined whether *in vitro* short-term IFN-β induction modified the sIFNAR2 gene expression in PBMC from MS patients. Increased expression of MxA after the short-term IFN-β induction was observed and considered as the positive control of the experiment. No changes were observed after 8 hours of IFN-β administration in the expression of sIFNAR2, but a significant increase was observed at 24 hours. This upregulation of sIFNAR2 mRNA was previously described in the murine cell line L929 after induction with type I and II IFN (38). Herein, we

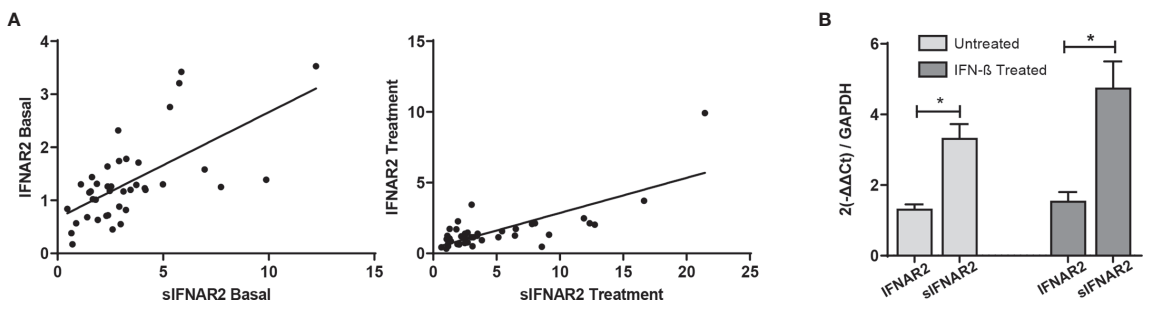

FIGURE 4 | IFNAR2 splice variants under IFN-β treatment. **(A)** Correlation analysis between the transmembrane (IFNAR2) and soluble (sIFNAR2) transcripts before (r=0.636 p< 0.001) and after 6 months of IFN-β therapy onset (r=0.749 p<0.001). **(B)** Comparison of the relative expression of IFNAR2 versus sIFNAR2 before and after 6 months of IFN-β therapy onset, using GAPDH as a raeference gene (N=41). Significant p-values are shown with asterisk.

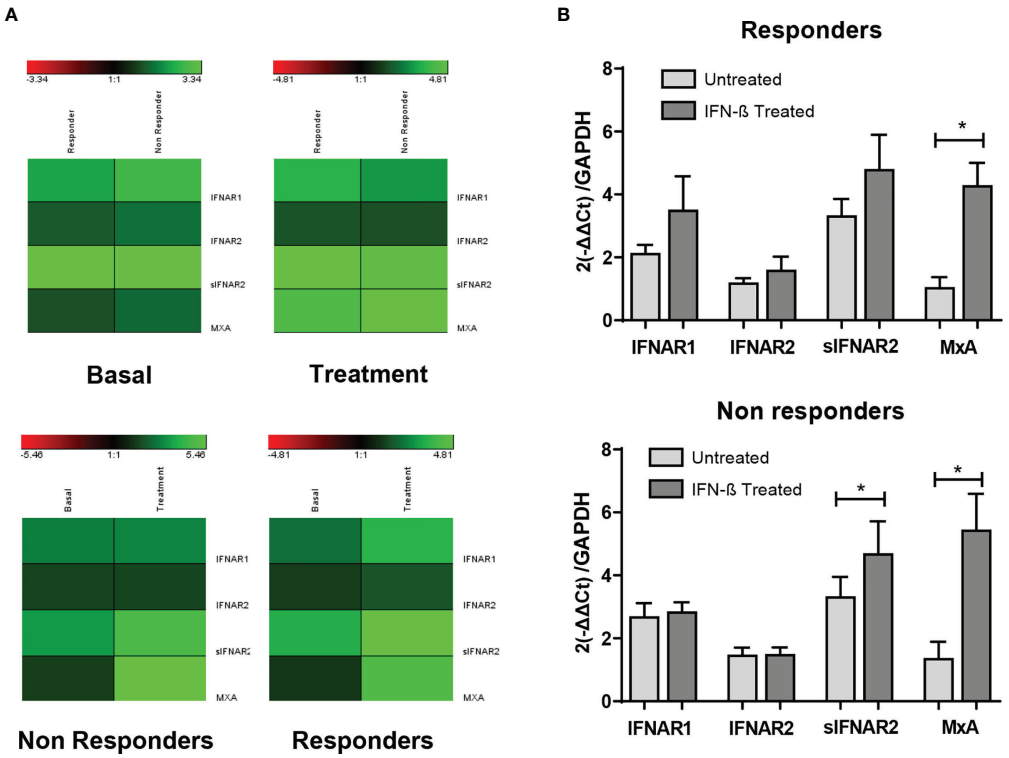

FIGURE 5 | Longitudinal assessment of IFNAR1, IFNAR2, sIFNAR2 and MxA gene expression in responder and non-responder patients. **(A)** Heat map representing the gene expression data of IFNAR1, IFNAR2, sIFNAR2, and MxA between responder and non-responder patients, at baseline and 6 months after the onset of IFN-β therapy. Unchanged proteins are displayed in black, up-regulated proteins are displayed in green while the down-regulated proteins are depicted in red. **(B)** Bar chart representing the gene expression for responders (N=22) and non-responders (N=19) using GAPDH as raeference gene. Significant p-values are shown with asterisk.

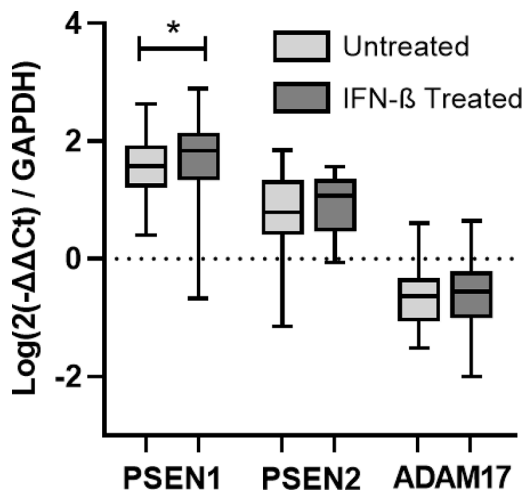

FIGURE 6 | Longitudinal assessment of PSEN1, PSEN2, and ADAM17 gene expression. RNA relative expression of PSEN1, PSEN2, and ADAM17 in PBMC from MS patients before and after 6 months of IFN-β treatment onset (N=41), assessed by real time-PCR using GAPDH as raeference gene. Significant p-values are shown with an asterisk. Logarithms are used to normalize and scale data for representation.

describe for the first time the up-regulation of sIFNAR2 mRNA in human PBMC, which could have important implications for IFN-β treatment optimization, due to the fact that it can act as an agonist or antagonist depending on its circulating levels.

Beyond MS, IFN-β is a pleiotropic cytokine, collectively having roles in both innate and adaptive immune responses. Thereby the function of IFNβ-sIFNAR2 mediated regulatory mechanisms could also exerts an important role in other diseases characterized by a dysregulation of the interferon pathway, named interferonopathies (39), although the complete functionality of sIFNAR2 in type I IFN signal transduction requires further elucidation.

A limitation of the study is that it is not possible to know if the absence of clinical response to IFN-β is the cause or the consequence of the up-regulation of sIFNAR2, so further studies including patients during the relapse and in remission are warranted. Also, it would necessary to carry out a replication study in a large cohort of responders and non-responders to confirm its use as biomarker of response. If confirmed, sIFNAR2 would be an easy ideal biomarker to implement in clinical practice because its determination is made by ELISA, which is a widely used technique in clinical laboratories, it requires a non-invasive method for the sample extraction and it is cost-effective.

In conclusion, our study demonstrates the induction of sIFNAR2 (protein and mRNA) by IFN-β administration,

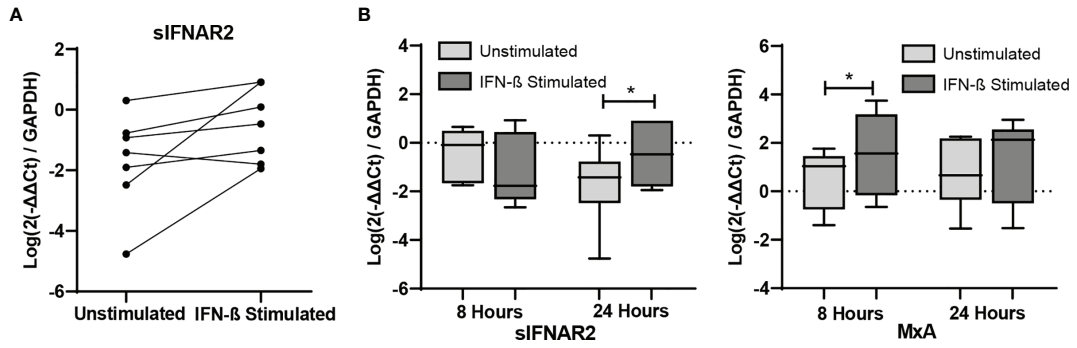

FIGURE 7 | *In vitro* study of IFNAR1, IFNAR2, sIFNAR2 and MxA gene expression. Representation of RNA relative expression of IFNAR1, IFNAR2, sIFNAR2 and MxA in PBMC from untreated MS patients cultured with or without IFN-β stimulus (N=7) during 8 and 24 hours. **(A)** sIFNAR2 expression in PBMC from each patient after 24 hours of culture in the presence or in the absence of IFN-β. **(B)** Boxplots comparing sIFNAR2 and MxA expression in unstimulated PBMC and IFN-β-stimulated PBMC during 8 and 24 hours of culture. Significant p values are marked with an asterisk. Logarithms are used to normalize and scale data for representation.

probably by inducing alternative splicing, which at higher levels it might be related to the reduction or absence of therapeutic response to IFN-β treatment. IFN-β activity should be tightly regulated and sIFNAR2 levels could open a new dimension for optimizing this treatment and give another opportunity for improved therapeutic interventions.

DATA AVAILABILITY STATEMENT

The raw data supporting the conclusions of this article will be made available by the authors, without undue reservation.

ETHICS STATEMENT

The studies involving human participants were reviewed and approved by Comité de Ética de la Investigación Málaga Nordeste. The patients/participants provided their written informed consent to participate in this study.

AUTHOR CONTRIBUTIONS

Conceptualization, BO-M and OF. Funding acquisition, BO-M. Methodology and data acquisition, PA-G, IH-G, JR-B, and I-BM. Patients' recruitment, NC-P, PU, VR, AA, RA, and LR-T. Data analysis, BO-M, PA-G, and IH-G. Writing – original draft, BO-M, IH-G, and PA-G. Writing –review and editing, OF, LL, RA-L, and EQ. All authors contributed to the article and approved the submitted version.

FUNDING

This research was funded by grants from the Instituto de Salud Carlos III and co-funded by European Regional Development Fund (ERDF), Technological Development Project in health DTS/1800045 to BO-M. BO-M holds a contract from Red Andaluza de Investigacion Clínica y Traslacional en Neurología (Neuro-reca) (RIC-0111-2019). PA-G is supported by Promoción de Empleo Joven e Implantación de la Garantía Juvenil 2018 (PEJ2018-002719-A). JR-B is supported by grants from Red Temática de Investigación Cooperativa, Red Española de Esclerosis Multiple REEM (RD16/0015/0010). LL holds a Nicolás Monardes research contract (RC-002-2019) from the Andalusian Ministry of Health and Family. IB-M holds a pFIS contract (FI19/00139) from the Spanish Science and Innovation Ministry.

SUPPLEMENTARY MATERIAL

The Supplementary Material for this article can be found online at: https://www.frontiersin.org/articles/10.3389/fimmu.2021.778204/full#supplementary-material

REFERENCES

1. Reich DS, Lucchinetti CF, Calabresi PA. Multiple Sclerosis. Edited by Dan L. Longo. *New Engl J Med* (2018) 378(2):169–80. doi: 10.1056/NEJMra1401483
2. Markowitz CE. Interferon-Beta: Mechanism of Action and Dosing Issues. *Neurology* (2007) 68(24 SUPPL. 4):8–11. doi: 10.1212/01.wnl.0000277703.74115.d2
3. Martínez-Aguilar L, Pérez-Ramírez C, Maldonado-Montoro MDM, Carrasco-Campos MI, Membrive-Jiménez C, Martínez-Martínez F, et al. Effect of Genetic Polymorphisms on Therapeutic Response in Multiple Sclerosis Relapsing-Remitting Patients Treated With Interferon-Beta. *Mutat Res* (2020) 785(July):108322. doi: 10.1016/J.MRREV.2020.108322
4. Lokau J, Garbers C. Biological Functions and Therapeutic Opportunities of Soluble Cytokine Receptors. *Cytokine Growth Factor Rev Elsevier Ltd* (2020) 55:94–108. doi: 10.1016/j.cytogfr.2020.04.003
5. Novick D, Rubinstein M. The Tale of Soluble Receptors and Binding Proteins: From Bench to Bedside. *Cytokine Growth Factor Rev* (2007) 18(5–6):525–33. doi: 10.1016/j.cytogfr.2007.06.024
6. Levine SJ. Molecular Mechanisms of Soluble Cytokine Receptor Generation. *J Biol Chem J Biol Chem* (2008) 283:14177–81. doi: 10.1074/jbc.R700052200

7. Lynch KW. Consequences of Regulated Pre-MRNA Splicing in the Immune System. *Nat Rev Immunol Nat Rev Immunol* (2004) 4:931–40. doi: 10.1038/nri1497
8. Rose-John S, Heinrich PC. Soluble Receptors for Cytokines and Growth Factors: Generation and Biological Function. *Biochem J Portland Press Ltd* (1994) 300:281–90. doi: 10.1042/bj3000281
9. Wang ET, Sandberg R, Luo S, Khrebtukova I, Zhang L, Mayr C, et al. Alternative Isoform Regulation in Human Tissue Transcriptomes. *Nature* (2008) 456(7221):470–76. doi: 10.1038/nature07509
10. Evsyukova I, Somarelli JA, Gregory SG, Garcia-Blanco MA. Alternative Splicing in Multiple Sclerosis and Other Autoimmune Diseases. *RNA Biol Taylor Francis Inc* (2010) 7:462–73. doi: 10.4161/rna.7.4.12301
11. Klein T, Eckhard U, Dufour A, Solis N, Overall CM. Proteolytic Cleavage - Mechanisms, Function, and 'Omic' Approaches for a Near-Ubiquitous Posttranslational Modification. *Chem Rev Am Chem Soc* (2018) 118:1137–68. doi: 10.1021/acs.chemrev.7b00120
12. Düsterhöft S, Lokau J, Garbers C. The Metalloprotease ADAM17 in Inflammation and Cancer. *Pathol Res Pract Elsevier GmbH* (2019) 215:152410. doi: 10.1016/j.prp.2019.04.002
13. Lambrecht BN, Vanderkerken M, Hammad H. The Emerging Role of ADAM Metalloproteinases in Immunity. *Nat Rev Immunol Nat Publish Group* (2018) 18:745–58. doi: 10.1038/s41577-018-0068-5
14. Uzé G, Schreiber G, Piehler J, Pellegrini S. The Receptor of the Type I Interferon Family. *Curr Topics Microbiol Immunol Springer Verlag* (2007) 316:71–95. doi: 10.1007/978-3-540-71329-6_5
15. Novick D, Cohen B, Tal N, Rubinstein M. Soluble and Membrane-Anchored Forms of the Human IFN-α/β Receptor. *In J Leukocyte Biol* (1995) 57:712–18. doi: 10.1002/jlb.57.5.712. Federation of American Societies for Experimental Biology.
16. Owczarek CM, Hwang SY, Holland KA, Gulluyan LM, Tavaria M, Weaver B, et al. Cloning and Characterization of Soluble and Transmembrane Isoforms of a Novel Component of the Murine Type I Interferon Receptor, IFNAR 2. *J Biol Chem* (1997) 272(38):23865–70. doi: 10.1074/jbc.272.38.23865
17. Pioli PD, Saleh AMZ, el Fiky A, Nastiuk KL, Krolewski JJ. Sequential Proteolytic Processing of an Interferon-Alpha Receptor Subunit by TNF-Alpha Converting Enzyme and Presenilins. *J Interferon Cytokine Res* (2012) 32(7):312–25. doi: 10.1089/jir.2011.0116
18. Saleh AZM, Fang AT, Arch AE, Neupane D, el Fiky A, Krolewski JJ. Regulated Proteolysis of the IFNaR2 Subunit of the Interferon-Alpha Receptor. *Oncogene* (2004) 23(42):7076–86. doi: 10.1038/sj.onc.1207955
19. Novick D, Cohen B, Rubinstein M. Soluble Interferon-α Receptor Molecules Are Present in Body Fluids. *FEBS Lett* (1992) 314(3):445–48. doi: 10.1016/0014-5793(92)81523-O
20. Hardy MP, Owczarek CM, Trajanovska S, Liu X, Kola I, Hertzog PJ. The Soluble Murine Type I Interferon Receptor Ifnar-2 Is Present in Serum, Is Independently Regulated, and Has Both Agonistic and Antagonistic Properties. *Blood* (2001) 97(2):473–82. doi: 10.1182/blood.V97.2.473
21. McKenna SD, Vergilis K, Arulanandam ARN, Weiser WY, Nabioullin R, Tepper MA. Formation of Human IFN-β Complex With the Soluble Type I Interferon Receptor IFNAR-2 Leads to Enhanced IFN Stability, Pharmacokinetics, and Antitumor Activity in Xenografted SCID Mice. *J Interferon Cytokine Res* (2004) 24(2):119–29. doi: 10.1089/107999004322813363
22. Samarajiwa SA, Mangan NE, Hardy MP, Najdovska M, Dubach D, Braniff S-J, et al. Soluble IFN Receptor Potentiates *In Vivo* Type I IFN Signaling and Exacerbates TLR4-Mediated Septic Shock. *J Immunol* (2014) 192(9):4425–35. doi: 10.4049/jimmunol.1302388
23. Órpez-Zafra T, Pavía J, Hurtado-Guerrero I, Pinto-Medel MJ, Luis Rodriguez Bada J, Urbaneja P, et al. Decreased Soluble IFN-β Receptor (SIFNAR2) in Multiple Sclerosis Patients: A Potential Serum Diagnostic Biomarker. *Multiple Sclerosis (Houndmills Basingstoke England)* (2017) 23(7):937–45. doi: 10.1177/1352458516667564
24. Polman CH, Reingold SC, Banwell B, Clanet M, Cohen JA, Filippi M, et al. Diagnostic Criteria for Multiple Sclerosis: 2010 Revisions to the McDonald Criteria. *Ann Neurol* (2011) 69(2):292–302. doi: 10.1002/ana.22366
25. Río J, Castilló J, Rovira A, Tintoré M, Sastre-Garriga J, Horga A, et al. Measures in the First Year of Therapy Predict the Response to Interferon β in MS. *Multiple Sclerosis* (2009) 15(7):848–53. doi: 10.1177/1352458509104591
26. Órpez-Zafra T, Paviá J, Pinto-Medel MJ, Hurtado-Guerrero I, Rodriguez-Bada JL, Martín Montañez E, et al. Development and Validation of an ELISA for Quantification of Soluble IFN-β Receptor: Assessment in Multiple Sclerosis. *Bioanalysis* (2015) 7(22):2869–80. doi: 10.4155/bio.15.208
27. Valentin MA, Ma S, Zhao A, Legay F, Avrameas A. Validation of Immunoassay for Protein Biomarkers: Bioanalytical Study Plan Implementation to Support Pre-Clinical and Clinical Studies. *J Pharm Biomed Anal* (2011) 55(5):869–77. doi: 10.1016/j.jpba.2011.03.033
28. Bustin SA, Benes V, Garson JA, Hellemans J, Huggett J, Kubista M, et al. The MIQE Guidelines: Minimum Information for Publication of Quantitative Real-Time PCR Experiments. *Clin Chem* (2009) 55(4):611–22. doi: 10.1373/clinchem.2008.112797
29. Oliver B, Órpez T, Mayorga C, Pinto-Medel MJ, Leyva L, López-Gómez C, et al. Neutralizing Antibodies Against IFN Beta in Patients With Multiple Sclerosis: A Comparative Study of Two Cytopathic Effect Tests (CPE) for Their Detection. *J Immunol Methods* (2009) 351(1–2):41–5. doi: 10.1016/J.JIM.2009.09.005
30. Kawade Y, Finter N, Grossberg SE. Neutralization of the Biological Activity of Cytokines and Other Protein Effectors by Antibody: Theoretical Formulation of Antibody Titration Curves in Relation to Antibody Affinity. *J Immunol Methods* (2003) 278(1–2):127–44. doi: 10.1016/S0022-1759(03)00203-5
31. Saber MA, Okasha H, Khorshed F, Samir S. A Novel Cell-Based *In Vitro* Assay for Antiviral Activity of Interferons α, β, and γ by QPCR of MxA Gene Expression. *Recent Patents Biotechnol* (2020) 15(1):67–75. doi: 10.2174/1872083146662011210505 3
32. Rommer PS, Zettl UK. Managing the Side Effects of Multiple Sclerosis Therapy: Pharmacotherapy Options for Patients. *Expert Opin Pharmacother Taylor Francis Ltd* (2018) 19:483–98. doi: 10.1080/14656566.2018.1446944
33. Calabresi PA, Kieseier BC, Arnold DL, Balcer LJ, Boyko A, Pelletier J, et al. Pegylated Interferon Beta-1a for Relapsing-Remitting Multiple Sclerosis (ADVANCE): A Randomised, Phase 3, Double-Blind Study. *Lancet Neurol* (2014) 13(7):657–65. doi: 10.1016/S1474-4422(14)70068-7
34. Hecker M, Rüge A, Putscher E, Boxberger N, Stefan Rommer P, Fitzner B, et al. Aberrant Expression of Alternative Splicing Variants in Multiple Sclerosis – A Systematic Review. *Autoimmun Rev Elsevier BV* (2019) 18:721–32. doi: 10.1016/j.autrev.2019.05.010
35. Hurtado-Guerrero I, Hernáez B, Pinto-Medel MJ, Calonge E, Rodriguez-Bada JL, Urbaneja P, et al. Antiviral, Immunomodulatory and Antiproliferative Activities of Recombinant Soluble IFNAR2 Without IFN-ß Mediation. *J Clin Med* (2020) 9(4):959. doi: 10.3390/jcm9040959
36. Mizukoshi E, Kaneko S, Kaji K, Terasaki S, Matsushita E, Muraguchi M, et al. Serum Levels of Soluble Interferon Alfa/Beta Receptor as an Inhibitory Factor of Interferon in the Patients With Chronic Hepatitis C. *Hepatology* (1999) 30(5):1325–31. doi: 10.1002/hep.510300516
37. Comabella M, Lünemann JD, Río J, Sánchez A, López C, Julià E, et al. A Type I Interferon Signature in Monocytes Is Associated With Poor Response to Interferon-Beta in Multiple Sclerosis. *Brain: A J Neurol* (2009) 132(Pt 12):3353–65. doi: 10.1093/BRAIN/AWP228
38. Hardy MP, Hertzog PJ, Owczarek CM. Multiple Regions Within the Promoter of the Murine Ifnar-2 Gene Confer Basal and Inducible Expression. *Biochem J* (2002) 365(2):355–67. doi: 10.1042/BJ20020105
39. Lee-Kirsch MA. The Type I Interferonopathies. *Annu Rev Med* (2017) 68(January):297–315. doi: 10.1146/ANNUREV-MED-050715-104506

Conflict of Interest: The authors declare that the research was conducted in the absence of any commercial or financial relationships that could be construed as a potential conflict of interest.

frontiers in Immunology

ORIGINAL RESEARCH
published: 13 January 2022
doi: 10.3389/fimmu.2021.770402

Tim-3 Relieves Experimental Autoimmune Encephalomyelitis by Suppressing MHC-II

Lili Tang[1†], Ge Li[1†], Yang Zheng[2], Chunmei Hou[1], Yang Gao[1], Ying Hao[1], Zhenfang Gao[1], Rongliang Mo[1], Yuxiang Li[1], Beifen Shen[1], Renxi Wang[4], Zhiding Wang[1,3*] and Gencheng Han[1*]*

[1] Beijing Institute of Basic Medical Sciences, Beijing, China, [2] Department of Oncology, First Hospital, Jilin University, Changchun, China, [3] Department of Hematology and Oncology, International Cancer Center, Shenzhen Key Laboratory of Precision Medicine for Hematological Malignancies, Shenzhen University General Hospital, Shenzhen University Clinical Medical Academy, Shenzhen University Health Science Center, Shenzhen, China, [4] Beijing Institute of Brain Disorders, Laboratory of Brain Disorders, Ministry of Science and Technology, Collaborative Innovation Center for Brain Disorders, Capital Medical University, Beijing, China

OPEN ACCESS

Edited by:
Roberta Magliozzi,
University of Verona, Italy

Reviewed by:
Alice Mariottini,
University of Florence, Italy
Annamaria Nigro,
San Raffaele Hospital (IRCCS), Italy
Mehdi Djelloul,
Karolinska Institutet (KI), Sweden

***Correspondence:**
Zhiding Wang
wzdfjfn@126.com
Gencheng Han
genchenghan@163.com
Renxi Wang
renxi_wang@ccmu.edu.cn

[†]These authors have contributed equally to this work

Specialty section:
This article was submitted to Multiple Sclerosis and Neuroimmunology, a section of the journal Frontiers in Immunology

Received: 03 September 2021
Accepted: 14 December 2021
Published: 13 January 2022

Citation:
Tang L, Li G, Zheng Y, Hou C, Gao Y, Hao Y, Gao Z, Mo R, Li Y, Shen B, Wang R, Wang Z and Han G (2022) Tim-3 Relieves Experimental Autoimmune Encephalomyelitis by Suppressing MHC-II. Front. Immunol. 12:770402. doi: 10.3389/fimmu.2021.770402

Tim-3, an immune checkpoint inhibitor, is widely expressed on the immune cells and contributes to immune tolerance. However, the mechanisms by which Tim-3 induces immune tolerance remain to be determined. Major histocompatibility complex II (MHC-II) plays a key role in antigen presentation and $CD4^+$T cell activation. Dysregulated expressions of Tim-3 and MHC-II are associated with the pathogenesis of many autoimmune diseases including multiple sclerosis. Here we demonstrated that, by suppressing MHC-II expression in macrophages *via* the STAT1/CIITA pathway, Tim-3 inhibits MHC-II-mediated autoantigen presentation and $CD4^+$T cell activation. As a result, overexpression or blockade of Tim-3 signaling in mice with experimental autoimmune encephalomyelitis (EAE) inhibited or increased MHC-II expression respectively and finally altered clinical outcomes. We thus identified a new mechanism by which Tim-3 induces immune tolerance *in vivo* and regulating the Tim-3-MHC-II signaling pathway is expected to provide a new solution for multiple sclerosis treatment.

Keywords: TIM-3, MHC-II, CIITA, EAE, antigen presentation, multiple sclerosis, T cell, macrophage

INTRODUCTION

T cell immunoglobulin mucin domain 3 (Tim-3) is widely expressed on the surface of many immune cells including T cells and macrophages (1, 2). As an immune checkpoint inhibitor, Tim-3 contributes to immune tolerance by inducing T cell apoptosis or by suppressing the activation of innate immune cells (1, 3). Deregulated upregulation of Tim-3 has been associated with many tumors or chronic infectious diseases, while dysregulated downregulation or dysfunction of Tim-3 leads to many kinds of autoimmune diseases such as multiple sclerosis (4) and rheumatoid arthritis (4–6). Recently, our findings and other reports showed that Tim-3 may control T cell response indirectly *via* regulating the function of innate immune cells (1, 3, 7). However, the mechanism by which Tim-3 mediates immune tolerance, especially innate immune tolerance, remains largely unclear.

MHC-II is expressed on many innate immune cells especially on professional antigen-presenting cells such as macrophages or dendritic cells. Following activation, MHC-II is upregulated and mediates antigen presentation and T cell activation. Unfortunately, dysregulated expression or variations of MHC-II lead to many immune disorders such as multiple sclerosis (8, 9). Investigations on the mechanisms by which MHC-II is regulated under different physiopathological conditions may provide useful solutions for many immune disorders. Multiple sclerosis (MS) is an autoimmune demyelinating and neurodegenerative disease of the central nervous system and the leading cause of non-traumatic neurological disability in young adults. Current therapeutic options for progressive multiple sclerosis remain comparatively disappointing and challenging.

The innate immune system is the first line of defense against antigens, and the adaptive immune system takes over by the innate immune system presentation of the antigens. Macrophages and microglia are important components of the innate immune system. They participate in the primary response to microorganisms and play a role in inflammatory responses, homeostasis, and tissue regeneration. In the initial phase of MS and EAE (an animal model of MS), macrophages from peripheral tissues infiltrate into the CNS and, together with residential microglia, contribute to the pathogenesis of MS. Strategies that target innate immune cells to prevent or treat immune disorders have shown therapeutical potential (10). Preventing multiple sclerosis by controlling the activity of macrophages/microglia may provide an alternative strategy.

Currently, it is found that the MHC-II molecule is the related gene for multiple sclerosis (11, 12). The expression of MHC-II is regulated by MHC class II transactivator (CIITA) (13). By reducing the MHC-II expression or blocking the MHC-II–peptide complex interaction on $CD4^+$T cells, the multiple sclerosis progression can be significantly alleviated (14, 15). These data suggested that MHC-II may act as a therapeutic target for immune disorders such as multiple sclerosis. However, how MHC-II is regulated during different physiopathological conditions remains to be determined.

Here using cell-based, molecular biology and *in vivo* approaches, we identified a new way of MHC-II regulation; that is, by suppressing CIITA expression, Tim-3 inhibits MHC-II expression in macrophages and then downregulates the presentation of autoantigen MOG to $CD4^+$T cells, finally leading to immune tolerance in mice with experimental autoimmune encephalomyelitis.

RESULTS

Tim-3 Inhibits MHC-II Expression in Macrophages/Monocytes

In our previous studies, we demonstrated that Tim-3 inhibits the activity of the phagocytosis (16) and MHC-I antigen presentation (7) of macrophages. There is great interest to keep on investigating whether Tim-3 inhibits other antigen presentation functions in macrophages and other immune functions. MHC-II expression was increased by anti-Tim-3 antibody inhibition in mouse macrophage cell line RAW264.7 (**Figure 1A**). Tim-3 was also knocked down by siRNA in RAW264.7, whose results (**Figure 1B**) showed that MHC-II expression was increased by Tim-3 knockdown. To test this further, the peritoneal macrophages of wild-type C57BL/6 mice (WT) mice, Tim-3-KO, and Tim-3-TG mice were extracted and analyzed. The MHC-II expression in Tim-3-KO mice was increased in macrophages compared with WT mice (**Figure 1C**), and MHC-II expression was decreased in macrophages from Tim-3-TG mice compared with WT mice (**Figure 1D**). WT mice were intraperitoneally injected with anti-Tim-3 antibody or control antibody, and peritoneal macrophages were harvested after 48 h. The MHC-II expression was increased after anti-Tim-3 antibody inhibition (**Figure 1E**). In addition, the expression of MHC-II on Tim-3 transgenic HEK-293T cells was decreased at both the mRNA and protein levels (**Figure 1F**). To find out whether Tim-3 also inhibited MHC-II expression on human monocytes/macrophages, Tim-3 and HLA-DR mRNA expression data from the GEO dataset (GSE34151) (7, 17) were collected. The 67 healthy individual samples were analyzed and showed an inverse correlation ($r = -0.2458$, $p = 0.0450$) between the expression of Tim-3 and MHC-II (HLA-DR) in CD14+ monocytes/macrophages (**Figure 1G**). These results suggest that Tim-3 signaling inhibited MHC-II expression not only in mouse macrophages but also in human macrophages.

Tim-3 Inhibits CIITA Expression in Macrophages

Tim-3 signaling inhibited MHC-II expression, but how Tim-3 inhibits MHC-II is still unclear. CIITA is the transcription factor of MHC-II (13), and Tim-3 may also inhibit the CIITA expression. To test the hypothesis, the Tim-3 function to CIITA was explored. CIITA expression was increased by anti-Tim-3 antibody inhibition in RAW264.7 (**Figure 2A**). Tim-3 was also knocked down by siRNA, whose results (**Figure 2B**) showed that CIITA expression was increased. To test this further, the peritoneal macrophages of WT, Tim-3-KO, and Tim-3-TG mice were extracted and analyzed. The CIITA expression in Tim-3-KO mice was increased in macrophages compared with WT mice (**Figure 2C**), and CIITA expression was decreased in macrophages from Tim-3-TG mice compared with WT mice (**Figure 2D**). The CIITA expression was increased after anti-Tim-3 antibody inhibition in mice (**Figure 2E**). These results suggest that Tim-3 signaling inhibited CIITA expression in macrophages.

Tim-3 Signaling Inhibits MHC-II Expression Through CIITA in Macrophages

After determining the inhibitory effects of Tim-3 on CIITA, we examined whether Tim-3 inhibits MHC-II expression through CIITA. To test this hypothesis, we silenced CIITA in RAW264.7 cells by siRNA (**Figure 2F**). Knockdown of CIITA led to decreased MHC-II mRNA and protein expression, which cannot be reversed by Tim-3 antibody blockage in RAW264.7 (**Figure 2G**). In addition, the dual-luciferase reporter assay

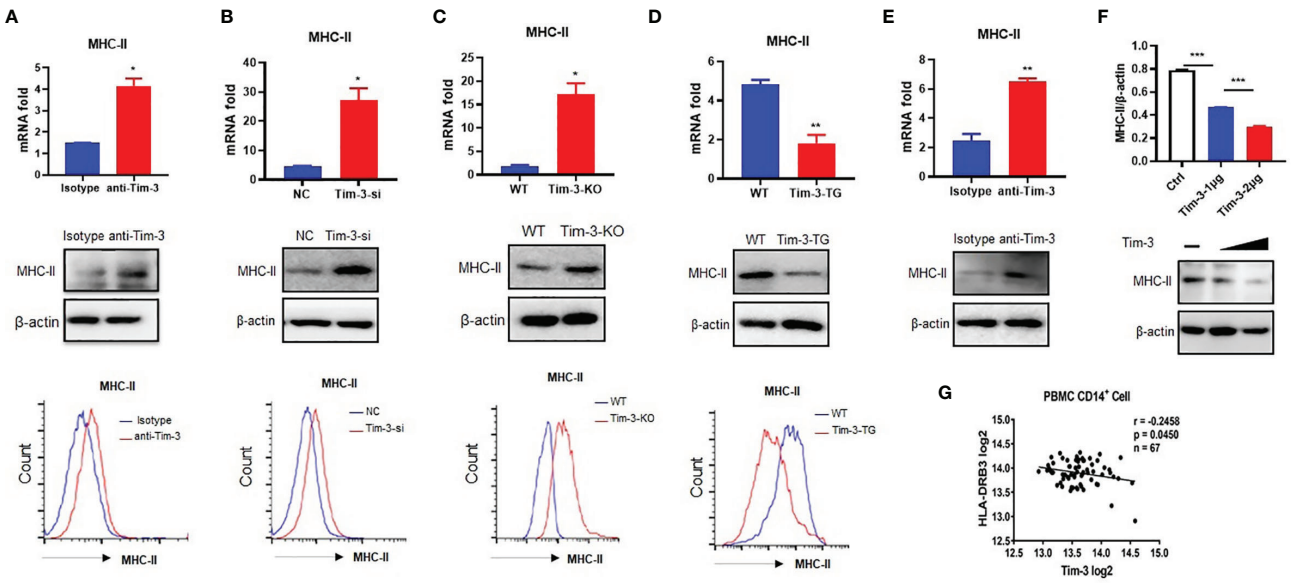

FIGURE 1 | Tim-3 inhibits MHC-II expression in macrophages. **(A)** The MHC-II expression of RAW264.7 cells cocultured with anti-Tim-3 antibody (20 μg/ml) or isotype antibody for 24 h (upper, mean ± SD, n = 3). **(B)** Tim-3 knockdown (Tim-3-si) RAW264.7 cells and (negative control, NC) RAW264.7 cells (upper, mean ± SD, n = 3). **(C)** The peritoneal macrophages from Tim-3 knockout mice (Tim-3-KO) and WT mice (upper, mean ± SD, n = 6). **(D)** The peritoneal macrophages from Tim-3 transgenic (Tim-3-TG) mice and wild-type (WT) mice. The MHC-II expression was detected by cytometry, Western blot, and RT-PCR (mean ± SD, n = 6). **(E)** WT mice were treated with anti-Tim-3 antibody or isotype antibody (10 mg/kg) by intraperitoneal injection at 0 and 24 h, and peritoneal macrophages were collected at 48 h to detect MHC-II protein and gene levels (mean ± SD, n = 6). **(F)** 1 and 2 μg of Tim-3 plasmid and 2 μg of vector plasmid were transferred into HEK-293T cells, respectively, and MHC-II protein level was detected at 48 h. **(G)** The expression data of Tim-3 and MHC-II in CD14+ monocytes/macrophages from 67 healthy individuals were collected from the GEO dataset (GSE34151), and their correlation was analyzed (*$p < 0.05$; **$p < 0.01$; ***$p < 0.001$).

revealed that CIITA-induced upregulation of MHC-II in HEK-293T cells could be reversed when Tim-3 was co-transfected (**Figure 2H**). These results showed that Tim-3 signaling inhibits MHC-II expression in macrophages through CIITA.

STAT1 Acts as a Signaling Adaptor for Tim-3-Mediated Suppression on the CIITA-MHC-II Pathway

We previously found that STAT1 helps Tim-3 to transduce signal (7). The STAT1-CIITA signaling pathway is involved in the regulation of MHC-II transcription (18–20). To test whether Tim-3 inhibits CIITA expression *via* STAT1, we first examined the Tim-3 and STAT1 signal to CIITA. The results showed that the expression of CIITA mRNA in RAW264.7 cells increased after Tim-3 antibody blockage, which could be reversed by the STAT1 inhibitor fludarabine (**Figure 3A**). CIITA and MHC-II mRNA increased after STAT1 transgenetic overexpression and reversed by Tim-3 co-overexpression (**Figure 3B**). Furthermore, the CIITA and MHC-II expression in protein level can be reversed by Tim-3 co-overexpression (**Figure 3C**). These results showed that Tim-3 signaling inhibits MHC-II expression in macrophages through STAT1-CIITA.

Tim-3 Inhibits MHC-II and Ameliorates the EAE Mouse Model

To study whether Tim-3 inhibits the macrophage MHC-II expression and antigen presentation *in vivo*, the EAE model was constructed on wild-type (WT) or Tim-3-TG C57BL/6 mice. The dynamic development and progression of EAE were monitored for the disease scores and body weights. MHC-II and CIITA expression was decreased in EAE mice macrophages from Tim-3-TG mice compared with WT mice (**Figures 4A, B**). CD4+ T cells in the Tim-3-TG group differentiate fewer IFN-γ+CD4+ T (Th1) cells and IL17+CD4+ T (Th17) cells, with more Foxp3+CD4+ T (Treg) cells (**Figure 4C**). Tim-3-TG significantly reduced the development and severity of EAE by disease score and weight loss, with less inflammatory cell infiltration and demyelination lesions in white matter by H&E and LFB staining (**Figures 4D, E**). These data indicated Tim-3 can attenuate the development and progression of EAE in mice.

CIITA and MHC-II expression in peritoneal macrophages of EAE mice was upregulated in the Tim-3 blockage group (**Figures 5A, B**). CD4+ T cells in the anti-Tim-3 group differentiate more IFN-γ+CD4+ T (Th1) cells and IL17+CD4+ T (Th17) cells, with few Foxp3+CD4+ T (Treg) cells (**Figure 5C**). After Tim-3 signaling blockage, the severity of EAE is significantly developed by disease score and weight loss (**Figure 5D**). H&E and LFB staining showed that inflammatory cell infiltration and demyelination lesions in white matter were significantly increased in the Tim-3 blockage group (**Figure 5E**). The data indicated that Tim-3 blockage exacerbated the development and progression of EAE in mice.

These data indicate that Tim-3 could inhibit MHC-II expression, which decreased macrophage antigen presentation

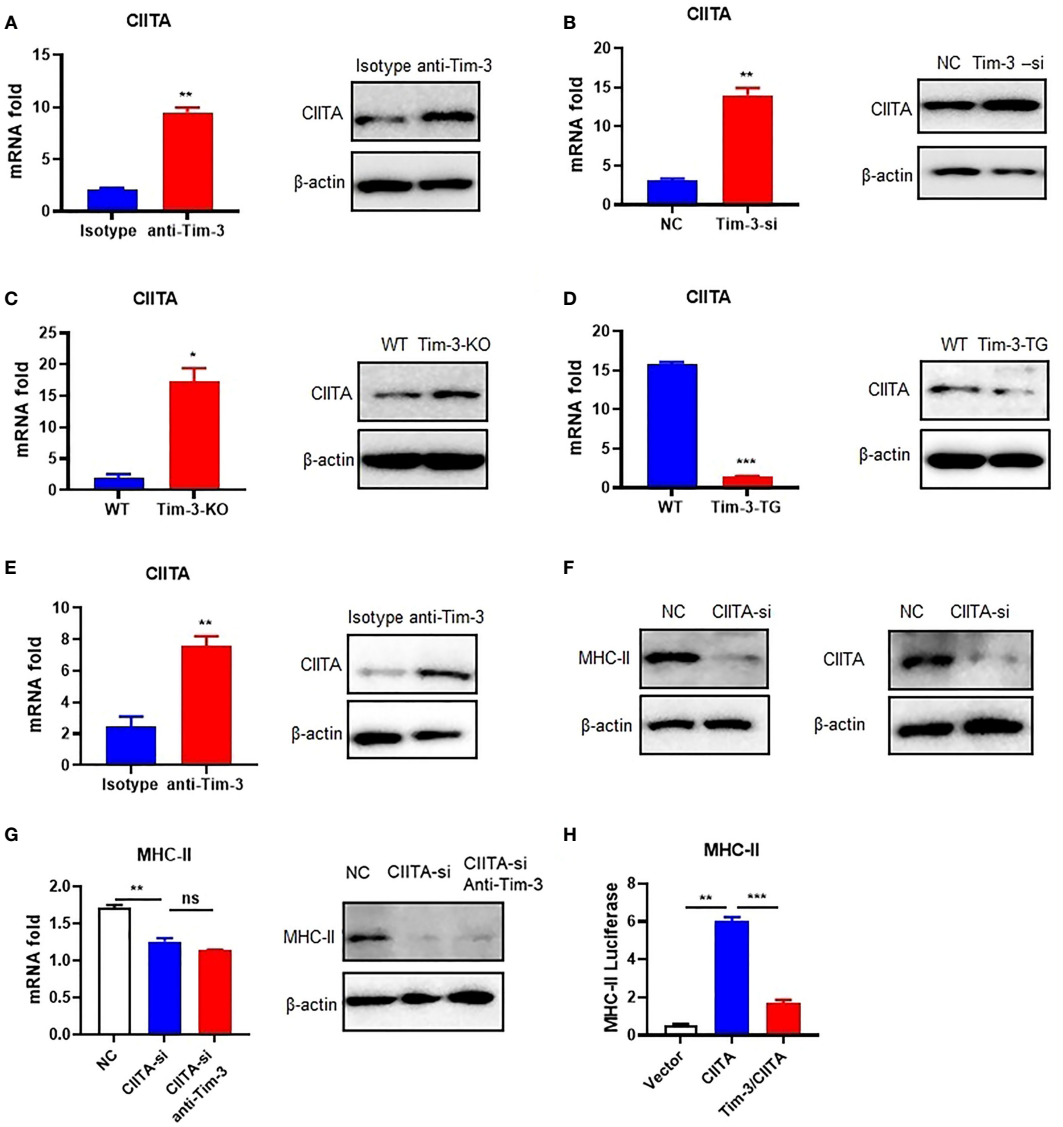

FIGURE 2 | Tim-3 signaling inhibits MHC-II expression through CIITA in macrophages. **(A)** The CIITA expression of RAW264.7 cells cocultured with anti-Tim-3 antibody (20 μg/ml) or isotype antibody for 24 h (left, mean ± SD, n = 3). **(B)** Tim-3-si RAW264.7 cells and RAW264.7 cells (left, mean ± SD, n = 3). **(C)** The peritoneal macrophages from Tim-3-KO and WT mice. The CIITA expression was detected by Western blot and RT-PCR (mean ± SD, n = 6). **(D)** The peritoneal macrophages from Tim-3-TG mice and WT mice (left, mean ± SD, n = 6). **(E)** WT mice were treated with anti-Tim-3 antibody or isotype antibody (10 mg/kg) by intraperitoneal injection at 0 and 24 h, and peritoneal macrophages were collected at 48 h to detect CIITA protein and gene levels (mean ± SD, n = 6). **(F)** siRNA-CIITA was transfection with RAW264.7 cells; CIITA and MHC-II expression was detected by Western blot at 48 h. **(G)** siRNA-CIITA was transfection with RAW264.7 cells cocultured with or without anti-Tim-3 antibody, and MHC-II expression was detected by RT-PCR (mean ± SD, n = 3) and Western blot at 48 h. **(H)** HEK-293T cells were transferred into pGL3-MHC-II reporter plasmid and CIITA plasmid, with or without Tim-3 plasmid for 48 h. Dual-fluorescence was analyzed (mean ± SD, n = 3). (*$p < 0.05$; **$p < 0.01$; ***$p < 0.001$). ns, Not Significant.

and stimulation to CD4+ T cells with increased anti-inflammatory Treg and decreased pro-inflammatory Th1 and Th17 CD4+ T cells. Tim-3 can relieve EAE mouse spinal cord demyelination and improve clinical scores by inhibiting MHC-II expression and CD4+ T cell stimulation.

MHC-II plays a critical role in antigen presentation and CD4+ T cell activation. To verify if Tim-3 regulates the MHC-II antigen presentation function and control, anti-Tim-3 antibody was added to peritoneal macrophages and incubated with the MOG35-55 peptide for MHC-II presentation. Then, mouse spleen cells were added to the macrophages with or without anti-MHC-II antibody blockage. The result is analyzed by FACS, which showed that Tim-3 signal blockage could decrease anti-inflammatory Treg (**Figure 6C**) and increased pro-inflammatory Th1 (**Figure 6B**) and Th17 CD4+ T (**Figure 6A**) cells through MHC-II presentation. The spleen cells were also had more proliferation by inhibiting the Tim-3 signal through MHC-II presentation (**Figure 6D**). The results

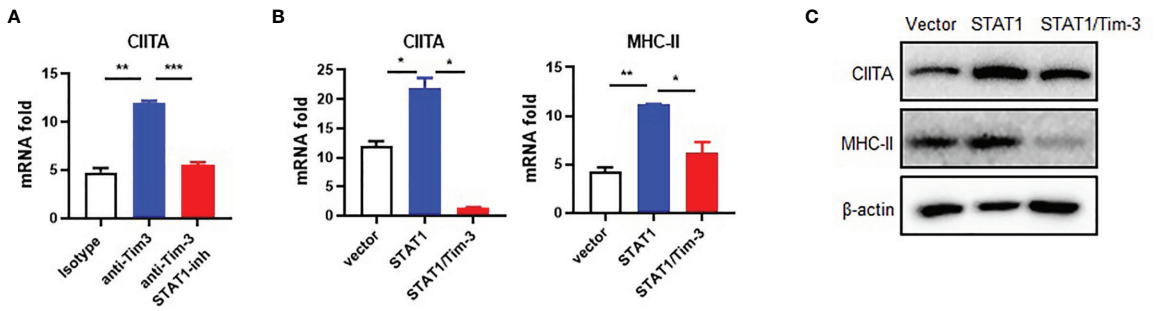

FIGURE 3 | Tim-3 signaling inhibits CIITA expression through STAT1 in macrophages. **(A)** RAW264.7 cells were incubated with 20 μg/ml anti-Tim-3 antibody or control antibody for 24 h in the presence of the STAT1 inhibitor fludarabine (10 μM) or dimethyl sulfoxide control and then were collected, and CIITA mRNA levels were examined by RT-PCR (mean ± SD, n = 3). **(B)** HEK-293T cells were transfected with STAT1 plasmid, with or without Tim-3 plasmid for 48 h, and the mRNA levels of CIITA (mean ± SD, n = 3) and MHC-II (mean ± SD, n = 3) were detected. **(C)** HEK-293T cells were transfected with STAT1 plasmid, with or without Tim-3 plasmid and lysed, and the protein levels of CIITA and MHC-II were analyzed at 48 h (*p < 0.05; **p < 0.01; ***p < 0.001).

showed that Tim-3 can inhibit macrophage MHC-II antigen presentation to CD4+ T cells *in vitro*.

DISCUSSION

In this study, we found that Tim-3 inhibits MHC-II expression in macrophages *via* the STAT1/CIITA pathway and inhibits antigen presentation and CD4+T cell activation in the EAE model. Moreover, blockade of Tim-3 signaling in EAE mice increased MHC-II expression and altered clinical outcomes. We identified a new mechanism that Tim-3 induces immune tolerance by MHC-II presentation, which paves a new way for multiple sclerosis treatment and other MHC-II related diseases.

In our previous studies, Tim-3 inhibits the MHC-I expression and antigen presentation function. Wang et al. (7) found that MHC-I-restricted antigen presentation by macrophages was inhibited by Tim-3-NLRC5 both *in vitro* and in a Listeria monocytogenes infection model *in vivo*. Li et al. (21) also found that Tim-3 blockage increases the expression of MHC-I on macrophages and promotes the activation of VSV-specific CD8+ T cells and also markedly attenuates vesicular stomatitis virus (VSV) encephalitis by decreased mortality and improved neuroethology in mice. In this study, we found that Tim-3 can inhibit the MHC-II expression and antigen presentation to CD4+ T cells, which relieves EAE mouse spinal cord demyelination and improves clinical scores. Tim-3 could also shift CD4+ T cells from a proinflammatory Th1 and Th17 phenotype to a less damaging, antiinflammatory Treg phenotype. These studies showed that Tim-3 inhibits not only MHC-I expression and function but also MHC-II in different animal models, which suggests that Tim-3 may have more function and potential in macrophage antigen function.

Understanding MHC-II antigen presentation in health and disease may be critical for developing tools to control autoimmune responses and to modulate strong responses against infections and cancer (8). CD4+ T cells that interact with MHC-II–bound peptides then promote B cell differentiation and antibody production, as well as CD8+ T cell responses. The immune process of MHC-II is vital and tightly controlled, with one step of unregulated responses that can promote infectious diseases, autoimmune diseases, and cancer. MHC-II alleles are indeed associated with autoimmune diseases and are often the strongest risk factors (22), such as MS, type 1 diabetes, systemic lupus erythematosus, ulcerative colitis, Crohn's disease, and rheumatoid arthritis. In this study, we found that Tim-3 inhibits MHC-II expression and antigen presentation with EAE model amelioration, which indicates that the Tim-3-targeting therapeutic strategy could have more potential for cancers and infectious and autoimmune diseases. There are two possible solutions to the design of a Tim-3-targeting therapy (2). One is IgG4 monoclonal antibodies, which could inhibit Tim-3 signaling in the immune system. The other is the use of IgG1 Tim-3 antibodies with CDC and ADCC function, which could kill dysfunctional immune cells with Tim-3 expression and differentiated monocytes. Elimination of dysfunctional Tim-3-expressing immune cells could be a new way to address immune tolerance (2). These problems are still waiting to be solved.

Multiple sclerosis (MS) is a chronic inflammatory disease of the central nervous system that involves demyelination and axonal degeneration. The multiple sclerosis treatment began with the approval of IFN-β and glatiramer acetate, then the first monoclonal antibody natalizumab, followed by oral medications (fingolimod, teriflunomide, dimethyl fumarate, and cladribine). Recently, new monoclonal antibodies (alemtuzumab and ocrelizumab) have been approved (23). MS treatment remains some problems. One is that progressive MS degenerative mechanisms differ from RRMS inflammatory mechanisms and that the neurodegenerative processes are not resolved by immunomodulatory compounds (24). Another is that animal models limit the understanding of pathophysiological mechanisms in progressive MS (25, 26). The current understanding is that progressive MS is characterized by chronic inflammation behind a closed blood–brain barrier with activation of microglia and continued involvement of T cells and B cells (24).

The goal of therapeutic modulation of T cell composition and differentiation in progressive MS is generally to normalize inflammation and minimize any involvement of T cell infiltrates.

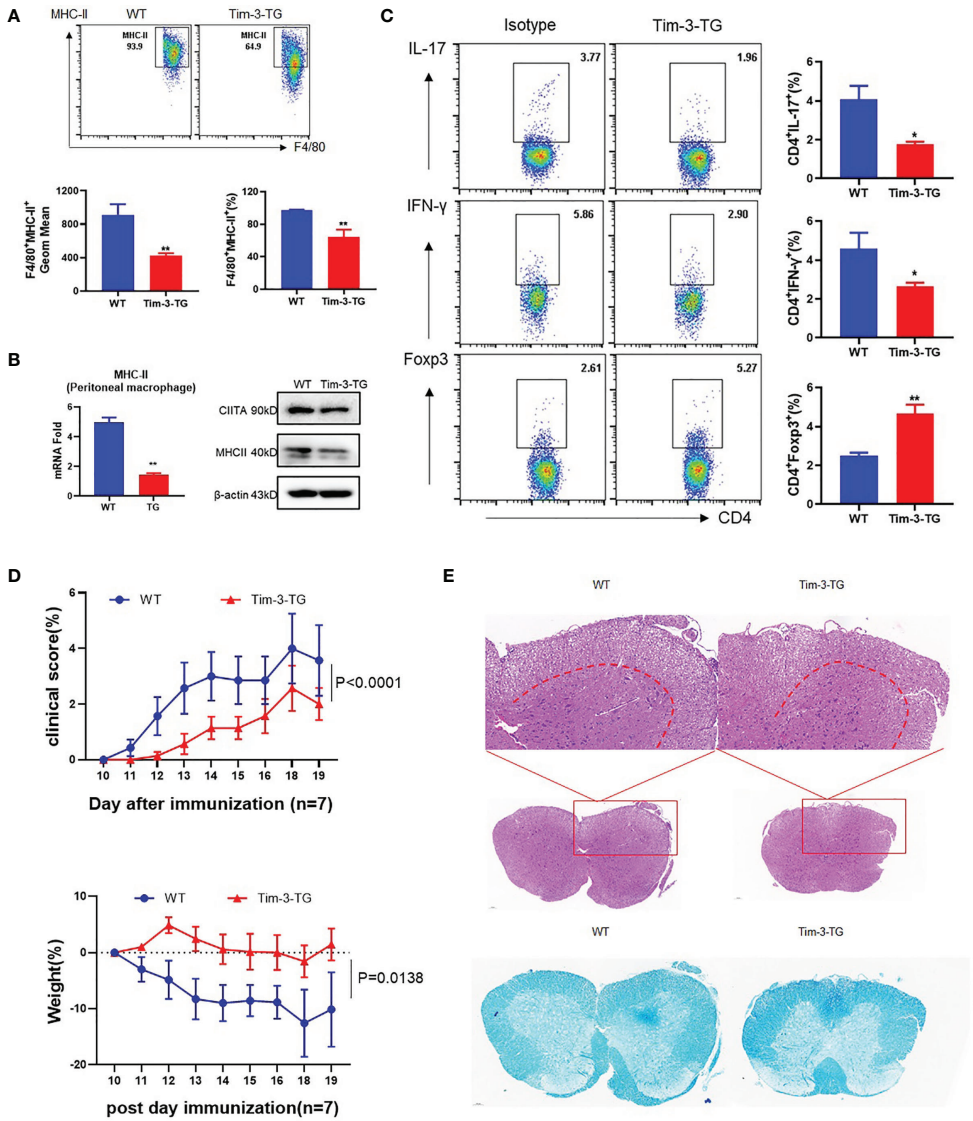

FIGURE 4 | Tim-3 inhibits MHC-II and ameliorates the EAE mouse model. MOG was emulsified into CFA, WT, and Tim-3-TG mice (n = 8) were immunized subcutaneously, and pertussis toxin (500 ng/mouse) was injected intraperitoneally at 2 and 48 h after immunization. On the 20th day after immunization, the mouse spinal cords, peritoneal macrophages, and spleens were harvested. **(A)** Flow cytometry was used to detect the expression of MHC-II on the surface of macrophages. The percentage of MHC-II and the GeoMean were counted (mean ± SD, n = 6–8), **(B)** and the expression level of MHC-II was detected by RT-PCR (mean ± SD, n = 6) and Western blotting. **(C)** Flow cytometry was used to detect the activation levels of IL-17$^+$CD4$^+$T, IFN-γ$^+$CD4$^+$T, and Foxp3$^+$CD4$^+$Tcells in splenic lymphocytes (mean ± SD, n = 8–10). **(D)** The weight and clinical scores of the EAE mice were recorded from the 10th day. **(E)** The mouse spinal cord tissue was isolated and stained with HE and LFB (*p < 0.05; **p < 0.01).

T cells can be found in the brain and spinal cord parenchyma of patients with PPMS and RRMS (27). Targeting T cells to slow disease progression needs more research. However, several interesting approaches could effectively target T cells, some of which are under investigation.

In summary, this study aims at finding the mechanism that Tim-3 could inhibit MHC-II expression and antigen presentation function through STAT1-CIITA, which relieves the EAE model (**Figure 7**), paving the way for Tim-3 as a potential therapeutic target to clinical usage.

MATERIALS AND METHODS

Animals

Female 6–8-week-old C57BL/6J mice were purchased from Sibefu; Tim-3 transgenic mice were obtained from Cyagen Biosciences (Guangzhou, China). All mice were raised in a specific pathogen-free condition with free access to food and water. All experiments were performed according to the protocol approved by the Animal Ethics Committee of the Academy of Military Sciences (permit number: 2020-715).

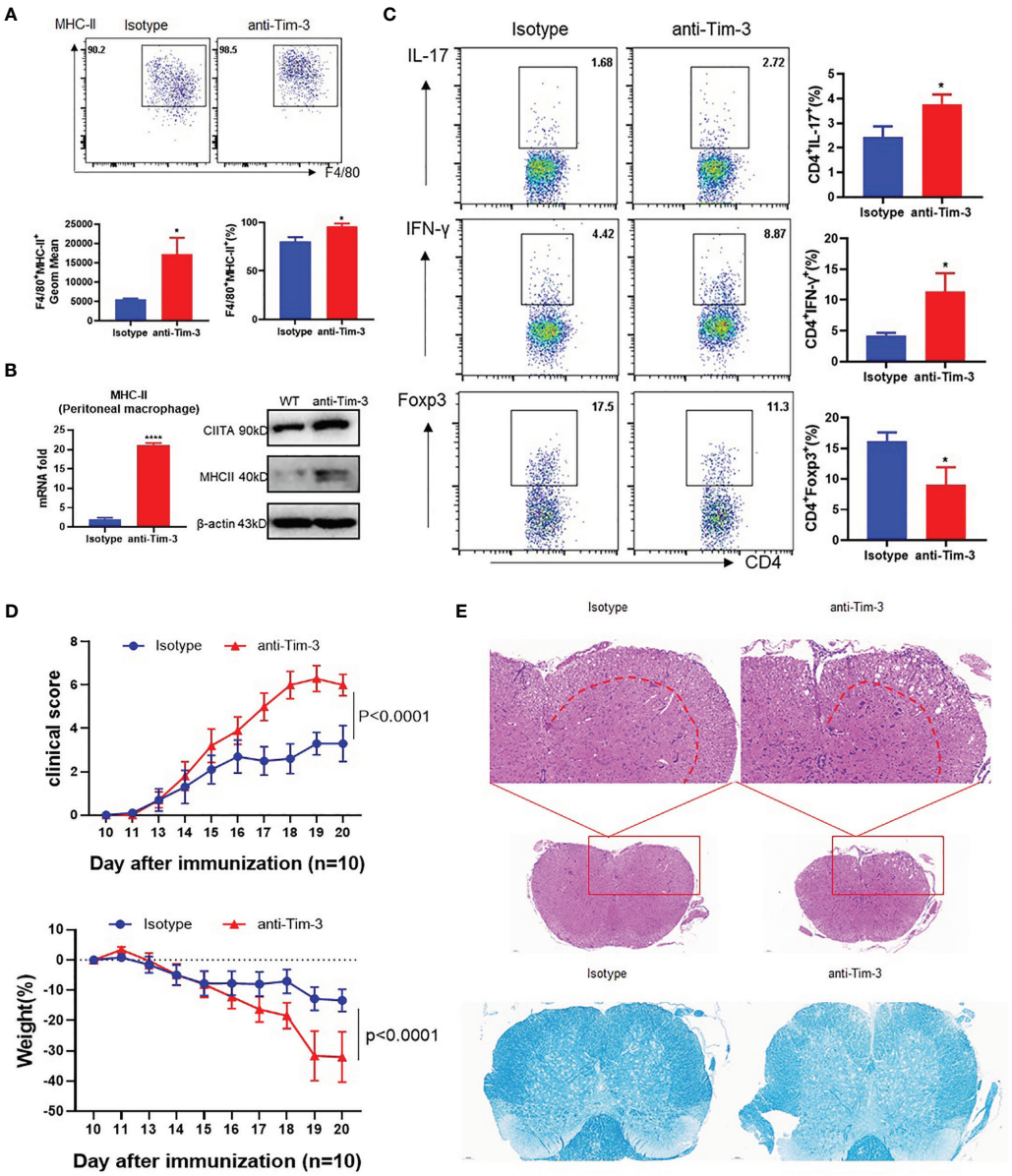

FIGURE 5 | Blockade of Tim-3 exacerbated multiple sclerosis in the EAE model. MOG was emulsified into CFA, mice were immunized subcutaneously, and pertussis toxin (500 ng/mouse) was injected intraperitoneally at 2 and 48 h after immunization. The immunized WT mice were divided into two groups (n = 10): one group is injected with anti-Tim-3 antibody, and the other group is injected with isotype antibody (10 mg/kg, intraperitoneal injection every other day. On the 20th day after immunization, the mouse spinal cords, peritoneal macrophages, and spleens were harvested. **(A)** Flow cytometry was used to detect the expression of MHC-II on the surface of macrophages. The percentage of MHC-II and the GeoMean were counted (mean ± SD, n = 5), **(B)** and the expression level of MHC-II was detected by RT-PCR (mean ± SD, n = 6) and Western blotting. **(C)** Flow cytometry was used to detect the activation levels of IL-17$^+$CD4$^+$T, IFN-γ$^+$CD4$^+$T, and Foxp3$^+$CD4$^+$T cells in splenic lymphocytes (mean ± SD, n = 6–10). **(D)** The weight and clinical scores of the EAE mice were recorded from the 10th day. **(E)** The mouse spinal cord tissue was isolated and stained with HE and LFB (*p < 0.05; ****p < 0.0001).

EAE Induction

EAE was established as described in the literature (28, 29). Briefly, the complete Freund's adjuvant (CFA, Sigma, F5881) was added with 50 mg of Mycobacterium tuberculosis (H37Ra, BD, 0052519) to prepare a final concentration of 6 mg/ml. MOG_{35-55} (SBS Genetech, Beijing) was emulsified with CFA (0.3 mg MOG_{35-55} and 0.6 mg H37Ra per mouse). The mice were immunized subcutaneously on the back, and Pertussis toxin (PTX, List Biological Laboratories, 180243A1) was injected intraperitoneally at 0 and 48 h after immunization (500 ng PTX per mouse each time). Groping, twenty C57BL/6J mice were immunized and randomly divided into two groups: anti-Tim-3 antibody (21) group and control antibody group (10 mg/kg, i.p, every other day). Eight Tim-3-TG mice and eight WT

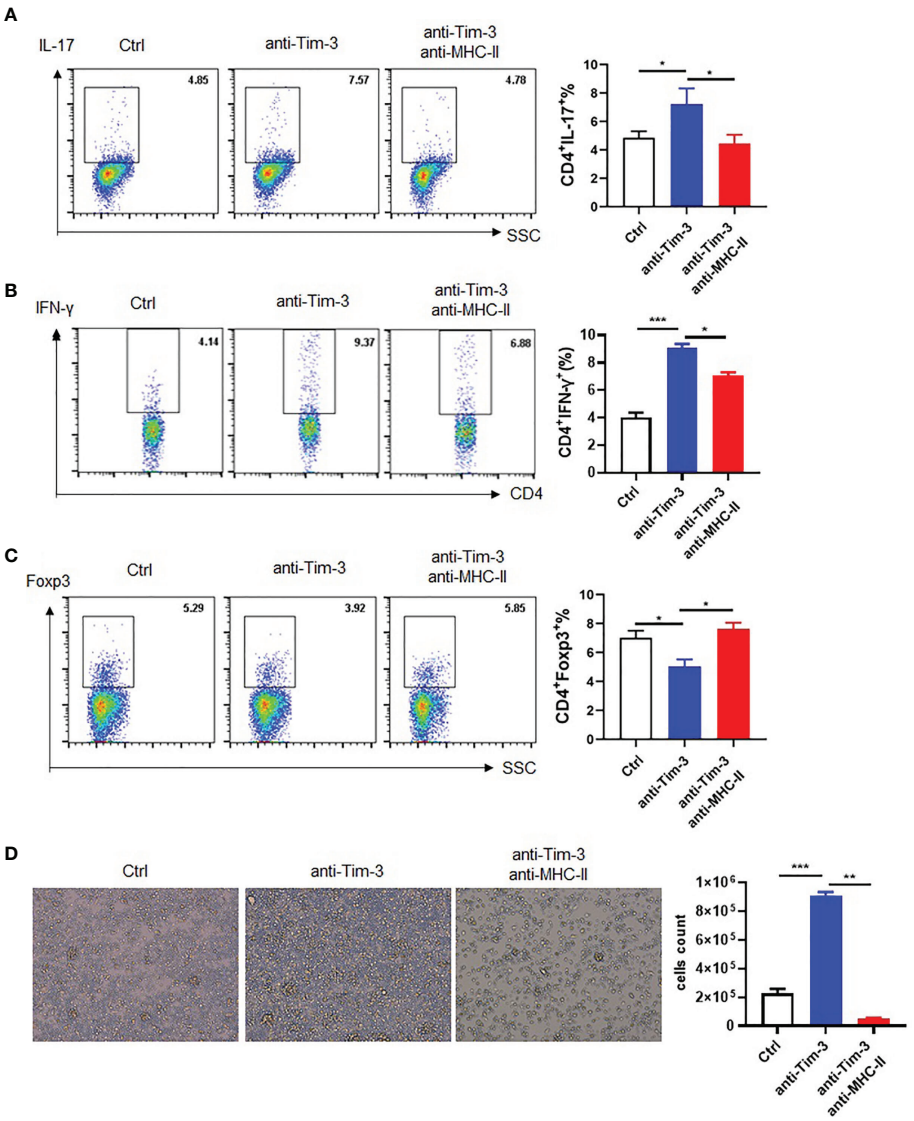

FIGURE 6 | Tim-3 inhibits macrophage MHC-II antigen presentation *in vitro*. Peritoneal macrophages were collected from WT mice, and anti-Tim-3 antibody (10 μg/ml) was added to culture overnight then incubated with MOG (10 μg/ml) for 4 h. Moreover, they were incubated with or without anti-MHC-II antibody (10 μg/ml) for 30 min, and then splenic lymphocytes were added to coculture for 24 h. The splenic lymphocyte suspension was collected to detect the ratio of **(A)** IL-17$^+$CD4$^+$T (mean ± SD, n = 4), **(B)** IFN-γ$^+$CD4$^+$T (mean ± SD, n = 4), and **(C)** Foxp3$^+$CD4$^+$T cells by flow cytometry (mean ± SD, n = 3). **(D)** Splenic lymphocytes of WT mice were cocultured for 3 days and photographed with a microscope, and then spleen cells were for collected for counting (mean ± SD, n = 3) (*p < 0.05; ***p < 0.001).

mice were immunized. The weight and clinical score of the EAE were recorded from the 10th day after immunization (30, 31).

H&E and LFB Staining

The mice were sacrificed on the 20th day after immunization. The mouse spinal cord was obtained and fixed with 4% paraformaldehyde, then paraffin embedding and tissue sectioning were performed. Perform hematoxylin and eosin staining was done to assess the state of the cortical and neuronal cells of the parenchymal. The Luxol fast blue method is used to stain myelin integrity. The microscope image was scanned with Pannoramic DESK, P-MIDI, P250 (Hungary, 3DHISTECH), and analyzed with Pannoramic Scanner software.

Cell Culture and Transfection

RAW264.7 cells and HEK-293T cells were from ATCC and were cultured under the culture guidelines. si-RAW264.7 cells (stably knocked out Tim-3) come from our laboratory (16). All cells using Dulbecco's modified Eagle's medium supplemented with 10% fetal bovine serum, streptomycin (50 μg/ml), and erythromycin (5 μg/ml) were cultured in an incubator (37°C, 5% CO2).

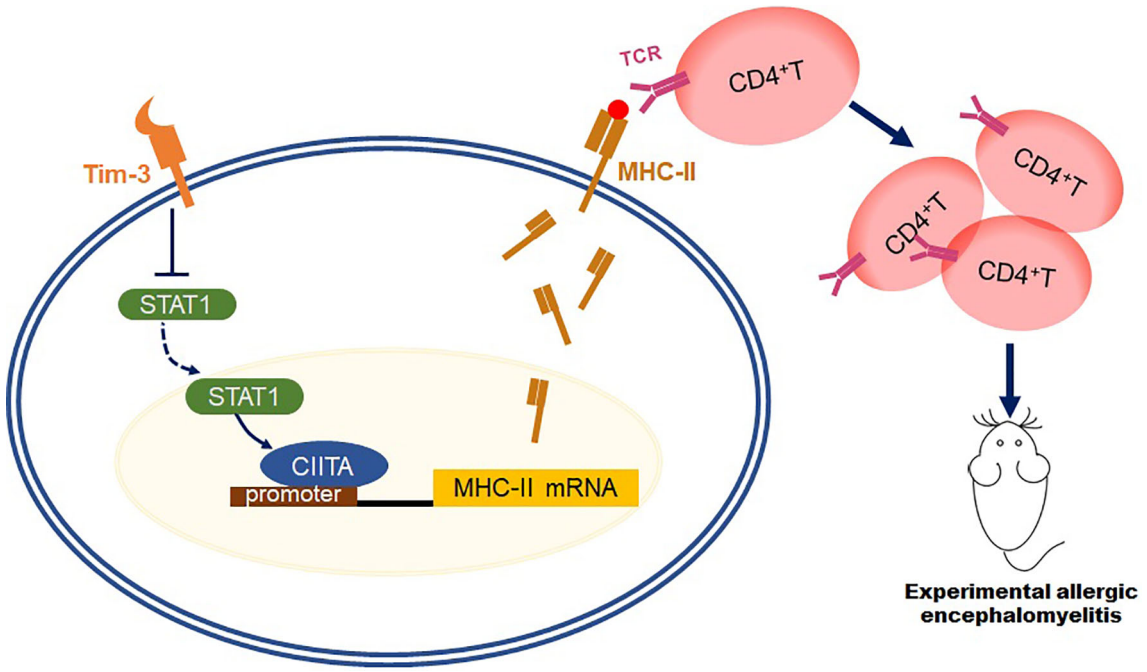

FIGURE 7 | Schematic diagram of how Tim-3 inhibits MHC-II expression and relieves the EAE model. This schematic diagram demonstrated that Tim-3 suppresses MHC-II expression in macrophages *via* the STAT1/CIITA pathway, and Tim-3 inhibits MHC-II-mediated autoantigen presentation and CD4+T cell activation, which facilitated experimental autoimmune encephalomyelitis in mice.

For cell transfection, Tim-3 plasmid gradient transfection was as follows: Vector or 1- and 2-μg Tim-3 plasmids were transfected into HEK-293T cells, respectively. Tim-3, CIITA, and STAT1 plasmids were transfected into HEK-293T cells alone or in combination and cultured for 48 h after transfection. The plasmid was previously stored in our laboratory. The CIITA knockdown, Vector, and CIITA siRNA (Guangzhou Ribobio, S1105) were transfected into RAW264.7 cells for 48 h. In the cell blocking experiment, RAW264.7 cells were cocultured with anti-Tim-3 antibody (20 μg/ml) or isotype antibody for 24 h. Also, 10 μM fludarabine (STAT1 inhibitor) was added on RAW264.7 cells which were then cocultured with anti-Tim-3 antibody (20 μg/ml) for 24 h.

Western Blotting

The cells were collected and lysed with the lysis buffer, in which protease and phosphatase inhibitors were added, then the supernatant was centrifuged and collected. The loading buffer was added and boiled for 10 min and then stored at -20°C. The protein concentrations of the sample were assessed using BCA Protein Analysis Kit (Thermo Fisher, TF268083). The protein sample was boiled for 5 min and was electrophoresed by SDS-PAGE (sodium dodecyl sulfate-polyacrylamide gel electrophoresis) and then transferred to a polyvinylidene difluoride (PVDF) membrane. Then, the membrane was blocked for 1 h with TBST containing 5% milk at room temperature. The blots were incubated with the following primary antibodies overnight at 4°C: anti-CIITA antibody (Abcam, ab49132), anti-MHC-II antibody (Abcam, ab180779), and anti-mouse β-actin antibody (Abcam, ab8227). The dilution method of the above antibodies is according to the instructions. Afterward, the membrane was washed three times with TBST, 10 min each time, then incubated with Goat anti-rabbit IgG or Goat anti-mouse IgG antibodies for 40 min at room temperature, then washed three times with TBST for 10 min each time.

Real-Time PCR

The peritoneal macrophages of Tim-3-TG and WT EAE mice were collected, and RNA was extracted according to the TRIzol instructions (Ambion, 28218) (32). The concentration and purity of RNA were assessed by a Q5000 ultraviolet spectrophotometer (Quawell Technology Inc., Sunnyvale, USA). The RNA was reverse-transcribed by using TransScript First-Strand cDNA Synthesis SuperMix (TransGen Biotech, N20730). Quantitative real-time PCR was performed using UltraSYBR One-Step RT-qPCR Kit (Beijing ComWin Biotech, CW0659) and a LightCycler 480 PCR system. The relative expression of interesting genes was detected using the $2^{-\Delta\Delta Ct}$ method, and internal control (18S ribosomal mRNA) was used for normalization of the target genes (7). The interesting primer sequences were shown as follows:

18S: sense 5′-TTGACGGAAGGGCACCACCAG-3′
Anti-sense 5′-GCACCACCACCACGGAATCG-3′
MHC-II: sense 5′-GCGGAGAGTTGAGCCTACG-3′
Anti-sense 5′-CCAGGAGGTTGTGGTGTTCC-3′
CIITA: sense 5′-TGTTTTGGATGCTGCAAGGC-3′
Anti-sense 5′-AAGGCACAGTGGTATTCCCG-3′

Dual-Luciferase Reporter Assay

The pGL3-MHC-II (1 μg) and pGL3-CIITA (1 μg) plasmids (Shenggong, Beijing, China) were transferred into HEK-293T cells, with or without Tim-3 plasmid, and cultured for 48 h. The luminescence was detected with the Dual-Luciferase Report Assay System (Promega, E1910). Briefly, the cells were washed with PBS once and 200 μl lysis buffer was added, then 20 μl was added to a 96-well plate, 50 μl 1× Gold's reagent was added to each well, and firefly luciferin was measured immediately, and then 50 μl 1× Stop reagent was added to measure Renilla luciferase. Finally, the relative of firefly fluorescein/renilla fluorescein was calculated (33).

FACS Analysis

The spleen lymphocytes of EAE mice (on the 20th day after immunization) were separated with Ficoll density gradient centrifugation. Peritoneal macrophages were isolated as previously described (7), washed twice with FACS (containing 2% fetal bovine serum), then stained with APC anti-mouse F4/80 antibody (BioLegend, 123116) and PE anti-mouse MHC-II antibody (BioLegend, B117132), incubated at 37°C for 30 min, and then washed once with FASC and resuspended in 1% paraformaldehyde. For staining of spleen cells, firstly, the cells were incubated with cell stimulation cocktail plus protein transport inhibitors (Invitrogen, 2260623) for 4–6 h, washed with FACS once for staining with PerCP anti-mouse CD4 antibody (BioLegend, 100538), and then washed with FACS; 200 μl fixation/permer buffer (Invitrogen, 2220750) was added at 4°C overnight, and then permer buffer dilution washing and staining were done on the APC anti-mouse IFN-γ antibody (BioLegend, 505810), PE anti-mouse IL-17 antibody (BioLegend, 506904), and APC anti-mouse Foxp3 antibody (eBioscience, E07303-1635), and finally washing with permer buffer and resuspension were performed.

MHC-II Neutralization Experiment *In Vitro*

Peritoneal macrophages and spleen cells of wild-type mice were obtained according to the above method. Then, anti-Tim-3 antibody was added to the peritoneal macrophages to incubate overnight, then MOG_{35-55} was also added to incubate for 4 h, and then anti-MHC-II antibody (Invitrogen, 2190425) was added to incubate for 30 min, and splenic lymphocytes were finally added and, after 24 h, photographed with a microscope; then, spleen cells for were collected for counting and then stained with PerCP anti-mouse CD4 antibody and APC anti-mouse IFN-γ antibody.

Statistical Analysis

Data analysis was analyzed with GraphPad Prism software version 8. Data were expressed with mean ± standard error of mean (SEM). Differences between groups were analyzed using repeated-measure analysis of variance or t-test. A p value of less than 0.05 is considered statistically significant.

DATA AVAILABILITY STATEMENT

The original contributions presented in the study are included in the article/supplementary material. Further inquiries can be directed to the corresponding authors.

AUTHOR CONTRIBUTIONS

Conception and design of the study: GH, ZW, RW. Acquisition, analysis, and interpretation of data: LT, GL. Contribution of administrative, experimental, analytic, or material support: YZ, CH, YG, ZG, YH, RM, YL, BS. Writing—original draft preparation: LT, ZW. Editing: GH. All authors contributed to the article and approved the submitted version.

FUNDING

This work was supported by the National Natural Sciences Foundation of China (grant nos. 81971473, 81771684, 82171753) and the Beijing Natural Sciences Foundation (grant no. 7192145).

REFERENCES

1. Han G, Chen G, Shen B, Li Y. Tim-3: An Activation Marker and Activation Limiter of Innate Immune Cells. *Front Immunol* (2013) 4:449. doi: 10.3389/fimmu.2013.00449
2. Wang Z, Chen J, Wang M, Zhang L, Yu L. One Stone, Two Birds: The Roles of Tim-3 in Acute Myeloid Leukemia. *Front Immunol* (2021) 12:618710. doi: 10.3389/fimmu.2021.618710
3. Ocana-Guzman R, Torre-Bouscoulet L, Sada-Ovalle I. TIM-3 Regulates Distinct Functions in Macrophages. *Front Immunol* (2016) 7:229. doi: 10.3389/fimmu.2016.00229
4. Mohammadzadeh A, Rad IA, Ahmadi-Salmasi B. CTLA-4, PD-1 and TIM-3 Expression Predominantly Downregulated in MS Patients. *J Neuroimmunol* (2018) 323:105–8. doi: 10.1016/j.jneuroim.2018.08.004
5. Afshar B, Khalifehzadeh-Esfahani Z, Seyfizadeh N, Rezaei Danbaran G, Hemmatzadeh M, Mohammadi H. The Role of Immune Regulatory Molecules in Multiple Sclerosis. *J Neuroimmunol* (2019) 337:577061. doi: 10.1016/j.jneuroim.2019.577061
6. Zhang R, Li H, Bai L, Duan J. Association Between T-Cell Immunoglobulin and Mucin Domain 3 (TIM-3) Genetic Polymorphisms and Susceptibility to Autoimmune Diseases. *Immunol Invest* (2019) 48(6):563–76. doi: 10.1080/08820139.2019.1599009
7. Wang Z, Li G, Dou S, Zhang Y, Liu Y, Zhang J, et al. Tim-3 Promotes Listeria Monocytogenes Immune Evasion by Suppressing Major Histocompatibility Complex Class I. *J Infect Dis* (2020) 221(5):830–40. doi: 10.1093/infdis/jiz512
8. Unanue ER, Turk V, Neefjes J. Variations in MHC Class II Antigen Processing and Presentation in Health and Disease. *Annu Rev Immunol* (2016) 34:265–97. doi: 10.1146/annurev-immunol-041015-055420
9. Yau AC, Piehl F, Olsson T, Holmdahl R. Effects of C2ta Genetic Polymorphisms on MHC Class II Expression and Autoimmune Diseases. *Immunology* (2017) 150(4):408–17. doi: 10.1111/imm.12692
10. DeNardo DG, Ruffell B. Macrophages as Regulators of Tumour Immunity and Immunotherapy. *Nat Rev Immunol* (2019) 19(6):369–82. doi: 10.1038/s41577-019-0127-6
11. International Multiple Sclerosis Genetics C and Wellcome Trust Case Control C, Sawcer S, Hellenthal G, Pirinen M, Spencer CC, et al. Genetic Risk and a

Primary Role for Cell-Mediated Immune Mechanisms in Multiple Sclerosis. *Nature* (2011) 476(7359):214–9. doi: 10.1038/nature10251
12. Kaskow BJ, Baecher-Allan C. Effector T Cells in Multiple Sclerosis. *Cold Spring Harb Perspect Med* (2018) 8(4):a029025. doi: 10.1101/cshperspect.a029025
13. Masternak K, Muhlethaler-Mottet A, Villard J, Zufferey M, Steimle V, Reith W. CIITA Is a Transcriptional Coactivator That Is Recruited to MHC Class II Promoters by Multiple Synergistic Interactions With an Enhanceosome Complex. *Genes Dev* (2000) 14(9):1156–66. doi: 10.1101/gad.14.9.1156
14. Badawi AH, Kiptoo P, Siahaan TJ. Immune Tolerance Induction Against Experimental Autoimmune Encephalomyelitis (EAE) Using A New PLP-B7AP Conjugate That Simultaneously Targets B7/CD28 Costimulatory Signal and TCR/MHC-II Signal. *J Mult Scler (Foster City)* (2015) 2(1):1000131. doi: 10.4172/2376-0389.1000131
15. Schmitz K, Wilken-Schmitz A, Vasic V, Brunkhorst R, Schmidt M, Tegeder I. Progranulin Deficiency Confers Resistance to Autoimmune Encephalomyelitis in Mice. *Cell Mol Immunol* (2020) 17(10):1077–91. doi: 10.1038/s41423-019-0274-5
16. Wang Z, Sun D, Chen G, Li G, Dou S, Wang R, et al. Tim-3 Inhibits Macrophage Control of Listeria Monocytogenes by Inhibiting Nrf2. *Sci Rep* (2017) 7:42095. doi: 10.1038/srep42095
17. Barreiro LB, Tailleux L, Pai AA, Gicquel B, Marioni JC, Gilad Y. Deciphering the Genetic Architecture of Variation in the Immune Response to Mycobacterium Tuberculosis Infection. *Proc Natl Acad Sci USA* (2012) 109 (4):1204–9. doi: 10.1073/pnas.1115761109
18. Miller S, Tsou PS, Coit P, Gensterblum-Miller E, Renauer P, Rohraff DM, et al. Hypomethylation of STAT1 and HLA-DRB1 Is Associated With Type-I Interferon-Dependent HLA-DRB1 Expression in Lupus CD8+ T Cells. *Ann Rheum Dis* (2019) 78(4):519–28. doi: 10.1136/annrheumdis-2018-214323
19. Coste C, Gerard N, Dinh CP, Bruguiere A, Rouger C, Leong ST, et al. Targeting MHC Regulation Using Polycyclic Polyprenylated Acylphloroglucinols Isolated From Garcinia Bancana. *Biomolecules* (2020) 10(9):1266. doi: 10.3390/biom10091266
20. Liang J, Wang L, Wang C, Shen J, Su B, Marisetty AL, et al. Verteporfin Inhibits PD-L1 Through Autophagy and the STAT1-IRF1-TRIM28 Signaling Axis, Exerting Antitumor Efficacy. *Cancer Immunol Res* (2020) 8(7):952–65. doi: 10.1158/2326-6066.CIR-19-0159
21. Li G, Tang L, Hou C, Wang Z, Gao Y, Dou S, et al. Peripheral Injection of Tim-3 Antibody Attenuates VSV Encephalitis by Enhancing MHC-I Presentation. *Front Immunol* (2021) 12:667478. doi: 10.3389/fimmu.2021.667478
22. Fernando MM, Stevens CR, Walsh EC, De Jager PL, Goyette P, Plenge RM, et al. Defining the Role of the MHC in Autoimmunity: A Review and Pooled Analysis. *PLoS Genet* (2008) 4(4):e1000024. doi: 10.1371/journal.pgen.1000024
23. Tintore M, Vidal-Jordana A, Sastre-Garriga J. Treatment of Multiple Sclerosis - Success From Bench to Bedside. *Nat Rev Neurol* (2019) 15(1):53–8. doi: 10.1038/s41582-018-0082-z
24. Faissner S, Plemel JR, Gold R, Yong VW. Progressive Multiple Sclerosis: From Pathophysiology to Therapeutic Strategies. *Nat Rev Drug Discov* (2019) 18 (12):905–22. doi: 10.1038/s41573-019-0035-2
25. Stys PK, Zamponi GW, van Minnen J, Geurts JJ. Will the Real Multiple Sclerosis Please Stand Up? *Nat Rev Neurosci* (2012) 13(7):507–14. doi: 10.1038/nrn3275
26. Lodygin D, Hermann M, Schweingruber N, Flugel-Koch C, Watanabe T, Schlosser C, et al. Publisher Correction: Beta-Synuclein-Reactive T Cells Induce Autoimmune CNS Grey Matter Degeneration. *Nature* (2019) 567 (7749):E15. doi: 10.1038/s41586-019-1047-0
27. Androdias G, Reynolds R, Chanal M, Ritleng C, Confavreux C, Nataf S. Meningeal T Cells Associate With Diffuse Axonal Loss in Multiple Sclerosis Spinal Cords. *Ann Neurol* (2010) 68(4):465–76. doi: 10.1002/ana.22054
28. Giralt M, Molinero A, Hidalgo J. Active Induction of Experimental Autoimmune Encephalomyelitis (EAE) With MOG35-55 in the Mouse. *Methods Mol Biol* (2018) 1791:227–32. doi: 10.1007/978-1-4939-7862-5_17
29. Glatigny S, Bettelli E. Experimental Autoimmune Encephalomyelitis (EAE) as Animal Models of Multiple Sclerosis (MS). *Cold Spring Harb Perspect Med* (2018) 8(11):a028977. doi: 10.1101/cshperspect.a028977
30. Enders U, Lobb R, Pepinsky RB, Hartung HP, Toyka KV, Gold R. The Role of the Very Late Antigen-4 and its Counterligand Vascular Cell Adhesion Molecule-1 in the Pathogenesis of Experimental Autoimmune Neuritis of the Lewis Rat. *Brain* (1998) 121(Pt 7):1257–66. doi: 10.1093/brain/121.7.1257
31. Wilmes AT, Reinehr S, Kuhn S, Pedreiturria X, Petrikowski L, Faissner S, et al. Laquinimod Protects the Optic Nerve and Retina in an Experimental Autoimmune Encephalomyelitis Model. *J Neuroinflamm* (2018) 15(1):183. doi: 10.1186/s12974-018-1208-3
32. Xiao Y, Chen J, Wang J, Guan W, Wang M, Zhang L, et al. Acute Myeloid Leukemia Epigenetic Immune Escape From Nature Killer Cells by ICAM-1. *Front Oncol* (2021) 11:751834. doi: 10.3389/fonc.2021.751834
33. Wang Z, Guan W, Wang M, Chen J, Zhang L, Xiao Y, et al. AML1-ETO Inhibits Acute Myeloid Leukemia Immune Escape by CD48. *Leuk Lymphoma* (2021) 62(4):937–43. doi: 10.1080/10428194.2020.1849680

Conflict of Interest: The authors declare that the research was conducted in the absence of any commercial or financial relationships that could be construed as a potential conflict of interest.

Publisher's Note: All claims expressed in this article are solely those of the authors and do not necessarily represent those of their affiliated organizations, or those of the publisher, the editors and the reviewers. Any product that may be evaluated in this article, or claim that may be made by its manufacturer, is not guaranteed or endorsed by the publisher.

frontiers in Neurology

ORIGINAL RESEARCH
published: 20 January 2022
doi: 10.3389/fneur.2021.721788

Constructing a Multiple Sclerosis Diagnosis Model Based on Microarray

Haoran Li[1], *Hongyun Wu*[2], *Weiying Li*[3], *Jiapei Zhou*[1], *Jie Yang*[1] *and Wei Peng*[2]*

[1] College of Traditional Chinese Medicine, Shandong University of Traditional Chinese Medicine, Jinan, China, [2] Department of Neurology, Affiliated Hospital of Shandong University of Traditional Chinese Medicine, Jinan, China, [3] Department of Comprehensive Surgery, Weifang Maternal and Child Health Hospital, Weifang, China

Introduction: Multiple sclerosis is an immune-mediated demyelinating disorder of the central nervous system. Because of the complexity of etiology, pathology, clinical manifestations, and the diversity of classification, the diagnosis of MS is very difficult. We found that McDonald Criteria is very strict and relies heavily on the evidence for DIS and DIT. Therefore, we hope to find a new method to supplement the evidence and improve the accuracy of MS diagnosis.

Results: We finally selected GSE61240, GSE18781, and GSE185047 based on the GPL570 platform to build a diagnosis model. We initially selected 54 MS susceptibility locus genes identified by IMSGC and WTCCC2 as predictors for the model. After Random Forests and other series of screening, the logistic regression model was established with 4 genes as the final predictors. In external validation, the model showed high accuracy with an AUC of 0.96 and an accuracy of 86.30%. Finally, we established a nomogram and an online prediction tool to better display the diagnosis model.

Conclusion: The diagnosis model based on microarray data in this study has a high degree of discrimination and calibration in the validation set, which is helpful for diagnosis in the absence of evidence for DIS and DIT. Only one SLE case was misdiagnosed as MS, indicating that the model has a high specificity (93.93%), which is useful for differential diagnosis. The significance of the study lies in proving that it is feasible to identify MS by peripheral blood RNA, and the further application of the model and be used as a supplement to McDonald Criteria still need to be trained with larger sample size.

Keywords: multiple sclerosis, diagnosis model, microarray, Random Forest, logistic regression, Area Under Curve, Calibration Curve, McDonald Criteria

OPEN ACCESS

Edited by:
Maria Teresa Cencioni, Imperial College London, United Kingdom

Reviewed by:
Dejan Jakimovski, Buffalo Neuroimaging Analysis Center, United States
Chandra Das, Netaji Subhash Engineering College (NSEC), India
Francesca Gobbin, University of Verona, Italy

***Correspondence:**
Wei Peng
szypengwei@163.com
orcid.org/0000-0003-1384-9014

Specialty section:
This article was submitted to Multiple Sclerosis and Neuroimmunology, a section of the journal Frontiers in Neurology

Received: *07 June 2021*
Accepted: *27 December 2021*
Published: *20 January 2022*

Citation:
Li H, Wu H, Li W, Zhou J, Yang J and Peng W (2022) Constructing a Multiple Sclerosis Diagnosis Model Based on Microarray. Front. Neurol. 12:721788. doi: 10.3389/fneur.2021.721788

INTRODUCTION

Multiple sclerosis (MS) is an immune-mediated demyelinating disorder of the central nervous system (CNS). The most frequently involved parts of the disease are periventricular white matter, optic nerve, spinal cord, brainstem, and cerebellum, characterized by limb weakness, sensory abnormalities, ataxia and visual, and cognitive changes. The pathological mechanism of MS is still unknown, but its occurrence is closely related to autoimmunity and environmental factors (1). MS usually occurs in young adults, and it is more common in women (2). MS has a great impact on the motor function and economy of early adult life, thus significantly reducing the quality of life. Disease-modifying treatments have mostly failed as treatments for progressive multiple

sclerosis (3). However, early diagnosis and treatment are still very effective in reducing recurrence and disability rates in relapsing-remitting MS (RRMS).

The diagnosis of MS is based on symptoms and signs of the central nervous system, as well as CNS demyelination evidence for dissemination in space (DIS) and dissemination in time (DIT). The detection of MRI and cerebrospinal fluid (CSF) has greatly improved the accuracy of diagnosis and differential diagnosis of MS from other diseases, but there were still some misdiagnoses (4). At present, an increasing number of studies have found that the biomarkers in blood have obvious specificity in patients with MS (5, 6). The International Multiple Sclerosis Genetics Consortium (IMSGC) and the Wellcome Trust Case Control Consortium 2 (WTCCC2) identified more than 50 MS susceptibility loci in genome-wide association studies (GWAS) with a large sample size (n = 9,772) (7). With the increasing maturity of microarray technology, economical and convenient gene detection makes the gene diagnosis of MS possible. In this study, the probe microarray data of blood samples of MS, healthy control, and other inflammatory CNS diseases were obtained from the Gene Expression Omnibus (GEO) database, and an MS diagnosis model based on gene expression was constructed.

RESULTS

Data Processing

We finally selected GSE61240, GSE18781, and GSE185047 based on the GPL570 platform (Affymetrix Human Genome U133 Plus 2.0 Array) to build a diagnosis model. We unified the raw probe data of the three series to get the matrix data of gene expression. We have drawn a boxplot based on gene expression, which shows that 147 arrays are at the same expression level, and there was no systematic error between the three series (as shown in **Figure 1** and **Supplementary Table 1**). One hundred and forty-seven arrays in the above three series were divided into a training set and a validation set. The training set contains samples of 39 RRMS (one RRMS was eliminated after inspection), 6 sarcoidosis, 10 systemic lupus erythematosus (SLE), and 18 healthy control. The validation set contains samples of 40 RRMS, 6 sarcoidosis, 10 SLE, and 17 healthy control. The training set is used to construct the prediction model, and the validation set is used to verify the accuracy and reliability of the model prediction (as shown in **Supplementary Tables 2, 3**).

Screening Predictors of the Model

We adopted the conclusions of the MS genome-wide association studies of IMSGC and WTCCC2 and used 54 MS susceptibility locus genes as the predictors preliminarily included in the model (7). Subsequently, we rigorously screened 54 predictors using Random Forests and obtained 8 predictors with a Gini index greater than 1 (as shown in **Figure 2**) (8, 9). We used the restricted cubic spline (RCS) to test the non-linearity of the 8 predictors and found that CD58 and MMEL1 did not satisfy the linear relation with the dependent variable while the P-value is 0.0041 and 0.0492 ($P < 0.05$), so both predictors were eliminated. Multicollinearity refers to the high correlation between variables in the linear regression model, which makes the model difficult to estimate accurately. We used variance expansion factors (VIF) to evaluate the multicollinearity of variables (10). The VIFs of STAT3 and RPS6KB1 were greater than 5 and were eliminated, and it was considered that there was multicollinearity between them. Finally, we selected 4 genes (DKKL1, BATF, PTGER4, MPHOSPH9) as final predictors of the model and used them in the subsequent model construction.

Model Establishment and Evaluation

The influential point in the data has a great influence on the stability and authenticity of parameter estimation. Therefore, this study used Cook's distance to evaluate the influential point in the data. When the Cook's distance is less than 1, it is considered that there is no influential point (11). After inspection, the Cook's distance of sample GSM1500092 is greater than 3, so GSM1500092 was excluded (as shown in **Figure 2**). The actual clinical manifestations of the diagnosis model constructed according to the training set should refer to its prediction accuracy in the independent validation set. We used the diagnosis model to predict the training set and validation set and evaluated the accuracy of the model according to the discrimination and calibration. The original training set and B-fold cross-validation were predicted, respectively. The C-statistics of the diagnosis model in the original training set and in B-fold cross-validation were both 0.99. The Calibration Curve drawn with R can directly indicate that the diagnosis model has a high calibration in the original training set, and also has a good performance in B-fold cross-validation (as shown in **Figure 3**). Subsequently, the diagnosis model was used to predict the validation set, and the receiver operating characteristic curve (ROC) and a Calibration Curve were drawn (as shown in **Figure 3**). The Area Under Curve (AUC) is 0.96, and the performance of the model in the Calibration Curve is close to that in the B-fold cross-validation of the training set. After determining that the diagnosis model has a good performance, we used the final model to build a nomogram (as shown in **Figure 4**) and an online prediction tool (https://acireman.shinyapps.io/dynnomapp/).

We have drawn a histogram of the output probability, and it can be seen that the distribution of the predicted probability is concentrated at both ends (as shown in **Figure 5**). In order to show the prediction accuracy of the model, we drew a confusion matrix based on all samples in the validation set (as shown in **Figure 5**). With the probability threshold set to 0.5, 63 out of the 73 samples were correctly classified, with an accuracy of 86.30%. Eight cases of RRMS were wrongly judged as non-MS, one case of healthy control and one case of SLE were wrongly judged as RRMS with a sensitivity of 80.0%, specificity of 93.93%, positive prediction value (PPV) of 94.11%, negative prediction value (NPV) of 79.48%. Similarly, we also drew a confusion matrix for the prediction of the model in the training set (as shown in **Figure 5**).

DISCUSSION

The McDonald Criteria in 2017 is very strict and complicated. Firstly, it is suitable for patients with a typical clinically isolated syndrome (CIS) (12). Secondly, evidence of DIS and DIT are

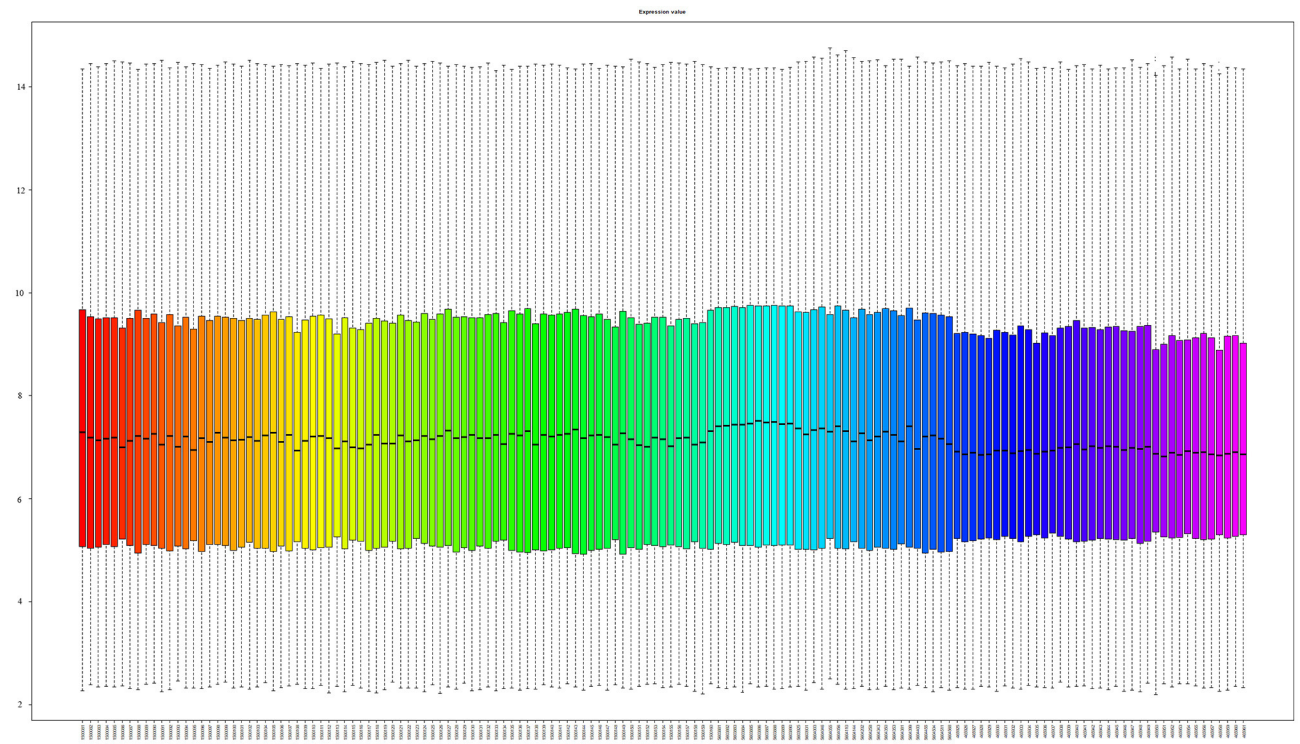

FIGURE 1 | Boxplot of 147 gene chips. The median gene expression of 147 samples is almost at the same level.

required to confirm the diagnosis, which refers to the multiple locations of lesions and the relapsing-remitting course (13, 14). Therefore, the difficulties of McDonald Criteria lie in three aspects: identifying demyelinating lesions of the CNS, identifying different positions of the lesions, and identifying the course of relapse and remission (or coexistence of old and new lesions).

The current development of imaging greatly improves the diagnosis of MS. For example, susceptibility-weighted sequences at 3T can identify the paramagnetic rim lesions and central vein sign (15, 16), which are the characteristic lesions of MS. However, since the related devices have not been widely used in clinical practice and the difficulties to determine the threshold for their diagnosis (17), they are only recommended as differential diagnostic markers, but not for clinical apply (18). Aside from neuromyelitis optica spectrum disorders (NMOSDs), non-specific MRI findings of common diseases (such as age-related vascular white matter lesion and migraine with a single periventricular lesion, which is not uncommon) are the most common misdiagnosis of MS (12). Therefore, the specificity of MRI in differentiating demyelinating lesions cannot meet clinical needs.

It is sometimes difficult to find evidence of lesions for DIS and DIT. Although both cortical lesions and juxtacortical lesions can be used as evidence of DIS, the ability of MRI to identify demyelinating lesions of cortex and distinguish them from other cortical lesions is limited at present. As evidence of DIS, the number of paraventricular lesions has been changing for years. Although the 2016 MAGNIMS Criteria found that the specificity of a single paraventricular lesion was low (19), the 2017 McDonald Criteria still used a single paraventricular lesion as evidence of DIS, which improved the sensitivity but reduced the specificity (12). Because of the lack of clinical symptoms or MRI (spinal cord MRI is not usually listed as routine imaging), the lesions in the spinal cord may be neglected. In the absence of contemporaneous or current objective evidence, historical events should be carefully accepted. Especially for patients with a first demyelinating attack or primary-progressive MS, the lack of evidence of DIT will affect the definitive diagnosis and the beginning of long-term disease-modifying treatment.

Based on the above objective restrictions, McDonald Criteria in 2017 suggests that CSF-specific oligoclonal bands (OCB) can be used as evidence of DIT, and suggests that spinal cord MRI should be performed as soon as possible in the absence of evidence or typical clinical manifestation (12). Similarly, we hope to develop a new dimension of evidence as a supplement when DIS or DIT evidence is insufficient under McDonald Criteria, even as a differential diagnosis of MS from other inflammatory demyelinating diseases or other CNS diseases. The MS genome-wide association studies of IMSGC and WTCCC2 identified more than 50 susceptibility locus genes among 9,722 cases of European descent (7), which makes it possible to identify MS from a genome.

On the other hand, brain MRI is not accurate for evaluating subcortical demyelination and spinal cord MRI is not as sensitive as the brain in detecting lesions (20), while CSF OCB has received more and more attention in the diagnosis of MS, and the lack of

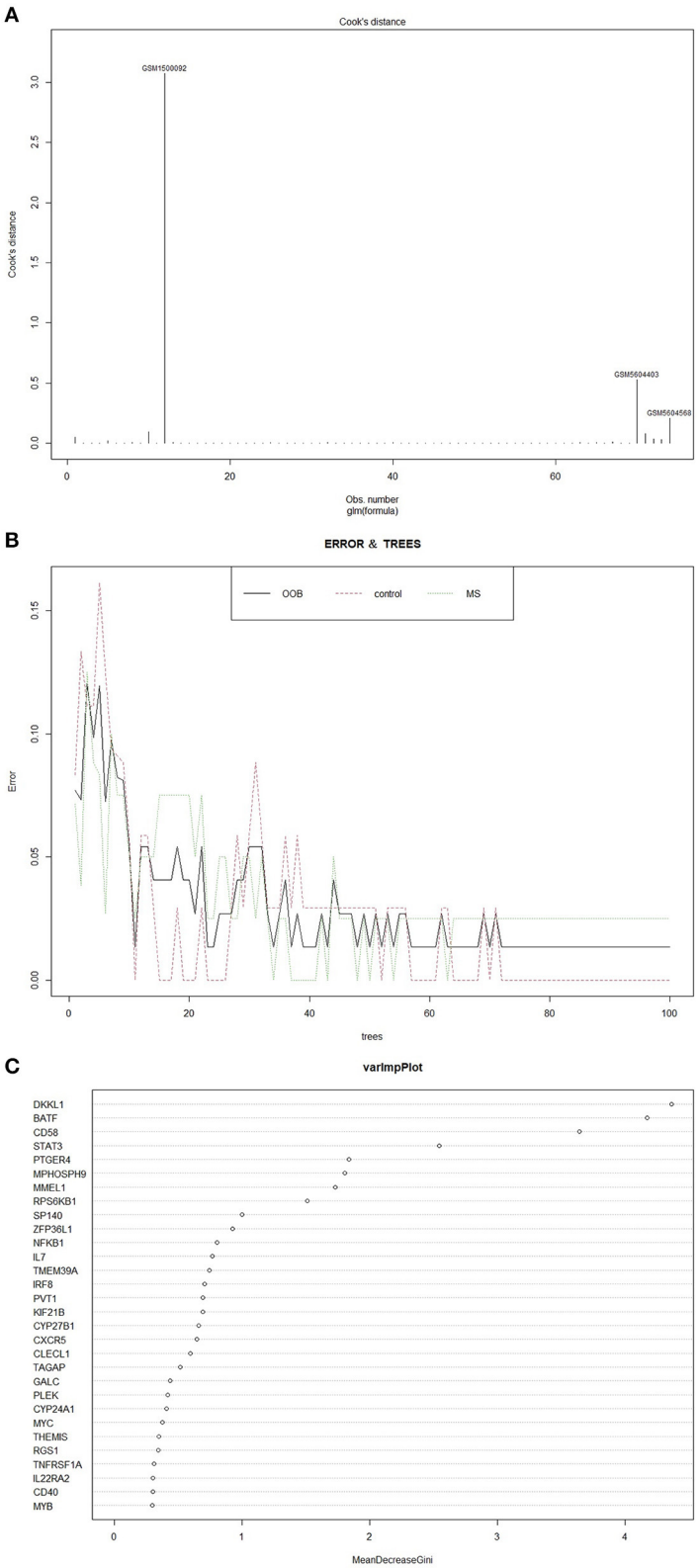

FIGURE 2 | (A) Cook's Distance describes the influence of a single sample on the entire regression model. The greater the Cook's distance, the greater the influence. **(B)** The relationship between the number of classification trees and the error in Random Forests. With the increase of the number of classification trees, the classification error gradually decreases, and the model gradually tends to be stable. **(C)** Gini index of predictors in the model, which reflects the importance of predictors.

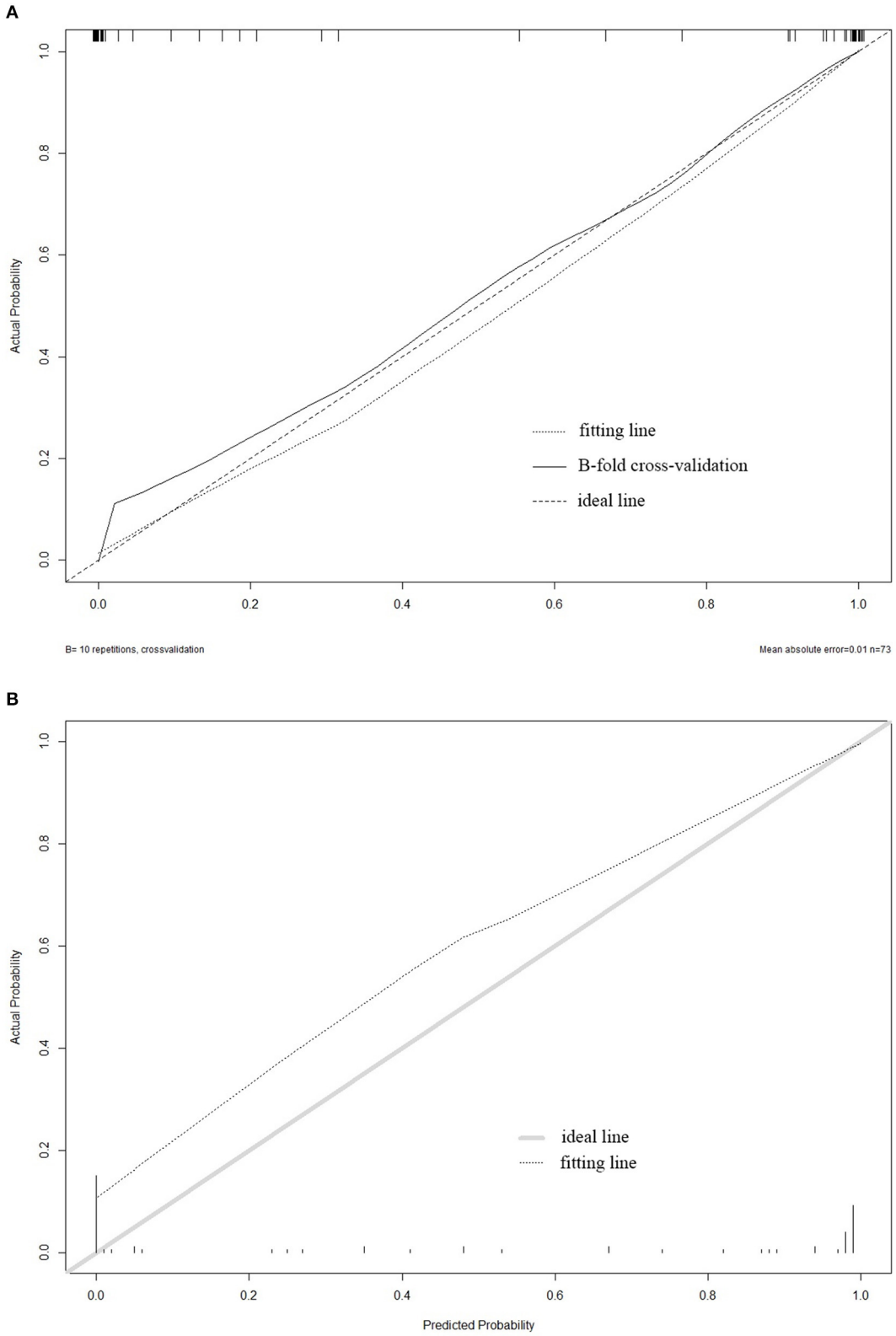

FIGURE 3 | (A) The Calibration Curve of the training set. **(B)** The Calibration Curve of the validation set. The abscissa of the graph is the predicted probability, and the ordinate is the actual probability. The ideal line indicates that the actual probability and the predicted probability are perfectly coincident under an ideal situation. The fitting line represents the predicted probability corresponding to the actual probability. If the predicted probability is greater than the actual probability, that is, the risk is

(Continued)

FIGURE 3 | overestimated, then the fitting line is under the ideal line. If the predicted probability is less than the actual probability, that is, the risk is underestimated, then the fitting line is above the ideal line. The graph also shows the performance of the model in B-fold cross-validation ($B = 10$).

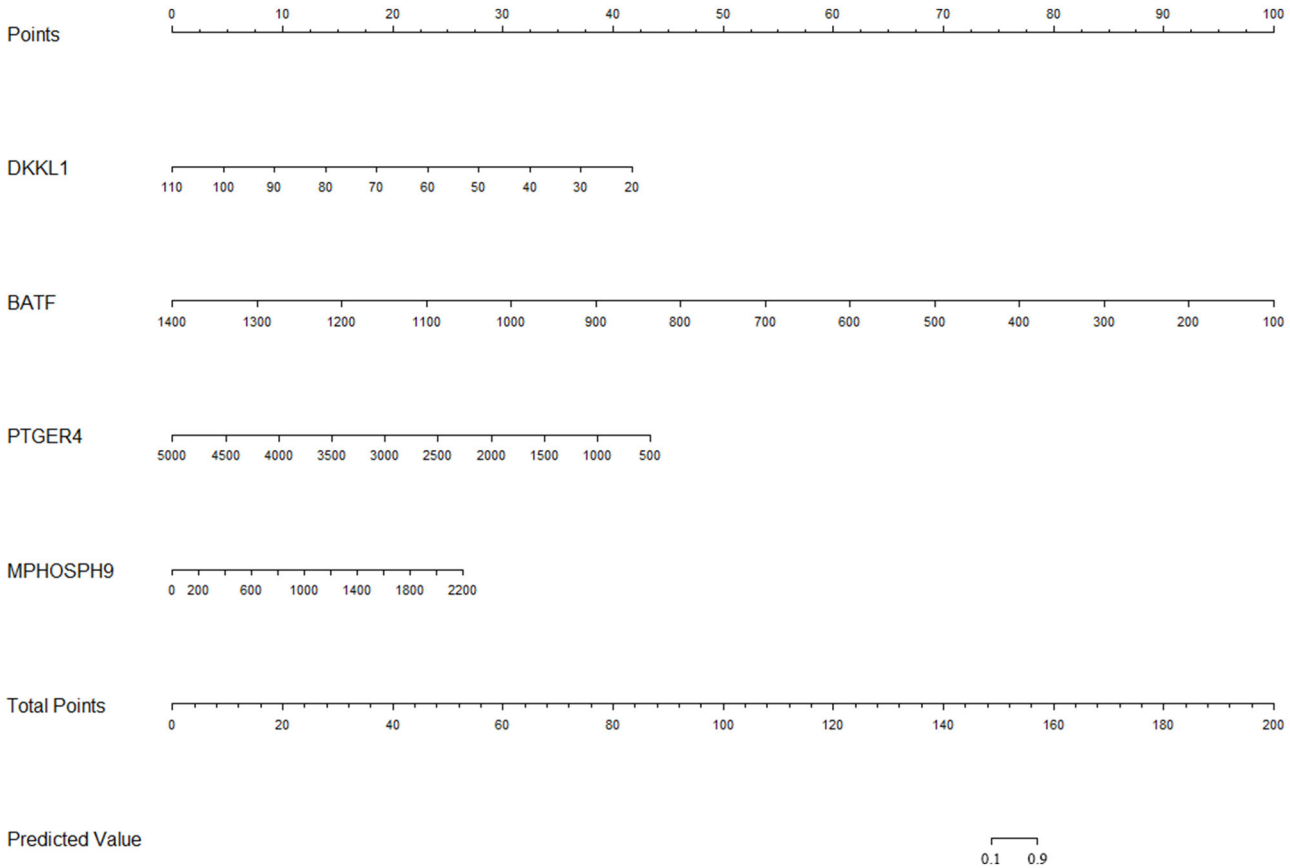

FIGURE 4 | The nomogram of the diagnosis model. Nomogram is a simple tool to calculate the output probability of the model. For more accurate probability calculation, please refer to the online prediction tool.

OCB has a very high negative predictive value, indicating other diagnoses should be considered (21). The detection of aquaporin-4 (AQP4) antibody can be used to distinguish MS and NMOSDs (22). For MS with the complexity of etiology, pathology, clinical manifestations, and the diversity of classification, it may be difficult to diagnose from a single aspect, and the combination of multiple evidence will improve the accuracy of the diagnosis. The inspiration for us is, a single gene may not be able to diagnose MS, but the diagnostic model based on the expression of multiple genes can significantly improve the accuracy.

At present, the auxiliary examination of MS mainly involves MRI, CSF electrophysiological evidence, and CSF immunological evidence. The blood biomarkers and the evidence based on peripheral blood gene expression have not reached a consensus in the diagnosis of MS. However, as an invasive examination, lumbar puncture increases the risk of hemorrhage and infection and has many complications such as cerebral hernia and low intracranial pressure. In addition, the blood sample is more inexpensive, more convenient to obtain, and more acceptable than a CSF sample. Therefore, based on the peripheral blood gene expression, the diagnosis model of MS was established, which provides a new dimension and a supplement for the diagnosis of MS.

At present, there are many popular methods applied to the diagnosis model, including support vector machine, artificial neural network, logical regression, and so on. Compared with the other model (23), the reason for choosing logistic regression in this study is that the linear regression model can output linear predicted probability, so as to provide a reference for clinical diagnosis. And the prediction accuracy is similar to other models. In addition, the nomogram and online prediction tool based on the logistic regression model can provide convenience for clinical diagnosis and are closely combined with the selected gene expression. The predicted probability of MS can be output by inputting the expression of 4 genes into the online prediction tool. Both machine learning and the logistic regression model selected in this study needed large data to train a model with excellent classification and prediction function. At present, the

A

Training set	Real MS	Real non-MS	total	Validation set	Real MS	Real non-MS	total
Predict MS	37	2	39	Predict MS	32	2	34
Predict non-MS	2	32	34	Predict non-MS	8	31	39
Total	39	34	73	Total	40	33	73

B

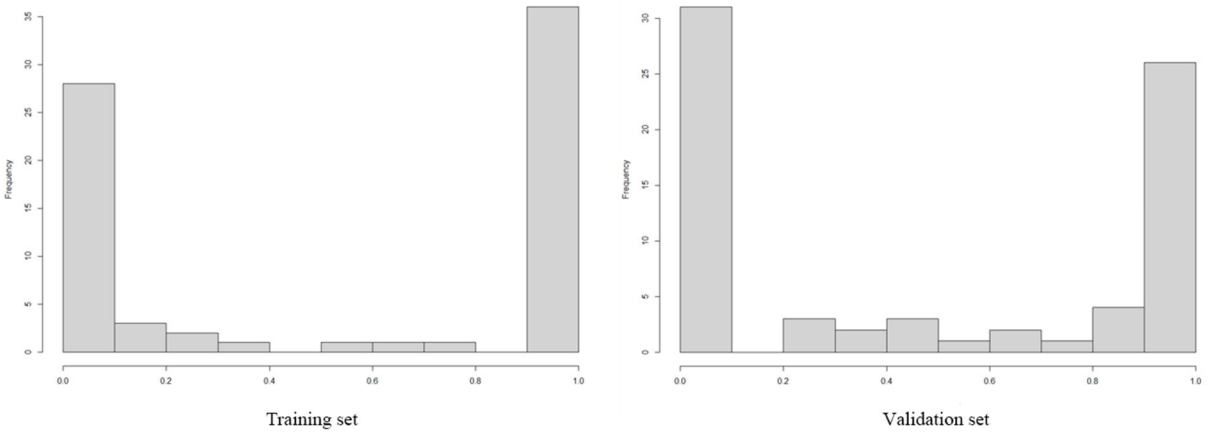

C

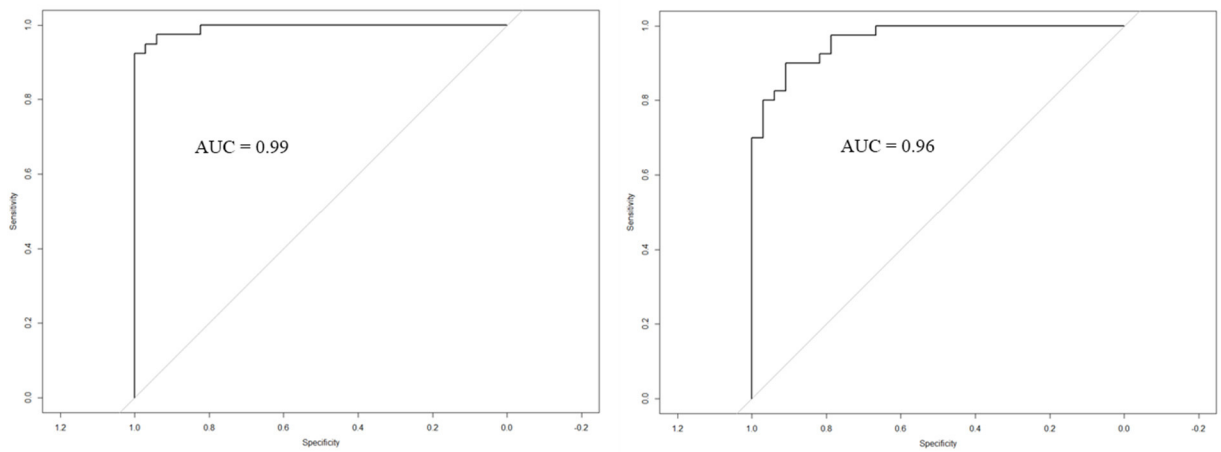

FIGURE 5 | (A) The confusion matrix of the prediction model. **(B)** The histogram of the output predicted probability, and it can be seen that the distribution of the predicted probability is concentrated at both ends. **(C)** The receiver operating characteristic curve (ROC). AUC is the size of the area under ROC.

sample size of a single microarray in GEO is often small. Therefore, most bioinformatics research adopted the method of combining microarray data from different data sets (but based on the same platform) to increase the sample size. For example, the SVA package of R is often used to remove the batch effect of the microarray from different data sets, which is widely used in data mining (24). However, eliminating the batch effect will inevitably modify the probe expression in the raw data as a whole. Whether there is a significant difference between the final model with the modified data as the training set and the final model with the raw data, and which of the final prediction accuracy of the two methods is better, the relevant literature support has not been found. Therefore, we chose to analyze the raw data of 147 gene chip arrays from three series in a unified way, so as to reduce the systematic error caused by directly merging the microarray matrix and the correction of batch effect.

BATF is a transcription factor that regulates IL-17 expression and Th17 differentiation. And early growth response gene-2 (Egr-2) is an intrinsic regulator that controls Th17 differentiation by inhibiting BATF activation, which may be important in controlling the development of multiple sclerosis (25). Dickkopf (Dkk) gene includes four members of a small gene family

(Dkk1-4) and a unique Dkk3-related gene DKKL1, which plays an important role in vertebrate development, and they locally inhibit Wnt regulated process. In adults, Dkks is related to bone formation and bone diseases, various tumors (including gliomas), and Alzheimer's disease (26). Although the expression of DKKL1 is necessary for normal nerve development, the over-expression of DKKL1 is the characteristic of many neurodegenerative diseases, such as stroke, Alzheimer's disease, Parkinson's disease, and temporal lobe epilepsy (27), and it can play an important role in pathological conditions such as tumorigenesis and cancer progression (28). Prostaglandin E2 receptor EP4 subtype (PTGER4) is highly correlated with immune response and inflammatory response (29), but its role in MS has not been systematically studied.

Unfortunately, the GPL570 chip does not annotate the probes of HLA-DRB1. However, studies on the relationship between HLA and diseases have shown that the incidence of some diseases is related to the detection rate of some special types of HLA. Most of these patients are diseases with unknown pathogenesis, abnormal immune function, and genetic tendency. Therefore, analyzing the expression of HLA antigen is not only helpful for understanding the pathogenesis but also is of great significance to the diagnosis, prevention, and prognosis of diseases. HLA class II encoded molecules are cell surface glycoproteins whose primary role in an immune response is to display and present short antigenic peptide fragments to peptide/MHC-specific T cells (30). In populations of European descent, allele DRB1*15:01 has the strongest association with multiple sclerosis among all HLA class II alleles (7).

The significance of the study lies in proving that it is feasible to identify MS by blood RNA, and the specificity of the model is still relatively high. In the future, it may be possible to combine image evidence, laboratory evidence, and genetic evidence into a diagnosis model based on machine learning. However, the sample size of the diagnostic model is too small for independent diagnosis and other CNS demyelinating diseases were not included in the training set (since no demyelination microarray data other than MS could be found in the GEO database). For further clinical application, it is still necessary to establish a larger sample cohort to include more other CNS diseases, especially inflammatory demyelinating diseases. In addition, the diagnosis model established in this study is only suitable for the gene chip based on the GPL570, which is a limitation for clinical use.

CONCLUSION

The diagnosis model based on microarray data in this study has a high accuracy of 86.30% in the validation set, which is helpful for diagnosis in the absence of evidence for DIS and DIT. Only one SLE case was misdiagnosed as MS, indicating that the model has high specificity (93.93%), which is useful for differential diagnosis. The significance of the study lies in proving that it is feasible to identify MS by peripheral blood RNA, and the further application of the model and be used as a supplement to McDonald Criteria still need to be trained with larger sample size.

METHODS

Data Retrieval Strategy

GEO is a public functional genomics database, which accepts microarray and sequence-based data. We searched with "demyelinating" and "blood" as the keywords, and preferred the data with large sample size, including MS, healthy control, and other inflammatory CNS diseases. In order to ensure the reliable prediction effect of the diagnosis model, we selected a training set to establish the model, and a validation set to verify the discrimination and calibration of the model. Considering the differences in the manufacturing process of chip manufacturers, we must ensure that the series of data comes from the same platform (Affymetrix Human Genome U133 Plus 2.0 Array, which is named GPL570 in GEO).

Processing of Raw Data

We downloaded the original probe files of GSE 61240, GSE 18781, and GSE 185047, with a total of 147 arrays. We used the RMA function of the R package "affy" to uniformly process the raw data, including background correction, standardization, summarization, and log-transformed. Through the above steps, we have got a matrix based on the expression of probes. Then, we annotated the probe matrix with R package "hgu133plus2.db," thus transforming the matrix from probe level to gene level. Since the data were log-transformed by the RMA function, we restored the data to facilitate the construction of the linear regression model. Finally, we obtained a microarray matrix with 20,862 rows and 147 columns. It is worth mentioning that there are 3 processed microarray matrixes in the GEO database for the three series. However, after being processed by different senders and batches, the microarray matrixes have a large systematic error, which is not conducive to the model construction and validation. Therefore, we must uniformly process the original 147 gene chip arrays so that the expression levels of the 147 chips of the three series are at the same level (as shown in **Figure 1**).

Screening Predictors by Random Forests

According to stratified random sampling, we divided the microarray matrix into a training set and a validation set. The training set and the validation set do not contain repeated samples. We initially selected 55 MS susceptibility locus genes identified by IMSGC and WTCCC2 as predictors for the model. Therefore, we excluded the other genes in the microarray matrix to reduce the amount of computation. Since GPL 570 does not have a probe to annotate TNFRSF6B, there are only 54 genes in the training set and the validation set. After importing data into R, the "status" was transformed into a classification variable and no missing values were found in the data. Subsequently, we further screened the predictors through Random Forests based on the R package "randomForest." When the classification tree reaches about 100 trees, the classification of Random Forests tends to be stable (as shown in **Figure 2**). At this point, we got the Gini index of the predictors and screened out the first 8 genes with a Gini index greater than 1.

Further Screening of Predictors and Establishment of Logistic Regression Model

The restricted cubic spline (RCS) was used for further non-linear tests of the selected predictors. After eliminating the predictors that do not satisfy the monotonicity, only the linear predictors were retained for the establishment of the logistic regression model. We found that there were influential points and multicollinearity in the model, and we excluded the samples with a Cook's distance greater than 1 to ensure that the data in the training set were reasonable. The predictors with multicollinearity were excluded to improve the stability of the model. After multiple screenings, only 4 out of the 55 initial predictors were used to construct the logistic regression model and the logistic regression model was established based on R packages "rms" and "glmnet."

Internal and External Validation of the Diagnosis Model

The logistic regression model is a powerful tool for the prediction of clinical events and allows both classified variables and continuous variables to be included in the model. In order to avoid underfitting or overfitting of the model, we carried out internal and external validation of the diagnosis model and measured the accuracy of the prediction results of the model through discrimination and calibration (31). In the internal validation, we used the original training set for validation and then carried out B-fold cross-validation. Before external validation, the data of the validation set was imported into R to identify the missing values and outliers of the data, and the classification variables were transformed into factor form. Finally, the validation set data was used for external validation of the model.

Establishment of Nomogram and Online Prediction Tool

After confirming that the diagnosis model has excellent prediction performance in both training set and validation set, the nomogram based on the logistic regression model is established by using the R package "rms." Nomogram is an imprecise calculation tool based on an image. After synthesizing the scores of all predictors, the total score is corresponding to the probability of the prediction result. The nomogram can roughly estimate the probability of disease occurrence of each clinical sample, which is simple and convenient. In order to further increase the accuracy of the prediction results, an online prediction tool was developed based on a dynamic nomogram to facilitate the further verification of the diagnosis model.

DATA AVAILABILITY STATEMENT

The datasets presented in this study can be found in online repositories. The names of the repositories and accession numbers can be found in the article.

AUTHOR CONTRIBUTIONS

WP: conception and design, funding and administrative support. WL and JY: provision of study materials. HL, HW, and JZ: collection and assembly of data. HL: data analysis and interpretation. All authors: manuscript writing and final approval.

FUNDING

This work was supported by the Shandong Provincial TCM Cardiovascular and Cerebrovascular Disease Clinical Medicine Research Center (2018103).

ACKNOWLEDGMENTS

We are very grateful to GEO database and all selfless researchers for their outstanding contributions.

SUPPLEMENTARY MATERIAL

The Supplementary Material for this article can be found online at: https://www.frontiersin.org/articles/10.3389/fneur.2021.721788/full#supplementary-material

REFERENCES

1. Howard J, Trevick S, Younger DS. Epidemiology of multiple sclerosis. *Neurol Clin.* (2016) 34:919–39. doi: 10.1016/j.ncl.2016.06.016
2. McGinley MP, Goldschmidt CH, Rae-Grant AD. Diagnosis and treatment of multiple sclerosis: a review. *JAMA.* (2021) 325:765–79. doi: 10.1001/jama.2020.26858
3. Feinstein A, Freeman J, Lo AC. Treatment of progressive multiple sclerosis: what works, what does not, and what is needed. *Lancet Neurol.* (2015) 14:194–207. doi: 10.1016/S1474-4422(14)70231-5
4. Brownlee WJ, Hardy TA, Fazekas F, Miller DH. Diagnosis of multiple sclerosis: progress and challenges. *Lancet.* (2017) 389:1336–46. doi: 10.1016/S0140-6736(16)30959-X
5. Labib DA, Ashmawy I, Elmazny A, Helmy H, Ismail RS. Toll-like receptors 2 and 4 expression on peripheral blood lymphocytes and neutrophils of Egyptian multiple sclerosis patients. *Int J Neurosci.* (2020) 26:1–5. doi: 10.1080/00207454.2020.1812601
6. Lavon I, Heli C, Brill L, Charbit H, Vaknin-Dembinsky A. Blood levels of co-inhibitory-receptors: a biomarker of disease prognosis in multiple sclerosis. *Front Immunol.* (2019) 10:835. doi: 10.3389/fimmu.2019.00835
7. Sawcer S, Hellenthal G, Pirinen M, Spencer CCA, Patsopoulos NA, Moutsianas L, et al. Genetic risk and a primary role for cell-mediated immune mechanisms in multiple sclerosis. *Nature.* (2011) 476:214–9. doi: 10.1038/nature10251
8. Ceriani L, Verme P. The origins of the Gini index: extracts from Variabilità e Mutabilità (1912) by Corrado Gini. *J Econ Inequal.* (2012) 10:421–43. doi: 10.1007/s10888-011-9188-x
9. Jin Z, Shang J, Zhu Q, Ling C, Xie W, Qiang B. RFRSF: employee turnover prediction based on random forests and survival analysis. In: *Web Information Systems Engineering – WISE 2020.* Cham (2020). doi: 10.1007/978-3-030-62008-0_35

10. Midi H, Sarkar SK, Rana S. Collinearity diagnostics of binary logistic regression model. *J Interdiscip Math.* (2010) 13:253–67. doi: 10.1080/09720502.2010.10700699
11. Kim C, Lee Y, Park BU. Cook's distance in local polynomial regression. *Stat Probab Lett.* (2001) 54:33–40. doi: 10.1016/S0167-7152(01)00031-1
12. Thompson AJ, Banwell BL, Barkhof F, Carroll WM, Coetzee T, Comi G, et al. Diagnosis of multiple sclerosis: 2017 revisions of the McDonald criteria. *Lancet Neurol.* (2018) 17:162–73. doi: 10.1016/S1474-4422(17)30470-2
13. Weinshenker BG, Bass B, Rice GP, Noseworthy J, Carriere W, Baskerville J, et al. The natural history of multiple sclerosis: a geographically based study. 2. Predictive value of the early clinical course. *Brain.* (1989) 112(Pt 6):1419–28. doi: 10.1093/brain/112.6.1419
14. Weinshenker BG, Bass B, Rice GP, Noseworthy J, Carriere W, Baskerville J, et al. The natural history of multiple sclerosis: a geographically based study. I. Clinical course and disability. *Brain.* (1989) 112(Pt 1):133–46. doi: 10.1093/brain/112.1.133
15. Clarke MA, Pareto D, Pessini-Ferreira L, Arrambide G, Alberich M, Crescenzo F, et al. Value of 3T susceptibility-weighted imaging in the diagnosis of multiple sclerosis. *AJNR Am J Neuroradiol.* (2020) 41:1001–8. doi: 10.3174/ajnr.A6547
16. Absinta M, Nair G, Monaco MCG, Maric D, Lee NJ, Ha S-K, et al. The "central vein sign" in inflammatory demyelination: the role of fibrillar collagen type I. *Ann Neurol.* (2019) 85:934–42. doi: 10.1002/ana.25461
17. Sinnecker T, Clarke MA, Meier D, Enzinger C, Calabrese M, De Stefano N, et al. Evaluation of the central vein sign as a diagnostic imaging biomarker in multiple sclerosis. *JAMA Neurol.* (2019) 76:1446–56. doi: 10.1001/jamaneurol.2019.2478
18. Wattjes MP, Ciccarelli O, Reich DS, Banwell B, de Stefano N, Enzinger C, et al. 2021 MAGNIMS–CMSC–NAIMS consensus recommendations on the use of MRI in patients with multiple sclerosis. *Lancet Neurol.* (2021) 20:653–70. doi: 10.1016/S1474-4422(21)00095-8
19. Filippi M, Rocca MA, Ciccarelli O, De Stefano N, Evangelou N, Kappos L, et al. MRI criteria for the diagnosis of multiple sclerosis: MAGNIMS consensus guidelines. *Lancet Neurol.* (2016) 15:292–303. doi: 10.1016/S1474-4422(15)00393-2
20. D'Ambrosio A, Pontecorvo S, Colasanti T, Zamboni S, Francia A, Margutti P. Peripheral blood biomarkers in multiple sclerosis. *Autoimmun Rev.* (2015) 14:1097–110. doi: 10.1016/j.autrev.2015.07.014
21. Deisenhammer F, Zetterberg H, Fitzner B, Zettl UK. The Cerebrospinal Fluid in Multiple Sclerosis. *Front Immunol.* (2019) 10:726. doi: 10.3389/fimmu.2019.00726
22. Polman CH, Reingold SC, Banwell B, Clanet M, Cohen JA, Filippi M, et al. Diagnostic criteria for multiple sclerosis: 2010 revisions to the McDonald criteria. *Ann Neurol.* (2011) 69:292–302. doi: 10.1002/ana.22366
23. Chen X, Hou H, Qiao H, Fan H, Zhao T, Dong M. Identification of blood-derived candidate gene markers and a new 7-gene diagnostic model for multiple sclerosis. *Biol Res.* (2021) 54:12. doi: 10.1186/s40659-021-00334-6
24. Leek JT, Johnson WE, Parker HS, Jaffe AE, Storey JD. The sva package for removing batch effects and other unwanted variation in high-throughput experiments. *Bioinformatics.* (2012) 28:882–3. doi: 10.1093/bioinformatics/bts034
25. Miao T, Raymond M, Bhullar P, Ghaffari E, Symonds ALJ, Meier UC, et al. Early growth response gene-2 controls IL-17 expression and Th17 differentiation by negatively regulating Batf. *J Immunol.* (2013) 190:58–65. doi: 10.4049/jimmunol.1200868
26. Niehrs C. Function and biological roles of the Dickkopf family of Wnt modulators. *Oncogene.* (2006) 25:7469–81. doi: 10.1038/sj.onc.1210054
27. Scott EL, Brann DW. Estrogen regulation of Dkk1 and Wnt/β-Catenin signaling in neurodegenerative disease. *Brain Res.* (2013) 1514:63–74. doi: 10.1016/j.brainres.2012.12.015
28. Sibbe M, Jarowyj J. Region-specific expression of Dickkopf-like1 in the adult brain. Abbreviated title: Dkkl1 in the adult brain. *Neurosci Lett.* (2013) 535:84–9. doi: 10.1016/j.neulet.2012.12.040
29. Gaudet P, Livstone MS, Lewis SE, Thomas PD. Phylogenetic-based propagation of functional annotations within the Gene Ontology consortium. *Brief Bioinform.* (2011) 12:449–62. doi: 10.1093/bib/bbr042
30. Hollenbach JA, Oksenberg JR. The immunogenetics of multiple sclerosis: a comprehensive review. *J Autoimmun.* (2015) 64:13–25. doi: 10.1016/j.jaut.2015.06.010
31. Harrell FEJ, Lee KL, Mark DB. Multivariable prognostic models: issues in developing models, evaluating assumptions and adequacy, and measuring and reducing errors. *Stat Med.* (1996) 15:361–87. doi: 10.1002/(SICI)1097-0258(19960229)15:4<361::AID-SIM168>3.0.CO;2-4

Conflict of Interest: The authors declare that the research was conducted in the absence of any commercial or financial relationships that could be construed as a potential conflict of interest.

Publisher's Note: All claims expressed in this article are solely those of the authors and do not necessarily represent those of their affiliated organizations, or those of the publisher, the editors and the reviewers. Any product that may be evaluated in this article, or claim that may be made by its manufacturer, is not guaranteed or endorsed by the publisher.

frontiers in Immunology

BRIEF RESEARCH REPORT
published: 01 February 2022
doi: 10.3389/fimmu.2022.819224

CCR6 and CXCR6 Identify the Th17 Cells With Cytotoxicity in Experimental Autoimmune Encephalomyelitis

Lifei Hou [1,2*] *and Koichi Yuki* [1,2*]

[1] *Department of Anesthesiology, Critical Care and Pain Medicine, Boston Children's Hospital, Boston, MA, United States,*
[2] *Department of Anaesthesia and Department of Immunology, Harvard Medical School., Boston, MA, United States*

Due to the plasticity of IL-17-producing CD4 T cells (Th17 cells), a long-standing challenge in studying Th17-driven autoimmune is the lack of specific surface marker to identify the pathogenic Th17 cells *in vivo*. Recently, we discovered that pathogenic CD4 T cells were CXCR6 positive in experimental autoimmune encephalomyelitis (EAE), a commonly used Th17-driven autoimmune model. Herein, we further revealed that peripheral CXCR6^{+}CD4 T cells contain a functionally distinct subpopulation, which is CCR6 positive and enriched for conventional Th17 molecules (IL-23R and RORγt) and cytotoxic signatures. Additionally, spinal cord-infiltrating CD4 T cells were highly cytotoxic by expressing Granzyme(s) along with IFNγ and GM-CSF. Collectively, this study suggested that peripheral CCR6^{+}CXCR6^{+}CD4 T cells were Th17 cells with cytotoxic property in EAE model, and highlighted the cytotoxic granzymes for EAE pathology.

Keywords: CXCR6, CCR6, Th17, cytotoxicity, EAE, Multiple Sclerosis

OPEN ACCESS

Edited by:
Luisa María Villar, Ramón y Cajal University Hospital, Spain

Reviewed by:
Luc Van Kaer, Vanderbilt University, United States
Iain Comerford, University of Adelaide, Australia

***Correspondence:**
Lifei Hou
Lifei.Hou@childrens.harvard.edu
Koichi Yuki
Koichi.Yuki@childrens.harvard.edu

Specialty section:
This article was submitted to Multiple Sclerosis and Neuroimmunology, a section of the journal Frontiers in Immunology

Received: *21 November 2021*
Accepted: *11 January 2022*
Published: *01 February 2022*

Citation:
Hou L and Yuki K (2022) CCR6 and CXCR6 Identify the Th17 Cells With Cytotoxicity in Experimental Autoimmune Encephalomyelitis. Front. Immunol. 13:819224. doi: 10.3389/fimmu.2022.819224

INTRODUCTION

Multiple sclerosis (MS) is a devastating autoimmune disease with progressive neurological dysfunction due to demyelination of the central nerve system (CNS) (1). EAE is the most commonly used murine MS model and driven by self-reactive CD4 T cells (CD4 cells thereafter) (1). The disease-inducing CD4 cells were initially thought to be Th1 cells, but later were described as Th17 cells (2, 3). Indeed, Th17 cells themselves are not pathogenic (4), but are converted, under the priming of myeloid cell-derived IL-1 and IL-23 (5–7), into pathogenic CD4 cells, which lose IL-17-producing ability and alternatively produce IFNγ and GM-CSF (8–12). Despite their cytokine profiles, little else is known about the pathogenic CD4 cells, mainly due to the lack of specific marker to precisely identify them *in vivo*.

We previously found SerpinB1 (sb1, Serine Protease Inhibitor B1), an endogenous protease inhibitor (13), to be a signature gene of IL-17-producing γδ T cells (14) and Th17 cells (15). Subsequent studies showed that *sb1-ko* mice were resistant to EAE with a paucity of CXCR6^{+}CD4 cells (16), which were highly enriched in the spinal cord, secreted inflammatory cytokine IFNγ and GM-CSF, contained cytotoxic Granzyme-C, and proliferated rapidly (16). Depleting CXCR6^{+}CD4 cells by anti-CXCR6 antibody dramatically ameliorated established EAE, confirming the

CXCR6+CD4 cells as the driver of EAE pathology (16). In this study, we further characterized CXCR6+CD4 cells.

MATERIAL AND METHOD

Mice

Wild type C57BL/6J mice (*wild type*, *wt*) were originally purchased from the Jackson laboratory and maintained in an animal facility at the Boston Children's Hospital. Animal protocols were approved by the Institutional Animal Care and Use Committee of Boston Children's Hospital. EAE model induction, flow cytometry, cell sorting, q-PCR analysis, cell counting, and RNA sequencing were performed as previously described (16). In brief, to induce EAE, *wt* mice in the C57BL/6J background were injected with MOG_{35-55} emulsified with complete Freund's adjuvant followed by 200 ng pertussis toxin on days 0 and 2.

RNAseq Analysis

CD4 effector cells (CD44+CD4) were sort-purified from pooled draining lymph node (dLN) cells and spinal cords of MOG-immunized *wt* mice by FACSAria system at the disease onset. The cells were stimulated for 4 h with PMA (50 ng/ml) and ionomycin (750 ng/ml) (Sigma-Aldrich), and RNA was purified using QIAGEN RNeasy Plus Mini kits and quantified by optical density at 260/280/230 nm. TruSeq RNA V2 kits were used to construct transcript-specific libraries that were sequenced on Illumina HiSeq2500. The resulting 4.5 Gb/genotype of raw data was trimmed, and 20 million reads were mapped. Genes that had expression levels (FPKM) ≥1.0 were analyzed for differential expression (https://www.ncbi.nlm.nih.gov/geo/query/acc.cgi?acc=GSE192878)

Reverse Transcription and qPCR Analysis

CCR6+CXCR6-CD44+CD4, CCR6+CXCR6+CD44+CD4, CCR6-CXCR6+CD44+CD4 were sort-purified from pooled lymph node cells of MOG-immunized *wt* mice by FACSAria system at disease onset. RNA was isolated using RNeasy Plus kits (74134, Qiagen) according to the manufacturer's protocol and reverse-transcribed using the iScript™ cDNA Synthesis kit (Bio-Rad). The qPCR assays were performed on the CFX96™ Real-Time System (Bio-Rad) with the iTaq™ Universal SYBR Green Supermix (Bio-Rad) using 30 s denaturation at 95°C and 40 cycles of 5 s at 95°C and 30 s at 61°C using the primers. Relative expression level for each gene was calculated by using the $^{\Delta\Delta}$Ct method and normalizing to *Actb*.

Flow Cytometry

Cells were stained with fluorochrome-conjugated antibodies to surface markers. Fluorochrome-conjugated antibodies were from Biolegend: FITC- or PE-Cy7-anti-mCD3 (145-2C11), Pacific blue- or PE-anti-mCD45 (30-F11), Pacific blue- or PE-Cy7- or APC- anti-mCD4 (GK1.5), PE-anti-mIL1R1 (JAMA-147), FITC-anti-mCD44 (IM7), APC-anti-mCXCR6 (SA051D1), APC- or PE-Cy7-anti-mCCR6 (29-2L17). From R&D system: PE-anti-mIL-23R (753317). Data were acquired on a Canto II cytometer (BD Biosciences) and analyzed using FlowJo software (Tree Star). Cell counting was achieved by using AccuCount beads (Spherotech).

CyTOF Assay

After red blood cell lysis, both draining lymph node cells and peripheral blood cells were stimulated for 4 h with PMA (50 ng/ml) and ionomycin (750 ng/ml) (Sigma-Aldrich) in the presence of Brefeldin A. Cells were then collected and resuspended in cell staining buffer (Fluidigm; San Francisco, CA). After centrifugation, Fc receptor blocking reagent (clone 93, Biolegend) was used at a 1:100 dilution in for 10 min, followed by incubation with metal conjugated surface antibodies for 30 min. Then the cells were fixed and permeabilized by using fixation/permeabilization reagents (BD Bioscience). The permeabilization buffer was made by diluting the 10× stock solution (51-2091, BD Biosciences) in UltraPure distilled water (Invitrogen). All antibodies were purchased from the CyTOF core facility at Brigham and Women's Hospital. DNA was labeled with iridium intercalator solution (Fluidigm). Samples were subsequently washed and reconstituted in Milli-Q filtered distilled water in the presence of EQ Four Element Calibration beads (Fluidigm, catalog 201078). Samples were acquired on a Helios CyTOF Mass Cytometer (Fluidigm) at Cellular Profiling Core Facility (School of Public Health, Harvard Medical School, Boston, MA, USA); Data were analyzed by using spanning-tree progression analysis of density-normalized events (SPADE) and vi stochastic neighbor embedding (SNE) on Cytobank software.

Statistical Analysis

Statistical analyses were performed using Prism 4 (Graphpad Software). Student's *t*-test was used. P-values <0.05 were considered significant.

RESULTS

We immunized the wild type (wt) mice with MOG to induce EAE and monitored the CXCR6+CD4 cells in the blood. Results showed that CXCR6+CD4 cells did not exist in naïve *wt* mice, but were dramatically induced in the blood with EAE induction (**Figures 1A, B**). Although CXCR6+CD4 cells dramatically accumulated in the peripheral blood of EAE mice, *Cxcr6-ko* and *wt* mice developed comparable EAE symptom (17), suggesting that CXCR6 might only serve as a marker and be dispensable for CD4 cell chemotaxis in EAE. Since CCR6 has been well established as a chemokine receptor preferentially expressed on conventional Th17 cells (18), especially the one generated *in vitro*, we then co-stained the CCR6 and CXCR6 on draining lymph node (dLN)-derived CD4 cells at EAE onset. Strikingly, we found CXCR6+CD4 cells could be divided into two subpopulations: CCR6 positive and CCR6 negative ones (**Figure 1C**). We then sorted out the CCR6+CXCR6- (as control), CCR6+CXCR6+, and CCR6-CXCR6+ effector CD4 cells from dLN at EAE onset. Q-PCR experiment showed that CCR6+CXCR6+ effector CD4 cells

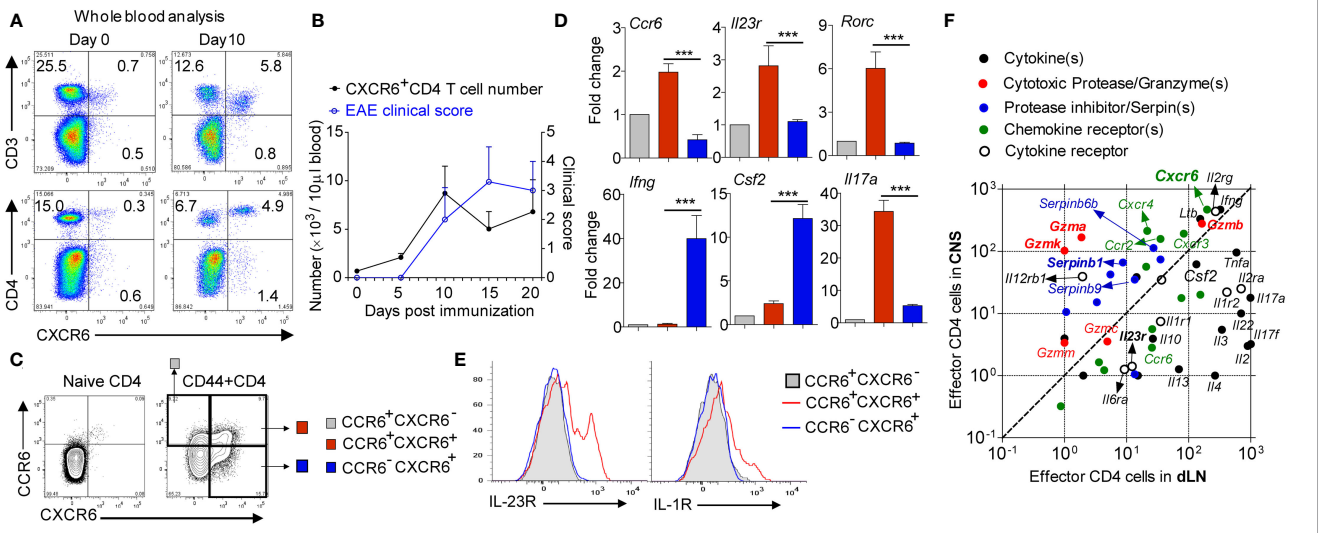

FIGURE 1 | CXCR6+CD4 cells in EAE. **(A)** Representative FACS data gating on blood leukocyte. **(B)** Cell number. N = 4 in each time points. **(C)** Gating strategy for FACS sorting or analysis of CD4 cells in dLN at EAE onset. **(D)** Relative gene expression of CCR6+CXCR6–, CCR6+CXCR6+and CCR6–CXCR6+ effector CD4 cells; CCR6+CXCR6– was used as control. Data are mean ± SEM of 3 independent experiments. ***p <0.001. **(E)** Representative FACS data showing IL23R and IL1R expression on CD4 cells in dLN at EAE onset. **(F)** Effector CD4 cells were isolated from both dLN and spinal cord at EAE onset, and subjected to bulk RNAseq. Data are presented by FMPK.

majorly expressed conventional Th17 signatures including *Il23r*, *Il17a* and *Rorc*, while CCR6$^-$CXCR6$^+$ ones majorly expressed *Ifng* and *Csf2* (encoding GM-CSF), a typical ex-Th17 phenotype (**Figure 1D**). Flow cytometry analysis further confirmed that IL-23R and IL-1R were exclusively expressed on CCR6$^+$CXCR6$^+$CD4 cells (**Figure 1E**).

A long-standing difficulty in treating autoimmune disease, such as MS, is the lack of understanding of inflammatory tissue-infiltrating CD4 cells. Given that most of CNS-infiltrating CD4 cells are CXCR6 positive, we compared the transcriptome profile between CNS-infiltrating CD4 cells and peripheral effector CD4 cells in EAE. We sorted out the spinal cord-infiltrated CD4 cells, and compared them with effector CD4 from dLN at EAE onset and discovered that all of *Il17a*, *Ccr6*, and *Il23r* were downregulated in spinal cord-infiltrated CD4 cells, suggesting a terminal differentiated effector status. Interestingly, we found that CD4 cells in the spinal cord were cytotoxic by highly expressing Granzyme(s) and cognate serine protease inhibitor Serpin(s) along with IFNγ and GM-CSF (**Figure 1F**). Indeed, this finding matches with the human MS study that CD4 cells from human secondary progressive MS autopsy brain samples are cytotoxic by co-expression of Eomes and Granzyme-B (19).

To further confirm the existence of distinct subpopulation within CXCR6$^+$CD4 cells in the periphery at EAE onset, cytometry by time of flight (CyTOF) was applied (20), which is a powerful discovery tool in identifying rare cell population and cluster. A CyTOF study of 22 markers for effector CD4 cells showed that all of IFNγ (IL-2 negative portion), GM-CSF, IL-17, IL-23R, CD107a, Granzyme-B, IL-1R1 and CCR6 and partial of T-bet and RORγt overlapped with CXCR6 expression, suggesting CXCR6 as a marker for pathogenic CD4 cells (**Figure 2A**). We then focused on CXCR6$^+$CD44$^+$CD4 cells, and finally confirmed that they contained a distinct CCR6 positive subpopulation, which was enriched with conventional Th17 molecules (IL-1R, IL-17, IL-23R, and RORγt), and also highly cytotoxic by expressing Perforin, CD107a and Granzyme-B (**Figure 2B**). We observed partial overlap among IFNγ, IL-17 and GM-CSF, which might suggest the co-existence of conventional Th17 and ex-Th17 cells. Interestingly, IFNγ staining did not match with T-bet well, deemed as Th1 transcriptional factor responsible for IFNγ expression. Similarly, IL-17 staining did not match with RORγt well. This discrepancy between cytokines and corresponding transcriptional factors might be due to that PMA and ionomycin stimulation will preferentially accumulate the cytokine, not the transcriptional factors, for detection. It also could be due to the complex roles of transcriptional factors involved in the CD4 cell plasticity in autoimmunity. Purified PBMC from the peripheral blood were subjected to CyTOF analysis in parallel and showed identical profile as dLN (data not shown).

DISCUSSION

Recently, we identified that chemokine receptor CXCR6 was preferentially expressed on pathogenic CD4 cells in EAE model (16), which i) secreted inflammatory cytokine IFNγ and GM-CSF, ii) contained cytotoxic granules, and iii) proliferated rapidly. In the current study, we further revealed that CXCR6$^+$CD4 cells in EAE mice were heterogeneous, divided into two distinct subpopulations. One was CCR6 positive, enriched for cytotoxic signatures (Perforin, CD107a and

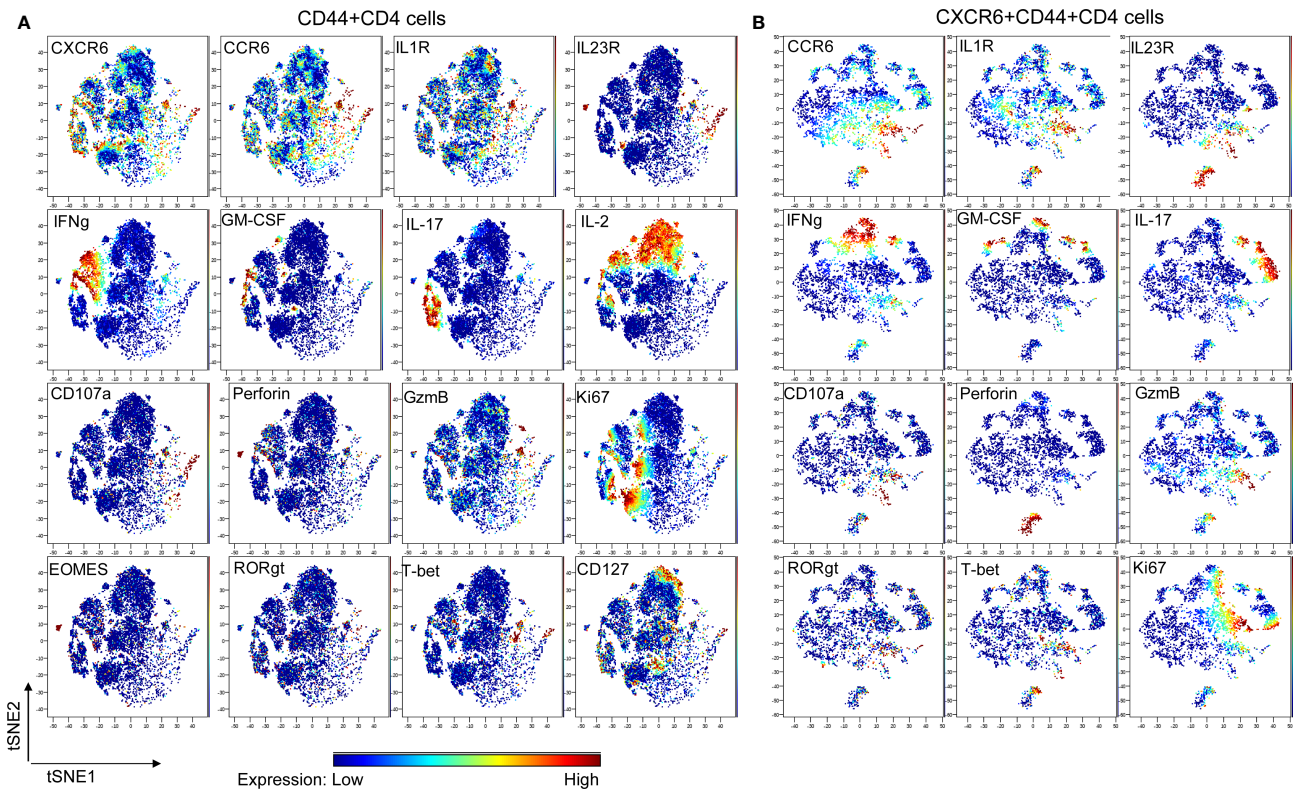

FIGURE 2 | CyTOF study. *Wt* mice were induced to develop EAE and sacrificed at the disease onset (N = 9; dLN from every 3 mice were pooled and deemed as one biological sample). Lymphocytes were stimulated with PMA & Ionomycin for 4 h in the presence of Brefeldin A, then were stained with metal-conjugated mAbs and subjected to CyTOF analysis. CXCR6 mAb and CD107a mAb were added during the stimulation. Shown are viSNE plots of CyTOF of effector CD4 **(A)** and CXCR6$^+$ effector CD4 **(B)** of one of 3 biological samples with the same pattern. The color indicates expression level of labeled marker.

GzmB) and conventional Th17 molecules (IL-17, IL-23R and RORγt); while the other was CCR6 negative, enriched solely for cytokine IFNγ and GM-CSF. Of note, although CCR6 has been established as a chemokine receptor of conventional Th17 cells, its role in EAE is still controversial since EAE disease varies from total absence (21, 22) to be delayed but more severe or totally normal (23, 24) in *ccr6*-deficient mice.

Regarding the EAE pathology, the current perception is that CD4 cells mainly interact with myeloid cells to indirectly induce the myelin sheath damage in EAE. It is unknown whether CD4 cells directly mediate the CNS damage and which molecule(s) mediate the process when that is the case. Although CD4 cell-derived GM-CSF is thought to be essential for EAE development, GM-CSF-deficient mice develop comparable EAE disease as wild type (*wt*) mice when regulatory T cells are depleted (25), suggesting that GM-CSF might function through peripheral priming step to mediate EAE. Indeed, the clinical trial of anti-GM-CSF antibody hasn't been successful to date for MS. Thus, it is possible that EAE pathology is induced by GM-CSF-producing CD4 cells, rather than GM-CSF itself, and there might be other factors that are responsible for CD4 cell pathogenicity in EAE and human MS.

In this study, we discovered that CNS-infiltrated CD4 cells were highly cytotoxic by highly expressing various cytotoxic granzymes and cognate inhibitor Serpin(s). Granzyme(s) possesses broad pathological functions, such as triggering apoptosis of target cells (26), degrading the extracellular matrix (27), activating the myeloid cells (28, 29), and inducing self-inflicted cell death (30, 31). The finding that CNS-infiltrated CD4 cells highly expressed all of Gzm-A, -B, -K and endogenous inhibitor Serpin(s) strongly suggests that the pathogenic CD4 cells may use the Granzyme(s) to directly mediate CNS damage or to induce activation-induced cell death to maintain the homeostasis.

Overall, in the current study, we identified two distinct subpopulations in CXCR6$^+$CD4 cells in EAE: CCR6$^+$ cells (enriched for conventional Th17 signature with unexpected cytotoxic signature) and CCR6$^-$ cells (enriched for cytokine IFNγ and GM-CSF, an ex-Th17 signature). The discovery of these two subpopulations makes *in vivo* generated pathogenic CD4 cells amenable for direct investigation. Our study also highlights the existence of cytotoxic protease(s) of encephalitogenic CD4 cells, which might be the mediator to directly mediate the CNS damage in MS. The relationship between Th17 programming and acquisition of cytotoxicity is not understood; the co-existence of these two functionally distinct subpopulations is elusive and intriguing, which requires the further investigations.

DATA AVAILABILITY STATEMENT

The datasets presented in this study can be found in online repositories. The names of the repository/repositories and accession number(s) can be found below: NCBI GEO, GSE192878 https://www.ncbi.nlm.nih.gov/geo/query/acc.cgi?acc=GSE192878.

ETHICS STATEMENT

The animal study was reviewed and approved by the Institutional Animal Care and Use Committee of Boston Children's Hospital.

AUTHOR CONTRIBUTIONS

Both authors, LH and KY, designed the research, did the experiment, analyzed the data and wrote the manuscript. All authors listed have made a substantial, direct, and intellectual contribution to the work and approved it for publication.

ACKNOWLEDGMENTS

We thank Dr. Eileen Remold-O'Donnell for providing the essential reagents and discussion, and XiaoDong Wang for assisting the CyTOF. This study is partially funded by the Anesthesia Research Distinguished Ignition Award (LH).

REFERENCES

1. Compston A, Coles A. Multiple Sclerosis. *Lancet* (2008) 372(9648):1502–17. doi: 10.1016/S0140-6736(08)61620-7
2. Cua DJ, Sherlock J, Chen Y, Murphy CA, Joyce B, Seymour B, et al. Interleukin-23 Rather Than Interleukin-12 is the Critical Cytokine for Autoimmune Inflammation of the Brain. *Nature* (2003) 421(6924):744–8. doi: 10.1038/nature01355
3. Ivanov II, McKenzie BS, Zhou L, Tadokoro CE, Lepelley A, Lafaille JJ, et al. The Orphan Nuclear Receptor RORgammat Directs the Differentiation Program of Proinflammatory IL-17+ T Helper Cells. *Cell* (2006) 126 (6):1121–33. doi: 10.1016/j.cell.2006.07.035
4. Haak S, Croxford AL, Kreymborg K, Heppner FL, Pouly S, Becher B, et al. IL-17A and IL-17F do Not Contribute Vitally to Autoimmune Neuro-Inflammation in Mice. *J Clin Invest* (2009) 119(1):61–9. doi: 10.1172/JCI35997
5. Sutton C, Brereton C, Keogh B, Mills KH, Lavelle EC. A Crucial Role for Interleukin (IL)-1 in the Induction of IL-17-Producing T Cells That Mediate Autoimmune Encephalomyelitis. *J Exp Med* (2006) 203(7):1685–91. doi: 10.1084/jem.20060285
6. McGeachy MJ, Chen Y, Tato CM, Laurence A, Joyce-Shaikh B, Blumenschein WM, et al. The Interleukin 23 Receptor Is Essential for the Terminal Differentiation of Interleukin 17-Producing Effector T Helper Cells. *vivo Nat Immunol* (2009) 10(3):314–24. doi: 10.1038/ni.1698
7. Ronchi F, Basso C, Preite S, Reboldi A, Baumjohann D, Perlini L, et al. Experimental Priming of Encephalitogenic Th1/Th17 Cells Requires Pertussis Toxin-Driven IL-1beta Production by Myeloid Cells. *Nat Commun* (2016) 7:11541. doi: 10.1038/ncomms11541
8. Codarri L, Gyülvészi G, Tosevski V, Hesske L, Fontana A, Magnenat L, et al. RORgammat Drives Production of the Cytokine GM-CSF in Helper T Cells, Which Is Essential for the Effector Phase of Autoimmune Neuroinflammation. *Nat Immunol* (2011) 12(6):560–7. doi: 10.1038/ni.2027
9. El-Behi M, Ciric B, Dai H, Yan Y, Cullimore M, Safavi F, et al. The Encephalitogenicity of T(H)17 Cells Is Dependent on IL-1- and IL-23-Induced Production of the Cytokine GM-CSF. *Nat Immunol* (2011) 12 (6):568–75. doi: 10.1038/ni.2031
10. McQualter JL, Darwiche R, Ewing C, Onuki M, Kay TW, Hamilton JA, et al. Granulocyte Macrophage Colony-Stimulating Factor: A New Putative Therapeutic Target in Multiple Sclerosis. *J Exp Med* (2001) 194(7):873–82. doi: 10.1084/jem.194.7.873
11. Ghoreschi K, Laurence A, Yang XP, Tato CM, McGeachy MJ, Konkel JE, et al. Generation of Pathogenic T(H)17 Cells in the Absence of TGF-Beta Signalling. *Nature* (2010) 467(7318):967–71. doi: 10.1038/nature09447
12. Hirota K, Duarte JH, Veldhoen M, Hornsby E, Li Y, Cua DJ, et al. Fate Mapping of IL-17-Producing T Cells in Inflammatory Responses. *Nat Immunol* (2011) 12(3):255–63. doi: 10.1038/ni.1993
13. Remold-O'Donnell E, Chin J, Alberts M. Sequence and Molecular Characterization of Human Monocyte/Neutrophil Elastase Inhibitor. *Proc Natl Acad Sci USA* (1992) 89(12):5635–9. doi: 10.1073/pnas.89.12.5635
14. Zhao P, Hou L, Farley K, Sundrud MS, Remold-O'Donnell E. SerpinB1 Regulates Homeostatic Expansion of IL-17+ Gammadelta and CD4+ Th17 Cells. *J Leukoc Biol* (2014) 95(3):521–30. doi: 10.1189/jlb.0613331
15. Hou L, Cooley J, Swanson R, Ong PC, Pike RN, Bogyo M, et al. The Protease Cathepsin L Regulates Th17 Cell Differentiation. *J Autoimmun* (2015) 65:56–63. doi: 10.1016/j.jaut.2015.08.006
16. Hou L, Rao DA, Yuki K, Cooley J, Henderson LA, Jonsson AH, et al. SerpinB1 Controls Encephalitogenic T Helper Cells in Neuroinflammation. *Proc Natl Acad Sci U S A* (2019) 116(41):20635–43. doi: 10.1073/pnas.1905762116
17. Kim JV, Jiang N, Tadokoro CE, Liu L, Ransohoff RM, Lafaille JJ, et al. Two-Photon Laser Scanning Microscopy Imaging of Intact Spinal Cord and Cerebral Cortex Reveals Requirement for CXCR6 and Neuroinflammation in Immune Cell Infiltration of Cortical Injury Sites. *J Immunol Methods* (2010) 352(1-2):89–100. doi: 10.1016/j.jim.2009.09.007
18. Annunziato F, Cosmi L, Santarlasci V, Maggi L, Liotta F, Mazzinghi B, et al. Phenotypic and Functional Features of Human Th17 Cells. *J Exp Med* (2007) 204(8):1849–61. doi: 10.1084/jem.20070663
19. Raveney BJE, Sato W, Takewaki D, Zhang C, Kanazawa T, Lin Y, et al. Involvement of Cytotoxic Eomes-Expressing CD4(+) T Cells in Secondary Progressive Multiple Sclerosis. *Proc Natl Acad Sci U S A* (2021) 118(11): e2021818118. doi: 10.1073/pnas.2021818118
20. Kimball AK, Oko LM, Bullock BL, Nemenoff RA, van Dyk LF, Clambey ET. A Beginner's Guide to Analyzing and Visualizing Mass Cytometry Data. *J Immunol* (2018) 200(1):3–22. doi: 10.4049/jimmunol.1701494
21. Reboldi A, Coisne C, Baumjohann D, Benvenuto F, Bottinelli D, Lira S, et al. C-C Chemokine Receptor 6-Regulated Entry of TH-17 Cells Into the CNS Through the Choroid Plexus is Required for the Initiation of EAE. *Nat Immunol* (2009) 10(5):514–23. doi: 10.1038/ni.1716
22. Liston A, Kohler RE, Townley S, Haylock-Jacobs S, Comerford I, Caon AC, et al. Inhibition of CCR6 Function Reduces the Severity of Experimental Autoimmune Encephalomyelitis via Effects on the Priming Phase of the Immune Response. *J Immunol* (2009) 182(5):3121–30. doi: 10.4049/jimmunol.0713169
23. Villares R, Cadenas V, Lozano M, Almonacid L, Zaballos A, Martínez AC, et al. CCR6 Regulates EAE Pathogenesis by Controlling Regulatory CD4+ T-Cell Recruitment to Target Tissues. *Eur J Immunol* (2009) 39(6):1671–81. doi: 10.1002/eji.200839123
24. Elhofy A, Depaolo RW, Lira SA, Lukacs NW, Karpus WJ. Mice Deficient for CCR6 Fail to Control Chronic Experimental Autoimmune Encephalomyelitis. *J Neuroimmunol* (2009) 213(1-2):91–9. doi: 10.1016/j.jneuroim.2009.05.011
25. Ghosh D, Curtis AD2nd, Wilkinson DS, Mannie MD. Depletion of CD4+ CD25+ Regulatory T Cells Confers Susceptibility to Experimental Autoimmune Encephalomyelitis (EAE) in GM-CSF-Deficient Csf2-/- Mice. *J Leukoc Biol* (2016) 100(4):747–60. doi: 10.1189/jlb.3A0815-359R
26. Bird CH, Christensen ME, Mangan MS, Prakash MD, Sedelies KA, Smyth MJ, et al. The Granzyme B-Serpinb9 Axis Controls the Fate of Lymphocytes After Lysosomal Stress. *Cell Death Differ* (2014) 21(6):876–87. doi: 10.1038/cdd.2014.7

27. Buzza MS, Zamurs L, Sun J, Bird CH, Smith AI, Trapani JA, et al. Extracellular Matrix Remodeling by Human Granzyme B via Cleavage of Vitronectin, Fibronectin, and Laminin. *J Biol Chem* (2005) 280(25):23549–58. doi: 10.1074/jbc.M412001200
28. Metkar SS, Menaa C, Pardo J, Wang B, Wallich R, Freudenberg M, et al. Human and Mouse Granzyme A Induce a Proinflammatory Cytokine Response. *Immunity* (2008) 29(5):720–33. doi: 10.1016/j.immuni.2008.08.014
29. Wensink AC, Hack CE, Bovenschen N. Granzymes Regulate Proinflammatory Cytokine Responses. *J Immunol* (2015) 194(2):491–7. doi: 10.4049/jimmunol.1401214
30. Phillips T, Opferman JT, Shah R, Liu N, Froelich CJ, Ashton-Rickardt PG. A Role for the Granzyme B Inhibitor Serine Protease Inhibitor 6 in CD8+ Memory Cell Homeostasis. *J Immunol* (2004) 173(6):3801–9. doi: 10.4049/jimmunol.173.6.3801
31. Zhang M, Park SM, Wang Y, Shah R, Liu N, Murmann AE, et al. Serine Protease Inhibitor 6 Protects Cytotoxic T Cells From Self-Inflicted Injury by Ensuring the Integrity of Cytotoxic Granules. *Immunity* (2006) 24(4):451–61. doi: 10.1016/j.immuni.2006.02.002

Conflict of Interest: Author LH is a cofounder and shareholder of Edelweiss Immune Inc. Both authors declare that the research was conducted in the absence of any other commercial or financial relationships that could be construed as a potential conflict of interest.

frontiers in Immunology

BRIEF RESEARCH REPORT
published: 07 February 2022
doi: 10.3389/fimmu.2022.750660

Cytotoxic B Cells in Relapsing-Remitting Multiple Sclerosis Patients

Vinícius O. Boldrini[1,2], Ana M. Marques[1], Raphael P. S. Quintiliano[2], Adriel S. Moraes[2], Carla R. A. V. Stella[2,3], Ana Leda F. Longhini[2,4], Irene Santos[2], Marília Andrade[2], Breno Ferrari[2], Alfredo Damasceno[3], Rafael P. D. Carneiro[2,5], Carlos Otávio Brandão[2,3], Alessandro S. Farias[1,2,6,7*] and Leonilda M. B. Santos[2,6*]*

[1] Autoimmune Research Laboratory, Department of Genetics, Evolution, Microbiology and Immunology, Institute of Biology, University of Campinas, Campinas, Brazil, [2] Neuroimmunology Unit, Department of Genetics, Evolution, Microbiology and Immunology, Institute of Biology, University of Campinas, Campinas, Brazil, [3] Department of Neurology, University of Campinas, Campinas, Brazil, [4] Department of Immunology and Rheumatology, University of Alabama at Birmingham, Birmingham, AL, United States, [5] MS Clinic of Santa Casa de São Paulo (CATEM), Irmandade da Santa Casa de Misericordia de São Paulo, São Paulo, Brazil, [6] National Institute of Science and Technology on Neuroimmunomodulation (INCT-NIM), Rio de Janeiro, Brazil, [7] Experimental Medicine Research Cluster (EMRC), São Paulo, Brazil

OPEN ACCESS

Edited by:
Luisa María Villar,
Ramón y Cajal University Hospital, Spain

Reviewed by:
Miriam Laura Fichtner,
Yale Medicine, United States
Barbara M.P. Willekens,
Antwerp University Hospital, Belgium

***Correspondence:**
Vinícius O. Boldrini
vi_boldrini@hotmail.com
Alessandro S. Farias
asfarias@unicamp.br
Leonilda M. B. Santos
leonilda@unicamp.br

Specialty section:
This article was submitted to Multiple Sclerosis and Neuroimmunology, a section of the journal Frontiers in Immunology

Received: 30 July 2021
Accepted: 13 January 2022
Published: 07 February 2022

Citation:
Boldrini VO, Marques AM, Quintiliano RPS, Moraes AS, Stella CRAV, Longhini ALF, Santos I, Andrade M, Ferrari B, Damasceno A, Carneiro RPD, Brandão CO, Farias AS and Santos LMB (2022) Cytotoxic B Cells in Relapsing-Remitting Multiple Sclerosis Patients. Front. Immunol. 13:750660. doi: 10.3389/fimmu.2022.750660

Background: Emerging evidence of antibody-independent functions, as well as the clinical efficacy of anti-CD20 depleting therapies, helped to reassess the contribution of B cells during multiple sclerosis (MS) pathogenesis.

Objective: To investigate whether $CD19^+$ B cells may share expression of the serine-protease granzyme-B (GzmB), resembling classical cytotoxic $CD8^+$ T lymphocytes, in the peripheral blood from relapsing-remitting MS (RRMS) patients.

Methods: In this study, 104 RRMS patients during different treatments and 58 healthy donors were included. CD8, CD19, Runx3, and GzmB expression was assessed by flow cytometry analyses.

Results: RRMS patients during fingolimod (FTY) and natalizumab (NTZ) treatment showed increased percentage of circulating $CD8^+GzmB^+$ T lymphocytes when compared to healthy volunteers. An increase in circulating $CD19^+GzmB^+$ B cells was observed in RRMS patients during FTY and NTZ therapies when compared to glatiramer (GA), untreated RRMS patients, and healthy donors but not when compared to interferon-β (IFN). Moreover, regarding Runx3, the transcriptional factor classically associated with cytotoxicity in $CD8^+$ T lymphocytes, the expression of GzmB was significantly higher in $CD19^+Runx3^+$-expressing B cells when compared to $CD19^+Runx3^-$ counterparts in RRMS patients.

Conclusions: $CD19^+$ B cells may exhibit cytotoxic behavior resembling $CD8^+$ T lymphocytes in MS patients during different treatments. In the future, monitoring "cytotoxic" subsets might become an accessible marker for investigating MS pathophysiology and even for the development of new therapeutic interventions.

Keywords: cytotoxicity, granzyme B, neuroinflammation, neurodegeneration, MS treatment

INTRODUCTION

Multiple sclerosis (MS) is an autoimmune-mediated demyelinating disease of the central nervous system (CNS). Early evidence showed the presence of $CD8^+$ T lymphocytes in the cerebrospinal fluid (CSF) and in perivascular leukocyte infiltration from white matter in chronic and active MS lesions (1–5). Thus, since there are few natural killer (NK) cells compared with T cells in the CSF of MS patients (6) and also effector T populations may be even more potent than NK cells in releasing cytotoxic granules (7); the expression of cytotoxic-associated molecules such as serine-protease granzyme-B (GzmB), during MS, seems to almost be exclusively originating from $CD8^+$ T lymphocytes. Interestingly, Runx3, which is a crucial transcriptional factor related to the expression of cytotoxic molecules in effector $CD8^+$ T subsets (8, 9), is reported as an MS-associated gene (10). In parallel, neurons express the mannose-6-phosphate receptor (M6PR), responsible for internalizing GzmB, which then makes them vulnerable to cell death triggered by this protease. *In vitro* evidence suggests that serine-protease inhibitors can dampen neuronal cell death associated with GzmB internalization (11). Supporting these findings, it was shown that MS patients exhibit higher GzmB levels in the CSF during relapses that tend to persist higher at 1–3 months into clinical remission (12). Also, increased circulating T lymphocytes with the ability to express GzmB were found in the peripheral blood from relapsing-remitting MS (RRMS) patients treated with fingolimod (FTY), and particularly during relapses, when compared to RRMS patients without FTY (13). Similarly, massive infiltration of cytotoxic $CD8^+GzmB^+$ T lymphocytes was found in the CNS parenchyma from two MS patients who suffered fulminant relapses after natalizumab (NTZ) discontinuation (14, 15). On the other hand, regarding progressive MS courses, not only the CSF from secondary progressive MS (SPMS) patients showed *in vitro* neurotoxicity due to the expression of GzmB (16) but also cytotoxic $CD8^+CD57^+$ T lymphocytes seem to be present in inflamed meninges in these patients with rapidly progressive disease (4). Altogether, these findings reinforce that cytotoxic mechanisms derived from $CD8^+$ T lymphocytes are pivotal drivers of CNS damage during MS (12, 17, 18).

Despite this, successful outcomes in the last few years by the use of anti-CD20 monoclonal antibodies (mAbs) (rituximab, ocrelizumab, or ofatumumab) reassessed the importance of B cells during both relapsing-remitting (RRMS) and progressive MS courses (4). Indeed, oligoclonal band (OCB) synthesis, compartmentalized clonal expansion, and increased levels of chemoattractants for B cells and/or plasma cells in the CSF (19–22) were extensively described in MS patients. Nevertheless, since the CD20 molecule is not expressed on pro-B cells or differentiated plasma cells, the beneficial effect of anti-CD20 treatment appears to be extended beyond autoantibody production and release. For instance, in the last few years, increasing evidence supports that B subsets can express and release anti- and pro-inflammatory cytokines, evidencing their antibody-independent functions during MS pathophysiology (23, 24). Considering it, in the present study, we evaluated whether $CD19^+$ B subsets may also exhibit the capacity to express and release GzmB similarly resembling the cytotoxic activity described for T lymphocytes in RRMS patients.

METHODS

Study Participants

A total of 104 RRMS patients [19 Untreated, 15 Glatiramer Acetate (GA), 24 Interferon-β (IFN), 14 FTY, and 32 NTZ], according to the McDonald criteria were recruited in the Neurology Clinic at the University of Campinas Hospital (UNICAMP). Also, 58 healthy subjects were included in the control group (**Table 1**). All subjects signed a term of consent approved by the University Committee for Ethical Research (CAAE: 53022516.3.0000.5404).

Blood Sample Collection and Lymphocyte Separation

Peripheral blood (25 ml) samples were collected from RRMS patients and healthy volunteers. Peripheral blood mononuclear cells (PBMCs) were separated by Ficoll-Hypaque® gradient and resuspended after centrifugation on RPMI-1640 supplemented with 10% heat-inactivated fetal bovine serum, 100 U/ml penicillin, and 100 µg/ml streptomycin. Then, PBMCs were used fresh or cryopreserved according to each experiment.

TABLE 1 | Demographic and baseline clinical characteristics of MS patients and controls.

Subjects	Sample size	Gender ♀:♂	Age	Time after first relapse (years)	Time after last relapse (months)	Treatment duration (years)	EDSS	OCB CSF (+/-)*
Healthy	58	40:18	28 (19-50)	–	–	–	–	
RRMS	104	80:24	37 (18-65)	9 (0.5-32)	27 (0-166)	3.0	2.0 +- 1.9	60/30
RRMS patients								
Untreated	19	14:5	27 (18-59)	5 (0.5-19)	4.5 (0-146)	–	1.5 +- 2.0	12/6*
Glatiramer Acetate (GA)	15	13:2	42 (23-58)	12.5 (1-32)	21 (5- 93)	4.0	1.5 +- 1.4	7/5*
Interferon-β (IFN)	24	20:4	41 (28-65)	12.5 (1-22)	40 (1-166)	6.5	2.0 +- 1.6	12/8*
Fingolimod (FTY)	14	10:4	39 (22-65)	11 (4-25)	102 (32-132)	3.0	2.0 +- 1.6	8/5*
Natalizumab (NTZ)	32	23:9	35 (23-62)	9 (2-15)	48 (24-120)	2.0	2.0 +- 2.0	21/6*

All data are represented in median (max – min values).

**Not all patients were tested for oligoclonal bands (Tested: n = 90; 66% OCB positive in the CSF).*

CSF, Cerebrospinal Fluid; OCBs, Oligoclonal Bands; EDSS, Expanded Disease Scale Status.

Flow Cytometry Analyses (FCA)

According to each experiment, PBMCs were stained with different anti-human mAbs: CD3-5.5 PerCP (clone SP34-2), CD3 BUV496 (clone UCHT1), CD8 PE (clone RPA-T8), CD8 BUV563 (clone RPAT8), CD19 FITC (clone HIB19), CD19 BV510 (clone SJ25C1), CD20 BV750 (clone 2H7), CD25 BUV805 (clone 2A3), CD27 BV711 (clone M7271), CD28 BUV737 (clone CD28.2), CD38 BB790 (clone HIT2), IgD BUV615 (clone IA6-2), CD45RA BB515 (clone HI100), CD56 APC-R700 (clone NCAM16.2), CD57 PECF594 (clone NK-1), CD94 BB630 (clone HP-3D9), CD127 BV650 (clone hIL-7R-M21), CD138 BB700 (clone MI15), CD150 BUV395 (clone A12), CD195 (CCR5) BB660 (clone 3A9), CD215 BV605 (clone JM7A4), T-bet BV786 (clone 04-46), RORγT BV421 (clone Q21-559), GzmB PE (clone GB11), GzmB Alexa700 (clone GB11) (all from BD Biosciences®), and Runx3-eFluor660 (clone R3-5G4) (eBioscience™). After incubation with specific antibodies against relevant surface molecules, PBMCs were fixed in BD Cytofix/CytoPerm solution for 30 min, washed with BD Perm/Wash buffer (BD Bioscience, San Diego, CA, USA), and then incubated overnight with intracellular markers. The acquisition was performed in FACSVerse® and FACSymphony® flow cytometers (BD Biosciences®), and the analysis used the FlowJo® software.

Isolating B Cells and *In Vitro* Stimulation

After the isolation from PBMCs using the EasySep® Human B Cell Enrichment Kit with EasySep® magnet, 2×10^4 B cells were stimulated for 16 h in culture, with CPG-ODN (2.5 µl/ml) and human recombinant IL-21 (50 ng/ml) according to the literature (25, 26).

Quantitative PCR

mRNA from isolated B cells was extracted using the RNeasy micro kit (QIAGEN) and reverse transcribed to cDNA. We used SYBR® Green manufacturer's instructions (BioRad, USA) to assess the expression of *GzmB* [*Forward* (F): CCATCC ATCCAAGCCTATAATCCTA, *Reverse* (R): CCTGCACTGTC ATCTTCACCT], *PRF1* (*F*: TGGAGTGCCGCTTCTACAGTT, *R*: GTGGGTGCCGTAGTTGGAGAT), and Runx3 (*F*: GAGTT TCACCCTGACCATCACTGTG, *R*: GCCCATCACTGGTCTT GAAGGTTGT). Data were normalized using a housekeeping gene *HPRT* (*F*: GACCAGTCAACAGGGGACAT, *R*: AACCTTCGTGGGGTCCTTTTC).

Cytometric Bead Array

A total of 50 µl of isolated and stimulated B-cell supernatants and solutions for calibration curve construction were incubated with beads containing mAbs to GzmB. After incubation for 2 h, revealing antibody conjugated to the fluorochrome PE was added. The acquisition was performed in FACSCanto (BD Bioscience®) flow cytometer, and the analysis used the FCAP Array software (BD Bioscience®).

Statistical Analyses

The statistical significance of the results was determined using a nonparametric analysis of variance (Kruskal–Wallis test) and a Mann–Whitney test (U-test). Dunn's multiple comparison test was used as *post-hoc* of Kruskal–Wallis. The ROUT (Q = 1%)' test was used to determine the presence of outlier values. $p < 0.05$ values were considered statistically significant.

RESULTS

Granzyme B Expression in CD8⁺ T Lymphocytes From Relapsing-Remitting Multiple Sclerosis Patients

Flow cytometry analysis of PBMCs (**Figure 1A**) showed no differences in the percentage of circulating $CD8^+$ T lymphocytes from RRMS patients when compared to healthy donors. Subgroups from untreated RRMS or treated patients (GA, IFN, FTY, and NTZ) also showed no differences in comparison with healthy volunteers (**Figures 1B, C**). However, an increased percentage of $CD8^+GzmB^+$ was found in the RRMS group vs. healthy donors (34.5 vs. 20.8, mean; 95% CI) ($p < 0.0003$) (**Figure 1D**). The expression of GzmB was also significantly higher in $CD8^+$ T lymphocytes from patients treated with FTY (43.2, mean; 95% CI) ($p = 0.0163$) and NTZ (40.5, mean; 95% CI) ($p = 0.0048$) vs. healthy donors, but not in treated RRMS patients during first-line immunomodulatory therapies, GA and IFN (26.8 and 25.5, means; 95% CI) nor in untreated RRMS patients (31.9, mean; 95% CI) vs. healthy donors, respectively (**Figure 1E**). We then performed Uniform Manifold Approximation and Projection (UMAP) analyses in $CD3^+CD8^+$ T lymphocytes from untreated RRMS patients and treated RRMS patients during FTY or NTZ therapies. Various surface [CD25, CD27, CD28, CD38, CD45RA, CD56, CD57, CD94, CD127, CD150, CD195 (CCR5), CD215] and intracellular (RORγT, T-bet, Runx3) markers were used, aiming to concomitantly identify expression with GzmB. Using this strategy, we found senescent-associated markers such as $CD28^-$ and $CD57^+$, and more broadly $CD27^-$ and $CD94^+$, associated with GzmB expression in $CD8^+$ T subsets from MS patients (**Figure 1F**). Upon confirming this, we assessed increased expression of GzmB in $CD27^-$ vs. $CD27^+$ (57.0 vs. 22.0, mean; 95% CI) ($p = 0.0003$) (**Figure 1G**), $CD28^-$ vs. $CD28^+$ (59.1 vs. 20.4, mean; 95% CI) ($p < 0.0001$) (**Figure 1H**), $CD57^+$ vs. $CD57^-$ (70.4 vs. 14.4, mean; 95% CI) ($p < 0.0001$) (**Figure 1I**), and $CD94^+$ vs. $CD94^-$ (62.9 vs. 21.3, mean; 95% CI) ($p < 0.0001$) (**Figure 1J**) markers of $CD8^+$ T lymphocytes from RRMS patients. Moreover, heatmap analyses showed that $CD27^{low}CD28^{low}$ and $CD27^+CD28^{low}$ compose almost the totality of $CD8^+$ T subsets from the investigated RRMS patients. Similar frequencies of these subsets were found in untreated RRMS patients and also in treated RRMS patients during FTY and NTZ (**Figures 1K, L**).

Granzyme B Expression in CD19⁺ B Cells From Relapsing-Remitting Multiple Sclerosis Patients

Flow cytometry analysis (**Figure 2A**) did not reveal differences in the percentage of total circulating $CD19^+$ B cells between RRMS patients and healthy donors (**Figure 2B**), nor among RRMS subgroups, despite the tendency of diminished circulating $CD19^+$ B cells in FTY-treated patients (**Figure 2C**). However, an increased percentage of circulating $CD19^+GzmB^+$ B cells was found in RRMS patients vs. healthy donors (13.6 vs. 1.8, mean; 95% CI) ($p < 0.0001$)

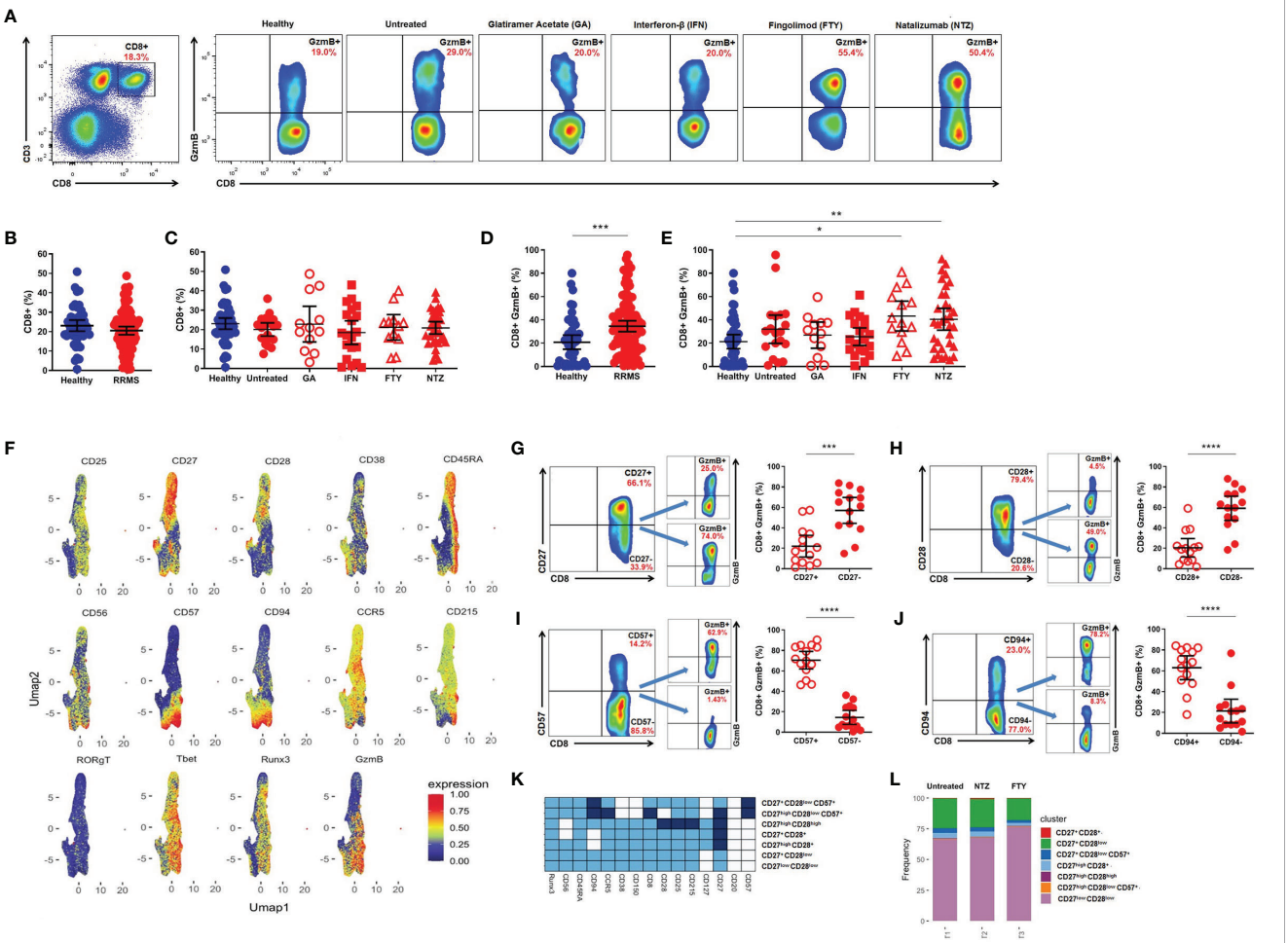

FIGURE 1 | Cytotoxic CD8$^+$ T lymphocytes in relapsing-remitting multiple sclerosis (RRMS) patients. **(A)** Gate strategy for total CD8$^+$ and CD8$^+$GzmB$^+$ T lymphocytes from healthy donors, untreated RRMS, and treated [Glatiramer Acetate (GA), Interferon-β (IFN), Fingolimod (FTY), and Natalizumab (NTZ)] RRMS patients. **(B)** Proportion (%) of total CD8$^+$ T lymphocytes in healthy donors (blue) and RRMS patients (red). **(C)** Proportion (%) of CD8$^+$ T lymphocytes in healthy donors (blue), untreated RRMS (red), and treated RRMS patients (GA, IFN, FTY, NTZ) (red). **(D)** Proportion (%) of circulating CD8$^+$GzmB$^+$ T lymphocytes in healthy donors (blue) and RRMS patients (red). **(E)** Proportion (%) of circulating CD8$^+$GzmB$^+$ T lymphocytes in healthy donors (blue), untreated RRMS (red), and treated RRMS patients (GA, IFN, FTY, NTZ) (red). Bars represent mean values. Each column represents mean (95% CI). *$p < 0.05$; **$p < 0.01$; ***$p < 0.001$; ****$p < 0.0001$. **(F)** Uniform Manifold Approximation and Projection (UMAP) gated in CD3$^+$CD8$^+$ T lymphocytes from RRMS patients with different conditions non-identified and based on the Arcsinh-transformed expression of the markers. Gate strategy and proportion (%) of granzyme B (GzmB) derived from circulating **(G)** CD8$^+$CD27$^+$ vs. CD8$^+$CD27$^-$, **(H)** CD8$^+$CD28$^+$ vs. CD8$^+$CD28$^-$, **(I)** CD8$^+$CD57$^+$ vs. CD8$^+$CD57$^-$, **(J)** CD8$^+$CD94$^+$ vs. CD8$^+$CD94$^-$ T lymphocytes in RRMS patients (red). Bars represent mean values. Each column represents mean (95% CI). *$p < 0.05$; **$p < 0.01$; ***$p < 0.001$; ****$p < 0.0001$. **(K)** Heatmap of the expression of the markers in subpopulations manually identified in CD3$^+$CD8$^+$ T lymphocytes from RRMS patients. **(L)** Barplot representing the frequency of each subpopulation in CD3$^+$CD8$^+$ T lymphocytes.

(**Figure 2D**). The expression of GzmB was also significantly higher in CD19$^+$ B cells from patients treated with FTY when compared to GA (25.7 vs. 2.9, mean; 95% CI) ($p = 0.0124$), untreated patients (2.5, mean; 95% CI) ($p = 0.0059$), and healthy donors (1.8, mean; 95% CI) ($p < 0.0001$). Similarly, CD19$^+$GzmB$^+$ B cells were significantly higher in NTZ-treated patients (25.8, mean; 95% CI) concerning the first-line immunomodulatory therapy GA ($p = 0.0109$), untreated patients ($p = 0.0037$), and healthy donors ($p < 0.0001$) (**Figure 2E**). Statistical differences were not observed in FTY and NTZ subgroups when compared to IFN-treated patients (4.4, mean; 95% CI). Resembling the strategy for CD8$^+$ T lymphocytes, we performed UMAP analyses in CD3$^-$CD19$^+$ B cells from untreated RRMS patients and treated RRMS patients during FTY or NTZ therapies. B cell-associated surface markers (CD20, CD25, CD27, CD38, CD138, IgD), as well as intracellular Runx3, were used, aiming to identify B subsets with the ability to express GzmB. Thus, we found that main GzmB-expressing B subsets lack the expression of CD20 marker but strongly correspond to CD38$^+$ activation marker and CD138$^+$ plasma cells (**Figure 2F**). We also notice a strong expression of Runx3 in B cells that concomitantly express GzmB. Upon confirming this, we assessed increased circulating CD19$^+$Runx3$^+$ in RRMS patients when compared to

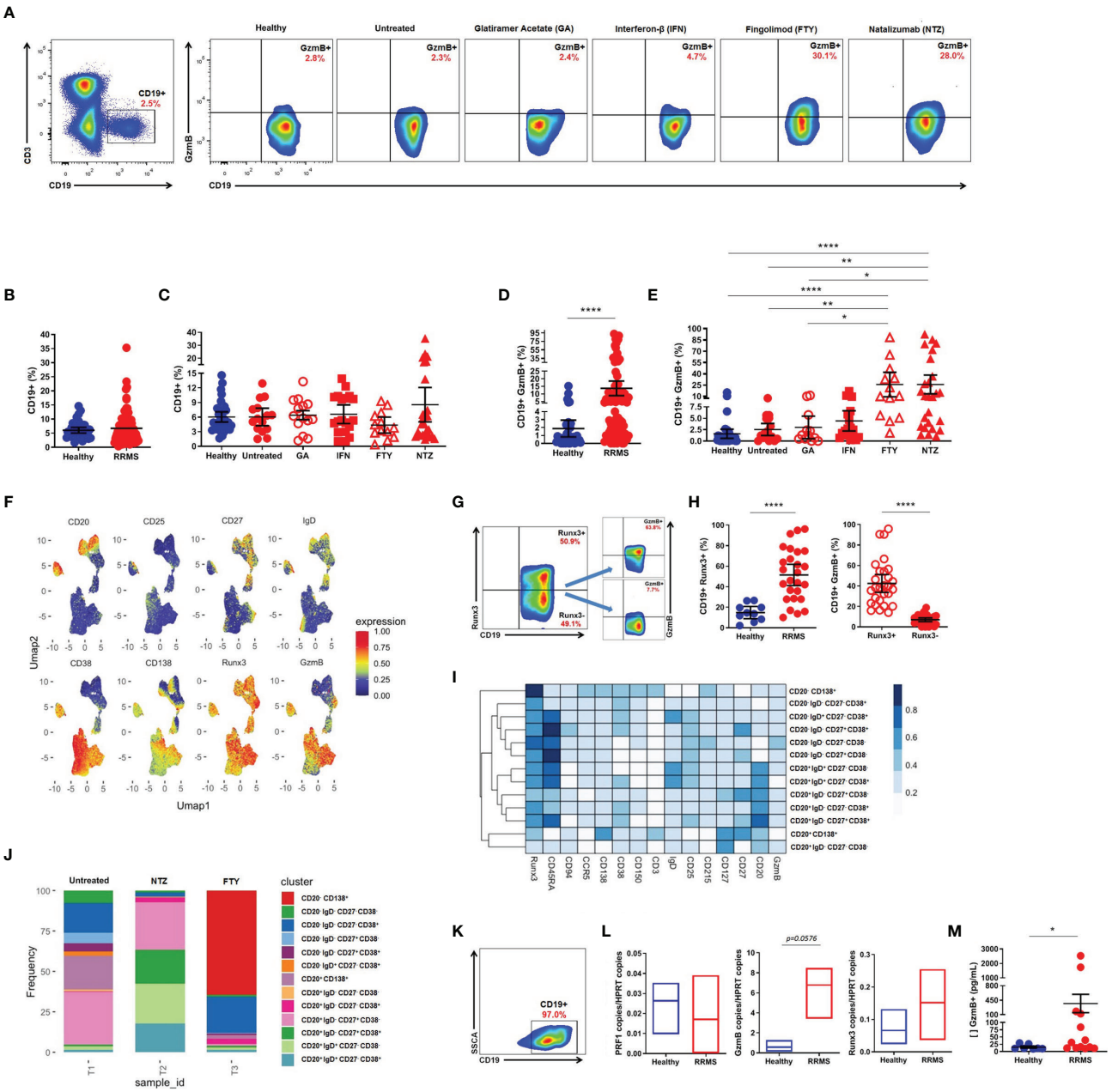

FIGURE 2 | Cytotoxic CD19$^+$ B cells in relapsing-remitting multiple sclerosis (RRMS) patients. **(A)** Gate strategy for total CD19$^+$ and CD19$^+$GzmB$^+$ B cells from healthy donors, untreated RRMS, and treated [Glatiramer Acetate (GA), Interferon-β (IFN), Fingolimod (FTY), and Natalizumab (NTZ)] RRMS patients. **(B)** Proportion (%) of total CD19$^+$ B cells in healthy donors (blue) and RRMS patients (red). **(C)** Proportion (%) of total CD19$^+$ B cells in healthy donors (blue), untreated RRMS (red), and treated RRMS patients (GA, IFN, FTY, NTZ) (red). **(D)** Proportion (%) of circulating CD19$^+$GzmB$^+$ B cells in healthy donors (blue) and RRMS patients (red). **(E)** Proportion (%) of circulating CD19$^+$GzmB$^+$ B cells in healthy donors (blue), untreated RRMS (red), and treated RRMS patients (GA, IFN, FTY, NTZ) (red). Bars represent mean values. Each column represents mean (95% CI). *$p < 0.05$; **$p < 0.01$; ****$p < 0.0001$. **(F)** Uniform Manifold Approximation and Projection (UMAP) gated in CD3$^-$CD19$^+$ B cells from RRMS patients with different conditions non-identified and based on the Arcsinh-transformed expression of the markers. **(G)** Gate strategy for granzyme B (GzmB)-derived CD19$^+$Runx3$^+$ B cells. **(H)** Proportion (%) of GzmB-derived from circulating CD19$^+$Runx3$^+$ vs. CD19$^+$Runx3$^-$ B cells in healthy donors (blue) and RRMS patients (red). **(I)** Proportion (%) of GzmB derived from circulating CD19$^+$Runx3$^+$ vs. CD19$^+$Runx3$^-$ in RRMS patients (red). Each column represents mean (95% CI). *$p < 0.05$; **$p < 0.01$; ****$p < 0.0001$. **(I)** Heatmap of the expression of the markers in subpopulations manually identified in CD3$^-$CD19$^+$ B cells from RRMS patients. **(J)** Barplot representing the frequency of each subpopulation in CD3$^-$CD19$^+$ B cells. **(K)** Gate strategy for isolated CD19$^+$ B cells. **(L)** Quantitative PCR for *PRF1*, *GzmB*, and *Runx3* in isolated B cells from healthy donors (blue) and RRMS patients (red). **(M)** Concentration (pg/ml) of GzmB in supernatants of stimulated CD19$^+$ B cells from healthy donors (blue) and RRMS patients (red). Each column represents mean (SEM). *$p < 0.05$; **$p < 0.01$; ***$p < 0.001$; ****$p < 0.0001$.

healthy donors (51.4 vs. 14.8, mean; 95% CI) ($p < 0.0001$). Moreover, we observed increased circulating GzmB-derived $CD19^+Runx3^+$ when compared to $CD19^+Runx3^-$ B cells from RRMS patients (42.4.8 vs. 6.9, mean; 95% CI) ($p < 0.0001$) (**Figures 2G, H**). Furthermore, including the previously mentioned markers, we were able to define distinct subsets of B cells in untreated and also in treated (FTY or NTZ) RRMS patients. Untreated RRMS patients mainly seem to exhibit $CD20^+$ B subsets suggestive of antigen-activated switched memory phenotype ($CD20^+IgD^-CD27^+CD38^-$), non-classical plasma cells ($CD20^+CD138^+$), and $CD20^-$ subsets also with atypical memory features ($CD20^-IgD^-CD27^-CD38^{+/-}$). Almost total of B subsets from NTZ-treated patients were $CD20^+$ in which approximately half of them exhibited naive phenotype ($CD20^+IgD^+CD27^-CD38^{+/-}$) followed by memory subsets ($CD20^+IgD^-CD27^-CD38^{+/-}$). Finally, FTY-treated patients exhibited almost all of the B subsets lacking CD20 expression, suggesting well-known defined plasma cells ($CD20^-CD138^+$) and a few suggestive of early plasmablasts or memory cells ($CD20^-IgD^-CD27^-CD38^+$) (**Figures 2I, J**).

Release of Granzyme B by $CD19^+$ B Cells Isolated From Relapsing-Remitting Multiple Sclerosis Patients

We sorted out $CD19^+$ B cells to evaluate the *in vitro* cytotoxic activity (**Figure 2K**). After ODN-CPG and IL-21 stimulation, no differences regarding Perforin (*PRF1*), *GzmB*, or *Runx3* mRNA expression were found between isolated B cells from RRMS patients and healthy donors (**Figure 2L**). However, supernatants of purified $CD19^+$ B cells from RRMS patients presented significantly higher amounts of GzmB in comparison with $CD19^+$ B cells from healthy individuals (368.9 vs. 15.1, mean; SEM) ($p = 0.0145$) (**Figure 2M**).

DISCUSSION

Herein, we demonstrated that $CD19^+$ B cells from RRMS patients share the ability to express serine-protease GzmB, similarly resembling classical $CD8^+$ T lymphocytes.

Regarding T lymphocytes, we show here that RRMS patients exhibit an increased percentage of circulating $CD8^+GzmB^+$ T lymphocytes when compared to healthy volunteers. Moreover, treated RRMS patients, particularly FTY and NTZ subgroups, showed higher $CD8^+GzmB^+$ T lymphocytes than healthy subjects.

Enhanced cytotoxic behavior derived from T lymphocytes has been suggested as a mechanism for controlling latent Epstein–Barr virus (EBV) infection and preventing viral replication during MS (27). However, sustained cytotoxic $CD8^+$ T cell activity would also be implicated in CNS lesions during disease. Indeed, infiltration of $CD8^+GzmB^+$ T lymphocytes that respond against EBV-infected B cells/plasma cells was recently found in the CNS lesions from two MS patients who died after suffering fulminant relapses following NTZ withdrawal (14, 28).

In addition, Cencioni et al. (4) showed that cytotoxic $CD57^+$ T subsets occur in inflamed meninges from progressive MS patients and are negatively correlated with disease progression/age of death. Interestingly, higher expression of programmed death-1 (PD-1) in circulating $CD8^+CD57^+$ T lymphocytes correlates with disease stability. *In vitro* blockade of PD-1 enhanced the release of IFN-γ, Perforin, and GzmB by these terminally differentiated cytotoxic T subsets from MS patients (4).

According to previous reports (4, 29), RRMS patients in our cohort showed increased expression of GzmB in $CD8^+$ T lymphocytes markedly associated with senescent T phenotype exhibiting $CD27^-$, $CD28^-$, $CD57^+$, and $CD94^+$ markers.

Indeed, diverse evidence suggests that cytotoxic subsets including those exhibiting senescent $CD28^-$ and $CD57^+$ markers restrain the migration ability into inflamed tissues in response to chemokines and also to express and release GzmB and other pro-inflammatory cytokines supporting tissue damage in diverse conditions (30).

Considering this, in the last few years, these subsets seemed to have emerged as candidates for predicting disease worsening in several diseases. The prognostic value of $CD4^+CD28^-$ T subset during MS was recently suggested for progressive disease (31). However, there is still a lack of studies investigating the potential of cytotoxic behavior in subsets other than T lymphocytes and its possible implications regarding different MS clinical courses/treatments.

On the other hand, the role of B cells during MS has been more deeply investigated in the context of antibody-independent functions. For instance, IL-21, which is known to promote B cell differentiation to memory and plasma cells in the presence of both BCR or Toll-like receptor (TLR) signaling and CD40L co-stimulation, may also promote GzmB-secreting B cells in the absence of CD40L co-stimulation (26, 32, 33).

Thus, considering that B cells may differentiate into GzmB-producing cells upon insufficient T cell help, herein, we have provided evidence that this phenomenon may occur during MS. Similar to $CD8^+$ T lymphocytes, we found no differences in total circulating $CD19^+$ B cells. However, our results show an increased percentage of circulating $CD19^+GzmB^+$ B cells in RRMS patients vs. healthy. Treated RRMS subgroup patients showed higher amounts of $CD19^+GzmB^+$ B cells during FTY and NTZ when compared to patients during first-line immunomodulatory therapy (GA), untreated RRMS patients, and healthy donors. We were able to assess which B-cell markers in $CD3^-CD19^+$ subsets were associated with the cytotoxic phenotype using flow cytometry high-dimensional analyses high-dimensional analyses. Accordingly, with previous literature, we observed that not $CD20^+$ but $CD38^+$ activated and $CD138^+$ plasma cells seem to identify GzmB-expressing phenotype in B subsets (26, 34, 35). Moreover, Runx3, a master regulator associated with cytotoxic behavior in $CD8^+$ T lymphocytes (8, 9) positively correlated with the GzmB-expressing phenotype.

As previously suggested by De Andrés et al. (36), these results reinforce a possible antibody-independent pathophysiological mechanism derived from B-cell subsets with the ability to express GzmB during MS. Beyond this, and considering the clinical efficacy of both FTY and NTZ, we may hypothesize that cytotoxicity may represent or even coexist with other tolerogenic functions in B subsets. Resembling our MS cohort, similar

percentages of circulating $CD19^+GzmB^+$ B cells, in the absence of IL-10 coexpression, were described during HIV infection (37). Also, regulatory activity of GzmB-derived circulating $CD19^+$ B cells was suggested due to degradation of TCR-ζ–chain that promotes a significant decrease in T-cell proliferation (32, 37, 38). As our results suggest, by now, it seems that GzmB expression is mainly derived from $CD20^-$ B subsets with $CD38^+$ and $CD138^+$ markers. Indeed, beyond several changes regarding the total percentage of $CD19^+$ B cells comprehending naive and memory phenotypes, as well as regulatory B subsets, increased circulating plasma cells were already described during highly effective MS treatments (39). Interestingly, reduced tumor necrosis factor (TNF)-α and enhanced interleukin (IL)-10 expression by B subsets were also reported during FTY. Yet, these regulatory IL-10-expressing B cells seem to be increased in the CSF from FTY-treated patients (24, 40).

It is noteworthy that despite $CD20^+$ B cells being found in CNS lesions from different stages of the disease, many authors have proposed that B cells would take a later role in MS pathophysiology, since, in 2004, $CD20^+$ B cells, $CD138^+$ plasma cells, and follicular dendritic cells were described in tertiary lymphoid organs in inflamed meninges from progressive MS patients (5, 27).

Further investigation in progressive MS courses may identify whether or not GzmB-derived B cells occur during chronic disease pathogenesis. So far, cytotoxicity derived from B cells was shown to cause damage in oligodendrocytes and neurons (41, 42), eventually sustaining a silent and continuous CNS-restricted inflammatory process. Supporting this, anti-CD20 mAbs seem to be effective for managing progressive MS mainly during early disease course (24, 40, 43) and have also been suggested for mitigating the increased risk of relapses in RRMS patients after NTZ washout (44).

Thus, since anti-CD20 mAbs mainly deplete naive and memory B cells, preserving antibody-secreting (CD138+) plasma cells, cytotoxic behavior derived from $CD20^-$ B subsets would be preserved during these treatments. Further investigations of cytotoxic behavior in $CD19^+$ may address, for instance, eventual important mechanisms associated with the clinical efficacy of emerging anti-CD19 mAbs and oral drugs targeting Bruton's tyrosine kinase (BTK) for MS patients (45).

Conclusions

Our findings collectively support that beyond classical $CD8^+$ T subsets, $CD19^+$ B cells may be an alternative source of lytic factors such as GzmB in the context of antibody-independent functions during MS.

Limitations

The size of cohort and the cross-sectional nature of our study did not allow us to understand the clinical relevance of our findings better. Although we were able to establish a strong correlation between Runx3 and GzmB expression, *in vitro* generation of cytotoxic B cells will be necessary to clarify the role of Runx3 expression in this subset.

DATA AVAILABILITY STATEMENT

The raw data supporting the conclusions of this article will be made available by the authors without undue reservation.

ETHICS STATEMENT

The studies involving human participants were reviewed and approved by the University of Campinas Committee for Ethical Research (CAAE: 53022516.3.0000.5404). The patients/participants provided their written informed consent to participate in this study.

AUTHOR CONTRIBUTIONS

VB, RQ, and ASM performed most of the experiments. CS, AD, RC, and CB diagnosed, treated, and selected MS patients as well as recruited all healthy donors. VB, AMM, ASM, MA, and BF designed and performed flow cytometry. VB, AMM, and AF analyzed flow cytometry data. AL and IS performed CBA experiments. AF and LS designed the experimental work. AF coordinated the study. VB, AMM, AF, and LS wrote the article with inputs from co-authors. All authors contributed to the article and approved the submitted version.

FUNDING

This work was supported by grants from Sao Paulo Research Foundation (FAPESP) (#2014/26431-0, 2015/22052-8, #2017/21363-5, #2019/06372-3, #2019/16116-4). This study was also partly financed in part by the Coordenação de Aperfeiçoamento de Pessoal de Nível Superior-Brasil (CAPES)-Finance Code 001 (2015/22052-8).

REFERENCES

1. Neumann H, Medana IM, Bauer J, Lassmann H. Cytotoxic T Lymphocytes in Autoimmune and Degenerative CNS Diseases. *Trends Neurosci* (2002) 25:313–9. doi: 10.1016/S0166-2236(02)02154-9
2. Skulina C, Schmidt S, Dornmair K, Babbe H, Roers A, Rajewsky K, et al. Multiple Sclerosis: Brain-Infiltrating CD8+ T Cells Persist as Clonal Expansions in the Cerebrospinal Fluid and Blood. *Proc Comput Sci* (2004) 101:2428–33. doi: 10.1073/PNAS.0308689100
3. Ifergan I, Kebir H, Alvarez JI, Marceau G, Bernard M, Bourbonniere L, et al. Central Nervous System Recruitment of Effector Memory CD8+ T Lymphocytes During Neuroinflammation is Dependent on 4 Integrin. *Brain* (2011) 134:3560–77. doi: 10.1093/brain/awr268
4. Cencioni MT, Magliozzi R, Nicholas R, Ali R, Malik O, Reynolds R, et al. Programmed Death 1 is Highly Expressed on CD8+ CD57+ T Cells in Patients With Stable Multiple Sclerosis and Inhibits Their Cytotoxic Response to Epstein–Barr Virus. *Immunology* (2017) 152:660–76. doi: 10.1111/imm.12808
5. Lassmann H. Pathogenic Mechanisms Associated With Different Clinical Courses of Multiple Sclerosis. *Front Immunol* (2019) 9:3116. doi: 10.3389/fimmu.2018.03116
6. Merelli E, Sola P, Faglioni P, Giordani S, Mussini D, Montagnani G. Natural Killer Cells and Lymphocyte Subsets in Active MS and Acute Inflammation of

the CNS. *Acta Neurol Scand* (1991) 84:127–31. doi: 10.1111/j.1600-0404.1991.tb04920.x
7. Chiang SCC, Theorell J, Entesarian M, Meeths M, Mastafa M, Al-Herz W, et al. Comparison of Primary Human Cytotoxic T-Cell and Natural Killer Cell Responses Reveal Similar Molecular Requirements for Lytic Granule Exocytosis But Differences in Cytokine Production. *Blood* (2013) 121:1345–56. doi: 10.1182/blood-2012-07-442558
8. Cruz-Guilloty F, Pipkin ME, Djuretic IM, Levanon D, Lotem J, Lichtenheld MG, et al. Runx3 and T-Box Proteins Cooperate to Establish the Transcriptional Program of Effector CTLs. *J Exp Med* (2009) 206:51–9. doi: 10.1084/jem.20081242
9. Behr FM, Chuwonpad A, Stark R, van Gisbergen KPJM. Armed and Ready: Transcriptional Regulation of Tissue-Resident Memory CD8 T Cells. *Front Immunol* (2018) 9:1770. doi: 10.3389/fimmu.2018.01770
10. Himmelstein DS, Baranzini SE. Heterogeneous Network Edge Prediction : A Data Integration Approach to Prioritize Disease-Associated Genes. *PLoS Comput Biol* (2015) 11(7):e1004259. doi: 10.1371/journal.pcbi.1004259
11. Haile Y, Carmine-Simmen K, Olechowski C, Kerr B, Bleackley RC, Giuliani F. Granzyme B-Inhibitor Serpina3n Induces Neuroprotection *In Vitro* and *In Vivo*. *J Neuroinflamm* (2015) 12:1–10. doi: 10.1186/s12974-015-0376-7
12. Malmeström C, Lycke J, Haghighi S, Andersen O, Carlsson L, Wadenvik H, et al. Relapses in Multiple Sclerosis are Associated With Increased CD8+ T-Cell Mediated Cytotoxicity in CSF. *J Neuroimmunol* (2008) 196:159–65. doi: 10.1016/j.jneuroim.2008.03.001
13. Fujii C, Kondo T, Ochi H, Okada Y, Hashi Y, Adachi T, et al. Altered T Cell Phenotypes Associated With Clinical Relapse of Multiple Sclerosis Patients Receiving Fingolimod Therapy. *Sci Rep* (2016) 6:35314. doi: 10.1038/srep35314
14. Serafini B, Scorsi E, Rosicarelli B, Rigau V, Thouvenot E, Aloisi F. Massive Intracerebral Epstein-Barr Virus Reactivation in Lethal Multiple Sclerosis Relapse After Natalizumab Withdrawal. *J Neuroimmunol* (2017) 307:14–7. doi: 10.1016/j.jneuroim.2017.03.013
15. Larochelle C, Metz I, Lécuyer M, Terouz S, Roger M, Arbour N, et al. Immunological and Pathological Characterization of Fatal Rebound MS Activity Following Natalizumab Withdrawal. *Mult Scler J* (2017) 23:72–81. doi: 10.1177/1352458516641775
16. Lee PR, Johnson TP, Gnanapavan S, Giovannoni G, Wang T, Steiner JP, et al. Protease-Activated Receptor-1 Activation by Granzyme B Causes Neurotoxicity That is Augmented by Interleukin-1β. *J Neuroinflamm* (2017) 14:1–18. doi: 10.1186/s12974-017-0901-y
17. Sauer BM, Schmalstieg WF, Howe CL. Axons are Injured by Antigen-Specific CD8+ T Cells Through a MHC Class I- and Granzyme B-Dependent Mechanism. *Neurobiol Dis* (2013) 59:194–205. doi: 10.1016/j.nbd.2013.07.010
18. Salou M, Nicol B, Garcia A, Laplaud D-A. Involvement of CD8+ T Cells in Multiple Sclerosis. *Front Immunol* (2015) 6:604. doi: 10.3389/fimmu.2015.00604
19. Sellebjerg F, Bornsen L, Khademi M, Krakauer M, Olsson T, Frederiksen JL, et al. Increased Cerebrospinal Fluid Concentrations of the Chemokine CXCL13 in Active MS. *Neurology* (2009) 73:2003–10. doi: 10.1212/WNL.0b013e3181c5b457
20. Krumbholz M, Derfuss T, Hohlfeld R, Meinl E. B Cells and Antibodies in Multiple Sclerosis Pathogenesis and Therapy. *Nat Rev Neurol* (2012) 8:613–23. doi: 10.1038/nrneurol.2012.203
21. Ferraro D, Simone AM, Bedin R, Galli V, Vitetta F, Federzoni L, et al. Cerebrospinal Fluid Oligoclonal IgM Bands Predict Early Conversion to Clinically Definite Multiple Sclerosis in Patients With Clinically Isolated Syndrome. *J Neuroimmunol* (2013) 257:76–81. doi: 10.1016/j.jneuroim.2013.01.011
22. Krumbholz M, Meinl E. B Cells in MS and NMO: Pathogenesis and Therapy. *Semin Immunopathol* (2014) 36:339–50. doi: 10.1007/s00281-014-0424-x
23. Holloman JP, Axtell RC, Monson NL, Wu GF. The Role of B Cells in Primary Progressive Multiple Sclerosis. *Front Neurol* (2021) 12:680581. doi: 10.3389/fneur.2021.680581
24. Li R, Rezk A, Healy LM, Muirhead G, Prat A, Gommerman JL, et al. Cytokine-Defined B Cell Responses as Therapeutic Targets in Multiple Sclerosis. *Front Immunol* (2016) 6:626. doi: 10.3389/fimmu.2015.00626
25. Jahrsdörfer B, Vollmer A, Blackwell SE, Maier J, Sontheimer K, Beyer T, et al. Granzyme B Produced by Human Plasmacytoid Dendritic Cells Suppresses T-Cell Expansion. *Blood* (2010) 115:1156–65. doi: 10.1182/blood-2009-07-235382
26. Cupi ML, Sarra M, Marafini I, Monteleone I, Franze E, Ortenzi A, et al. Plasma Cells in the Mucosa of Patients With Inflammatory Bowel Disease Produce Granzyme B and Possess Cytotoxic Activities. *J Immunol* (2014) 192:6083–91. doi: 10.4049/jimmunol.1302238
27. Serafini B, Rosicarelli B, Magliozzi R, Stigliano E, Aloisi F. Detection of Ectopic B-Cell Follicles With Germinal Centers in the Meninges of Patients With Secondary Progressive Multiple Sclerosis. *Brain Pathol* (2004) 14:164–74. doi: 10.1111/j.1750-3639.2004.tb00049.x
28. Serafini B, Zandee S, Rosicarelli B, Scorsi E, Veroni C, Larochelle C, et al. Epstein-Barr Virus-Associated Immune Reconstitution Inflammatory Syndrome as Possible Cause of Fulminant Multiple Sclerosis Relapse After Natalizumab Interruption. *J Neuroimmunol* (2018) 319:9–12. doi: 10.1016/j.jneuroim.2018.03.011
29. Broux B, Mizee MR, Vanheusden M, van der Pol S, van Horssen J, Van Wijmeersch B, et al. IL-15 Amplifies the Pathogenic Properties of CD4 + CD28 – T Cells in Multiple Sclerosis. *J Immunol* (2015) 194:2099–109. doi: 10.4049/jimmunol.1401547
30. Darrah E, Rosen A. Granzyme B Cleavage of Autoantigens in Autoimmunity. *Cell Death Differ* (2010) 17:624–32. doi: 10.1038/cdd.2009.197
31. Peeters LM, Vanheusden M, Somers V, van Wijmeersch B, Stinissen P, Broux B, et al. Cytotoxic CD4+ T Cells Drive Multiple Sclerosis Progression. *Front Immunol* (2017) 8:1160. doi: 10.3389/fimmu.2017.01160
32. Hagn M, Jahrsdörfer B. Why do Human B Cells Secrete Granzyme B? Insights Into a Novel B-Cell Differentiation Pathway. *Oncoimmunology* (2012) 1:1368–75. doi: 10.4161/onci.22354
33. Hagn M, Sontheimer K, Dahlke K, Brueggemann S, Kaltenmeier C, Beyer T, et al. Human B Cells Differentiate Into Granzyme B-Secreting Cytotoxic B Lymphocytes Upon Incomplete T-Cell Help. *Immunol Cell Biol* (2012) 90:457–67. doi: 10.1038/icb.2011.64
34. Chesneau M, Michel L, Dugast E, Chenouard A, Baron D, Pallier A, et al. Tolerant Kidney Transplant Patients Produce B Cells With Regulatory Properties. *J Am Soc Nephrol* (2015) 26:2588–98. doi: 10.1681/ASN.2014040404
35. Chesneau M, Le MH, Danger R, Le Bot S, Nguyen T-V-H, Bernard J, et al. Efficient Expansion of Human Granzyme B–Expressing B Cells With Potent Regulatory Properties. *J Immunol* (2020) 205:2391–401. doi: 10.4049/jimmunol.2000335
36. De Andrés C, Tejera-Alhambra M, Alonso B, Valor L, Teijeiro R, Ramos-Medina R, et al. New Regulatory CD19+CD25+B-Cell Subset in Clinically Isolated Syndrome and Multiple Sclerosis Relapse. Changes After Glucocorticoids. *J Neuroimmunol* (2014) 270:37–44. doi: 10.1016/j.jneuroim.2014.02.003
37. Kaltenmeier C, Gawanbacht A, Beyer T, Lindner S, Trzaska T, van der Merwe JA, et al. CD4+ T Cell-Derived IL-21 and Deprivation of CD40 Signaling Favor the *In Vivo* Development of Granzyme B-Expressing Regulatory B Cells in HIV Patients. *J Immunol* (2015) 194:3768–77. doi: 10.4049/jimmunol.1402568
38. Lindner S, Dahlke K, Sontheimer K, Hagn M, Kaltenmeier C, Barth TFE, et al. Interleukin 21-Induced Granzyme B-Expressing B Cells Infiltrate Tumors and Regulate T Cells. *Cancer Res* (2013) 73:2468–79. doi: 10.1158/0008-5472.CAN-12-3450
39. Nakamura M, Matsuoka T, Chihara N, Miyake S, Sato W, Araki M, et al. Differential Effects of Fingolimod on B-Cell Populations in Multiple Sclerosis. *Mult Scler J* (2014) 20:1371–80. doi: 10.1177/1352458514523496
40. Li R, Patterson KR, Bar-Or A. Reassessing B Cell Contributions in Multiple Sclerosis. *Nat Immunol* (2018) 19:696–707. doi: 10.1038/s41590-018-0135-x
41. Lisak RP, Benjamins JA, Nedelkoska L, Barger JL, Ragheb S, Fan B, et al. Secretory Products of Multiple Sclerosis B Cells are Cytotoxic to Oligodendroglia. *Vitro J Neuroimmunol* (2012) 246:85–95. doi: 10.1016/j.jneuroim.2012.02.015
42. Lisak RP, Nedelkoska L, Benjamins JA, Schalk D, Bealmear B, Touil H, et al. B Cells From Patients With Multiple Sclerosis Induce Cell Death *via* Apoptosis in Neurons *In Vitro*. *J Neuroimmunol* (2017) 309:88–99. doi: 10.1016/j.jneuroim.2017.05.004
43. Filippi M, Bar-Or A, Piehl F, Preziosa P, Solari A, Vukusic S, et al. Multiple Sclerosis. *Nat Rev Dis Prim* (2018) 4:43. doi: 10.1038/s41572-018-0041-4
44. Alping P, Frisell T, Novakova L, Islam-Jakobsson P, Salzer J, Björck A, et al. Rituximab Versus Fingolimod After Natalizumab in Multiple Sclerosis Patients. *Ann Neurol* (2016) 79:950–8. doi: 10.1002/ana.24651

45. Sellebjerg F, Blinkenberg M, Sorensen PS. Anti-CD20 Monoclonal Antibodies for Relapsingand Progressive Multiple Sclerosis. *CNS Drugs* (2020) 34:269–80. doi: 10.1007/s40263-02000704-w

Conflict of Interest: LS received a research grant from Biogen and a consultation honorarium from Biogen and Roche.

The remaining authors declare that the research was conducted in the absence of any commercial or financial relationships that could be construed as a potential conflict of interest.

Publisher's Note: All claims expressed in this article are solely those of the authors and do not necessarily represent those of their affiliated organizations, or those of the publisher, the editors and the reviewers. Any product that may be evaluated in this article, or claim that may be made by its manufacturer, is not guaranteed or endorsed by the publisher.

frontiers in Neurology

ORIGINAL RESEARCH
published: 24 February 2022
doi: 10.3389/fneur.2022.820256

Intermediate-Intensity Autologous Hematopoietic Stem Cell Transplantation Reduces Serum Neurofilament Light Chains and Brain Atrophy in Aggressive Multiple Sclerosis

Alice Mariottini[1,2], Leonardo Marchi[1], Chiara Innocenti[3], Maria Di Cristinzi[1], Matteo Pasca[1], Stefano Filippini[1], Alessandro Barilaro[2], Claudia Mechi[2], Arianna Fani[3], Benedetta Mazzanti[3], Tiziana Biagioli[4], Francesca Materozzi[3], Riccardo Saccardi[3], Luca Massacesi[1,2] and Anna Maria Repice[2]*

[1] Department of Neurosciences, Drug and Child Health, University of Florence, Florence, Italy, [2] Department of Neurology 2 and Tuscan Region Multiple Sclerosis Referral Centre, Careggi University Hospital, Florence, Italy, [3] Cell Therapy and Transfusion Medicine Unit, Careggi University Hospital, Florence, Italy, [4] General Laboratory, Careggi University Hospital, Florence, Italy

OPEN ACCESS

Edited by:
Maria Teresa Cencioni,
Imperial College London,
United Kingdom

Reviewed by:
Christian Barro,
Brigham and Women's Hospital and
Harvard Medical School,
United States
Roland Martin,
University of Zurich, Switzerland
Giulio Disanto,
Neurocenter of Southern
Switzerland, Switzerland

***Correspondence:**
Luca Massacesi
luca.massacesi@unifi.it

Specialty section:
This article was submitted to
Multiple Sclerosis and
Neuroimmunology,
a section of the journal
Frontiers in Neurology

Received: 22 November 2021
Accepted: 31 January 2022
Published: 24 February 2022

Citation:
Mariottini A, Marchi L, Innocenti C, Di Cristinzi M, Pasca M, Filippini S, Barilaro A, Mechi C, Fani A, Mazzanti B, Biagioli T, Materozzi F, Saccardi R, Massacesi L and Repice AM (2022) Intermediate-Intensity Autologous Hematopoietic Stem Cell Transplantation Reduces Serum Neurofilament Light Chains and Brain Atrophy in Aggressive Multiple Sclerosis. Front. Neurol. 13:820256. doi: 10.3389/fneur.2022.820256

Background: Autologous haematopoietic stem cell transplantation (AHSCT) is highly effective in reducing new inflammatory activity in aggressive multiple sclerosis (MS). A remarkable decrease of serum neurofilament light chains (sNfL) concentration, a marker of axonal damage, was reported in MS following high-intensity regimen AHSCT, but hints for potential neurotoxicity had emerged. sNfL and brain atrophy were therefore analysed in a cohort of patients with aggressive MS treated with intermediate-intensity AHSCT, exploring whether sNfL might be a reliable marker of disability progression independent from new inflammation (i.e. relapses and/or new/gadolinium-enhancing MRI focal lesions).

Methods: sNfL concentrations were measured using SIMOA methodology in peripheral blood from relapsing-remitting (RR-) or secondary-progressive (SP-) MS patients undergoing AHSCT (MS AHSCT), collected before transplant and at months 6 and 24 following the procedure. sNfL measured at a single timepoint in SP-MS patients not treated with AHSCT without recent inflammatory activity (SP-MS CTRL) and healthy subjects (HD) were used as controls. The rate of brain volume loss (AR-BVL) was also evaluated by MRI in MS AHSCT cases.

Results: Thirty-eight MS AHSCT (28 RR-MS; 10 SP-MS), 22 SP-MS CTRL and 19 HD were included. Baseline median sNfL concentrations were remarkably higher in the MS AHSCT than in the SP-MS CTRL and HD groups ($p = 0.005$ and <0.0001, respectively), and levels correlated with recent inflammatory activity. After a marginal (not significant) median increase observed at month 6, at month 24 following AHSCT sNfL concentrations decreased compared to baseline by median 42.8 pg/mL (range 2.4–217.3; $p = 0.039$), reducing by at least 50% in 13 cases, and did not differ from SP-MS CTRL ($p = 0.110$)

but were still higher than in HD ($p < 0.0001$). Post-AHSCT AR-BVL normalised in 55% of RR-MS and in 30% of SP-MS. The effectiveness and safety of AHSCT were aligned with the literature.

Conclusion: sNfL concentrations correlated with recent inflammatory activity and were massively and persistently reduced by intermediate-intensity AHSCT. Association with response to treatment assessed by clinical or MRI outcomes was not observed, suggesting a good sensitivity of sNfL for recent inflammatory activity but low sensitivity in detecting ongoing axonal damage independent from new focal inflammation.

Keywords: hematopoietic (stem) cell transplantation (HSCT), multiple sclerosis, neurofilament light (NfL), biomarker, brain atrophy, PIRA, progression independent of relapse activity

INTRODUCTION

Autologous haematopoietic stem cell transplantation (AHSCT) is a treatment option for a selected population of patients with aggressive multiple sclerosis (aMS), endorsed as "standard of care" for treatment-refractory relapsing MS (1, 2). AHSCT virtually eradicates new inflammatory activity in MS, and its risk-benefit ratio is highly favourable in early inflammatory phases of the disease (relapsing-remitting, RR-), whereas efficacy in secondary-progressive (SP-) MS is still controversial and long-term stabilisation of disability is achieved only in a moderate proportion of cases (3).

Neurofilament light chain (NfL) concentrations, which can be reliably evaluated in cerebrospinal fluid (CSF) and serum, are associated in MS patients with inflammatory activity, disability accrual, and accelerated brain atrophy; serum NfL (sNfL) has been proposed as a useful biomarker for treatment monitoring (4–6). A remarkable decrease in NfL levels was recently reported in paired CSF and serum samples of aMS treated with high-intensity conditioning AHSCT (7), but a possible transient neurotoxic effect of this protocol was suggested by a temporary increase in NfL detected shortly after the procedure (8). Similarly, hints of potential neurotoxicity of high-intensity conditioning AHSCT emerged from other studies (9, 10), but no data are available so far on intermediate-intensity regimens AHSCT. We hence present the results of a monocentric study evaluating the effect of intermediate intensity regimen AHSCT on sNfL and brain atrophy in aMS, exploring whether in this cohort sNfL might be a reliable marker of disability progression independent from new focal inflammation, thus identifying MS patients non-responding to the procedure.

MATERIALS AND METHODS

Patient and Control Populations

MS AHSCT

RR-MS or SP-MS patients diagnosed according to the Poser and Mc Donald criteria (11–13) who had been enrolled in an open-label monocentric study of AHSCT in Florence and who had frozen-stored serum samples previously collected at pre-defined timepoints (baseline, i.e. before haematopoietic stem cells mobilisation, months 6 and 24 after transplant) were included as the MS AHSCT group, according to the inclusion/exclusion criteria of the transplant centre. Briefly, RR-MS patients were considered for the procedure if they showed highly active MS despite treatment with disease-modifying treatments (DMTs) (i.e. occurrence of a disabling relapse or of at least two clinical relapses in the year prior to enrolment, associated with signs of new focal inflammatory activity at brain MRI in the previous year); or had history of highly active disease and scheduled withdrawal of a second line DMT. SP-MS were included if they had experienced a confirmed EDSS worsening in the previous year coupled with clinical or radiological evidence of new inflammatory activity in the year prior to inclusion (signs of new inflammation were not required if receiving active treatment). The main exclusion criteria were the following: primary progressive MS, pregnancy or other medical conditions that could contraindicate AHSCT, acute infections, malignancies, relevant comorbidity (e.g. liver disease, kidney failure, …), inability to provide adequate informed consent to participate to the study. Treatments were performed between 2007 and 2018 at the Cellular Therapies and Transplant Unit of the Careggi University Hospital in Florence, Italy, in collaboration with the Tuscan Region MS Referral Centre of the same hospital. Briefly, mobilisation of haematopoietic stem cells was obtained with IV cyclophosphamide (4 g/m^2) and granulocyte colony-stimulating factor. The conditioning regimen used was BEAM+ATG, an intermediate intensity regimen according to the EBMT classification (2), for all the patients except for two individuals who received either melphalan-carmustine-ATG or BEAM without melphalan and ATG for safety issues. Standardised haematological and neurological evaluations were performed at baseline, at months 6 and 12 after transplant and then yearly. Disability was assessed as Expanded Disability Status Scale (EDSS) (14) worsening (i.e. occurrence of one single episode of EDSS deterioration, defined as an increase of at least 1.0 or 0.5 EDSS point if baseline EDSS was <5.5 or ≥ 5.5, respectively) and continuous disability accrual (CDA, i.e. at least two confirmed episodes of EDSS worsening associated with continuous progression of disability between timepoints), as previously reported (15). Baseline, 6-month and 24-month samples were available for 37, 33 and 37 cases, respectively. sNfL measurement at all the timepoints was available for 31 patients.

Control Groups

In order to explore the accuracy of sNfL concentration in detecting axonal damage independent from new focal inflammation, SP-MS patients without signs of recent inflammatory activity (relapses and/or gadolinium-enhancing—Gd+–brain lesions in the 6 months before the collection of the serum sample), of age similar to the AHSCT SP-MS cases at month 24 after treatment were included (SP-MS CTRL). In addition, people not affected by any neurological disorders (healthy controls—HD) were included as normal controls. Serum samples in these two control groups were collected at one timepoint only and frozen-stored until their utilisation.

Laboratoristic and MRI Assessments

sNfL Measurement

sNfL were measured using single-molecule array (SIMOA) technology in cryopreserved serum samples stored in the same conditions; a quantification in duplicate was performed according to the manufacturer's instructions (16). Variation in absolute values within 20% was considered as not significant.

Magnetic Resonance Imaging Analysis

Brain magnetic resonance imaging (MRI) was performed at baseline, and then at least yearly up to the last follow-up. An additional scan at month 6 following AHSCT was available for a subset of cases.

MRI inflammatory activity was defined as the occurrence of new T2 lesions and/or Gd+ lesions in a follow-up brain MRI, compared to the baseline scan. T2 lesion load was evaluated using MIPAV software. Two-timepoint percentage brain volume change was estimated using the Structural Image Evaluation using Normalisation of Atrophy (SIENA) methodology (17, 18); whole brain volume at a timepoint (normalised for subject head size) was calculated with SIENAX, FSL-suite. The annualised rate of brain volume loss (AR-BVL) was then calculated as follows: (PBVC/100+1)^(365.25/days)−1)*100, where PBVC is the percentage brain volume change obtained with SIENA; AR-BVL was calculated up to last available MRI. A brain volume change >-0.4%/year was considered pathological, according to normative data (19).

Aims of the Study

The main aim of the study was to explore the impact of intermediate-intensity regimen AHSCT on sNfL in aMS patients, exploring if AHSCT could reduce sNfL to levels similar to SP-MS patients without signs of recent focal inflammation, or to healthy controls. As exploratory endpoint, potential correlations between response to AHSCT and sNfL were analysed, investigating whether in MS AHSCT treated patients sNfL could be a marker of disability accrual independent from new focal inflammation.

Statistical Methods

Baseline characteristics of the cases are reported as median and range, or as mean and 95% CI, as appropriate. Non parametric tests were adopted to compare baseline characteristics

TABLE 1 | Baseline clinical and demographic characteristics of the MS patients included in the study.

	RR-MS AHSCT ($n = 28$)		SP-MS AHSCT ($n = 10$)		SP-MS CTRL ($n = 22$)		SP-MS AHSCT vs. SP-MS CTRL
	Median	**(Range)**	**Median**	**(Range)**	**Median**	**(Range)**	***p* Value**
Age at baseline, y	34	(20–53)	43	(26–57)	49.5	(33–64)	0.039*
Disease duration from the onset, y	9.5	(1–22)	11	(6–23)	21.5	(6–36)	0.010*
Progressive phase duration, m	N/A	N/A	18.5	(7–79)	68	(3–181)	0.010*
Previous treatment duration with DMTs, y	6	(0–21)	7.5	(4–21)	15	(5–28)	0.006*
DMTs received, *n*	3	(0–7)	3	(2–6)	3	(1–5)	0.572
Baseline EDSS	4.0	(1.0–7.0)	5.75	(4.0–6.0)	6.25	(3.5–7.5)	0.182
Delta EDSS in the previous year	0.5	(-1.5–1.5)	0	(0–1.0)	0.25	(0–2.5)	0.257
Progression Index[a]	0.92	(0.43–1.41)	0.64	(0.34–0.94)	0.41	(0.31–0.50)	0.044*
Relapses in the previous year, *n*	1.5	(0–6)	0.5	(0–2)	0	(0–1)	0.002*
Gd+ lesions at last brain MRI, *n*	1.5	(0–31)	0.5	(0–3)	0	(0–0)	<0.001*
	n	**(%)**	***n***	**(%)**	***n***	**(%)**	***p* value**
Sex, female	22	(79%)	8	(80%)	14	(64%)	0.440
Cases with relapse in the previous 6 months	17	(61%)	3	(30%)	0	(0%)	0.024*
Cases with EDSS worsening in the previous year	6	(21%)	3	(30%)	8	(36%)	1.000
Cases receiving DMTs at blood sampling	17	(61%)	8	(80%)	13	(59%)	0.425
Cases showing Gd+ lesions in pre-treatment brain MRI	18	(64%)	5	(50%)	0	(0%)	0.001*

[a]*Mean (95% confidence interval—CI). N/A: not applicable. Significant values ($p < 0.05$) are marked with *.*

AHSCT, autologous haematopoietic stem cell transplantation; DMTs, disease-modifying treatments; EDSS, Expanded Disability Status Scale; Gd, gadolinium; MRI, magnetic resonance imaging; MS, multiple sclerosis; MS AHSCT, MS patients treated with AHSCT; RR-, relapsing-remitting; SP-, secondary-progressive; SP-MS CTRL, SP-MS control group (i.e. not treated with AHSCT).

between groups (Mann-Whitney test for continuous and Chi-square test for dichotomic variables). Correlation between sNfL concentration and the other variables were explored using partial correlation after adjusting for age at the sample. Event-free survival was estimated using the Kaplan–Meier survival analysis. A Cox regression model was adopted to explore the effect of baseline variables on the outcomes. The statistics software used were SPSS (IBM SPSS Statistics, RRID:SCR_019096) version 25 and Origin Pro for Windows. A two-tailed p-value < 0.05 was considered significant.

RESULTS

Patient and Control Group Characteristics

Thirty-eight aMS patients (28 RR-MS and 10 SP-MS) treated with AHSCT were included (MS AHSCT). Twenty-two SP-MS patients not treated with AHSCT and 19 healthy individuals (68% females) were included in the SP-MS CTRL and HD groups, respectively. Baseline clinical and demographic characteristics of MS patients included in the study are reported in **Table 1**. In the AHSCT group, age at baseline was similar to that of HD (median 35 years, range 20–57, vs. median 36 years, range 26–65, respectively; $p = 0.260$); the median age in the SP-MS AHSCT group at 24 months serum collection was similar to that of the SP-MS CTRL group (median 45, range 28–59, and median 49.5, range 33–64, respectively; $p = 0.070$).

At baseline serum collection (corresponding to pre-mobilisation for AHSCT patients, and to the single blood sample available for cases in the control groups), SP-MS AHSCT and SP-MS CTRL groups differed in the following characteristics: age ($p = 0.039$), disease duration ($p = 0.010$) and disability accrual rate ($p = 0.044$, **Table 1**).

At baseline serum collection, 25/38 (66%) patients in the AHSCT group were receiving DMTs, either second-line ($n = 22$) or first-line ones ($n = 3$); the remaining cases were off-treatment and had discontinued DMTs a median of 5.5 months (range 1–42) before transplant. In the SP-MS CTRL group, 13/22 (59%) patients were receiving DMTs at the time of sample collection (a second-line treatment in nine cases), while the remaining nine patients had been off-treatment for at least 6 months (median 11.5 months, range 7–84; data not shown).

sNfL Concentration Analysis

sNfL Concentration in the Control Groups

Median sNfL concentration was higher in the SP-MS CTRL group than the HD group, being 10.25 (5.2–22.6) pg/mL and 6.4 (4.0–18.4) pg/mL, respectively, $p = 0.003$ (**Figure 1**). No differences were observed between SP-MS CTRL patients who were receiving DMTs at the time of blood sampling and those who were not: 9.39 (range 5.2–12.4) pg/mL and 11.2 (range 7–22.7) pg/mL, respectively ($p = 0.235$; data not shown). A moderate correlation between sNfL concentrations and age at sample was observed in both groups, with r=0.56 in SP-MS CTRL ($p = 0.007$) and $r = 0.46$ in HD ($p = 0.045$; data not shown).

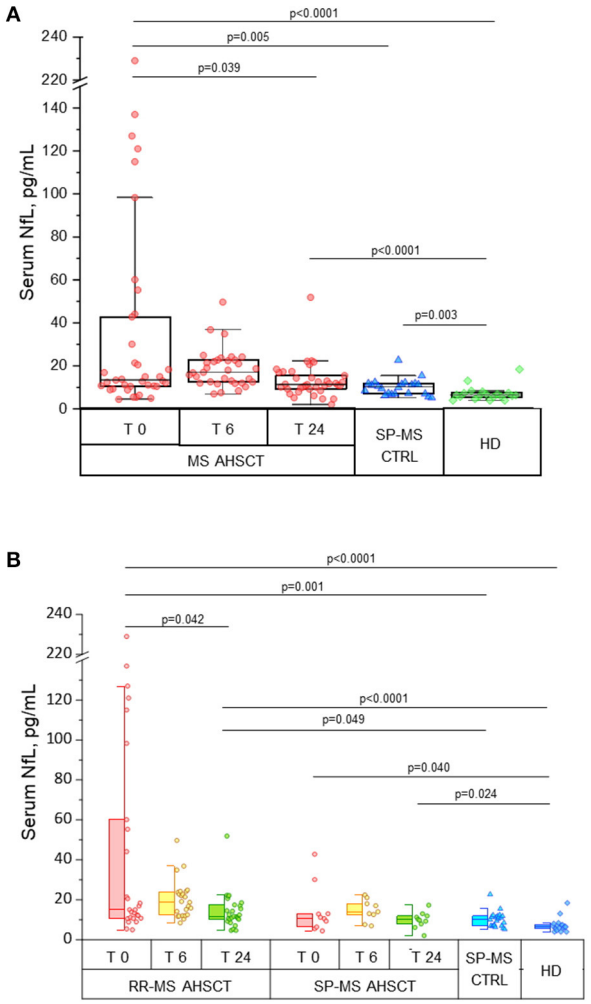

FIGURE 1 | Intermediate-intensity autologous haematopoietic stem cell transplantation reduces serum neurofilament light chain concentrations in treated MS patients. Serum neurofilament light chain (sNfL) concentrations in patients affected by aggressive relapsing-remitting (RR-) or secondary-progressive (SP-) multiple sclerosis (MS) before (T 0) and at months 6 (T 6) and 24 (T 24) following autologous haematopoietic stem cell transplantation (AHSCT, $n = 38$), compared with inactive SP-MS patients (i.e. without signs of recent clinical or radiological disease activity, SP-MS CTRL, $n = 22$) and with healthy individuals (HD, $n = 19$). **(A)** Overall MS AHSCT cohort. In AHSCT patients, baseline values of sNfL (median 13.4 pg/mL, range 4.4–229) were higher than in both SP-MS CTRL and HD groups (median 10.25 pg/mL, range 5.2–22.6, and median 6.4 pg/mL, range 4.0–18.4, $p = 0.005$ and <0.0001, respectively). SNfL at month 6 after transplant did not change compared to baseline ($p = 0.427$), but at T24 a reduction compared to baseline was observed (p=0.039), reaching levels similar to SP-MS CTRL ($p = 0.110$) but being still higher than in HD ($p < 0.0001$). **(B)** RR-MS and SP-MS AHSCT subgroups. At baseline, sNfL concentration in RR-MS cases was higher than in SP-MS CTRL ($p = 0.001$) and HD groups ($p < 0.0001$), whereas SP-MS AHSCT cases showed sNfL levels different from HD only ($p = 0.040$). SNfL concentrations at month 24 were reduced compared to baseline in the RR-MS AHSCT group ($n = 28$; 11.7 pg/mL, range 4.6–51.9, and 15 pg/mL, range 4.9–229, respectively; $p = 0.042$), whereas they did not differ from baseline in the SP-MS AHSCT group ($n = 10$; 10 pg/mL, range 2.0–17.3, and 10.8 pg/mL, range 4.4–42.8, respectively; $p = 0.721$). sNfL at month 24 were higher in RR-MS AHSCT cases compared both to SP-MS CTRL ($p = 0.049$) and HD ($p < 0.0001$); in SP-MS AHSCT group, values were higher than HD ($p = 0.024$).

TABLE 2 | Correlation between serum neurofilament light chain levels at baseline and clinical-radiological characteristics of the MS AHSCT patients corrected for age at sampling.

	R	*p* value
Relapses previous year, n	0.53	0.001
Days since last relapse	−0.40	0.030
Relapse in the previous 6 months, yes	0.38	0.026
Gd+ lesions, *n*	0.48	0.003
Gd+ lesions, volume	0.66	<0.001
Delta-EDSS in the previous year	0.37	0.029
EDSS worsening in the previous year, yes	0.46	0.006
T2 lesion load at baseline, mm^3	0.54	0.004

Baseline sNfL Concentrations in the MS AHSCT Group

In AHSCT patients, median sNfL concentration at baseline was 13.4 (range 4.4–229) pg/mL (**Figure 1A**), being 15 (range 4.9–229) pg/mL in RR-MS and 10.8 (range 4.4–42.8) pg/mL in SP-MS cases (**Figure 1B**). Median sNfL at baseline were higher in the MS AHSCT group compared to the SP-MS CTRL and HD groups, both considering the whole AHSCT cohort (p value 0.005 and <0.0001, respectively; **Figure 1A**) and the RR-MS AHSCT subgroup ($p = 0.001$ and <0.0001, respectively; **Figure 1B**). In the SP-MS AHSCT subgroup, median baseline sNfL concentration was similar to that of the SP-MS CTRL group ($p = 0.665$; **Figure 1B**) but it was higher than in HD ($p = 0.040$).

No differences in baseline sNfL were observed between MS AHSCT patients who were receiving DMTs at the time of baseline sample collection and those who were not (13.6 pg/mL, range 4.9–137, and 12.4 pg/mL, range 4.4–229, respectively, $p = 0.404$; data not shown). sNfL concentrations at baseline correlated with clinical and/or MRI markers of recent inflammatory disease activity (**Table 2**).

sNfL Variation Following AHSCT

In the MS AHSCT group, median sNfL concentration at month 24 (11.3 pg/mL, range 2.0–51.9) was remarkably reduced compared to baseline ($p = 0.039$), whereas levels at month 6 (17 pg/mL, range 6.9–49.7) did not differ from baseline ($p = 0.427$; **Figure 1A**). At month 24, median sNfL concentration in the MS ASHCT group was similar to that of the SP-MS CTRL group (p=0.110), but it was still higher than in HD ($p < 0.0001$; **Figure 1A**). Variation of individual values of MS AHSCT patients are reported in **Figure 2**. A median decrease by 13% (median 42.8 pg/mL, range 2.4–217.3) of the baseline value was observed, which was by at least 50% in 13 patients (10 RR-MS, 3 SP-MS), reaching up to 90% in four cases.

In the RR-MS AHSCT subgroup, median sNfL concentrations were reduced at month 24 (11.7 pg/mL, range 4.6–51.9) compared to baseline (15 pg/mL, range 4.9–229; $p = 0.042$) (**Figure 1B**).

In the SP-MS AHSCT subgroup, sNfL levels at months 24 (10 pg/mL, range 2.0–17.3) were similar to baseline (10.8 pg/mL, range 4.4–42.8; $p = 0.721$) (**Figure 1B**).

A remarkable elevation in sNfL at month 24 (51.9 pg/mL) compared to month 6 (22.7 pg/mL) was observed in one single case (RR-MS) who had experienced a clinical and radiological disease reactivation (i.e. relapse associated with occurrence of new Gd+ lesions at brain MRI) 2 months before the blood sample collection. This patient had received BEAM without melphalan and ATG for safety issues.

Baseline sNfL concentrations correlated with those at month 6 ($r = 0.56$, $p = 0.001$), but not with 24-months values ($p = 0.547$; data not shown).

Relapses and Disability Following AHSCT

ARR dropped from 1.13 in the two years before AHSCT to 0.0054 up to the last follow-up after transplant (median 49 months, range 24–153). All the cases except for one were relapse-free up to the last follow-up, being relapse-free survival from year 2 to last follow-up 97%. At month 24, EDSS worsening was observed in 8/38 cases (21%, 1/28 RR-MS−4%, and 7/10 SP-MS−70%, $p < 0.0001$), occurring at a median of 10 months (2–24) after the procedure. One additional worsening was reported in one SP-MS case at month 66. Four aMS patients (all SP-MS) experienced CDA and the second confirmed episode of progression was reported at a median of 27 months (range 25–37) of follow-up. In the RR-MS subgroup, EDSS improved at last follow-up in 13/28 (46%) cases, stabilised 14/28 (50%) and worsened in 1 case (4%). Median EDSS in the RR-MS AHSCT subgroup improved at all the timepoints following AHSCT compared to baseline ($p < 0.005$, **Figure 3**), with a confirmed decrease up to −4.0 EDSS points. Following AHSCT, a slight deterioration of disability was observed in the SP-MS subgroup, which was significant at month 24 compared to baseline ($p = 0.047$; **Figure 3**), being the median worsening of 1.0 EDSS point (range 0.5–1.5).

Safety

No fatalities or life-threatening complications were observed; common adverse events following transplant were aligned with the literature (20).

MRI Activity and Brain Atrophy

One case (RR-MS) showed new Gd+ lesions at month 22, associated with clinical relapse. All the remaining cases were free from both new and Gd+ lesions up to the last follow-up.

Brain volume loss after transplant was evaluated in 32 patients (22 RR-MS and 10 SP-MS) who had scans of adequate quality to perform the analysis. Mean PBVC was −1.15 (95%CI −1.55, −0.75) and −1.56 (95%CI −2.04, −1.09) at months 12 and 24, respectively (**Figure 4A**). MRI scan at month 6 following AHSCT was available for 18 cases (14 RR-MS, 4 SP-MS), and mean PBVC at this timepoint was −0.6 (95%CI −1.02, −0.17). At year 2 following AHSCT, 15/32 cases (47%) showed normalisation of AR-BVL, without re-baseline (median AR-BVL −0.24%, range −0.4–0.0); at this timepoint, the observed AR-BVL was within normal values for age (i.e. below−0.4%) in 55% of the RR-MS AHSCT and 30% of the SP-MS AHSCT cases analysed ($p = 0.197$, **Figure 4B**). The normalisation of AR-BVL did not correlate with EDSS worsening following transplant (data not shown). AR-BVL

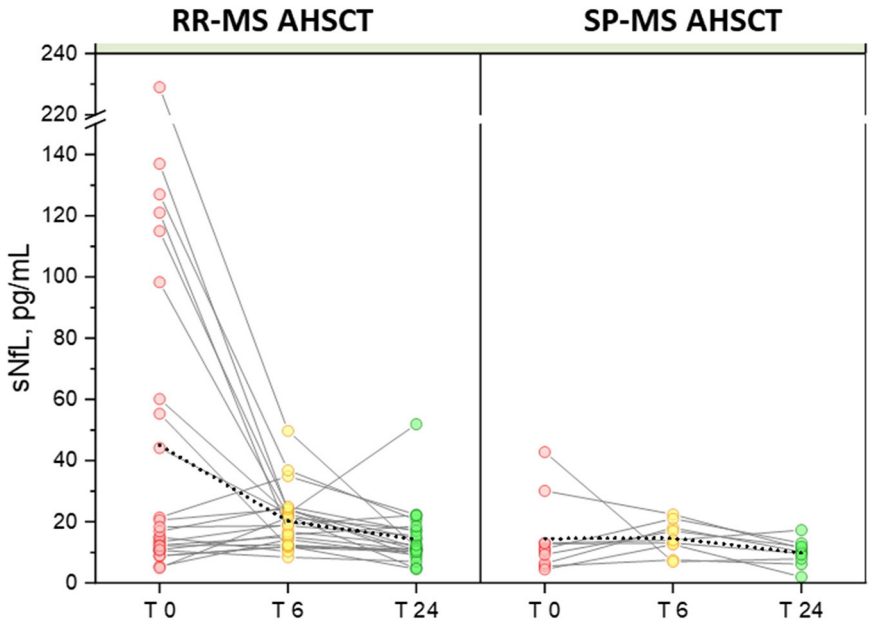

FIGURE 2 | Variation in serum NfL following AHSCT. Individual values of pre- and post-AHSCT sNfL for RR-MS **(left)** and SP-MS AHSCT patients **(right)** are connected with solid colour lines. Mean values of each group are connected with a dotted line, showing high sensitivity of the mean to the outliers with a significant reduction in the RR-MS group at months 6 (20.23 pg/mL) and 24 of follow-up (14.33 pg/mL) compared to baseline (45.06 pg/mL), *p* values 0.012 and 0.010 for month 6 and 24, respectively.

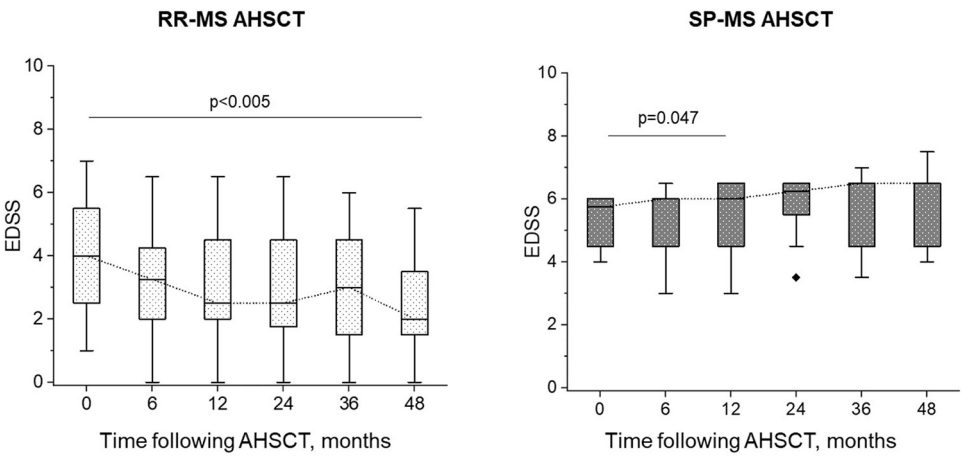

FIGURE 3 | EDSS change following AHSCT. In the RR-MS AHSCT subgroup, EDSS decreased compared to baseline at each timepoint (p <0.005), whereas in the SP-MS AHSCT subgroup, median EDSS increased compared to baseline at month 24 after AHSCT ($p = 0.047$).

up to the last follow-up beyond year 2 (median 7 years, range 3–12) was available for eight RR-MS and five SP-MS cases and it normalised in 75% and 60% of the cases, respectively, $p = 0.207$ (**Figure 4B**).

Association Between sNfL Concentration and Outcomes

No correlations between sNfL concentrations either at baseline or follow-up and disability accrual or AR-BVL normalisation were observed. In the SP-MS AHSCT subgroup, baseline sNfL concentration did not predict subsequent disability accrual up to the last follow-up (HR 1.02, 95%CI 0.97–1.08, $p = 0.442$), nor did month 6 sNfL levels (HR 1.12, 95%CI 0.90–1.40, $p = 0.306$). sNfL concentration at month 24 did not differ between patients who had shown disability accrual within 24 months from AHSCT and those who had not ($p = 0.299$ for the MS AHSCT and 0.667 for SP-MS AHSCT groups; data not shown).

sNfL at month 24 did not correlated with T2 lesion load at the same timepoint (R −0.24, $p = 0.187$; data not shown).

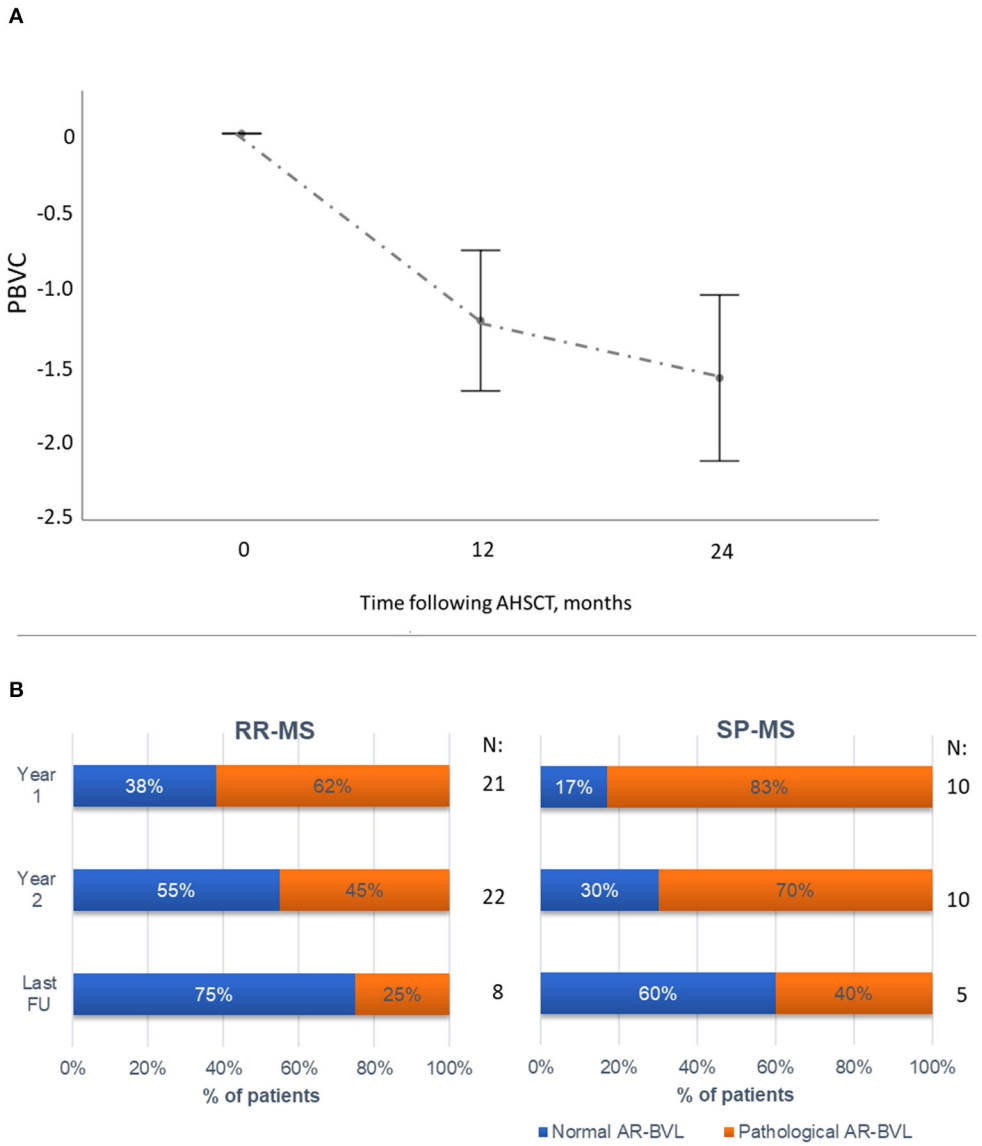

FIGURE 4 | Brain atrophy following AHSCT. **(A)** Mean (95% CI) percentage of brain volume change (PBVC) in the first two years following AHSCT in the RR-MS and SP-MS AHSCT cases, compared to the baseline scan. The greatest reduction in PBVC was observed during the first year following AHSCT, followed by a reduction in AR-BVL. **(B)** Annualised rate of brain volume loss (AR-BVL) in RR- and SP-MS AHSCT cases at year 1, 2 and up to last follow-up available beyond year 2. The proportion of patients with normalisation of AR-BVL tended to be higher in RR vs. SP-MS cases and increased over follow-up.

DISCUSSION

sNfL concentrations were evaluated in 38 aMS patients who underwent intermediate-intensity AHSCT at our centre, and the results were compared with those detected in two control groups: SP-MS cases without recent inflammatory activity (i.e. relapses or new/Gd+ lesions in the previous 6 months) and individuals not affected by neurological diseases (HD). The main aim of the study was to assess the impact of intermediate-intensity AHSCT on sNfL in RR-MS and SP-MS patients undergoing the procedure, exploring whether transplant could induce a reduction in sNfL to levels similar to the control groups. The potential role of sNfL as a marker of disability accrual independent from new focal inflammation was also investigated in AHSCT treated MS patients.

Patients enrolled in the transplant program showed highly active disease, refractory to DMTs in most of the cases. The procedure was effective in halting relapses and new inflammatory MRI activity in all the patients except for one RR-MS, who relapsed at month 22, after being treated with BEAM without melphalan and ATG for safety issues.

SP-MS AHSCT patients had a more aggressive disease course than SP-MS CTRL, as expected for a selection bias due to the enrolment in the AHSCT program. Treatment with DMTs

did not influence sNfL concentrations in our sample, both in the SP-MS CTRL and MS AHSCT groups, and two opposite explanations can be offered: the lack of recent inflammatory activity in all the cases in the SP-MS CTRL group and the occurrence of breakthrough disease activity despite treatment in the MS AHSCT group. Superimposed inflammatory activity which could overcome the small age-related increase in sNfL concentration might explain the lack of correlation between sNfL and age at sampling in the MS AHSCT group only (21).

Aligned with previous works (5), sNfL reflected recent inflammatory activity: values were higher in RR-MS compared to SP-MS patients, consistent with the differences in recent relapses and MRI activity between the groups. The transient although not significant increase in median sNfL concentration detected at month 6 after AHSCT might mirror transient neuronal damage with consequent release of NfL in the CSF and serum. However, the interpretation of these data is not univocal and two not mutually exclusive scenarios can be hypothesised: a transient neuro-toxic effect of the chemotherapy, or accelerated neuronal damage induced by a rapid suppression of inflammation. Potential neurotoxicity of AHSCT in MS patients was suggested by previous studies, which however were limited to high-intensity conditioning regimens only. An increase in serum neurofilament heavy chains was reported in SP-MS patients treated with cyclophosphamide and total body irradiation, a protocol no longer used due to safety concerns (10). More recently, a transient increase in sNfL was observed 3 months after busulfan-cyclophosphamide AHSCT, followed by a decrease to levels similar to baseline starting in month 6 (8). Albeit valuable, caution should be adopted in inferring these observations to intermediate- or low-intensity regimen AHSCT, and no evidence of neurotoxicity of these protocols is available so far. Furthermore, the observed increase in sNfL might be due to an MS-specific process rather than to a neurotoxic effect of the chemotherapy, i.e. the consolidation of baseline axonal damage in a CNS affected by inflammation could be the main driver of NfL release. If this latter hypothesis was true, the transient increase in sNfL observed could be an epiphenomenon of the glial scarring of MS lesions "de-activated" by the procedure. Potentially supporting this hypothesis, a transient increase in sNfL was reported in a proportion of MS patients receiving alemtuzumab at months 2–3 following either the first or second course of treatment (5/15 patients and 3/15 cases, respectively) (22). Finally, in either case, indirect proof of the ability of the drugs adopted during mobilisation and/or conditioning to cross the blood-brain barrier might be provided, thus suggesting that AHSCT might be effective also on compartmentalised inflammation. If this latter hypothesis is true, AHSCT could become a suitable treatment option for patients in progressive phases of MS with signs of ongoing compartmentalised inflammation, where the lack of effective approved DMTs is still an unmet clinical need.

Furthermore, potential pleiotropic effects of AHSCT have been suggested, such as a possible contribution to tissue repair mediated by putative trans differentiation of the graft in neural/glia cells and trophic/protective effects on CNS tissue, although further research is needed to explore this issue (23, 24).

The significant decrease of sNfL detected at month 24 compared to baseline confirms that the procedure exerts a long-standing effect in reducing inflammation-related axonal damage, at least in the RR-MS form, where the greatest reduction was observed. The amount of decrease in sNfL levels detected is similar to that previously reported in a cohort of patients treated with high-intensity AHSCT (7), suggesting that BEAM-AHSCT might be as effective as the former protocol in suppressing inflammation-related axonal damage. Notably, the great reduction in sNfL after transplant is remarkable considering that most of the MS AHSCT cases in the present cohort were receiving DMTs at the time of baseline sample collection, providing further evidence on AHSCT as an effective escalating therapy.

sNfL concentrations at month 24 did not differ between MS AHSCT cases and SP-MS CTRL, thus reflecting the resolution of new inflammatory activity in all the cases, except for one patient who experienced a disease reactivation. Indeed, this latter was the only case that showed a marked increase at month 24 compared to month 6.

Correlation between sNfL levels and disability accrual and brain atrophy has been reported in large cohorts of non-AHSCT treated MS patients (4, 25), whereas in the present study baseline sNfL were not able to predict response to AHSCT in terms of disability progression or brain atrophy, and sNfL reflected mainly new focal inflammatory activity. Although the small sample size could have prevented us from finding significant correlations, it could be speculated that this difference might be due, at least in part, to a different persistence of new focal inflammatory activity in untreated or various DMTs treated patients described in other studies (4, 25) and AHSCT-treated patients, being new focal inflammation virtually suppressed in these latter. It could be hypothesised that sNfL concentrations might correlate with prognosis in MS as long as new inflammation (relapses and/or new MRI lesions) is the main driver of disability accrual. Following AHSCT, the persistence of median values of sNfL higher than in HD could be explained by a background of axonal damage persisting in a subset of treated patients despite the suppression of new inflammatory activity, and possibly due to non-inflammation driven neurodegeneration or by compartmentalised inflammation not eradicated by AHSCT. However, the lack of correlation with clinical outcomes partially argues against this hypothesis, even if the study might be underpowered for this purpose. Moreover, the measurement of NfL in the serum, where values are considerably lower than in CSF, might have a low sensitivity to detect pathological release of small amounts of NfL promoted by neurodegeneration or smouldering inflammation, suggesting that sNfL might not be a sensitive surrogate marker of these latter phenomena in progressive disease.

In this study, the effectiveness of AHSCT on ARR and MRI activity was aligned with the literature (26–28). A significant improvement in median EDSS was observed in the RR-MS AHSCT subgroup, while disability progression occurred exclusively in SP-MS cases. AR-BVL was high during the first

year following treatment and this could be due, at least in part, to pseudoatrophy, i.e. shrinking of brain tissue due to rapid resolution of inflammation and of the associated oedema. A normalisation of AR-BVL two years after transplant was observed in 15 out of 32 evaluable cases (47%), mostly RR-MS (12/15, 80%). The safety of the procedure was overall acceptable.

Our study has several limitations. First of all, the lack of a control group of active MS patients not undergoing AHSCT does not allow to compare the relative effect of AHSCT on sNfL; moreover, as MS AHSCT patients showed highly active disease before the enrolment, a regression to the mean could, at least in part, influence the reduction in sNfL observed shortly after transplant. Despite broad experience in AHSCT for MS in our centre, the relatively small sample size could have prevented us from identifying significant correlations between sNfL and the outcomes. Furthermore, the lack of blood samples collected shortly after transplant could have underestimated a potential increase in sNfL occurring early after the procedure, as already pointed out by other authors (8), therefore no conclusive data on a potential neuro-toxicity of intermediate-intensity AHSCT in MS could be provided.

CONCLUSION

The present study provides class IV evidence on the efficacy of intermediate intensity AHSCT in inducing suppression of new inflammatory activity in aggressive MS, both on clinical and para-clinical parameters. The remarkable reduction in sNfL observed in aMS patients who were receiving DMTs at baseline strengthens the role of AHSCT as an effective escalating therapy, providing that the switch to transplant is performed timely before the occurrence of irreversible disability accrual. Further data are needed to properly answer the question as to whether an early (although not significant) increase in sNfL after AHSCT might harbour a neurotoxic effect of the procedure vs. consolidation of pre-existing axonal damage induced by a rapid suppression of inflammation.

In our sample, sNfL did not perform as a sensitive surrogate marker of inflammation-independent neurodegeneration but was reliably associated with recent focal inflammatory activity, and baseline levels could not predict response to treatment in terms of disability accrual or brain atrophy. The individuation of a biomarker that could identify MS patients in whom axonal damage is still related to inflammation (and could therefore be eradicated by maximal immunosuppression) is of pivotal importance to allow a better selection of the patients who might benefit from anti-inflammatory treatments, including transplant.

DATA AVAILABILITY STATEMENT

The raw data supporting the conclusions of this article will be made available by the authors, without undue reservation.

ETHICS STATEMENT

The studies involving human participants were reviewed and approved by Comitato Etico Area Vasta Centro, University Hospital of Careggi. The patients/participants provided their written informed consent to participate in this study.

AUTHOR CONTRIBUTIONS

AM contributed to the conception and design of the study, acquired and analysed data, and wrote the first draft of the manuscript. LeM, SF, and MP performed imaging analyses and acquired related data. CI, AB, CM, and RS acquired clinical data. MD contributed to the database. FM, BM, and TB acquired laboratoristic data. LuM and AR contributed to the conception and design of the study and reviewed the manuscript. All authors contributed to manuscript revision, read, and approved the submitted version.

ACKNOWLEDGMENTS

The authors thank the trial nurse Serena Mariotti for the dedicated time in this project, and all the haematological and neurological team that contributed to patient caring.

REFERENCES

1. Cohen JA, Baldassari LE, Atkins HL, Bowen JD, Bredeson C, Carpenter PA, et al. Autologous hematopoietic cell transplantation for treatment-refractory relapsing multiple sclerosis: position statement from the American Society for Blood and Marrow Transplantation. *Biol Blood Marrow Transplant.* (2019) 25:845–54. doi: 10.1016/j.bbmt.2019.02.014
2. Sharrack B, Saccardi R, Alexander T, Badoglio M, Burman J, Farge D, et al. Autologous haematopoietic stem cell transplantation and other cellular therapy in multiple sclerosis and immune-mediated neurological diseases: updated guidelines and recommendations from the EBMT Autoimmune Diseases Working Party (ADWP) and the Joint Accreditation Committee of EBMT and ISCT (JACIE). *Bone Marrow Transplant.* (2019). doi: 10.1038/s41409-019-0684-0
3. Muraro PA, Pasquini M, Atkins HL, Bowen JD, Farge D, Fassas A, et al. Long-term outcomes after autologous hematopoietic stem cell transplantation for multiple sclerosis. *JAMA Neurol.* (2017) 74:459–69. doi: 10.1001/jamaneurol.2016.5867
4. Barro C, Benkert P, Disanto G, Tsagkas C, Amann M, Naegelin Y, et al. Serum neurofilament as a predictor of disease worsening and brain and spinal cord atrophy in multiple sclerosis. *Brain.* (2018) 141:2382–91. doi: 10.1093/brain/awy154
5. Novakova L, Zetterberg H, Sundstrom P, Axelsson M, Khademi M, Gunnarsson M, et al. Monitoring disease activity in multiple sclerosis using serum neurofilament light protein. *Neurology.* (2017) 89:2230–7. doi: 10.1212/WNL.0000000000004683
6. Leppert D, Kuhle J. Serum NfL levels should be used to monitor multiple sclerosis evolution - Yes. *Mult Scler.* (2020) 26:17–9. doi: 10.1177/1352458519872921
7. Thebault S. Tessier DR, Lee H, Bowman M, Bar-Or A, Arnold DL, et al. High serum neurofilament light chain normalizes after hematopoietic stem

cell transplantation for MS. *Neurol Neuroimmunol Neuroinflamm.* (2019) 6:e598. doi: 10.1212/NXI.0000000000000598
8. Thebault S, Lee H, Bose G, Tessier D, Abdoli M, Bowman M, et al. Neurotoxicity after hematopoietic stem cell transplant in multiple sclerosis. *Ann Clin Transl Neurol.* (2020) 7:767–75. doi: 10.1002/acn3.51045
9. Lee H, Nakamura K, Narayanan S, Brown R, Chen J, Atkins HL, et al. Impact of immunoablation and autologous hematopoietic stem cell transplantation on gray and white matter atrophy in multiple sclerosis. *Mult Scler.* (2018) 24:1055–66. doi: 10.1177/1352458517715811
10. Petzold A, Mondria T, Kuhle J, Rocca MA, Cornelissen J. te Boekhorst P, et al. Evidence for acute neurotoxicity after chemotherapy. *Ann Neurol.* (2010) 68:806–15. doi: 10.1002/ana.22169
11. Polman CH, Reingold SC, Edan G, Filippi M, Hartung HP, Kappos L, et al. Diagnostic criteria for multiple sclerosis: 2005 revisions to the "McDonald Criteria." *Ann Neurol.* (2005) 58:840–6. doi: 10.1002/ana.20703
12. Polman CH, Reingold SC, Banwell B, Clanet M, Cohen JA, Filippi M, et al. Diagnostic criteria for multiple sclerosis: 2010 revisions to the McDonald criteria. *Ann Neurol.* (2011) 69:292–302. doi: 10.1002/ana.22366
13. Poser CM, Paty DW, Scheinberg L, McDonald WI, Davis FA, Ebers GC, et al. New diagnostic criteria for multiple sclerosis: guidelines for research protocols. *Ann Neurol.* (1983) 13:227–31. doi: 10.1002/ana.410130302
14. Kurtzke JF. Rating neurologic impairment in multiple sclerosis: an expanded disability status scale (EDSS). *Neurology.* (1983) 33:1444–52. doi: 10.1212/WNL.33.11.1444
15. Mariottini A, Filippini S, Innocenti C, Forci B, Mechi C, Barilaro A, et al. Impact of autologous haematopoietic stem cell transplantation on disability and brain atrophy in secondary progressive multiple sclerosis. *Mult Scler.* (2021) 27:61–70. doi: 10.1177/1352458520902392
16. Hendricks R, Baker D, Brumm J, Davancaze T, Harp C, Herman A, et al. Establishment of neurofilament light chain Simoa assay in cerebrospinal fluid and blood. *Bioanalysis.* (2019) 11:1405–18. doi: 10.4155/bio-2019-0163
17. Smith SM, Zhang Y, Jenkinson M, Chen J, Matthews PM, Federico A, et al. Accurate, robust, and automated longitudinal and cross-sectional brain change analysis. *Neuroimage.* (2002) 17:479–89. doi: 10.1006/nimg.2002.1040
18. Smith SM, Jenkinson M, Woolrich MW, Beckmann CF, Behrens TE, Johansen-Berg H, et al. Advances in functional and structural MR image analysis and implementation as FSL. *Neuroimage.* (2004) 23 Suppl 1:S208–19. doi: 10.1016/j.neuroimage.2004.07.051
19. De Stefano N, Stromillo ML, Giorgio A, Bartolozzi ML, Battaglini M, Baldini M, et al. Establishing pathological cut-offs of brain atrophy rates in multiple sclerosis. *J Neurol Neurosurg Psychiatry.* (2016) 87:93–9.
20. Muraro PA, Martin R, Mancardi GL, Nicholas R, Sormani MP, Saccardi R. Autologous haematopoietic stem cell transplantation for treatment of multiple sclerosis. *Nat Rev Neurol.* (2017) 13:391–405. doi: 10.1038/nrneurol.2017.81
21. Khalil M, Pirpamer L, Hofer E, Voortman MM, Barro C, Leppert D, et al. Serum neurofilament light levels in normal aging and their association with morphologic brain changes. *Nat Commun.* (2020) 11:812. doi: 10.1038/s41467-020-14612-6
22. Akgun K, Kretschmann N, Haase R, Proschmann U, Kitzler HH, Reichmann H, et al. Profiling individual clinical responses by high-frequency serum neurofilament assessment in MS. *Neurol Neuroimmunol Neuroinflamm.* (2019) 6:e555. doi: 10.1212/NXI.0000000000000555
23. Bossolasco P, Cova L, Calzarossa C, Rimoldi SG, Borsotti C, Deliliers GL, et al. Neuro-glial differentiation of human bone marrow stem cells in vitro. *Exp Neurol.* (2005) 193:312–25. doi: 10.1016/j.expneurol.2004.12.013
24. Daley GQ, Goodell MA, Snyder EY. Realistic prospects for stem cell therapeutics. *ASH Educ. Program Book.* (2003) 2003:398–418. doi: 10.1182/asheducation-2003.1.398
25. Kuhle J, Kropshofer H, Haering DA, Kundu U, Meinert R, Barro C, et al. Blood neurofilament light chain as a biomarker of MS disease activity and treatment response. *Neurology.* (2019) 92:e1007–e15. doi: 10.1212/WNL.0000000000007032
26. Atkins HL, Bowman M, Allan D, Anstee G, Arnold DL, Bar-Or A, et al. Immunoablation and autologous haemopoietic stem-cell transplantation for aggressive multiple sclerosis: a multicentre single-group phase 2 trial. *Lancet.* (2016) 388:576–85. doi: 10.1016/S0140-6736(16)30169-6
27. Burt RK, Balabanov R, Han X, Sharrack B, Morgan A, Quigley K, et al. Association of nonmyeloablative hematopoietic stem cell transplantation with neurological disability in patients with relapsing-remitting multiple sclerosis. *Jama.* (2015) 313:275–84. doi: 10.1001/jama.2014.17986
28. Moore JJ, Massey JC, Ford CD, Khoo ML, Zaunders JJ, Hendrawan K, et al. Prospective phase II clinical trial of autologous haematopoietic stem cell transplant for treatment refractory multiple sclerosis. *J Neurol Neurosurg Psychiatry.* (2019) 90:514–21. doi: 10.1136/jnnp-2018-319446

Conflict of Interest: The authors declare that the research was conducted in the absence of any commercial or financial relationships that could be construed as a potential conflict of interest.

Publisher's Note: All claims expressed in this article are solely those of the authors and do not necessarily represent those of their affiliated organizations, or those of the publisher, the editors and the reviewers. Any product that may be evaluated in this article, or claim that may be made by its manufacturer, is not guaranteed or endorsed by the publisher.

frontiers in Immunology

ORIGINAL RESEARCH
published: 28 February 2022
doi: 10.3389/fimmu.2022.818325

Long-Term Effects of Alemtuzumab on CD4+ Lymphocytes in Multiple Sclerosis Patients: A 72-Month Follow-Up

Simona Rolla[1†], Stefania Federica De Mercanti[1†], Valentina Bardina[1,2], Alessandro Maglione[1], Daniela Taverna[3], Francesco Novelli[3], Eleonora Cocco[4], Anton Vladic[5], Mario Habek[6,7], Ivan Adamec[6,7], Pietro Osvaldo Luigi Annovazzi[8], Dana Horakova[9] and Marinella Clerico[1]*

[1] Department of Clinical and Biological Sciences, University of Torino, Torino, Italy, [2] Laboratory of Microbiology and Virology, Amedeo di Savoia Hospital, Torino, Italy, [3] Department of Molecular Biotechnology and Health Sciences, University of Torino, Torino, Italy, [4] Department of Medical Science and Public Health, University of Cagliari and Multiple Sclerosis Center, Cagliari, Italy, [5] Department of Neurology, Clinical Hospital Sveti Duh Zagreb and Medical Faculty, University J.J Strossmayer Osijek, Prague, Croatia, [6] Referral Center for Autonomic Nervous System, University Hospital Center Zagreb, Zagreb, Croatia, [7] School of Medicine, University of Zagreb, Zagreb, Croatia, [8] Multiple Sclerosis Centre, Gallarate Hospital, ASST Valle Olona, Gallarate, Italy, [9] Department of Neurology and Center of Clinical Neuroscience, First Faculty of Medicine, Charles University and General University Hospital, Prague, Czechia

Introduction: Alemtuzumab is highly effective in the treatment of patients with relapsing multiple sclerosis (PwRMS) and selectively targets the CD52 antigen, with a consequent profound lymphopenia, particularly of CD4+ T lymphocytes. However, the immunological basis of its long-term efficacy has not been clearly elucidated.

Methods: We followed up 29 alemtuzumab-treated RMS patients over a period of 72 months and studied the immunological reconstitution of their CD4+ T cell subsets by means of phenotypic and functional analysis and through mRNA-related molecule expression, comparing them to healthy subject (HS) values (rate 2:1).

Results: In patients receiving only two-course alemtuzumab, the percentage of CD4+ lymphocytes decreased and returned to basal levels only at month 48. Immune reconstitution of the CD4+ subsets was characterized by a significant increase ($p < 0.001$) in Treg cell percentage at month 24, when compared to baseline, and was accompanied by restoration of the Treg suppressor function that increased within a range from 2- to 6.5-fold compared to baseline and that persisted through to the end of the follow-up. Furthermore, a significant decrease in self-reactive myelin basic protein-specific Th17 ($p < 0.0001$) and Th1 ($p < 0.05$) cells reaching HS values was observed starting from month 12. There was a change in mRNA of cytokines, chemokines, and transcriptional factors related to Th17, Th1, and Treg cell subset changes, consequently suggesting a shift toward immunoregulation and a reduction of T cell recruitment to the central nervous system.

OPEN ACCESS

Edited by:
Luisa María Villar, Ramón y Cajal University Hospital, Spain

Reviewed by:
Emanuele D'amico, University of Catania, Italy
Ayman Rezk, University of Pennsylvania, United States

***Correspondence:**
Simona Rolla
simona.rolla@unito.it

[†]These authors have contributed equally to this work

Specialty section:
This article was submitted to Multiple Sclerosis and Neuroimmunology, a section of the journal Frontiers in Immunology

Received: *19 November 2021*
Accepted: *07 February 2022*
Published: *28 February 2022*

Citation:
Rolla S, De Mercanti SF, Bardina V, Maglione A, Taverna D, Novelli F, Cocco E, Vladic A, Habek M, Adamec I, Annovazzi POL, Horakova D and Clerico M (2022) Long-Term Effects of Alemtuzumab on CD4+ Lymphocytes in Multiple Sclerosis Patients: A 72-Month Follow-Up. Front. Immunol. 13:818325. doi: 10.3389/fimmu.2022.818325

Conclusions: These data provide further insight into the mechanism that could contribute to the long-term 6-year persistence of the clinical effect of alemtuzumab on RMS disease activity.

Keywords: multiple sclerosis, alemtuzumab, immune reconstitution, Treg cells, MBP (myelin basic protein)

INTRODUCTION

Alemtuzumab, a monoclonal antibody that targets the CD52 antigen, is the first immune reconstitution therapy in Europe and the USA to be approved for patients with relapsing multiple sclerosis (PwRMS). Alemtuzumab administration determines a rapid and marked reduction in peripheral T and B lymphocytes, which express CD52 molecules at high levels on their membrane, due to antibody-dependent cell-mediated cytotoxicity, complement-dependent cytolysis, and induction of apoptosis (1) with a subsequent beneficial reconstitution of the immune system (2). The lack of CD52 expression on bone marrow-derived hematopoietic cells enables immune reconstitution, which is obtained over several months (3, 4), and return of immune competency (5). Specific immune repopulation patterns appear to be responsible for the long-term efficacy of alemtuzumab that persists even years after the last course of therapy: B lymphocytes recover first, followed by CD8+ and CD4+ T lymphocytes (2–6). As immune reconstitution proceeds, Tregs represent the majority of the T lymphocyte population and thus are believed to be one of the reasons for long-term alemtuzumab effectiveness (6–8).

We had previously organized a multicenter 24-month study (7) to analyze the changes in Th subsets, Treg proportion and function, and mRNA levels of cytokines and other immunologically related molecules in 29 patients from phase III trials CARE-MS I (3) and CARE-MS II (4). The data showed a different T cell repopulation among the CD4+ T cells: while the percentage of Th1 and Th17 cells did not have any relevant change, a significant increase in Treg cell percentage with restored suppressive function was observed at 24 months post treatment. Moreover, mRNA levels of pro-inflammatory and anti-inflammatory cytokines were downregulated and upregulated respectively following treatment, which may also favor the drug's long-term efficacy in RMS (7, 9). In this paper, we herewith report the now complete long-term follow-up of 72 months focusing on the study of the CD4+ immune cell reconstitution in those 24 patients who had received the two classical alemtuzumab administrations at months 0 and 12, and studying the CD4+ immune cell reconstitution so as to compare it to the healthy subjects (HS).

MATERIALS AND METHODS

Patients and Clinical Study Design

Twenty-nine PwRMS participating in CARE-MS I (3) and II (4) trials in 6 European MS centers were enrolled and evaluated at baseline and for 72 months after alemtuzumab treatment. Inclusion and exclusion criteria were described in the original articles (3, 4). Patients were treated with 12 mg/d IV alemtuzumab in 2 annual courses (5 administrations at month 0 and 3 administrations at month 12). Patients' demographic and clinical characteristics are reported in **Table 1**. Neurologic assessments, performed by blinded investigators, were done at baseline and repeated every month or in case of relapses. Clinical data were collected in clinical research forms (CRF) and sent to the coordinating center located at the University of Torino. Blood samples were taken at baseline (before the first alemtuzumab course) and at months 6, 12 (before the second alemtuzumab course), 18, 24, 36, 48, 60, and 72. Fresh blood was collected in heparin-treated vacutainers and immediately sent to the coordinating center located at the University of Torino for immunologic testing. All samples were received and processed within 48 h from the blood withdrawal. Twelve sex- and age-matched healthy subjects were also enrolled from every center (rate cases/controls: 2:1).

Standard Protocol Approvals, Registrations, and Patient Consents

The institutional review board of the participating centers approved the study, and all subjects gave written informed consent (protocol number Bio2009001).

Flow Cytometry (Fluorescence-Activated Cell Sorting)

We used the same methodology as the one employed in our previous study (7). Peripheral blood mononuclear cells (PBMC) were isolated by density gradient centrifugation from heparinized venous blood. PBMC were stained for Treg cells with anti-CD4, anti-CD25, anti-CD127, anti-CD45RO, and anti-CD45RA monoclonal antibodies (mAb) (BioLegend, San Diego, CA) on the cell surface. For detection of the transcriptional factor FoxP3, cells were fixed with fixation and permeabilization buffers (eBioscience, San Diego, CA). PBMC were cultured in Iscove's modified Dulbecco's medium (BioWhittaker, Walkersville, MD) supplemented with 10% fetal bovine serum (Invitrogen, Carlsbad, CA) and stimulated for 5 h with phorbol 12-myristate 13-acetate PMA (50 ng/ml) and ionomycin (500 ng/ml) in the presence of brefeldin A (10 mg/ml, Sigma-Aldrich, St. Louis, MO). Cells were first stained for the surface antigen CD4 (BioLegend) and then fixed with 4% paraformaldehyde, permeabilized with 0.5% saponin, followed by intracellular staining with anti-IL-17 and anti-IFN-γ mAbs (BioLegend) (10, 11). Stained PBMC were acquired on a FACSCalibur (BD Biosciences, San Jose, CA) and analyzed with FlowJo software (Ashland, OR). For detection of Treg cells, stained PBMC were first gated on CD4 and CD25. CD4+CD25^{high} T cells were

TABLE 1 | Demographic and clinical data.

Demographic data		
	PwRMS	**HS**
No. of subject	29	12
Sex (% of female)	58%	62%
Age at baseline	34.0 ± 8.7	31.0 ± 5.7
Previous treatment	IFNβ (27). GA (1). none (1)	–
Disease duration (years)	5.0 ± 3.4	–
EDSS at baseline	2.0 (1.5–3.5)	–
EDSS at month 72	1.7 (1.5–3.5)	–
Number of patients who experienced relapses	13	–
Numbers of relapses in the 6-year follow up	1.6 ± 0.9	–
Number of patients who developed secondary autoimmunity	9	–

Values are percentages or mean ± SD and median and interquartile range for EDSS.

analyzed for co-expression of FOXP3 and CD127low identifying CD4+CD25^{high}CD127^{low}FOXP3+Tregs (**Supplementary Figure 1A**). Tregs were then analyzed for expression of CD45RA and CD45R0. For detection of Th17 and Th1 cells, stained PBMC were first gated on CD4 and then analyzed for IL-17 or IFN-γ production (**Supplementary Figure 1B**). Absolute values of Treg, Th17, and Th1 cells were calculated normalizing the percentage of CD25^{high}CD127^{low}FOXP3+, IL-17-producing cells, and IFN-γ-producing cells on the CD4 T cell count obtained from complete blood count with formula and expressed as cells/μL of blood.

Cytokine mRNA Analysis

We used the same methodology as the one employed in our previous study (7). Aliquots (0.5 ml each) of blood were mixed with 1.3 ml RNAlater (Ambion, Life Technologies, Carlsbad, CA) immediately after arrival at the coordinating canter and stored at 280°C. To determine mRNA levels, samples were treated as previously described (12): RNA was extracted with the RiboPure Blood Kit (Ambion, Foster City, CA, USA) and cDNA obtained with the High-Capacity cDNA Reverse Transcription Kit (Applied Biosystems, Life Technologies, Monza, Italy) (12).

We assessed the mRNA levels of the following 26 immunologically relevant molecules whose function in MS has been documented by using TaqMan low-density arrays (Applied Biosystems 7900HT Real-Time PCR System) (12): molecules with pro-inflammatory function including IL-1b, IL-2, IL-6, IL-12, IL-17A, IL-17F, IL-21, IL-22, IL-23, IL-26, IFN-γ, T-box expressed in T cells (Tbet), retinoid-related orphan receptor g (RORC), tumor necrosis factor-a (TNF-α), C–C chemokine receptor type 3 (CCR3), CCR4, CCR5, CCR6, C–X–C chemokine receptor type 3 (CXCR3), C–X–C motif ligand 10 (CXCL10), C–C motif ligand 20 (CCL20), and very late antigen 4 (VLA4), and molecules with anti-inflammatory function, including IL-10, IL-27, transforming growth factor–b (TGF-β), and forkhead box P3 (FoxP3). Glyceraldehyde-3 phosphate dehydrogenase served as the housekeeping gene for normalization. The relative expression of each gene was calculated using the comparative threshold cycle method as directed by the manufacturer (User Bulletin No. 2, Applied Biosystems, Foster City, CA, USA) and expressed in arbitrary units as previously described in detail (7).

Enzyme-Linked Immunospot Assay

Antigen-specific IFN-γ and IL-17-producing cells and antigen-specific suppressor activity of Treg cells were assessed by enzyme-linked immunospot (ELISPOT) (eBioscience) at months 0, 12, 24, 36, 48, 60, and 72. We used the same methodology as the one employed in our previous study (7). To remove Treg cells from PBMC (PBMC^{CD25-}), the CD25^{+} fraction was depleted using immunomagnetic beads (CD4^{+} CD25^{+} Regulatory T Cell Isolation Kit, Miltenyi Biotec, Bergisch Gladbach, Germany). The purity of the depleted fraction was immediately analyzed by fluorescence-activated cell sorting (FACS) staining and ranged from 92 to 95%. 1 × 10^{5} total PBMC or PBMC^{CD25-} was seeded in 96-well ELISPOT assay plates (Millipore, Darmstadt, Germany) in triplicate and incubated for 48 h at 37°C either with myelin basic protein (MBP, 40 mg/ml, Sigma-Aldrich), with the purified protein derivative of tuberculin (PPD, 40 mg/ml, Sigma-Aldrich) as negative control, or with anti-CD3 and anti-CD28 mAbs (10 and 1 μg/ml, respectively) as an internal test control. IFN-γ-specific or IL-17-specific spots were counted by computer-assisted image analysis (Transtec 1300 ELISpot Reader; AMI Bioline, Buttigliera Alta, Italy). The number of IFN-γ or IL-17 spots produced spontaneously was subtracted from the number of spots produced by antigen-stimulated cells to obtain the number of IFN-γ and IL-17 antigen-specific spots in the PBMC or in the PBMC^{CD25-}, as previously described (7). Median values for the triplicates, adjusted as the number of IL-17- and IFN-γ-producing cells/10^{6} PBMC, were used.

Statistical Analysis

Statistical analysis was performed using GraphPad Prism 8.0 (La Jolla, CA) software. For the longitudinal follow-up, statistical significance was calculated concerning baseline and to HS by using one-way analysis of variance for repeated measures followed by the Bonferroni multiple-comparison post-test. The Pearson t-test was used to analyze the differences between groups. p values < 0.05 were considered statistically significant.

RESULTS

Clinical Characteristics of the Cohort

This study represents the continuation of the one previously published (7). Thirteen patients experienced a total of 16 clinical relapses (at months 1, 9, 10, 12, 20, 25, 28, 29, 30, 36, 41, 70) which brought 5 patients to receive additional courses of the drug. The median of Expanded Disease Status Scale (EDSS) score did not change significantly during the 72-month follow-up (EDSS median score from 2 at baseline to 1, 7 at month 72). Secondary autoimmune thyroiditis occurred in 9 patients at months 24, 30, 36, 42, and 59.

Of the 29 patients recruited in this study, only patients who had received the "classical" two courses of alemtuzumab were analyzed in this new study (24 patients). Two patients, described in a different paper (13), were excluded from the analysis due to their atypical CD4+ T population behavior after alemtuzumab administration: they showed persistent disease activity despite repeated alemtuzumab treatment and, while lymphocyte count decreased and fluctuated according to alemtuzumab administration, their CD4+ cell percentage was not affected or was barely affected and was slightly below the lowest normal limit prior to alemtuzumab (13). The other 3 patients had been excluded as they had received a third course of alemtuzumab at month 30 or 36 due to a relapse.

Pro-Inflammatory Th17 and Th1 Cells and Their Related Molecules Decreased Persistently Throughout the 72 Months

As previously observed, the percentage of CD4+ T cells in the PBMC rapidly decreased after the first administration (7) course and returned to the lowest normal limit (LNL) only at month 48 (13), and this was maintained over months 60 (40.78 ± 2.97%) and 72 (39.37 ± 2.40%) where the LNL was 34 (**Figure 1A**). Within the CD4+ cell fraction, we did not observe any significant change in the percentage of pro-inflammatory Th17 and Th1 cells (defined by the production of IL-17 and IFN-γ, respectively, in the CD4+ T cell fraction) at any time point of the follow-up, when compared to HS (**Figure 1B**). However, the absolute number of circulating Th17 had significantly decreased after alemtuzumab (i.e., month 0: 1,100 ± 610; month 24: 380 ± 300; month 72: 410 ± 270 cells/ml) compared to the number obtained in HS (270 ± 210 cells/ml; **Figure 1C** upper panel). The absolute number of circulating Th1 had significantly decreased after alemtuzumab until month 48, compared to baseline (6,341 ± 3,182 at month 0 vs. 3,422 ± 1,581 cells/ml at month 48), but all the values assessed during the follow-up were not different from those of HS (5,292 ± 3,378 cells/ml; **Figure 1C** lower panel). To better evaluate the immune response involved in RMS, we also evaluated the antigen-specific response directed against MBP. One should note that MBP-specific IL-17-producing cells and IFN-γ-producing cells significantly decreased after alemtuzumab administration and were comparable (not statistically different) to HS starting from months 36 (2.85 ± 3.79 vs. 0.27 ± 0.64 IL-17 spots) and 12 (21.50 ± 23.47 vs. 1.1 ± 2.03 IFN-γ spots), respectively (**Figure 1D**).

Accordingly, mRNA levels of pro-inflammatory cytokines produced by Th17 cells, IL-17A (14), IL-17F (14), IL-21 (15), IL-22 (11), IL-26 (16), and by Th1 cells, IFN-γ (17), and their related transcriptional factors, RORC (18) and Tbet (19),

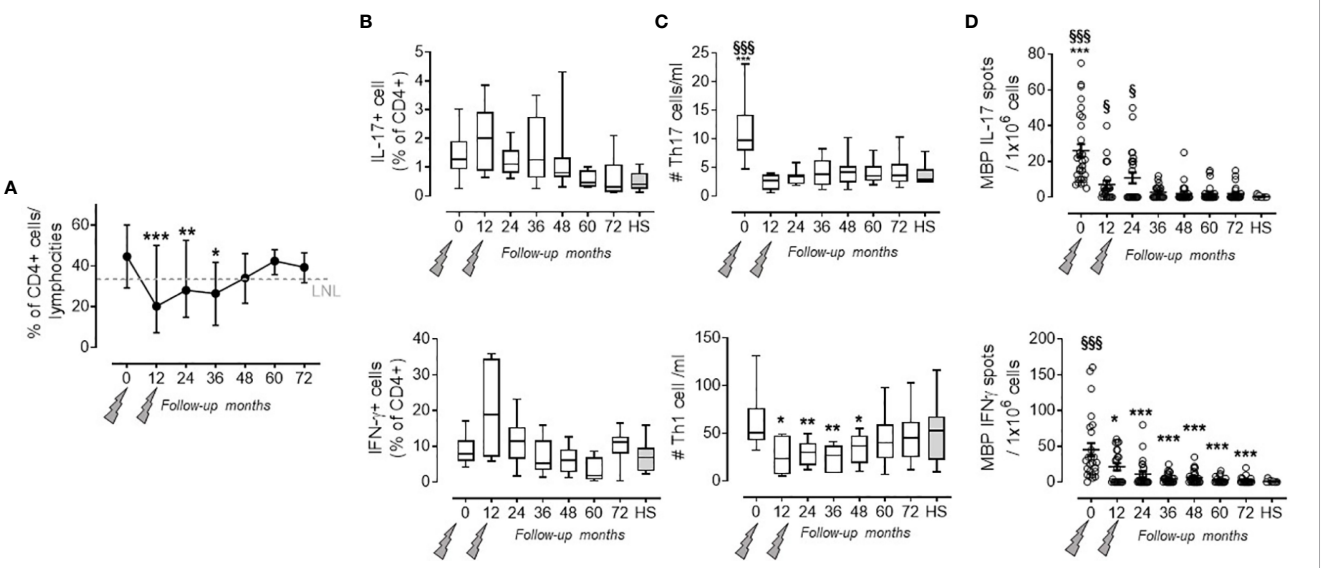

FIGURE 1 | Pro-inflammatory Th17 and Th1 cells in the PB of PwRMS treated with alemtuzumab and in HS. **(A)** % of CD4 lymphocytes on total lymphocytes. **(B)** Th17 and Th1 cell (identified as IL-17-producing CD4+ T cells and IFN-γ-producing CD4+ T cells, respectively) percentage among the CD4+ fraction. **(C)** Absolute numbers of Th17 and Th1 cells circulating in the PB. **(D)** IL-17 and IFN-γ MBP-specific spots in the PBMC. Months after alemtuzumab administration and HS are indicated in the X-axis. Whiskers represent minimum to maximum values. Statistical significance (one-way ANOVA) was calculated with respect to month 0 (*$p < 0.05$; **$p < 0.001$; ***$p < 0.0001$) and to HS ($^{§}p < 0.05$; $^{§§§}p < 0.0001$, gray bars and dots). The arrows indicate infusion of alemtuzumab.

significantly declined to the values of HS at each time point of the follow-up when compared to baseline (**Table 2**). A similar behavior was observed for their chemokines and chemokine receptors, CCL20 (20) and CXCL10 (21), CCR6 (22), CCR5, and CXCR3 (23), involved in T cell recruitment into the CNS (**Table 2**). Alemtuzumab administration also reduced mRNA levels of cytokines known to guide Th17 [IL-1β (24), IL-6 (25), IL-23 (26)], and Th1 [IL-12 (27)] differentiation, but their levels remained higher compared to HS, suggesting that a pro-inflammatory environment could persist in these 24 patients.

TABLE 2 | mRNA levels of pro- and anti-inflammatory molecules evaluated at months 0, 12, 24, 36, 48, 60, and 72 after alemtuzumab administration and in HS.

	0	12	24	36	48	60	72	HS
IL-17A	50.50 ± 2.50 §§§	0.05 ± 0.01 ***	0.01 ± 0.01 ***	0.02 ± 0.01 ***	0.02 ± 0.01 ***	0.01 ± 0.01 ***	0.01 ± 0.01 ***	0.01 ± 0.01
IL-17F	25.60 ± 10.7 §§§	0.03 ± 0.01 ***	0.03 ± 0.01 ***	nd ***	nd ***	nd ***	Nd ***	0.36 ± 0.80
IL-21	0.02 ± 0.02 §§§	nd ***	nd ***	nd ***	nd ***	nd ***	Nd ***	0.48 ± 0.19
IL-22	15.58 ± 3.10 §§§	0.05 ± 0.01 ***	0.04 ± 0.01 ***	0.05 ± 0.01 ***	0.05 ± 0.01 ***	nd ***	Nd ***	0.96 ± 0.58
IL-23	374.00 ± 6.70 §§§	76.00 ± 2.00 *** §§§	65.42 ± 3.80 *** §§§	67.34 ± 2.10 *** §§§	69.07 ± 19.05 *** §§§	60.81 ± 2.70 *** §§§	59.31 ± 5.30 *** §§§	0.58 ± 0.38
IL-26	11.39 ± 1.87 §§§	0.01 ± 0.01 ***	0.01 ± 0.01 ***	nd ***	nd ***	nd ***	Nd ***	0.36 ± 0.11
IL-1β	373.60 ± 9.30 §§§	88.70 ± 2.20 *** §§§	88.70 ± 2.20 *** §§§	64.20 ± 2.60 *** §§§	69.80 ± 2.70 *** §§§	62.26 ± 3.30 *** §§§	63.15 ± 3.17 *** §§§	1.10 ± 0.22
IL-6	503.80 ± 9.30 §§§	47.20 ± 2.30 *** §§	56.100 ± 1.3 *** §§	55.13 ± 1.50 *** §§	52.53 ± 1.80 *** §§	47.32 ± 2.20 *** §§	51.73 ± 2.10 *** §§	0.02 ± 0.01
TNF-α	830.60 ± 18.70 §§§	96.07 ± 2.40 *** §§	72.90 ± 2.70 *** §§	74.44 ± 2.50 *** §§	72.10 ± 3.40 *** §§	76.64 ± 5.10 *** §§	69.54 ± 3.7 *** §§	0.21 ± 0.03
RORC	11.30 ± 0.60 §§§	0.01 ± 0.01 ***	0.01 ± 0.01 ***	nd ***	nd ***	nd ***	Nd ***	0.01 ± 0.01
CCR6	473.70 ± 24.80 §§§	80.90 ± 1.80 *** §§	82.65 ± 5.70 *** §§	77.90 ± 5.30 *** §§	71.90 ± 4.20 *** §§	16.90 ± 3.50 *** §§	17.23 ± 3.80 *** §§	0.24 ± 0.10
CCL20	23.50 ± 2.05 §§§	0.80 ± 0.07 ***	0.01 ± 0.01 ***	0.10 ± 0.01 ***	nd ***	nd ***	Nd ***	0.10 ± 0.01
INF-γ	217.10 ± 6.10 §§§	51.50 ± 2.20 ***	35.80 ± 1.40 ***	38.30 ± 3.80 ***	36.10 ± 1.20 ***	35.50 ± 3.20 ***	32.80 ± 1.40 ***	49.30 ± 5.10
IL-12	436.40 ± 11.41 §§§	93.20 ± 2.20 *** §§§	69.40 ± 2.40 *** §§§	66.20 ± 2.50 *** §§§	64.70 ± 3.10 *** §§§	58.12 ± 4.50 *** §§§	61.70 ± 3.91 *** §§§	1.10 ± 0.06
Tbet	764.30 ± 17.00 §§§	40.40 ± 1.60 ***	24.58 ± 2.30 ***	26.21 ± 2.00 ***	25.47 ± 2.10 ***	29.50 ± 3.90 ***	20.70 ± 1.60 ***	1.10 ± 0.11
CCR5	77.50 ± 5.10 §§§	19.41 ± 0.90 ***	11.82 ± 1.40 ***	12.92 ± 1.30 ***	13.80 ± 1.11 ***	11.42 ± 1.91 ***	10.30 ± 1.80 ***	11.30 ± 0.60
CXCR-3	150.01 ± 4.70 §§§	53.30 ± 1.70 ***	54.10 ± 5.10 ***	46.6 ± 1.8 ***	42.61 ± 2.10 ***	36.70 ± 6.11 ***	26.11 ± 6.20 ***	0.30 ± 0.02
CXCL-10	72.20 ± 3.11 §§§	21.50 ± 1.20 ***	22.10 ± 1.70 ***	21.50 ± 1.38 ***	21.28 ± 1.70 ***	14.80 ± 3.70 ***	14.30 ± 3.10 ***	14.20 ± 2.90
FoxP3	13.50 ± 0.80 §§§	205.60 ± 27.11 *** §§§	328.80 ± 18.10 *** §§§	342.50 ± 12.10*** §§§	339.40 ± 12.10 *** §§§	291.30 ± 15.90*** §§§	332.50 ± 10.51 *** §§§	1.70 ± 0.20
IL-10	47.31 ± 0.70 §§§	494.90 ± 14.10 *** §§§	526.00 ± 16.70 *** §§§	495.00 ± 18.01 *** §§§	524.00 ± 23.90 *** §§§	509.20 ± 13.70 *** §§§	491.51 ± 21.30 *** §§§	0.46 ± 0.13
TGF-β	46.40 ± 1.80	894.80 ± 40.10 *** §§§	994.10 ± 24.10 *** §§§	892.70 ± 30.31*** §§§	837.80 ± 34.10*** §§§	806.90 ± 36.11 *** §§§	818.11 ± 28.90 *** §§§	5.40 ± 0.11
IL-27	116.30 ± 1.80 §§§	1189.01 ± 40.80 ***§§§	1181.00 ± 57.50 ***§§§	1073.0 ± 28.10 ***§§§	1060.00 ± 32.10 ***§§§	1038.0 ± 40.91 ***§§§	908.50 ± 79.21 ***§§§	4.20 ± 0.71

Results are shown as AU (see Methods) ± SEM; statistical significance was calculated by one-way ANOVA.

****p < 0.0001 compared to baseline.*

§§p < 0.001 compared to HS.

§§§p < 0.0001 compared to HS.

nd, not detectable.

Treg Cell Function Is Restored and Persists Throughout the 72-Month Follow-Up

As previously reported, a significant increase in Treg cell percentage (evaluated as CD4+ $CD25^{high}$ $CD127^{low}$ FoxP3+ cells) was detected at month 24 when compared to baseline (7). Afterward, the values of Treg cell percentage revert back to their basal levels which are similar to those observed in HS (i.e., month 36: 3.48 ± 1.48 in PwRMS vs. 2.55 ± 1.25% in HS; **Figure 2A**). This behavior is reflected by the Treg cell absolute count in the blood that, after an initial decrease at month 12, then reaches levels similar to HS as of month 24. Up to month 36, the majority of Treg cells exhibited a memory phenotype as indicated by the significant increase in the percentage of memory CD45RO+FoxP3+CD4+lymphocytes, accompanied by a relative contraction of the percentage of naive CD45RA+ FoxP3+CD4+ cells (**Figure 2B**). mRNA levels of Treg transcription factor FoxP3 (28), and of anti-inflammatory cytokines related to Treg subset IL-10, TGFβ (29), and IL-27 (30), had increased throughout all time points of the follow-up compared both to baseline and to HS (**Table 2**).

Treg suppressor function was assessed by measuring the MBP-specific IL-17 and IFN-γ production in the PBMC both before and after CD4+CD25+ depletion. This method allowed us to test the presence of functional Treg cells also in months with high lymphopenia, through the increase in IL-17 and IFN-γ spot production by $PBMC^{CD25-}$. Treg suppressor function, expressed as fold change over PBMC (**Figure 2C**), was restored at month 24 (as previously observed in 7) and persisted through to the end of the follow-up, even if their functions remain significantly lower compared to HS (**Figure 2C** and **Supplementary Figure 2**). Furthermore, the increase in suppressive capacity of Treg cells was confirmed both by FoxP3 expression in Treg cells (**Figure 2D**) and by the increase of FoxP3 mRNA levels in the blood (**Table 2**).

Correlation of Immunological Evaluation With Clinical Parameters

As thirteen PwRMS had one or more relapses during the follow-up, we wondered if some of the immunological parameters we had evaluated differed in "responders" (i.e., PwRMS that did not develop any relapses) versus "relapsing PwRMS" before starting alemtuzumab. Clinical data of these subgroups are reported in **Table 3**. Interestingly, we observed a significantly higher percentage of Th17 cells (1.76 ± 0.77 vs. 0.93 ± 0.38%), but not of Th1, and a low percentage of Treg (2.40 ± 1.05 vs. 3.70 ± 0.82%) cells in "relapsing PwRMS" compared to "responders" at month 0 (**Figure 3A**). In the same way, the Th17/Treg cell ratio was highest in "relapsing PwRMS" (**Figure 3B**). The same analysis was performed on the patient who developed secondary autoimmunity; a significant increase in the mRNA levels of IL-21 was detected at baseline in the subject who developed thyroiditis compared with subjects who did not develop secondary autoimmunity (**Figure 3C**).

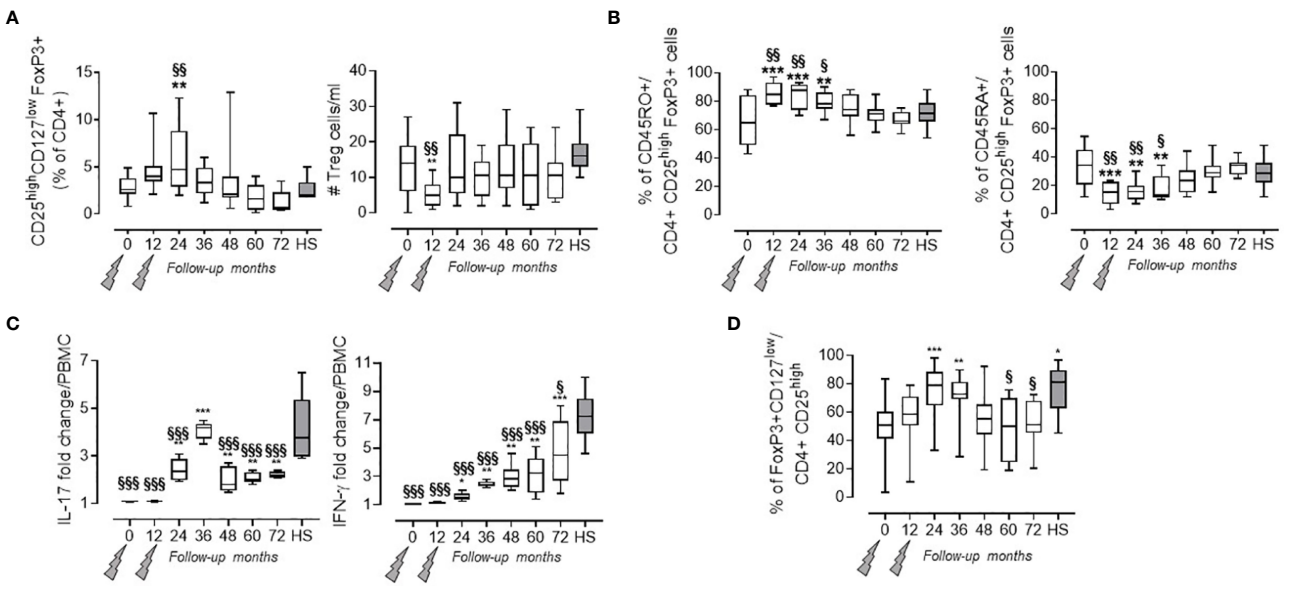

FIGURE 2 | Treg cells in the PB of PwRMS treated with alemtuzumab and in HS. **(A)** Treg cells percentage among the CD4+ fraction and absolute numbers in the blood. **(B)** Percentage of Treg cells expressing CD45RO and CD45RA. Statistical significance (one-way ANOVA) was calculated with respect to month 0 (**p < 0.001) and to HS (§§p < 0.001). **(C)** % of change of MBP-specific spots in the $PBMC^{CD25-}$ over PBMC after background subtraction of unstimulated PBMC or $PBMC^{CD25-}$. **(D)** FoxP3 expression in Treg cells expressed as % of FoxP3 + on CD4 + CD25 + cells. Whiskers represent minimum to maximum values. Statistical significance (one-way ANOVA) was calculated with respect to month 0 (*p < 0.05; **p < 0.001; ***p < 0.0001) and to HS (§p < 0.05; §§p < 0.001; §§§p < 0.0001, gray bars and dots). Months after alemtuzumab administration and HS are indicated in the X-axis. The arrows indicate infusion of alemtuzumab.

TABLE 3 | Clinical data of responders vs. relapsing PwMS.

	Responders (n = 16)	Relapsing PwMS (n = 13)	Statistics
Age at baseline	37.13 ± 8.23	30.77 ± 8.31	p = 0.04
Sex (% of female)	56.21%	61.56%	–
Disease duration (years)	6.32 ± 3.31	5.84 ± 3.48	p = 0.67
EDSS at baseline	2.25 (1.50–3.87)	2.00 (1.50–3.50)	p = 0.76
EDSS at month 72	2.00 (1.00–3.50)	1.50 (1.50–3.75)	p = 0.92
Worst EDSS at relapse	–	3.50 (3.00–3.50)	–

Values of demographic data are percentages or mean ± SD. EDSS is indicated as median and interqualtile range. Statistcal significance was assesed by Mann-Whitney T test.

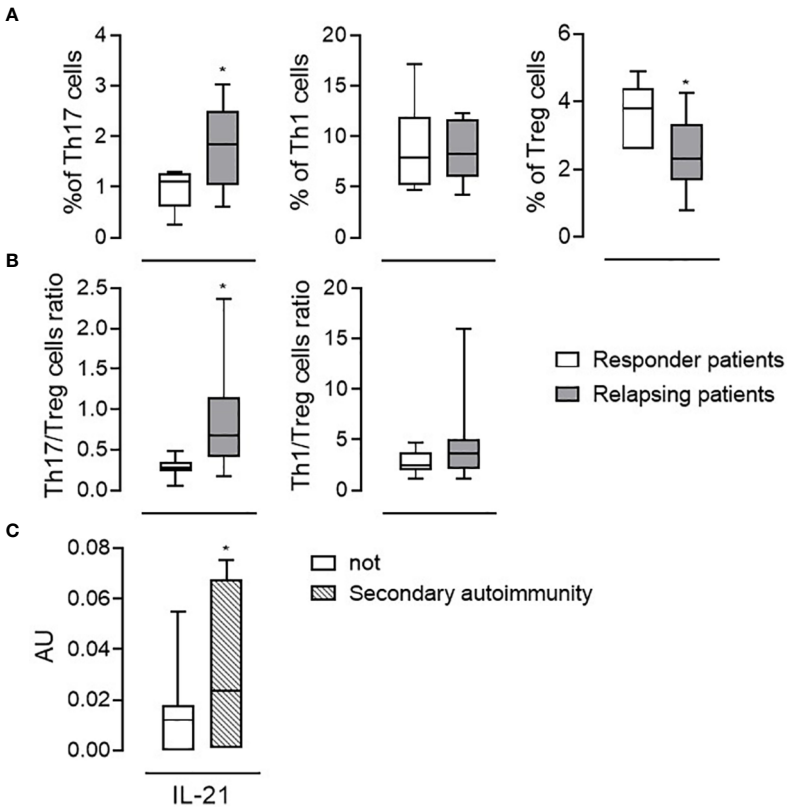

FIGURE 3 | Immunological features associated with relapses or autoimmunity. Th17, Th1, and Treg cell percentage among the CD4+ fraction **(A)** and Th17/Treg Th1/Treg cell ratios **(B)** evaluated at the baseline (month 0) in responder patients (white bars, n = 16) and in patients in which relapses occurred (relapsing patients, gray bars, n = 13). **(C)** mRNA levels of IL-21 in the blood of patients who developed autoimmunity (dashed bars; n = 9) and not (white bars; n = 20). Whiskers represent minimum to maximum values. *p < 0.05, Pearson t-test.

DISCUSSION

Alemtuzumab is a recombinant humanized immunoglobulin G1 (IgG1) monoclonal antibody directed against the CD52 antigen, a small protein of undefined function (31) expressed at a high level on the surface of T and B lymphocytes, to a lesser extent on NK cells, monocytes, macrophages, and eosinophils, while it is absent or barely expressed in neutrophils, dendritic cells (DCs), and hematopoietic stem cells (32, 33). The specific repopulation pattern of T and B cells accounts for its long-term efficacy; furthermore, growing evidence suggests a rearrangement of the T and B cell network. Here, we investigated the numbers and function of the three main subsets of CD4+ cells in PwRMS patients in a 6-year follow-up study after the classical two cycles of alemtuzumab. Our results indicate that alemtuzumab's long-lasting therapeutic effect is associated with a reconstitution of the CD4+ T cell subsets characterized by an initial expansion of memory Treg cells and mainly by a persistent restoration of their suppressive function, accompanied by a shift in the cytokine balance from inflammation toward immune tolerance.

Th17 cells, Th1 cells, and Treg cells are amply recognized as having a pivotal role in the pathogenesis and in the course of RMS (34). Myelin-reactive Th17 and Th1 cells are probably the main effectors involved in the final pathogenetic pathway

(10, 35). On the other hand, Treg cells are believed to counteract Th1 and Th17 proinflammatory effects (36) and, in the context of autoimmune diseases, they possess plasticity and instability that allow them to acquire effector-like and tissue-specific properties (37). In our previous work, we observed that the number of Th17 cells and Th1 cells in the blood and the mRNA transcript of immunological molecules related to these subsets decreased at months 6, 12, 18, and 24 after alemtuzumab administration, when compared to baseline. This peculiar effect of alemtuzumab is maintained through to month 72, in agreement with other recent reports (38, 39). Furthermore, alemtuzumab brings the number of Th17 and Th1 cells back to those present in HS. In line with these results, also the mRNA levels of cytokines produced by Th17 and Th1 cells, of cytokines involved in their differentiation, of chemokines, and of chemokine receptors involved in their migration to CNS decrease after alemtuzumab administration, confirming that the long-term effect of alemtuzumab could rely on the reduction of both pro-inflammatory cytokines and T cell-recruitment into the CNS (7). However, mRNA levels of IL-1β, IL-6, TNF-α, IL-23, and IL-12 involved in Th17 or Th1 differentiation were higher compared to HS also after alemtuzumab administration. This phenomenon could relay in the peculiar ability of alemtuzumab to target specific immune cells. These cytokines are mainly produced by mature DCs that, in RMS, skew the immune response toward an autoreactive Th17 and Th1 phenotype (40). Thus, even though alemtuzumab treatment strongly depletes the pro-inflammatory T cells, this does not occur for DCs because of their low CD52 expression. A study by Gross and colleagues found a reduced number of circulating plasmacytoid-DC, a particular subset of DC able to elicit a pro-inflammatory immune response, at month 6 of alemtuzumab treatment, when compared to baseline, although the production of GM-CSF and IL-23 in these cells remained unchanged (41). In line with these observations, we could suggest an inflammatory persistence in these patients despite alemtuzumab. However, the mRNA amount of anti-inflammatory cytokines IL-10, TGF-β, and IL-27 is strongly upregulated and the ratio of pro/anti-inflammatory cytokines (not shown) significantly decreases after alemtuzumab and through to the end of the follow-up, indicating that, on the whole, alemtuzumab acts by shifting the immune response toward the production of anti-inflammatory cytokines. IL-27 production by DCs is an important inhibitor of Th17 and Th1 response (42). The production of the potent anti-inflammatory cytokine IL-10 by DCs is crucial for Treg induction. In the steady state, some of the peripheral Treg cells appear from peripheral $CD4^{+}CD25^{-}FOXP3^{-}$ T cells that are exposed to antigen in the presence of TGF-β as well as IL-10 without IL-6 or IL-1β, which promote the upregulation of FoxP3 (43). In the same way, the mRNA level of FoxP3, the master regulator of the regulatory pathway in the development and function of Treg cells, was upregulated after alemtuzumab, reaching its highest values at month 24 and maintaining similar value ranges through to month 72.

Of particular meaning and interest are the results concerning the Treg cells. Several studies have shown a preferential expansion of the $CD4+CD25^{high}CD127^{low}FoxP3+$ Treg cells among the CD4+ cells at the early stage of recovery, reaching peak expansion at month 1 (6) and month 5 (38) and becoming significantly higher, compared to baseline, at month 24 (7). Our findings can now extend these observations to month 72, showing that the Treg cell percentage reverts back to its basal level, similar to the one observed in HS. They are mainly memory Treg cells that can specifically suppress the myelin-induced immune response starting from month 24, as in HS. These data show that the Treg cells increase in the CD4+ population occurs through homeostatic proliferation from the pool of lymphocytes that escape depletion rather than from new cells originating from non-depleted stem cells (6, 44, 45). Similarly, through classical Treg proliferation inhibition assay, other data showed a significant rebound proliferation at months 5 and 12 in PHA-activated PBMC depleted from the CD25 component (38) and the recovery of Treg cell competence at months 36 and 48 (44). Further evidence that supports the restoration of Treg cell suppressive ability was discussed by Gilmore and colleagues showing that the majority of Treg cells express CD39, an ectoenzyme able to promote and stabilize the functional capacity of Treg cells (38). Functional Treg cells can suppress pathogenic Th1 and Th17 responses, especially in the presence of high levels of IL-10 (46), which is also produced by Treg cells themselves. However, the reason why Treg cells recover their function to suppress autoreactive immune response during the repopulation period, as also occurs in HS, still needs to be investigated further, as it is unclear whether it is the result of an enhanced cytokine production on the part of the Treg cells themselves, rather than an altered composition and reactivity of repopulated CD4+ T cells that are more susceptible to regulation, or whether it is a combination of both.

Despite the fact that the primary objective of our study was to determine how CD4+ T cell subsets reconstitute after the administration of alemtuzumab, interestingly, data suggest that, although still early, there may be a role for Th17 and Treg cells in predicting the responsiveness of PwRMS to the treatment in question. The identification of immunological markers able to distinguish responding patients to the classical two courses of alemtuzumab from patients who will develop relapses, and therefore require further alemtuzumab infusions is one of the major challenges for neurologists when setting up the best therapy for their patients. The majority of papers addressing this concern have focused their studies on the identification of markers able to predict the appearance of clinical or radiological relapse (7, 38, 39). In all these reports, Th17 cells were shown to increase some months before the manifestation of the relapse, suggesting they are potential biomarkers. On the other hand, the percentage of Th17 cells in the PBMCs of our study is already higher at baseline in "non-responder" patients and is accompanied by a lower percentage of Treg cells, paving the way for further studies aimed at thoroughly immune profiling patients before starting the therapy. One of the major limitations of this study is indeed the relatively small number of subjects included. Nonetheless, our results represent a new piece of the puzzle concerning immunological reconstitution after

alemtuzumab, and, piecing it all together with other similar ones, will be the basis for the correct design of further studies.

Summarizing therefore, our data confirm that the efficacy of alemtuzumab is associated with a reshuffle of the CD4+ immune response from pro- to anti-inflammatory, more or less in line with that of a healthy subject. Besides quantitative changes of the cell repertoire, qualitative alterations of CD4+ T cell subsets were also observed and can be described through two major phenomena: on the one hand, there is a durable decrease of the inflammatory pathways characterized by the disappearance of Th17 and Th1 self-reactive responses, the reduced expression of master regulator factors, and the cytokines related to those subsets and of chemokines and their receptor-connected to CNS recruitment. On the other hand, the restoration of Treg cell suppressor function and the increase of anti-inflammatory cytokines contribute to immune-tolerance promotion versus CNS antigens. Overall, this peculiar mode of action of alemtuzumab is reflected in its durable effect that is maintained for up to 6 years, without the need for further treatment during that period.

DATA AVAILABILITY STATEMENT

The original contributions presented in the study are included in the article/**Supplementary Material**. Further inquiries can be directed to the corresponding author.

ETHICS STATEMENT

The studies involving human participants were reviewed and approved by Comitato Etico Interaziendale, AOU San Luigi Gonzaga. The patients/participants provided their written informed consent to participate in this study.

AUTHOR CONTRIBUTIONS

SR and SD: designed and conceptualized the study; interpreted the data; drafted the manuscript for intellectual content. VB: major role in the acquisition of data and analyzed the data. AM, DT, and FN: interpreted the data; revised the manuscript for intellectual content. EC, AV, MH, IA, PA, and DH: patient enrolment and follow-up; revised the manuscript for intellectual content. MC: designed and conceptualized the study; revised the manuscript for intellectual content. All authors contributed to the article and approved the submitted version.

FUNDING

This study was partially supported by Genzyme (Bio2009001) and the Federazione Italiana Sclerosi Multipla (FISM, 2011/R/28). None of the funding sources had a role in the study design; collection, analysis, and interpretation of data; or the decision to submit the paper for publication.

ACKNOWLEDGMENTS

We thank the patients and healthy donors for participation in this study. We also acknowledge the financial support by Genzyme and FISM.

SUPPLEMENTARY MATERIAL

The Supplementary Material for this article can be found online at: https://www.frontiersin.org/articles/10.3389/fimmu.2022.818325/full#supplementary-material

REFERENCES

1. Xia MQ, Hale G, Lifely MR, Campbell D, Packman L, Waldmann H. Structure of the CAMPATH-1 Antigen, a Glycosylphosphatidylinositol-Anchored Glycoprotein Which Is an Exceptionally Good Target for Complement Lysis. *Biochem J* (1993) 293:633–40. doi: 10.1042/bj2930633
2. Hill-Cawthorne GA, Button T, Tuohy O, Jones JL, May K, Somerfield J, et al. Long Term Lymphocyte Reconstitution After Alemtuzumab Treatment of Multiple Sclerosis. *J Neurol Neurosurg Psychiatry* (2012) 83(3):298–304. doi: 10.1136/jnnp-2011-300826
3. Cohen JA, Coles AJ, Arnold DL, Confavreux C, Fox EJ, Hartung HP, et al. Alemtuzumab Versus Interferon Beta 1a as First-Line Treatment for Patients With Relapsing-Remitting Multiple Sclerosis: A Randomised Controlled Phase 3 Trial. *Lancet* (2012) 380(9856):1819–28. doi: 10.1016/S0140-6736(12)61769-3
4. Coles AJ, Twyman CL, Arnold DL, Cohen JA, Confavreux C, Fox EJ, et al. Alemtuzumab for Patients With Relapsing Multiple Sclerosis After Disease-Modifying Therapy: A Randomised Controlled Phase 3 Trial. *Lancet* (2012) 380(9856):1829–39. doi: 10.1016/S0140-6736(12)61768-1
5. McCarthy CL, Tuohy O, Compston DA, Kumararatne DS, Coles AJ, Jones JL. Immune Competence After Alemtuzumab Treatment of Multiple Sclerosis. *Neurology* (2013) 81(10):872–6. doi: 10.1212/WNL.0b013e3182a35215
6. Zhang X, Tao Y, Chopra M, Ahn M, Marcus KL, Choudhary N, et al. Differential Reconstitution of T Cell Subsets Following Immunodepleting Treatment With Alemtuzumab (Anti-CD52 Monoclonal Antibody) in Patients With Relapsing-Remitting Multiple Sclerosis. *J Immunol* (2013) 191(12):5867–74. doi: 10.4049/jimmunol.1301926
7. De Mercanti S, Rolla S, Cucci A, Bardina V, Cocco E, Vladic A, et al. Alemtuzumab Long-Term Immunologic Effect: Treg Suppressor Function Increases Up to 24 Months. *Neurol Neuroimmunol Neuroinflamm* (2016) 3(1):e194. doi: 10.1212/NXI.0000000000000194
8. Cox AL, Thompson SA, Jones JL, Robertson VH, Hale G, Waldmann H, et al. Lymphocyte Homeostasis Following Therapeutic Lymphocyte Depletion in Multiple Sclerosis. *Eur J Immunol* (2005) 35(11):3332–42. doi: 10.1002/eji.200535075
9. Coles AJ, Cohen JA, Fox EJ, Robertson VH, Hale G, Waldmann H, et al. Alemtuzumab CARE-MS II 5-Year Follow-Up: Efficacy and Safety Findings. *Neurology* (2017) 89(11):1117–26. doi: 10.1212/WNL.0000000000004354
10. Durelli L, Conti L, Clerico M, Boselli D, Contessa G, Ripellino P, et al. T-Helper 17 Cells Expand in Multiple Sclerosis and are Inhibited by Interferon-Beta. *Ann Neurol* (2009) 65(5):499–509. doi: 10.1002/ana.21652
11. Rolla S, Bardina V, De Mercanti S, Quaglino P, De Palma R, Gned D, et al. Th22 Cells Are Expanded in Multiple Sclerosis and Are Resistant to IFN-β. *J Leukoc Biol* (2014) 96(6):1155–64. doi: 10.1189/jlb.5A0813-463R
12. Cucci A, Barbero P, Clerico M, Ferrero B, Versino E, Contessa G, et al. Pro-Inflammatory Cytokine and Chemokine mRNA Blood Level in Multiple Sclerosis Is Related to Treatment Response and Interferon-Beta Dose. *J Neuroimmunol* (2010) 226(1-2):150–7. doi: 10.1016/j.jneuroim.2010.05.038

13. Rolla S, De Mercanti SF, Bardina V, Horakova D, Habek M, Adamec I, et al. Lack of CD4+ T Cell Percent Decrease in Alemtuzumab-Treated Multiple Sclerosis Patients With Persistent Relapses. *J Neuroimmunol* (2017) 313:89–91. doi: 10.1016/j.jneuroim.2017.10.009
14. Moser T, Akgün K, Proschmann U, Sellner J, Ziemssen T. The Role of TH17 Cells in Multiple Sclerosis: Therapeutic Implications. *Autoimmun Rev* (2020) 19(10):102647. doi: 10.1016/j.autrev.2020.102647
15. Tzartos JS, Craner MJ, Friese MA, Jakobsen KB, Newcombe J, Esiri MM, et al. IL-21 and IL-21 Receptor Expression in Lymphocytes and Neurons in Multiple Sclerosis Brain. *Am J Pathol* (2011) 178(2):794–802. doi: 10.1016/j.ajpath.2010.10.043
16. Broux B, Zandee S, Gowing E, Charabati M, Lécuyer MA, Tastet O, et al. Interleukin-26, Preferentially Produced by TH17 Lymphocytes, Regulates CNS Barrier Function. *Neurol Neuroimmunol Neuroinflamm* (2020) 7(6): e870. doi: 10.1212/NXI.0000000000000870
17. Lees JR, Cross AH. A Little Stress is Good: IFN-Gamma, Demyelination, and Multiple Sclerosis. *J Clin Invest* (2007) 117(2):297–9. doi: 10.1172/JCI31254
18. Ivanov II, McKenzie BS, Zhou L, adokoro CE, Lepelley A, Lafaille JJ, et al. The Orphan Nuclear Receptor RORgammat Directs the Differentiation Program of Proinflammatory IL-17+ T Helper Cells. *Cell* (2006) 126(6):1121–33. doi: 10.1016/j.cell.2006.07.035
19. Basdeo SA, Kelly S, O'Connell K, Tubridy N, McGuigan C, Fletcher JM. Increased Expression of Tbet in CD4(+) T Cells From Clinically Isolated Syndrome Patients at High Risk of Conversion to Clinically Definite MS. *Springerplus* (2016) 5(1):779. doi: 10.1186/s40064-016-2510-0
20. Jafarzadeh A, Bagherzadeh S, Ebrahimi HA, Hajghani H, Bazrafshani MR, Khosravimashizi A, et al. Higher Circulating Levels of Chemokine CCL20 in Patients With Multiple Sclerosis: Evaluation of the Influences of Chemokine Gene Polymorphism, Gender, Treatment and Disease Pattern. *J Mol Neurosci* (2014) 53(3):500–5. doi: 10.1007/s12031-013-0214-2
21. Vazirinejad R, Ahmadi Z, Kazemi Arababadi M, Hassanshahi G, Kennedy D. The Biological Functions, Structure and Sources of CXCL10 and Its Outstanding Part in the Pathophysiology of Multiple Sclerosis. *Neuroimmunomodulation* (2014) 21(6):322–30. doi: 10.1159/000357780
22. Reboldi A, Coisne C, Baumjohann D, Benvenuto F, Bottinelli D, Lira S, et al. C-C Chemokine Receptor 6-Regulated Entry of TH-17 Cells Into the CNS Through the Choroid Plexus is Required for the Initiation of EAE. *Nat Immunol* (2009) 10(5):514–23. doi: 10.1038/ni.1716
23. Balashov KE, Rottman JB, Weiner HL, Hancock WW. CCR5(+) and CXCR3 (+) T Cells are Increased in Multiple Sclerosis and Their Ligands MIP-1alpha and IP-10 are Expressed in Demyelinating Brain Lesions. *Proc Natl Acad Sci USA* (1999) 96(12):6873–8. doi: 10.1073/pnas.96.12.6873
24. Sutton C, Brereton C, Keogh B, Mills KH, Lavelle EC. A Crucial Role for Interleukin (IL)-1 in the Induction of IL-17-Producing T Cells That Mediate Autoimmune Encephalomyelitis. *J Exp Med* (2006) 203(7):1685–91. doi: 10.1084/jem.20060285
25. Acosta-Rodriguez EV, Napolitani G, Lanzavecchia A, Sallusto F. Interleukins 1beta and 6 But Not Transforming Growth Factor-Beta Are Essential for the Differentiation of Interleukin 17-Producing Human T Helper Cells. *Nat Immunol* (2007) 8(9):942–9. doi: 10.1038/ni1496
26. Langrish CL, Chen Y, Blumenschein WM, Mattson J, Basham B, Sedgwick JD, et al. IL-23 Drives a Pathogenic T Cell Population That Induces Autoimmune Inflammation. *J Exp Med* (2005) 201(2):233–40. doi: 10.1084/jem.20041257
27. Annunziato F, Cosmi L, Liotta F, Maggi E, Romagnani S. Human Th1 Dichotomy: Origin, Phenotype and Biologic Activities. *Immunology* (2014) 144(3):343–51. doi: 10.1111/imm.12399
28. Fontenot JD, Gavin MA, Rudensky AY. Foxp3 Programs the Development and Function of CD4+CD25+ Regulatory T Cells. *Nat Immunol* (2003) 4 (4):330–6. doi: 10.1038/ni904
29. Povoleri GA, Scottà C, Nova-Lamperti EA, John S, Lombardi G, Afzali B. Thymic Versus Induced Regulatory T Cells - Who Regulates the Regulators? *Front Immunol* (2013) 4:169. doi: 10.3389/fimmu.2013.00169
30. Kim D, Le HT, Nguyen QT, Kim S, Lee J, Min B. Cutting Edge: IL-27 Attenuates Autoimmune Neuroinflammation *via* Regulatory T Cell/Lag3-Dependent But IL-10-Independent Mechanisms In Vivo. *J Immunol* (2019) 202(6):1680–5. doi: 10.4049/jimmunol.1800898
31. Chatenoud L. Chapter 81 - Treatment of Autoimmune Disease: Biological and Molecular Therapies. In: NR Rose, IR Mackay, editors. *The Autoimmune Diseases*, *Fifth Edition*. Boston: Academic Press (2014). p. 1221–45.
32. Hu Y, Turner MJ, Shields J, Gale MS, Hutto E, Roberts BL, et al. Investigation of the Mechanism of Action of Alemtuzumab in a Human CD52 Transgenic Mouse Model. *Immunology* (2009) 128(2):260–70. doi: 10.1111/j.1365-2567.2009.03115.x
33. Buggins AG, Mufti GJ, Salisbury J, Codd J, Westwood N, Arno M, et al. Peripheral Blood But Not Tissue Dendritic Cells Express CD52 and Are Depleted by Treatment With Alemtuzumab. *Blood* (2002) 100(5):1715–20. doi: 10.1182/blood.V100.5.1715.h81702001715_1715_1720
34. Kunkl M, Frascolla S, Amormino C, Volpe E, Tuosto L. T Helper Cells: The Modulators of Inflammation in Multiple Sclerosis. *Cells* (2020) 9(2):482. doi: 10.3390/cells9020482
35. Kebir H, Ifergan I, Alvarez JI, Bernard M, Poirier J, Arbour N, et al. Preferential Recruitment of Interferon-Gamma-Expressing TH17 Cells in Multiple Sclerosis. *Ann Neurol* (2009) 66(3):390–402. doi: 10.1002/ana.21748
36. Zozulya AL, Wiendl H. The Role of Regulatory T Cells in Multiple Sclerosis. *Nat Clin Pract Neurol* (2008) 4(7):384–98. doi: 10.1038/ncpneuro0832
37. Dominguez-Villar M, Hafler DA. Regulatory T Cells in Autoimmune Disease. *Nat Immunol* (2018) 19(7):665–73. doi: 10.1038/s41590-018-0120-4
38. Gilmore W, Lund BT, Li P, Levy AM, Kelland EE, Akbari O, et al. Repopulation of T, B, and NK Cells Following Alemtuzumab Treatment in Relapsing-Remitting Multiple Sclerosis. *J Neuroinflamm* (2020) 17(1):189. doi: 10.1186/s12974-020-01847-9
39. Akgün K, Blankenburg J, Marggraf M, Haase R, Ziemssen T. Event-Driven Immunoprofiling Predicts Return of Disease Activity in Alemtuzumab-Treated Multiple Sclerosis. *Front Immunol* (2020) 11:56. doi: 10.3389/fimmu.2020.00056
40. Dendrou CA, Fugger L, Friese MA. Immunopathology of Multiple Sclerosis. *Nat Rev Immunol* (2015) 15(9):545–58. doi: 10.1038/nri3871
41. Gross CC, Ahmetspahic D, Ruck T, Schulte-Mecklenbeck A, Schwarte K, Jörgens S, et al. Alemtuzumab Treatment Alters Circulating Innate Immune Cells in Multiple Sclerosis. *Neurol Neuroimmunol Neuroinflamm* (2016) 3(6): e289. doi: 10.1212/NXI.0000000000000289
42. Chong WP, Horai R, Mattapallil MJ, Silver PB, Chen J, Zhou R, et al. IL-27p28 Inhibits Central Nervous System Autoimmunity by Concurrently Antagonizing Th1 and Th17 Responses. *J Autoimmun* (2014) 50:12–22. doi: 10.1016/j.jaut.2013.08.003
43. Papadopoulos MC, Verkman AS. Aquaporin 4 and Neuromyelitis Optica. *Lancet Neurol* (2012) 11(6):535–44. doi: 10.1016/S1474-4422(12)70133-3
44. Jones JL, Thompson SA, Loh P, Davies JL, Tuohy OC, Curry AJ, et al. Human Autoimmunity After Lymphocyte Depletion Is Caused by Homeostatic T-Cell Proliferation. *Proc Natl Acad Sci USA* (2013) 110(50):20200–5. doi: 10.1073/pnas.1313654110
45. Haas J, Würthwein C, Korporal-Kuhnke M, Viehoever A, Jarius S, Ruck T, et al. Alemtuzumab in Multiple Sclerosis: Short- and Long-Term Effects of Immunodepletion on the Peripheral Treg Compartment. *Front Immunol* (2019) 10:1204. doi: 10.3389/fimmu.2019.01204
46. Chaudhry A, Samstein RM, Treuting P, Liang Y, Pils MC, Heinrich JM, et al. Interleukin-10 Signaling in Regulatory T Cells Is Required for Suppression of Th17 Cell-Mediated Inflammation. *Immunity* (2011) 34(4):566–78. doi: 10.1016/j.immuni.2011.03.018

Conflict of Interest: The authors declare that the research was conducted in the absence of any commercial or financial relationships that could be construed as a potential conflict of interest.

frontiers in Immunology

ORIGINAL RESEARCH
published: 21 March 2022
doi: 10.3389/fimmu.2022.842354

Baseline Inflammatory Status Reveals Dichotomic Immune Mechanisms Involved In Primary-Progressive Multiple Sclerosis Pathology

*José I. Fernández-Velasco[1], Enric Monreal[2], Jens Kuhle[3], Virginia Meca-Lallana[4], José Meca-Lallana[5], Guillermo Izquierdo[6], Celia Oreja-Guevara[7], Francisco Gascón-Giménez[8], Susana Sainz de la Maza[2], Paulette E. Walo-Delgado[1], Paloma Lapuente-Suanzes[1], Aleksandra Maceski[3], Eulalia Rodríguez-Martín[1], Ernesto Roldán[1], Noelia Villarrubia[1], Albert Saiz[9], Yolanda Blanco[9], Carolina Diaz-Pérez[4], Gabriel Valero-López[5], Judit Diaz-Diaz[7], Yolanda Aladro[10], Luis Brieva[11], Cristina Íñiguez[12], Inés González-Suárez[13], Luis A Rodríguez de Antonio[14], José M. García-Domínguez[15], Julia Sabin[16], Sara Llufriu[9], Jaime Masjuan[2], Lucienne Costa-Frossard[2] and Luisa M. Villar[1]**

[1] Immunology Department, Ramon y Cajal University Hospital, Madrid, Spain, [2] Neurology Department, Ramon y Cajal University Hospital, Madrid, Spain, [3] Neurologic Clinic and Policlinic, Departments of Medicine, Biomedicine, and Clinical Research, University Hospital Basel, University of Basel, Basel, Switzerland, [4] Neurology Department, La Princesa University Hospital, Madrid, Spain, [5] Multiple Sclerosis and Clinical Neuroimmunology Unit, Virgen de la Arrixaca University Hospital, Murcia, Spain, [6] Multiple Sclerosis Unit, Vithas Nisa Sevilla Hospital, Sevilla, Spain, [7] Neurology Department, Clíinico San Carlos Hospital, Instituto de Investigación Sanitaria San Carlos (IdISSC), Madrid, Spain, [8] Neurology Department, Valencia Clinic University Hospital, Valencia, Spain, [9] Center of Neuroimmunology, Neurology Department, Clínic of Barcelona Hospital, Institut d'Investigacions Biomèdiques August Pi i Sunyer (IDIBAPS), and Institut de Neurociències, Universitat de Barcelona, Barcelona, Spain, [10] Neurology Department, Getafe University Hospital, Madrid, Spain, [11] Neurology Department, Arnau de Vilanova Hospital, Lleida, Spain, [12] Neurology Department, Lozano Blesa Clinic University Hospital, Zaragoza, Spain, [13] Neurology Department, Alvaro Cunqueiro Hospital, Vigo, Spain, [14] Neurology Department, Fuenlabrada University Hospital, Madrid, Spain, [15] Neurology Department, Gregorio Marañón University Hospital, Madrid, Spain, [16] Neurology Department, Puerta de Hierro University Hospital, Madrid, Spain

Objective: To ascertain the role of inflammation in the response to ocrelizumab in primary-progressive multiple sclerosis (PPMS).

Methods: Multicenter prospective study including 69 patients with PPMS who initiated ocrelizumab treatment, classified according to baseline presence [Gd+, n=16] or absence [Gd-, n=53] of gadolinium-enhancing lesions in brain MRI. Ten Gd+ (62.5%) and 41 Gd- patients (77.4%) showed non-evidence of disease activity (NEDA) defined as no disability progression or new MRI lesions after 1 year of treatment. Blood immune cell subsets were characterized by flow cytometry, serum immunoglobulins by nephelometry, and serum neurofilament light-chains (sNfL) by SIMOA. Statistical analyses were corrected with the Bonferroni formula.

Results: More than 60% of patients reached NEDA after a year of treatment, regardless of their baseline characteristics. In Gd+ patients, it associated with a low repopulation rate of inflammatory B cells accompanied by a reduction of sNfL values 6 months after their first ocrelizumab dose. Patients in Gd- group also had low B cell numbers and sNfL values 6 months after initiating treatment, independent of their treatment response. In these

OPEN ACCESS

Edited by:
Bert A 'T Hart, University Medical Center Groningen, Netherlands

Reviewed by:
Ayman Rezk, University of Pennsylvania, United States
Nancy Monson, University of Texas Southwestern Medical Center, United States

***Correspondence:**
Luisa M. Villar
luisamaria.villar@salud.madrid.org
orcid.org/0000-0002-9067-3668

Specialty section:
This article was submitted to Multiple Sclerosis and Neuroimmunology, a section of the journal Frontiers in Immunology

Received: *23 December 2021*
Accepted: *28 February 2022*
Published: *21 March 2022*

Citation:
Fernández-Velasco JI, Monreal E, Kuhle J, Meca-Lallana V, Meca-Lallana J, Izquierdo G, Oreja-Guevara C, Gascón-Giménez F, Sainz de la Maza S, Walo-Delgado PE, Lapuente-Suanzes P, Maceski A, Rodríguez-Martín E, Roldán E, Villarrubia N, Saiz A, Blanco Y, Diaz-Pérez C, Valero-López G, Diaz-Diaz J, Aladro Y, Brieva L, Íñiguez C, González-Suárez I, Rodríguez de Antonio LA, García-Domínguez JM, Sabin J, Llufriu S, Masjuan J, Costa-Frossard L and Villar LM (2022) Baseline Inflammatory Status Reveals Dichotomic Immune Mechanisms Involved In Primary-Progressive Multiple Sclerosis Pathology. Front. Immunol. 13:842354. doi: 10.3389/fimmu.2022.842354

patients, NEDA status was associated with a tolerogenic remodeling of the T and innate immune cell compartments, and with a clear increase of serum IgA levels.

Conclusion: Baseline inflammation influences which immunological pathways predominate in patients with PPMS. Inflammatory B cells played a pivotal role in the Gd+ group and inflammatory T and innate immune cells in Gd- patients. B cell depletion can modulate both mechanisms.

Keywords: multiple sclerosis, demyelinating diseases, ocrelizumab, B cells, biomarkers

1 INTRODUCTION

Multiple sclerosis (MS) is the most common demyelinating disease of the central nervous system (1). It induces demyelination, inflammation, and axonal damage, responsible for the permanent neurological deficits suffered by patients with MS (2). Primary progressive MS (PPMS) represents about 10-15% (3) of all MS cases and is characterized by a disease progression that remains continuous since disease onset (4), with or without concomitant visible inflammation by conventional MRI. Although many therapeutic options are available for relapsing remitting MS (RRMS), this is not the case for PPMS. Most of the anti-inflammatory drugs found useful for patients with RRMS are not effective among those with PPMS (5). However, the anti CD20 antibody rituximab showed efficacy in depleting cerebrospinal fluid and peripheral blood B cells in PPMS (6) and results of the OLYMPUS clinical trial suggested that B cell depletion could be effective in those PPMS patients exhibiting signs of inflammation as demonstrated by the occurrence of contrast-enhancing lesions at baseline on MRI (7). Recently, results of the ORATORIO clinical trial with ocrelizumab, a humanized anti CD20 antibody, showed that patients with PPMS responded to this drug, independent of the presence of clinically demonstrable inflammation (8), and it was approved for the treatment of PPMS patients. Ocrelizumab not only induces B cell depletion but modulates T cell compartment toward adopting a more tolerogenic status (9).

Therefore, we aimed to explore the mechanisms associated with favorable response to ocrelizumab in inflammatory and non-inflammatory PPMS cases, toward facilitating the early identification of ocrelizumab responders and revealing new putative therapeutic targets in PPMS.

2 MATERIALS AND METHODS

2.1 Patients

This multicenter, prospective longitudinal study included 69 patients with PPMS diagnosed according to the McDonald criteria (10) who consecutively initiated ocrelizumab treatment in 13 Spanish University Hospitals. Patients were subdivided into four groups based on their inflammatory status (presence [Gd+, n=16] or absence [Gd-, n=53] of gadolinium-enhancing lesions at baseline) and their response to 1 year of ocrelizumab treatment. Non evidence of disease activity (NEDA) was defined as the absence of further Expanded Disability-Status Scale (EDSS) progression with no new MRI lesions at 1 year; in contrast, evidence of disease activity (EDA) patients as having at least one of the above-mentioned conditions. We considered patients as having an increase in the EDSS score when this was confirmed three months after the first assessment. The maximum gap between baseline MRI and treatment initiation was a month.

2.2 Sample Collection

Blood samples were collected in heparinized tubes immediately before (baseline) and 6 months after (before the second dose) ocrelizumab treatment. In both cases they were obtained the day Ocrelizumab was administered, just before initiating the infusion. Samples were then sent to the Immunology Department at Ramón y Cajal University Hospital (Madrid). Peripheral blood mononuclear cells (PBMCs) were isolated from 20 mL of heparinized whole blood as previously described (9) and cryopreserved in fetal bovine serum (HyClone Laboratories) supplemented with 10% DMSO (dimethyl sulfoxide) until further analysis. The samples collected at baseline and 6 months were analyzed simultaneously to avoid inter-assay variability. Serum samples were also collected and stored at -80°C while awaiting analysis. Total lymphocyte and monocyte counts were determined using a Coulter Counter from 10 mL of fresh EDTA-treated blood.

2.3 Monoclonal Antibodies

The monoclonal antibodies used in this study are listed in **Supplementary Table 1**. No differences were observed in plasmablast counts in any of the groups studied (**Figure 1E**; **Supplementary Table 2**).

2.4 Labelling Surface Antigens

Aliquots of 10^6 PBMCs were thawed by a 37°C thermostatic bath and washed twice in RPMI 1640 medium (Thermo Fisher Scientific). Samples were processed and stained as described (9) prior to being analyzed by flow cytometry.

2.5 *In Vitro* Stimulation and Intracellular Cytokine Staining

Thawed aliquots to analyze intracellular cytokine production were subdivided in three polypropylene tubes. To study cytokine production by monocytes, an aliquot of $3x10^5$ PBMCs was resuspended in 1 mL of RPMI 1640 medium and incubated with 1 mg/mL lipopolysaccharide (from Escherichia coli O111: B4; Merck) in presence of 2 μg/ml Brefeldin A (GolgiPlug, BD

Biosciences) and 2.1 µM Monensin (Golgi Stop, BD Biosciences) during 4 hours at 37ºC in 5% CO_2 atmosphere.

To study cytokine production by T and B cells (Except IL-10 producing B cells) an aliquot of $3x10^5$ PBMCs was resuspended and incubated in 1 mL RPMI 1640 medium and stimulated with 50 ng/mL of Phorbol 12-myristate 13-acetate (PMA, Merck) and 750 ng/mL Ionomycin (Merck) in presence of 2 µg/ml Brefeldin A and 2.1 µM Monensin during 4 hours at 37°C in 5% CO_2 atmosphere.

To identify IL-10 producing B cells, an aliquot of $3x10^5$ PBMCs was preincubated in 1 mL RPMI 1640 medium with 3 µg/mL of CpG oligonucleotide (*In vivo*Gen) during 20h at 37°C in 5% CO2 atmosphere. After this, it was stimulated with 50 ng/mL of Phorbol 12-myristate 13-acetate (PMA, Merck) and 750 ng/mL Ionomycin (Merck) in presence of 2 µg/ml Brefeldin A and 2.1 µM Monensin during 4 hours at 37°C in 5% CO_2 atmosphere.

After incubation, the three aliquots were stained with the two-step protocol described previously (9). PBMCs were analyzed in a FACSCanto II flow cytometer (BD Biosciences).

2.6 Flow Cytometry

Cells were always analyzed within a maximum period of 1h after staining. Mean autofluorescence values were set using appropriate negative isotype controls. Data analysis was performed using FACSDiva Software V.8.0 (BD Biosciences). A minimum amount of $5x10^4$ events were analyzed. We followed the strategy showed in **Supplementary Figure 1** to identify the different subpopulations. We set a gate including cells with high to intermediate CD45 and low to intermediate side scatter and excluding debris and apoptotic cells. CD4 and CD8 T cells were classified as: naïve (CCR7+ CD45RO−), central memory (CM) (CCR7+ CD45RO+), effector memory (EM) (CCR7− CD45RO+), and terminally differentiated (TD) (CCR7− CD45RO−). Regulatory CD4 T cells (Treg) were defined as CD3+ CD4+ $CD25^{hi}$ $CD127^{-/low}$. CD56 NK cells were classified as: NKT cells (CD3+ $CD56^{dim}$), CD56dim NK cells (CD3- $CD56^{dim}$) and CD56bright NK cells (CD3- $CD56^{br}$). B cells were classified as: naïve (CD19+ $CD38^{dim}$ CD27-), memory (CD19+ $CD27^{dim}$ $CD38^{dim}$), plasmablasts (CD19 + $CD27^{hi}$ $CD38^{hi}$), transitional B cells (CD19+ CD27- $CD24^{hi}$ $CD38^{hi}$) cells or regulatory B cells (Breg) (CD19+ IL-10+) cells. PD-L1 was explored in monocytes by studying its co-expression with CD14 in PBMCs. We also explored intracellular production of IL-1β, IL-6, IL-10, IL-12 and TNFα by monocytes.IL-1β and TNFα represent innate cell activation, IL-12 induces Th1 responses, IL-6 represent innate cell activation and induces Th17 responses and finally, IL-10 is an anti-inflammatory cytokine. We also explored in CD4 and CD8 T cells the production of IFNγ and TNFα, products of Th1 response; IL-17, a product of the Th17 response; GM-CSF, which induces innate cell activation; and IL-10 that has a regulatory function. Finally, we explored B cells producing IL-6, a pro-inflammatory cytokine that induces Th17 cells; TNFα, an inflammatory cytokine; GM-CSF, inducing innate cell activation; and IL-10 a regulatory cytokine. Representative dot plots showing cytokine production by monocytes, B and T cells are shown in **Supplementary Figure 2**.

2.7 Flow Cytometry Analyses

We recorded for every leukocyte subset total cell counts per mL of blood, calculated by measuring total lymphocyte and monocyte numbers by a coulter counter, and the percentages of every subset over total mononuclear cells. To avoid bias due to B cell depletion, we also recorded the values of every T, B, NK and monocyte subset relative to total T, B, NK and monocyte cells, respectively.

2.8 Immunoglobulin and sNfL Quantification

Serum levels of immunoglobulins (IgG, IgA, and IgM) were measured by nephelometry using a DimensionVista analyzer (Siemens Healthcare Diagnostics) and serum neurofilament light chain (sNfL) levels were measured using the single molecule array (Simoa) NF-light® Assay (Quanterix).

2.9 Statistical Analyses

Statistical analyses were performed using GraphPad Prism 8.0 software (GraphPad Prism Inc.). Wilcoxon matched pairs test was used to assess differences between the samples collected at baseline and after 6 months from the same patient. Mann-Whitney-U test was used to compare the subgroups of patients. *P*-values were adjusted using the Bonferroni correction and *p*-values less than 0.05 were considered statistically significant.

The association between NfL and age has been modelled using a Generalized Additive Model for Location, Scale and Shape (GAMLSS) model and age-normalized measures were obtained for each data point. Z score was used as a continuous measure for the number of standard deviations a given datapoint is above/below the mean in samples of healthy controls of the same age.

2.10 Ethical Considerations

Written informed consent was obtained from every patient prior to their inclusion in the present study, which was approved by the Ethics Committee of each center participating in this study.

2.11 Data Availability Statement

Any anonymized data collected for the purpose of this study will be shared with qualified investigators for 3 years from the initial publication of the study upon reasonable request to the corresponding author.

3 RESULTS

Sixty-nine patients with PPMS (53% female) treated with ocrelizumab were included in this study. Age and disease duration [median (range)] were, respectively, 52.0 (33.0-71.0) and 9.2 (1.3-24.1) years and basal EDSS score was 5.5 (1.0-8.0). All patients were followed for 1 year. Fifty-one (73.9%) remained NEDA 1 year after ocrelizumab initiation. Using MRI data collected at baseline, we further classified the patients according to their inflammatory status into Gd+ (at least one

Gd-enhancing lesion) and Gd- (no Gd-enhancing lesions) groups. Ten Gd+ (62.5%) and 41 Gd- (77.4%) patients were NEDA at the one-year follow-up. We found no significant differences between the four patient subgroups in terms of baseline clinical characteristics except for the MRI data (**Table 1**).

At baseline, few differences were found between Gd+ and Gd- patients (**Supplementary Figure 3**). sNfL levels were higher in Gd+ group, (p=0.019). Likewise, plasmablast numbers trended to be higher in this group of patients (p=0.029) but significance was lost after Bonferroni correction. By contrast, percentages of B naïve cells with respect to total CD19+ cells were higher (p=0.015) in Gd- patients. No differences were found between those Gd+ and Gd- patients in monocytes, T or NK cell subsets analyzed nor in intracellular cytokine production (data not shown).

We next explored differences in the PBMCs induced by ocrelizumab according to patient group after 6 months of ocrelizumab treatment by addressing its impact on the absolute numbers (**Supplementary Table 2**) and relative percentages (**Supplementary Table 3**) of each cellular subtype.

3.1 B Cells

As expected, after 6 months of treatment, ocrelizumab reduced the total numbers of B cells in all groups (**Supplementary Table 2**). After applying the Bonferroni correction, these differences remained statistically significant in the Gd+ NEDA group and the Gd- EDA and NEDA groups (**Figure 1A** and **Supplementary Table 2**). These differences were mainly due to decreased naïve and memory B cell numbers (**Figures 1B, C**, **Supplementary Table 2**). However, there was no statistically significant reduction in any B cell subpopulation in EDA patients in the Gd+ group (**Supplementary Table 2**). This may be partly due to the low number of patients included in this group. However, it should be noted that this patient subgroup had significantly more total (p=0.030) and transitional (p=0.030) B cells than the NEDA patients in the same Gd+ group at the 6-month follow-up (**Figures 1A, D**, respectively; **Supplementary Table 2**). This could also imply a more rapid B cell repopulation in this group. These differences were not observed in the Gd- patients (**Supplementary Table 2**).

We next evaluated intracellular cytokine production in B cells. Again, after applying the Bonferroni correction, a drastic reduction in IL-10, IL-6, GM-CSF, and TNFα B cell numbers (**Figures 2A–D**, respectively, **Supplementary Table 2**) was observed in the Gd+ NEDA group and in both Gd- EDA and NEDA patients. However, this was not observed in Gd+ EDA patients, who at 6 months of follow-up showed increased numbers of B cells producing TNFα than NEDA patients of the same group (p=0.04, **Figure 2D** and **Supplementary Table 2**). At 6 months, B cell numbers were very low and thus establishing percentages respective to total B cells with such a small quantity of cells could result highly imprecise. Consequently, we decided not to analyze differences relative to total B cells percentages, contrary to what we did with the rest of the leukocyte populations.

3.2 T Cells

3.2.1 Total Cell Counts

We next studied the effect of ocrelizumab in the different T cell subpopulations after 6 months of ocrelizumab treatment. We only found significant differences in the CD20+ T cell subset. It decreased in all groups but after Bonferroni correction differences only remained significant in the Gd+ NEDA group and in both Gd- EDA and NEDA groups (**Figure 1F** and **Supplementary Table 2**). Results were similar when studied separately CD4+ and CD8+ subsets (**Supplementary Figure 4**).

3.2.2 Percentages Relative to CD4+ and CD8+ Subsets

No differences were observed in the Gd+ group (**Supplementary Table 3**). However, ocrelizumab treatment modified the T cell compartment in NEDA patients of the Gd- group. We found an increase in the proportion of naïve CD4+ T cells (p=0.004, **Supplementary Table 3**) accompanied by decreases in the percentages of TD (p=0.002, **Supplementary Table 3**) and EM (p=0.041, **Supplementary Table 3**) CD4+ T subsets related to the total CD4+ T cell population. Accordingly, we found

TABLE 1 | Baseline data and patient characteristics.

	All patients (n=69)	Gd+ (n=16)		Gd- (n=53)		p value
		EDA (n=6)	NEDA (n=10)	EDA (n=12)	NEDA (n=41)	
Age [years] – median (range).	52.0 (33.0 – 71.0)	51.0 (40.0 – 54.0)	49.0 (33.0 – 58.0)	50.0 (38.0 – 63.0)	54.0 (36.0 – 71.0)	0.204
Sex (F/M).	37/32	3/3	5/5	6/6	23/18	0.970
Disease duration [years] – median (range).	9.2 (1.3 – 24.1)	10.7 (2.1 – 15.4)	7.0 (1.3 – 13.3)	6.6 (1.6 – 19.0)	10.2 (1.7 – 24.2)	0.490
EDSS score – median (range).	5.5 (1.0 – 8.0)	5.5 (3.0 – 8.0)	6.0 (3.5 – 6.0)	4.0 (1.0 – 6.0)	6.0 (2.0 – 7.0)	0.160
Gd lesions – median (range).	0.0 (0.0 – 4.0)	1.0 (1.0 – 3.0)	1.0 (1.0 – 4.0)	0.0 (0.0 – 0.0)	0.0 (0.0 – 0.0)	**$1.6x10^{-14}$**

F, Female; M, male; EDSS, Expanded Disability Status Scale; n, number of patients; Gd+/-, presence/absence of gadolinium enhancing lesions at baseline; EDA, evidence of disease activity patients at 1 year of follow-up; NEDA, non-evidence of disease activity patients at 1 year of follow-up.
Bold values are significant values (p < 0.05).

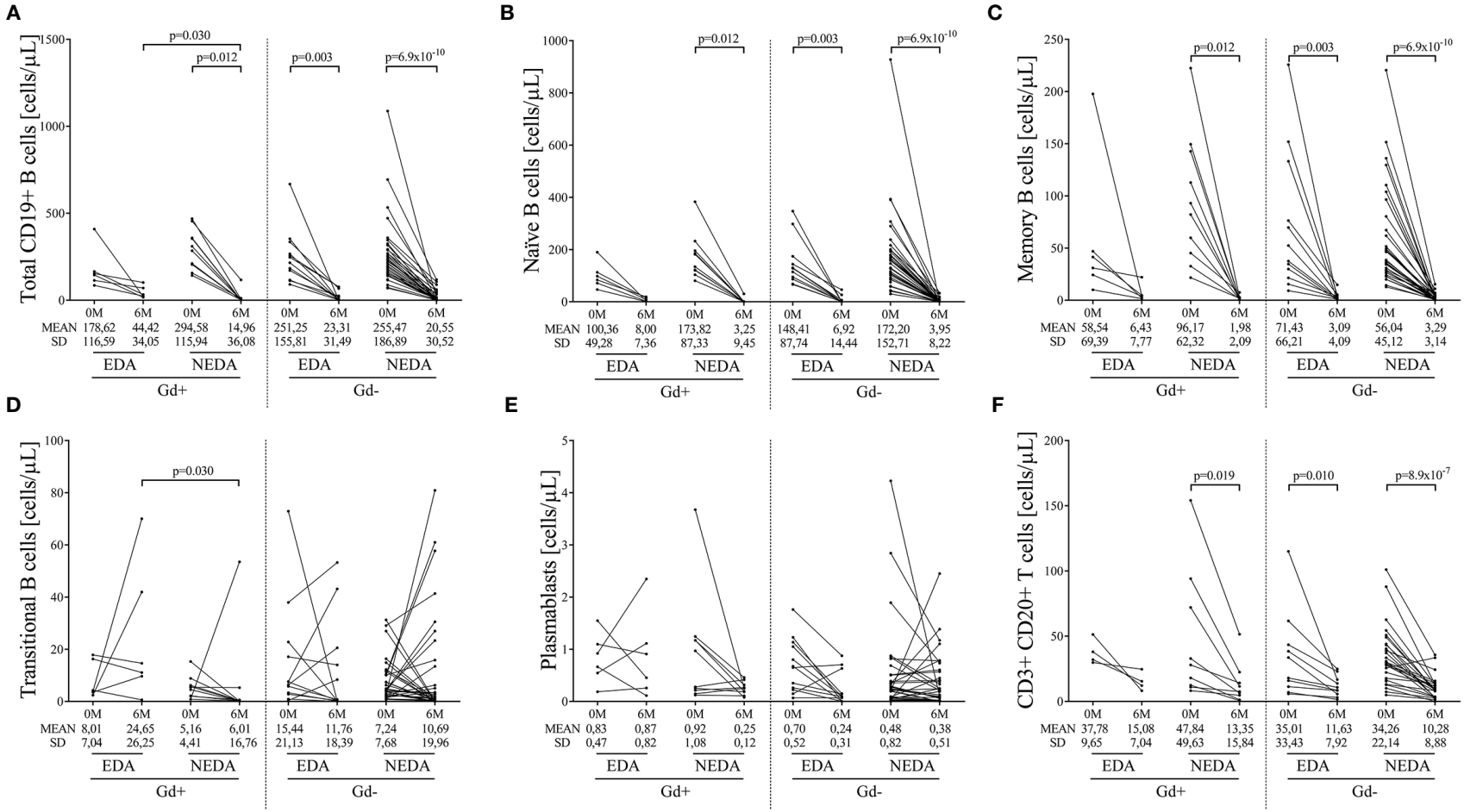

FIGURE 1 | Changes in blood B cell subsets induced by ocrelizumab treatment. Total and B-cell subsets were obtained before (0M) and at 6 months (6M) of ocrelizumab treatment and classified based on their inflammatory status (presence [Gd+] or absence [Gd-] of gadolinium enhancing lesions at baseline) and response (optimal NEDA or suboptimal EDA) to treatment at one year of follow-up. N was 6, 10, 12 and 41 in Gd+ EDA, Gd+ NEDA, Gd- EDA and Gd- NEDA, respectively. Graphs showing changes in absolute numbers (cells/µL) of total CD19+ B cells **(A)**, naïve B cells **(B)**, memory B cells **(C)**, transitional B cells **(D)**, plasmablasts **(E)** and CD20 T cells **(F)**. SD, Standard deviation. Bonferroni-corrected p-values are shown.

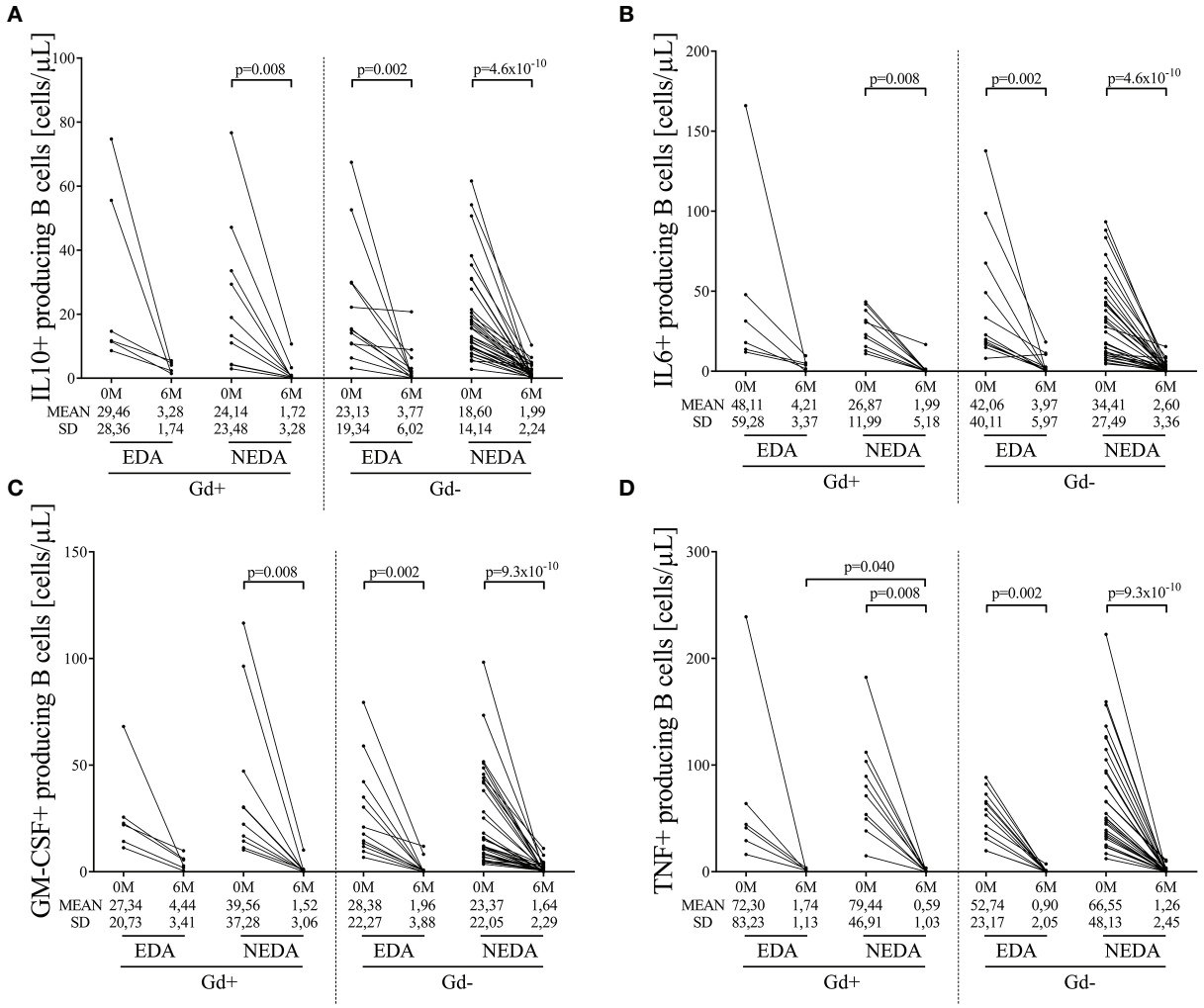

FIGURE 2 | Changes in blood cytokine-producing B cells on ocrelizumab treatment. Cytokine-producing B cells were obtained before (0M) and at 6 months (6M) of ocrelizumab treatment and classified based on their inflammatory status (presence [Gd+] or absence [Gd-] of gadolinium enhancing lesions at baseline) and response (NEDA or EDA) to treatment at one year of follow-up. N was 6, 10, 12 and 41 in Gd+ EDA, Gd+ NEDA, Gd- EDA and Gd- NEDA, respectively. Graphs showing changes in absolute numbers (cells/µL) of IL-10 **(A)**, IL-6 **(B)**, GM-CSF **(C)**, and TNFα **(D)**-producing B cells. IL, interleukin; GM-CSF, granulocyte-macrophage colony-stimulating factor; TNF, tumor necrosis factor alpha; SD, Standard deviation. Bonferroni-corrected p-values are shown.

increases in the naïve/EM (p=0.004, **Figure 3A**) and naïve/TD (p<0.0001, **Figure 3A**) ratios.

We also found an increase in naïve CD8+ T cell percentages relative to total T CD8+ cells (p=0.031, **Supplementary Table 3**). Although, in this case, it was not associated with significant decreases in effector and TD subpopulations, again, NEDA patients showed an increase in the naïve/EM (p=0.011, **Figure 3B**) and naïve/TD (p=0.005, **Figure 3B**) ratios.

Finally, we studied the relative changes in intracellular cytokine production by CD4+ and CD8+ T cells. No differences were found in cytokine production from CD4+ T cells. However, in the Gd- group, the NEDA patients experienced a decrease in the proportion of CD8+ T cells producing IFNγ (p=0.004, **Figure 3C** and **Supplementary Table 3**) relative to the total CD8+ T cell population.

By contrast, no changes were observed in EDA Gd- group in any T cell subset after six months of ocrelizumab treatment. This suggests that the remodeling of the T cell compartment is important for the response to ocrelizumab in these patients.

3.3 Innate Immune Cells

An increase in the total monocyte counts was found in Gd- NEDA patients 6 months after ocrelizumab treatment with the differences being higher in the NEDA group (p=0.034, **Supplementary Table 2**). We next explored if this increase was associated with the total numbers of monocytes producing IL-1, IL-6, IL-10, IL-12, and TNF-alpha or expressing PD-L1. The only significant differences were found in PD-L1+ monocytes. Gd- NEDA patients experienced an increase of the numbers of this subset after ocrelizumab treatment (p=0.013,

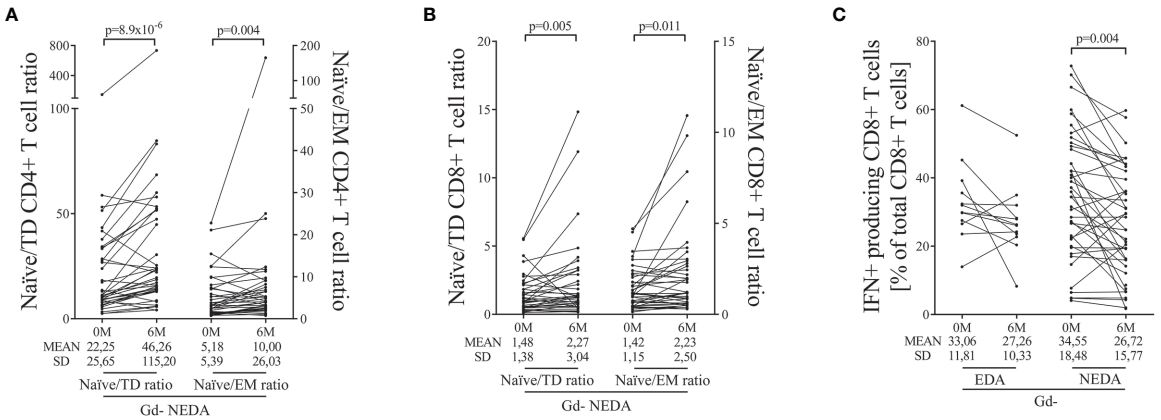

FIGURE 3 | Main changes in blood T cells after ocrelizumab treatment. T cells were obtained before (0M) and at 6 months (6M) of ocrelizumab treatment and classified based on their inflammatory status (presence [Gd+] or absence [Gd-] of gadolinium enhancing lesions at baseline) and response (NEDA or EDA) to treatment at one year of follow-up. N was 6, 10, 12 and 41 in Gd+ EDA, Gd+ NEDA, Gd- EDA and Gd- NEDA, respectively. Graphs showing changes in naïve/effector ratios of CD4 **(A)** and CD8 **(B)** T cells, and changes in percentage of IFNγ-producing CD8 T cells **(C)** relative to total CD8+ T cells. TD, terminally differentiated; EM, effector memory; IFN, gamma-interferon; SD, Standard deviation. Bonferroni-corrected p-values are shown.

Supplementary Table 2). No significant changes were observed in the proportions of any subset relative to total monocytes. We observed a decrease in the number of CD56bright NK cells (p=0.023, **Supplementary Table 2**) in the Gd- NEDA group after treatment with no variations in the relative proportions of the NK subsets analyzed (**Supplementary Table 3**).

3.4 Serum NfL Levels

Baseline sNfL levels were higher in the Gd+ EDA group compared with the Gd- EDA (p=0.014) and Gd- NEDA (p=0.007) groups (**Figure 4**). They also trended toward higher values than those observed in the Gd+ NEDA patients (p=0.07). Six months after ocrelizumab treatment, sNfL levels were only significantly lower than basal values in the Gd+ NEDA group (**Figure 4**). They did not decrease significantly in the Gd+ EDA patients. The Gd- NEDA and EDA groups, whose baseline sNfL values were not elevated, did not vary significantly from each other upon treatment. When explored the z score normalized by patient age, we observed that in most Gd+ EDA patients, baseline sNfL values were higher than 2 z score levels (median values=2.411) whilst they were mostly between 0 and 2 z score values in most patients from the other three groups (**Table 2**).

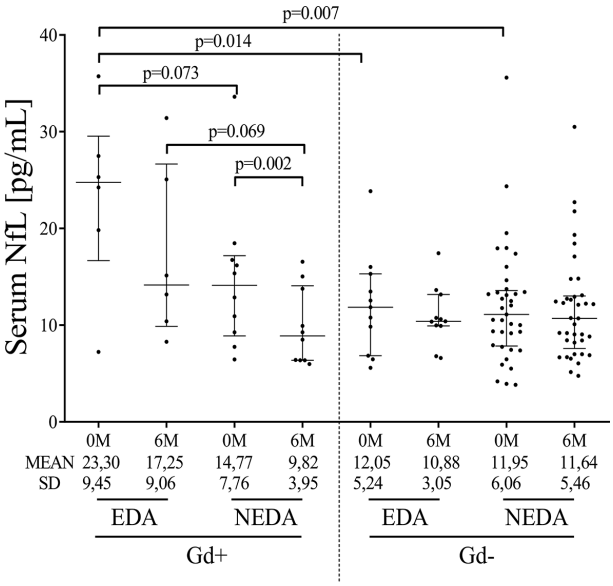

FIGURE 4 | Ocrelizumab treatment induces changes in sNfL levels. sNfL levels (pg/mL) measured before (0M) and at 6 months (6M) of ocrelizumab treatment and classified based on their inflammatory status (presence [Gd+] or absence [Gd-] of gadolinium enhancing lesions at baseline) and response (NEDA or EDA) to treatment at one year of follow-up. N was 6, 10, 12 and 41 in Gd+ EDA, Gd+ NEDA, Gd- EDA and Gd- NEDA, respectively. sNfL, serum neurofilament light-chains; SD, Standard deviation.

3.5 Serum Immunoglobulin Values

We explored changes in serum immunoglobulin concentrations 6 months after the first dose of ocrelizumab. The levels of IgG remained stable, while significant decreases in serum IgM levels were observed in all of them (**Table 3**). Additionally, increased serum IgA levels were observed in the Gd- NEDA group (p=0.006, **Table 3**). However, the most interesting results were observed when the changes in the ratios of the different serum immunoglobulins were explored. The IgA to IgM ratio was augmented in all groups (**Figure 5B**) with these changes highly relevant in Gd- NEDA group ($p=4x10^{-12}$). The IgG to IgM ratio also increased (**Figure 5A**), being again the most prominent changes observed in the Gd- NEDA group ($p=2.5x10^{-11}$). Remarkably, this group of patients experienced an increase in the IgA to IgG ratio (p=0.0011; **Figure 5C**) not observed in any other group.

TABLE 2 | Cohort summary of age-normalized sNfL values.

	0M			6M		
		NfL.zscore			NfL.zscore	
Group	**n**	**Median**	**IQR**	**n**	**Median**	**IQR**
Gd- NEDA	41	0.305	[-0.361, 1.495]	41	0.176	[-0.496, 1.175]
Gd- EDA	12	0.440	[-0.101, 1.243]	12	0.210	[-0.319, 0.948]
Gd+ NEDA	10	1.422	[0.515, 1.642]	10	0.151	[-0.422, 0.812]
Gd+ EDA	6	2.411	[2.074, 2.750]	6	1.646	[0.775, 2.395]
All	69	0.569	[-0.094, 1.801]	69	0.228	[-0.358, 1.282]

Results of NfL z score are shown as median [25-75% IQR]. Gd+/-, presence/absence of gadolinium enhancing lesions at baseline; EDA, evidence of disease activity patients at 1 year of follow-up; NEDA, non-evidence of disease activity patients at 1 year of follow-up; 0M, 0 Months (pre-ocrelizumab treatment); 6M, 6 Months of ocrelizumab treatment.

TABLE 3 | Ocrelizumab induced changes in serum immunoglobulin levels.

		EDA (n=18)			NEDA (n=51)		
		0M	**6M**	***p**	**0M**	**6M**	***p**
IgG [mg/dL]	**Gd+**	1113 (795-1573)	1125 (748-1478)	*>0.99*	1095 (744-1120)	995 (737-1133)	*>0.99*
	Gd-	880 (750-1023)	927 (791-1010)	*>0.99*	955 (825-1090)	984 (870-1195)	*>0.99*
IgA [mg/dL]	**Gd+**	233 (206-324)	237 (210-361)	*>0.99*	179 (138-225)	170 (155-215)	*>0.99*
	Gd-	172 (133-196)	177 (144-188)	*>0.99*	199 (139-228)	208 (155-251)	***0.006***
IgM [mg/dL]	**Gd+**	72 (63-186)	60 (37-168)	*>0.99*	95 (51-244)	77 (40-157)	***0.018***
	Gd-	124 (60-160)	99 (36-134)	***0.009***	102 (80-159)	84 (67-131)	***$4.8*10^{-4}$***

*Results are shown as Median [25-75% IQR]. P values were corrected by using Bonferroni test. Gd+/-, presence/absence of gadolinium enhancing lesions at baseline; EDA, evidence of disease activity patients at 1 year of follow-up; NEDA, non-evidence of disease activity patients at 1 year of follow-up; 0M, 0 Months (pre-ocrelizumab treatment); 6M, 6 Months of ocrelizumab treatment; *p, corrected p value.*
Bold values are significant values ($p < 0.05$).

4 DISCUSSION

Ocrelizumab selectively depletes CD20+ cells while maintaining B cell reconstitution and pre-existing humoral immunity (11). In patients with PPMS, ocrelizumab not only induces B cell depletion, but reshapes the T cell response toward a low inflammatory profile, resulting in decreased sNfL levels (9).

However, the influence of baseline inflammatory status on these changes has not been fully ascertained. Inflammation is used in the classification of patients with progressive MS. In fact, current guidelines for diagnosing PPMS include two qualifiers: disease activity, defined by MRI or clinical evidence of inflammatory lesions or relapses; and disability progression, defined as a gradually worsening disability independent of relapses (12).

Inflammatory status can also play a role in DMT effectiveness. Overall subgroup analyses evaluating Rituximab in patients with PPMS (OLYMPUS trial) suggested that this drug may affect disease progression in younger patients, particularly those with inflammatory lesions (7). However, results from the ORATORIO trial with ocrelizumab showed that anti-CD20 antibodies are effective in non-inflammatory patients with PPMS (8). This agrees with our results. We explored response to ocrelizumab in a multicenter prospective cohort of 69 patients with PPMS treated with this drug. NEDA patients at 1 year of treatment represented 62% of the inflammatory group (10 out of 16) and 75% of the non-inflammatory one (41 of 53) in our study.

We first explored baseline differences in patients classified according to their inflammatory status (presence [Gd+]/absence [Gd-] of gadolinium-enhancing lesions at baseline). We studied different leukocyte subsets (B cells, T cells, NK cells and monocytes) and sNfL values. As expected, Gd+ patients showed high sNfL values. They also showed a trend to higher plasmablast numbers. The association of plasmablasts with inflammation in MS has been widely documented in the CSF (13). Probably peripheral blood is not the best compartment to study these cells in MS, but our data seem to confirm the role of plasmablasts in inflammation in MS. On the other hand, we found increased values of naïve B cells in Gd- patients. This suggests other function for B cells in non-inflammatory PPMS patients, as antigen presentation. No other differences were found between Gd+ and Gd- patients.

We next studied changes associated with NEDA status in both groups of patients by analyzing T, B, NK, and monocyte cell subsets at baseline and 6 months after receiving the first dose of treatment, before receiving the second one. Patients were classified according to their inflammatory condition (Gd+ or Gd-) and to their response to treatment (NEDA or EDA).

Although B cells clearly diminished in all groups of patients 6 months after the first ocrelizumab dose, in the EDA inflammatory group, total B cell counts were higher at this point. This increase was mainly due to transitional B cells, thus indicating a higher rate of B cell repopulation for these patients, and to TNF-alpha-producing B cells, thus indicating a rapid differentiation into pro-inflammatory B cells. Another characteristic of EDA Gd+ patients was the increased levels of sNfL levels at baseline compared with the non-inflammatory groups, with a trend also observed for higher values than NEDA Gd+ patients. These data show that baseline Gd enhancing lesions and especially high serum neurofilament levels associate in PPMS with a high rate of B cell repopulation and

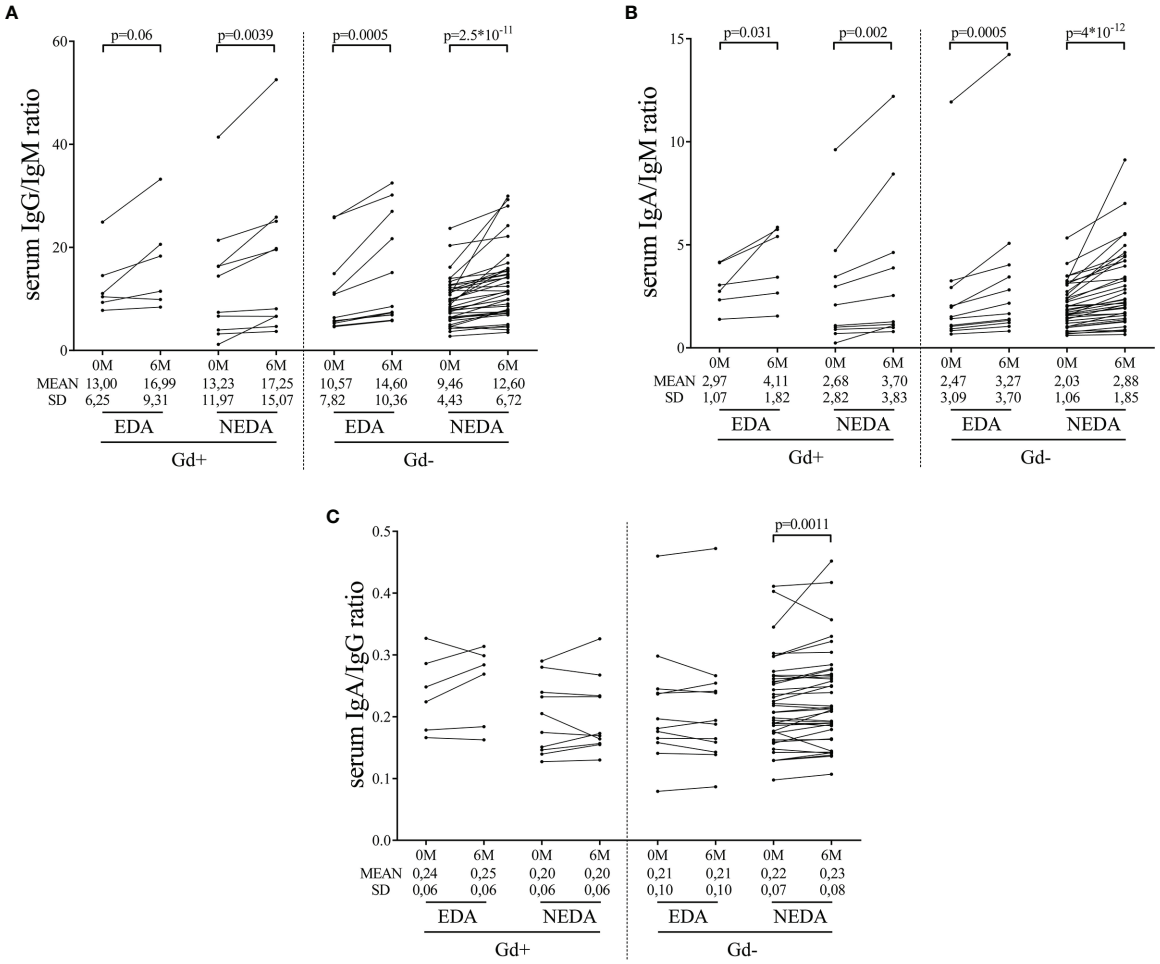

FIGURE 5 | Changes in serum immunoglobulin ratios induced by ocrelizumab treatment. Serum samples were analyzed before (0M) and at 6 months (6M) of ocrelizumab treatment and classified based on their inflammatory status (presence [Gd+] or absence [Gd-] of gadolinium enhancing lesions at baseline) and response (NEDA or EDA) to treatment at one year of follow-up. N was 6, 10, 12 and 41 in Gd+ EDA, Gd+ NEDA, Gd- EDA and Gd- NEDA, respectively. Graphs showing IgG/IgM **(A)**, IgA/IgM **(B)** and IgA/IgG **(C)** ratios. SD, Standard deviation.

strongly suggest that these patients should benefit from early re-treatment or dose adjustment. By contrast, in NEDA Gd+ patients, the low B cell counts at 6 months were associated with a significant reduction of the sNfL levels 6 months after the first ocrelizumab dose. Finally, in NEDA and EDA Gd- patients, sNfL levels did not change significantly after ocrelizumab treatment, despite the reduction in B cell counts or response to treatment. This is important, since NfL is being proposed as a biomarker for response to different drugs in MS (14) and this could be not the case in patients with low inflammatory activity.

T cell activation and cytokine production are also affected by anti-CD20 DMTs (9, 15). We first studied absolute T cell counts. Only CD20+ T cells decreased in number. This occurred in the four patient groups, with Gd+ EDA being the only one in which the reduction did not reach statistical significance, probably due to the low sample size. The CD20+ T cell subset has been proposed to play an important role in MS pathology because of its highly activated phenotype and proinflammatory and migratory properties (16) and a reduction in these cells, described also for alemtuzumab, fingolimod, and dimethyl fumarate (16), can be beneficial for patients with PPMS treated with ocrelizumab, independent of their baseline inflammatory status.

We next explored the changes in the proportions of the different T cell subsets after 6 months of treatment relative to the total CD4+ and CD8+ T cells. Variations were restricted to the Gd- NEDA group. These patients exhibited a reduction in TD and EM CD4+ T effector cells and increases in naïve CD4+ and CD8+ T cells and in the ratios of naïve/EM and naïve/TD in CD4+ and CD8+ T cells. Likewise, they experienced a decrease in the proportion of CD8+ T cells producing IFNγ. These data show that response to ocrelizumab in Gd- patients is conditioned by reshaping the T cell compartment to a more tolerogenic profile. The activation of the T cell compartment by B cells may play an important role in the pathology of Gd- PPMS. Furthermore, the beneficial effects of different drugs in patients with MS with low inflammatory contribution to their disease may be reflected by

changes in other biomarkers aside from sNfL, especially in those with low baseline levels of this protein.

Regarding to Gd- EDA patients, we did not find any clear explanation for the lack of changes in the T cell compartment they showed upon Ocrelizumab treatment. They had no differences on epidemiological, clinical or immune cell subsets at baseline with NEDA group. Exploring antigen presenting B cells and activated dendritic cells in both groups could help to elucidate this conundrum. Future research will demonstrate if antigen presenting B cells could be a biomarker of response to Ocrelizumab in Gd- PPMS patients, as suggested by the remodeling in the T cell compartment showed by NEDA patients.

We also explored changes in innate immune cells at baseline and after 6 months of treatment. Again, we only found significant changes in NEDA Gd- patients. They showed a significant increase in total monocyte counts. This increase was mainly due to PD-L1-expressing monocytes. This molecule is a ligand of the PD-1 receptor, which promotes self-tolerance by suppressing T cell inflammatory activity (17). Its increase has been described in response to other drugs in MS (18). Its up-regulation upon B cell depletion further demonstrates the role of inflammatory B cells in inducing inflammation in cells of the innate immune response and how this can be changed by B cell depletion (19). The up-regulation of PD-L1 expression by monocytes may contribute to the remodeling of the T cell compartment observed in these patients.

Regarding serum immunoglobulins in the four groups of patients, ocrelizumab induced a decrease in serum IgM levels, with no changes in IgG values, as previously reported for patients treated with anti-CD20 antibodies (9, 20). Likewise, all groups of patients showed a decrease in the IgG/IgM and IgA/IgM ratios. Most IgM molecules present in serum are natural antibodies that react against non-protein antigens, anti-lipid specificity being the most frequent (21, 22). Intrathecal synthesis of anti-lipid IgM antibodies associates with an aggressive MS course (22, 23). Thus, the down regulation of the B cells producing these antibodies may have a beneficial effect in MS. Additionally, our data contain interesting results with IgA antibodies. Gd- NEDA patients showed an increase of the levels of this immunoglobulin upon ocrelizumab treatment, and raised values of the ratio IgA/IgG. IgA, produced mostly at mucosal surfaces, functions as a critical mediator of intestinal homeostasis (24) and gut-microbiota reactive IgA plasma cells can migrate to peripheral organs with potential roles in extraintestinal autoimmune diseases (25). In MS, gut microbiota-specific IgA cells are considered a systemic mediator of the disease behaving as an informative biomarker during active neuroinflammation (26). In the experimental model of the disease, migration of IgA-producing plasma cells from the intestinal mucosa to the CNS has proven to down-modulate disease activity. This was attributed to IL-10 production in these cells (27), but often, natural IgA antibodies produced by plasma cells of the gut mucosa recognize similar antigens that natural IgM antibodies present in serum (28, 29). These IgA antibodies could block antigens recognized by IgM, thus avoiding complement fixation and diminishing axonal damage.

In summary this study shows that baseline inflammation could determine the immunological pathways that drive the response to Ocrelizumab in PPMS and that, regardless of baseline MRI activity, B cell depletion with ocrelizumab can modify both underlying mechanisms, and be effective in more than 60% of patients.

DATA AVAILABILITY STATEMENT

The original contributions presented in the study are included in the article/**Supplementary Material**. Further inquiries can be directed to the corresponding author.

ETHICS STATEMENT

The studies involving human participants were reviewed and approved by Ethics Committee of each participating hospital. The patients/participants provided their written informed consent to participate in this study.

AUTHOR CONTRIBUTIONS

JF-V drafted the manuscript, major role in performing experiments, acquisition and analysis of data. PW-D, PL-S, and NV collected samples and performed flow cytometry experiments. JK and AM contributed to sNfL measurement. ER-M and ER supervised flow cytometry studies. EM, VM-L, JM-L, GI, CO-G, FG-G, SS, AS, YB, CD-P, GV-L, JD-D, YA, LB, CÍ, IG-S, LR, JG-D, JS, SL, JM, and LC-F visited MS patients, contributed by sending samples or collected clinical data. LV designed and supervised the study. All authors revised the manuscript and approved the final version.

FUNDING

This work was supported by Red Española de Esclerosis Múltiple (REEM) (RD16/0015/0001; RD16/0015/0002; RD16/0015/0003; RD16/0015/0008; RD16/0015/0013) and PI18/00572 integrated in the Plan Estatal I+D+I and co-funded by ISCIII-Subdirección General de Evaluación and Fondo Europeo de Desarrollo Regional (FEDER, "Una manera de hacer Europa").

ACKNOWLEDGMENTS

Authors acknowledge AI Pérez Macías and S Ortega for their excellent technical support.

SUPPLEMENTARY MATERIAL

The Supplementary Material for this article can be found online at: https://www.frontiersin.org/articles/10.3389/fimmu.2022.842354/full#supplementary-material

REFERENCES

1. Filippi M, Bar-Or A, Piehl F, Preziosa P, Solari A, Vukusic S, et al. Multiple Sclerosis. *Nat Rev Dis Primers* (2018) 4(1):43. doi: 10.1038/s41572-018-0041-4
2. Faissner S, Plemel JR, Gold R, Yong VW. Progressive Multiple Sclerosis: From Pathophysiology to Therapeutic Strategies. *Nat Rev Drug Discovery* (2019) 18 (12):905–22. doi: 10.1038/s41573-019-0035-2
3. Miller DH, Leary SM. Primary-Progressive Multiple Sclerosis. *Lancet Neurol* (2007) 6(10):903–12. doi: 10.1016/S1474-4422(07)70243-0
4. Baldassari LE, Fox RJ. Therapeutic Advances and Challenges in the Treatment of Progressive Multiple Sclerosis. *Drugs* (2018) 78(15):1549–66. doi: 10.1007/s40265-018-0984-5
5. Goldschmidt C, McGinley MP. Advances in the Treatment of Multiple Sclerosis. *Neurol Clin* (2021) 39(1):21–33. doi: 10.1016/j.ncl.2020.09.002
6. Monson NL, Cravens PD, Frohman EM, Hawker K, Racke MK. Effect of Rituximab on the Peripheral Blood and Cerebrospinal Fluid B Cells in Patients With Primary Progressive Multiple Sclerosis. *Arch Neurol* (2005) 62(2):258–64. doi: 10.1001/archneur.62.2.258
7. Hawker K, O'Connor P, Freedman MS, Calabresi PA, Antel J, Simon J, et al. Rituximab in Patients With Primary Progressive Multiple Sclerosis: Results of a Randomized Double-Blind Placebo-Controlled Multicenter Trial. *Ann Neurol* (2009) 66(4):460–71. doi: 10.1002/ana.21867
8. Montalban X, Hauser SL, Kappos L, Arnold DL, Bar-Or A, Comi G, et al. Ocrelizumab Versus Placebo in Primary Progressive Multiple Sclerosis. *N Engl J Med* (2017) 376(3):209–20. doi: 10.1056/NEJMoa1606468
9. Fernández-Velasco JI, Kuhle J, Monreal E, Meca-Lallana V, Meca-Lallana J, Izquierdo G, et al. Effect of Ocrelizumab in Blood Leukocytes of Patients With Primary Progressive Ms. *Neurol Neuroimmunol Neuroinflamm* (2021) 8(2): e940. doi: 10.1212/NXI.0000000000000940
10. Thompson AJ, Banwell BL, Barkhof F, Carroll WM, Coetzee T, Comi G, et al. Diagnosis of Multiple Sclerosis: 2017 Revisions of the McDonald Criteria. *Lancet Neurol* (2018) 17(2):162–73. doi: 10.1016/S1474-4422(17)30470-2
11. Greenfield AL, Hauser SL. B-Cell Therapy for Multiple Sclerosis: Entering an Era. *Ann Neurol* (2018) 83(1):13–26. doi: 10.1002/ana.25119
12. Lublin FD, Reingold SC, Cohen JA, Cutter GR, Sørensen PS, Thompson AJ, et al. Defining the Clinical Course of Multiple Sclerosis: The 2013 Revisions. *Neurology* (2014) 83(3):278–86. doi: 10.1212/WNL.0000000000000560
13. Cepok S, Rosche B, Grummel V, Vogel F, Zhou D, Sayn J, et al. Short-Lived Plasma Blasts are the Main B Cell Effector Subset During the Course of Multiple Sclerosis. *Brain* (2005) 128(7):1667–76. doi: 10.1093/brain/awh486
14. Disanto G, Barro C, Benkert P, Naegelin Y, Schädelin S, Giardiello A, et al. Serum Neurofilament Light: A Biomarker of Neuronal Damage in Multiple Sclerosis. *Ann Neurol* (2017) 81(6):857–70. doi: 10.1002/ana.24954
15. Bar-Or A, Fawaz L, Fan B, Darlington PJ, Rieger A, Ghorayeb C, et al. Abnormal B-Cell Cytokine Responses a Trigger of T-Cell-Mediated Disease in MS? *Ann Neurol* (2010) 67(4):452–61. doi: 10.1002/ana.21939
16. Schuh E, Berer K, Mulazzani M, Feil K, Meinl I, Lahm H, et al. Features of Human CD3+CD20+ T Cells. *J Immunol* (2016) 197(4):1111–7. doi: 10.4049/jimmunol.1600089
17. Goodman A, Patel SP, Kurzrock R. PD-1-PD-L1 Immune-Checkpoint Blockade in B-Cell Lymphomas. *Nat Rev Clin Oncol* (2017) 14(4):203–20. doi: 10.1038/nrclinonc.2016.168
18. Medina S, Sainz de la Maza S, Villarrubia N, Álvarez-Lafuente R, Costa-Frossard L, Arroyo R, et al. Teriflunomide Induces a Tolerogenic Bias in Blood Immune Cells of MS Patients. *Ann Clin Transl Neurol* (2019) 6(2):355–63. doi: 10.1002/acn3.711
19. Li R, Bar-Or A. The Multiple Roles of B Cells in Multiple Sclerosis and Their Implications in Multiple Sclerosis Therapies. *Cold Spring Harb Perspect Med* (2019) 9(4):a029108. doi: 10.1101/cshperspect.a029108
20. Oksbjerg NR, Nielsen SD, Blinkenberg M, Magyari M, Sellebjerg F. Anti-CD20 Antibody Therapy and Risk of Infection in Patients With Demyelinating Diseases. *Mult Scler Relat Disord* (2021) 52:102988. doi: 10.1016/j.msard.2021.102988
21. Boes M. Role of Natural and Immune IgM Antibodies in Immune Responses. *Mol Immunol* (2000) 37(18):1141–9. doi: 10.1016/s0161-5890(01)00025-6
22. Villar LM, Sádaba MC, Roldán E, Masjuan J, González-Porqué P, Villarrubia N, et al. Intrathecal Synthesis of Oligoclonal IgM Against Myelin Lipids Predicts an Aggressive Disease Course in MS. *J Clin Invest* (2005) 115(1):187–94. doi: 10.1172/JCI22833
23. Monreal E, Sainz de la Maza S, Costa-Frossard L, Walo-Delgado P, Zamora J, Fernández-Velasco JI, et al. Predicting Aggressive Multiple Sclerosis With Intrathecal IgM Synthesis Among Patients With a Clinically Isolated Syndrome. *Neurol Neuroimmunol Neuroinflamm* (2021) 8(5):e1047. doi: 10.1212/NXI.0000000000001047
24. Pabst O, Slack E. IgA and the Intestinal Microbiota: The Importance of Being Specific. *Mucosal Immunol* (2020) 13(1):12–21. doi: 10.1038/s41385-019-0227-4
25. Shalapour S, Lin XJ, Bastian IN, Brain J, Burt AD, Aksenov AA, et al. Inflammation-Induced IgA+ Cells Dismantle Anti-Liver Cancer Immunity. *Nature* (2017) 551(7680):340–5. doi: 10.1038/nature24302
26. Pröbstel AK, Zhou X, Baumann R, Wischnewski S, Kutza M, Rojas OL, et al. Gut Microbiota-Specific IgA+ B Cells Traffic to the CNS in Active Multiple Sclerosis. *Sci Immunol* (2020) 5(53):eabc7191. doi: 10.1126/sciimmunol.abc7191
27. Rojas OL, Pröbstel AK, Porfilio EA, Wang AA, Charabati M, Sun T, et al. Recirculating Intestinal IgA-Producing Cells Regulate Neuroinflammation *via* IL-10. *Cell* (2019) 177(2):492–3. doi: 10.1016/j.cell.2019.03.037
28. Grönwall C, Silverman GJ. Natural IgM: Beneficial Autoantibodies for the Control of Inflammatory and Autoimmune Disease. *J Clin Immunol* (2014) 34Suppl1:S12–21. doi: 10.1007/s10875-014-0025-4
29. Palma J, Tokarz-Deptuła B, Deptuła J, Deptuła W. Natural Antibodies-Facts Known and Unknown. *Cent Eur J Immunol* (2018) 43(4):466–75. doi: 10.5114/ceji.2018.81354

Conflict of Interest: EM received research grants, travel support or honoraria for speaking engagements from Biogen, Merck, Novartis, Roche, and Sanofi-Genzyme; JK received speaker fees, research support, travel support, and/or served on advisory boards by ECTRIMS, Swiss MS Society, Swiss National Research Foundation (320030_189140/1), University of Basel, Bayer, Biogen, Celgene, Merck, Novartis, Roche, Sanofi; VM-L received grants and consulting or speaking fees from Almirall, Biogen, Celgene, Genzyme, Merck, Novartis, Roche and Teva; JM-L has received grants and consulting or speaking fees from Almirall, Biogen, Bristol-Myers-Squibb, Genzyme, Merck, Novartis, Roche and Teva; GI has received consultancy/advice and Conference- travel support from Bayer, Novartis, Sanofi, Merck Serono, Roche, Actelion Celgene and Teva; CO-G has received speaker and consulting fees from Biogen, Celgene, Merck KGaA (Darmstadt, Germany), Novartis, Roche, Sanofi Genzyme and Teva; FG-G has received funding for research grants, travel support and honoraria for speaking engagements from: Bayer, Biogen, Roche, Merck, Novartis, Almirall, Teva and Genzyme-Sanofi; SS received research grants, travel support, or honoraria for speaking engagements from Almirall, Bayer, Biogen, Merck, Mylan, Novartis, Roche, Sanofi-Genzyme and Teva; AS reports compensation for consulting services and speaker honoraria from Merck-Serono, Biogen-Idec, Sanofi-Aventis, Teva Pharmaceutical Industries Ltd, Novartis, Roche, and Alexion; YB received speaking honoraria from Biogen, Novartis and Genzyme; LB received funding for research projects or in the form of conference fees, mentoring, and assistance for conference attendance from: Bayer, Biogen, Roche, Merk, Novartis, Almirall, Celgen and Sanofi; IG-S received research grants, travel support and honoraria for speaking engagements from Biogen, Merck, Novartis, Roche, Sanofi-Genzyme, TEVA and Alexion; LR received travel support, and honoraria for speaking engagements from Biogen, Merck, Roche and Sanofi-Genzyme; JS received funding for research projects and conference fees, mentoring, and assistance for conference attendance from: Teva, Merck, Biogen, Roche, Novartis, and Sanofi; SL received compensation for consulting services and speaking honoraria from Merck-Serono, Biogen-Idec, Sanofi-Aventis, Teva Pharmaceutical Industries Ltd, Novartis and Roche; LC-F received speaker fees, travel support, and/or served on advisory boards by Biogen, Sanofi, Merck, Bayer, Novartis, Roche, Teva, Celgene, Ipsen, Biopas, Almirall; LV received research grants, travel support or honoraria for speaking engagements from Biogen, Merck, Novartis, Roche, Sanofi-Genzyme and Bristol-Myers.

The remaining authors declare that the research was conducted in the absence of any commercial or financial relationships that could be construed as a potential conflict of interest.

Publisher's Note: All claims expressed in this article are solely those of the authors and do not necessarily represent those of their affiliated organizations, or those of the publisher, the editors and the reviewers. Any product that may be evaluated in this article, or claim that may be made by its manufacturer, is not guaranteed or endorsed by the publisher.

frontiers | Frontiers in Immunology

TYPE Original Research
PUBLISHED 16 August 2022
DOI 10.3389/fimmu.2022.803229

OPEN ACCESS

EDITED BY
Luisa María Villar,
Ramón y Cajal University Hospital,
Spain

REVIEWED BY
Ayman Rezk,
University of Pennsylvania,
United States
Francisco Carrillo-Salinas,
Tufts University School of Medicine,
United States

*CORRESPONDENCE
Alexey A. Belogurov Jr.
belogurov@ibch.ru
Alexander G. Gabibov
gabibov@gmail.com

SPECIALTY SECTION
This article was submitted to Multiple Sclerosis and Neuroimmunology, a section of the journal Frontiers in Immunology

RECEIVED 27 October 2021
ACCEPTED 20 June 2022
PUBLISHED 16 August 2022

CITATION
Lomakin YA, Zvyagin IV, Ovchinnikova LA, Kabilov MR, Staroverov DB, Mikelov A, Tupikin AE, Zakharova MY, Bykova NA, Mukhina VS, Favorov AV, Ivanova M, Simaniv T, Rubtsov YP, Chudakov DM, Zakharova MN, Illarioshkin SN, Belogurov AA Jr. and Gabibov AG (2022) Deconvolution of B cell receptor repertoire in multiple sclerosis patients revealed a delay in tBreg maturation.
Front. Immunol. 13:803229.
doi: 10.3389/fimmu.2022.803229

Deconvolution of B cell receptor repertoire in multiple sclerosis patients revealed a delay in tBreg maturation

Yakov A. Lomakin[1], Ivan V. Zvyagin[1], Leyla A. Ovchinnikova[1], Marsel R. Kabilov[2], Dmitriy B. Staroverov[1], Artem Mikelov[1,3], Alexey E. Tupikin[2], Maria Y. Zakharova[1,4], Nadezda A. Bykova[5], Vera S. Mukhina[5,6], Alexander V. Favorov[6,7], Maria Ivanova[8], Taras Simaniv[8], Yury P. Rubtsov[1], Dmitriy M. Chudakov[1,4], Maria N. Zakharova[8], Sergey N. Illarioshkin[8], Alexey A. Belogurov Jr.[1,9]* and Alexander G. Gabibov[1,10,11]*

[1]Shemyakin-Ovchinnikov Institute of Bioorganic Chemistry Russian Academy of Sciences (RAS), Moscow, Russia, [2]Institute of Chemical Biology and Fundamental Medicine, Siberian Branch Russian Academy of Sciences (RAS), Novosibirsk, Russia, [3]Skolkovo Institute of Science and Technology, Moscow, Russia, [4]Department of Molecular Technologies, Institute of Translational Medicine, Pirogov Russian National Research Medical University, Moscow, Russia, [5]Institute for Information Transmission Problems (Kharkevich Institute), Russian Academy of Sciences (RAS), Moscow, Russia, [6]Vavilov Institute of General Genetics, Russian Academy of Sciences (RAS), Moscow, Russia, [7]Quantitative Sciences Division, Department of Oncology, Johns Hopkins University, Baltimore, MD, United States, [8]Neuroinfection Department of the Research Center of Neurology, Moscow, Russia, [9]Department of Biological Chemistry, Evdokimov Moscow State University of Medicine and Dentistry, Moscow, Russia, [10]Department of Life Sciences, Higher School of Economics, Moscow, Russia, [11]Department of Chemistry, Lomonosov Moscow State University, Moscow, Russia

Background: B lymphocytes play a pivotal regulatory role in the development of the immune response. It was previously shown that deficiency in B regulatory cells (Bregs) or a decrease in their anti-inflammatory activity can lead to immunological dysfunctions. However, the exact mechanisms of Bregs development and functioning are only partially resolved. For instance, only a little is known about the structure of their B cell receptor (BCR) repertoires in autoimmune disorders, including multiple sclerosis (MS), a severe neuroinflammatory disease with a yet unknown etiology. Here, we elucidate specific properties of B regulatory cells in MS.

Methods: We performed a prospective study of the transitional Breg (tBreg) subpopulations with the $CD19^{+}CD24^{high}CD38^{high}$ phenotype from MS patients and healthy donors by (i) measuring their content during two diverging courses of relapsing-remitting MS: benign multiple sclerosis (BMS) and highly active multiple sclerosis (HAMS); (ii) analyzing BCR repertoires of circulating B cells by high-throughput sequencing; and (iii) measuring the percentage of $CD27^{+}$ cells in tBregs.

Results: The tBregs from HAMS patients carry the heavy chain with a lower amount of hypermutations than tBregs from healthy donors. The percentage of

transitional $CD24^{high}CD38^{high}$ B cells is elevated, whereas the frequency of differentiated $CD27^{+}$ cells in this transitional B cell subset was decreased in the MS patients as compared with healthy donors.

Conclusions: Impaired maturation of regulatory B cells is associated with MS progression.

KEYWORDS

B regulatory cells, BCR, CD19+CD24highCD38high, multiple sclerosis, MS, transitional Breg, TrB, activated memory-like transitional cells

Introduction

Multiple sclerosis is a highly heterogenous severe autoimmune neurodegenerative disorder with an evident inflammation component (1). Despite considerable advances in this field, the mechanism triggering it remains elusive, hindering the development of effective therapeutics (2–8). MS progression is mostly associated with the promotion of the T cell response (9, 10). Yet the contribution of B cells to various autoimmune disorders, including MS, should not be underestimated (11–16). Apart from antibody production and antigen presentation, B cells play a crucial role in regulating the immune response through their antibody-independent effector functions (17, 18).

In 1974, professor James Turk and coauthors suggested that B cells could inhibit inflammation during delayed hypersensitivity reactions (19). Further on, regulatory properties of B cells were confirmed in experimental autoimmune encephalomyelitis (EAE), an animal model of MS (20). The subpopulation of B cells performing regulatory functions were termed Bregs. In mice, the Breg population constitutes up to 5% of total B cells in the spleen and lymph nodes, and their number significantly increases during inflammation development (21–23). In humans, Bregs account for less than 5% of blood B cells (24). Abnormalities in the Breg counts or their function were observed in patients with autoimmune diseases (25–29) and allergies (30).

Different phenotypes of Bregs are described so far. Transitional Bregs (tBreg cells) $CD19^{+}CD24^{high}CD38^{high}$ (24, 26, 29, 31) and memory Bregs $CD19^{+}CD24^{high}CD27^{+}$ are the most studied regulatory B cell subpopulations that modulate the immune response in humans (32, 33). Meanwhile, several other Breg phenotypes are reported: $CD19^{+}CD25^{+}CD71^{+}CD73^{-}$ (34), $CD19^{+}CD27^{int}CD38^{+}IgM^{+}$ (35), $CD19^{+}CD24^{high}CD27^{+}CD39^{high}IgD^{-}IgM^{+}CD1c^{+}$ (36), $CD19^{+}CD5^{+}Foxp3^{+}$ (37), and $CD19^{+}CD38^{+}CD1d^{+}IgM^{+}CD147^{+}$ (38). Transitional $CD19^{+}CD24^{high}CD38^{high}$ Bregs can be found in the peripheral blood of healthy adults representing a minor subset (approximately 4%) of all circulating B cells (39). This tBreg subset was previously shown to produce IL-10, regulate $CD4^{+}$ T cell proliferation/differentiation toward T helper effector cells (40), and contribute to the cytokine imbalance during autoimmune diseases (41).

Since the molecular underpinnings of MS onset and progression were revealed, T cell–mediated immunity was believed to play the leading role in it. However, it is evident now that B cells are crucial for MS pathogenesis as well (42, 43). Autoreactive B cells in MS may produce catalytic antibodies, hydrolyzing myelin basic protein (13, 44, 45), and cause humoral cross-reactivity between myelin and viral antigens (46–50). Still, the existing studies on Bregs functioning in MS are controversial and far from conclusive. The percentages of IL-10–producing Bregs in MS patients are shown to be lower than in healthy controls (28, 51). Other works report either unaltered (52, 53) or even increased (25, 54) Breg numbers during MS progression. A recent study shows no association between the reduced peripheral blood Bregs levels and the Expanded Disability Status Scale (EDSS) score in MS (51).

These inconsistencies most likely arise from several Breg populations coexisting (55, 56). Indeed, these regulatory subpopulations can comprise B cells at different stages of development; therefore, the level of certain BCR hypermutations can be lower at the earlier stages of maturation of these B cells. The specificity of Bregs' BCRs and pathways that mediate their maturation are still poorly elucidated. It is still not known whether the specificity of Bregs BCRs undergoes alteration in autoimmune disorders.

This study aims to identify the possible abnormalities in the structure of BCRs in the tBregs isolated from peripheral blood of MS patients as compared with HD. Thus, we suggest that analyzing BCR repertoires of tBregs may reveal the disease-related alterations occurring at the early stage of B cell development.

10.3389/fimmu.2022.803229

Materials and methods

Patients and healthy donors

Peripheral blood was obtained from the Neuroinfection Department of the Research Center of Neurology, Moscow, Russia. Venous blood was collected in EDTA Vacutainers (BD) from 19 MS patients (nine with BMS (57) and 10 with HAMS) (58) and 16 HD (Table 1). The age of the MS patients ranged between 23 and 70 years old. Their EDSS scores ranged between 1.5 and 8.5. The EDSS values (scored on a scale of 0 to 10) were calculated based on the Kurtzke EDSS scale (59). BMS was diagnosed if the EDSS score was less than 4 for at least 10 years after the disease onset in the absence of

TABLE 1 Baseline and clinical characteristics of patients with multiple sclerosis and healthy donors.

MS phenotype	Age, years	Gender	EDSS	Treatment	Disease duration, years	BCR repertoire analysis	$CD27^+$ phenotypic analysis
BMS	56	female	2.5	No treatment	11	+	–
BMS	61	female	3	No treatment	26	+	–
BMS	43	female	1.5	No treatment	12	+	–
BMS	36	male	2.5	No treatment	14	+	–
BMS	46	female	2	No treatment	27	–	+
BMS	43	female	2.5	No treatment	27	–	+
BMS	43	male	4.0	No treatment	18	–	+
BMS	58	female	3.5	No treatment	30	–	+
BMS	70	female	4.0	No treatment	30	–	+
HAMS	33	male	6	IFNβ1b (2006-2011; 2014-2017)	12	+	–
HAMS	23	male	5	No treatment	3	+	–
HAMS	37	female	5	IFNβ1b (2014-2016) GA (2016-2017)	5	+	–
HAMS	29	female	8	GA (2012-2014) IVIG (2014) IFNβ1b (2015-2016)	12	+	–
HAMS	39	female	8.5	No treatment	8	+	–
HAMS	22	female	4.5	No treatment	1	–	+
HAMS	46	male	6	IFNβ1b (2019)	2	–	+
HAMS	44	male	8.5	IFNβ1b (2014-2015)	13	–	+
HAMS	24	male	4.0	No treatment	2	–	+
HAMS	44	female	4.5	No treatment	2	–	+
Healthy	24	female	N/A	N/A	N/A	+	–
Healthy	40	female	N/A	N/A	N/A	+	–
Healthy	36	male	N/A	N/A	N/A	+	–
Healthy	27	female	N/A	N/A	N/A	+	–
Healthy	42	female	N/A	N/A	N/A	+	–
Healthy	25	female	N/A	N/A	N/A	+	–
Healthy	39	male	N/A	N/A	N/A	–	+
Healthy	42	female	N/A	N/A	N/A	–	+
Healthy	35	female	N/A	N/A	N/A	–	+
Healthy	51	female	N/A	N/A	N/A	–	+
Healthy	24	female	N/A	N/A	N/A	–	+
Healthy	34	male	N/A	N/A	N/A	–	–
Healthy	24	female	N/A	N/A	N/A	–	–
Healthy	35	male	N/A	N/A	N/A	–	+
Healthy	68	female	N/A	N/A	N/A	–	+
Healthy	47	male	N/A	N/A	N/A	–	+

IFNβ1b, interferon-β-1b; GA, glatiramer acetate; IVIG, intravenous immunoglobulin; HAMS, highly active MS; BMS, benign MS; HD, healthy donors; N/A, not applicable.
"+" indicates that the corresponding analysis has been carried out.
"-" indicates that the corresponding analysis has not been performed.

treatment; HAMS relapsing-remitting MS was diagnosed based on an EDSS score of 4.0 within five years after the disease onset, poor response to disease-modifying treatments, and two or more relapses with incomplete recovery during one year. None of the patients received glucocorticoid treatment or immunomodulatory treatment for at least six months prior to blood collection. Data on the course of the disease, its duration, and history of administration of disease-modifying treatments are presented in Table 1. HDs (24–68 years old) had neither autoimmune nor oncology diseases nor recent infections. The study was approved by the Local Ethics Committee of the Research Center of Neurology and was conducted in full compliance with the WMA Declaration of Helsinki, ICH GCP, and appropriate local legislation. All patients provided written informed consent for enrollment, followed by a discussion of the study with the investigators.

FACS sorting of tBreg and total B cell subsets

Blood samples were diluted two times in PBS with 2 mM EDTA and layered onto Ficoll–Paque Plus (GE Healthcare) and then centrifuged at 900 g for 40 minutes at room temperature. PBMC isolated from MS patients were incubated with ACK lysing buffer for complete removal of red blood cells. Cells were washed with PBS, incubated with α-CD19-PE-Cy7, α-CD24-PE, α-CD38-APC, α-CD27-FITC, and α-CD45-APC-Cy7 antibodies (Biolegend, USA) or α-CD19-PE-Cy7, α-CD24-PE, α-CD38-APC, α-CD45-APC-Cy7, and sytox green dead cell stain (ThermoFisher Scientific) for 60 minutes at +4°C in the dark. Human Fc-blocker (Miltenyi Biotec) was added to all samples before cell staining. B cell subsets were identified by the following markers on their surface: transitional Bregs ($CD19^+CD24^{high}CD38^{high}$), T1 transitional cells ($CD19^+CD24^{+++}CD38^{+++}$), T2 transitional cells ($CD19^+CD24^{++}CD38^{++}$), memory Bregs ($CD19^+CD24^{high}CD27^+$), and memory ($CD19^+CD24^{+/high}CD38^{+/low}CD27^+$) or naïve ($CD19^+CD24^+CD38^{+/low}CD27^-$) peripheral B cells (60). Following incubation, the cells were washed with PBS and resuspended in PBS. To distinguish T1 and T2 cells by CD24 and CD38 expression, we used gates for flow cytometry analysis, which provided a T2/T1 ratio of approximately 3:1 in HDs (61). Leukocyte and total lymphocyte counts per mm^3 were determined using a hematology analyzer (Nihon Kohden MEK-7222, Nihon Kohden, Japan). All samples were analyzed for B cell and tBreg frequencies by flow cytometry. For nine MS patients (four with BMS and five with HAMS) and six healthy donors, a live $CD19^+$ pool of total B cells or $CD19^+CD24^{high}CD38^{high}$ tBreg was sorted into two distinct populations (Table 1). The cells were sorted directly into 1.5-mL microcentrifuge tubes containing Qiazol lysis reagent (Qiagen, Germany). Sorting was carried out using a BD FACSAria III, and the data were analyzed using FlowJo software 9.7.5 (TreeStar, Ashland, OR, USA).

Library preparation for immunoglobulin sequencing (RT-PCR)

RNA extraction was performed using the RNeasy Mini Kit (Qiagen, Germany) according to the manufacturer's protocol. Reverse transcription (RT) was performed in 20 μL reaction volume using MMLV RT according to the manufacturer's protocol (Evrogen, Russian Federation). Multiplex PCR with a modified set of the previously described VH- and VL-specific primers was used for cDNA amplification (62). The primers included 15 human VH-specific forward primers and four human JH-specific reverse primers for the IGH chain, 13 human Vκ-forward primers and two Jκ-reverse primers for Vκ genes, and 16 human Vλ-forward primers and three Jλ-reverse primers for Vλ genes (Table S1). Each VH, Vκ, and Vλ primer pair was added to a separate 50 μl reaction mix with an appropriate equimolar mixture of the four JH, two Jκ, or three Jλ reverse primers. Then, 0.5 ng cDNA was used in each PCR reaction using the Hot Start Taq Master Mix Kit (Evrogen, Russian Federation). The conditions of PCR were as follows: 1 step (94°C—3 min), 1 cycle (94°C—25 s, 62°C—25 s, 72°C—25 s), 2 cycles (94°C—25 s, 60°C—25 s, 72°C—25 s), 2 cycles (94°C—25 s, 58°C—25 s, 72°C—25 s), 3 cycles (94°C—25 s, 56°C—25 s, 72°C—25 s), 3 cycles (94°C—25 s, 54°C—25 s, 72°C—25 s), 30 cycles (94°C—25 s, 52°C—25 s, 72°C—25 s), and 1 step (72°C—4 min). The products of 15 PCR reactions for VH genes, 13 PCR reactions for Vκ genes, and 16 PCR reactions for Vλ genes were combined for each chain and concentrated to 50–80 μl using Amicon 30 kDa (Merck, Millipore). The PCR products (~400 bp length) of VH, Vκ, and Vλ were loaded on 1.5% agarose gels and purified with the Gel Extraction Kit (Monarch, NEB).

Deep sequencing of VH and VL genes from individual patients

Next, 1 μg of the PCR product was ligated with adapters using the NEBNext Ultra DNA Library Prep Kit for Illumina with the NEBNext Multiplex Oligos set (NEB). Libraries were sequenced on Miseq using a 2x300 bp paired-ends sequencing kit (Illumina) in the SB RAS Genomics Core Facility (ICBFM SB RAS, Novosibirsk, Russia).

Sequencing data processing and repertoire analysis

MiXCR (63) software was used to extract BCR clonotypes from raw sequencing data. Raw reads were aligned to the standard reference set of V, D (for heavy chain), and J gene-segment sequences. Successfully aligned reads were used for

clonotype sequence assembly with the following parameters: OassemblingFeatures="{CDR1Begin : CDR3End}" -OmaxBadPointsPercent=0. To normalize the repertoire analysis depth, equal numbers (13,000 for IGVH or IGVK and 7000 for IGVL) of read pairs covering the full target sequence (CDR1+FR2+CDR2+FR3+CDR3) were randomly sampled from each data set. A BCR clonotype is referred to here as a unique nucleotide sequence covering BCR from the beginning of CDR1 to the end of CDR3. Repertoire sequencing results are summarized in Table S2.

Repertoire data analysis was performed using the R programming language (R Core Team (2017) R: the language and environment for statistical computing (R Foundation for Statistical Computing, Vienna, Austria. URL https://www.R-project.org/). Unproductive IGVH/IGVK/IGVL sequences were filtered out before analysis. To characterize the germline identity for each clonotype, a nucleotide sequence covering the CDR1-FR3 part was used for calculating the percentage of identity with the corresponding reference V-segment sequence. The VDJ tools software (64) with the CalcCdrAaStats subroutine was used to obtain the statistics on composition and physical-chemical properties of amino acids in the CDR3 region. For CDR3 length analysis, we defined the length as a number of amino acids from conservative Cys at the end of the part encoded by the V-segment to the conservative Phe/Trp encoded by the J-segment (65).

IL-10 secretion assay

B cells from isolated PBMC were enriched using magnetic Dynabeads (negative selection; Invitrogen, Thermo Fisher) following the manufacturer's instructions with >95% purity. Enriched B cells were maintained in the complete glutamine-enriched RPMI-1640 medium supplemented with 10% fetal bovine serum (FBS) and 10 mM HEPES at a concentration of $0.5 \bullet 10^6$ cells/mL in six-well culture plates at 37°C with 5% CO_2. IL-10 production was induced by the incubation with 10 μg/mL CpG-B ODN 2006 for 20 hours. CpG-stimulated B cells were restimulated by adding up to 50 ng/mL PMA (Sigma-Aldrich) and 0.5 μg/mL ionomycin (Sigma-Aldrich) for four hours.

Stimulated B cells were washed twice with PBS and stained for assessing the cell viability with Zombie Violet Fixable Viability Kit (Biolegend, USA) according to the manufacturer's instructions. Next, B cells were washed with cold (MACS) buffer containing PBS supplemented with 0.5% BSA and 2 mM EDTA; 10^6 of B cells were then resuspended in 90 μl of cold RPMI-1640 medium supplemented with 10% FBS and incubated with 10 μl IL-10 Catch Reagent (IL-10 secretion assay, Miltenyi Biotec) for five minutes on ice. Subsequently, 1 mL of warm (37°C) RPMI-1640 medium supplemented with 10% FBS was added, and cells were kept for 45 minutes at 37°C under slow continuous rotation. B cells were washed twice with a cold (MACS) buffer, resuspended in 80 μl cold (MACS) buffer with the addition of 10 μl IL-10 detection antibody (APC) (IL-10 secretion assay, Miltenyi Biotec) and 10 μl of the antibody mix (α-CD19-PE-Cy7, α-CD24-PE, and α-CD38-AlexaFluor700). After 20 minutes of incubation on ice, B cells were washed with cold buffer and resuspended in PBS. IL-10^+ and IL-10^- B cells were analyzed using FACS Aria III (BD Biosciences).

Statistical analysis

The data were analyzed using Prism 9 software. The significance of differences was assessed using the two-tailed Student's t-test, Mann Whitney U-test, or ANOVA. p-values <.05 were considered to be significant.

Results

The elevated level of transitional $CD19^+CD24^{high}CD38^{high}$ Bregs in peripheral blood correlates with MS severity

We analyzed patients with two diverging courses of relapsing-remitting MS (RRMS): (*i*) BMS (57), characterized by an infrequent relapse and low levels of disability over long periods of time, and (*ii*) HAMS (58) with elevated levels of inflammatory activity and rapid progression that facilitate a shift to secondary progressive MS with severely disrupted control of the immune response. The peripheral blood samples were obtained from 19 MS patients and 16 HDs (Table 1). To gain further insight into the nature of Breg development and maturation, we analyzed the $CD19^+CD24^{high}CD38^{high}$ subpopulation, which is the most studied phenotype of tBreg (26, 66). Mononuclear cells were stained against CD45, CD19, CD24, and CD38 markers. A gating strategy is shown in Figure 1A. We found that the cell number and frequency of $CD19^+CD24^{high}CD38^{high}$ B cells were significantly increased in the MS patients (4.5 ± 2.4%) as compared with the HDs (2.6% ± 1.8%). This upregulation was most pronounced in the HAMS patients (5.5% ± 2.7%) (Figures 1B, C). Wherein we observed no differences in the absolute counts for B cells between HDs and MS patients with various courses of MS (Table 2).

Previously, Cherukuri and colleagues showed that the activity of regulatory B cells varies depending on the composition of the tBreg subpopulation (67). A reduced T2/T1 ratio is associated with elevated IL-10 production and the most efficient T cell suppression (61). We studied the ratio between the transitional T1 and T2 subsets (the gating strategy is shown on Figure 4) distinguished by CD24 and CD38 expression (Table 2). The absolute T1 count was significantly elevated in the MS patients (p = .037) in

10.3389/fimmu.2022.803229

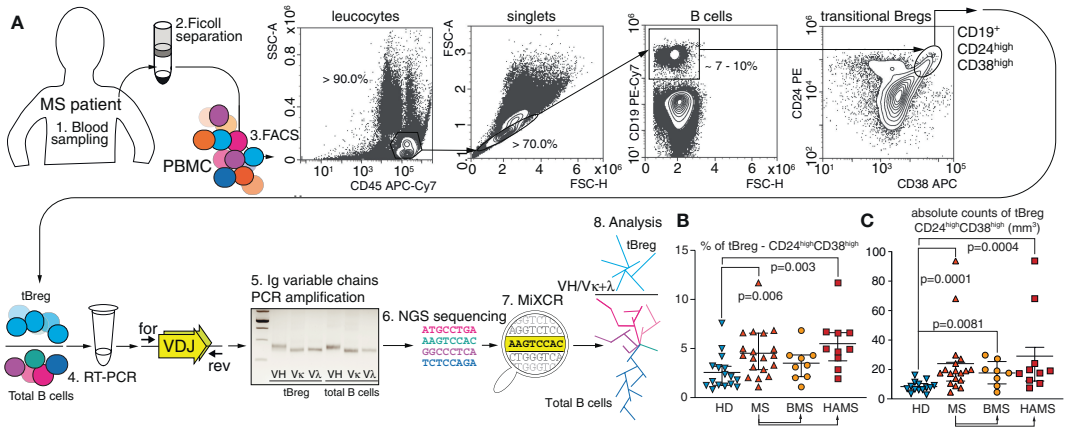

FIGURE 1
MS severity correlates with the elevated level of transitional CD19^{+}CD24^{high}CD38^{high} Bregs in peripheral blood. **(A)** Total CD19^{+} B cell pool and transitional regulatory CD19^{+}CD24^{high}CD38^{high} subpopulation (tBregs) from peripheral blood were sorted individually for subsequent RNA isolation and RT-PCR amplification of IGVH, IGVK and IGVL followed by high-throughput sequencing and subsequent bioinformatic clustering and analysis. **(B)** The percentage and **(C)** absolute cell count of transitional Bregs in MS patients (MS) and healthy donors (HD). BMS denotes benign multiple sclerosis, HAMS is highly active multiple sclerosis. Data are shown as mean values, interquartile range, and *p*-values. The statistical significance was evaluated with the Mann Whitney test (only significant *p*-values are shown).

comparison with healthy donors. The absolute T2 counts in peripheral blood were also significantly increased in the MS patients as compared with HDs (p = .0007), especially during HAMS (p = .0002). Whereas the mean value of the T2/T1 ratio is elevated during MS progression, no statistically significant difference in comparison to healthy donors was observed. To carefully distinguish between T1 and T2 cells, we analyzed CD24 and CD38 expression as well as the expression of IgD, being an important marker of B cell developmental stage and maturation (68, 69). We observed no significant difference in the T2(CD24^{high}CD38^{high}IgD^{+})/T1(CD24^{high}CD38^{high}IgD$^{low/-}$) ratio between the two groups of six MS and four HDs, respectively (Figure S3).

To characterize the BCR repertoire of tBregs cells, we sorted total CD19^{+} B cells and CD19^{+}CD24^{high}CD38^{high} subpopulations and performed high-throughput sequencing of BCR cDNA libraries for variable heavy (VH) and light (VL) chains in these cell subsets. On average, we obtained ~40,000 and ~37,000 IGVH- and IGVK-containing reads for tBregs and total B cells, respectively. We obtained ~25,000 and ~17,000 IGVL-containing reads for tBregs and total B cells, respectively. We achieved the minimum depth of two IG sequence-containing reads per cell in most samples. Heavy and light chain clonotypes were assembled by the MiXCR with sequencing error correction (63). To reduce a potential bias, we used the equal repertoire analysis depth for all individuals (see Material and Methods section). For the CD19^{+}CD24^{high}CD38^{high} B cell subpopulation, we obtained and included in our analysis ≈4500 functional clonotypes for the heavy chain, ≈3500 for the kappa, and ≈550 for lambda chains for individuals in the MS and HD cohorts. For total B cells (the CD19+ subpopulation), we obtained ≈4000 functional clonotypes for heavy chain, ≈4300 for kappa, and ≈830 for lambda chains from the raw sequencing data and included this in our analysis for the individuals from the MS and HD cohorts (Table S2).

TABLE 2 Total numbers and frequency of T1/T2 subpopulations of transitional B cells in peripheral blood from the MS patients and healthy donors.

Clinical group	HD	MS	BMS	HAMS
Absolute counts B cells per mm^3	455 ± 52	508 ± 74	508 ± 98	508 ± 112
Absolute counts tBreg cells per mm^3	8.4 ± 1.0*	24.0 ± 5.2*	17.7 ± 3.0*	29.1 ± 9.0*
T2/T1 ratio	2.8 ± 0.2	3.9 ± 0.7	3.2 ± 0.3	4.4 ± 1.1
Absolute counts T1 cells per mm^3	2.3 ± 0.3*	6.6 ± 2.1*	3.5 ± 0.8	8.1 ± 3.1
Absolute counts T2 cells per mm^3	6.1 ± 0.7*	16.3 ± 3.6*	9.9 ± 2.2	19.4 ± 5.1*

All values are expressed as mean values ± SEM. Significantly different values evaluated by a Mann Whitney test between the healthy donors and MS patients are indicated with asterisks.

Transitional CD19^{+}CD24^{high}CD38^{high} Bregs of MS patients are characterized by a lower number of hypermutations compared with the healthy individuals

The tBregs are suggested to be the exogenous antigen-naïve cell population, therefore exhibiting fewer somatic hypermutations than the total pool of CD19^{+} B cells from peripheral blood (Figure 2A). V_H and Vκ genes of CD19^{+}CD24^{high}CD38^{high} tBregs from MS patients are generally less mutated as compared with the HDs. There was a statistically significant difference between the HDs and HAMS patients yet not between the donors and BMS patients (Figure 2A). These data are in line with an increased level of tBregs in the peripheral blood from the HAMS patients. We observed approximately the same number of the IGH clonotypes in tBregs and total CD19^{+} B cells in the MS patients and healthy donors (Figure 2B). Analysis of repertoire diversity of the light chains showed that in the HDs the ratio in number of the IGK and IGL clonotypes in the total CD19^{+} pool was higher than in tBregs, whereas it remained unchanged in MS patients (Figure 2B). The lowest repertoire diversity was observed for the lambda light chain. The ratio of tBreg/total B cell clonotypes between MS patients and HDs was different only for the lambda chain (Figure 2C).

Because in the MS patients we observed fewer somatic hypermutations in the tBreg clonotypes, one could suggest a higher number of CDR3 in this cell subset shared among MS patients. However, we detected only a few tBreg IGH clonotypes common for at least two different donors. Furthermore, we did not observe any significant differences in the number of shared amino acid CDR3 sequences between MS and HD (data not shown).

Characteristics of the CDR3 region of tBreg clonotypes do not vary between MS and healthy states

CDR3 is the most variable region of immunoglobulin molecules. It can be used for identifying clonal lineages and characterizing their functional repertoire (70). First, we examined CDR3 characteristics by comparing the amino acid CDR3 length of the heavy, kappa, and lambda chains among HDs, HAMS, and BMS disease states in tBregs and total peripheral B cells. In line with our expectations, we detected a significant difference in amino acid length between the heavy chain (18.3 ± 0.7 a.a.) and both light chain types (11.2 ± 0.1 a.a. for the kappa chain and 11.5 ± 0.3 a.a. for the lambda chain) due to the presence of the D-segment in the IGH.

For the heavy chain, the CDR3 length significantly varied between the tBreg and the total B cell populations (Figure 3A) in contrast to the previously reported data (71). Nonetheless, there was no statistically significant difference in the CDR3 length

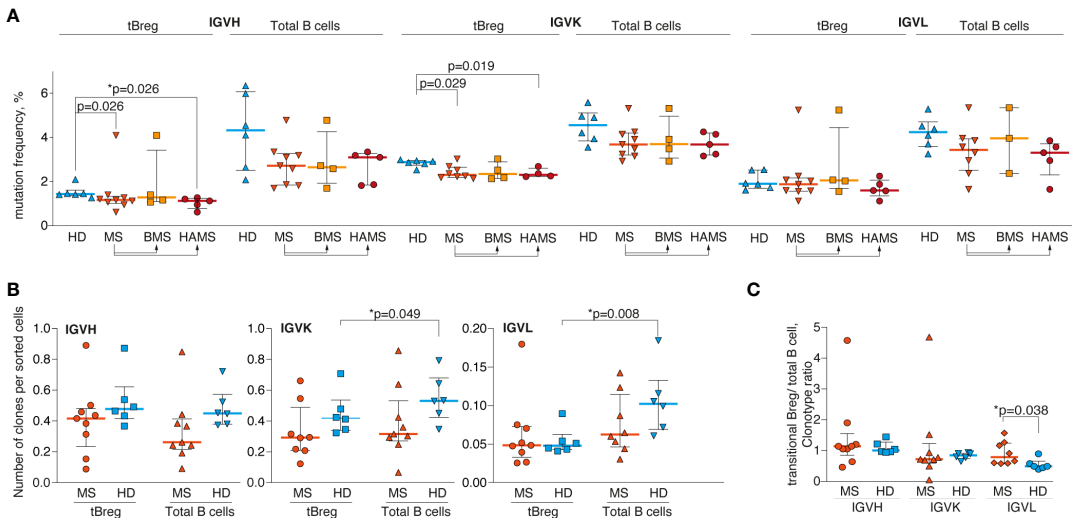

FIGURE 2
Delayed maturation of CD24^{high}CD38^{high} transitional B lymphocytes in the MS patients. **(A)** Mutation frequency for V_H, Vκ, and Vλ genes; **(B)** the number of unique clonotypes per sorted cells; and **(C)** the tBreg/total B cell clonotype ratio of the total blood B cells and CD24^{high}CD38^{high} transitional Bregs from the multiple sclerosis patients (MS) and healthy donors (HD). Mutation frequency refers to the percentage of clonotype sequence different from the corresponding germline V- and J-segment sequences excluding CDR3 region. BMS denotes benign multiple sclerosis, HAMS is highly active multiple sclerosis. Bar and line plots represent a median and interquartile range. Statistical significance of the differences between donor groups was assessed using the Mann-Whitney test **(A, B)** and ratio paired *T*-test **(C)**. *p*-values <.05 after correction for multiple comparisons were considered statistically significant and designated with asterisks.

10.3389/fimmu.2022.803229

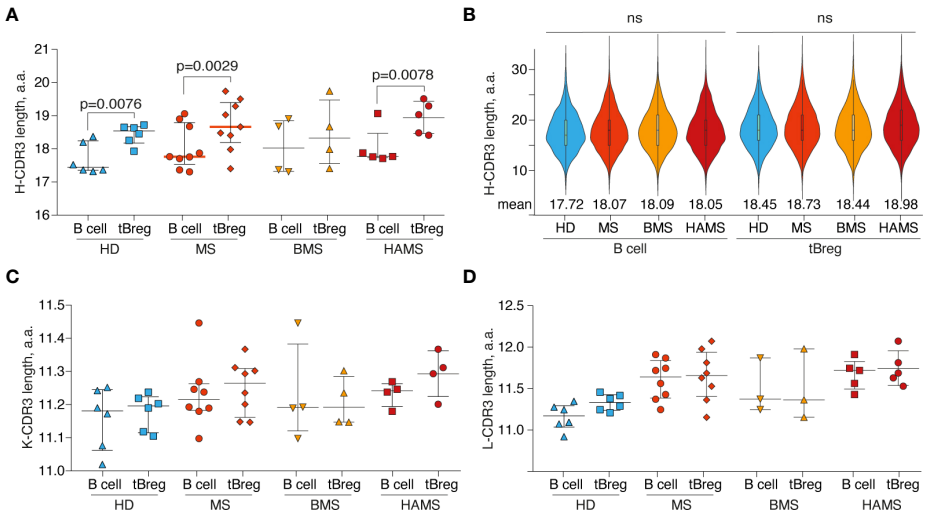

FIGURE 3
Differences in CDR3 length. The distribution of B cell subset CDR3 amino acid length for heavy **(A)**, kappa **(C)**, and lambda **(D)** light chains. Bar and line plots show mean ± SD. **(B)** The CDR3 amino acid length distribution for IGVH clonotypes in different B cell subsets. To balance the sample size, an equal number of clonotypes (n = 1000) were randomly sampled from each donor repertoire. Rare clonotypes with CDR3 length <6 a.a. or >35 a.a. were excluded. Mean values are displayed by numbers. The difference in CDR3 length between tBreg and total B cell fraction was analyzed by the ratio paired T-test. The difference in CDR3 length between donor groups was assessed using the Mann Whitney test. Only statistically significant p-values are indicated. The total $CD19^+$ B cell pool and transitional regulatory $CD19^+CD24^{high}CD38^{high}$ subpopulation from peripheral blood are designated as B cells and tBregs, respectively. ns , not significant.

between the MS patients and healthy individuals (Figure 3B). We did not detect any significant differences in the length of CDR3 of the kappa and lambda light chains between the tBreg subset and total B cells (Figures 3C, D, S1).

Furthermore, we compared the physicochemical properties of the CDR3 amino acids for the clonotypes from tBregs and total peripheral B cells. We observed no significant differences in the charge and hydrophobicity or amino acid usage in the CDR3 regions between the B cell subsets of the MS patients and HDs (data not shown).

The $CD19^+CD24^{high}CD38^{high}$ subpopulation in MS patients is characterized by less mature phenotype

It is previously reported that the number of mature memory $CD27^+$ peripheral B cells (72) in MS patients tends to decrease as compared with healthy individuals (73). Importantly, the ratio of different B cell populations and especially of the memory B cells varies with age (74). To avoid any age-related bias, the samples from sex- and age-matched MS patients (44 ± 14 y.o.) and HDs (43 ± 13 y.o.) were enrolled in this study (Table 1; Figure 4C). To examine the phenotypic stage of tBreg maturation, we analyzed the percentage of CD27 positive cells in this subpopulation (Figure 4A). We found that the $CD27^+$ cell content in the $CD19^+CD24^{high}CD38^{high}$ tBregs cells was significantly reduced in the MS patients (1.0% ± 0.5%) as compared with healthy individuals (2.2% ± 1.4%). We observed no correlation between age and the frequency of $CD27^+$ cells in the $CD19^+CD24^{high}CD38^{high}$ subpopulation (Figure S2). Our findings correlate well with previously reported data suggesting that Bregs ($CD19^+IL10^+$) mostly had the $CD27^-$ phenotype in HD and MS patients in remission (28), whereas the percentage as well as the absolute counts of memory Bregs ($CD24^{high}CD27^+$) and naïve and memory B cells were similar in the HDs and MS patients (Figure 4B; Table 3).

$CD19^+CD24^{high}CD38^{high}$ B cells are characterized by an elevated production of IL-10 in MS patients and HDs

Because the regulatory properties of B cells are not limited exclusively to the $CD19^+CD24^{high}CD38^{high}$ subpopulation (55, 56), we analyzed the frequencies of the IL-10-positive cells among the total pool of B lymphocytes after a short CpG stimulation. Such rapid stimulation (less than 24 hours) allows estimating IL-10 production only in Bregs and not in the B cells predisposed for the IL-10 expression. There were no statistically significant differences in the IL-10–producing B cell subsets between MS and HD, whereas more IL-10–positive B cells were observed in the $CD19^+CD24^{high}CD38^{high}$ subpopulation than in total B cells for both MS and HD (Figure 5A).

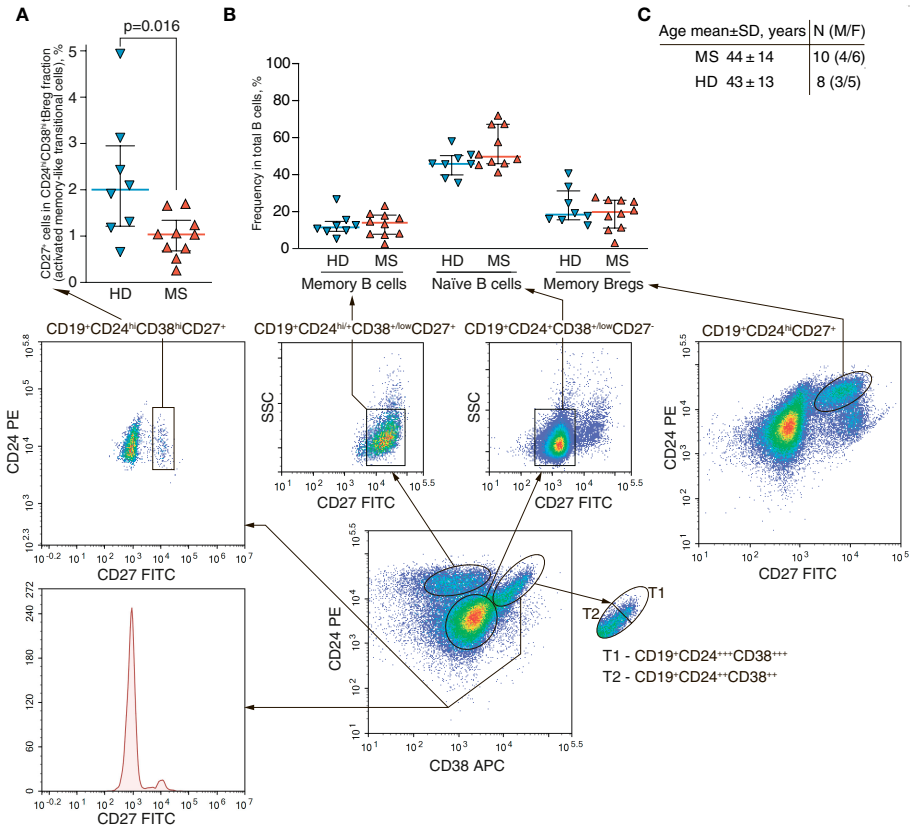

FIGURE 4
Frequencies of the CD27-positive B cells in peripheral blood of MS patients and healthy individuals. **(A)** The percentage of CD27-positive activated memory-like transitional cells in $CD19^+CD24^{high}CD38^{high}$ tBreg subpopulation and **(B)** the frequency of memory ($CD19^+CD24^{+/high}CD38^{+/low}CD27^+$), naïve ($CD19^+CD24^+CD38^{+/low}CD27^-$) or memory Breg ($CD24^{high}CD27^+$) among peripheral B cells in multiple sclerosis patients (MS) and healthy donors (HD). The bottom panel shows the gating strategy of flow cytometric analysis. **(C)** Age and gender comparison of MS and HD analyzed in the same experiment. The difference in cell frequency was analyzed by Mann Whitney test. Statistically significant *p*-values are shown.

Conversely, IL-10–positive B cells in MS and HD were enriched with $CD19^+CD24^{high}CD38^{high}$ cells (Figure 5B).

Discussion

The existence of several alternative methods of Breg differentiation might lead to different subsets of B cells with regulatory functions coexisting in an inflammatory milieu (75). The Breg population can originate from either multiple or a limited set of independent pre-Bregs progenitors. Furthermore, it results in either a diverse or restricted clonal repertoire, the latter being ensured by the clonally related Bregs. Moreover, almost any B cell can become a regulatory B cell at a certain stage of its development upon exposure to permissive environmental stimuli (35, 55). In the present study, we focus on the repertoire of tBregs with the $CD19^+CD24^{high}CD38^{high}$ phenotype.

The mechanism of immune regulation mediated by B cells was first proposed by S. Fillatreau and colleagues. They first identified a subpopulation of B cells (B10 cells) that produced IL-

TABLE 3 Total numbers of B cell subpopulations in peripheral blood of the MS patients and healthy donors (gating strategy is shown in Figure 4).

Clinical group	HD	MS	BMS	HAMS
Memory B cells	51 ± 9	41 ± 6	34 ± 5	46 ± 9
Naïve B cells	192 ± 40	216 ± 47	172 ± 42	246 ± 75
Memory Breg cells	89 ± 17	77 ± 22	44 ± 6	100 ± 34

All values are given as absolute counts per mm^3 and presented as mean ± SEM.

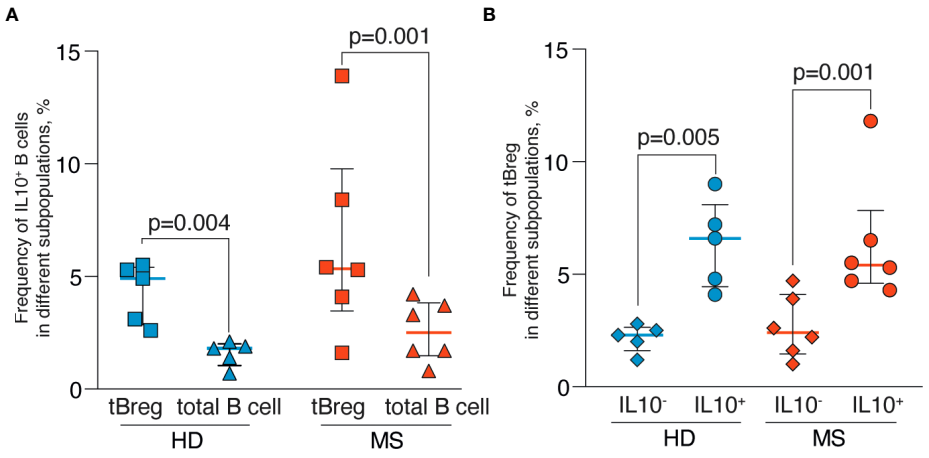

FIGURE 5
Frequencies of the IL-10–positive B cells in peripheral blood of MS patients and healthy individuals after rapid CpG stimulation. **(A)** The percentage of IL-10–positive cells in $CD19^{+}CD24^{high}CD38^{high}$ tBreg subpopulation and total B cells. **(B)** The percentage of $CD19^{+}CD24^{high}CD38^{high}$ tBreg in IL-10–positive and IL-10–negative B cells. Results are expressed as a median, interquartile range, and *p*-values analyzed by ratio paired *T*-test. Statistical significance of the differences between donor groups was assessed by the Mann Whitney test, and significance of differences between B cell subpopulations was assessed by the ratio paired *T*-test. Statistically significant *p*-values ($p < .05$) are shown.

10, alleviating the clinical manifestations of EAE (76). Bregs can also affect the differentiation of T cells to T regulatory cells (Tregs) (24) and inhibit differentiation of the effector T cells *via* the IL-10–driven suppression of dendritic cells (35). Bregs are shown to suppress inflammation by producing transforming growth factor-β (TGF-β) (77), IL-35 (i35 Breg) (78), IgM, IgG4, the co-inhibitory receptor TIGIT (T cell immunoreceptor with Ig and ITIM domains) (36), and *BTLA* (B and T lymphocyte attenuator or CD272) (79). Nonetheless, IL-10 production is still believed to be the key mechanism for Bregs to control the immune response in healthy individuals as well as during immune-related disorders (26, 27, 80–82) and organ transplantation (83).

Breg maturation may be induced *via* BCR and/or TLR signaling (84). Using EAE, the experimental mouse model of autoimmune diseases, a significant impact of TLR-signaling on B cells was revealed (85). TLR-4 and TLR-9 induce a significant increase in IL-10 secretion by B cells in a MyD88-dependent manner. Their activation *via* TLR and CD40 ligands is also described for infectious diseases of viral (HIV (31), HBV (86)), bacterial (87, 88), and parasitic origins (89). Exposure of PBMC from both healthy donors and patients with rheumatoid arthritis to CD40L and CpG led to an increased number of IL-10–producing Bregs (90). A significantly lower level of IL-10 production by B cells stimulated in the presence of CD40L was found in the groups with relapsing-remitting (29) and secondary-progressive MS as compared with HDs. A similar effect was observed in the CpG-stimulated B cells (82). The fact that CD40 ligation on B cells plays an important role in this process promoting cell survival (91) is in line with the inductive model of Breg formation. The latter implies that B cells may become regulatory and exhibit suppressive capacity in response to specific environmental stimuli.

Another mechanism to induce Bregs is to activate them through BCR signaling (76). Matsumoto et al. demonstrate the importance of correct antigen recognition by Breg BCR (92). The antigen-mediated calcium influx in Bregs is shown to depend on STIM-1 (stromal interaction molecule) and STIM-2. A deficiency in these molecules impairs the ability of Bregs to produce IL-10, disrupts T cell activation, and eventually prevents alleviating EAE in mice. The number of Bregs was reduced in CD19-deficient mice with disrupted BCR-signaling, whereas CD19 overexpression resulted in an increased number of B10 cells (93–95). The antigen-specific interaction between $CD4^{+}$ T cells and B10 cells is crucial for generating B10 effector cells, whereas antigen-specific T cell response is downregulated by B10-mediated IL-10 production (96). Therefore, the B10 cell effector function primarily depends on antigen specificity; however, it might also be mediated by suppressing antigen presentation by dendritic cells and macrophages (97).

We observed that $CD19^{+}CD24^{high}CD38^{high}$ tBregs have a significantly longer CDR3 in the heavy chain as compared with the total pool of peripheral B cells. Antigen-experienced B cells were previously shown to have shorter CDR3 than naïve or immature B cells (98, 99), thus indicating that, in tBregs, longer CDR3 can point at their immature state. This can also be related to the differences in V/J-usage between tBregs and total B cells (100, 101). Finally, in tBregs, longer CDR3 may reflect the higher poly-/self-reactive potential of their BCRs (102).

Another piece of evidence underlying the importance of BCR during Breg activation is that human B10 cells are often defined as $CD27^+$. This allows for classifying them as memory cells, which is in line with their *in vivo* antigen experience (25). Of note, in the RRMS patients at the relapse stage, the ratio of naïve and memory Bregs is decreased, resulting in an elevated memory/naïve ratio (28). The presence of the $CD27^+$ subpopulation in early immature transitional B cells could be explained by the recently proposed class-switching of antibodies in early human B cell development (71). Therefore, even transitional cells can undergo early maturation or, according to the alternative hypothesis, the $CD19^+CD24^{high}CD38^{high}CD27^+$ subset might belong in the IgM memory population (103, 104). Here, we show that the $CD19^+CD24^{high}CD38^{high}$ tBregs from MS patients contain a statistically lower number of CD27-positive cells as compared with HDs.

Our findings allow us to conclude that the elevated absolute number and frequency of $CD19^+CD24^{high}CD38^{high}$ tBregs observed in MS patients is characterized by a greater germline identity as compared with HD. At the same time, the absolute cell counts of the recently immigrated from the bone marrow T1 and more mature T2 cells both increased, thus more or less maintaining the overall T1/T2 ratio as in a healthy state. We propose at least three scenarios explaining these findings: (i) deficient maturation of transitional B cells (TrB); (ii) delayed TrB maturation, and (iii) elevated TrB counts that compensate for deficient maturation (Figure 6). The latter seems to be the most likely scenario because the T1/T2 ratio and, especially, percentage and absolute counts of TrB are increased in MS patients, whereas the numbers of memory and naïve B cells remain unaltered. Nonetheless, current evidence is not conclusive yet.

The tBregs maturation failure could arise from either an intrinsic defect in pre-Bregs or insufficient antigen-induced maturation. The BCR sequences of B10 cells were recently shown to be closer to germline and harbor only rare mutations (105). The authors state that, similarly to the splenic B10 cells, the peritoneal cavity B10 cells expressed clonally diverse BCRs that were predominantly germline encoded. Despite the germline proximity, B10 cells are shown to produce IgG as well as IgM (106). Thus, the so-termed "low differentiated" BCR may provide low-affinity antigen-BCR stimulation during chronic disease and development of the B10 precursor to B10, whereas a strong stimulation may switch the Breg precursor to another differentiation pathway (25, 94, 105). In the present work, we revealed no differences in IL-10 production between MS and HD *via* functional analysis. Therefore, increased tBreg counts along with the absence of increased IL-10 production can serve as indirect evidence in favor of their disrupted functioning and altered inflammatory profile during MS development. We suggest that, in future studies, tBregs should be analyzed for IL-10 production as well

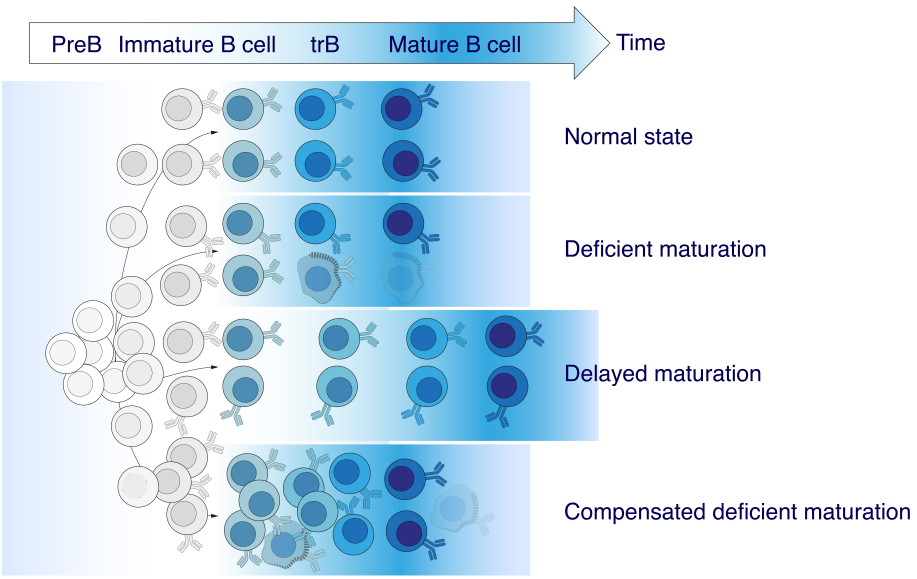

FIGURE 6
Abnormalities in transitional B cell maturation in MS. An elevated frequency of $CD19^+CD24^{high}CD38^{high}$ transitional B cells (TrB) observed in MS patients is characterized by greater germline identity compared with healthy donors. There are least three possible coexisting or independent scenarios explaining these findings: (*i*) deficient maturation of TrB, (*ii*) delayed TrB maturation, and (*iii*) an increased number of TrB compensating deficient maturation.

as co-expression of other cytokines as IL-10$^+$ B cells are previously shown to co-express pro-inflammatory cytokines such as IL-6 and tumor necrosis factor alpha (TNFa) (55).

Here, we put forward that the observed stagnation in the maturation of the transitional Bregs potentially may be the first step in the fatal sequence of events leading to the systemic failure of humoral regulative immunity. Being accompanied by one or multiple factors, such as HLA haplotype, cytokine background, abnormal T cell negative selection, enhanced blood–brain barrier permeability, or lack of vitamin D, it may trigger the uncontrolled breakdown of the immunological tolerance toward myelin antigens. On the other hand, the elevated absolute count of tBregs and T1/T2 B cell subset ratio may be a sign of the already activated compensatory mechanisms, which may be monitored on the border of a clinically isolated syndrome and clinically defined multiple sclerosis. Further studies should elucidate if modulating the immunological checkpoints regulating B cell development may be regarded as opening up the avenue for putative therapeutical applications in MS treatment.

Data availability statement

The datasets presented in this study can be found in online repositories. The names of the repository/repositories and accession number(s) can be found below: https://www.ebi.ac.uk/arrayexpress/, E-MTAB-10859.

Ethics statement

The studies involving human participants were reviewed and approved by Local Ethic Committee of the Research Center of Neurology, Moscow, Russia. The patients/participants provided their written informed consent to participate in this study.

Author contributions

YL, ABJr and AG designed the research and wrote the paper. MNZ, MI and TS performed blood sample acquisition, patient data management and MS diagnosis. YL, LO, MK, AT, MYZ and DS performed research. YL, IZ, LO, AM, ABJr and AG analyzed data. YR, IZ, DC, NB, VM, AF and SI made intellectual contributions to data analysis. All authors contributed to the article and approved the submitted version.

Funding

This study was supported by Russian Science Foundation, grant #17-74-30019. Cell sorting experiments were carried out using the equipment provided by the IBCH core facility (CKP IBCH, supported by grant of the Ministry of Science and Higher Education of the Russian Federation no. 075-15-2020-807 (to DMC, in part of BCR repertoire analysis). ABJr would like to acknowledge personal fellowship MD-5902.2021.1.4 and Project 075-15-2021-1033 (13.2251.21.0111) for NGS.

Conflict of interest

The authors declare that the research was conducted in the absence of any commercial or financial relationships that could be construed as a potential conflict of interest.

Publisher's note

Supplementary material

The Supplementary Material for this article can be found online at: https://www.frontiersin.org/articles/10.3389/fimmu.2022.803229/full#supplementary-material

References

1. McGinley MP, Goldschmidt CH, Rae-Grant AD. Diagnosis and treatment of multiple sclerosis. *JAMA* (2021) 325:765. doi: 10.1001/jama.2020.26858

2. Aharoni R, Eilam R, Schottlender N, Radomir L, Leistner-Segal S, Feferman T, et al. Glatiramer acetate increases T- and b -regulatory cells and decreases granulocyte-macrophage colony-stimulating factor (GM-CSF) in an animal model of multiple sclerosis. *J Neuroimmunol* (2020) 345:577281. doi: 10.1016/j.jneuroim.2020.577281

3. From R, Eilam R, Bar-Lev DD, Levin-Zaidman S, Tsoory M, LoPresti P, et al. Oligodendrogenesis and myelinogenesis during postnatal development effect of glatiramer acetate. *Glia* (2014) 62:649–65. doi: 10.1002/glia.22632

4. Belogurov A, Kuzina E, Kudriaeva A, Kononikhin A, Kovalchuk S, Surina Y, et al. Ubiquitin-independent proteosomal degradation of myelin basic protein contributes to development of neurodegenerative autoimmunity. *FASEB J* (2015) 29:1901–13. doi: 10.1096/fj.14-259333

5. Belogurov AA, Stepanov AV, Smirnov IV, Melamed D, Bacon A, Mamedov AE, et al. Liposome-encapsulated peptides protect against experimental allergic encephalitis. *FASEB J* (2013) 27:222–31. doi: 10.1096/fj.12-213975

6. Belogurov A, Zakharov K, Lomakin Y, Surkov K, Avtushenko S, Kruglyakov P, et al. CD206-targeted liposomal myelin basic protein peptides in patients with multiple sclerosis resistant to first-line disease-modifying therapies: A first-in-Human, proof-of-Concept dose-escalation study. *Neurotherapeutics* (2016) 13:895–904. doi: 10.1007/s13311-016-0448-0

7. Walo-Delgado PE, Monreal E, Medina S, Quintana E, de la Maza SS, Fernández-Velasco JI, et al. Role of b cell profile for predicting secondary autoimmunity in patients treated with alemtuzumab. *Front Immunol* (2021) 12:760546. doi: 10.3389/fimmu.2021.760546

8. Fernández-Velasco JI, Kuhle J, Monreal E, Meca-Lallana V, Meca-Lallana J, Izquierdo G, et al. Effect of ocrelizumab in blood leukocytes of patients with primary progressive MS. *Neurol - Neuroimmunol Neuroinflamm* (2021) 8:e940. doi: 10.1212/NXI.0000000000000940

9. Hohlfeld R, Wekerle H. Immunological update on multiple sclerosis. *Curr Opin Neurol* (2001) 14:299–304. doi: 10.1097/00019052-200106000-00006

10. Junker A, Ivanidze J, Malotka J, Eiglmeier I, Lassmann H, Wekerle H, et al. Multiple sclerosis: T-cell receptor expression in distinct brain regions. *Brain* (2007) 130:2789–99. doi: 10.1093/brain/awm214

11. Hasler P, Zouali M. B cell receptor signaling and autoimmunity. *FASEB J* (2001) 15:2085–98. doi: 10.1096/fj.00-0860rev

12. Lomakin YA, Zakharova MY, Stepanov AV, Dronina MA, Smirnov IV, Bobik TV, et al. Heavy-light chain interrelations of MS-associated immunoglobulins probed by deep sequencing and rational variation. *Mol Immunol* (2014) 62:305–14. doi: 10.1016/j.molimm.2014.01.013

13. Ponomarenko NA, Durova OM, Vorobiev II, Belogurov AA, Kurkova IN, Petrenko AG, et al. Autoantibodies to myelin basic protein catalyze site-specific degradation of their antigen. *Proc Natl Acad Sci U.S.A.* (2006) 103:281–6. doi: 10.1073/pnas.0509849103

14. Villar LM, Sádaba MC, Roldán E, Masjuan J, González-Porqué P, Villarrubia N, et al. Intrathecal synthesis of oligoclonal IgM against myelin lipids predicts an aggressive disease course in MS. *J Clin Invest* (2005) 115:187–94. doi: 10.1172/JCI22833

15. Reali C, Magliozzi R, Roncaroli F, Nicholas R, Howell OW, Reynolds R. B cell rich meningeal inflammation associates with increased spinal cord pathology in multiple sclerosis. *Brain Pathol* (2020) 30:779–93. doi: 10.1111/bpa.12841

16. Cencioni MT, Mattoscio M, Magliozzi R, Bar-Or A, Muraro PA. B cells in multiple sclerosis — from targeted depletion to immune reconstitution therapies. *Nat Rev Neurol* (2021) 17:399–414. doi: 10.1038/s41582-021-00498-5

17. Mauri C, Menon M. Human regulatory b cells in health and disease: Therapeutic potential. *J Clin Invest* (2017) 127:772–9. doi: 10.1172/JCI85113

18. Sokolov AV, Shmidt AA, Lomakin YA. B Cell regulation in autoimmune diseases. *Acta Naturae* (2018) 10:11–22. doi: 10.32607/20758251-2018-10-3-11-22

19. Katz SI, Parker D, Turk JL. B-cell suppression of delayed hypersensitivity reactions. *Nature* (1974) 251:550–1. doi: 10.1038/251550a0

20. Wolf SD, Dittel BN, Hardardottir F, Janeway CA. Experimental autoimmune encephalomyelitis induction in genetically b cell–deficient mice. *J Exp Med* (1996) 184:2271–8. doi: 10.1084/jem.184.6.2271

21. Matsushita T, Horikawa M, Iwata Y, Tedder TF. Regulatory b cells (B10 cells) and regulatory T cells have independent roles in controlling experimental autoimmune encephalomyelitis initiation and late-phase immunopathogenesis. *J Immunol* (2010) 185:2240–52. doi: 10.4049/jimmunol.1001307

22. Mauri C, Gray D, Mushtaq N, Londei M. Prevention of arthritis by interleukin 10–producing b cells. *J Exp Med* (2003) 197:489–501. doi: 10.1084/jem.20021293

23. Mangan NE, van Rooijen N, McKenzie ANJ, Fallon PG. Helminth-modified pulmonary immune response protects mice from allergen-induced airway hyperresponsiveness. *J Immunol* (2006) 176:138–47. doi: 10.4049/jimmunol.176.1.138

24. Flores-Borja F, Bosma A, Ng D, Reddy V, Ehrenstein MR, Isenberg DA, et al. CD19+CD24hiCD38hi b cells maintain regulatory T cells while limiting TH1 and TH17 differentiation. *Sci Transl Med* (2013) 5(173):173ra23. doi: 10.1126/scitranslmed.3005407

25. Iwata Y, Matsushita T, Horikawa M, DiLillo DJ, Yanaba K, Venturi GM, et al. Characterization of a rare IL-10–competent b-cell subset in humans that parallels mouse regulatory B10 cells. *Blood* (2011) 117:530–41. doi: 10.1182/blood-2010-07-294249

26. Blair PA, Noreña LY, Flores-Borja F, Rawlings DJ, Isenberg DA, Ehrenstein MR, et al. CD19+CD24hiCD38hi b cells exhibit regulatory capacity in healthy individuals but are functionally impaired in systemic lupus erythematosus patients. *Immunity* (2010) 32:129–40. doi: 10.1016/j.immuni.2009.11.009

27. Sun F, Ladha SS, Yang L, Liu Q, Shi SX, Su N, et al. Interleukin-10 producing-b cells and their association with responsiveness to rituximab in myasthenia gravis. *Muscle Nerve* (2014) 49:487–94. doi: 10.1002/mus.23951

28. Knippenberg S, Peelen E, Smolders J, Thewissen M, Menheere P, Cohen Tervaert JW, et al. Reduction in IL-10 producing b cells (Breg) in multiple sclerosis is accompanied by a reduced naïve/memory breg ratio during a relapse but not in remission. *J Neuroimmunol* (2011) 239:80–6. doi: 10.1016/j.jneuroim.2011.08.019

29. Cencioni MT, Ali R, Nicholas R, Muraro PA. Defective CD19+CD24 hi CD38 hi transitional b-cell function in patients with relapsing-remitting MS. *Mult Scler J* (2021) 27:1187–97. doi: 10.1177/1352458520951536

30. Ma S, Satitsuksanoa P, Jansen K, Cevhertas L, van de Veen W, Akdis M. B regulatory cells in allergy. *Immunol Rev* (2021) 299:10–30. doi: 10.1111/imr.12937

31. Siewe B, Stapleton JT, Martinson J, Keshavarzian A, Kazmi N, Demarais PM, et al. Regulatory b cell frequency correlates with markers of HIV disease progression and attenuates anti-HIV CD8 + T cell function *in vitro*. *J Leukoc Biol* (2013) 93:811–8. doi: 10.1189/jlb.0912436

32. Rosser EC, Mauri C. Regulatory b cells: Origin, phenotype, and function. *Immunity* (2015) 42:607–12. doi: 10.1016/j.immuni.2015.04.005

33. Hasan MM, Thompson-Snipes L, Klintmalm G, Demetris AJ, O'Leary J, Oh S, et al. CD24 hi CD38 hi and CD24 hi CD27 + human regulatory b cells display common and distinct functional characteristics. *J Immunol* (2019) 203:2110–20. doi: 10.4049/jimmunol.1900488

34. van de Veen W, Stanic B, Yaman G, Wawrzyniak M, Söllner S, Akdis DG, et al. IgG4 production is confined to human IL-10–producing regulatory b cells that suppress antigen-specific immune responses. *J Allergy Clin Immunol* (2013) 131:1204–12. doi: 10.1016/j.jaci.2013.01.014

35. Matsumoto M, Baba A, Yokota T, Nishikawa H, Ohkawa Y, Kayama H, et al. Interleukin-10-Producing plasmablasts exert regulatory function in autoimmune inflammation. *Immunity* (2014) 41:1040–51. doi: 10.1016/j.immuni.2014.10.016

36. Hasan MM, Nair SS, O'Leary JG, Thompson-Snipes L, Nyarige V, Wang J, et al. Implication of TIGIT+ human memory b cells in immune regulation. *Nat Commun* (2021) 12:1534. doi: 10.1038/s41467-021-21413-y

37. Noh J, Choi WS, Noh G, Lee JH. Presence of Foxp3-expressing CD19(+) CD5(+) b cells in human peripheral blood mononuclear cells: Human CD19(+) CD5(+)Foxp3(+) regulatory b cell (Breg). *Immune Netw* (2010) 10:247–9. doi: 10.4110/in.2010.10.6.247

38. Lindner S, Dahlke K, Sontheimer K, Hagn M, Kaltenmeier C, Barth TFE, et al. Interleukin 21–induced granzyme b–expressing b cells infiltrate tumors and regulate T cells. *Cancer Res* (2013) 73:2468–79. doi: 10.1158/0008-5472.CAN-12-3450

39. Marie-Cardine A, Divay F, Dutot I, Green A, Perdrix A, Boyer O, et al. Transitional b cells in humans: Characterization and insight from b lymphocyte reconstitution after hematopoietic stem cell transplantation. *Clin Immunol* (2008) 127:14–25. doi: 10.1016/j.clim.2007.11.013

40. Simon Q, Pers J-O, Cornec D, Le Pottier L, Mageed RA, Hillion S. In-depth characterization of CD24 high CD38 high transitional human b cells reveals different regulatory profiles. *J Allergy Clin Immunol* (2016) 137:1577–1584.e10. doi: 10.1016/j.jaci.2015.09.014

41. Guerrier T, Labalette M, Launay D, Lee-Chang C, Outteryck O, Lefèvre G, et al. Proinflammatory b-cell profile in the early phases of MS predicts an active disease. *Neurol - Neuroimmunol Neuroinflamm* (2018) 5:e431. doi: 10.1212/NXI.0000000000000431

42. von Büdingen H-C, Palanichamy A, Lehmann-Horn K, Michel BA, Zamvil SS. Update on the autoimmune pathology of multiple sclerosis: B-cells as disease-drivers and therapeutic targets. *Eur Neurol* (2015) 73:238–46. doi: 10.1159/000377675

43. McFarland HF. The b cell — old player, new position on the team. *N Engl J Med* (2008) 358:664–5. doi: 10.1056/NEJMp0708143

44. Belogurov AA, Kurkova IN, Friboulet A, Thomas D, Misikov VK, Zakharova MY, et al. Recognition and degradation of myelin basic protein peptides by serum autoantibodies: Novel biomarker for multiple sclerosis. *J Immunol* (2008) 180:1258–67. doi: 10.4049/jimmunol.180.2.1258

45. Lomakin Y, Kudriaeva A, Kostin N, Terekhov S, Kaminskaya A, Chernov A, et al. Diagnostics of autoimmune neurodegeneration using fluorescent probing. *Sci Rep* (2018) 8:12679. doi: 10.1038/s41598-018-30938-0

46. Gabibov AG, Belogurov AA, Lomakin YA, Zakharova MY, Avakyan ME, Dubrovskaya VV, et al. Combinatorial antibody library from multiple sclerosis patients reveals antibodies that cross-react with myelin basic protein and EBV antigen. *FASEB J* (2011) 25:4211–21. doi: 10.1096/fj.11-190769

47. Lomakin Y, Arapidi GP, Chernov A, Ziganshin R, Tcyganov E, Lyadova I, et al. Exposure to the Epstein–Barr viral antigen latent membrane protein 1 induces myelin-reactive antibodies *in vivo*. *Front Immunol* (2017) 8:777. doi: 10.3389/fimmu.2017.00777

48. Tejada-Simon MV, Zang YCQ, Hong J, Rivera VM, Zhang JZ. Cross-reactivity with myelin basic protein and human herpesvirus-6 in multiple sclerosis. *Ann Neurol* (2003) 53:189–97. doi: 10.1002/ana.10425

49. Tengvall K, Huang J, Hellström C, Kammer P, Biström M, Ayoglu B, et al. Molecular mimicry between anoctamin 2 and Epstein-Barr virus nuclear antigen 1 associates with multiple sclerosis risk. *Proc Natl Acad Sci* (2019) 116:16955–60. doi: 10.1073/pnas.1902623116

50. Bjornevik K, Cortese M, Healy BC, Kuhle J, Mina MJ, Leng Y, et al. Longitudinal analysis reveals high prevalence of Epstein-Barr virus associated with multiple sclerosis. *Science* (2022) 375:296–301. doi: 10.1126/science.abj8222

51. Guo S, Chen Q, Liang X, Mu M, He J, Fang Q, et al. Reduced peripheral blood regulatory b cell levels are not associated with the expanded disability status scale score in multiple sclerosis. *J Int Med Res* (2018) 46:3970–8. doi: 10.1177/0300060518783083

52. Michel L, Chesneau M, Manceau P, Genty A, Garcia A, Salou M, et al. Unaltered regulatory b-cell frequency and function in patients with multiple sclerosis. *Clin Immunol* (2014) 155:198–208. doi: 10.1016/j.clim.2014.09.011

53. Jiusheng Deng JH. Blood b cell and regulatory subset content in multiple sclerosis patients. *J Mult Scler* (2015) 2(2):1000139. doi: 10.4172/2376-0389.1000139

54. de Andrés C, Tejera-Alhambra M, Alonso B, Valor L, Teijeiro R, Ramos-Medina R, et al. New regulatory CD19+CD25+ b-cell subset in clinically isolated syndrome and multiple sclerosis relapse. changes after glucocorticoids. *J Neuroimmunol* (2014) 270:37–44. doi: 10.1016/j.jneuroim.2014.02.003

55. Glass MC, Glass DR, Oliveria J-P, Mbiribindi B, Esquivel CO, Krams SM, et al. Human IL-10-producing b cells have diverse states that are induced from multiple b cell subsets. *Cell Rep* (2022) 39:110728. doi: 10.1016/j.celrep.2022.110728

56. Lighaam LC, Unger P-PA, Vredevoogd DW, Verhoeven D, Vermeulen E, Turksma AW, et al. *In vitro*-induced human IL-10+ b cells do not show a subset-defining marker signature and plastically Co-express IL-10 with pro-inflammatory cytokines. *Front Immunol* (2018) 9:1913. doi: 10.3389/fimmu.2018.01913

57. Schaefer LM, Poettgen J, Fischer A, Gold S, Stellmann JP, Heesen C. Impairment and restrictions in possibly benign multiple sclerosis. *Brain Behav* (2019) 9(4):e01259. doi: 10.1002/brb3.1259

58. Díaz C, Zarco LA, Rivera DM. Highly active multiple sclerosis: An update. *Mult Scler Relat Disord* (2019) 30:215–24. doi: 10.1016/j.msard.2019.01.039

59. Kurtzke JF. Rating neurologic impairment in multiple sclerosis: An expanded disability status scale (EDSS). *Neurology* (1983) 33:1444–52. doi: 10.1212/WNL.33.11.1444

60. Sanz I, Wei C, Jenks SA, Cashman KS, Tipton C, Woodruff MC, et al. Challenges and opportunities for consistent classification of human b cell and plasma cell populations. *Front Immunol* (2019) 10:2458. doi: 10.3389/fimmu.2019.02458

61. Burton H, Dorling A. Transitional b cell subsets–a convincing predictive biomarker for allograft loss? *Kidney Int* (2017) 91:18–20. doi: 10.1016/j.kint.2016.10.028

62. Cheng J, Torkamani A, Grover RK, Jones TM, Ruiz DI, Schork NJ, et al. Ectopic b-cell clusters that infiltrate transplanted human kidneys are clonal. *Proc Natl Acad Sci* (2011) 108:5560–5. doi: 10.1073/pnas.1101148108

63. Bolotin DA, Poslavsky S, Mitrophanov I, Shugay M, Mamedov IZ, Putintseva EV, et al. MiXCR: Software for comprehensive adaptive immunity profiling. *Nat Methods* (2015) 12:380–1. doi: 10.1038/nmeth.3364

64. Shugay M, Bagaev DV, Turchaninova MA, Bolotin DA, Britanova OV, Putintseva EV, et al. VDJtools: Unifying post-analysis of T cell receptor repertoires. *PloS Comput Biol* (2015) 11:e1004503. doi: 10.1371/journal.pcbi.1004503

65. Lefranc M-P, Pommié C, Ruiz M, Giudicelli V, Foulquier E, Truong L, et al. IMGT unique numbering for immunoglobulin and T cell receptor variable domains and ig superfamily V-like domains. *Dev Comp Immunol* (2003) 27:55–77. doi: 10.1016/s0145-305x(02)00039-3

66. Zhu H-Q, Xu R-C, Chen Y-Y, Yuan H-J, Cao H, Zhao X-Q, et al. Impaired function of CD19 + CD24 hi CD38 hi regulatory b cells in patients with pemphigus. *Br J Dermatol* (2015) 172:101–10. doi: 10.1111/bjd.13192

67. Cherukuri A, Salama AD, Carter CR, Landsittel D, Arumugakani G, Clark B, et al. Reduced human transitional b cell T1/T2 ratio is associated with subsequent deterioration in renal allograft function. *Kidney Int* (2017) 91:183–95. doi: 10.1016/j.kint.2016.08.028

68. Duong BH, Ota T, Aït-Azzouzene D, Aoki-Ota M, Vela JL, Huber C, et al. Peripheral b cell tolerance and function in transgenic mice expressing an IgD superantigen. *J Immunol* (2010) 184:4143–58. doi: 10.4049/jimmunol.0903564

69. Zhou Y, Zhang Y, Han J, Yang M, Zhu J, Jin T. Transitional b cells involved in autoimmunity and their impact on neuroimmunological diseases. *J Transl Med* (2020) 18:131. doi: 10.1186/s12967-020-02289-w

70. Chaudhary N, Wesemann DR. Analyzing immunoglobulin repertoires. *Front Immunol* (2018) 9:462. doi: 10.3389/fimmu.2018.00462

71. Mitsunaga EM, Snyder MP. Deep characterization of the human antibody response to natural infection using longitudinal immune repertoire sequencing. *Mol Cell Proteomics* (2020) 19:278–93. doi: 10.1074/mcp.RA119.001633

72. Klein U, Rajewsky K, Küppers R. Human immunoglobulin (Ig)M+IgD+ peripheral blood b cells expressing the CD27 cell surface antigen carry somatically mutated variable region genes: CD27 as a general marker for somatically mutated (memory) b cells. *J Exp Med* (1998) 188:1679–89. doi: 10.1084/jem.188.9.1679

73. Niino M, Hirotani M, Miyazaki Y, Sasaki H. Memory and naïve b-cell subsets in patients with multiple sclerosis. *Neurosci Lett* (2009) 464:74–8. doi: 10.1016/j.neulet.2009.08.010

74. Ciocca M, Zaffina S, Fernandez Salinas A, Bocci C, Palomba P, Conti MG, et al. Evolution of human memory b cells from childhood to old age. *Front Immunol* (2021) 12:690534. doi: 10.3389/fimmu.2021.690534

75. Mauri C, Menon M. The expanding family of regulatory b cells. *Int Immunol* (2015) 27:479–86. doi: 10.1093/intimm/dxv038

76. Fillatreau S, Sweenie CH, McGeachy MJ, Gray D, Anderton SM. B cells regulate autoimmunity by provision of IL-10. *Nat Immunol* (2002) 3:944–50. doi: 10.1038/ni833

77. Natarajan P, Singh A, McNamara JT, Secor ER, Guernsey LA, Thrall RS, et al. Regulatory b cells from hilar lymph nodes of tolerant mice in a murine model of allergic airway disease are CD5+, express TGF-β, and co-localize with CD4 +Foxp3+ T cells. *Mucosal Immunol* (2012) 5:691–701. doi: 10.1038/mi.2012.42

78. Zhang Y, Li J, Zhou N, Zhang Y, Wu M, Xu J, et al. The unknown aspect of BAFF: Inducing IL-35 production by a CD5+CD1dhiFcγRIIbhi regulatory b-cell subset in lupus. *J Invest Dermatol* (2017) 137:2532–43. doi: 10.1016/j.jid.2017.07.843

79. Murphy KM, Nelson CA, Šedý JR. Balancing co-stimulation and inhibition with BTLA and HVEM. *Nat Rev Immunol* (2006) 6:671–81. doi: 10.1038/nri1917

80. Oleinika K, Mauri C, Salama AD. Effector and regulatory b cells in immune-mediated kidney disease. *Nat Rev Nephrol* (2019) 15:11–26. doi: 10.1038/s41581-018-0074-7

81. Duddy M, Niino M, Adatia F, Hebert S, Freedman M, Atkins H, et al. Distinct effector cytokine profiles of memory and naive human b cell subsets and implication in multiple sclerosis. *J Immunol* (2007) 178:6092–9. doi: 10.4049/jimmunol.178.10.6092

82. Hirotani M, Niino M, Fukazawa T, Kikuchi S, Yabe I, Hamada S, et al. Decreased IL-10 production mediated by toll-like receptor 9 in b cells in multiple sclerosis. *J Neuroimmunol* (2010) 221:95–100. doi: 10.1016/j.jneuroim.2010.02.012

83. Luo Y, Luo F, Zhang K, Wang S, Zhang H, Yang X, et al. Elevated circulating IL-10 producing breg, but not regulatory b cell levels, restrain antibody-mediated rejection after kidney transplantation. *Front Immunol* (2020) 11:627496. doi: 10.3389/fimmu.2020.627496

84. Dai Y-C, Zhong J, Xu J-F. Regulatory b cells in infectious disease. *Mol Med Rep* (2017) 16:3–10. doi: 10.3892/mmr.2017.6605

85. Lampropoulou V, Hoehlig K, Roch T, Neves P, Gómez EC, Sweenie CH, et al. TLR-activated b cells suppress T cell-mediated autoimmunity. *J Immunol* (2008) 180:4763–73. doi: 10.4049/jimmunol.180.7.4763

86. Das A, Ellis G, Pallant C, Lopes AR, Khanna P, Peppa D, et al. IL-10–producing regulatory b cells in the pathogenesis of chronic hepatitis b virus infection. *J Immunol* (2012) 189:3925–35. doi: 10.4049/jimmunol.1103139

87. Horikawa M, Weimer ET, DiLillo DJ, Venturi GM, Spolski R, Leonard WJ, et al. Regulatory b cell (B10 cell) expansion during listeria infection governs innate and cellular immune responses in mice. *J Immunol* (2013) 190:1158–68. doi: 10.4049/jimmunol.1201427

88. Neves P, Lampropoulou V, Calderon-Gomez E, Roch T, Stervbo U, Shen P, et al. Signaling *via* the MyD88 adaptor protein in b cells suppresses protective immunity during salmonella typhimurium infection. *Immunity* (2010) 33:777–90. doi: 10.1016/j.immuni.2010.10.016

89. Hussaarts L, van der Vlugt LEPM, Yazdanbakhsh M, Smits HH. Regulatory b-cell induction by helminths: Implications for allergic disease. *J Allergy Clin Immunol* (2011) 128:733–9. doi: 10.1016/j.jaci.2011.05.012

90. Bankó Z, Pozsgay J, Szili D, Tóth M, Gáti T, Nagy G, et al. Induction and differentiation of IL-10–producing regulatory b cells from healthy blood donors and rheumatoid arthritis patients. *J Immunol* (2017) 198:1512–20. doi: 10.4049/jimmunol.1600218

91. Tsubata T, Wu J, Honjo T. B-cell apoptosis induced by antigen receptor crosslinking is blocked by a T-cell signal through CD40. *Nature* (1993) 364:645–8. doi: 10.1038/364645a0

92. Matsumoto M, Fujii Y, Baba A, Hikida M, Kurosaki T, Baba Y. The calcium sensors STIM1 and STIM2 control b cell regulatory function through interleukin-10 production. *Immunity* (2011) 34:703–14. doi: 10.1016/j.immuni.2011.03.016

93. Yanaba K, Bouaziz J-D, Haas KM, Poe JC, Fujimoto M, Tedder TF. A regulatory b cell subset with a unique CD1dhiCD5+ phenotype controls T cell-dependent inflammatory responses. *Immunity* (2008) 28:639–50. doi: 10.1016/j.immuni.2008.03.017

94. Yanaba K, Bouaziz J-D, Matsushita T, Tsubata T, Tedder TF. The development and function of regulatory b cells expressing IL-10 (B10 cells) requires antigen receptor diversity and TLR signals. *J Immunol* (2009) 182:7459–72. doi: 10.4049/jimmunol.0900270

95. Tedder TF. B10 cells: A functionally defined regulatory b cell subset. *J Immunol* (2015) 194:1395–401. doi: 10.4049/jimmunol.1401329

96. Lykken JM, Candando KM, Tedder TF. Regulatory B10 cell development and function: Fig. *L Int Immunol* (2015) 27:471–7. doi: 10.1093/intimm/dxv046

97. Mittal SK, Roche PA. Suppression of antigen presentation by IL-10. *Curr Opin Immunol* (2015) 34:22–7. doi: 10.1016/j.coi.2014.12.009

98. Kitaura K, Yamashita H, Ayabe H, Shini T, Matsutani T, Suzuki R. Different somatic hypermutation levels among antibody subclasses disclosed by a new next-generation sequencing-based antibody repertoire analysis. *Front Immunol* (2017) 8:389. doi: 10.3389/fimmu.2017.00389

99. Galson JD, Trück J, Fowler A, Clutterbuck EA, Münz M, Cerundolo V, et al. Analysis of b cell repertoire dynamics following hepatitis b vaccination in humans, and enrichment of vaccine-specific antibody sequences. *EBioMedicine* (2015) 2:2070–9. doi: 10.1016/j.ebiom.2015.11.034

100. Kaplinsky J, Li A, Sun A, Coffre M, Koralov SB, Arnaout R. Antibody repertoire deep sequencing reveals antigen-independent selection in maturing b cells. *Proc Natl Acad Sci* (2014) 111:E2622–9. doi: 10.1073/pnas.1403278111

101. Sankar K, Hoi KH, Hötzel I. Dynamics of heavy chain junctional length biases in antibody repertoires. *Commun Biol* (2020) 3:207. doi: 10.1038/s42003-020-0931-3

102. Meffre E, Milili M, Blanco-Betancourt C, Antunes H, Nussenzweig MC, Schiff C. Immunoglobulin heavy chain expression shapes the b cell receptor repertoire in human b cell development. *J Clin Invest* (2001) 108:879–86. doi: 10.1172/JCI13051

103. Boyd SD, Liu Y, Wang C, Martin V, Dunn-Walters DK. Human lymphocyte repertoires in ageing. *Curr Opin Immunol* (2013) 25:511–5. doi: 10.1016/j.coi.2013.07.007

104. Martin VG, Wu Y-CB, Townsend CL, Lu GHC, O'Hare JS, Mozeika A, et al. Transitional b cells in early human b cell development – time to revisit the paradigm? *Front Immunol* (2016) 7:546. doi: 10.3389/fimmu.2016.00546

105. Maseda D, Candando KM, Smith SH, Kalampokis I, Weaver CT, Plevy SE, et al. Peritoneal cavity regulatory b cells (B10 cells) modulate IFN-γ + CD4 + T cell numbers during colitis development in mice. *J Immunol* (2013) 191:2780–95. doi: 10.4049/jimmunol.1300649

106. Maseda D, Smith SH, DiLillo DJ, Bryant JM, Candando KM, Weaver CT, et al. Regulatory B10 cells differentiate into antibody-secreting cells after transient IL-10 production *in vivo*. *J Immunol* (2012) 188:1036–48. doi: 10.4049/jimmunol.1102500

Frontiers in Immunology

Explores novel approaches and diagnoses to treat immune disorders.

The official journal of the International Union of Immunological Societies (IUIS) and the most cited in its field, leading the way for research across basic, translational and clinical immunology.

Discover the latest Research Topics

See more →

Frontiers

Avenue du Tribunal-Fédéral 34
1005 Lausanne, Switzerland
frontiersin.org

Contact us

+41 (0)21 510 17 00
frontiersin.org/about/contact